Type VI secretion system mediated competition in *Pseudomonas aeruginosa*: modulation of system activity, contribution of individual toxins and bacterial intermixing.

Marta Rudzite

Department of Life Sciences
Imperial College London

2023

This thesis is submitted in fulfilment of the requirements for the degree of Doctor of Philosophy

Statement of Originality

I, Marta Rudzite, hereby confirm that the work presented in this thesis is my own and that the contributions of others are duly acknowledged and appropriately referenced.

Copyright Declaration

The copyright of this thesis rests with the author. Unless otherwise indicated, its contents are licensed under a Creative Commons Attribution-Non Commercial-No Derivatives 4.0 International Licence (CC BY-NC-ND).

Under this licence, you may copy and redistribute the material in any medium or format on the condition that; you credit the author, do not use it for commercial purposes and do not distribute modified versions of the work.

When reusing or sharing this work, ensure you make the licence terms clear to others by naming the licence and linking to the licence text.

Please seek permission from the copyright holder for uses of this work that are not included in this licence or permitted under UK Copyright Law.

Abstract

The type VI secretion system (T6SS) is a macromolecular weapon that is used by numerous Gram-negative bacteria and allows to inject toxins directly into adjacent cells. *Pseudomonas aeruginosa* is an opportunistic pathogen and uses T6SS for bacterial competition that allows it to establish and persist within dense polymicrobial biofilm communities. *P. aeruginosa* possesses 3 distinct T6SSs and a set of more than 20 toxic effectors with diverse functions including disruption of cell wall integrity, degradation of nucleic acids, or metabolic impairment. We generated a collection of mutants with various degrees of T6SS activity and/or sensitivity to each of the individual T6SS toxins and through disruption of genes encoding Gac-Rsm cascade components we generate a set of strains with graduated T6SS activity and killing capacity. By imaging whole mixed bacterial macrocolonies, we observed that the efficacy of individual T6SS toxins is highly variable and synergistic use maximises impact on prey growth. We show that competition mediated by as little as a single toxin delivered at low doses enables restriction of prey bacterial expansion while increase in toxin delivery rate enables a near complete elimination of prey bacteria. Remarkably, the degree of intermixing between prey and attacker populations is also key determinant of the competition outcome, as active intermixing promotes the frequency of contacts between competitors, and prey populations can use type IV pili-dependent twitching motility to move away from the attacking population. Finally, we implemented a computational model to better understand how changes in T6SS firing behaviours or cell-cell contacts lead to population-level competitive advantages. Overall, furthering the understanding of how highly local contact-based interactions between individuals shape the structure of whole populations, thus providing conceptual insight applicable to all types of contact-based competition.

Acknowledgments

I would like to thank my supervisors Prof Alain Filloux and Prof Robert Endres for giving me the opportunity to undertake my PhD studies.

I want to extent my thanks to all lab members from the Filloux lab and many other within CMBI, for exchanges both scientific and not so science related, it has been great being part of this community.

I would also like to acknowledge the technical help provided by FILM facility staff who helped me with both the initial microscopy setup and later troubleshooting along the way. Further, I would like to thank Dr Suhail Islam for help with computational access and data handling as well as Prof Knut Drescher for helpful discussion.

Contents

List of Figures **13**

List of Tables **17**

1 Introduction **20**

1.1 *Pseudomonas aeruginosa* 20

1.1.1 *Pseudomonas aeruginosa* in infection 21

1.1.2 Virulence factors 22

1.1.3 Antibiotic resistance and niche adaptation 24

1.1.4 Target for design of novel therapeutic approaches 26

1.2 Bacterial communities 29

1.2.1 Two bacterial lifestyles - planktonic and biofilm 29

1.2.2 c-di-GMP and biofilm formation 29

1.2.3 Gac-Rsm regulatory cascade 32

1.2.3.1 RNA binding proteins RsmA and RsmN 32

1.2.3.2 Small RNAs controlling Rsm protein availability 36

1.2.3.3 GacS/GacA two component system and impact of sensory kinases RetS, PA1611, and LadS 39

1.2.4 *Pseudomonas aeruginosa* motility 40

1.2.4.1 Flagella mediated motility 40

1.2.4.2 Type IV pili mediated motility and impact on community organisation 42

1.2.5 Biofilms 45

1.2.5.1 Biofilm formation 46

1.2.6 Extracellular matrix 49

1.2.6.1 Alginate . . . 50
1.2.6.2 Psl . . . 51
1.2.6.3 Pel . . . 52
1.2.6.4 eDNA . . . 53
1.2.6.5 Summary of exopolymeric substances . . . 54
1.3 Bacterial interactions . . . 55
1.3.1 Types of bacterial interactions . . . 55
1.3.2 Tools used in bacterial competition . . . 58
1.3.3 Type V secretion system . . . 59
1.3.4 Type IV secretion system . . . 61
1.3.5 Type VII Secretion system . . . 63
1.3.6 Toxin-antitoxin systems contribute to polymorphic toxin effector pool . . . 65
1.3.7 Bacteriocins - tailocins and pyocins . . . 66
1.3.8 Extracellular contractile injection systems . . . 69
1.3.9 *P. aeruginosa* small molecule products with antimicrobial impact . . . 70
1.3.10 Outer membrane vesicles . . . 73
1.4 Type VI secretion system . . . 74
1.4.1 T6SS - a molecular machine for effector injection . . . 74
1.4.2 Modes of effector delivery . . . 77
1.4.3 T6SS in *P. aeruginosa* . . . 80
1.4.4 Control of T6SS firing . . . 82
1.4.5 T6SS toxin effectors . . . 84
1.4.5.1 Peptidoglycan targeting toxins . . . 85
1.4.5.2 Lipases . . . 86
1.4.5.3 Pore forming toxins . . . 87
1.4.5.4 Nucleases . . . 88
1.4.5.5 Metabolism targeting toxins . . . 89
1.4.6 Cognate toxin immunity . . . 90
1.4.7 Trans-kingdom effectors . . . 92
1.4.8 Common good effectors . . . 94
1.4.9 Identification of further effectors . . . 96
1.4.10 Non-immunity defences against T6SS . . . 97

1.4.10.1 Stress responses and damage repair . . . 98
1.4.10.2 Protection provided by EPS and cell envelopes . . . 100
1.4.10.3 Gram-positive resistance to T6SS attacks . . . 101
1.5 Using computational approaches to study bacterial community dynamics . . . 102
1.5.1 Approaches to modelling bacterial communities . . . 103
1.5.2 Theoretical modelling of dynamics within contact-mediated microbial competition . . . 106
1.5.2.1 Use of contact mediated competition enables niche domination, but species extinction events are rare . . . 107
1.5.2.2 Strain spatial segregation - emergent property and protective mechanism . . . 109
1.5.2.3 Population geometry determines competitive outcomes . . . 111
1.5.2.4 Comparing benefits of contact-mediated and long-range competition . . . 112
1.5.2.5 Competitive benefits of distinct T6SS firing-strategies . . . 114
1.6 Project aims . . . 116

2 Methods **117**

2.1 Bacterial strains and growth conditions . . . 117
2.2 DNA manipulation . . . 131
2.3 Plasmid delivery . . . 131
2.3.1 Transformation into competent cells . . . 131
2.3.2 Three partner conjugation . . . 132
2.3.3 Electroporation . . . 133
2.4 *P. aeruginosa* genomic manipulation . . . 134
2.4.1 Gene deletions and fusions . . . 134
2.4.2 Fluorescent tagging . . . 136
2.4.3 Measuring gene expression using plasmid based reporters . . . 136
2.5 CdrA reporter measurements . . . 138
2.6 Biofilm assay . . . 138
2.7 Motility assays . . . 139
2.7.1 Twitching assay . . . 139

2.7.2 Swimming assay . . . 140
2.7.3 Swarming assay . . . 140
2.8 T6SS expression and activity assays . . . 140
2.8.1 Protein sample preparation . . . 140
2.8.2 Western blotting . . . 141
2.9 Competition assay . . . 142
2.10 Microscopy . . . 143
2.10.1 Whole colony microscopy . . . 143
2.10.2 Single cell microscopy . . . 143
2.11 Data processing . . . 144
2.11.1 Image analysis . . . 144
2.12 Modelling . . . 145
2.12.1 Cell growth and movement . . . 147
2.12.2 T6SS interactions . . . 147
2.12.3 Model setups and analysis . . . 148

3 Role of c-di-GMP in regulation of *Pseudomonas aeruginosa* T6SS 149
3.1 Introduction . . . 149
3.2 Results . . . 152
3.2.1 Changes in relative c-di-GMP levels correlate with amounts of biofilm formed 152
3.2.2 Loss of SadC results in decreased H1-T6SS activity while H2- and H3-T6SS expression is elevated . . . 154
3.2.3 *P. aeruginosa* T6SS activity is modulated by c-di-GMP levels . . . 155
3.2.4 Mutation in *pppA* can "rescue" c-di-GMP mediated H1-T6SS firing impairment . . . 157
3.3 Discussion . . . 159

4 The Gac-Rsm cascade modulates expression, activity and killing capacity of *Pseudomonas aeruginosa* T6SSs 162
4.1 Introduction . . . 162
4.2 The Gac-Rsm cascade modulates expression and activity of all 3 *P. aeruginosa* T6SSs . . . 166
4.2.1 Gac-Rsm dependent changes in core T6SS promoter activity . . . 166

4.2.2 Gac-Rsm dependent elevation in Hcp abundance in cells and culture supernatant fraction . . . 169
4.2.3 *gac-rsm* mutants show increased TssBC sheath assembly dynamics . . . 170
4.2.4 *gac-rsm* mutants show increased H1- and H2-T6SS-dependent competitiveness . . . 172
4.3 Discussion . . . 176

5 Individual *Pseudomonas aeruginosa* T6SS toxin mediated killing determines lineage distribution within communities 179

5.1 Introduction . . . 179
5.2 Whole colony microscopy setup for imaging bacterial competition . . . 183
5.2.1 Bacterial distribution in mixed macrocolonies . . . 183
5.2.2 Ability to actively fire T6SS is not sufficient to provide a competitive advantage. . . . 186
5.3 Delivery of individual T6SS toxins restricts prey expansion within macrocolonies. 187
5.3.1 H1-T6SS toxin-mediated competition in different Gac-Rsm mutant strains 187
5.3.2 Analysis of changes in sensitive lineage spatial distribution upon T6SS attack . . . 191
5.3.3 T6SS toxins act synergistically . . . 193
5.3.3.1 *P. aeruginosa* engages in effective H1-T6SS toxin-mediated competition under nutrient limitation . . . 194
5.3.4 H1-T6SS toxin-mediated killing occurs independently of prey T6SS activity 196
5.3.5 Loss of *pppA* results in elevated H1-T6SS firing, but does not change toxin-mediated competition outcome within a context of mixed bacterial macrocolonies . . . 198
5.4 Growth temperature dictates outcome of H2-T6SS-dependent competition . . . 200
5.4.1 Low temperature promotes H2-T6SS sheath assembly . . . 200
5.4.2 Sensitivity to H2-T6SS toxins results in prey growth restriction at low temperatures . . . 201
5.4.3 Change in growth temperature has only minor impact on H1-T6SS toxin-mediated killing . . . 207

5.5 Theoretical model of T6SS interactions reveals how mode of toxin action is key determinant of competitive success . . . 208
5.5.1 Toxin lysis rate and attacker firing dynamics determine competition outcome 208
5.5.2 *P. aeruginosa* H1-T6SS-typical non-homogeneous firing behaviour is consistent with the ability to proficiently out-compete prey bacteria . . . 212
5.6 Discussion . . . 215
5.6.1 Increase in T6SS firing results in improved killing . . . 215
5.6.2 Differing toxin biochemical activity - importance of lytic toxins . . . 216
5.6.3 Toxin synergy . . . 218
5.6.4 Changes in growth conditions impact T6SS-mediated competition efficacy 220
5.6.5 Summary . . . 221

6 Prey-attacker contact assortment determines T6SS mediated competition outcome 222

6.1 Introduction . . . 222
6.2 Results . . . 226
6.2.1 Inoculum composition determines the number of prey-attacker contacts within macrocolony and subsequent survival of T6SS sensitive prey . . . 226
6.2.1.1 Inoculum density and strain ratio determines local contact assortment . . . 227
6.2.1.2 Effectiveness of T6SS killing is determined by the initial bacterial seeding density . . . 229
6.2.1.3 Effectiveness of T6SS killing is determined by the initial prey-attacker cells ratio . . . 234
6.2.2 Lineages in mixed macrocolonies formed by *gac-rsm* mutants show different levels of intermixing . . . 237
6.2.3 *P. aeruginosa* EPS impact on strain distribution in macrocolonies . . . 240
6.2.3.1 Loss of EPS has minor impact on mixed macrocolony structure. 240
6.2.4 Type IV pili impact on bacterial intermixing . . . 244
6.2.4.1 Gac-Rsm cascade mutants display decreased motility . . . 244
6.2.4.2 Loss of T4P results in decreased strain intermixing at both single-cell and whole-colony scale . . . 246

6.2.4.3 Surface growth and active intermixing promotes H1-T6SS sheath assembly and firing . . . 248
6.2.4.4 Loss of T4P interferes with *P. aeruginosa* T6SS-dependent competition . . . 251
6.2.4.5 Toxin sensitive prey strains use T4P to escape immobile attacker population . . . 253
6.3 Discussion . . . 256
6.3.1 Gac-Rsm cascade modulates gradual changes in whole community structure 256
6.3.2 Local contact assortment is a key determinant of population level competitive success . . . 257
6.3.3 EPS impact on *P. aeruginosa* community structure and T6SS-mediated interactions . . . 258
6.3.4 T4P in *P. aeruginosa* communities - attachment, intermixing and escape 260
6.3.5 Summary . . . 263

7 Discussion **265**

7.1 Impact of regulatory network on T6SS expression and activity . . . 266
7.2 T6SS toxins are the key determinants of the overall competitive success . . . 268
7.3 Active intermixing aids with effective T6SS killing . . . 269
7.4 Conclusion . . . 270

Bibliography **272**

List of Figures

1.1 *P. aeruginosa* virulence factors 23

1.2 *P. aeruginosa* planktonic-to-biofilm lifestyle switch 30

1.3 Physiological functions of c-di-GMP 31

1.4 Schematic showing core components of Gac-Rsm cascade. 33

1.5 Modes of action of CsrA regulatory proteins. 34

1.6 Regulation of RsmY/Z synthesis and turnover. 37

1.7 *P. aeruginosa* flagella. 41

1.8 Schematic of Type IV pili. 43

1.9 Schematic of Type IV pili functions in bacterial communities. 44

1.10 Model of biofilm formation. 48

1.11 Schematic showing types of pairwise bacterial interactions occurring in microbial communities. 56

1.12 Schematic showing CDI effector translocation. 60

1.13 Schematic of type IV secretion system. 62

1.14 Structure and dynamics of T7SS from *Mycobacterium tuberculosis*. 64

1.15 Diagram of R-type tailocin structure and mechanism of action. 67

1.16 Schematic of eCIS features and phylogeny. 69

1.17 Structure of T6SS. 75

1.18 Modes of T6SS effector delivery. 77

1.19 Schematic and structure of Tse6 in complex with VgrG1. 79

1.20 T6SS gene core and satellite clusters found in *P. aeruginosa* PAO1 genome. . . . 81

1.21 Schematic of TPP components and T6SS assembly. 83

1.22 Diagram of types of peptidoglycan degrading toxins. 85

1.23 Diagram of phospholipase effector cleavage sites. 87

1.24 Conservation of *tse7-tsi7* loci in *P. aeruginosa* PAO1, PAK, PA7, and PA14. . . 88
1.25 Genomic context of Tse6 in *P. aeruginosa* PAO1 and PA14. 89
1.26 Schematic illustration of anti-eukaryotic T6SS effector action. 93
1.27 Schematic showing T6SS effector mediated metal ion uptake. 94
1.28 Diagram of non-immunity T6SS defences. 98
1.29 Schematic depicting EPS protection from T6SS injection. 100
1.30 Schematic T6SS competition outcomes in scenarios where populations intermixed and spatially segregated. 109
1.31 Schematic T6SS competition outcomes depending on the type of toxin used. . . . 110
1.32 Schematic T6SS competition outcomes in dense and sparse communities. 113

2.1 Map of the pKNG101 plasmid. 133
2.2 Schematic of allelic exchange using pKNG101 plasmid. 135
2.3 Map of the miniCTX-pX2:mCherry plasmid. 136
2.4 Map of the pUCP22 plasmid. 137

3.1 Gac-Rsm cascade and c-di-GMP modulate *P. aeruginosa* planktonic-to-biofilm lifestyle switch. 150
3.2 Removal of SadC reverses high c-di-GMP phenotype of Δ*retS* mutant. 152
3.3 Validation of biofilm phenotype resulting from *sadC* deletion. 153
3.4 SadC has inverse impact on H1-T6SS and H2-/H3-T6SS expression in *P. aeruginosa*. 154
3.5 Validation of phenotype resulting from *sadC* deletion. 155
3.6 The differential modulation of H1- and H2-T6SS activity is dependent on the global c-di-GMP levels. 156
3.7 Loss of PppA leads to constitutive H1-T6SS activation regardless of the intracellular c-di-GMP content. 157

4.1 Schematic of Gac-Rsm regulatory cascade core components. 163
4.2 Diagram of fluorescent T6SS promoter reporters. 166
4.3 Disruption of Gac-Rsm regulatory cascade results in graduated elevation in T6SS expression and activity. 167
4.4 Gac-Rsm mutant strains show graduated increase in H3-T6SS promoter activity and expression. 168
4.5 Growth temperature impact on T6SS promoter activity. 169

4.6 Elevation in H1-T6SS expression and activity is reflected by increased dynamic sheath structure abundance. 171

4.7 Assessment of H1-T6SS toxin Tse5 mediated killing capacity of different Gac-Rsm mutants. 173

4.8 Assessment of H2-T6SS toxin TseT mediated killing capacity of different Gac-Rsm mutants. 174

5.1 Sub-population distribution within mixed macrocolony community. 184

5.2 Sub-population distribution within mixed macrocolonies is dependent on the media rigidity. 185

5.3 Bacteria within a drying inoculum spot distribute accordingly to 'coffee stain' pattern. 185

5.4 Ability to actively fire T6SS does not provide a marked competitive advantage between otherwise isogenic *P. aeruginosa* strains. 186

5.5 Growth of H1-T6SS toxin sensitised strains is spatially restricted in a manner dependent on the specific toxin used and the level of H1-T6SS activity. 188

5.6 T6SS toxin action impacts bacterial distribution within communities. 191

5.7 T6SS toxins act synergistically to further restrict prey growth. 193

5.8 *P. aeruginosa* is able to growth restrict H1-T6SS toxin-sensitive prey independently of nutrient limitation during competition. 195

5.9 *P. aeruginosa* used H1-T6SS to kill toxin-sensitive prey bacteria independently of active provocation by prey bacteria. 197

5.10 Loss of post-translational regulator PppA results in increased H1-T6SS activity, but does not ensure improved competitive fitness. 199

5.11 Decrease in growth temperature promotes H2-T6SS sheath structure assembly. . 202

5.12 Sensitivity to H2-T6SS toxins can be observed when growing colonies at 25^{o}C, but not 37^{o}C. 203

5.13 Increased H2-T6SS toxin-mediated prey growth restriction can be observed in Δ*retS* strains. 204

5.14 Mixed macrocolony setup can be used to assess competitive impact of putative T6SS toxins. 206

5.15 *P. aeruginosa* is able to use H1-T6SS toxins to restrict sensitive prey growth at 25^{o}C. 207
5.16 Schematic of toxin-sensitive and attacker lineage fate in simulations. 209
5.17 Both toxin mode of action and T6SS firing rate determine population distribution within mixed bacterial communities. 210
5.18 T6SS toxin killing efficacy increases with elevation in T6SS activity. 213

6.1 A schematic showing locally intermixed and spatially segregated communities. . . 227
6.2 Inoculum composition determines prey/attacker population contact assortment within macrocolony. 228
6.3 Theoretical modelling shows that decrease in founding population density allows for toxin sensitive bacteria survival. 231
6.4 Schematic showing protective effect provided through "corpse barrier". 232
6.5 Low inoculum density allows for establishment and survival of toxin sensitive prey. 233
6.6 Decrease in inter-population contacts protects T6SS sensitive prey. 234
6.7 Decrease in inter-population contacts protects T6SS sensitive prey. 235
6.8 Increased opportunity for toxin injection does not ensure improved killing. 236
6.9 Colony morphology is determined by strain regulatory background and bacterial density in inoculum. 239
6.10 Loss of EPS has minor impact on sub-population distribution within bacterial macrocolonies. 241
6.11 Loss of EPS has minor impact on Tse5-dependent competition. 242
6.12 Loss of EPS has minor impact on *P. aeruginosa* T6SS-dependent competition. . 243
6.13 Disruption of Gac-Rsm cascade results in impairment in both T4P and flagella dependent motility. 245
6.14 Loss of T4P results in reduced local intermixing at single-cell scale. 247
6.15 T4P mediate *P. aeruginosa* lineage lateral expansion on surfaces. 248
6.16 Contact with kin cells and active intermixing promotes assembly and firing of H1-T6SS sheaths. 250
6.17 Loss of T4P negatively impacts *P. aeruginosa* T6SS-mediated killing. 252
6.18 Toxin sensitive prey bacteria can escape H1- and H2-T6SS attack using type IV pili. 254

List of Tables

1 Abbreviations. 19

1.1 *P. aeruginosa* T6SS effectors. 84

2.1 Bacterial strains used in the study. 122

2.2 Plasmids used in the study. 125

2.3 Primers used in the study. 130

2.4 Simulations parameters. 146

5.1 T6SS effectors present in the genome of *P. aeruginosa* PAO1. 181

Abbreviations

ABM	Agent based model	PG	Peptidoglycan
AMR	Antimicrobial resistance	PQS	Pseudomonas quinolone signal
bp	Base pairs	PVC	Photorhabdus virulence cassettes
CDI	Contact dependent inhibition	QS	Quorum sensing
c-di-GMP	Cyclic di-GMP (cyclic dimeric guanosine 3',5'-monophosphate)	RBD	Receptor binding domain
CF	Cystic Fibrosis	RBS	Ribosome binding sequence
DGC	Diguanylate cyclase	Rhs	Rearrangement hotspot
eCIS	Extracellular contractile injection systems	ROS	Reactive oxygen species
ECM	Extracellular matrix	rpm	Rotations per minute
eDNA	Extracellular DNA	SD	Standard deviation
EPS	Exopolysaccharides	SmR	Streptomycin resistence
FIX	Found in type six effector	sRNA	Small RNA
g	Grams	T3SS	Type III secretion system
GmR	Gentamycin resistance	T4P	Type IV pili
h	Hours	T4P-	T4P lacking
kD	Kilodaltons	T4P+	T4P active
KmR	Kanamycin resistance	T4SS	Type IV secretion system
LB	Lysogeny Broth	T5SS	Type V secretion system
LPS	Lipopolysaccharides	T6SS	Type VI secretion system
MAC	Metamorphosis-associated contractile	T6SS-	T6SS inactive
MBIC	Minimal biofilm inhibitory concentration	T6SS+	T6SS active
Mbp	Megabasepairs	T7SS	Type VII secretion system
MDR	Multidrug-resistant	TA	Toxin-antitoxin
MIC	Minimal inhibitory concentration	Tag	Type six associated gene
min	Minutes	TcR	Tetracycline resistence
MIX	Marker for type six effectors	Tle	Type six lipase effector
mL	Millilitres	Tli	Type six lipase immunity
mRNA	Messenger RNA	TSB	Tryptic soy broth

μL	Microliters	Tse	Type six effector
NEB	New England Biolabs	Tsi	Type six immunity
OD	Optical density	Tss	Type six secretion
OMV	Outer membrane vesicle	VBM	Vogel-Bonner agar
PBS	Phosphate Buffered Saline	VPS	Vibrio polysaccharide
PCR	Polymerase chain reaction	w/v	Weight/ volume
PDE	Phosphodiesterase	WT	Wildtype

Table 1: **Abbreviations.**

Chapter 1

Introduction

1.1 *Pseudomonas aeruginosa*

Pseudomonas aeruginosa is a Gram-negative rod-shaped bacterium that can survive in a variety of environmental niches. It is of particular interest because it is an opportunistic pathogen capable of causing both acute and chronic infections in immune-compromised individuals (1). Simultaneously, free-living strains of *P. aeruginosa* can be isolated from various soil and aquatic environments, with increased abundance seen in niches that are exposed to human activity and contamination (2).

P. aeruginosa ability to thrive in a range of niches is due to its high level of adaptability and efficient use of various molecular tools that enable it to interact with the environment and compete with other organisms (1). These capabilities are facilitated by a relatively large genome, which ranges in size from 5.5 to 7Mbp depending on the isolate (3). The first *P. aeruginosa* genome to be sequenced was for the reference strain PAO1 (4), which is also the focus of this thesis. The PAO1 genome is 6.3Mbp in size and is predicted to encode approximately 5600 open reading frames (4, 5). *In silico* analysis of *P. aeruginosa* isolate genomes by (6) identified 5170 core genes present in more than 90% of strains, with an accessory genome of nearly 24,000 genes. This provides *P. aeruginosa* with capacity to encode a range of complex molecular tools,

flexibility in nutrient utilisation, production of secondary metabolites, and antibiotic resistance genes, with the specific skills varying between individual isolates (1, 7).

A large genome provides *P. aeruginosa* with a range of tools contributing to versatility when it comes to niche adaptation However, this also necessitates complex regulation that allows the bacterium to sense its surroundings and respond appropriately. Regulatory genes make up almost 10% of the *P. aeruginosa* genome (4), underlining the importance of sensory and regulatory pathways for the microbial adaptability. Two-component systems are key part of the bacterial ability to sense information about the surrounding environment and integrate this information, which is done through use of sensor kinase and response regulator sets. The presence of numerous two-component systems, and the many different associated sensors, underlies the bacterial capacity to adapt to various environments (8). The *P. aeruginosa* PAO1 genome contains 55 two-component systems, with are encoded in sensor-response regulator gene pairs, and additional orphan sensors and response regulators (9, 10). *P. aeruginosa* also has at least 25 sigma factors, many of which are involved in the regulation of virulence factor expression (11, 12). In addition, there are nearly 400 putative transcription factors and hundreds of non-coding RNAs (13, 14). The exact functions of many of these regulators are not yet known, and the possible dynamic interactions between them are likely to add even further complexity in the regulation of *P. aeruginosa* gene expression.

1.1.1 *Pseudomonas aeruginosa* in infection

P. aeruginosa is well-known for its nature as an opportunistic pathogen that is capable of causing both acute and chronic infections. It is particularly prevalent in healthcare settings and is responsible for as many as 10% of hospital-acquired infections (15). One of the most common infections associated with *P. aeruginosa* is healthcare-associated pneumonia, which has a poor prognosis (16, 17). *P. aeruginosa* is also closely associated with lung infections in individuals with cystic fibrosis (CF) (18). While initial infections may be transient and responsive to

antibiotic treatment, *P. aeruginosa* infections are often recurring, and often become chronic in nature due to failure to fully eradicate the bacterium (19, 20). *P. aeruginosa* is often the dominant organism in microbiome samples isolated from CF sputum and is one of the organisms that is best predictive of poor overall treatment outcome (21, 22). In addition to lung infections, *P. aeruginosa* is also linked to urinary tract infections, surgical site infections, and burn wound infections (17, 23). What makes *P. aeruginosa* an organism of special concern is that these infections are not only prevalent in immunocompromised individuals but are also predictive of poor outcomes and presents a continuous treatment challenge (24, 17, 25).

1.1.2 Virulence factors

P. aeruginosa has a range of virulence factors that it can use to cause toxicity to host cells, modify host cell behaviour, and evade immune clearance, which helps it establish and persist within an infection site (Figure 1.1) (26, 27). Its Gram-negative outer membrane contains lipopolysaccharides (LPS) with various glycoforms that both constitute a physical barrier and modulate interactions with host cells (28). *P. aeruginosa* also uses surface appendages such as type IV pili (T4P) and flagella for direct mechanistic interactions with environment including movement within niche and interactions with host cells (29, 30). *P. aeruginosa* has a single polar flagellum that it uses for swimming and directed movement, aiding not only with inducing early inflammatory response, but also epidermis invasion and persistence (31, 32). T4P are used for surface-based motility, adhesion, and help in the formation of structured biofilms (30). The type III secretion system (T3SS) is a tool specialized for delivering virulence factors directly into host cells (33). The T3SS delivers Exo effectors with varied biochemical functions, such as the ADP-ribosyltransferase ExoS and the phospholipase ExoT (34). ExoS has been shown to inhibit phagocytosis, while ExoT is highly cytotoxic (35, 36). Presence and high activity of T3SS is one of the key markers seen in early *P. aeruginosa* infections and trend towards lower T3SS activity marks transition towards chronic infection (37, 38). An alternative tool for

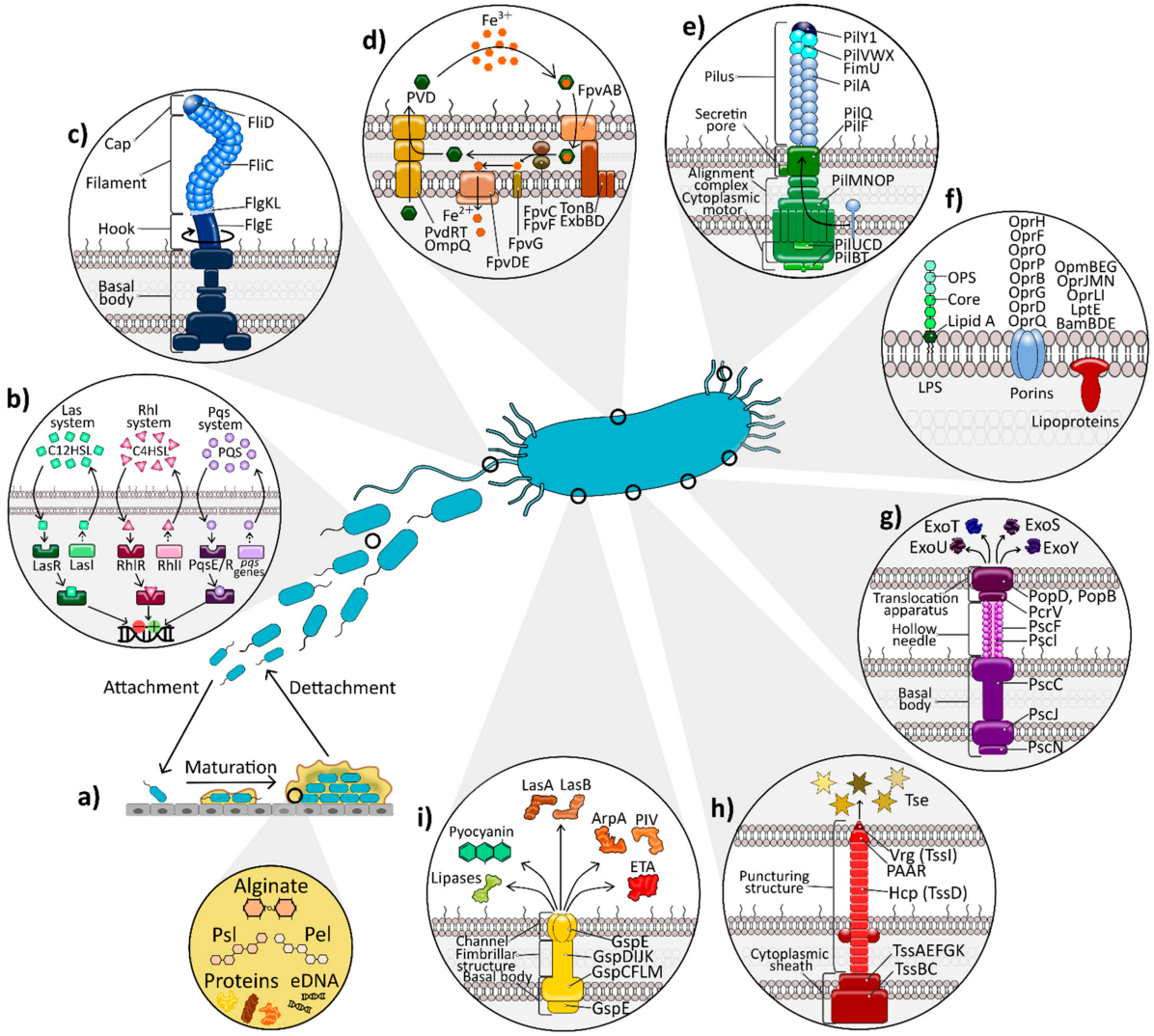

Figure 1.1: ***P. aeruginosa* virulence factors**
Schematic overview of *P. aeruginosa* virulence factors adapted from (26) under creative commons license. (**a**) Biofilm formation and extracellular matrix component production. (**b**) Quorum sensing systems used for co-ordination of collective behaviour. (**c**) Diagram of flagella and core flagellins - FliC and FliD. (**d**) Iron uptake systems and siderophore - pyoverdine. (**e**) Type IV pili (T4P). (**f**) Lipopolysaccharides and outer membrane proteins (OMPs). (**g**) Type III secretion system (T3SS). (**h**) Type VI secretion system (T6SS). (**i**) Type II secretion system (T2SS) and associated substrates - proteases (AprA, PIV), elastases (LasA, LasB), exotoxin A (ETA) and pyocyanin.

direct effector delivery is type VI secretion system (T6SS) that is primarily used as a bacterial competition tool, but also delivers host effectors, amongst these being a set of phospholipases (PldA, PldB, and Tle4) (39, 40). These phospholipase effectors have been shown to aid with internalization into non-phagocytic host cells (41, 42).

In addition to the virulence factors that work through direct cell-cell contact, *P. aeruginosa*

also produces virulence factors that are released into the extracellular milieu. These include phospholipase C, which can degrade eukaryotic membranes (43), and exported proteases. Examples of protease enzymes include elastases LasA and LasB that degrade host elastin or alkaline protease AprA that also degrade host connective tissue (26). *P. aeruginosa* also releases secondary metabolites that are cytotoxic to both host cells and adjacent microbiome, such as pyocyanin or hydrogen cyanide (44, 45). While siderophores pyoverdine and pyochelin are used for iron scavenging (46), rhamnolipids are multifunctional biosurfactants that contribute to microbial community structure and immune evasion through host cell toxicity (47, 48). To coordinate the collective behaviour of the population, including the expression of many of these virulence factors, *P. aeruginosa* uses three quorum sensing (QS) systems: Las, Rhl, and Pqs, which are also considered virulence factors in their own right (49, 50). The virulence factors listed here cover only a fraction of the tools at disposal of *P. aeruginosa* and this diversity of tools aids in explaining how this bacterium can take advantage of an opportunity to invade a host niche once one arises.

1.1.3 Antibiotic resistance and niche adaptation

P. aeruginosa is a bacterium that is naturally tolerant to exposure to a wide range of antibiotics and is one of the ESKAPE pathogens that is a global concern in clinical settings (15). It has an intrinsic resistome, which refers to the mechanisms that enable bacteria to tolerate exposure to antimicrobials. This set of characteristics includes presence of drug efflux pumps, low membrane permeability, the absence of specific sites that are susceptible to antibiotics, and in the case of biofilms, the presence of an extracellular matrix (ECM) that limits the diffusion of small molecules (51, 52, 53). In addition to its intrinsic resistome, *P. aeruginosa* can also acquire resistance to specific drugs through horizontal gene transfer or through the acquisition of pathoadaptive mutations that allow it to better tolerate treatments and the stresses present within infection niche (54, 55). Horizontal gene transfer is the evolutionary fastest mechanism for

the spread of antimicrobial resistance and can be mediated through both transfer of plasmids and chromosomally integrated mobile elements (56). Review of epidemiology of multidrug-resistant (MDR) *P. aeruginosa* by (57) highlights spread of β-lactamases and carbapenemases specifically as the most concerning due to high usage of these antibiotic classes.

Alternatively, to horizontal resistance gene transfer between strains or species, *P. aeruginosa* existing in infection niche may acquire a set of pathoadaptive mutations that allows bacteria to better tolerate stresses present and treatments applied (58, 59). This can include mutations in regulatory pathways that induce a permanent phenotypic shift, examples of this being acquisition of mucoid phenotype overproducing hygroscopic exopolysaccharide alginate (60) or emergence of hyper biofilm forming small rugose colony variants (61). Mucoidy has been associated with both increased antibiotic resistance and immune evasion (62, 63), and this phenotype is often a result of loss of function mutations in a gene encoding the anti-sigma factor MucA or the associated sigma-factor AlgU (64, 65). Review of studies looking at pathoadaptive mutations by (66) found *algU* and *mucA* genes to be the two most commonly identified mutational hot-spots. Rugose colony variants emerge from increased exopolysaccharide (EPS) production elicited by high levels of intracellular second messenger c-di-GMP. Several distinct loci have been linked to emergence of this phenotype including *wsp*, *yfi*, and some mutations associated with the Gac-Rsm pathway (61, 67, 68). Other examples of mutations resulting in increased antibiotic resistance are loss of expression of the repressor MexR that led to an increased expression of Mex drug efflux pumps (69, 70). Furthermore, mutations rendering the outer membrane Opr porins non-functional limit small molecule uptake and thus antibiotic uptake (71). Combination of intrinsic resistome with horizontal acquisition of resistance against specific drugs consistently places *P. aeruginosa* amongst the six leading pathogens for deaths associated with resistance, with more than 300 thousand *P. aeruginosa* AMR associated deaths in 2019 (72).

1.1.4 Target for design of novel therapeutic approaches

P. aeruginosa high antibiotic resistance has made it a focus for the development of new antimicrobial therapies, including the design of combination therapies using existing antimicrobials and the development of new antibiotic compounds (25). β-lactam antibiotics, which target peptidoglycan synthesis and are a commonly prescribed class of antibiotics, are particularly relevant in this regard (73). β-lactam resistance is mediated by specific hydrolases called β-lactamases, and the spread of β-lactamases is a current concern in the epidemiology of MDR *P. aeruginosa* (57). To combat the challenge presented by MDR *P. aeruginosa*, approaches such as co-delivering β-lactams with β-lactamase inhibitors, such as clavulanic acid and taniborbactam, both of these acting on multiple β-lactamase classes (74, 75). Another approach to developing new antimicrobials is through the creation of derivatives of existing compounds with the aim of overcoming emerging resistance or improving their safety profiles. An example of this is the class of lipopeptide antibiotics called polymyxins, which disrupt the outer membranes of Gram-negative bacteria but have been associated with human nephrotoxicity (76). A recent polymyxin derivative called SPR206 is currently in clinical trials and is seen as promising due to its effectiveness against MDR pathogens and improved toxicity profile (25). Similarly, existing medications can be repurposed for use as antimicrobials, this approach being beneficial as any medication in active use has already undergone safety testing and this can significantly shorten the time frame until use in clinical practice (77). Examples of such compounds under current investigation include an anti-fungal dimetridazole (78) and antiviral medication ribavirin (79), that have been shown to promote *P. aeruginosa* sensitivity to other antimicrobial compounds (80). Another approach to developing new antimicrobials is through the identification of novel molecular targets and new modes of action of natural toxins that can subsequently inspire drug design. Cefiderocol, a siderophore-antibiotic that was approved for limited use by the FDA in 2019, is an example of this (81, 82). Antibiotics have been historically isolated and derived from molecules used in competition between bacterial species

and this continues today, with inspiration for new antimicrobial strategies being taken from studies on bacterial competition.

Bacterial ability to exist as biofilms has been linked to increased antibiotic tolerance. In addition to this, antibiotic susceptibility testing performed in single species and polymicrobial biofilms reveals different impact. For example, research has shown that *P. aeruginosa* is less susceptible to colistins in the presence of *Staphylococcus aureus* and *Candida albicans* (83), and the presence of *Stenotrophomonas maltophilia* can protect *P. aeruginosa* from imipenem (84). These observations of biofilm communities behaving differently from planktonic cultures are leading researchers to increasingly test new antimicrobials within the context of biofilms aiming to better represent infection conditions (85, 86). This has led to increased testing of both minimal inhibitory concentrations (MIC) and minimal biofilm inhibitory concentrations (MBIC) when assessing efficacy of new antimicrobial compounds (87, 88, 85, 89). In addition to this, approaches aimed at disrupting the structure of biofilm communities and improving the delivery of existing antimicrobials are being developed to address the treatment challenges posed by biofilms. These approaches may involve directly degrading ECM components or indirectly disrupting biofilms, such as through the deprivation of essential nutrients like iron in the case of *P. aeruginosa* (25, 90). Some examples of biofilm eradication trough ECM degradation include application of alginate lyases, that have a potential to be highly effective against mucoid *P. aeruginosa* isolates (91). An interesting microbial delivery approach under current investigation is the use of outer membrane vesicles (OMVs). OMVs are membrane derived particles that carry a variety of molecules and can fuse with bacterial cell membranes resulting in internalisation of the vesicle contents (92). As OMVs could be loaded with exogenous antimicrobial agents, these are being investigated for use in targeted antimicrobial delivery (93).

Aside from furthering development of antibiotics, a variety of less traditional antimicrobial treatment approaches are under investigation. One of these is phage therapy, in which bacterial viruses that are known to kill specific types of bacteria are modified to treat infections caused

by MDR pathogens (94). Bacteriophages can be used both to kill bacteria and to break down the extracellular matrix, which increases the permeability aiding in delivery of small molecule antimicrobials (95). *In vitro* and animal studies have shown that phages can effectively disrupt biofilm structure and kill bacterial cells, but clinical trials testing their effectiveness in humans have not yet resulted in recommendations for wider use (25, 95).

Since infections with *P. aeruginosa* are only a concern for a small portion of the population, one of the strategic approaches being explored in management of these is the possibility of preventing infections through vaccination (25, 96). While there are currently no vaccines that have been approved for use, various targets have been explored, amongst these are *P. aeruginosa* lipopolysaccharides and flagellar proteins (25, 97). One of the most recent promising trials has focused on IC43 vaccine based on recombinant outer membrane porin proteins. While this vaccine was well tolerated and immunogenic it did not provide a significant advantage in regard to reduced mortality (98). Another immunology-based approach that is being studied is the use of antibodies to prevent or treat existing infections. Clinical trials are currently underway that are targeting exopolysaccharides and virulence factors with these antibodies (25).

1.2 Bacterial communities

1.2.1 Two bacterial lifestyles - planktonic and biofilm

With the exception of separate highly transmissible isolates, *P. aeruginosa* infections are typically acquired from environmental sources rather than through patient-to-patient transmission (99). This suggests that *P. aeruginosa* success within infection niche is not necessarily caused by the spread of highly transmissible strains, but rather by the bacteria's ability to adapt to the infection site. Longitudinal studies that compare the phenotypic features of *P. aeruginosa* isolates from early and chronic infections have identified characteristic shifts in gene expression patterns. Isolates from acute infections tend to express high levels of virulence factors and exist in a planktonic state (26). This is associated with high expression of motility devices such as flagella and pili, virulence factors such as pyocyanin or elastase, and increased activity of the T3SS (26). The production of these virulence factors also provokes a strong immune response. In contrast, during chronic infections, bacteria form aggregates or surface-attached biofilms and reduce the production of virulence factors, resulting in a more persistent and less immunogenic phenotype (1). This state is characterised by increased ECM production, reduced motility, and increased activation of the T6SS (100). This switch has been shown to be largely dependent on changes in intracellular c-di-GMP levels and activity of the Gac-Rsm regulatory cascade (Figure 1.2) (100, 101).

1.2.2 c-di-GMP and biofilm formation

c-di-GMP is an ubiquitous second messenger involved in determining whether bacteria exhibit planktonic or biofilm-like behaviour. High intracellular concentrations of c-di-GMP are associated with biofilm-like characteristics, while a decrease in c-di-GMP levels is linked to increased motility and virulence (102, 103, 104) (Figure 1.3). c-di-GMP is produced by enzymes called diguanylate cyclases (DGCs) and degraded by phosphodiesterases (PDEs) (105). There is

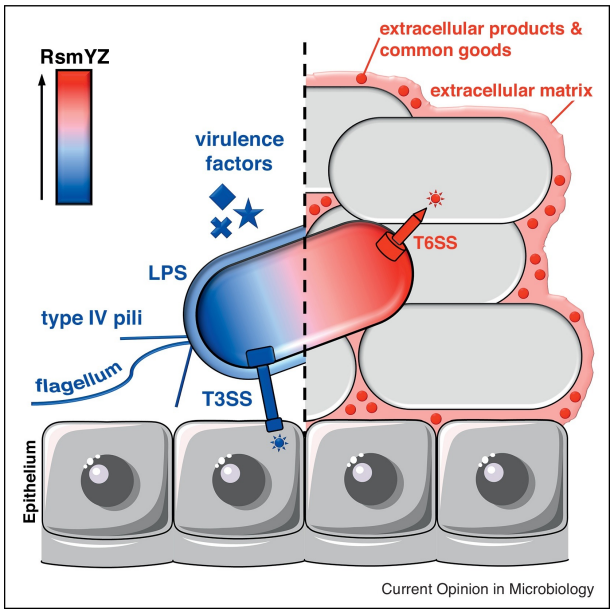

Figure 1.2: ***P. aeruginosa* planktonic-to-biofilm lifestyle switch**
Schematic showing features of *P. aeruginosa* planktonic and biofilm phenotypes. Virulence factors associated with acute infection shown in blue. Biofilm-associated features shown in red. The shift in phenotypic features is associated with differences in levels of RsmYZ snRNSs. Adapted from (100) with permission from Elsevier.

a total of 40 such enzymes encoded in the genome of *P. aeruginosa* reference strain PAO1 (106), with some diversity seen in genomes of other strain isolates. Although the overall role of c-di-GMP is in the transition between planktonic and biofilm phenotypes, the specific contributions of individual enzymes are much more complex. For example, WspR is a major DGC that contributes to biofilm formation and is activated through surface sensing and as a result of cell envelope stress (107, 108). Another DGC, SadC, is regulated by the Gac-Rsm cascade and influences biofilm formation, swarming motility, and virulence factor production (109, 110, 111). Among the major PDEs is BifA, which contributes to biofilm dispersal (112, 113). These are just a few examples of specific DGC/PDE enzymes, and further characterisation of how these enzymes contribute to both spatially localised changes and function of few c-di-GMP binding proteins and global pools of c-di-GMP, which introduce a broad phenotypic response across the whole cell, is an active area of research.

The presence of c-di-GMP is detected by a range of regulators that subsequently control specific phenotypic features. These regulators often contain a degenerated GGDEF or EAL

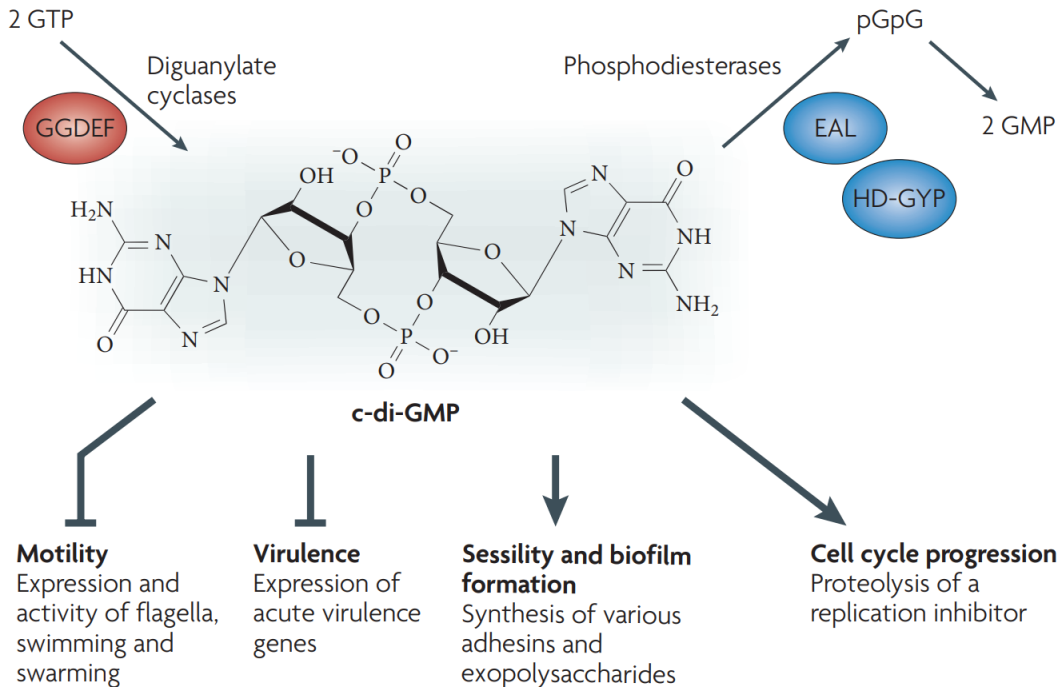

Figure 1.3: **Physiological functions of c-di-GMP**
Schematic showing structure of c-di-GMP. C-di-GMP is produced by GGDEF domain containing diguanylate cyclase enzymes, while degradation is performed by phosphodiesterases containing EAL or HD-GYP domains. Highlighting key physiological features associated with both high and low c-di-GMP levels in bacterial cells. Adapted from (104) with permission from Springer Nature.

domain with a c-di-GMP binding site that is no-longer capable of enzymatic function, but acts as a sensory domain (114, 115). One major regulator that directly binds c-di-GMP is the transcription factor FleQ (116, 114). FleQ is an enhancer-binding protein that controls the production of exopolysaccharide Pel, flagella, and surface adhesins, among other targets (116, 117, 118). In particular, FleQ can function as both a transcriptional activator and a repressor depending on its c-di-GMP binding state (119). The c-di-GMP-dependent control of T4P production is mediated through FimX, which is required for pili assembly (120). Alg44 is a membrane protein that is required for alginate export and mucoid phenotype transition, and c-di-GMP binding is essential for this activity (121). In addition, shifts in c-di-GMP levels have also been shown to control the preferential expression of the type III or type VI secretion systems of *P. aeruginosa* (101). Overall, c-di-GMP levels influence the expression of a range of *P. aeruginosa* biofilm-associated genes and virulence factors, which play a critical role in the

transition between planktonic and biofilm lifestyles (100).

1.2.3 Gac-Rsm regulatory cascade

In *P. aeruginosa* a pathway that is central in coordinating transition between planktonic and biofilm lifestyles is the Gac-Rsm regulatory cascade (Figure 1.4). RNA-binding proteins RsmA and RsmN directly or indirectly control the expression of hundreds of genes (122). Biological processes under direct control of RsmA/RsmN include exopolysaccharide biosynthesis, cell wall synthesis and remodelling, T3SS, T6SS and motility (123, 122). RsmA and RsmN activity is modulated by sRNAs RsmY and RsmZ, whose expression is consequently under GacS-GacA two component system (124). External signals that inform the transition between platonic and biofilm lifestyles are integrated through the sensory kinases RetS and LadS, which subsequently impact the activation of GacS-GacA (125, 126). Details of specific T6SS promoters under Gac-Rsm control will be discussed in further detail in chapter 4.1 of the thesis, while this section focuses on broader context surrounding regulation by this cascade.

1.2.3.1 RNA binding proteins RsmA and RsmN

RsmA and RsmN (also called RsmF) are two orthologous *P. aeruginosa* post-transcriptional regulators that belong to the CsrA protein family (128). CsrA orthologs are small proteins of approximately 60 amino acids that form functional homodimers to enable RNA binding (129). These proteins are widely conserved across many genera of both Gram-positive and Gram-negative bacteria (128). The first member of this family, CsrA, was identified in *E. coli* and is named for its role as a **c**arbon **s**torage **r**egulator **A** (130). It modulates the rate of translation and mRNA stability of many gene targets (131). CsrA proteins can act both as positive or negative regulators, through direct interactions or indirectly through regulation of other regulators (Figure 1.5). The CsrA protein binding motif is a core GGA sequence that is exposed as part of a single-stranded RNA stem-loop (132, 133, 134). Since the CsrA protein

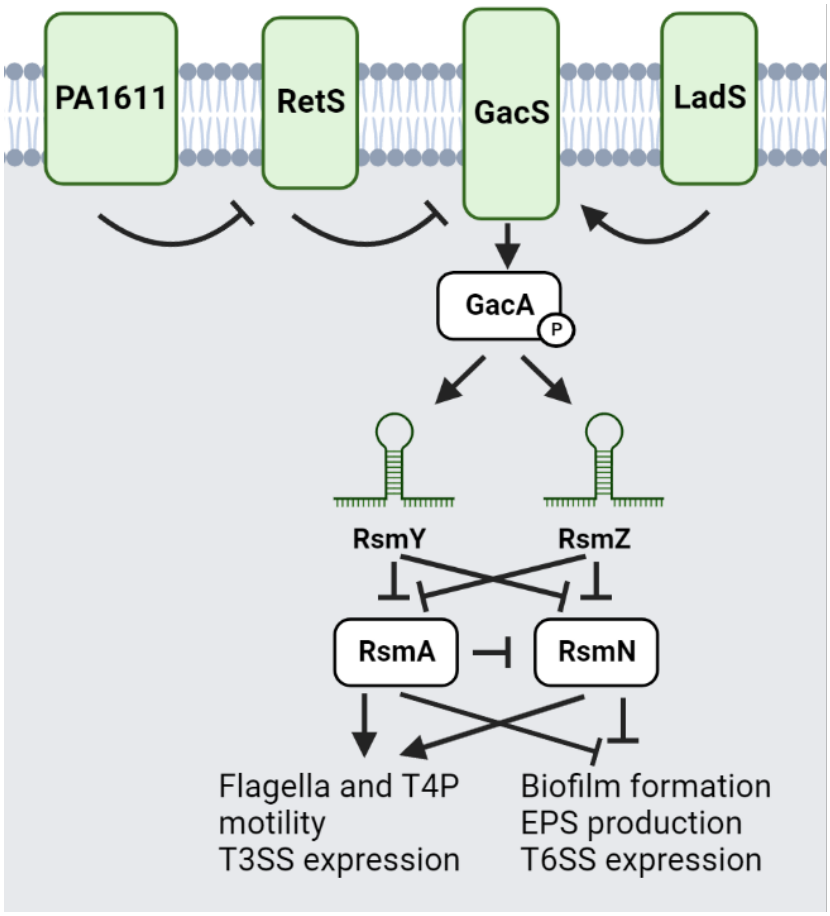

Figure 1.4: **Schematic showing core components of Gac-Rsm cascade.**
Sensory kinase RetS represses action of GacS-GacA two component system, while sensory kinase LadS acts antagonistically, and sensory kinase PA1611 inhibits RetS-GacS interaction. Upon phosphorylation by GacS, GacA induces expression of sRNAs RsmY and RsmZ. RsmY and RsmY titrate the availability of free translational repressors RsmA and RsmN. RsmA and RsmN negatively control expression of biofilm associated genes mediating transition between planktonic and biofilm lifestyles.

dimer contains two RNA binding sites located on opposite sides of the protein complex (135, 136, 137), it can bind to a secondary site located on the same RNA target (137). The most common mechanism of action is through direct inhibition of translation due to competition for binding to the ribosome binding sequence (RBS) or through the initiation of structural rearrangement that prevents ribosome binding (133, 137) (Figure 1.5A). CsrA proteins can also modulate the mRNA pool through actively promoting Rho-dependent transcription termination (138) (Figure 1.5C). CsrAs can also modulate the degradation of specific mRNAs, interestingly examples of both CsrA-mediated protection from degradation by RNase E and active targeting for recycling have been described (139, 140) (Figure 1.5D). Examples of positive translational regulation

by CsrAs are less common, but they include the protection of the *E. coli* flagella biosynthesis master regulator, *flhDC* mRNA, from degradation (140), and the increased rate of translational initiation seen in *E. coli ymdA* (141). Positive effects on gene transcription and translation can also be achieved indirectly, for example, through the repression of transcriptional/translational repressors, highlighting the importance of these proteins as broadly acting central regulators.

CsrA orthologs found in *Pseudomonas* species are called Rsm after Regulator of Secondary Metabolites (142). Phylogenetic analysis suggests that there are nine subfamilies of Rsm paralogues in the genus *Pseudomonas* (128). The best conserved RsmA, which was first described by (143), is widely distributed across most *Pseudomonas* species, including *P. aeruginosa* (128).

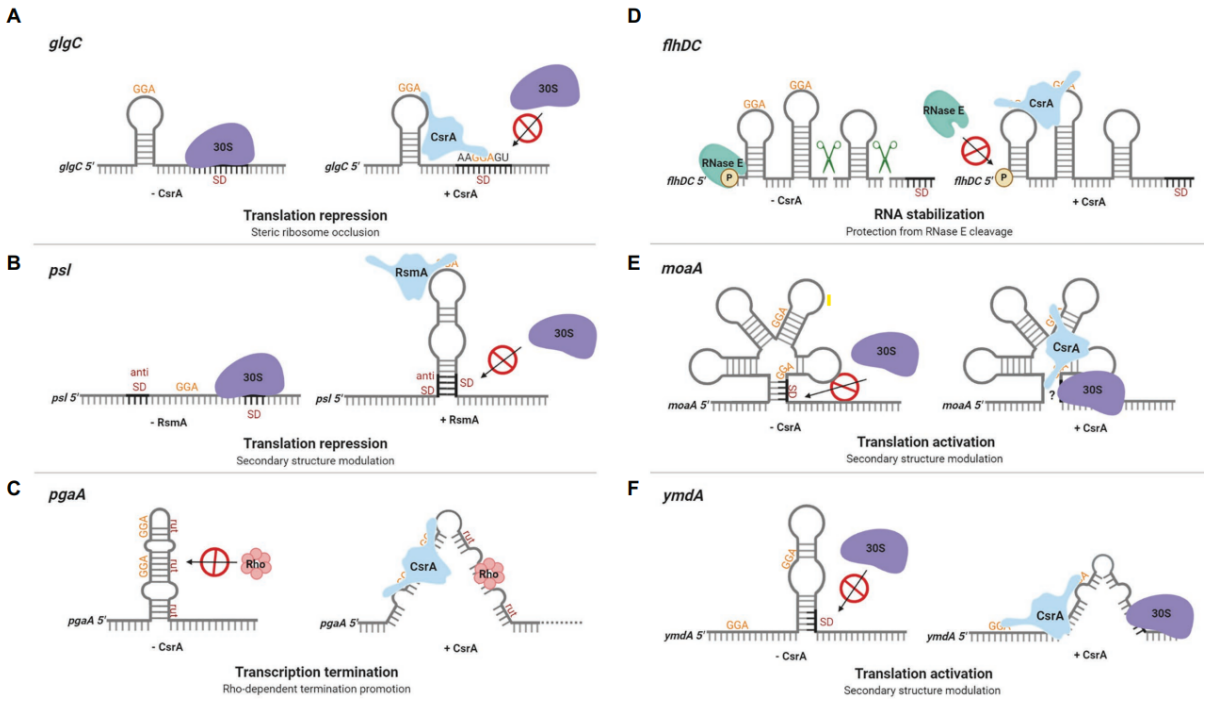

Figure 1.5: **Modes of action of CsrA regulatory proteins.**
(**A**) Translational repression through binding of Shine-Dalgarno sequence preventing ribosome binding and translation initiation.
(**B**) Translational repression through secondary structure modulation preventing ribosome binding and translation initiation.
(**C**) Transcription termination through enabling Rho-dependent transcription termination.
(**D**) mRNA stabilisation through protection from RNase E dependent degradation.
(**E**) Translational activation through disrupting repressor riboswitch enabling ribosome binding and translation initiation.
(**F**) Translational activation through secondary structure modulation enabling ribosome binding and translation initiation.
Adapted from (127) under a creative commons attribution license.

Another widely conserved paralogue, RsmE, is absent from the genome of *P. aeruginosa* and closely related species (128). Instead, *P. aeruginosa* species encode RsmN (RsmF) (136, 135). Whole transcriptome analysis studies have shown that the expression of approximately 500 genes, or 9% of the genome, is directly or indirectly affected in Δ*rsmA* strains. The regulatory targets of RsmA include virulence factors, including type III secretion system, HCN, flagella, type IV pili, proteases, elastases, and biofilm-associated features such as EPS or pyocyanin production and quorum sensing (144, 123, 145). Notably RsmA/N targets include other global regulators, one of these being the transcription factor AmrZ (145). AmrZ (**a**lginate and **m**otility **r**egulator **Z**) is a broadly acting virulence phenotype modulator that acts on hundreds of genes, including those associated with the production of EPS, flagella, c-di-GMP, T3SS, and T6SS, among others (146, 147). The example of AmrZ highlights the complexity of interpreting the direct regulatory impact of RsmA/N due to broad overlap in direct and indirect regulome. A notable target of RsmA is the DGC SadC, which has been implicated as a central contributor for the Gac-Rsm cascade mediated increase in c-di-GMP production (110). The production of SadC is under the control of RsmA; therefore, the loss of repression by RsmA results in a higher abundance of SadC and a corresponding increase in the production of c-di-GMP that subsequently promotes biofilm formation. Furthermore, it should be noted that RsmA regulates both the expression of genes *rsmN* and *retS*, as well as other mRNAs encoding upstream components of the Gac-Rsm cascade, indicating that these repressors are involved in a feedback loop within the cascade (122, 148). A study comparing the regulatory targets of RsmA and RsmN by (122) showed that the binding sites of both proteins are highly conserved and there is a significant overlap in target genes between the two regulators. However, the phenotypes associated with RsmN specifically have been less well characterised in the existing literature.

1.2.3.2 Small RNAs controlling Rsm protein availability

Impact of RsmA/N on gene expression is dependent on the amount of RsmA/N available to interact with mRNAs of specific gene targets. The available pool of RsmA/N is titrated by sRNAs, in *P. aeruginosa* these are mainly RsmY and RsmZ, but RsmA and RsmN have been shown to interact with 33 and 22 sRNAs, respectively (122). Each RsmY and RsmZ contain 7 GGA motifs that are essential for binding to RsmA or RsmN, and 3 of them are potentially exposed as part of stem-loop structures that match the extended binding sequence (CAnGGAyG) (149). Two of these RsmY GGA motifs are able to sequester both RsmA and RsmN, but the affinity for RsmN is about 10 times lower (149). In the case of RsmZ, four of the GGA motifs contribute to RsmA and RsmN repression, with 100-1000 times higher affinity for RsmA (149).

The expression of both RsmY and RsmZ is dependent on activation by the GacS-GacA two-component system, but each of the sRNAs has additional interaction partners that play a role in determining the amount of RsmY/Z in the sRNA pool (Figure 1.6). Both RsmY and RsmZ are under the control of the anaerobic response regulator Anr, and this has been shown to result in RsmA-dependent upregulation of T3SS under low oxygen conditions (150). An environmental signal with opposing impact on the control of Rsm-mediated T3SS is Mg^{2+} ions; the magnesium transporter MgtE inhibits T3SS gene expression by increasing RsmY and RsmZ transcription (151). These examples illustrate the co-regulation of RsmY and RsmZ, but several examples where a regulator interacts with only one of the two components have also been shown in the literature (152). For example, sRNA179 stimulates RsmY synthesis and inhibits T3SS (153), while the two-component system PmrA-PmrB acts as a transcriptional inhibitor (154). RsmZ transcription is under negative control of the histone-like nucleoid structuring proteins MvaT/MvaU (123, 155). CafA is a RNase G family expressed during the early stages of biofilm development and has been shown to degrade RsmZ, while the RsmY pool remains largely unaffected (156). A combination of these and other mechanisms results in condition-

specific titration of the free Rsm protein pool through the control by Rsm-binding sRNAs that integrate a range of specific environmental signals. When large amounts of Rsm sRNAs are present, RsmA and RsmN are sequestered and a more biofilm-like gene expression pattern can be observed (100).

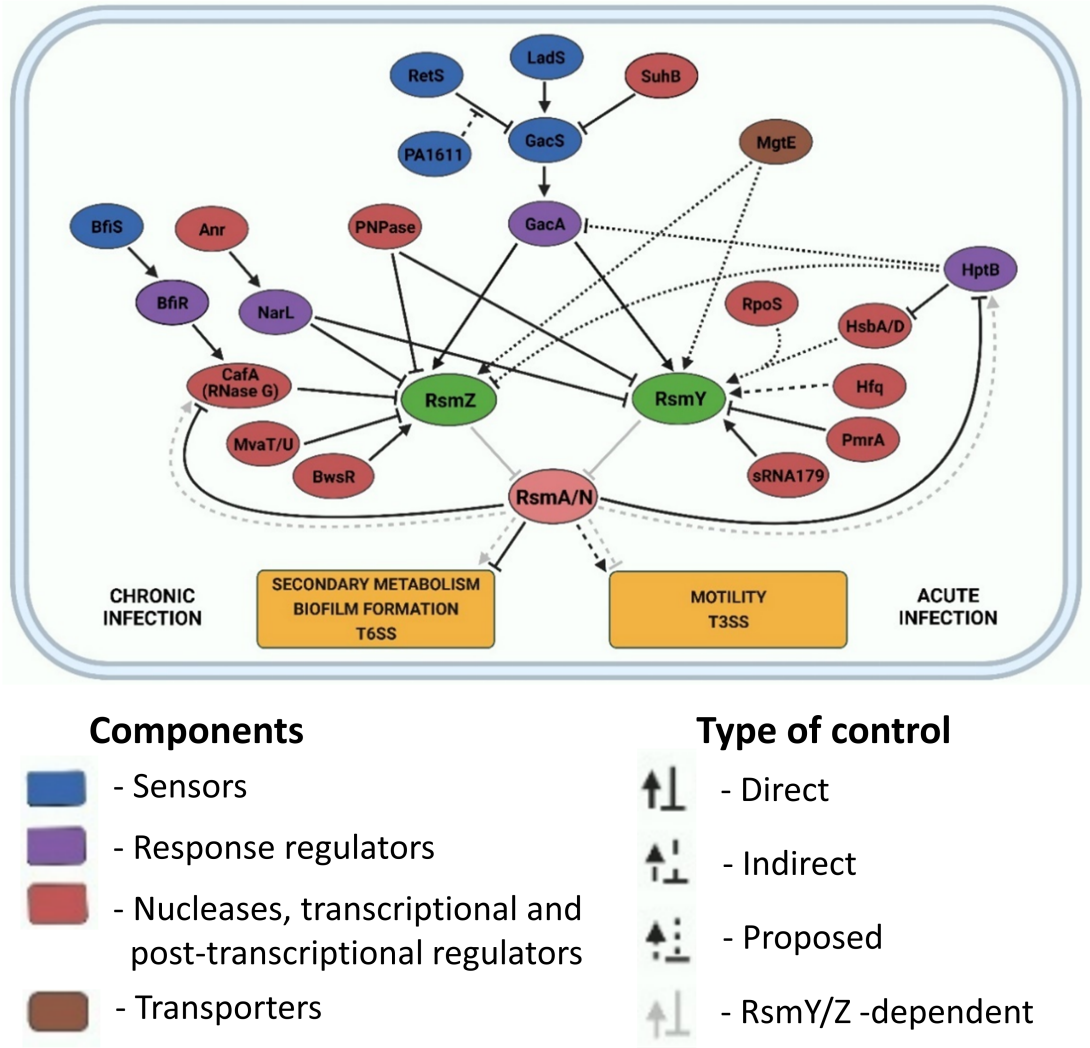

Figure 1.6: **Regulation of RsmY/Z synthesis and turnover.**
Schematic of regulators involved in modulation of cellular RsmY/Z pool adapted from (152) under Creative Commons Attribution license. Sowing sensors, response regulators, directly acting regulators and transporters, that have been shown impact RsmY/Z availability. Reviewed in further detail in (152).

RsmA and RsmN have been experimentally shown to be modulated by at least two more sRNAs, RsmW and RsmV. Both of these regulatory RNAs are GacS-GacA independent (149) and bind both RsmA and RsmN *in vitro* (157), while the impact under physiological concentrations and conditions remains as an open research question. RsmW (PA4570.1) was

first identified as a novel sRNA by (158), while named and characterised by (157). RsmW is preferentially expressed during the late growth phases and in biofilms, as well as under nutrient and iron limiting conditions (157, 149, 159, 160). A range of regulators including the alginate sigma factor (AlgU) and FleQ trancription factor have been predicted to potentially regulate RsmW production (157), implicating this sRNA with some of the regulators involved in the switch from planktonic to biofilm lifestyle, but any of these remain to be experimentally validated. Assessment of the RsmW function *in vivo* shows that overexpression can compensate for the loss of RsmY and RsmZ (157, 149).

RsmV (PA4033.1) was identified as sRNA through transcriptome sequencing studies (158, 161) and predicted as a sRNA binding RsmA/RsmN through use of *in silico* tools (149). Conserved in the *P. aeruginosa* genomes but absent from related species, RsmV shows a similar affinity for both RsmA and RsmN, but appears to be a comparably weak repressor compared to RsmY/RsmZ/RsmW (149). *In vivo* characterisation of the RsmV regulatory impact has been limited so far, but it has been shown that overexpression of RsmV in strain lacking RsmY/Z/V results in elevated T6SS promoter activity (149). The expression of these sRNAs is influenced by various environmental factors, such as oxygen levels, nutrient availability, and iron concentration. While *in vitro* binding studies have shown that these sRNAs can bind both RsmA and RsmN and can compensate for each other's absence when overexpressed (149), their specific *in vivo* functions and impact on RsmA and RsmN availability remain largely unknown. It has been observed that the expression of these sRNAs is temporally distinct, with RsmY and RsmZ increasing in the late stationary phase, RsmW increasing in early stationary phase, and RsmV gradually accumulating during successive growth stages (149). This suggests that the balance and concentration of these sRNAs may play a role in fine-tuning the activity of RsmA and RsmN.

1.2.3.3 GacS/GacA two component system and impact of sensory kinases RetS, PA1611, and LadS

Bacteria commonly use two-component systems (TCS) to detect and respond to changes in their environment. These systems are made up of a histidine kinase sensor and a cognate response regulator (162). GacS/GacA is one such sensor-regulator pair that has been closely linked to the Rsm system in *P. aeruginosa*. GacS is a membrane-associated kinase that controls the phosphorylation of the GacA response regulator (163). Phosphorylated GacA activates the transcription of non-coding RNAs RsmY and RsmZ (124). In *P. aeruginosa* GacS/GacA the two-component system has been shown to act exclusively through RsmY and RsmZ (124), but as discussed above, these sRNAs are not under the exclusive control of GacS/GacA. The periplasmic detector domain of GacS has been the focus of multiple studies, its presence has been shown to be essential for GacSA signalling and structural characterisation has seemingly pinpointed the specific amino acids involved in ligand binding (164, 165), yet to date, no known ligands for the sensory domain of *P. aeruginosa* GacS have been identified. However, the activation of GacS is controlled through kinase-kinase interactions with hybrid histidine kinases such as RetS, LadS, and PA1611 (166, 167, 168).

RetS is a sensory kinase that responds to the presence of mucin glycans and interacts with GacS to prevent the phosphorylation of GacA (169, 170). Multiple studies examining *P. aeruginosa* CF isolates strains have found that the *retS* gene is among pathoadaptive mutational hotspots (171, 54, 66). The loss of RetS has been shown to induce high biofilm formation and increase T6SS activity (101, 172, 167). This is a result of RetS forming heterodimers with GacS and this directly prevents phosphorylation of GacA (125, 169, 173). Another sensory kinase LadS responds to Ca^{2+} ions, which acts as an antagonist to RetS (174, 126). LadS activates Gac/Rsm cascade by directly phosphorylating GacS, triggering subsequent activation of GacA (126). Loss of LadS is associated with increased virulence, truncation of the *ladS* gene is the underlying reason for increased virulence seen in *P. aeruginosa* reference strains PA14 (175).

PA1611 is another hybrid kinase sensor that affects GacS activation, but unlike RetS or LadS, it does not interact with GacS directly. PA1611 interacts with RetS inhibiting its action and this results in a shift towards biofilm formation (176, 168). RetS, LadS, and PA1611 work together to integrate signals from the immediate environment and jointly modulate the activity of the GacS/GacA TC system, helping to determine whether current local environmental conditions favour planktonic or biofilm-like gene expression (177, 163).

1.2.4 *Pseudomonas aeruginosa* motility

P. aeruginosa can engage in three main types of motility: twitching, swimming, and swarming. Swimming is facilitated by flagella and is the dominant mode of motility in low viscosity environments (178). Twitching is a directed surface-based motility dependent on the use of type IV pili (T4P) (30). While both swimming and swarming can be described as activities performed by individual bacteria, swarming is a collective behaviour reliant on direct cell-to-cell coordination within the communities and can be observed on semisolid surfaces (179, 180). *P. aeruginosa* collective swarming is dependent on quorum sensing and use of both flagella and T4P (181). Each of these modes of motility is used under different environmental conditions. While flagella are preferentially associated with bacterial swimming in liquid, T4P are essential for surface attachment and formation of mature biofilm structures, where bacteria use T4P to "climb" over each other forming characteristic mushroom cap-like structures (Figure 1.7B) (182, 183, 184). Swarming is part of a broader adaptation in response to the viscous environment, which is distinct from planktonic or biofilm growth, and is associated with the expression of virulence factors that aid in host colonisation (185, 186).

1.2.4.1 Flagella mediated motility

Flagella are widespread bacterial motility devices that consist of an extended filament, a hook, and a basal body (178) (Figure 1.7A). The basal body of the flagella acts as a motor

that powers the rotation of the flagella and propels bacterial movement (189). The number and location of flagella vary among bacterial species. *P. aeruginosa* possesses a single flagellum located at one pole of the cell (190, 178). By changing the direction of rotation of the basal body motor, flagella can be used to both push and pull the bacterial cell (191) (Figure 1.7C). Additionally, it has been recently discovered that *P. aeruginosa* can wrap its flagellum around the cell body, enabling sudden changes in direction (188). The use of flagella allows for a fast, directed movement that enables the bacteria to explore its surroundings (187). Flagella-dependent motility is also involved in *P. aeruginosa* chemotaxis where bacteria ascends a gradient of chemoatractant molecule present in immediate environment (192). This process involves chemo-receptor proteins consisting of an extracytosolic ligand-binding domain and the cytosolic signal transduction domain (193, 194). *P. aeruginosa* PAO1 genome is predicted

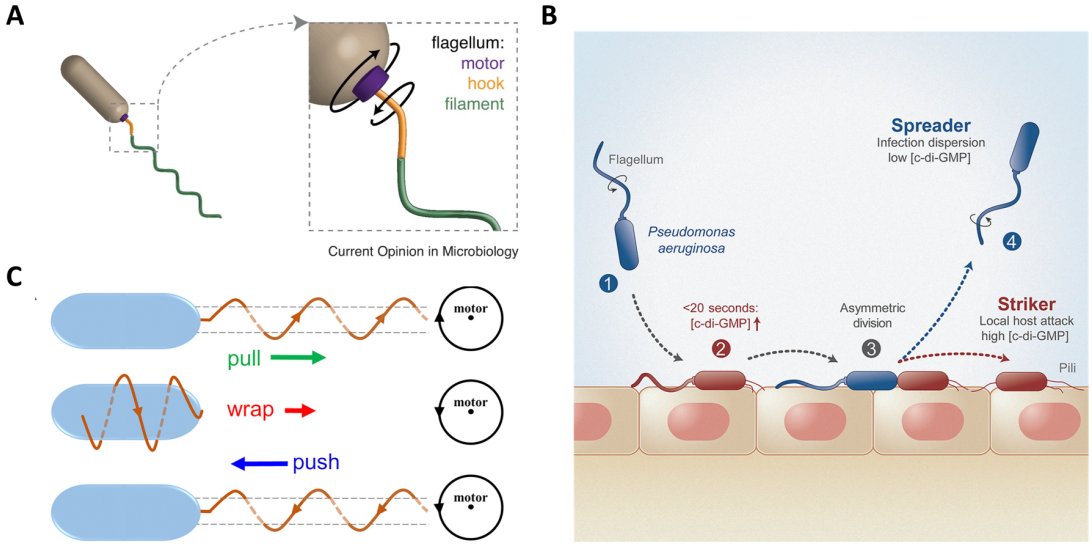

Figure 1.7: ***P. aeruginosa* flagella.**
(**A**) *P. aeruginosa* contains a single polar flagellum. Adapted from (187) under a creative commons attribution license.
(**B**) Flagella aids in biofilm initial establishment and dispersal in c-di-GMP dependent manner. Bacteria in planktonic culture exist in low c-di-GMP state, after encountering a surface c-di-GMP levels are elevated. After undergoing division on surface, cells with high intracellular c-di-GMP level continue surface colonisation, while low c-di-GMP cells use flagella to continued dispersal. Adapted from (183) under a creative commons attribution license.
(**C**) Flagella dynamics can be used to push or pull bacterial body depending on the direction of rotation in basal body motor, or to rapidly change direction of movement by wrapping flagella around bacterial body. Adapted from (188) under a creative commons attribution license.

to encode as many as 26 signal binding chemoreceptors (195). Some examples include CtpH and CtpL that respond to the presence of inorganic phosphate ions (196), PctA and PctB, both of which bind multiple amino acids aiding with nutrient uptake (197, 198), interestingly PctA as well as PctD can also respond to presence of neurotransmitter acetylcholine likely contributing to virulence in host niche (199). Flagella-mediated swimming is associated with a planktonic lifestyle and flagella proteins are considered one of the virulence factors of *P. aeruginosa* (32, 200). Flagella contribute to the initiation of biofilm formation by aiding in surface sensing and transition towards existence on solid surfaces and is required for biofilm dispersal and further dissemination in a c-di-GMP-dependent manner (183, 201) (Figure 1.7B).

1.2.4.2 Type IV pili mediated motility and impact on community organisation

T4P are flexible protein fibres that extend from the surface of bacterial cells. Pili structure and general mechanisms of action are broadly conserved in not only bacteria but also archaea (202). T4P are used for attachment to a variety of surfaces, including glass, metal, host cells, and other bacteria, promoting aggregation and mechanical surface sensing (30, 203). Pili fibres are made up of pilin subunits, the major pilin essential in the structure assembly is PilA but *P. aeruginosa* genome also encodes 5 additional minor pilins (204, 30). T4P fibres are anchored in the cell wall through alignment proteins, while cytoplasmically located ATPases act as assembly or retraction motors (205). T4P are dynamically polymerized and depolymerized, generating mechanical force (206, 207, 208). The combination of adhesive properties with active dynamics makes T4P a useful tool for bacterial motility and adhesion, both of which are highly beneficial for surface colonisation (203). Differential expression and incorporation of minor pilins allows bacteria to modulate binding affinity on different surfaces, such as the minor pilin PilY1 in *P. aeruginosa* that promotes host cell integrin binding and colonisation (209). T4P also contribute to DNA uptake and natural transformation in several Gram-negative species (210). Additionally, the adhesive properties of T4P enable the initial attachment of bacteria to the surface, while

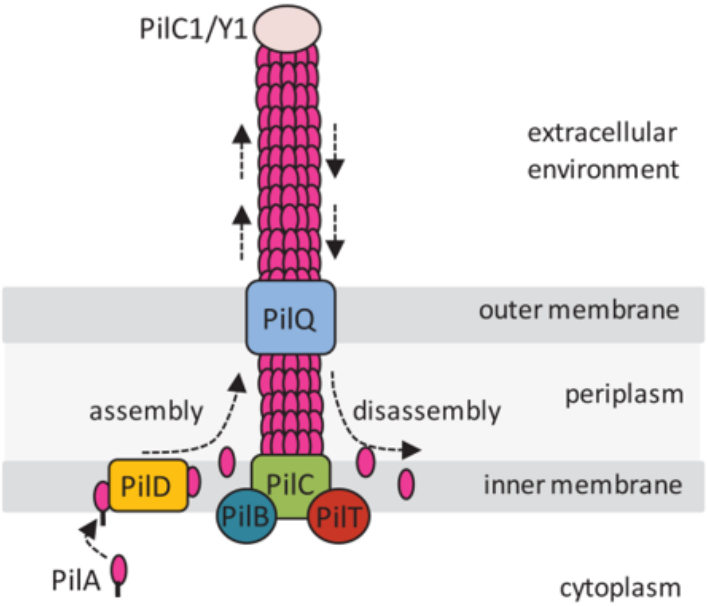

Figure 1.8: **Schematic of Type IV pili.**
The T4P filament is composed of major pilin PilA. The filament is attached to the inner membrane protein PilC and protrudes trough the outer membrane secretin PilQ. PilB and PilT are ATPases that are correspondingly responsible for pilus assembly and retraction, while PilD processes PilA before integration into pilus. Adapted from (212) under a creative commons attribution license.

their dynamic nature allows for the formation of a structured ECM that provides mechanical support for mature biofilms (30). To further emphasise the importance of T4P in bacterial community organisation, a study investigating *P. aeruginosa* clinical isolate biofilm formation correlated increased T4P production with strong aggregation and biofilm formation (211).

Type IV pili (T4P) of *P. aeruginosa* are preferentially expressed on rigid surfaces (213) and contribute to both twitching and swarming motility. During twitching, T4P are used to adhere to a substrate and pilus retraction allows the bacteria to exert mechanical force against the surface, propelling the bacterial body across surfaces (214). *P. aeruginosa* has been described to use T4P to engage both in "horizontal crawling" and "vertical walking" depending on the cell orientation relative to the substrate (215, 216). Surface motility helps bacteria to colonise surfaces, including movement in a direction opposing fluid flow, and ensure initial attachment during biofilm formation (216). In addition to aiding in surface colonization, T4P-mediated surface motility is also part of *P. aeruginosa* chemotaxis and exploratory motility that occurs

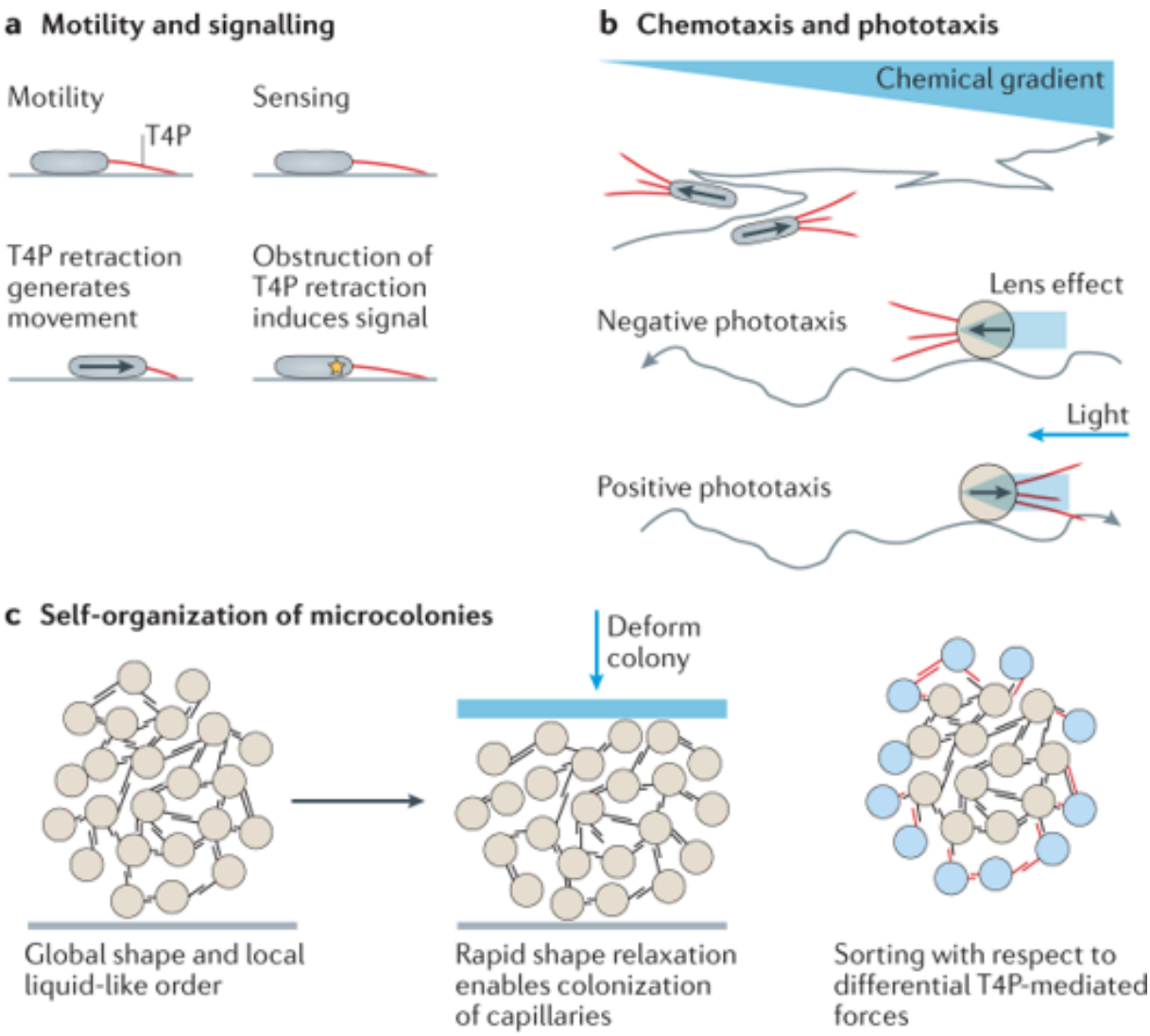

Figure 1.9: **Schematic of Type IV pili functions in bacterial communities.**
(**a**) T4P extension and retraction mediated surface motility. (**b**) Twitching motility enables directed movement in response to chemical gradients and other signals. (**c**) T4P-mediated cell-cell adhesion aids with aggregation and biofilm formation. This is essential for biofilm formation, contributes to the community organisation through specific adhesion mediated sorting and aids with withstanding stress from deformation forces.
Adapted from (205) with permission from Springer Nature.

upon exposure to other bacterial species (217, 218). While T4P are involved in swarming behaviour, unlike flagella, pili are not required for bacterial lateral expansion under swarming conditions, but aid in cohesion of bacterial groups during swarming (180). It is thought that, instead of acting as a motility device, during swarming pili-pili interactions aid with nematic ordering of adjacent bacteria, which likely helps coordinate the movement of whole *P. aeruginosa* clusters (179). Mutants lacking functional T4P will cover a larger swarming area than wild-type

strains and show high local alignment, while hyper-piliated mutants are swarming defective and lack local alignment (180). This role in local organisation highlights T4P role in adhesion, the importance of this function has also been shown in a study investigating *P. aeruginosa* clinical isolate biofilm formation correlated increased T4P production with strong aggregation and biofilm formation (211). Although T4P mediate surface motility at single-cell scale can be seen as highly individualistic behaviour, twitching motility is used for community expansion on surfaces and can be seen as a complex collective behaviour. Additionally T4P motility is responsive to environmental chemical signals aiding with colonisation (219). Chapter 6 of this thesis also investigates how T4P contribute to *P. aeruginosa* intermixing at both local and global scale, as well as demonstrates how T4P contribute to macrocolony expansion. Overall T4P are a surface appendage that is integral in *P. aeruginosa* existence on surfaces, aiding with both motility and community coherence.

1.2.5 Biofilms

The concept of bacterial biofilms has evolved from describing surface-colonizing microbial communities relevant to wastewater treatment and aquatic isolates, to bacterial communities developing in solid-liquid, liquid-gas, or solid-gas interfaces, to a somewhat ubiquitous sessile model of bacterial lifestyle that is highly prevalent in nature (220). The term "biofilm" is now more broadly used as a general designation for microbes engaging in sessile growth (221), and they are of broad interest in environmental, industrial, or medical sciences as both a cause of concern and a tool to be exploited for novel applications. Corrosion caused by marine biofilms is of significant economic concern in the shipping industry (222). Examples of beneficial industrial biofilm applications include the use of "activated sludge" for wastewater treatment (223). Biofilms and bacterial aggregates are also of clinical interest, with the most commonly used example being dental plaque formation (224). Aggregates of pathogenic bacteria can also be observed in isolates from chronic infections, as in the case with *P. aeruginosa* in CF sputum

(225). Another distinct example of naturally occurring biofilms is microbial aggregates found within soil (226). Biofilms are the dominant form of bacterial existence, and the above examples highlight just how diverse microbial communities referred to as "biofilms" can be (220).

The defining features of biofilm communities are a decrease in individual motility in favour of bacterial aggregate formation and the production of an extracellular matrix that encases the bacterial community (227). As bacteria transition from individualistic, free-living cells to collective systems, a range of defining collective features emerge. The formation of aggregates results in spatial heterogeneity, in the form of gradients in oxygen, nutrients, and waste products, which subsequently promotes phenotypic heterogeneity and specialisation (228). As the bacteria are spatially fixed, long-term synergistic interactions can establish (229, 230). The proximity also necessitates communication and coordination, which typically occurs through quorum sensing (231, 1). As part of physiological adaptation, quorum sensing allows for the coordination of a range of biofilm behaviours, including changes in virulence factor expression (147) and coordination of environmental adaptation (232).

Biofilm communities have also been shown to improve stress tolerance, including to abiotic stresses such as changes in pH and temperature fluctuations or exposure to mechanical shear stress (233, 234, 235). In the context of the host microbiome, the existence of a healthy microbiome is one of the key mechanisms providing resistance against invading species (236, 237). However, once infection has been established, existence in biofilm communities protects bacteria from host clearance (67, 238) and provides resistance against antibiotic treatment (52, 239).

1.2.5.1 Biofilm formation

Biofilm formation involves a process of transition from individualistic bacteria to existence within organised community consisting of varied micro-environments and phenotypically specialised bacteria. *P. aeruginosa* has been a key model organism for studying the process of biofilm establishment and maturation, and has been used to develop conceptual models for

biofilm development. These models have been refined over time, with (240) defining multiple phenotypic life-stages and (241) defining five steps of biofilm development. These five stages are reversible attachment, irreversible attachment coinciding with a broad switch in gene expression, and two stages of maturation, first characterised by the appearance of matrix-embedded clusters and second by the formation of structured microcolonies, finally followed by biofilm dispersal (241). Recently, this model was expanded by (227) to incorporate aggregates as an independent part of the biofilm lifestyle, separate from surface attachment.

When planktonic bacteria encounter a surface, they can undergo frequent polar attachment-detachment events that initiate the formation of surface-based biofilms (242). The "commitment" to switch towards biofilm formation is marked by an "irreversible" longitudinal attachment, which is accompanied by shifts in gene expression, including downregulation of flagellar motility (243, 244) and upregulation of antibiotic resistance-related gene expression (245), as well as early exopolysaccharide production (119, 246). In *P. aeruginosa*, this process is driven by changes in intracellular c-di-GMP levels upon surface contact. This leads to an asymmetric division event in which one of the cells with high c-di-GMP levels commits to a surface-attached existence, while the other detaches and continues as a planktonic cell (183). During surface-attached growth, these bacteria undergo subsequent rounds of division and form microcolonies that will subsequently evolve into large structures in which bacteria coordinate their behaviour through QS (247). Gradually, large three-dimensional biofilm structure will form, leading to the creation of internal gradients in nutrients, oxygen, and waste products (228). The change in local conditions drives further niche sub-specialization within the community (248). Although dispersal is often described as the final stage of biofilm formation, individual cells can detach from resident cells and leave the structure by switching to planktonic life at any time point during biofilm growth (227).

A striking structural feature of mature *P. aeruginosa* biofilms observed on flow-cell surfaces is the formation of large stalked mushroom body structures (184). However, it should be noted that

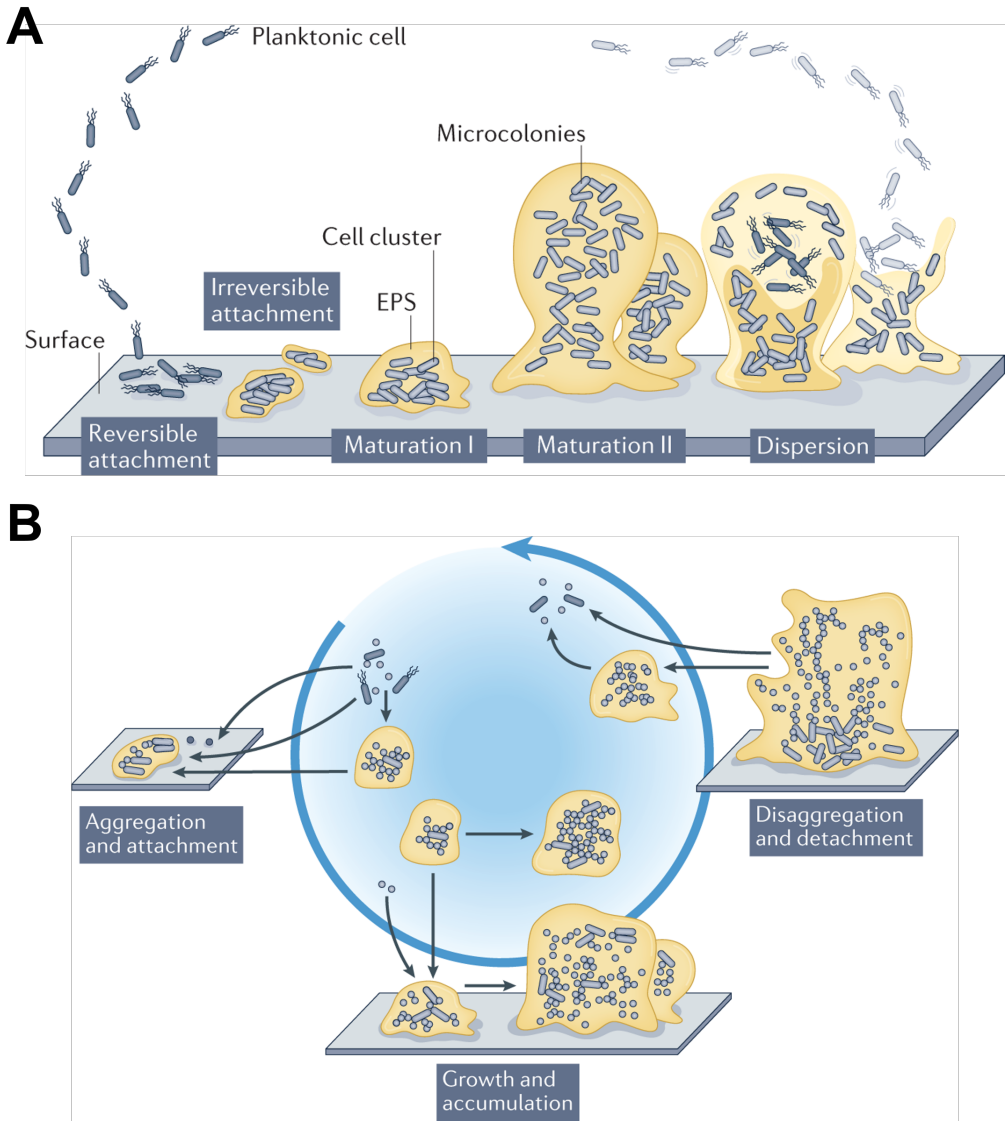

Figure 1.10: **Model of biofilm formation.**
(**A**) Conceptual model of biofilm formation defining five sequential stages of biofilm development from (241). 1. Upon encountering a surface planktonic cells undergo reversible attachment. 2. Irreversible attachment. 3. Maturation and microcolony formation. 4. Further maturation and structured biofilm formation. 5. Dispersal.
(**B**) Expanded conceptual model incorporating bacterial aggregate formation as per (227). Rather than sequential process, this is laid out as distinct micro-environments with associated characteristic features. Aggregation and attachment - during which bacteria attach to each other, biotic, or abiotic substrates. Growth and accumulation - during which aggregated bacteria grow forming structured communities. Disaggregation and detachment - during which bacteria leave the biofilm as single cells or aggregates.
Adapted from (227) with permission from Springer Nature.

biofilm formation is not dependent on a surface or interface and *P. aeruginosa* biofilm isolates from the CF lung environment would be better described as aggregates (249). Aggregates formed in the liquid phase exhibit many of the same properties as surface-attached structures, including

chemical gradients and sub-population specialization, and these structures are maintained by mechanisms like those present in surface-attached communities (250, 251). The distinguishing feature of these aggregates is their mode of assembly, which is often independent of surface attachment (252). Multiple mechanisms of bacterial aggregation have been described, including detachment of cell clusters from surface-attached biofilms, also known as sloughing, which can be induced by chemical and physical stresses (253). Aggregates can also be formed directly in the liquid phase when daughter cells remain attached through surface adhesins or extracellular polysaccharides (254), which may explain why regulatory mutant strains that over-express EPS-associated genes readily form aggregates grown in laboratory liquid culture under vigorous agitation (255). Alternatively, cells that produce sufficient amounts of attachment molecules in the liquid phase can also form co-aggregates (254), or use host polymers, such as fibronectin (256), to form coherent particles (257), both of which enable the formation of aggregate communities that are not strictly monoclonal. Although the specifics of aggregate formation and disintegration are still the subject of current research across a range of fields, it is clear that the key concepts remain the same independently of whether a biofilm is formed at an interface or within the liquid phase (227). A more general model can be split into three stages of biofilm formation: initial attachment to a surface or other population members, followed by growth and the establishment of more complex structured communities with heterogeneous microenvironments and sub-populations. The final broad stage of community development is detachment and disintegration, which allows the bacteria to spread to new environmental niches (Figure 1.10 B).

1.2.6 Extracellular matrix

The extracellular matrix (ECM) is a defining feature of bacterial biofilms and can make up more than 90% of the biofilm's dry mass (258). The ECM is composed of exopolysaccharides (EPS), extracellular DNA (eDNA), and secreted proteins, and increased production of all of

these is a hallmark of the transition to a biofilm lifestyle (100). The matrix provides structural support for the formation of complex 3D structures, facilitates the organisation of the microbial community, and serves as a physical barrier to protect the biofilm community (259, 260, 261, 262). EPS in particular forms a protective barrier that has been shown to help bacteria with immune evasion, resist antibiotic treatment, and withstand contact-based attacks (263, 264, 238). The combination of both EPS and eDNA results in viscoelastic matrix support that aids in protecting against mechanical stress introduced by liquid flow (265, 266). Furthermore, EPS production has been linked to increased fitness and persistence in polymicrobial contexts, while leading to reduced virulence (267, 236, 221). In *P. aeruginosa* the ECM contains 3 main exopolydasachrides - Pel, Psl, and alginate - with distinct but partially overlapping functions (268, 260).

1.2.6.1 Alginate

Alginate is a high molecular weight uncharged heteropolymer made up of β-d-mannuronic and α-l-guluronic acids (269). Alginate overproduction results in a mucoid phenotype, characterised by an increase in water retention and a distinctive colony morphology, which confers desiccation resistance and aids with nutrient retention (270, 271). Alginate contributes to both biofilm establishment and structural support in mature biofilms (272), but it is not essential for biofilm formation in *P. aeruginosa*. This is because a range of isolates with low alginate expression can form biofilms, including the reference strain PAO1 used in this study (273, 274). A shift toward mucoid phenotype is commonly found to have occurred in *P. aeruginosa* clinical isolates (60, 275). In the context of *P. aeruginosa* infections, alginate inhibits phagocytosis (276, 277, 278) and is a significant contributor to the formation of the biofilm's bulk biomass, which acts as a protective barrier that interferes with the delivery of antimicrobial drugs (279, 280). This mucoid phenotype is often caused by mutations in the *mucA* gene (64, 281), which are highly prevalent in CF patient isolates (281) and are associated

with a poor treatment prognosis (282, 283). Interestingly, mucoid *P. aeruginosa* lineages can be seen acquiring a secondary compensatory mutations, often in MucA interaction partner AlgU, resulting in a transition back toward the non-mucoid phenotype (284). This is through to occur due to high fitness costs imposed by overproduction of alginate (285). Mutations in *mucA* have also been associated with down-regulation of T3SS (286). The acquisition of these mutations marks a transition from a highly virulent planktonic lifestyle to a biofilm-associated chronic infection phenotype. The expression of T3SS is often inversely correlated with increased expression of T6SS (101), so it is of interest to determine if mutations within *mucA* affect the expression of T6SS. Previous research has shown that mucoidy is related to up-regulation of T6SS activity in *Pseudomonas fluorescens* (287) and H1-T6SS structural genes are suggested to be up-regulated in microarray studies using *mucA* mutants (288). However, further research is needed to confirm the impact of these mutations on T6SS expression.

1.2.6.2 Psl

Psl is a polysaccharide composed of D-mannose, D-glucose, and L-rhamnose (289). Genes responsible for Psl production and transport to the surface are encoded within **p**olysaccharide **s**ynthesis **l**ocus (290, 291). Psl can be anchored to the cell surface, where it promotes close cell-cell and cell-surface adhesion through polymer cross-linking (292), or it can be present in the extracellular matrix (289). Both forms of Psl contribute to the ECM elasticity and resistance to mechanical shear forces (293). Psl is preferentially produced during early biofilm formation and helps with the surface attachment (294, 246). Later in the maturation process, Psl expression can be found in the central part of the biofilm (295). Depletion of Psl can also cause mature biofilms to disintegrate, indicating that Psl is essential for the maintenance of biofilms at all stages (292). Psl also has a non-structural role in signalling, extracellular Psl serves as a "feed-forward" signal that activates diguanylate cyclases SadC and SiaD, leading to the production of c-di-GMP and the formation of biofilms (296).

Biofilm formation in different *P. aeruginosa* isolate strains can be primarily dependent on Pel or Psl. Psl is the primary exopolysaccharide in the majority of non-mucoid clinical isolates (246), including the reference strain PAO1 used in this study (297). Within the context of high alginate production in mucoid isolates, Psl remains crucial and is reacquired for both attachment to epithelial cells and the formation of robust mature biofilm structures (62). When attached to epithelial cells, Psl has been shown to provoke immune responses (298). In these cases, co-expression with alginate is key for protection against phagocytosis (62). Psl production has also been associated with an increase in tolerance to aminoglycoside antibiotics, the antiseptic chlorhexidine, and colistin at the population level, as well as an improved competitive advantage in polymicrobial biofilm contexts (299, 263, 300, 301). Loss of Psl production has been shown to compromise *P. aeruginosa* competitive fitness in mixed species biofilms (274, 236, 302). In the context of infection, Psl production aids in evasion of the host immune system in model systems (62, 303). Elevated Psl production has been associated with treatment failure to eradicate *P. aeruginosa* infection in childhood CF patients (304), leading to the consideration of Psl as a potential target for new therapies (305).

1.2.6.3 Pel

Pel is a positively charged polysaccharide made primarily of N-acetylgalactosamine and N-acetylglucosamine (306). Genes responsible for Pel production were identified by screening mutants defective in the formation of characteristic pellicles at the air-liquid interface and named thereafter (307). The requirement for Pel in biofilm formation depends on the specific strain of *P. aeruginosa* (297). Although Psl is the major exopolysaccharide produced in early biofilms, the loss of Pel will result in impaired attachment (308). Due to its positive charge, Pel interacts with extracellular DNA (306), and the structural properties of polymer cross-links are thought to contribute significantly to the viscous properties of the exopolysaccharides, allowing biofilms to withstand mechanical stress through deformation (293, 309). This is also essential for the

structural remodelling of mature biofilms, which is necessary for the formation of mushroom-like *P. aeruginosa* biofilm structures (293, 306). Here, Pel is localised at the periphery of pellicle stalks, providing structural support in mature biofilms (306). Pel interacts with eDNA and protects biofilms from eradication by treatment with DNases, aminoglycosides (297, 249), or polymyxin antibiotics (310). Pel and Psl have overlapping functions, and their production can compensate for each other to some extent, and the preference for their use varies among clinical isolates (246). Unlike Psl, the interruption of Pel production will not result in the disintegration of mature biofilms, but rather determines whether cells on the outer surface of the structure will remain attached and contribute to the formation of the existing structure or detach (297).

1.2.6.4 eDNA

Extracellular DNA (eDNA) is an essential ECM component in *P. aeruginosa* biofilms as DNase treatment is sufficient to induce biofilm dispersal (311) and closely interacts with EPS components. Due to their opposing charges, Pel and eDNA can bind to each other (312) and because of interactions with EPS, eDNA helps to maintain the structural rigidity (313, 314, 249). This interaction has implications for the design of future treatment therapies targeting both EPS or eDNA (249). Presence of eDNA aids in T4P-mediated expansion through coordination of local organisation (315). The eDNA pool also contributes to conjugative gene transfer that occurs with increased efficacy in biofilm context (316, 317). Additionally, eDNA can be used as a substrate for natural transformation (318). The negative charge of eDNA allows it to chelate cations present in the matrix, promoting cell-cell binding and acidification of the local environment (319, 320). In the context of infection, eDNA contributes to *P. aeruginosa* biofilm resistance to aminoglycoside treatment (321, 320, 249). Overall, eDNA is an essential component of *P. aeruginosa* biofilms that is intentionally released to act not only as a structural cross-linking aid but is also important for biofilm resiliency in the context of infection (322, 323, 324).

1.2.6.5 Summary of exopolymeric substances

Exopolymeric substances, including alginate, Pel, and Psl, are important components of the ECM of *P. aeruginosa* biofilms. While they have some overlapping functions, each EPS has a distinct contribution to the formation of structured biofilms. Psl is essential for early biofilm formation, including attachment and cell-cell coherence, while Pel contributes to the viscosity and elasticity of the overall structure. In mature biofilms, Psl interacts with eDNA and is present in the core of complex structures, where it is essential for maintaining cell-cell contacts that act as structural support. Levels of Pel expression determine whether cells located in the biofilm/media interface will detach or remain with the core structure enabling formation of complex biofilm structure in form of characteristic *Pseudomonas* pellicles. Another key contributor to biofilm formation and aggregation is the extracellular adhesin CdrA (325). The expression and release of CdrA is highly responsive to c-di-GMP and, through binding to Psl and Pel, shows strong self-aggregating properties (326, 327). Alginate, although not essential for structured biofilm formation, plays a key role in *P. aeruginosa* infections by forming a protective barrier that helps establish a stable microenvironment and protects against immune clearance. Mutations impacting EPS production are common in clinical isolate strains, and two commonly found pathoadaptive phenotypes are the mucoid and rugose phenotypes (66). Mucoidy is a result of overproduction of alginate while high Pel and Psl expression contribute to rugose *P. aeruginosa* phenotype (328, 68). Overall, the ECM is a defining feature of biofilms, aiding in community organisation and contributing to biofilm resiliency.

1.3 Bacterial interactions

Within the environment, microbes rarely exist as single species communities and polymicrobial biofilms are more common. For example, microbial communities found in the oral cavity or gut typically consist of hundreds of species (329, 330). Similarly, when present in lung infections, *P. aeruginosa* is part of a polymicrobial community consisting of tens of bacterial and fungal species, which it must compete with to invade the community and persist (331, 332, 333). In mixed-species biofilms, organisms often display improved stress tolerance and differ in their treatment response in the context of infection (86, 84). In addition to abiotic factors, the composition, structure, and response of communities to conditions are influenced by the presence of different species and their interactions with each other. The emergence of complex structures is dependent on individual interactions, which can include direct or indirect competition, positive feedback, and other social or physical interactions (334). Small differences in local cell dynamics can lead to significant structural changes at the colony or biofilm level, and profiling of community structural variation can be used as an indicator of phenotypic variation (335, 336). Structural changes are indicative of phenotype switching (67) and environmental adaptations (52), which can be used to aid in diagnostics, identify key pathogenesis features, as multiple pathoadaptive mutations can converge to similar phenotypes, or guide drug development and biotechnological applications (336, 337). To better understand the interactions in complex communities as a whole, it is important to further our understanding of the mechanisms underlying interactions between individuals.

1.3.1 Types of bacterial interactions

Ecological interactions within the niche can be broadly categorised as positive, negative, or neutral. Considering systems with two interaction partners, this leads to six possible ecological interactions summarised in Figure 1.11. First of these is direct cooperation or mutualism, where both species benefit from the presence of the other within the niche. A clear example of this

amino acid cross-feeding can be seen in the evolved community of *Salmonella* Typhimurium and *E. coli* in a study by (339). A naturally evolved example of positive cross-feeding seen between *Bacteroides* species in the gut of mice, where one of the species releases glycoside hydrolases in the extracellular milieu that allows the digestion of extracellular polysaccharides, and all bacteria present benefit from the increase in the availability of uptake-ready sugar, while other *Bacteroides* species provide another, currently unknown, benefit in return (340). An alternative example of positive inter-species interactions is the production of public goods such as siderophores that improve iron uptake (341, 342) or can result in increased biofilm-forming behaviour (230). However, cooperative interactions between species are predicted to be uncommon in naturally occurring mixed-communities and competition appears to be more prevalent (343, 344). Further interaction is commensalism, where one species benefits from the

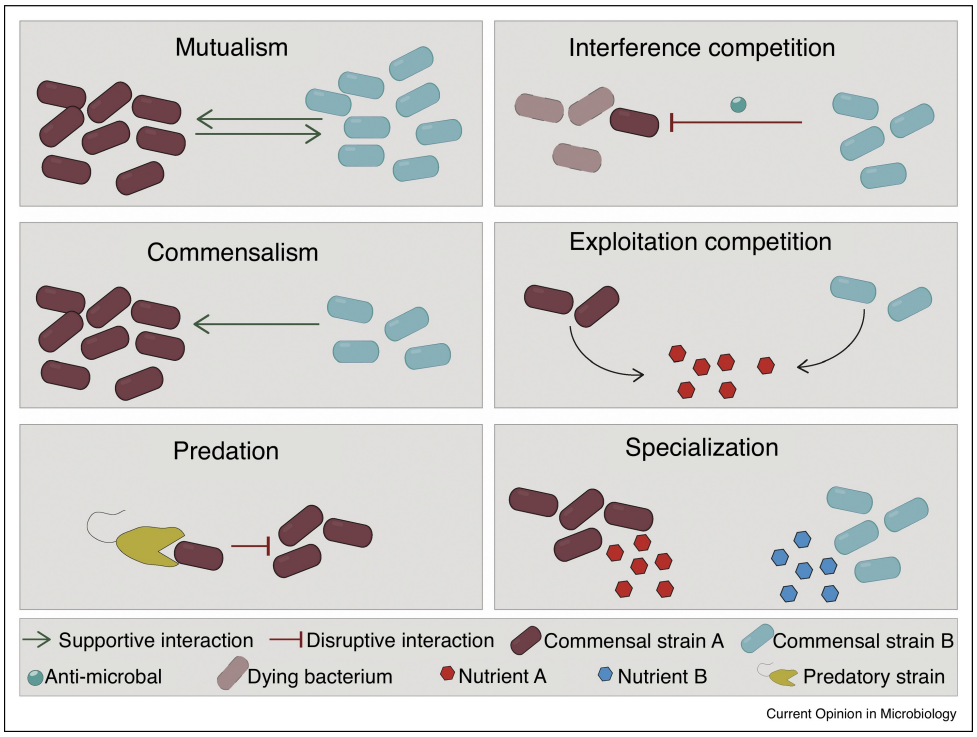

Figure 1.11: **Schematic showing types of pairwise bacterial interactions occurring in microbial communities.**
Interactions where both strains benefit are termed mutualism, while commensalism refers to interactions where only one of the strains gains fitness advantage. In cases of predation one of the organisms gains nutrients by killing another. Interference competition describes direct competition through killing, while exploitation competition is indirect and bacteria compete for better utilisation of a shared resource. Specialisation allows bacteria to avoid competition for resources. Adapted from (338) with permission from Elsevier.

presence of the other, but the other species is not affected. Although these interactions are rare in interactions between microbes within a community, they are important to consider in the context of interactions between the host and the healthy microbiome as a whole. As the host provides nutrients and a habitat for bacteria, while the bacteria do not have a negative impact on the host (338). The host often indirectly benefits from the presence of a healthy microbiome as a whole, rather than individual bacteria within the community. The presence of gut commensals has been shown to protect against pathogen colonisation, affect host immune function, and aid with micronutrient uptake (345, 346, 347, 338).

Competition, where the presence of one species reduces the fitness of the other seems to be the far more prevalent type of interactions seen in polymicrobial context (343). In mixed-species biofilms, competition has been shown to drive the emergence of structured communities, as individual cells or lineages compete for space and resources (344). Competition can take many forms, including direct competition, where both species are negatively impacted by the presence of the other, or indirect competition. Indirect competition can occurs when multiple species make use of the same resource. In cases such as this, the ability to grow faster or even marginal improvement in metabolism will lead to an overall competitive benefit (348, 349). Another form of competition is exploitation, where one species benefits at the expense of the other. Examples of this include predation, such as in case of *Bdellovibrio bacteriovorus* that invades a prey bacterium and uses it as a source of nutrients and a protective niche (350). It should also be considered that two bacteria within a niche may not engage in direct interactions, and instead by further specialising to make use of different nutrients, microorganisms can avoid the need to engage in antagonism. In general, competition and negative interactions are more common in mixed species communities, as both species are trying to maximise their own fitness at the expense of the other, and this is emphasised by the large number of molecular tools that bacteria have evolved specifically for use in bacterial competition (351, 352, 353).

1.3.2 Tools used in bacterial competition

Direct competition for space and resources is a common occurrence in the bacterial world, and as a result, bacteria have evolved a range of specialised tools to compete with each other (352, 351). These include small-molecule products such as poisons and protein effectors, as well as molecular machines that directly cause damage to other organisms within the same niche. These competition tools can be highly targeted towards specific species or lineages, as in the case with bacteriocins, or have a broader impact across kingdoms, as in the case of T6SS (354, 355). The range of impact, the need for cell-cell contact, and the potential for multipurpose use of effectors are all factors that can distinguish different competition tools and determine which is most effective in a given context. For example, long-range competition conducted through toxins released into the extracellular environment must overcome the challenge of entering target cells in sufficient amounts, while contact-dependent competition tools, such as T6SS, can directly translocate effector molecules to target cells. However, contact-dependent competition is limited by the need for spatial proximity and can be compromised if target bacteria manage to gain spatial separation through any means (356). Many competition systems and compounds are multipurpose, with common good effectors that aid with ion uptake in one species being detrimental to competitors (357). Alternatively, proteins with antibacterial activity can also function in host cell interactions, such as *P. aeruginosa* the T6SS effector VgrG2b, which both targets the peptidoglycan synthesis machinery of competing bacteria and aids with internalisation into host cells (358). The specific context in which an organism exists within likely determines which type of tool is most beneficial, which may explain the wide range of competition tools found in bacteria and the common occurrence of multiple competition weapons in individual bacterium (351). Below, aspects of different tools used for bacterial competition are reviewed, with the aim of both highlighting commonalities between the systems and distinguishing features that may lead to situation-specific advantages or disadvantages. As T6SS is the focus of this thesis, the mechanistic details and ecological role of this system will

be reviewed in more detail in section 1.4 of this report, while here focus is placed on other tools used in microbial competition, both ones present in *P. aeruginosa* and other bacterial species.

1.3.3 Type V secretion system

Type V secretion systems (T5SSs) are the most broadly distributed group of Gram-negative secretion systems and are present in around 62% of currently sequenced genomes (359). T5SSs are divided into several sub-classes based on the organisation of component protein domains, structural features, and differences in specific translocation mechanisms (360). These systems transport a variety of proteins, including proteases and lipases, adhesins, and factors involved in pathogen-host interactions (361). Of further note in the context of bacterial competition the T5SSb is also known as CDI or contact-dependent inhibition system.

CDI is a bacterial competition tool that was first described in *E. coli* by (363). It is present in various species of proteobacteria and consists of three components: the toxic passenger protein CdiA, the translocation protein CdiB, and the cognate immunity protein CdiI (364, 365). Both CdiA and CdiB are transported to the periplasm in a Sec-dependent manner, where β-barrel containing CdiB then forms a translocation pore by inserting itself into the outer membrane and this pore accommodates the passenger protein CdiA (366, 367). The C-terminal domain of CdiA encodes an antibacterial toxin, while CdiI is typically co-encoded within the same gene cluster as the other two proteins and protects the producer and kin cells from self-intoxication (368) (Figure 1.12A). The delivery of toxin to the prey cell is mediated by the receptor binding domain (RBD) of the CdiA protein, which binds to a cognate surface feature of a susceptible prey cell (369). The CdiA toxin domain is present in the periplasm of the inhibitor cell and is translocated to the target cell upon interaction of RBD with cognate outer membrane proteins present on the surface of the prey bacteria (370). After delivery to the target cell periplasm, cytoplasmic acting toxins are further transferred to the cytoplasm as a result of interactions with specific inner membrane proteins, examples of which include the protease FtsH or PtsG

that is involved in sugar uptake (371, 372) (Figure 1.12B).

CDI toxins have a variety of biochemical targets, including cell wall disruption and nucleic acid degradation (373, 365, 374). CDI allows for the delivery of the targeted toxin directly into the prey bacteria, making this a potentially very efficient bacterial competition tool. Yet a key aspect of interactions mediated through CDI is the requirement for a specific surface protein to be present, such as BamA or OmpC (372), on the prey cell, this can be beneficial, as an attacking bacterium is able to narrowly tailor toxin delivery to specific targets, limiting

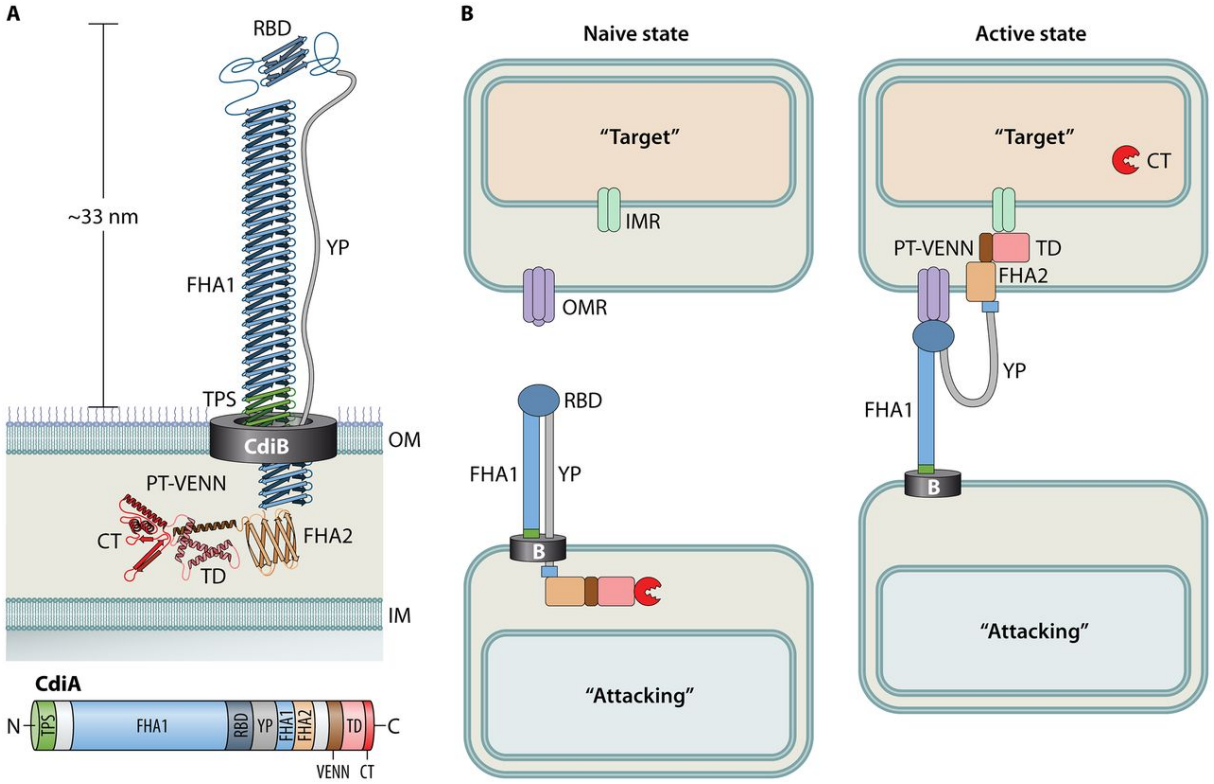

Figure 1.12: **Schematic showing CDI effector translocation.**
(**A**) Diagram of CdiA and CdiB localisation within attacker cell before formation of contact with target cell. Domain organisation of CdiA effector from right to left (N-terminal to C-terminal): two partner secretion (TPS) domain, FHA-1, receptor-binding domain (RBD), tyrosine-proline rich domain (YP), FHA-2, pretoxin (PT) domain, VENN motif, cytosol entry domain and toxin domain.
(**B**) CdiB forming a translocation pore in the outer membrane of inhibitor cell, with CdiA effector protruding from the pore. Upon binding CdiA-RBP forms contact with target cell surface features (OMR), C-terminal effector domain is trans-located and upon entry cleaved after the VENN motif. Subsequently entry domain recognises specific inner membrane protein of target cell and CdiA toxin domain is translocated across the target cell inner membrane and reaches the cytosol.
Adapted from (362) with permission from American Society for Microbiology - Journals.

the metabolic expenditure associated with toxin production. Simultaneously, this specific toxin targeting also allows prey bacteria to evolve escape mechanisms as a result of mutations in specific binding targets (369).

CDI can mediate competition between closely related bacterial strains within the same species as well as in inter-species competition (364, 365). An interesting example of CDI in action is the *Burkholderia thailandensis* CDI effector BcpA exhibits *in vitro* nuclease activity, which acts as a toxin and contributes to eDNA modification and structured biofilm formation (375, 376, 377). CDI systems are nearly ubiquitous in *P. aeruginosa* genomes, with genomes of 80% of strains containing two systems (373). Although presence of the CDI systems is widespread toxin domains are polymorphic and far less conserved (378). The CDI systems present in *P. aeruginosa* have been experimentally demonstrated to effectively kill strains lacking specific toxin immunity genes (378, 379). While the exact biochemical functions of the two CdiAs are unknown, bioinformatics analysis predicts CdiA1 to be a putative tRNase while CdiA2 is a putative nuclease (380). Additionally, *P. aeruginosa* CDIs have been shown to be used not only for bacteria-bacteria competition but also as virulence factors in host interactions (380, 379).

1.3.4 Type IV secretion system

It has been known for a long time that Type IV secretion systems (T4SSs) translocate a wide range of substrates to eukaryotic cells (381). A distinguishing feature of the T4SS is that is able to transport both proteins and DNA as a substrate, including plasmid transfer during bacterial conjugation events (382, 383). More recently, T4SS has also been shown to deliver protein toxins to other bacteria (384, 385). These systems are structurally diverse, and thus the specific mechanisms by which they transport their cargo can vary (381, 386). Briefly, T4SSs assemble a pilus structure anchored within the membrane of donor bacteria, cargo transport occurs when the pilus comes into contact with the target cell (385). Unlike the CDI system, T4SSs effector protein delivery does not appear to be dependent on binding of specific surface

proteins and allows for somewhat indiscriminate cargo delivery (387). Instead, the T4SS pilus is topped by the VirB5 protein pentamer, which bears structural similarities to pore-forming proteins (388). Different functional and structural classes of T4SS are distributed across a range of bacterial genera, but T4SS is not found to be encoded in *P. aeruginosa* genome.

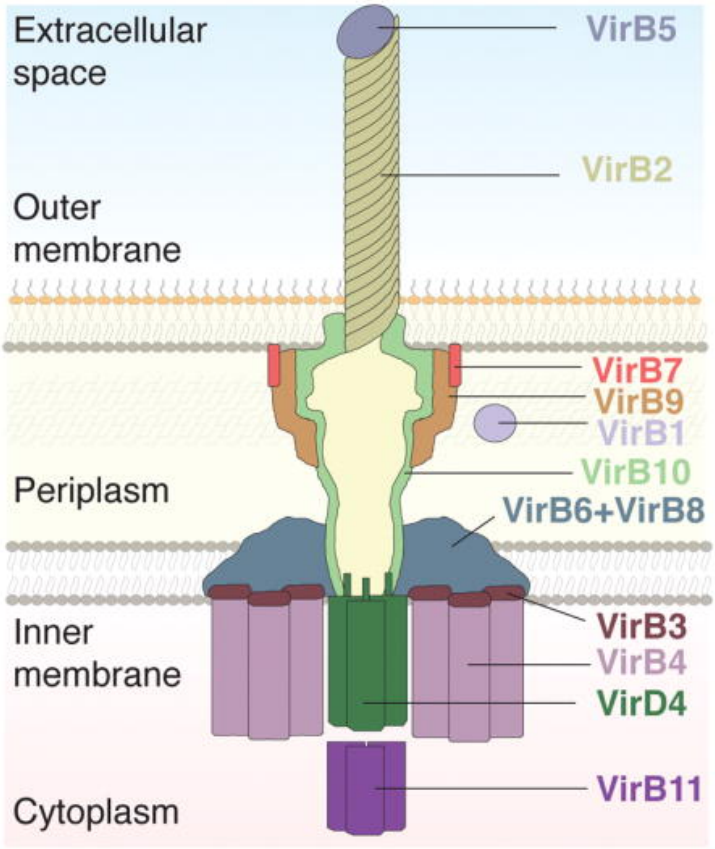

Figure 1.13: **Schematic of type IV secretion system.**
Schematic of T4SS showing localisation of core structural components. T4SS extends a pilus consisting of VirB2 into extracellular environment. The pilus is topped by VirB5 that aids in target cell recognition. Pilus is anchored into the cell wall through outer and inner membrane complexes, and system dynamics are powered by cytoplasmic ATPases.
Adapted from (387) with permission from John Wiley and Sons.

The function of the T4SS is thus very diverse, with a subset of T4SSs being involved in bacterial conjugation which has been suggested as one of the major mechanisms contributing to the spread of antimicrobial resistance plasmids (389). Some bacteria, such as *Agrobacterium tumefaciens*, use T4SSs to deliver oncogenic DNA to plant host cells (390). Furthermore, specialised T4SSs, such as those in *Helicobacter pylori*, can be used to take up DNA from the environment (391). Alternatively, T4SSs can deliver effector proteins directly to host cells and

other bacteria. Examples of T4SS-mediated delivery of virulence factors include the delivery of pertussis toxin by *Bordetella pertussis* (392) and CagA by *H. pylori*, later being associated with both peptic ulcers and gastric cancer (393). More recently, T4SS-mediated toxin translocation for direct bacterial competition has also been described (385). For example, the *Xanthomonas citri* T4SS has been shown to associate with a range of proteins containing domains bearing homology to to peptidoglycan hydrolases, phospholipases, metallopeptidase, and other proteins with known toxin properties (384). These toxins, called X-Tfe, are co-encoded with immunity proteins (X-Tfi) and were found to provide a competitive advantage in competition with *E. coli* (384). Similar T4SS-mediated contact-dependent killing of *E. coli* was observed in competition with *Stenotrophomonas maltophilia* (394). Further bio-informatics analysis has shown that X-Tfe homologues can be found in in other bacterial species and the ability to engage in direct bacterial competition using the T4SS could be a more broadly distributed capability (385).

1.3.5 Type VII Secretion system

Cell wall of Gram-positive bacteria consists of multi-layer peptidoglycan barrier or lipidated cell wall termed mycomembrane found in *Mycobacteria* or related species (395, 396). This cell wall provides protection from potential external stresses, but also pauses challenges for protein export (397). A molecular machine used for this is the type VII secretion system (T7SS), which was first identified in *Mycobacterium tuberculosis* (398) and analogous systems have since been described in other Gram-positive bacteria such as *Staphylococcus*, *Listeria*, and *Bacillus* sp. (399). For a substrate to be translocated to the extracellular space, protein effectors have to not only cross the inner membrane, but also additional mycomembrane or typical Gram-negative cell wall.

The exact molecular details of the T7SS effector translocation process are still under active investigation and to date, best structural characterisation is available for the *Mycobacterium* T7SS inner membrane components (400, 401, 402) (Figure 1.14). The T7SS core protein complex

resides in the inner membrane and is able to adopt multiple conformational states, forming a closed complex, gated membrane pore and potentially an additional open state enabling substrate passage (400, 401, 402, 403). The parts of complex protruding into the cytoplasm adapt an open confirmation or transiently form a cytosolic chamber below the membrane pore forming complex, and a similar closed chamber structure is seen on the periplasmic side (401). The exact mechanism of action of this complex require further validation, but it is known that effector translocation is dependent on action of ATPases, effectors interact with cytoplasmically exposed proteins and this is presumed to lead to subsequent conformational changes leading to the effector translocation through a central pore, or smaller priming pores (400, 401, 402). The mechanisms of further transport across periplasmic space and cell wall are still to be described.

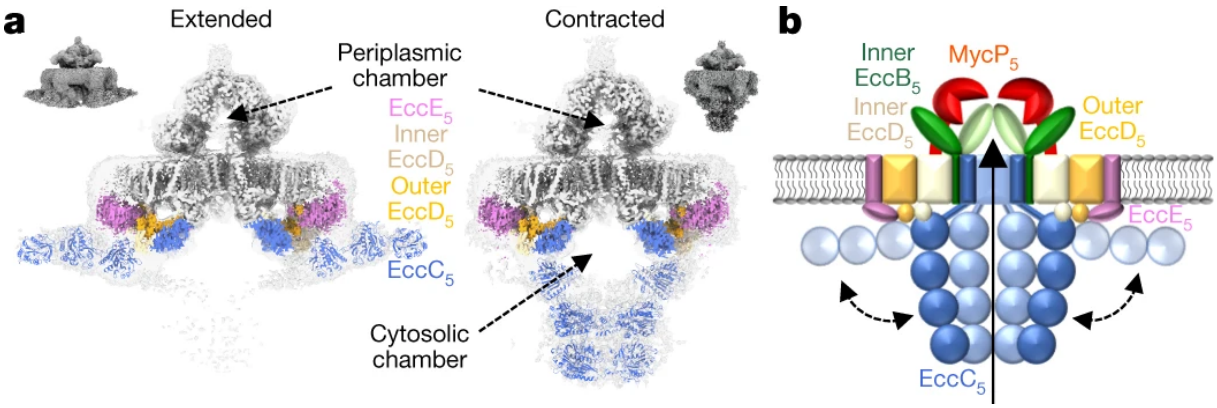

Figure 1.14: **Structure and dynamics of T7SS from *Mycobacterium tuberculosis*.**
(**a**) Side cross-section of density maps and homology models, showing the extended and contracted conformation of *Mycobacterium* T7SS core membrane complex components.
(**b**) Carton model of T7SS inner-membrane complex, highlighting two distinct conformational states of $EccC_5$ cytoplasmic domains.
Adapted from (401) under creative commons attributions license.

These systems have been shown to deliver a range of effectors involved in both bacterial-host and bacterial-bacterial interactions (404). For example, the T7SS of *M. tuberculosis* releases a NAD+ hydrolase called the tuberculosis necrotizing toxin, which significantly contributes to host cell death during *M. tuberculosis* infection (405). The T7SS of *S. aureus* delivers both host effectors that modulate apoptosis during infection and nuclease toxins that kill competing bacteria (406, 407). T7SSs in other bacteria, such as *B. subtilis*, have also been shown to

deliver putative RNase effectors that contribute to bacterial competition (408). Like other toxin delivery systems, T7SSs often encode corresponding immunity proteins to neutralised impact of self-produced toxins, and they appear to function analogously to T6SSs in Gram-negative bacteria by contributing to contact-based interactions with adjacent eukaryotic and prokaryotic cells.

1.3.6 Toxin-antitoxin systems contribute to polymorphic toxin effector pool

Toxin-antitoxin (TA) systems are two-gene modules found to be encoded on conjugative plasmids and were initially described for their role in the maintenance of plasmids (409, 410). When TA genes are present on a plasmid, the plasmid-containing cells actively express both the toxin and the associated antitoxin gene, protecting themselves from the toxin's effects. Upon loss of the plasmid during cell division, production of both genes ceases, leading to the degradation of the antitoxin component of the pair and the release of the toxin. This toxin can subsequently induce cell death in any bacteria that are unable to continue producing the antitoxin protein (411, 412). TA systems can be classified based on the mechanism of action of the antitoxin (413).

The modular makeup of cognate toxin-antitoxin gene sets in TA systems leads to a comparison with other polymorphic toxin systems (414). While TA systems are typically encoded on plasmids and are used to maintain plasmid stability (415, 416), homologues of TA genes have also been found to be encoded on the bacterial chromosome (417). Chromosomally encoded TA genes have been shown to induce programmed cell death as part of the general stress response and to induce dormancy, which helps bacteria persist during antibiotic treatment (418, 412). Although TA systems do not directly contribute to bacterial competition, they are still considered part of the polymorphic toxin systems, and the gene sets encoded in TA systems add to the overall toxin pool. Therefore, research on TA toxins can contribute to a better understanding of toxins involved in direct bacterial conflict.

1.3.7 Bacteriocins - tailocins and pyocins

Bacteriocins are toxic proteins produced and released by various bacterial species (419). The first group of bacteriocins to be described were the colicins, which were named after their discovery in *E. coli* by (420). Colicins are often pore-forming or poses an endonuclease activity, these toxins are released in the surrounding media as a result of cell lysis and subsequent action on prey cells is dependent on binding of specific surface receptors (421). Produced in some *E. coli* strains and released in media, colicins are often narrow spectrum and lethal to strains related to producer (343, 355). Later, it was discovered that a wide range of bacterial species produce bacteriocins, including both Gram-positive and Gram-negative bacteria (422). The production of toxic peptides appears to be a universal strategy employed by microbes to manipulate the composition of the microbiome (355). Bacteriocin diversity has also been used to inspire the development of new antimicrobial therapeutic approaches and to guide the design of antibiotics (419, 423).

Pyocins are bacteriocins produced by *P. aeruginosa* and similarly to colicins, these often cause lysis of same and closely related bacterial species (424). The first two classes of pyocins to be described were R-type and F-type tailocins, which are produced by 90% of *P. aeruginosa* strains (425). Tailocins are the largest bacteriocins, with protein assemblies ranging in size from 2 to 10MDa (426). These structures are made up of approximately eight to fourteen polypeptide subunits that are evolutionary related to and share morphological features with phage tails (427, 426) (Figure 1.15A). Due to their size, the release of these molecules requires the lysis of the producer cell, which is triggered by lytic proteins co-encoded within the same genomic cassette as the structural components and regulatory genes (428). The expression of R- and F-type tailocins is co-regulated and increased in response to DNA damage and SOS responses (429, 425, 430). This association with stress responses suggests that the release of toxins during cell death may be beneficial for the kin population under conditions where cell damage is likely to lead to lysis. Additionally, tailocin release is mediated through the same

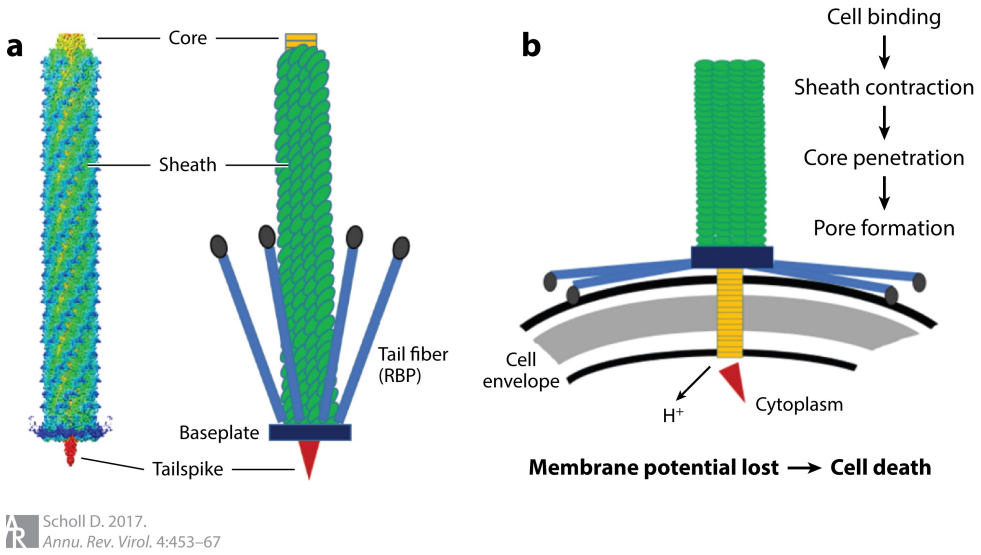

Figure 1.15: **Diagram of R-type tailocin structure and mechanism of action.**
(**A**) Schematic of R-type tailocin structure in extended confirmation. Highlighting core, contractile sheath, baseplate, tail-spike and tail fibres with RBPs.
(**B**) Proposed mechanism of action. Upon RBP binding to cognate surface features, sheath is contracted propelling core structure towards the cell body. With the aid of pointed tailspike, target cell wall is punctured and hollow core of the phage acts as a non-selective membrane pore leading to membrane depolarisation an cell death. Adapted from (426) with permission from Annual Reviews.

same set of endolysin genes that is associated eDNA release (322, 431). Therefore cells releasing pyocins not only damage competitors, but also contribute to extracellular matrix formation and biofilm structure maintenance. Tailocins are among the more narrowly tailored bacterial competition tools and have some interesting implications for community competition dynamics, as the production of these toxic molecules requires the lysis of the producing cell, allowing kin cells to gain a competitive advantage over more distantly related competitors within the same species.

R-type pyocins consist of a long tube surrounded by a contractile sheath and a baseplate structure, while F-type pyocins are made up of a non-contractile protein tube (426). Both have tail fibres with receptor binding proteins (RBPs) that mediate specific interactions with the target cell, likely recognising specific surface features of the target's lipopolysaccharides (LPS) (432, 433, 434). In both R- and F-type tailocins, once the RBPs make contact with the target cell, rapid lysis is induced as a result of disruption of the cell wall and membrane. R-type pyocins

have been studied in more detail, and it appears that a single structure is able to induce target cell lysis, likely through punching a hole in the cell membrane and inducing rapid membrane depolarisation and loss of proton motive force (435, 436) (Figure 1.15B). As the action of these molecules is reliant on RBPs making specific contacts with target cells O-antigens, tailocins are often narrow-spectrum and can kill only a subset of strains within the bacterial species producing the tailocin, while sister cells remain resistant (426, 437, 438). Tailocin sensitivity is determined by the composition of polysaccharides exposed on the cell surface (438), and resistance to pyocins can be mediated through multiple mechanisms. For example, incompatible LPS can prevent RBP binding in R- and F-type tailocins (432). Simultaneously, examples of killing in interspecies context exists, such as *Neisseria sp* killing by *P. aeruginosa* R-type pyocins and tailocin expression has been shown to be up-regulated in co-culture context (439, 440). Although initially described in *P. aeruginosa* (424, 441), tailocins have also been identified in other Gram-negative bacteria such as *V. cholerae* and *Yersinia enterocolitica* (442, 443), and in Gram-positive bacteria such as *Clostridium difficile* and *Listeria spp.* (444, 445).

A different class of smaller soluble class of bacteriocins termed S-type pyocins is found to be produced by more than 85% of *P. aeruginosa* strains (446, 447). These, as well as L- and M-type pyocins, were described later. They are much smaller in molecular weight and do not bear structural homology to phage tails (446, 448, 449). S-type pyocins have been found to have various activities including DNase, tRNase, rRNase, lipidase, and pore forming activity, and these vary between strains (428). Gene clusters encoding S-type pyocins do not contain a lysis gene, but are released in conjunction with R- and F-type pyocins (430), while the cell entry mechanism appears distinct and is dependent on iron uptake receptors (428). M-type pyocins are similar to the *E. coli* colicin ColM and have peptidoglycan hydrolase activity (449). The mechanism of toxicity for L-type pyocins, which resemble lectins (448), is unknown. Like other polymorphic toxin systems, S-, L-, and M-type pyocins are co-encoded with immunity proteins that protect the producer and sister cells from intoxication (450, 451).

1.3.8 Extracellular contractile injection systems

eCIS, which stands for extracellular contractile injection systems sometimes referred to as phage tail-like protein-protein translocation system, is a general designation of cell-free protein delivery systems (Figure 1.16). This can be used as an umbrella term that includes both tailocins and other less well-known examples of molecular devices with homology to phage tail structures. These are notable for the ability to specifically target delivery of cargo proteins and provide opportunities for biomedical engineering and novel therapeutic development (453). Multiple types of eCIS have been identified and bioinformatics analysis interlinks these with various types of T6SS and phages (452) (Figure 1.16B). Bioinformatics analysis notes that non-bacteriophage and non-R-type pyocin eCIS encoding loci can be found in 1-2% of bacterial and archaeal genomes (454). eCISs are distributed across a range of taxonomic phyla suggesting a spread through horizontal gene transfer and what is notable is that these appear to be preferentially

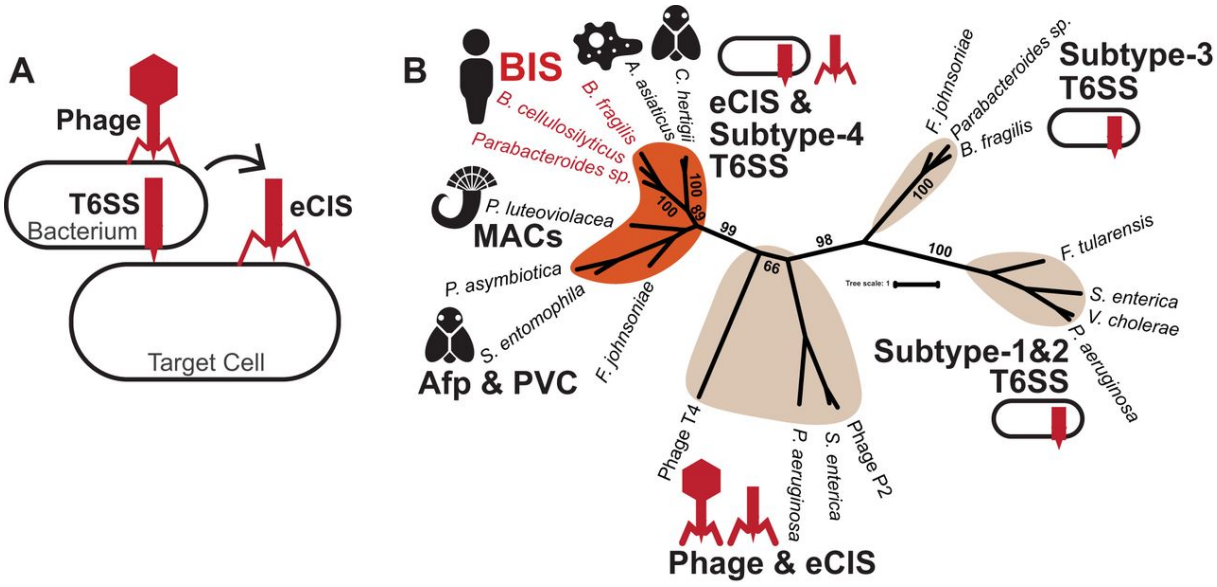

Figure 1.16: **Schematic of eCIS features and phylogeny.**
(**A**) Phages, T6SS and eCIS are evolutionary related and share common structural and mechanistic features. T6SS are anchored in the cell wall and assembled within the cell, while phages and eCIS are released as a result of cell lysis and bind target cells after surface feature recognition.
(**B**) Unrooted phylogeny of contractile sheath protein sequence conservation from (452), showing interrelation of T6SS, phages and minor eCIS systems from other bacteria.
Adapted from (452) under creative commons attributions license.

enriched in environmental microbes rather than ones commonly implicated in host-pathogen interactions (454). What is also notable in context of this report is that eCIS and T6SS are rarely found within the same genomes despite the systems sharing homologous components (455). Tailocins and T6SS are discussed in more detail in other sections, while here examples of less studied contractile systems are highlighted.

One well-studied eCIS is PVCs - termed as such for "*Photorhabdus* virulence cassette" described in *Photorhabdus luminescens* (456). *Photorhabdus* forms a symbiotic relationship with its nematode host, once these nematodes invade insect larvae *Photorhabdus* is released to aid in pathogenesis (457). The PVC tail-like structure is loaded with protein effectors, but unlike tailocins these are used to deliver effectors into eukaryotic cells (458). PVC effectors have been shown to have activity that results in degradation of cytoskeleton aiding in degradation of insect tissue providing nutrient source for both the host nematode and the symbiotic bacteria (458). Similarly insecticidal proteins have been shown to be delivered through AFP or aniti-feeding prophages released by *Serratia entomophila* (459). AFP effectors are key contributors to *Serratia entomophila* infection cycle and induce starvation response and death in insects such as grass grub and manuka beetle larvae (460). Yet, an example of eCIS effectors mediating host beneficial interactions is MAC arrays released by *Pseudoalteromonas luteoviolacea*. *P. luteoviolacea* is a marine bacterium that releases ordered arrays of contractile tailocins (461). These are termed MAC arrays and upon contact these induce morphogenesis that is essential for development of larvae of marine tubeworm *Hydroides elegans* (462).

1.3.9 *P. aeruginosa* small molecule products with antimicrobial impact

In the examples of toxin systems described above, toxicity appears to be the primary evolutionary function of these molecules, but other small molecule products that are primarily described for different purposes can also contribute to antimicrobial or anti-host toxicity. Both QS and nutrient uptake molecules were identified and have been characterised as having distinct

functions that aid in community survival through mechanisms that would not be categorised as direct competition, nevertheless further investigation has found that these secondary metabolites can be multi-functional. The physiological effects of small molecule products produced by *P. aeruginosa* appear to be largely dependent on context and dose.

Bacteria in dense communities communicate and coordinate their behaviour through the use of QS molecules. Amongst *P. aeruginosa* QS coordinated processes are production of both virulence factors and antimicrobials (27). While QS is typically characterized as a tool for communication and coordination in bacterial communities, small molecules used for these purposes have also been shown to have direct effects on the physiology of other bacterial species, including toxicity (463). In addition, bacteria can interfere with the QS of other species through a process called quorum quenching, which is thought to be employed by healthy microbiome communities to resist pathogen invasion (464). Quorum quenching appears to be one of the mechanisms that healthy microbiome communities employ to resist pathogen invasion and consequently the strategy of interference with QS is also being considered for its pharmaceutical potential (465).

Toxicity of individual QS compounds and related substrates is often target specific. The Las QS autoinducer molecule, 3-oxo-C12-HSL, has been shown to be toxic to fungal cells and certain Gram-positive bacterial species, but has no measurable impact on Gram-negatives (466). A degradation product of 3-oxo-C12-HSL, tetramic acid, can dissipate the membrane potential in Gram-positives and be toxic to Gram-negatives, including *P. aeruginosa*, at high concentrations (467, 468). The Las QS pathway also controls the production of the protease LasA, which can degrade the peptidoglycan of *S. aureus* and cause cell lysis (469). PQS impacts the growth of other bacterial species through a mechanism dependent on its iron-chelating ability and can inhibit respiration in some bacterial species (470). Furthermore, PQS precursors have antimicrobial activity against *S. aureus* (357).

Rhamnolipids are biosurfactants whose production is controlled by the Rhl QS system (471).

Due to their amphipathic nature, rhamnolipids have been proposed to disrupt cell membrane integrity and increase permeability, leading to broad-spectrum antibacterial toxicity (472). Externally applied rhamnolipids have been shown to disperse biofilms of various bacterial species (473, 474) and have been considered for their potential therapeutic applications (475, 476). Additionally, rhamnolipid micelles can also act as vesicles carrying toxic substances directly to cells of competing bacteria (477). Another secondary metabolite produced under the control of Rhl QS is hydrogen cyanide (HCN), which is a cytochrome C oxidase inhibitor and generally toxic to aerobic organisms. (478, 479). The production of this broad-spectrum toxin helps *P. aeruginosa* dominate its niche through use of cyanide insensitive terminal oxidases CiaAB (480). Interestingly, expression of *ciaAB* genes is under control of QS and is part of *P. aeruginosa* selection against emergence of QS-deficient social cheater lineages (480, 481).

Phenazines are pigmented secondary metabolites produced by *Pseudomonas* species (482). Phenazine-1-carboxylic acid is a yellow pigment that can cause lysis of bacterial cells and ROS-mediated fungal cell death (483, 484). Pyocyanin is a blue-green pigment responsible for the characteristic blue-green colour of *P. aeruginosa* laboratory-grown cultures. It has antimicrobial activity against a variety of Gram-positive and Gram-negative bacterial species and fungi (485, 486, 487). At high enough quantities and depending on the local microenvironment, pyocyanin can also be toxic to *P. aeruginosa* and contribute to cell lysis and the release of extracellular DNA, which aids in biofilm formation (488, 489). Other *P. aeruginosa* phenazines have also been found to have antimicrobial activity through mechanisms such as inhibiting protein synthesis or causing the accumulation of reactive oxygen species (490, 491). The production of both phenazines and pyocyanins has been shown to be dependent on the *P. aeruginosa* QS systems (492).

Iron chelating siderophores, specifically pyoverdine and pyochelin, are small molecule products that are key contributors to *P. aeruginosa* physiology (493). These siderophores are preferentially expressed and released under low iron concentrations and aid in *P. aeruginosa* iron

uptake, improving its survival in mixed bacterial communities (494, 46). The sequestration of iron from the local microenvironment can also increase nutrient stress for other bacteria present. Pyochelin has also been shown to generate ROS that are directly toxic to *Xanthomonas sp.* and *S. aureus* (495).

1.3.10 Outer membrane vesicles

Formation of outer membrane vesicles (OMVs) is observed to occur in cells across all phyla of life, where either through regulated membrane blebbing or rapid lysis, lipid-encapsulating spheres are released in the environment (496). These lipid vesicles can be loaded with a variety of proteins from both periplasmic space, inner membrane and cytoplasm providing a somewhat low constrain mechanism for release of a large variety of molecules in potentially high doses (497, 498). OMVs can release hydrolytic and proteolytic enzymes that can both aid in nutrient uptake and direct bacterial antagonism through release of toxic substances into the surrounding environment or by directly fusing with recipient cells (498, 497). Examples of OMV use in bacterial antagonism include *M. xanthus* release of alkaline phosphatase that kill *E. coli* (499) or *P. aeruginosa* release of peptidoglycan hydrolases (500). These have also been implicated with T6SS associated effector function - both *P. aeruginosa* H3-T6SS-associated TseF mediated iron and H2-T6SS ModA mediated molibdate uptake has been proposed to involve re-uptake of OMVs (501, 502). OMVs can also be utilised for cell-cell communication purposes as in case of *P. aeruginosa* PQS (503). Host interactions and pathogenesis involving *P. aeruginosa* OMVs have been shown to trigger host cell toxicity by releasing hemolytic phospholipase C (504) or provocation of immune response through sRNA release amongst others (505, 506). Overall OMVs are some of the most functionally versatile tools for mediating interactions with environment and surrounding organisms including release of toxins intro environment or for direct effector deliver to adjacent cells (507, 498, 496).

1.4 Type VI secretion system

1.4.1 T6SS - a molecular machine for effector injection

The Type VI secretion system (T6SS) is a macro-molecular machine used to inject effector proteins directly into adjacent cells. First identified in the bacterium *Vibrio cholerae* (508), T6SS is present in the genomes of 20-25% of Gram-negative bacteria, with the highest prevalence in γ- and β-proteobacteria (509, 510, 454). T6SS is found in both free-living environmental bacteria and in the genomes of plant or animal associated commensals and pathogens, with genera such as *Vibrio*, *Pseudomonas*, *Yersinia*, *Klebsiella*, *Serratia*, and *Escherichia* being some of the most T6SS-enriched (454). Additionally, entire sets of T6SS-associated genes and effectors can also be found encoded on plasmids (511), and have been shown to be functional upon transfer between organisms (512). T6SS allows for effector protein delivery to both prokaryotes and eukaryotes, including other microorganisms such as yeast (513, 514), as well as host cells (515). The diversity in targets is due to the fact that, unlike other effector translocation systems such as CDI, T6SS does not require the binding of specific features on the target surface for injection to occur. Instead, T6SS is anchored within the attacker cell's membrane, and the only prerequisite for effector translocation is close spatial proximity or direct cell-cell contact, substantially adding to the versatility of this tool.

Ecological roles of T6SS are varied, foremost being use in direct bacterial competition, where pathogenic bacteria can use T6SS to invade and establish within niches or where commensal bacteria use T6SS to provide protection against invasion (516, 517, 455). T6SS can also function in direct interactions with host cells, contributing to virulence and immune evasion during infection (39, 354). Additionally, T6SS can be used for resource acquisition, such as the use of T6SS effector proteins that can scavenge metal ions in the extracellular environment and aid in their subsequent re-uptake (482, 518). This function has likely led to the enrichment of T6SS proficient strains seen in nutrient-scarce marine environments (519). Returning to T6SS acting

in direct antagonism, the antimicrobial capacity provides opportunities for use in predation, or killing that results in DNA release for subsequent use in biofilm structural maintenance or for horizontal gene transfer (520, 455, 521). As T6SS has the capacity to deliver functionally diverse proteins, its specific effectors determine the broader ecological function of the system (522, 354). Overall, the use of T6SS has been associated with improved fitness in mixed bacterial biofilm communities (523, 524, 455, 525).

The T6SS is defined by 13 broadly conserved core proteins that are essential for constructing a functional firing machinery (510, 527). The structure and schematic of T6SS system assembly and firing is shown in Figure 1.17. Nomenclature convention commonly used for describing T6SS components in *P. aeruginosa* is Tss for **t**ype **s**ix **s**ecretion and Tag has been designated for **t**ype six secretion-**a**ssociated **g**ene. T6SS structure can be divided in three complexes - membrane, baseplate, and tail. The system assembly site is determined by the localisation of the membrane complex that consists of TssJLM proteins and which through association with the baseplate

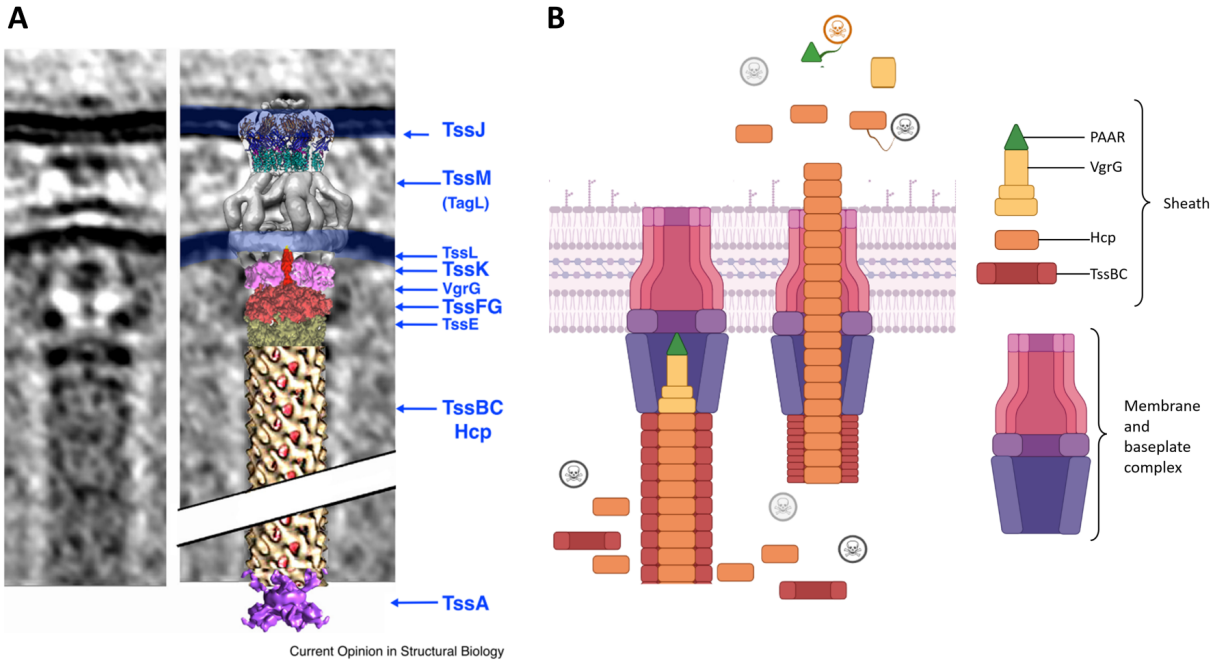

Figure 1.17: **Structure of T6SS.**
(**A**) Topograph of an extended T6SS structure from *Myxococcus xanthus*. With solved structures superimposed onto the topograph. Adapted from (526) with permission from Elsevier.
(**B**) Cartoon representation of T6SS assembly within a cell and contraction event that leads to explosion of Hcp, VgrG, and PAAR proteins as well as associated effectors into the extracellular milieu. Created using bioRender.

complex will anchor the system in the cell envelope (528). TssJ is inserted into the outer membrane inner leaflet while both TssM and TssL are anchored within the inner membrane (292). The periplasmic domain of TssM interacts with TssJ, while TssL provides a platform for assembly of the baseplate (529, 528). The baseplate complex consists of TssEFGK and is docked onto the membrane complex (530, 531). TssK makes connections with the cytoplasmic domains of TssL and TssM and it is the appearance of TssK that marks the location for new sheath assembly (531, 532, 533). TssF and TssG associate in two-to-one heterotrimer forming a wedge, that further oligomerises into a hexameric ring that interacts with TssK and sheath proteins TssBC (533, 530). TssE is the last of the baseplate proteins to bind the complex and this initiates sheath assembly (532). The T6SS tail consists of an internal Hcp spear surrounded by a contractile sheath made up of TssBC proteins (534, 535). The sheath structure is topped by a VgrG trimer and a single PAAR protein spike that serves as a puncturing device (536, 537). The lumen of the Hcp spear, VgrG and PAAR proteins are the system components that both directly and indirectly bind effector proteins to be delivered (538, 539). The VgrG/PAAR protein complex is accommodated within the baseplate structure and is the first to be added during the tail assembly (532, 540). Subsequent polymerisation of the tail proceeds under VgrG/PAAR gradually extending from baseplate towards the opposite side of the cell (541). Upon contraction of the TssBC sheath, the Hcp rings, as well as the VgrG/PAAR spike, are propelled into the extracellular space or a target cell (542). Once sheath contraction has occurred, a AAA+ ATPase ClpV is recruited and aids with the disassembly of sheath structure to allow component recycling (543).

The final core structural component is TssA, that forms a ring structure that initially interacts with the baseplate and subsequently is located at the distal-end of an extending sheath acting as an assembly chaperone (544, 545, 546). The type of TssA protein present and the nature of its interaction partners also appear to determine the firing dynamics of a T6SS (547). TssA proteins can be divided in two major classes - short (approx. 40kDa) and long (55 to 60

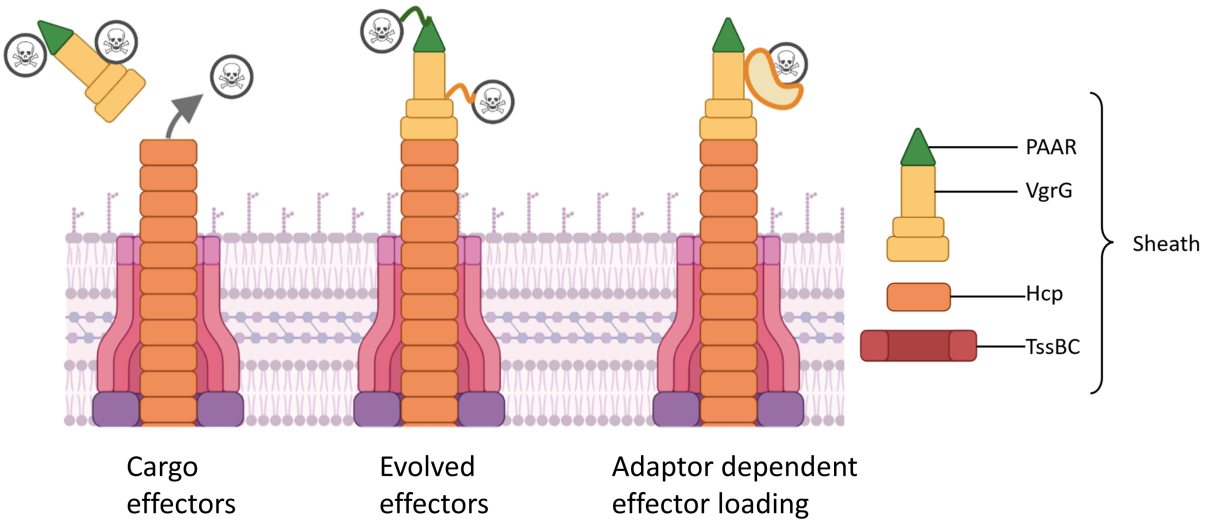

Figure 1.18: **Modes of T6SS effector delivery.** Schematic showing modes of T6SS effector delivery. Effectors proteins can be associated with Hcp, VgrG, and PAAR proteins. Cargo effectors bind to T6SS structural components through non-covalent interactions. Effectors loading may be dependent on presence of one or multiple adaptor proteins. Evolved effector proteins contain both structural and effector domains. Created using bioRender.

kDa), each of which has distinct set of interactions partners (548, 546, 547). Long TssA proteins interact with TagA, that aids with stabilisation of assembled T6SS sheath structures trough anchoring at the distal end (549). Sheath structures stabilised through TssA interacting with TagA have been shown to remain extended for minutes, before a firing event occurs (547, 546). While the dynamics of T6SSs containing short TssA proteins are much faster with multiple assembly/firing events occurring every minute (547).

1.4.2 Modes of effector delivery

T6SS effectors are delivered in several distinct ways and can be associated with any of the spike components expelled from the cell during a firing event, namely Hcp, VgrG, and PAAR proteins (Figure 1.18). The effector proteins can be classified into two categories: cargo effectors and evolved effectors. If an effector is associated with a T6SS structural component through non-covalent interactions or with the help of an adaptor protein it is classed as a cargo effector. While the evolved effectors contain both a functional toxin domain and a structural protein domain.

Evolved effectors often have a similar domain organisation, with a N-terminal structural domain and C-terminal effector domain. Most widespread are evolved effectors that carry PAAR or VgrG domains. Examples of this class of exported proteins include H1-T6SS associated PAAR encoding Tse5, Tse6, and Tse7 (550, 551, 552), and the H2-T6SS associated VgrG2b (553). Hcp associated evolved effectors are found in the genomes of some *Enterobacteriaceae* species (554, 454), but none are present in *P. aeruginosa*. Instead *P. aeruginosa* Hcp associated effectors - Tse1 to 4, PA2066 and PA0256 (555) - non-covalently bind Hcp proteins (556), with Hcp1 itself acting as stabilising chaperone in cases of Tse2 to 4 (556, 551). These cargo effectors engage in direct interactions with T6SS components and can be loaded within the lumen of Hcp (556). Alternatively, effectors can directly interact with spike proteins such as in the case of Tse8 that has been associated with VgrG1a (557). Other effector loading onto T6SS is dependent on presence of adaptor proteins. These proteins do not contain universally conserved T6SS structural domains or effector domains, but presence of the adaptors is essential for effector delivery. Notably, genes encoding adaptor proteins are genetically linked with the effector genes (Figure 1.20). In case of *P. aeruginosa* Tse6 contains a PAAR domain that is flanked by two trans-membrane domains (Figure 1.19). A pair of EagT6 adaptor proteins bind to these trans-membrane domains inhibiting protein aggregation and allowing for loading onto VgrG (558). Tse6 is also notable, because its toxicity appears to be dependent on presence of T6SS independent protein - elongation factor Tu (121). The delivery of *P. aeruginosa* TseT requires presence of two adaptor proteins - TecT and co-TecT (559). TseT loading onto PAAR4 appears to be facilitated by the chaperone TecT, while the stability of TecT before interacting with PAAR4 and TseT is dependent on co-chaperone co-TecT (559). A point of note for loading and delivery of T6SS associated antibacterial toxins is that once loaded onto T6SS, these proteins appear non-toxic due to interaction with structural components obstructing toxin catalytic sites or through localisation that interferes with effector-target interactions (551, 560).

The association with specific T6SS components determines the possible stoichiometry and

co-occurrence of toxins delivered in a single firing event. Each T6SS spike is topped by a single PAAR protein, meaning that delivery of PAAR-containing toxins is mutually exclusive. VgrGs form a functional trimer, and heterotrimer formation has been demonstrated to occur in case of *P. aeruginosa* H1-T6SS VgrG1abc (536), and requirement for VgrG heterotrimer formation for effective T6SS sheath assembly has also been seen in *Aeromonas dhakensis* (561). Presence of multiple of VgrG proteins is not a requirement in all T6SSs and presence of a single type of associated VgrG maybe be sufficient for system assembly, like in the case of H3-T6SS (Figure 1.20), but possible VgrG combinations provide an opportunity for co-delivery of effectors. Finally, a large number of Hcp rings are found within a single T6SS sheath (562) and no obvious limitation for loading Hcp's with different toxins has been shown, therefore a potential for simultaneous delivery of a number of Hcp-associated toxins might exist.

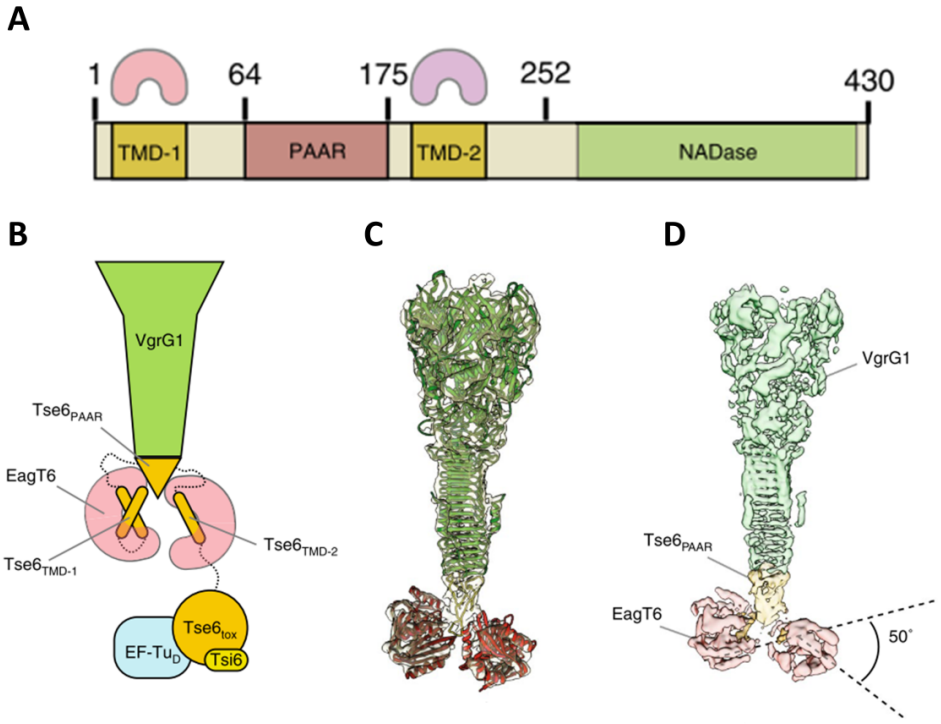

Figure 1.19: **Schematic and structure of Tse6 in complex with VgrG1.**
(**A**) Schematic of Tse6 domain organisation, with TMD corresponding to trans-membrane domains, and NADase toxin domain. (**B**) Schematic representation of VgrG1-Tse6-EagT6-EF-Tu-Tsi6 complex. Corresponding fit of available cryo-EM atomic structures (**C**) and colour-coded cryo-EM density map (**D**).
Adapted from (558) with permission from Springer Nature.

1.4.3 T6SS in *P. aeruginosa*

The *P. aeruginosa* genome encodes 3 distinct T6SS systems termed H1-, H2-, and H3-T6SS. The figure 1.20 shows organisation of the core T6SS genes and the associated orphan clusters found in *P. aeruginosa* PAO1 genome. Genes for core structural components for each of the systems are clustered in adjacent loci, while satellite genomic loci, or so-called orphan clusters, contain effector-immunity-adaptor gene sets and in some cases additional *vgrG* and *paar* genes. These gene clusters are distributed across the genome without notable preference in localisation. A notable feature is that H2-T6SS has three associated *hcp* genes - *hcpA* (PA1512), *hcpB* (PA5267), and *hcpC* (PA0263), however the gene product of these is referred to as Hcp2 protein and is 100% conserved in terms of amino acid sequence. Component multiplicity extends further to VgrG proteins, with 3 VgrGs being associated with H1-T6SS, 6 VgrGs with H2-T6SS and only VgrG3 being associated with H3-T6SS. An additional cluster containing one more H2-T6SS associated Hcp and VgrG protein is present in the genome of reference strain PA14 (563). These features and presence of multiple PAAR proteins highlights that T6SS is modular in makeup and the diversity in these components provides an increased capacity for binding and delivery of a wide range of distinct effectors.

All 3 of the *P. aeruginosa* T6SSs differ in their firing kinetics (547) and possibly have distinct ecological roles. H1-T6SS sheath dynamics are rapid with approx. 20s needed for system assembly and firing to occur, the system is also used to engage in retaliatory firing called Tit-for-Tat (547, 564). Additionally, H1-T6SS effector set is made up of several antibacterial toxins (Table 1.1). These features jointly position the H1-T6SS as primarily functioning in direct bacterial competition. Simultaneously, Hcp1 antibody titter has been shown to be elevated in sera of patients with long-term CF (172). Dynamics of H2-T6SS are much slower, with sheath structures remaining stationary for as long as 10min before a firing event occurs (547). Additionally, H2-T6SS effector repertoire includes both anti-host and antibacterial toxins as well as common good effectors as further discussed in the blow sections (Table 1.1). Notably

increased action of H2-T6SS is seen in strains isolated from severe acute infections (565). H3-T6SS is the least characterised of *P. aeruginosa* T6SSs, its expression is controlled by quorum sensing (566, 567, 568). The only H3-T6SS effector with known function is the common good effector TseF that aids in iron uptake (501). This points towards H3-T6SS being associated with environmental adaptation, but as the characterisation of the system and further effectors is still lacking this cannot be concluded with confidence.

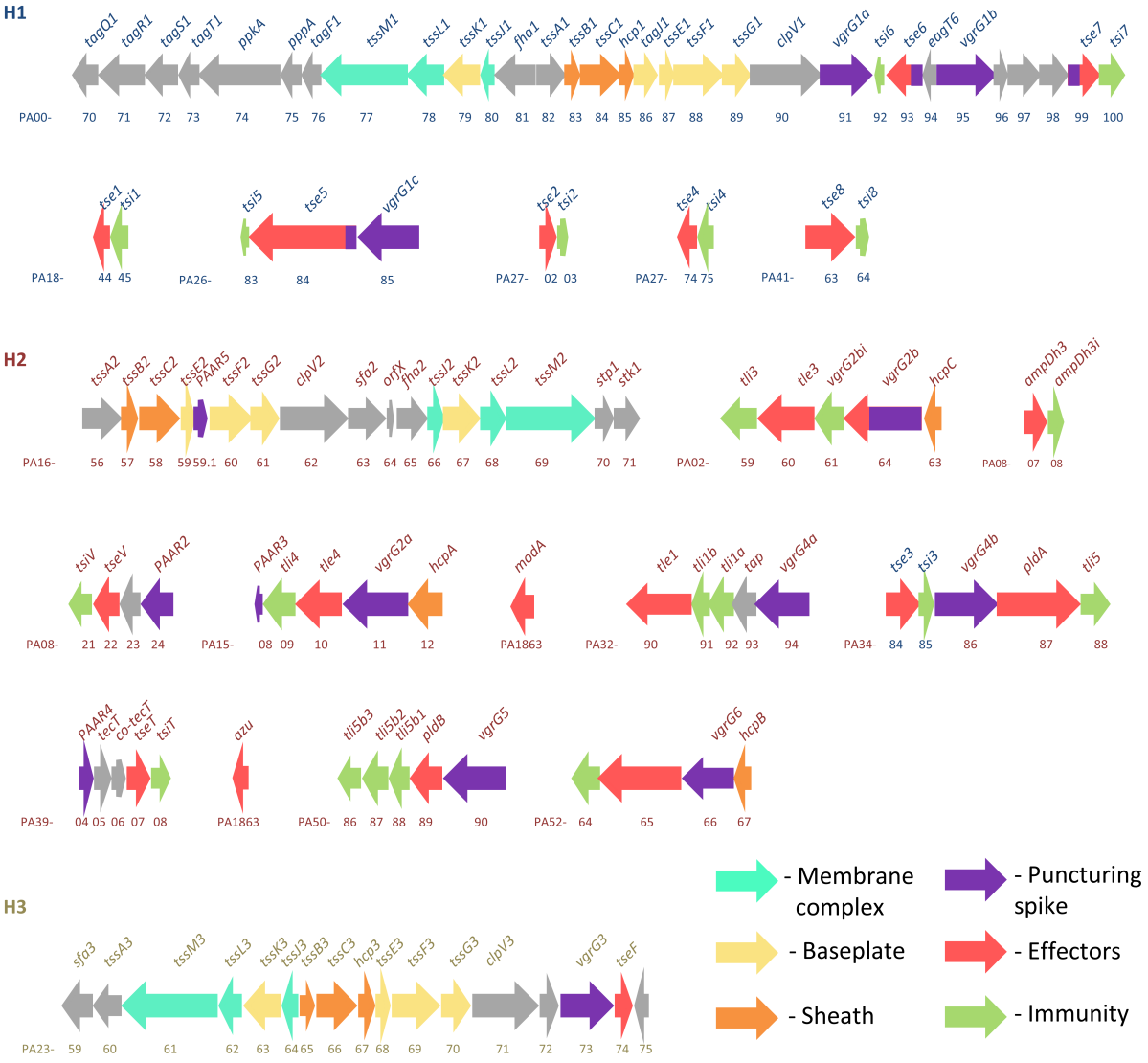

Figure 1.20: **T6SS gene core and satellite clusters found in *P. aeruginosa* PAO1 genome.**
Genes coloured accordingly with the corresponding protein function. Showing genes for all three T6SS systems, with associated gene names colour coded accordingly. Gene names specified above and gene numbers provided below schematics.

1.4.4 Control of T6SS firing

The *P. aeruginosa* T6SS system with best characterised post-translational control is the H1-T6SS. In this case, the system assembly and re-assembly is under control of TagQRST-PpkA-FhA1-PppA pathway (569), which is encoded in the same gene cluster as core H1-T6SS structural components (Figure 1.20). This was first shown to post-translationally regulate *P. aeruginosa* H1-T6SS by (569) and termed **t**hreonine **p**hos**p**horylation pathway (TPP). Since, TPP regulation has been shown to act on T6SS systems in other organisms such as *Agrobacterium tumefaciens* and *Serratia marcescens*, but the specific molecular impact is not necessarily well conserved between species (570, 571). The TagQRST proteins are located in the periplasmic space or associated with the inner-membrane and act as signal sensors that activate a kinase PpkA (569, 572) (Figure 1.21). The presence of the kinase PpkA is essential for H1-T6SS activity and PpkA acts through phosphorylation of Fha or TssL (569, 573). Instead, the phosphatase PppA dephosphorylates target proteins disrupting continued system re-assembly and results in sheath repositioning. Loss of PppA has been shown to result in constitutive H1-T6SS firing (531, 564). TagQ is a lipoprotein associated with the outer membrane and interacts with the periplasmic TagR protein (574). The interaction between TagR and PpkA has been proposed to trigger the kinase activity (572). TagS is an integral membrane protein and interacts with TagT that has ATPase activity (574). All TagQRST proteins are essential for H1-T6SS function (574). While TPP provides positive post-translational regulation, another accessory protein TagF has been shown to down-regulate H1-T6SS assembly (575). TagF interacts with Fha1 and this likely impedes phosphorylation by PpkA (575).

The H1-T6SS engages in retaliatory sheath assembly/firing termed "Tit-for-Tat" (564). This describes behaviour where T6SS sheaths are assembled at a location where exogenous T6SS contact has occurred and results in direct retaliation against a received T6SS injection. PppA-dependent H1-T6SS sheath re-positioning is essential for *P. aeruginosa* to engage in this behaviour and sensory input for localisation of new sheath assembly is gathered through

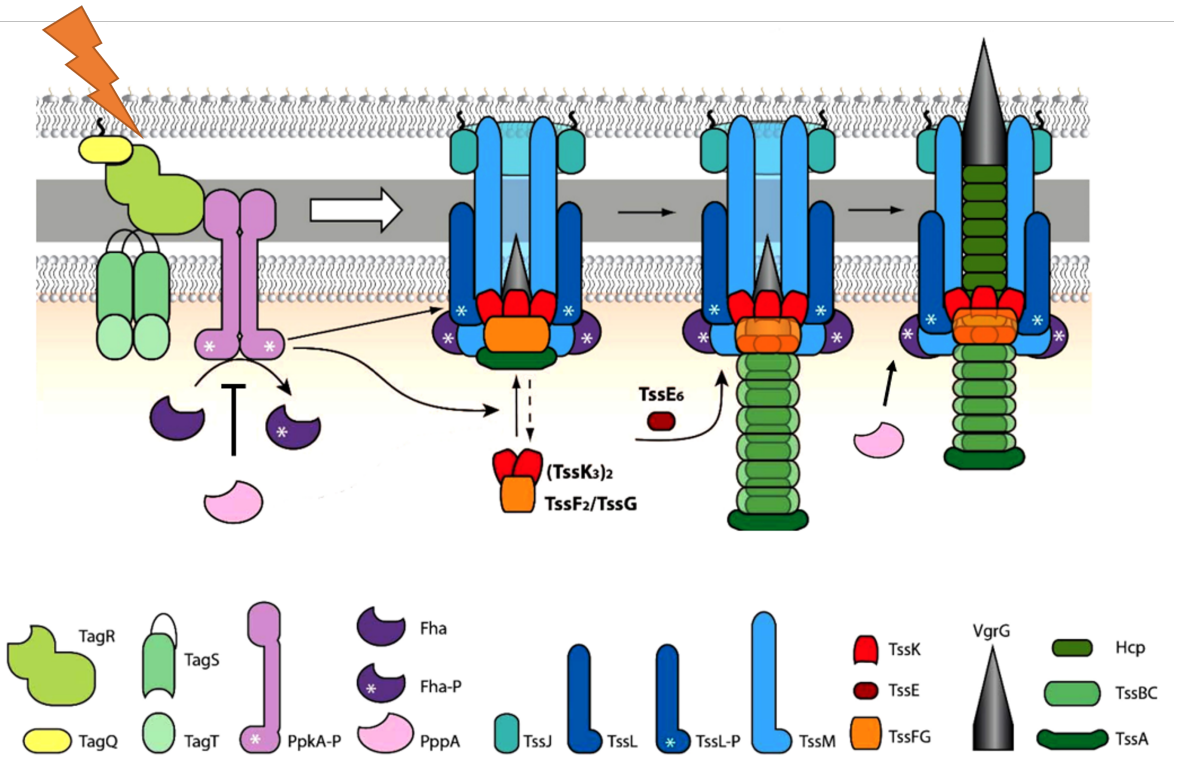

Figure 1.21: **Schematic of TPP components and T6SS assembly.** Cartoon schematic of proposed model of TagRQST-PpkA-PppA signal sensing-transduction. Where H1-T6SS assembly is dependent on Fha1 and TssL1 phosphorylation by PpkA.
Adapted from (531) under creative commons attributions license.

TagQRST proteins (564, 531). Both, the ability to precisely target T6SS injection and retaliatory firing in general has been shown to be an advantageous competitive strategy (576). A known signal that triggers assembly of H1-T6SS is membrane stress, this can be a result of exogenous delivery of T6SS effectors, such as in case of *V. cholerae* lipase effector TseL (577), or a response to antimicrobials such as polymixin B (578). H1-T6SS assembly can also be promoted by endogenous membrane stress caused by a knockdown of genes essential for membrane maintenance. TagT has been pinpointed as the component responsible for sensing membrane disruption (579). What is also notable, is that exogenous T6SS effector toxicity is not a pre-requisite for Tit-for-Tat firing behaviour, as retaliatory firing is also triggered by kin-cell T6SS injections (564).

1.4.5 T6SS toxin effectors

The T6SS is capable of delivering effectors to any adjacent cell, with the only prerequisite being close physical proximity, allowing for systems use in a range of different interactions. As previously mentioned, T6SS has been shown to deliver effector proteins to both prokaryotes and

	Effector	Cognate toxin immunity	Description	References
H1-T6SS	Tse1 (PA1844)	Tsi1 (PA1845)	Amidase that hydrolyses peptidoglycan crosslinks causing target cell lysis	(Hood *et al.*, 2010, Russell *et al.*, 2011)
	Tse2 (PA2702)	Tsi2 (PA2703)	NAD dependent ADP-ribosyltransferase that causes quiescence, toxic when expressed in eukaryotic cells	(Hood *et al.*, 2010, Li *et al.*, 2012, Robb *et al.*, 2016)
	Tse3 (PA3485)	Tsi3 (PA3485)	Muramidase that hydrolyses peptidoglycan backbone causing target cell lysis	(Hood *et al.*, 2010, Russell *et al.*, 2011)
	Tse4 (PA2774)	Tsi4 (PA2775)	Forms ion selective membrane pores that disrupt proton motive force	(Whitney *et al.*, 2014, LaCourse *et al.*, 2018)
	Tse5 /RhsP1 (PA2684)	Tsi5 /RhsP1i (PA2683.1)	Forms ion selective membrane pores resulting in loss of membrane potential, contains RHS and PAAR domains	(Hachani *et al.*, 2014, Whitney *et al.*, 2014, Gonzalez-Magana *et al.*, 2021)
	Tse6 (PA0093)	Tsi6 (PA0094)	NAD(P)+ glycohydrolase that depletes NAD(P)+ resulting in target bacteriostasis, contains PAAR domain	(Hachani *et al.*, 2014, Whitney *et al.*, 2014, Whitney *et al.*, 2015)
	$Tse6^{PA14}$ /Tas1 (PA14_01140)*	Tis1 (PA14_01130)*	(p)ppApp synthetase that rapidly depletes prey ATP/ADP pool, contains RHS and PAAR domains	(Ahmad *et al.*, 2019)
	Tse7 (PA0099)	Tsi7 (PA0100)	Tox-GHH2 nuclease, contains PAAR domain	(Hachani *et al.*, 2014, Pissaridou *et al.*, 2018)
	Tse8 (PA4163)	Tsi8 (PA4164)	Targets transamidosome complex disrupting protein synthesis	(Gonzalez-Magana *et al.*, 2020, Nolan *et al.*, 2021)
H2-T6SS	Tle1 (PA3290)	Tli1a (PA3291) Tli1b (PA3292)	Phospholipase A2 activity	(Russell *et al.*, 2013, Hu *et al.*, 2014, Flaugnatti *et al.*, 2016)
	Tle2 (PAK_03765)*	Tli2a (PAK_03766)* Tli2b (PAK_03767)*	Phospholipase A1 activity	(Russell *et al.*, 2013)
	Tle3 (PA0260)	Tli3 (PA0259)	Phospholipase	(Russell *et al.*, 2013, Berni *et al.*, 2019)
	Tle4 /TplE (PA1510)	Tli4 /TplEi (PA1509)	Phospholipase, contains PGAP1-like domain to aid internalisation into host cells and localisation at ER membrane inducing autophagy, both antibacterial and anti-host toxicity	(Russell *et al.*, 2013, Jiang *et al.*, 2014, Lu *et al.*, 2014)
	PldA /Tle5a (PA3487)	Tli5a (PA3488)	Phospholipase D with preference for PE (phosphatidylethanolamine) as substrate, activate PI3K/Akt pathway that promotes internalisation into host cells, both antibacterial and anti-host toxicity	(Wilderman *et al.*, 2001, Russell *et al.*, 2013, Jiang *et al.*, 2014, Spencer & Brown, 2015, Boulant *et al.*, 2018, Wettstadt *et al.*, 2019)
	PldB /Tle5b (PA5089)	$Tli5b_1$ (PA5088) $Tli5b_2$ (PA5087) $Tli5b_3$ (PA5086)	Phospholipase D, activates PI3K/Akt Pathway that promotes internalisation into host cells, both antibacterial and anti-host toxicity	(Russell *et al.*, 2013, Jiang *et al.*, 2014, Wettstadt *et al.*, 2019, Wen *et al.*, 2020)
	VgrG2b (PA0262)	VgrG2bi (PA0261)	Contains zinc- metallopeptidase domain, hydrolyses peptidoglycan in cell division plane causing target lysis. Interacts with α- and β-tubulins and γTuRC promoting internalisation into nonphagocytic cells, both antibacterial and anti-host toxicity	(Sana *et al.*, 2015, Berni *et al.*, 2019, Wood *et al.*, 2019)
	AmpDh3 (PA0807)	AmpDh3i (PA0808)	Cell wall remodelling amidase that contributes to β-lactam resistance, hydrolyses target cell peptidoglycan cross links	(Juan *et al.*, 2006, Zhang *et al.*, 2013, Wang *et al.*, 2020)
	TseT (PA3907)	TsiT (PA3908)	TOX-REase domain containing nuclease	(Burkinshaw *et al.*, 2018)
	TseV (PA0822)	TsiV (PA0821)	Putative VRR-NUC domain containing nuclease	(Wang *et al.*, 2021)
	PA5265	PA5264	Contains MIX (marker for type six effectors) motif	(Salomon *et al.*, 2014)
	RhsP2 (PA14_43100)*	RhsP2i (PA14_43090)*	RHS domain containing effector	(Hachani *et al.*, 2014, Jones *et al.*, 2014)
	PA2066	Unknown	Putative Hcp2 associated effector	(Howard *et al.*, 2021)
	Azu (PA4922)	-	Common good effector, copper binding and uptake	(Nar *et al.*, 1992, Han *et al.*, 2019)
	ModA (PA1863)	-	Common good effector, molybdite binding and uptake	(Self *et al.*, 2001, Wang *et al.*, 2021)
H3-T6SS	PA0256	Unknown	Putative Hcp3 associated effector	(Howard *et al.*, 2021)
	TseF (PA2374)	-	Common good effector, interacts with PQS and the siderophore receptor FptA aiding in iron uptake	(Lin *et al.*, 2017)

Table 1.1: ***P. aeruginosa* T6SS associated effectors.**
* T6SS effectors not present in genome of *P. aeruginosa* PAO1.

eukaryotes, making it a versatile system that can be used for interactions with both surrounding microbes and host cells (354). What defines the impact of a specific system are the associated effector proteins delivered. Some T6SS systems have just a few characterised effectors. One of the best characterised T6SSs is found in *V. cholerae* and delivers 3 effectors (580). In contrast, the T6SSs of *P. aeruginosa* are associated with more than 20 effectors, which include antibacterial toxins, anti-host, and common good effectors. All currently known effectors and their key features are listed in Table 1.1. Among these, antibacterial toxins are the most represented and belong to functionally diverse biochemical classes described below, including ones targeting cell wall components, nucleic acids, or various aspects of metabolism.

1.4.5.1 Peptidoglycan targeting toxins

A common target for antibacterial T6SS toxins is the bacterial cell wall. This includes peptidoglycan (PG) hydrolases, which have been found to be delivered by T6SSs from a range of bacterial genera, such as *Salmonella*, *Acinetobacter* or *Serratia* (582) and some of the first

Effector class	Groups	Activity	Distribution	Number
Tae	1-4	Amidase	Beta-, Gamma-and Deltaproteobacteria	53
Tge	1-3	Glycosidase	Beta- and Gammaproteobacteria	13
VgrG3	NA	Muramidase	Gammaproteobacteria	NA

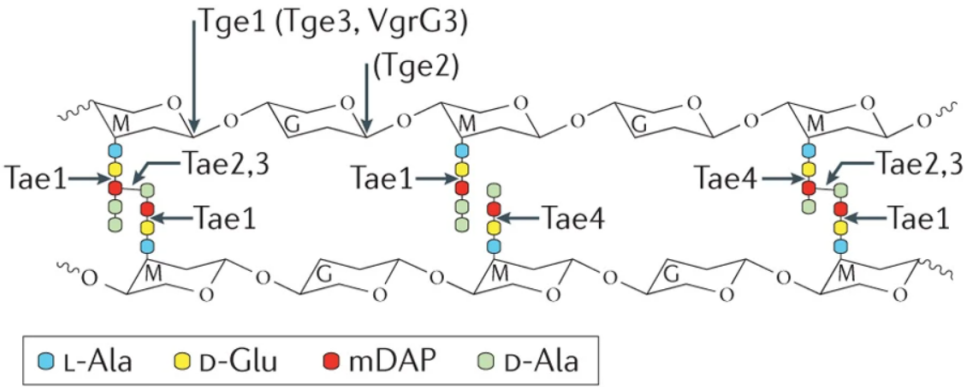

Figure 1.22: **Diagram of types of peptidoglycan degrading toxins.**
Enzymatic cleavage specificity of different types of peptidoglycan hydrolases. Adapted from (581) with permission from Springer Nature.

H1-T6SS toxins to be identified - Tse1 and Tse3 (583). Tse1 is an amidase that hydrolyses peptidic PG crosslinks, while Tse3 is a muramidase that attacks the PG sugar backbone (Figure 1.22) (584). Another example of PG degrading toxin is AmpDh3, an amidase known for its contribution to β-lactam resistance, and when delivered in an H2-T6SS-dependent manner, it is capable of killing prey by hydrolysing PG cross-links (585, 586, 587).

Alternatively to direct cell wall component degradation, toxins may cause damage indirectly through interfering with PG synthesis, remodelling or repair. The H2-T6SS dependent VgrG2b contains a zinc-metallopeptidase domain C-terminasl domain that is not involved in direct PG cleavage, but appears to interfere with PG biosynthesis related proteins acting in the cell division plane (553). The delivery of PG-targeting toxins has been shown to result in visible deformation and subsequent prey cells lysis following toxin injection (584). Tse1 has been shown to be the cause of *V. cholerae* cell rounding (564), while VgrG2b induces membrane blebbing in the cell division plane (553).

1.4.5.2 Lipases

A class of antibacterial T6SS effectors that are conserved across a range of Gram-negative bacteria is a group of phospholipases called Tle (for **T**6SS **l**ipase **e**ffector) (40). Tle effectors are classified into five families (Tle1 to Tle5) based on catalytic site sequence homology and each of these is represented among toxins associated with *P. aeruginosa* H2-T6SS (Figure 1.23). Tle1 and Tle2 have phospholipase A2 and A1 activity, respectively, and cleave fatty acid chains (40, 588, 589). Tle2 is homologous to the *V. cholerae* lipase effector TseL (580) and is present in the genomes of both PAK and PA7 reference strains but is absent from *P. aeruginosa* PAO1 (40, 41). PldA and PldB possess phospholipase D activity (Tle5) with PldA having a catalytic preference for phosphatidylethanolamine (PE) as a substrate (40, 590, 591). Both show antibacterial activity upon delivery in H2-T6SS-dependent manner (592). Additionally, both PldA and PldB activate the PI3K/Akt pathway that promotes internalisation into host

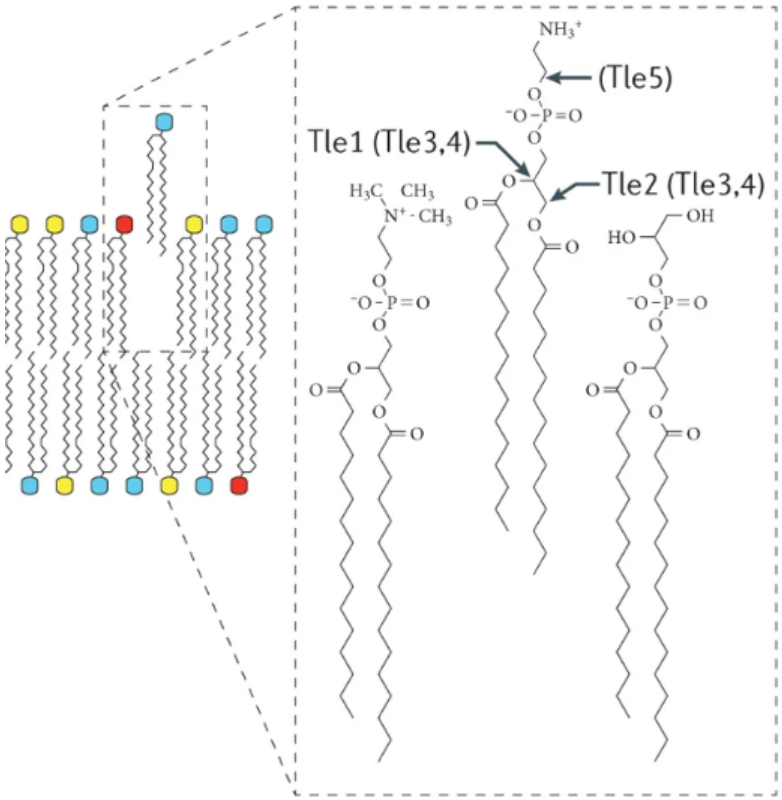

Figure 1.23: **Diagram of phospholipase effector cleavage sites.**
Schematic showing cleavage sites of phospholipases from distinct catalytic classes. Adapted from (581) with permission from Springer Nature.

cells (41), and have been associated with a high prevalence in multidrug-resistant *P. aeruginosa* clinical isolates (565). The exact catalytic mechanisms of Tle3 and Tle4 (TplE) are unknown, but Tle4 has been shown to aid with internalisation into host cells and localise at the endoplasmic reticulum membrane, which results in autophagy through a PGAP1-like domain (40, 593, 42). As lipase effectors target phospholipids found in any membrane, many of these effectors appear to show both antibacterial and anti-host toxicity.

1.4.5.3 Pore forming toxins

While PG hydrolases and phospholipases degrade cell wall components, an alternative method of disrupting cell wall integrity of prey bacterial is through pore formation. H1-T6SS-associated Tse4 and Tse5 both form ion selective pores that disrupt proton motive force, leading to membrane depolarisation and death (551, 550, 594, 595). Tse4 contains four transmembrane

helices and glycine zipper motifs, that promote multimerisation of transmembrane peptides and are a feature commonly seen in pore-forming proteins (596, 594). Tse5 is an evolved T6SS effector whose delivery is facilitated through an N-terminal PAAR domain (551, 550). Once inside the target cell, Tse5 is thought to undergo auto-cleavage just after RHS domain and the C-terminal toxin domain is capable of spontaneous insertion into the inner membrane, causing rapid depolarisation (597). Notably, efficacy of pore forming toxins has been shown to be dependent on the growth media composition and salinity (594).

1.4.5.4 Nucleases

T6SS toxins also target various cell components present in the cytoplasm, including nucleic acids. To date, three nucleases encoded in the PAO1 genome have been associated with T6SS: Tse7, TseT, and TseV. H1-T6SS-associated Tse7 contains Tox-GHH2 nuclease domain and is a notable example where toxin catalytic domains lack conservation between different reference strains (550, 552). A study by (552) showed that even though a T6SS toxin can be found within the *tse7* loci in PAO1, PAK, PA14, and PA7 reference strains, toxin domains of these effectors lack conservation (Figure 1.24) and the corresponding immunity proteins do not provide cross-

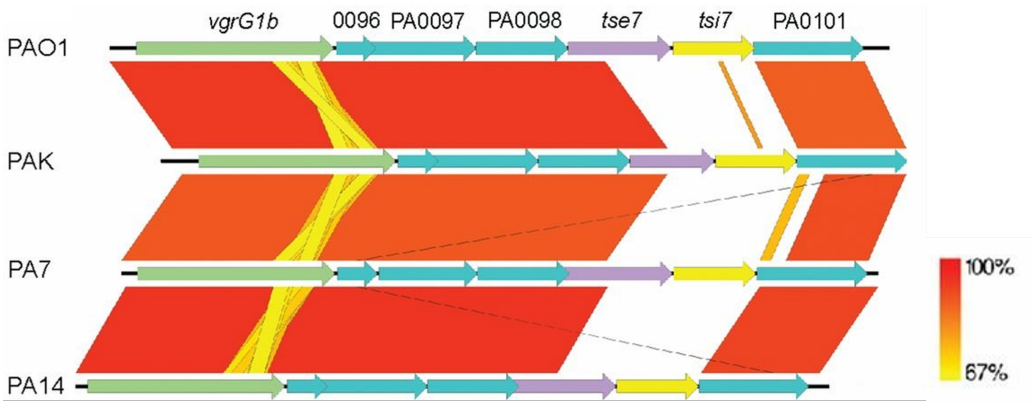

Figure 1.24: **Conservation of *tse7-tsi7* loci in *P. aeruginosa* PAO1, PAK, PA7, and PA14.**
Conservation of *tse7-tsi7* and flanking genes in genomes of *P. aeruginosa* PAO1, PAK, PA7, and PA14. N-terminal PAAR containing domain of Tse7 is highly homologous, while C-terminal toxin domain and *tsi7* lack sequence conservation.
Adapted from (552) under creative commons attributions license.

protection from the toxin's action. This variation in toxin set means that T6SS can be used for not only competition between distinct bacterial species, but also distantly related lineages within the same species. The H2-T6SS has been associated with two nucleases, first, TseT that contains TOX-REase domain shown to kill sensitive prey (559). Second, TseV contains VRR-NUC domain whose corresponding gene and is linked to H2-T6SS through genomic context (169), but the specific catalytic activity of this toxins and impact on prey bacteria as delivered by T6SS is yet to be experimentally demonstrated.

1.4.5.5 Metabolism targeting toxins

Another strategy of attack for antibacterial toxins is through the disruption of prey cell energy metabolism. Tse2 has been shown to be functional within prey bacteria cytoplasm in an NAD-dependent manner and leads to queiscence, additionally it is toxic when expressed in eukaryotic cells. Altrough catalytic function of Tse2 is yet to be experimentally validated, it bears structural homology to ADP-ribosylating toxins (583, 231, 599). Tse6 in *P. aeruginosa* PAO1 is an NAD(P)+ glycohydrolase that depletes NAD(P)+, causing prey bacteriostasis (550, 551). The toxin domain of Tse6 is not conserved among the different *P. aeruginosa* reference

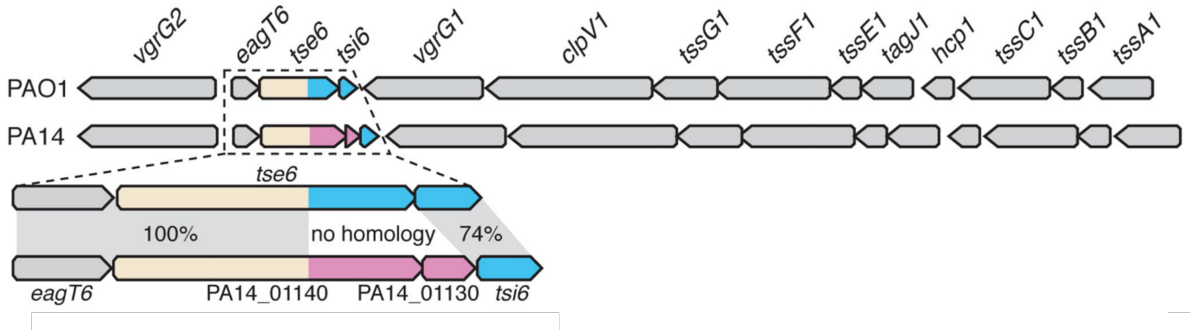

Figure 1.25: **Genomic context of Tse6 in *P. aeruginosa* PAO1 and PA14.**
Conservation of *tse6-tsi6* genes in genomes of *P. aeruginosa* PAO1 and PA14. In yellow, PAAR containing N-terminal domain of Tse6 shows 100% sequence homology. Tse6 C-terminal toxin domain lacks sequence homology between loci from the two strains. An additional *tsi6* gene with 74% seqeucence homology to $tsi6^{PAO1}$ is found in PA14 genome after the cognate $tse6\text{-}tsi6^{PA14}$ gene set.
Adapted from (598) with permission from Springer Nature.

strains (Figure 1.25), as the genome of PA14 encodes a Tse6^{PA14} also known as Tas1 with (p)ppApp synthetase activity, which results in a rapid depletion of prey ATP/ADP pool (598). A toxin with a rather original molecular target is the H1-T6SS dependent Tse8 that directly disrupts protein synthesis through targeting the transamidosome complex (557, 600). A further toxin, RhsP2, possesses ADP-ribosyltransferase activity and affects the non-coding RNA pool of prey cells (601). This toxin is not present in *P. aeruginosa* PAO1 but is co-encoded in an additional *vgrG*-containing satellite cluster found in *P. aeruginosa* PA14 genome (550, 563).

1.4.6 Cognate toxin immunity

As a large number of T6SS effectors are antibacterial toxins and the bacteria producing these effectors must possess protective mechanisms to avoid self- or sister-cell intoxication. T6SS toxin-encoding genes have thus evolved to be co-encoded with one or multiple cognate immunity proteins (583, 584, 602). This co-occurrence of toxin/immunity genes is most apparent when looking at the genomic context of T6SS effectors (Figure 1.20). The presence of cognate toxin immunity genes is beneficial as they are accumulated and maintained in genomes even in cases where specific effectors are lost (603, 604, 605). One such example is *P. aeruginosa* Tse6 described above (Figure 1.25). Although, *tse6* from PAO1 has been substituted with *tse6-tsi6*^{PA14}, the immunity gene *tsi6*^{PAO1} is still maintained within the genome of *P. aeruginosa* PA14.

Cognate immunity proteins often appear to act through forming complexes with the specific toxins. When an effector is acting in the periplasm, cognate immunity proteins are actively exported to this compartment and carry a Sec-dependent signal peptide to support this targeting (584, 358). Structures of multiple toxin-immunity protein complexes have been solved providing a mechanistic insight into immunity protein action. For example, in case of Tse2-Tsi2 and Tle4-Tli4, immunity proteins form complexes with the specific effector, disrupting the catalytic ability (593, 599). An alternative protective mechanism was shown in the

case of *Serratia proteamaculans*, where the ADP-ribosyltransferase effector 1 (Tre1) immunity protein Tri1 not only binds the effector in a manner that occludes the active site but also cleaves a post-translational modification permanently deactivating toxin catalytic ability (606). Furthermore, *P. aeruginosa* TseT-associated immunity protein TsiT is proposed to act by preventing oligomerization of the TseT toxin (607).

Examples of a single effector being co-encoded with multiple immunity proteins are also common, with PldB-Tli5b$_{1-3}$ and Tle1-Tli$_{ab}$ being two such effector/immunity sets present in *P. aeruginosa* genome (Figure 1.20). Each of the three PldB immunity proteins has been shown to individually contribute to protection against toxin action (41), while sequence and structural characterisation of the three immunity proteins shows these to be highly conserved with main differences found in surface electrostatic charge (608). Authors of the study suggest that presence of multiple similar immunity proteins could provide added protection through being able to bind similar toxins from other species (608). It is notable that although both PldA and PldB are trans-kingdom effectors categorized within the same PLD phospholipase family (42), the associated immunity proteins lack structural conservation (608, 609). This is likely due to the fact that phospholipases are classified accordingly to conservation of catalytic motifs, while the proteins as a whole can be phylogenetically and structurally divergent (40).

As evidenced by the high variation in effector/immunity gene sets between closely related bacterial strains, these genes are subject to frequent horizontal gene transfer events and this can lead to accumulation of arrays of immunity genes (603, 610, 605). As bacteria are protected from the action of their own toxins by specific cognate immunity proteins, they can in turn be sensitised to the action of these toxins by a deletion of the immunity gene and this is a strategy commonly employed while characterising new T6SS effectors.

1.4.7 Trans-kingdom effectors

T6SS effector examples described above are focused on cases where the system is used for bacterial interactions. Similarly, in addition to direct competition with other bacteria, T6SS can be used in competition with eukaryotic microbes. For example, anti-fungal effectors delivered by the T6SS of *S. marcescens* have been shown to aid in competition against *Candida* species (514). While anti-amoebae activity of *V. cholerae* T6SS being protective against *Dictyostelium discoideum* predation was amongst the very first examples of T6SS impact characterised (508).

Rather than just competing with eukaryotic microbes, T6SS can also be used for interactions with host cells. Among the *P. aeruginosa* anti-bacterial effectors described above, H2-T6SS effectors Tle4, PldA, PldB, and VgrG2b have been shown to provide host cell toxicity and promote internalisation (42, 611, 41). This can often be accomplished by use of effectors that interact with host cytoskeleton components. VgrG2b specifically promotes internalisation into non-phagocytic host cells through interactions with α- and β-tubulins as well as γTuRC complex (611, 612, 553). For example, *A. hydrophila* uses VgrG1 to inhibit actin polymerization, leading to subsequent apoptosis (613), while *V. cholerae* VgrG-1 and *B. cenocepacia* TecA use different mechanisms to interfere with cytoskeleton remodelling, with both resulting in pro-inflammatory responses (614, 615).

Another use of T6SS in bacterial pathogenesis is in host immune evasion. When host immune cells attempt to clear bacteria through phagocytosis, bacteria can be captured within ROS and lysozyme filled vesicles. Some bacteria have been shown to cope with ROS-induced damage in a T6SS-dependent manner. For example, the enterohemorrhagic *E. coli* catalase KatN effector degrades H_2O_2 while *Y. pseudotuberculosis* Zn^{2+} binding YezP acts through yet to be characterised indirect mechanism, both have been shown to aid in coping with ROS damage and promote *in vivo* virulence (616, 617). Both pathogenic *Edwardsiella tarda* and the intracellular bacterial pathogen *Francisella tularensis* use T6SS effectors for phagosomal escape, which enables intracellular replication and is a key part of pathogenesis in both bacteria

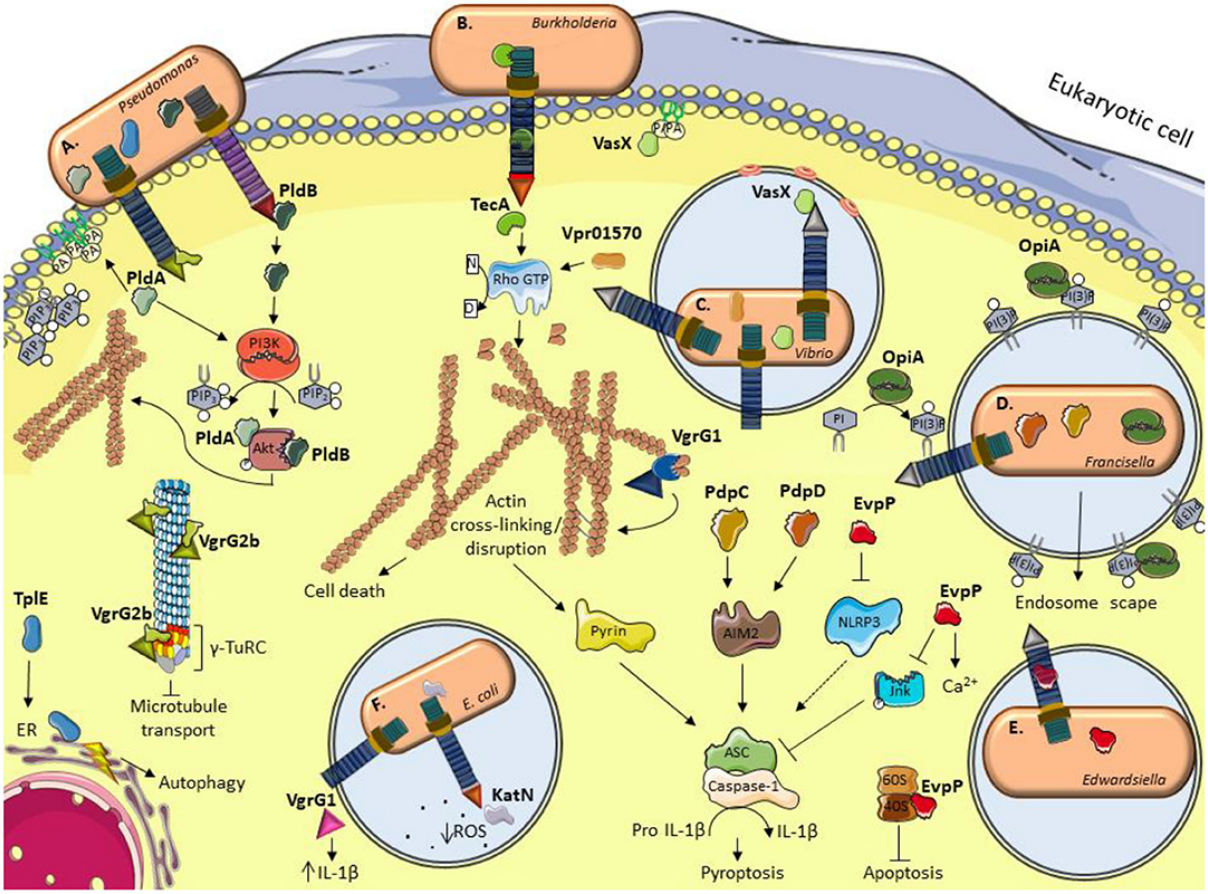

Figure 1.26: **Schematic illustration of anti-eukaryotic T6SS effector action.** (**A**) *P. aeruginosa* T6SS effector interactions aid with internalisation into host cells, PldA and PldB interacts with Atk and induces PI3K pathway, VgrG2b interacts with microtubulin and γ-TuRC complex, while Tle4 (TplE) targets endoplasmic reticulum. (**B**) *B. cenocepacia* activates Pyrin inflammasome and disrupts actin cytroskeletion. (**C**) *V. cholerae* VgrG1 cross-links actin disrupting host cell morphology, while VasX is proposed to be pore-forming. (**D**) *F. tularensis* PdpC and PdpD activate inflammasome and while OpiA kinase aids in endosomal recruitment through PI3P pathway. (**E**) *E. tarda* uses EvpP to inhibit NLRP3 inflammasome by modifying calcium ion influx. (**F**) *E. coli* (EHEC) KatN hydrolases reactive oxygen species and aids in survival within macrophages, while VgrG1 alters IL-1β levels. Adapted from (39) under creative commons attributions license.

(618, 619, 620, 621).

T6SS is not only significant in the context of animal but also plant hosts interactions. For example, the plant commensal bacteria, such as *Pseudomonas putida*, use the T6SS to prevent colonization by pathogens (622). T6SS is also prevalent in plant pathogens, such as *Pantoea ananatis* and *Ralstonia solanacearum*, both of which use T6SS for host pathogenesis (623, 624). However, currently, effector translocation directly to plant cells has not been shown. Therefore, it has been proposed that T6SS dependent pathogenesis is likely a result of plant pathogens

actively killing plant commensal bacteria enabling niche invasion (624).

1.4.8 Common good effectors

Aside from anti-host or antibacterial toxins, T6SS also delivers common good effectors that aid in binding and uptake of metal ions. To date, T6SS in *P. aeruginosa* has been linked with three common good effectors: the H3-T6SS-associated TseF and the H2-T6SS-associated Azu and ModA (501, 625, 169). The action of common good effectors is not dependent on delivery to adjacent cells but rather release within the surrounding environment. TseF is released from the cell in a H3-T6SS-dependent manner, where it interacts with the iron-chelating extracellular signalling molecule PQS (501) (Figure 1.27). TseF interacts with membrane porin OprF, that has

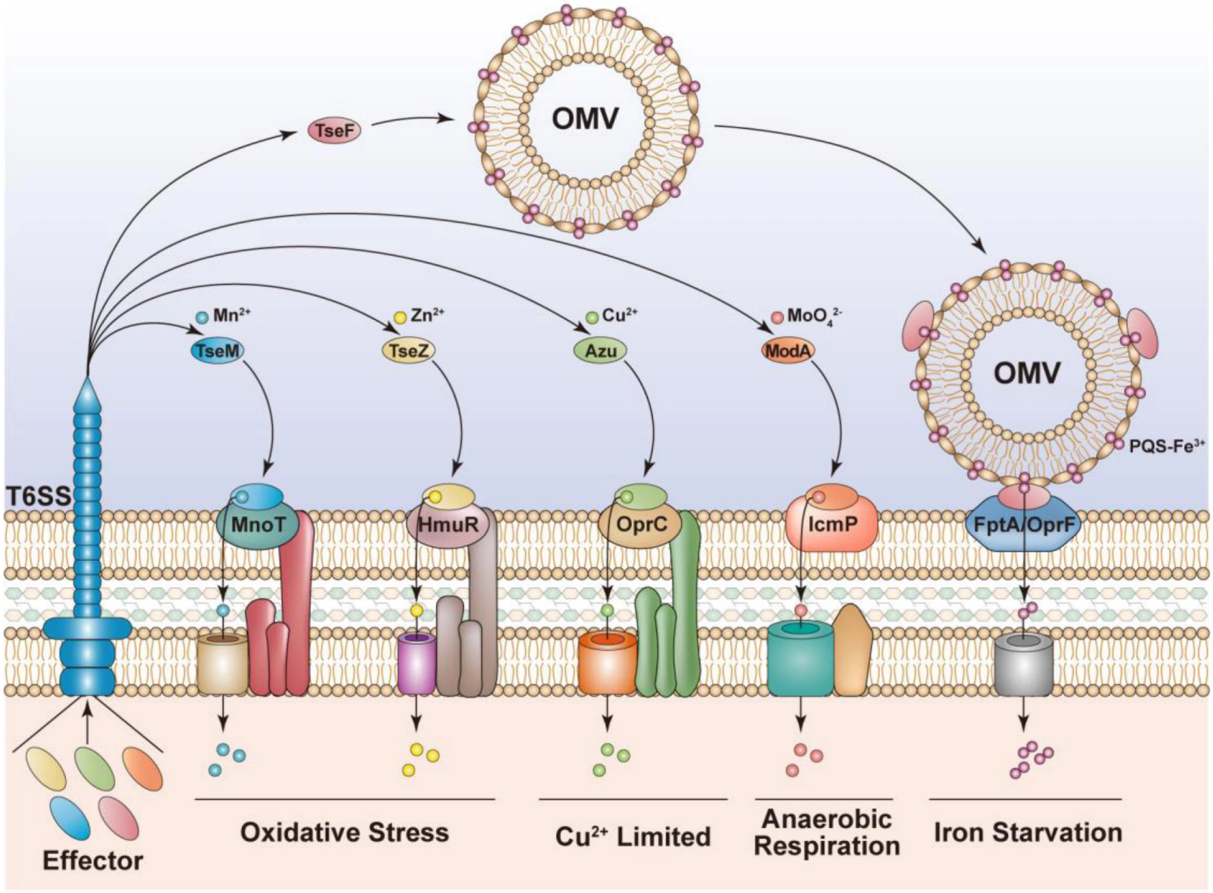

Figure 1.27: **Schematic showing T6SS effector mediated metal ion uptake.** *P. aeruginosa* H3-T6SS dependent TseF is involved in reuptake of PQS-Fe3+ vesicles, while H2-T6SS dependent Azu and ModA directly bind to copper and molybdate ions respectively. TseM and TseZ are *B. thailandensis* effectors that bind manganese and zinc ions respectively. Adapted from (518) under creative commons license.

been associated with both increased virulence and siderophore-mediated iron uptake (626, 627), and FptA, a Fe(III)-pyochelin receptor (628). PQS is highly hydrophobic, but are found to associate with *P. aeruginosa* OMVs (629), as TseF interacts with both Fe-PQS and iron uptake associated surface receptors, it has been proposed to be the protein recruiting Fe-PQS to OMVs for subsequent re-uptake (501). TseF aids in iron uptake, in a manner that is not dependent on direct Fe ion binding, but other T6SS common good effectors have been shown to aid in nutrient scavenging by directly binding metal ions. The uptake of molybdate ions has been linked to improved competitiveness of *P. aeruginosa* within the context of CF lung infection (630), and this is mediated through the ModABC uptake system initially characterised in *E. coli* (631). Only later this system was connected with the T6SS, as (169) demonstrated that ModA is secreted into the extracellular milieu by H2-T6SS where it directly binds $MoO_4{}^{2-}$ ions. Another H2-T6SS associated metal ion uptake effector is Azu that has been shown to bind Cu^{2+} ions (632, 625).

The link between T6SS and metal ion uptake extends beyond *P. aeruginosa* and has been described in a range of other bacteria (633). T6SS effector-associated zinc and manganese ion uptake has been observed in *Yersinia pseudotuberculosis* and *Burkholderia* species (617, 634, 635, 636, 637). In all of these examples, the T6SS expels the effectors into the extracellular space for subsequent re-uptake through mechanisms that are not dependent on T6SS firing. This aids more effective nutrient scavenging and contributes to indirect competition, improving survival in nutrient-limited host niches (633). Additionally, these ion-binding effectors can also aid in direct contact-dependent toxicity, such as in the case of *Y. pseudotuberculosis* TssS which binds Mn^{2+} ions and when injected into host cells, its ion chelating ability results in the inhibition of STING immune response aiding with immune evasion (637).

1.4.9 Identification of further effectors

Identifying T6SS effectors can be challenging due to the lack of specific, universally conserved motifs associated with their translocation. One approach to identifying these effectors is to examine the genomic organisation of T6SS genes, as sets of effector-immunity-chaperone genes are often found encoded within the same cluster as T6SS structural genes (Figure 1.20). For example, in the case of *P. aeruginosa*, the genes *eagT6-tse6-tsi6* (PA0092-94) are found alongside H1-T6SS core components, or *pldA-tli5* (PA3487-88) genes are co-encoded with *vgrG4b* (PA3486) in an orphan cluster associated with the H2-T6SS. Alternatively, evolved T6SS effectors that contain domains corresponding to structural components, such as PAAR in case of Tse7, or VgrG proteins as in VgrG2b, can be easily recognisable through bioinformatics analysis.

Another bioinformatics approach for identifying novel T6SS effectors is through the use of common marker domains. Rhs is one such domain,termed for **r**earrangement **h**ot**s**pot (638). Proteins that possess an Rhs or a different toxin domain have been identified as effector proteins not only for T6SSs in various bacterial species, such as *Dickeya dadantii* and *S. marcescens* (639, 640), but also for CDI effector proteins (368), and toxin-antitoxin system of *Salmonella Typhimurium* (641), or the exported Gram-positive toxin WapA found in *Bacillus subtilis* (642). The presence of an Rhs domain is one of the markers for effector proteins in polymorphic toxin systems of any kind and are not exclusive to T6SS (639, 643, 644). T6SS-specific recognition motifs such as MIX (**m**arker for type s**ix** effectors) and FIX (**f**ound in type s**ix** effector) have also been identified (645, 646). For example, the as-yet unnamed *P. aeruginosa* T6SS toxin PA5265 contains the MIX motif and is linked to H2-T6SS as it is encoded in a satellite cluster containing the genes *vgrG6* and *hcpB* (Figure 1.20). Deletion of predicted toxin-immunity genes pair *PA5264-65* is shown to render bacteria sensitive to eradication by a competitor in H2-T6SS dependent manner in Section 5 of this report.

Many of the T6SS effectors that have been characterised to date lack these markers and have been identified experimentally. The first *P. aeruginosa* T6SS effectors Tse1 to Tse3 were

identified through mass spectrometry analysis comparing the supernatant fraction of strains with and without active T6SS (583). A different approach for novel *P. aeruginosa* T6SS effector identification was taken in case of Tse8, where transposon directed insertion–site sequencing (TraDIS) was performed in strains with and without T6SS to detect mutations that are tolerated only in one of the backgrounds (557), with Tn hit suggesting a putative T6SS immunity gene. A more direct proteomics approach was used in a study by (555) for identification of *P. aeruginosa* Hcp associated effectors, where putative effectors were identified using pull-down assay with Hcp as bait protein. This study identified the putative H2-T6SS-associated effector PA2066 and the H3-T6SS associated effector PA0256. The variety of methods needed for identifying T6SS effectors shown here illustrates that more remain to be identified and characterised.

1.4.10 Non-immunity defences against T6SS

T6SS is widespread in Gram-negative bacteria and as discussed above, it delivers effectors with antimicrobial properties positioning it as a common direct bacterial competition tool. To defend against these toxins, bacteria employ a variety of protective mechanisms and strategies. The best understood defence against T6SS toxins is the use of specific cognate immunity proteins described in the above section. However, due to the large and functionally diverse set of toxins, more generic mechanisms are also useful (356) (Figure 1.28). These mechanisms can include general stress response and damage repair systems or adaptations evolved in response to other types of stress. For example, peptidoglycan adaptations evolved to resist antibiotics can also render peptidoglycan-targeting effectors delivered by less effective (647). Additionally, highly specific T6SS defence mechanisms exist, such as retaliatory or Tit-for-Tat T6SS firing (564, 576). The impact of EPS and stress responses on T6SS competition are discussed here, while impact of spatial segregation and different T6SS firing strategies on competitive fitness are addressed in further detail in section 1.5.

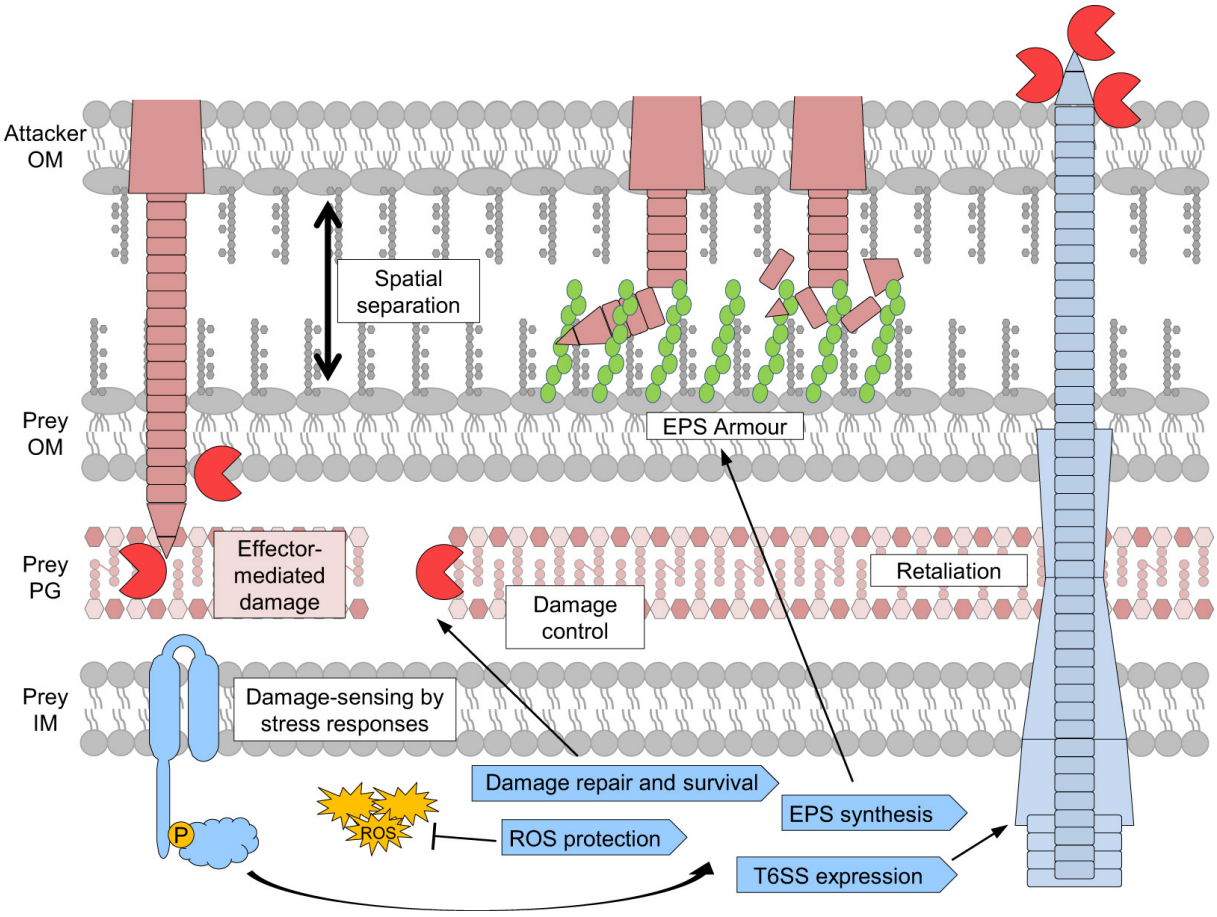

Figure 1.28: **Diagram of non-immunity T6SS defences.**
Schematic showing how EPS provide protection through introducing a physical barrier in the extracellular space and by increasing the distance between cells. Alternatively, bacteria may use generic stress response and damage repair mechanisms to cope with T6SS effector induced damage in the same way it would cope with any other cellular damage.
Adapted from (356) under creative commons attributions license.

1.4.10.1 Stress responses and damage repair

T6SS injections puncture prey cell membrane and many of the T6SS-associated toxins target cell wall components directly. This type of damage triggers stress responses in prey bacteria that subsequently act to mitigate T6SS toxin-induced damage (648, 579). For example, in *V. cholerae*, cell wall damage response is mediated by the sensor-response regulator pair WigK-WigR (VxrA-VxrB) that act to maintain cell wall integrity upon exposure to β-lactam antibiotics (649). WigK-WigR is a two-component system that regulates expression of 320 genes, with large fraction of the upregulated genes encoding proteins involved in cell wall component synthesis and maintenance (649). This two-component system has been shown to protect *V. cholerae* TseH

immunity (TsiH) lacking strains from killing by a parental strain, and is essential for survival of the strain producing both the effector and immunity proteins (650). It appears that *V. cholerae* uses the same damage sensing and repair machinery when exposed to antibiotic stress and T6SS attack.

A widely used mechanism for damage repair is the SOS response, a DNA repair system known to be associated with tolerance of antibiotic and environmental stress factors (651). This system has been shown to be triggered upon damage caused by *P. aeruginosa* nuclease Tse7 (552), with similar responses being induced by other T6SS-associated nucleases (652). In case of competition between *E. coli* and *Acenitobacter baylyi*, T6SS-dependent death and lysis of *E. coli* results in release of DNA that is subsequently taken up by competent *A. baylyi* (521). Interestingly, this DNA uptake results in activation of SOS response, that can lead to growth arrest and decreases the overall competitive fitness of attacker population (521).

Increased production of reactive oxygen species (ROS) is a universal signal of bacterial distress. ROS production can be linked to exposure to antibiotics (653), and has been seen to occur *K. pneumoniae* or *A. baylyi* prey bacteria exposed to to T6SS attacks by *V. cholerae* (654, 655). This leads to the idea that shared damage repair mechanisms can be employed to cope with both types of stress, and conversely the same conditions rendering bacteria more sensitive to antibiotic toxicity, may lead to increased sensitivity to T6SS attacks. In *E.coli*, exposure to T6SS attacks promotes the action of the SoxR-SoxS sensor-transcription activator pair (654), which coordinates the ROS response (656). The result is that loss of envelope stress response regulators SoxR-SoxS renders *E.coli* sensitive to *V.cholerae* T6SS toxin TseH (650). It has been proposed that mechanistic reason behind this is the loss of ability to trigger synthesis of protective EPS in the form of colanic acid. If colanic adic is produced in high levels, this results in a mucoid phenotype that appears to be protective against T6SS attacks (650).

1.4.10.2 Protection provided by EPS and cell envelopes

Biofilms are communities of bacteria embedded in an extracellular matrix that acts as a structural support and protective barrier. This, along with the cell envelope encasing individual bacterium, are mechanisms that protect sensitive prey from T6SS-mediated toxin injection (Figure 1.29). Similarly to colanic acid providing T6SS protection for *E. coli* (650), production of Vibrio polysaccharide has been shown to form a type of "protective armour" that shields *V. cholerae* from exogenous T6SS attacks by *A. baylyi* or *P. aeruginosa*, while simultaneously having no apparent effect on the T6SS killing ability of the EPS producing strain (264) (Figure 1.29). An interesting counterexample of EPS capsule interfering with producers T6SS injection is that of *Campylobacter jejuni*, where the presence of polysaccharide capsule has been shown to interfere with T6SS-mediated lysis of red blood cells (657). The formation of a polysaccharide capsule is a defining feature of many *Klebsiella* species and its presence has been shown to be sufficient to protect *Klebsiella* from T6SS attacks by *V. cholerae*, *E. coli* and *A. baumannii* (560). Additionally, this EPS capsule has also been shown to provide T6SS protection to an *E. coli* commensal isolate Ec300, that carries a horizontally acquired capsule biosynthesis pathway

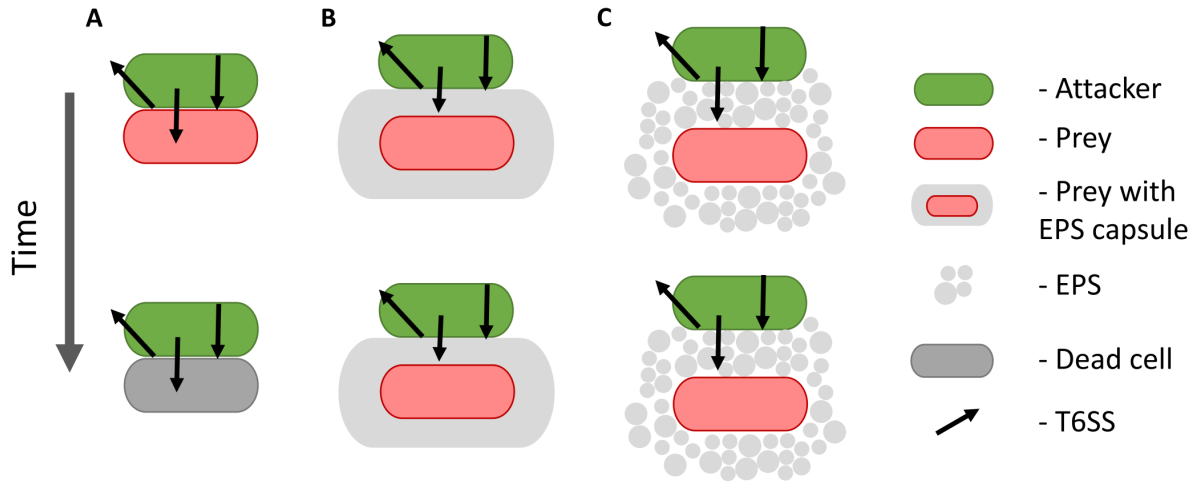

Figure 1.29: **Schematic depicting EPS protection from T6SS injection.**
EPS has been proposed to provide protection from T6SS attacks through multiple distinct mechanisms. In absence of EPS (**A**) bacteria are proposed to be in close contact, while EPS capsule (**B**) or cell-free EPS (**C**) could increase intracellular distance or act as a physical barrier preventing injection of T6SS.

(560, 658). The proposed mechanism of protection is that of increase in cell-cell distance or through physically obstructing T6SS injection (Figure 1.29). A point of interest in this study was the investigation of how changes in EPS content affect strain distribution within community and how loss of EPS affects T6SS-mediated competition in case of *P. aeruginosa* (Section 6).

1.4.10.3 Gram-positive resistance to T6SS attacks

The prime example of cell envelope/ cell wall that is believed to act as a barrier against T6SS attacks preventing direct toxin injection is that of Gram-positive bacteria. However, recent literature has described some cases of T6SS-mediated interactions with Gram-positives. For example, the plant-beneficial bacteria *B. subtilis* and *Pseudomonas chlororaphis* engage in antagonistic interactions that limit co-existence *in planta* (659, 660). These interactions are in part mediated through T6SS of *P. chlororaphis*, as *B. subtilis* has been shown to undergo sporulation when exposed to T6SS attack by *P. chlororaphis* (660). Similarly, P. aeruginosa H1-T6SS associated peptidoglycan hydrolase Tse1 has been shown to induce sporulation in *B. subtilis* (661) Furthermore, a T6SS effector Tse4$^{A.\ baumannii}$ identified in *A. baumannii* was found to kill *B. subtilis*, *Listeria monocytogenes*, and *S. aureus* in a contact-dependent manner (662). To date, the only known example of a cytoplasmic T6SS toxin with activity against Gram-positive prey is a nuclease, RhsB, found in the plant pathogen *Acidovorax citrulli* (513). RhsB and RhsE (a toxin of unknown function) contribute to T6SS-dependent killing of both Gram-negative *E. coli*, Gram-positive *B. subtilis*, as well as *Mycobacterium smegmatis* whose cell wall outer layer is made up of a mycomembrane (513). Although a few examples of T6SS toxin impact on Gram-positives have been identified, the mechanisms behind these interactions are still not well understood. Additionally, while these examples suggest a need for contact, there is currently no evidence for T6SS effector translocation to or action within the cytoplasm of Gram-positive bacteria.

1.5 Using computational approaches to study bacterial community dynamics

Biofilm communities are complex, organised systems in which the constituent microbes gain an overall fitness benefit. These systems are highly heterogeneous and dynamic, and individuals within communities behave differently depending on the specific microenvironment (663, 664). This heterogeneity emerges as biofilms develop from a few individual bacteria into a dynamic system with many interactions taking place, resulting in development of collective properties. Biofilms can be considered emerging systems, since, acting together, bacteria behave in a manner that cannot be explained through the study of individual cells under planktonic conditions alone (665). The study of interactions and local responses within biofilms can be difficult experimentally, as it is challenging to consistently control and manipulate all of the relevant variables and isolate specific interactions. However, theoretical simulations can be a powerful tool in the study of microbial biofilms, as they allow researchers to comprehensively address the impact of individual aspects of interactions within these complex and organised systems (666, 667, 668).

Simulations can be used to gain insight in how a complex bacterial communities emerge from establishment by just a few individual bacteria and to gain a deeper understanding of how different interactions contribute to the overall behaviour of the community. Laboratory models reduce complexity of the interacting bacterial system to enable the study of individual aspects of bacterial communities. This can be done by studies both at the single-cell scale as well as the level of whole community structures, but is technically challenging to include both of these within a single study. Additionally, when investigating the impact of specific phenotypic changes it is often difficult to disentangle a specific impact from compounding factors, as even a single gene will often elicit a change in multiple phenotypic features. This is exemplified by *P. aeruginosa* T6SS activation as a part of transition towards biofilm phenotype (100). Simulations can be

used to bridge experimental observations by fitting these with specific mechanistic explanations.

Theoretical simulations can be a powerful tool that allows us to explore a wide range of scenarios and to guide subsequent experimental design. For example, simulations can be used to study how biofilm communities respond to changes in environmental conditions, such as changes in nutrient availability or flow rate (669). This can help researchers to understand how these factors influence biofilm formation and structure and how they may be harnessed to control biofilm growth in practical applications. Conceptual explanations for behaviour of biological communities are based on studies conducted within laboratory setting aiming to reduce variability, but there are a large number of confounding factors that exist in natural systems. This includes the specifics of study of how the biofilm formation occurs. The formation of complex structures of *P. aeruginosa* biofilms within a flow-cell is determined by available carbon source (184) and the media flow rate. The latter is needed to facilitate both supply of fresh media and waste removal, while flow also imposes physical shear stress (670, 669). These experimental models enable a reliable study of specific bacterial behaviours, but do not accurately depict the existence of *P. aeruginosa* within the infection niche (249). By simplifying the system and reducing the number of confounding factors, simulations can help researchers identify key concepts that can be subsequently interpreted within the context of more complex "real-world" problems. With the gradual advancement of study techniques, observations from simplified systems can subsequently be applied to more complex systems to refine and adjust conceptual models.

1.5.1 Approaches to modelling bacterial communities

There are three main approaches for simulating microbial communities: continuous, individual-based, and mixed models. Each of these approaches describes the organisms within a system, key aspects of the environment at a given point in time and sets out rules on how bacteria are to behave accordingly to the conditions of its environment and how any given behaviour

impacts its surroundings. Computational simulations allow to iteratively solve question of how organisms behave depending on the specific information about its continuously changing surroundings at any given point in time and what are the local and global consequences of any behaviour. Different simulation approaches are better suited to look at certain aspects of microbial behaviour and interactions with its surroundings (667, 666). Some of the aspects to consider when choosing a theoretical modelling approach are time and spatial resolution. Spatial resolution refers to geometry of individuals and community size as a whole, while time resolution looks at both how frequently meaningful actions occur and decisions are made, as well as the overall timescale of community existence.

Continuous grid-based models can provide detailed descriptions of continuously changing biochemistry while allowing for the implementation of large system sizes and a high number of simulation iterations. However, these types of models are limited in their ability to implement mechanistic interactions and aspects of localised community structure due to grid constraints (671). Simultaneously, these are most useful for recreating large systems, often used in microbial ecology or studies of community metabolic dynamics (672, 673, 674). Individual or agent-based models, on the other hand, offer detailed descriptions of the physical interactions of single bacteria while simplifying the chemical environment (675). They are better suited for addressing questions involving spatially explicit interactions and the impact of bacterial geometry (668). These models can be used to understand how changes in system-level dynamics emerge from differences in highly localised interactions and changes in individual cell behaviour (676). Mixed modelling platforms combine the benefits of both continuous and individual-based models by implementing a high-resolution chemical concentration grid and individual cell objects that are coupled to locations in the grid. This allows for the implementation of stochastic cellular behaviour that is highly dependent on the local environment, such as nutrient concentrations or growth-inhibiting substances.

A range of simulation tools have been developed to investigate dynamics of bacterial

populations, the reviews by (668) and (667) conduct a detailed assessment of capabilities of many currently available tools, with a selection discussed here. Some of the main aspects of microbial systems that these models aim to address growth dynamics, internal metabolism, interactions with external chemical fields, physical interactions with the environment and other cells, motility, chemotaxis, fluid dynamics, extracellular polymeric substances, direct interactions, and conjugation. But it is more common to focus on only a few key aspects at a time, when addressing a particular question. BSocial is a tool specifically designed to analyse the effects of social interactions on the fitness of polymicrobial communities (677). Simbiotics includes explicit cell geometry, chemical gradients as an environment, and intracellular processes (676). Gro is a programming language that allows for the explicit description of individual cell behaviours and genetic circuits, as well as the integration of information about the environment and current internal cell state to produce an appropriate response (678, 679). LAAMPS (Large-Scale Atomic/Molecular Massively Parallel Simulator) is a tool originally designed for simulations of materials and molecular dynamics (680), has been adopted for use in studying the dynamics of the microbial community in the form of NUFEB, which enables efficient simulations of large numbers of bacterial agents (620). McComedy, a more recent addition to the available simulation tools, is designed to enable the modelling of spatially explicit bacterial interactions without requiring programming expertise (681). Overall, these simulation tools offer a range of capabilities for studying the dynamics of bacterial populations, including the effects of social interactions, explicit cell geometry, programming language for describing cell behaviours, and spatially explicit bacterial interactions.

T6SS-mediated interactions rely on direct cell contact, and the local geometry of bacteria has significant effects on community structure and competition that relies on contact. Therefore, it was important to select a simulation approach that could describe mechanistic bacterial interactions for this project. CellModeller, initially developed by (682) as an agent-based simulation platform, has been used to study the impact of intercellular dynamics within mixed

species communities on the overall makeup of the community. It has also been used to investigate the impact of CDI and T6SS interactions on bacterial communities (683, 684). CellModeller was chosen as the simulation tool for this study.

1.5.2 Theoretical modelling of dynamics within contact-mediated microbial competition

Bacterial ability to expand within a niche is limited by two key factors - space and nutrient availability. The use of T6SS allows bacteria to actively compete for both space, by killing adjacent competitors, and nutrients, through the use of ion uptake associated effectors. Although T6SS-based interactions are highly localised, species encoding T6SS have been shown to establish and even dominate host niches (685, 686, 524). For example, a *Shigella sonnei* clinical isolate strain has been shown to use T6SS not only to outperform *E. coli* and *Shigella flexneri in vitro*, but also in mouse colon infection (686). Biophysical simulations can be used to identify the key mechanistic parameters and competitive strategies behind successful T6SS competition.

Multiple computational studies on different aspects of T6SS competition can be found in literature to date. These include continuum models and mechanically simplistic lattice-based simulations (687, 688, 689), as well as more recent agent-based models that consider aspects of local geometry of individual bacteria and how these influence competition outcomes (684, 689, 690, 518). Interactions mediated through CDI and T6SS can be abstracted in similar terms within the context of biophysical simulations, as both require direct contact between individuals of opposing populations, while the frequency of interactions and the impact of toxin are described through differences in parameters, rather than general rules of engagement (691, 683). In the following section, studies investigating both CDI and T6SS-mediated interactions are included for a more comprehensive general perspective on modelling contact-mediated microbial competition.

1.5.2.1 Use of contact mediated competition enables niche domination, but species extinction events are rare

T6SS-mediated killing is dependent on direct contact between the attacker and the prey, which allows efficient delivery of toxin directly into prey cells and eradication of adjacent competitors, thus giving the individual attacking bacterium an immediate and direct benefit. However, this also makes T6SS-mediated competition vulnerable to defences through spatial separation, where prey can persist if it remains inaccessible to direct T6SS attack. Nevertheless, T6SS has been shown to allow invasion of host niches, as T6SS has been shown to aid with host gut invasion by *Salmonella* Typhimurium, *Shigella sonnei*, and *V. cholerae* amongst others (692, 686, 693). One of the experimental systems used to investigate how T6SS is utilised to enable niche takeover is the squid light organ. *Euprymna scolopes* is a species of marine squid whose light organ crypts are often found to be dominated by only a few strains of symbiotic *Vibrio fischeri* (694). The ability of *V. fischeri* to achieve niche domination in this context has been pinpointed to use of antibacterial T6SS (524). This study also notes that both T6SS active and toxin sensitive strains can be co-isolated from the same host organism, indicating that despite attacker population being able to achieve general dominance complete prey elimination does not occur. Rather, mutual killing will drive sub-population segregation and enable co-existence of competing species. This balance can also be perturbed by actively mixing competitors after the initial establishment (524). Therefore, one of the first questions to be addressed using theoretical simulations was whether the use of T6SS always leads to invasion and complete takeover of the niche through eventual elimination of the sensitive prey or whether this is just one of multiple possible stable outcomes.

Assuming a sufficiently high toxin delivery rate, the use of contact-dependent competition tools can drive sensitive strains toward extinction, but this is dependent on populations being well mixed and small. If mixing is limited, then localised prey aggregation and survival may occur (691, 688, 683). The overall fraction of the space occupied by competitors is determined

by the strength of the inhibition and the cost balance (691, 683, 684). In large enough systems, spatial heterogeneity seems to inevitably lead to localised prey survival, and complete extinction events are rare (691, 684). One scenario in which sensitive sub-populations may be able to escape is when competitors expand laterally within a spatially unconstrained system; if the sensitive bacteria are localised on an edge of the population, it may keep expanding, leading to sensitive population persistence (687, 683). In a study by (690), an opposing scenario of T6SS killing under spatial containment was explored. This work combines agent-based theoretical modelling approach with *P. aeruginosa* H1-T6SS-mediated competition in microarray wells to examine population dynamics in a spatially confined niche. Interestingly, this work shows that even in space-constrained dense communities, complete elimination of sensitive bacteria is rare, and spatial growth constraints (limiting the ability for bacteria to spatially segregate) do not necessarily translate into the dominance of the T6SS+ strain, but the variation in population composition does still increase with community size (690). A different study by (683) combines an agent-based modelling approach with experiments focusing on *E. coli* CDI-mediated competition. These studies show that although direct contact-dependent antagonism is a mechanism that can enable niche domination, complete eradication of the sensitive bacteria is expected to occur only rarely. With the rate of toxin action being the main determinant of the competitive outcome, it is also notable that experimental work used to support simulations shows that although fast-acting toxins are more effective at restricting the growth of sensitive bacteria, complete eradication of sensitive bacteria within these systems is rare. One of the reasons for this being local heterogeneity - although most of the community may be dominated by one of the competitors, spatial segregation can consistently enable localised prey population survival (683).

1.5.2.2 Strain spatial segregation - emergent property and protective mechanism

Theoretical modelling of contact-mediated killing shows that stable co-existence of competing strains is achieved through spatial segregation and this can occur even in cases where the attacking population achieves overall spatial and numerical dominance within the niche (691, 689, 695, 518, 684, 683). The study by (689) pinpoints this as an emerging feature through the use of deterministic PDEs, lattice-based simulations, and individual-based models and corroborates this through experimental observations of T6SS-mediated competition between two *V. cholerae* strains. Similarly, T6SS proficient *V. cholerae* and *A. hydrophila* engage in bi-directional competition and coexistence can be achieved through spatial segregation (695).

Spatial segregation describes a scenario in which, starting from a homogeneous species mix, bacterial communities develop such that sub-populations exist in spatially distinct regions. This state can be characterised by a reduction in intermixing between individuals and a decrease in the total interaction surface between populations (Figure 1.30). While mutualistic interactions have been shown to result in communities where species remain intermixed (696), spatial segregation appears to commonly emerge in populations where mutual antagonistic interactions are present. The study by (687) uses 2D lattice-based simulations to depict interactions between a T6SS+ and

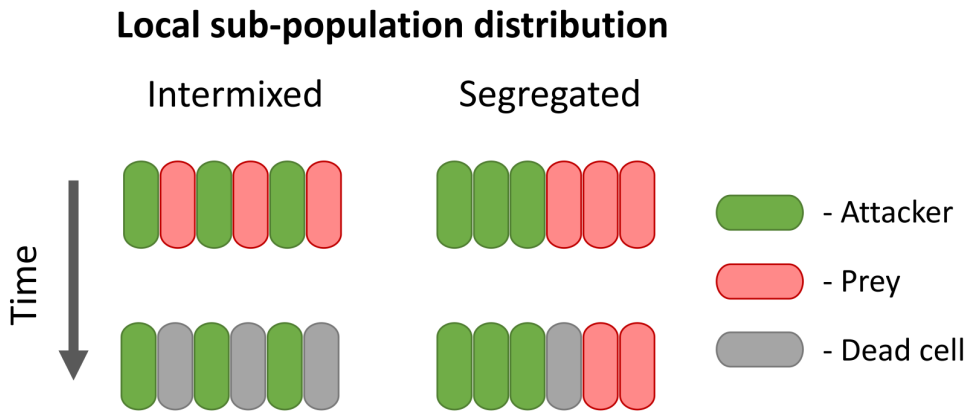

Figure 1.30: **Schematic T6SS competition outcomes in scenarios where populations intermixed and spatially segregated.**
Different communities develop as a result of contact-mediated competition in highly intermixed communities (left) and spatially segregated communities (right). Showing attacker population in green, toxin sensitive prey cells in red and accumulated dead cells in grey.

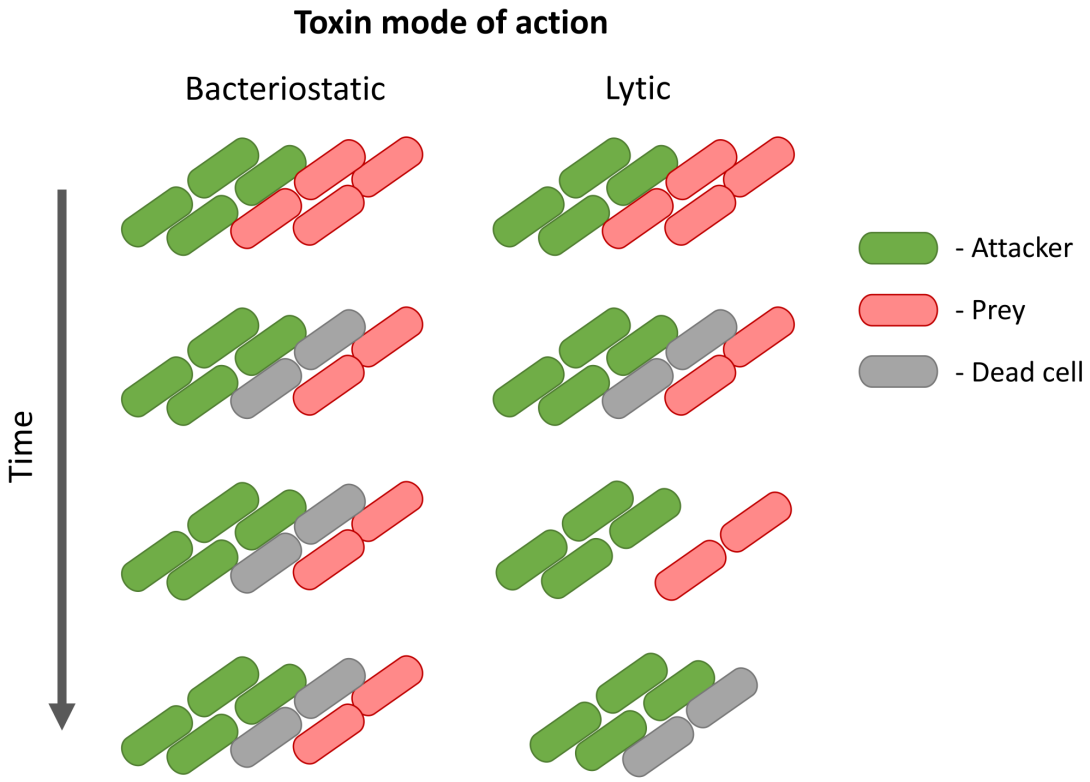

Figure 1.31: **Schematic T6SS competition outcomes depending on the type of toxin used.**
Different communities development as a result of contact-mediated competition conducted through bacterostatic toxins leading to accumulation of protective layer of dead cells (left) and highly lytic toxins (right). Showing attacker population in green, toxin sensitive prey cells in red and accumulated dead cells in grey.

sensitive populations. These simple models incorporate information only about the frequency of T6SS attacks and the growth rate differences between the two competitors. An assumption made is that bacteria producing T6SS will have to pay a metabolic cost that is likely to result in slower growth rate. These simulations show that prey survival is inversely correlated to rate of T6SS attack and shows that spatial separation aids in prey survival (687). Similarly, herd protection is observed in both interspecies competition mediated through T6SS and use a proof-of-principle lattice simulations to illustrate how presence of bacterial debris interferes with T6SS-dependent niche takeover (695). Impact of physical perturbation on the competitive dynamics in pre-established communities was also investigated within context of surface grown mixed species macrocolonies of *P. aeruginosa* competing with *Pseudomonas protegens* or *K. pneumoniae* (697).

The mechanistic explanation behind spatial segregation and how this enables competitor co-existence is that this is a result of accumulation of dead cells that prevent direct contact between prey and attacker populations (698). This accumulation of dead cells at competing population interfaces was the focus of study by (684), that termed this phenomenon the "corpse barrier effect". The protective sub-population segregation mediated by accumulation of dead bacteria at the interface between the susceptible prey and T6SS attacker was termed the "corpse barrier effect" (684). This shielding of susceptible prey occurred in cases where T6SS toxins delivered did not cause immediate prey lysis and this supports the evolutionary advantage in favour of using lytic toxins that will enable attacker to continuously gain access to sensitive prey bacteria (684). This limitation can be overcome by use of lytic toxins, which are capable not only of killing adjacent bacteria, but also of resulting in near complete removal of dead cells (Figure 1.31). Toxin mode of action determines the overall competitive outcome, as use of lytic toxins enables bacteria to overcome the limitations presented by spatial separation (684).

1.5.2.3 Population geometry determines competitive outcomes

As much as spatial separation can emerge from homogeneous systems as a result of competition, scenarios in which natural communities are established from a homogeneous mix are rare. In a pristine niche, a population is likely to establish from just a few bacteria, while most bacteria likely face existence of pre-established microbiome and to establish in a niche, invading bacteria must outcompete the current resident flora. The presence of healthy commensal microbiome is particularly important as it provides protection from pathogen invasion (604, 516, 686). This also extends to examples of T6SS use for invasion resistance, as T6SS gene clusters are enriched in genomes of commensal gut bacteria (699). Both the bacterial distribution within the initial populations and presence of pre-established prey population lead to a single question of the impact of population geometry on contact-mediated competition.

Cell configuration within the founding population has a substantial impact on the

distribution of sub-populations within an established community, with populations established from sparsely placed bacteria being more varied (700, 701). Depending on how individual bacteria from competing populations are spaced, they will immediately encounter competing population or will be able to undergo prior establishment before engaging in direct competition (Figure 1.32). Once sub-populations encounter each other, killing will still occur, but prior establishment has been shown to interfere with the clearance of T6SS sensitive bacteria (687, 695), and this is likely to result in attacking bacteria being unable to establish contact with susceptible prey populations. The degree of sub-population intermixing or local contact assortment has been shown to be one of the determining factors for success in bacterial competition mediated through T6SS, CDI, and diffusible toxins (683, 416, 684, 700, 688, 702). The impact of sub-population contact assortment within context of *P. aeruginosa* T6SS-mediated competition is one of the questions addressed in chapter 6 of this study.

1.5.2.4 Comparing benefits of contact-mediated and long-range competition

The main limitation of contact-dependent competition is the ability to establish direct contact between interacting bacteria. Use of long-range competitive tools enables bacteria to overcome these limitations. A study by (416) compares outcomes of bi-directional competition conducted through CDI and CcdB toxin from the type II toxin-antitoxin system for long-range inhibition in *E. coli* (415) with individual based simulations. Depending on the set-up conditions, it appears that either weapon can aid in achieving complete community dominance, with stable co-existence being rare. In general, long-distance inhibition is seen as being more likely to result in complete elimination of sensitive bacteria, while contact-dependent antagonism allows for sensitive prey survival (416). A more recent study by (703) assesses the impact of both short and long-range inhibition through the use of agent-based simulations and *P. aeruginosa* CDI and tailocin experimental systems to further investigate how opposition through contact-mediated competition and diffusible toxins influence the distribution of sub-populations within

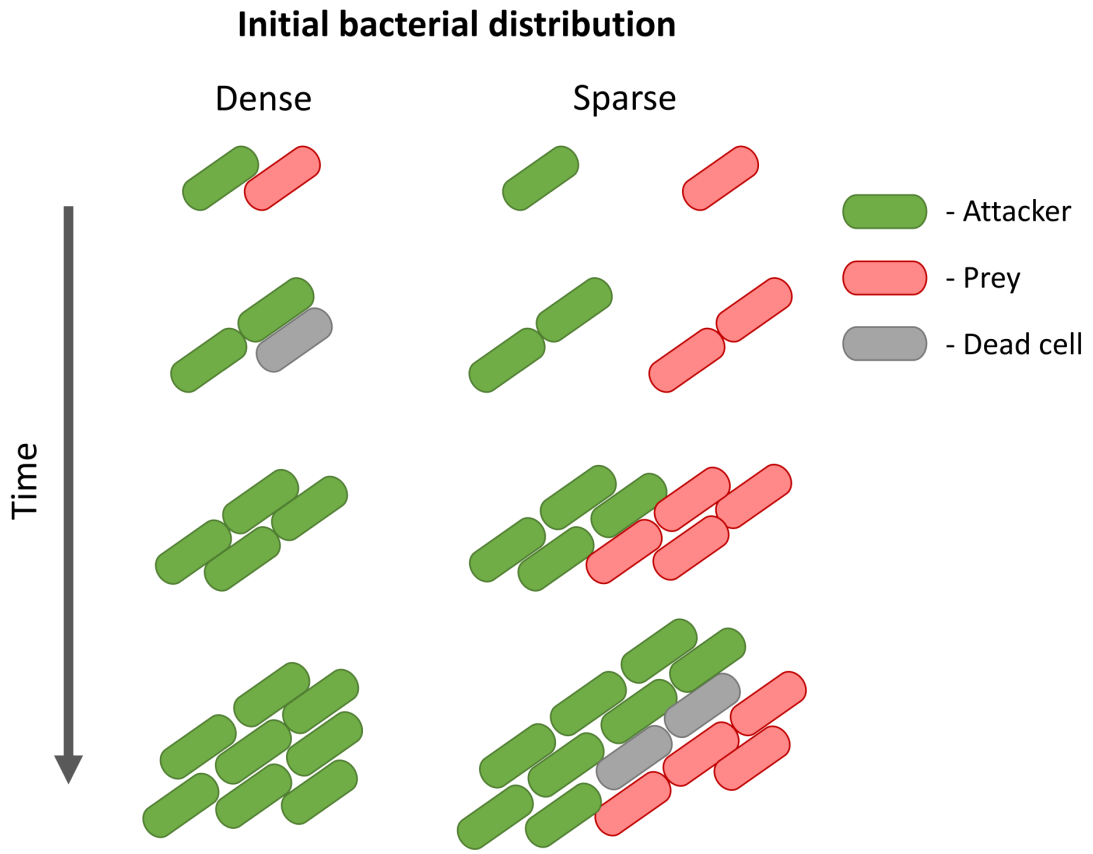

Figure 1.32: **Schematic T6SS competition outcomes in dense and sparse communities.** Different in communities development as a result of contact-mediated competition in dense community (left) and sparse community allowing for establishment (right). Showing attacker population in green, toxin sensitive prey cells in red and accumulated dead cells in grey.

community. Contact-mediated competition is advantageous in dense well-mixed communities and allow for persistence even when sub-population is placed at an initial numerical disadvantage. While successful use of tailocins requires high concentration that can be reached through high bacterial densities and frequent toxin release. When both weapons are pitted against each other experimentally, contact-based competition is strongly favoured. Admittedly, CDI and tailocin systems are also very distinct in their mode of action, the release of the latter requiring cell lysis; therefore, an individual cell sacrifices itself for a population-level benefit (704). The overall takeaways from these two studies indicate that although general competitive outcome is dependent on the type of tool used, the specific toxin used is likely to be more impactful in determining the overall outcome.

1.5.2.5 Competitive benefits of distinct T6SS firing-strategies

When faced with a direct attack rather than defending against a toxin action or mitigating damage, bacteria can engage in direct retaliation. As long as bacteria retaliating is able to cope with the initial provocation and can respond quickly, this is a highly effective competitive strategy (576). The foremost example of this is the Tit-for-Tat firing behaviour displayed by *P. aeruginosa* H1-T6SS (564). This describes a scenario where bacteria up-regulate T6SS firing in direct response to sensing a T6SS attack. What is notable is that this is not a general stress response that leads to an overall up-regulation in T6SS activity; instead bacteria are able to precisely position and assembly T6SS sheaths to enable directed retaliatory firing. Details of the molecular mechanisms involved in *P. aeruginosa* sensing of exogenous T6SS injections are described in section 1.4.4. Retaliatory and condition-specific T6SS firing has also been observed in other bacterial species. *S. marcescens* proportionally modulates T6SS expression levels in response to increase in exogenous T6SS attack rates, while *K. pneumoniae* T6SS activity is modulated in response to a variety of abiotic stress factors (705, 655). Studies pitting bacteria with different T6SS firing behaviours against each other have been used to evaluate the factors that contribute to the competitive success of the population. In a study by (706) in which a range of marine bacterial isolates were challenged in competition with T6SS active *V. cholerae*, one of the most successful competitors was *Vibrio coralliilyticus* surviving through use of its own T6SS. Similarly in a study by (560) where this time T6SS active *V. cholerae* strain was competed against human gut commensals, multiple strains from the *Enterobacter cloacae* complex were able to not only withstand the T6SS attack, but to out-compete *V. cholerae* through use of offensive T6SS firing.

The evaluation of the benefits of the different firing strathegies of T6SS was a focus of computational study by (576). Simulations show that random undirected T6SS firing is effective when it comes to competing with prey bacteria that do not fire T6SS. Interestingly, if random T6SS attack is met with directly proportional directed retaliation, competitor firing randomly

will still succeed. Instead, for a retaliatory T6SS firing to be successful, a single T6SS hit has to be met with multiple response firing events (576). In addition, bacteria that engage in retaliation must be able to withstand the initial T6SS attack.

A different study looking at how differences in T6SS firing dynamics lead to different competitive outcomes was conducted by (707). Here the experimental system of squid light organ was used in conjunction with agent-based modelling of the T6SS interactions. The competition between two distinct strains of *V. fischeri* is assessed, and what is notable is that these bacteria upregulate T6SS in response to environmental stimuli, but the response rates are varied (707). T6SS systems are often activated only when certain environmental stimulia are present, in practice, a certain delay is involved between sensing in change within local environment, shifting gene expression profile to upregulate T6SS activity. This type of delay can substantially impact the ability to eliminate prey using T6SS, if initial T6SS attack is delayed, prey population can take advantage of this window of opportunity to establish (707).

In summary, existing theoretical studies of T6SS mediated competition cover a range of questions surrounding T6SS-dependent competition dynamics, but a few joint key themes emerge. Use of T6SS-dependent competition can be a very efficient competitive strategy, but is entirely dependent on the community geometry. Subsequently, cases where use of T6SS alone would allow for complete elimination of sensitive bacteria are rare. And most importantly, although different T6SS firing strategies can be advantageous in different competition scenarios, the properties of toxins used are likely to be the main determinant of the overall competitive success.

1.6 Project aims

The overall aim of this project is to investigate how *P. aeruginosa* T6SS-mediated competition shapes community structure. This will involve:

- To investigate the impact of c-di-GMP level on the expression and activity of all three *P. aeruginosa* T6SSs.
- To construct and characterize strains with mutations in Gac-Rsm cascade, aiming to assemble a strain set with gradually modulated T6SS activity.
- To develop an experimental assay that can investigate the impact of T6SS-dependent competition on large mixed community structure.
- To evaluate the contribution of individual T6SS toxins to bacterial competition.
- To use biophysical simulations to evaluate the key parameters that determine T6SS-dependent competition outcome.
- To investigate how changed in the local contact assortment impact T6SS-dependent competition outcomes.
- To assess how Type IV pili-mediated motility affects T6SS-dependent competition in *P. aeruginosa*.

Chapter 2

Methods

2.1 Bacterial strains and growth conditions

P. aeruginosa and *E. coli* strains used in the study are listed in Table 2.1. Plasmids listed in the Table 2.2 and primers used for cloning listed in the Table 2.3.

Strain	**Features**	**Source**
PAK	Wild type strain	Laboratory collection
Δ*retS*	Deletion of *retS* (PA4856)	Laboratory collection
Δ*retS* Δ*sadC*	Deletion of *retS* (PA4856) and *sadC* (PA4332)	Laboratory collection
Δ*retS* Δ*sadC*::*sadC*	Deletion of *retS* (PA4856) and *sadC* (PA4332), where WT *sadC* gene gas been restored	This study
Δ*retS* Δ*pppA*	Deletion of *retS* (PA4856) and *pppA* (PA0075)	Laboratory collection
Δ*retS* Δ*sadC* Δ*pppA*	Deletion of *retS* (PA4856), *sadC* (PA4332) and *pppA* (PA0075)	This study
PAO1	Wild type strain	Laboratory collection
Δ*rsmN*	Deletion of *rsmN* (PA5183.1)	This study
Δ*rsmA*	Deletion of *rsmA* (PA0905)	Laboratory collection
Δ*retS*	Deletion of *retS* (PA4856)	Laboratory collection

Strain	**Features**	**Source**
Δ*rsmA* Δ*rsmN*	Deletion of *rsmA* (PA0905) and *rsmN* (PA5183.1)	This study
Δ*tssB1* Δ*tssB2* Δ*tssB3*	Deletion of *rsmN* (PA5183.1), *tssB1* (PA0083), *tssB2* (PA1657) and *tssB3* (PA2365)	Laboratory collection
Δ*rsmN* Δ*tssB1* Δ*tssB2* Δ*tssB3*	Deletion of *tssB1* (PA0083), *tssB2* (PA1657) and *tssB3* (PA2365)	This study
Δ*rsmA* Δ*tssB1* Δ*tssB2* Δ*tssB3*	Deletion of *rsmA* (PA0905), *tssB1* (PA0083), *tssB2* (PA1657) and *tssB3* (PA2365)	Laboratory collection
Δ*retS* Δ*tssB1* Δ*tssB2* Δ*tssB3*	Deletion of *retS* (PA4856), *tssB1* (PA0083), *tssB2* (PA1657) and *tssB3* (PA2365)	This study
Δ*rsmA* Δ*rsmN* Δ*tssB1* Δ*tssB2* Δ*tssB3*	Deletion of *rsmA* (PA0905), *rsmN* (PA5183.1), *tssB1* (PA0083), *tssB2* (PA1657) and *tssB3* (PA2365)	This study
Δ*rsmA tssB1*:mScarlet-I	Deletion of *rsmA* (PA0905), C-terminal mScarlet-I fusion to *tssB1* (PA0083) at native locus	Laboratory collection
Δ*retS tssB1*:mScarlet-I	Deletion of *retS* (PA4856), C-terminal mScarlet-I fusion to *tssB1* (PA0083) at native locus	Laboratory collection
Δ*rsmA* Δ*rsmN tssB1*:mScarlet-I	Deletion of *rsmA* (PA0905) and *rsmN* (PA5183.1), C-terminal mScarlet-I fusion to *tssB1* (PA0083) at native locus	This study
Δ*tse1_tsi1*	Deletion of *tse1* and *tsi1* (PA1844-45)	This study
Δ*tse2_tsi2*	Deletion of *tse2* and *tsi2* (PA2702-03)	This study
Δ*tse3_tsi3*	Deletion of *tse3* and *tsi3* (PA3484-85)	This study
Δ*tse4_tsi4*	Deletion of *tse4* and *tsi4* (PA2774-75)	This study
Δ*tse5_tsi5*	Deletion of *tse5* and *tsi5* (PA2683-84)	This study
Δ*tse6_tsi6*	Deletion of *tse6* and *tsi6* (PA0092-93)	This study
Δ*tse7_tsi7*	Deletion of *tse7* and *tsi7* (PA0099-0100)	This study
Δ*tse8_tsi8*	Deletion of *tse8* and *tsi8* (PA4163-64)	This study
Δ*rsmA* Δ*tse1_tsi1*	Deletion of *rsmA* (PA0905), *tse1* and *tsi1* (PA1844-45)	Laboratory collection
Δ*rsmA* Δ*tse2_tsi2*	Deletion of *rsmA* (PA0905), *tse2* and *tsi2* (PA2702-03)	Laboratory collection
Δ*rsmA* Δ*tse3_tsi3*	Deletion of *rsmA* (PA0905), *tse3* and *tsi3* (PA3484-85)	Laboratory collection
Δ*rsmA* Δ*tse4_tsi4*	Deletion of *rsmA* (PA0905), *tse4* and *tsi4* (PA2774-75)	This study
Δ*rsmA* Δ*tse5_tsi5*	Deletion of *rsmA* (PA0905), *tse5* and *tsi5* (PA2683-84)	This study

Strain	**Features**	**Source**
Δ*rsmA* Δ*tse6_tsi6*	Deletion of *rsmA* (PA0905), *tse6* and *tsi6* (PA0092-93)	This study
Δ*rsmA* Δ*tse7_tsi7*	Deletion of *rsmA* (PA0905), *tse7* and *tsi7* (PA0099-0100)	This study
Δ*rsmA* Δ*tse8_tsi8*	Deletion of *rsmA* (PA0905), *tse8* and *tsi8* (PA4163-63)	This study
Δ*retS* Δ*tse1_tsi1*	Deletion of *retS* (PA4856), *tse1* and *tsi1* (PA1844-45)	This study
Δ*retS* Δ*tse2_tsi2*	Deletion of *retS* (PA4856), *tse2* and *tsi2* (PA2702-03)	This study
Δ*retS* Δ*tse3_tsi3*	Deletion of *retS* (PA4856), *tse3* and *tsi3* (PA3484-85)	This study
Δ*retS* Δ*tse4_tsi4*	Deletion of *retS* (PA4856), *tse4* and *tsi4* (PA2774-75)	This study
Δ*retS* Δ*tse5_tsi5*	Deletion of *retS* (PA4856), *tse5* and *tsi5* (PA2683-84)	This study
Δ*retS* Δ*tse6_tsi6*	Deletion of *retS* (PA4856), *tse6* and *tsi6* (PA0092-93)	This study
Δ*retS* Δ*tse7_tsi7*	Deletion of *retS* (PA4856), *tse7* and *tsi7* (PA0099-0100)	This study
Δ*retS* Δ*tse8_tsi8*	Deletion of *retS* (PA4856), *tse8* and *tsi8* (PA4163-64)	This study
Δ*rsmA* Δ*rsmN* Δ*tse1_tsi1*	Deletion of *rsmA* (PA0905), *rsmN* (PA5183.1), *tse1* and *tsi1* (PA1844-45)	This study
Δ*rsmA* Δ*rsmN* Δ*tse2_tsi2*	Deletion of *rsmA* (PA0905), *rsmN* (PA5183.1), *tse2* and *tsi2* (PA2702-03)	This study
Δ*rsmA* Δ*rsmN* Δ*tse3_tsi3*	Deletion of *rsmA* (PA0905), *rsmN* (PA5183.1), *tse3* and *tsi3* (PA3484-85)	This study
Δ*rsmA* Δ*rsmN* Δ*tse4_tsi4*	Deletion of *rsmA* (PA0905), *rsmN* (PA5183.1), *tse4* and *tsi4* (PA2774-75)	This study
Δ*rsmA* Δ*rsmN* Δ*tse5_tsi5*	Deletion of *rsmA* (PA0905), *rsmN* (PA5183.1), *tse5* and *tsi5* (PA2683-84)	This study
Δ*rsmA* Δ*rsmN* Δ*tse6_tsi6*	Deletion of *rsmA* (PA0905), *rsmN* (PA5183.1), *tse6* and *tsi6* (PA0092-93)	This study
Δ*rsmA* Δ*rsmN* Δ*tse7_tsi7*	Deletion of *rsmA* (PA0905), *rsmN* (PA5183.1), *tse7* and *tsi7* (PA0099-0100)	This study
Δ*rsmA* Δ*rsmN* Δ*tse8_tsi8*	Deletion of *rsmA* (PA0905), *rsmN* (PA5183.1), *tse8* and *tsi8* (PA4163-64)	This study
Δ*rsmA* Δ*tse1_tsi1* Δ*tse3_tsi3*	Deletion of *rsmA* (PA0905), *tse1* and *tsi1* (PA1844-45), *tse3* and *tsi3* (PA3484-85)	Laboratory collection

Strain	**Features**	**Source**
Δ*rsmA* Δ*tssB1* Δ*tssB2* Δ*tssB3* Δ*tse2_tsi2*	Deletion of *rsmA* (PA0905), *tssB1* (PA0083), *tssB2* (PA1657), *tssB3* (PA2365), *tse2* and *tsi2* (PA2702-03)	This study
Δ*rsmA* Δ*tssB1* Δ*tssB2* Δ*tssB3* Δ*tse5_tsi5*	Deletion of *rsmA* (PA0905), *tssB1* (PA0083), *tssB2* (PA1657), *tssB3* (PA2365), *tse5* and *tsi5* (PA2683-84)	This study
Δ*rsmA* Δ*pppA*	Deletion of *rsmA* (PA0905) and *pppA* (PA0075)	Laboratory collection
Δ*rsmA* Δ*pppA* Δ*tssB1*	Deletion of *rsmA* (PA0905), *pppA* (PA0075) and *tssB1* (PA0083)	Laboratory collectio
Δ*retS* Δ*pppA*	Deletion of *retS* (PA4856) and *pppA* (PA0075)	Laboratory collectio
Δ*retS* Δ*pppA* Δ*tssB1*	Deletion of *retS* (PA4856), *pppA* (PA0075) and *tssB1* (PA0083)	Laboratory collectio
Δ*rsmA* Δ*rsmN* Δ*pppA*	Deletion of *rsmA* (PA0905) *rsmN* (PA5183.1) and *pppA* (PA0075)	This study
Δ*rsmA* Δ*rsmN* Δ*pppA* Δ*tssB1*	Deletion of *rsmA* (PA0905), *rsmN* (PA5183.1), *pppA* (PA0075) and *tssB1* (PA0083)	This study
Δ*retS* Δ*pppA* Δ*tse1_tsi1*	Deletion of *retS* (PA4856), *pppA* (PA0075), *tse1* and *tsi1* (PA1844-45)	This study
Δ*retS* Δ*pppA* Δ*tse3_tsi3*	Deletion of *retS* (PA4856), *pppA* (PA0075), *tse3* and *tsi3* (PA3484-85)	This study
Δ*retS* Δ*pppA* Δ*tse4_tsi4*	Deletion of *retS* (PA4856), *pppA* (PA0075), *tse4* and *tsi4* (PA2774-75)	This study
Δ*retS* Δ*pppA* Δ*tse8_tsi8*	Deletion of *retS* (PA4856), *pppA* (PA0075), *tse8* and *tsi8* (PA4163-64)	This study
Δ*retS* *tssB1*-mScarlet-I *tssB2*-sfGFP	Deletion of *retS* (PA4856), C-terminal mScarlet-I fusion to *tssB1* (PA0083) at native locus, C-terminal sfGFP fusion to *tssB2* (PA1657) at the native locus	This study
Δ*tseT_tsiT*	Deletion of *tseT* and *tsiT* (PA3907-08)	This study
Δ*rsmN* Δ*tseT_tsiT*	Deletion of *rsmN* (PA5183.1), *tseT* and *tsiT* (PA3907-08)	This study
Δ*retS* Δ*tseT_tsiT*	Deletion of *retS* (PA4856), *tseT* and *tsiT* (PA3907-08)	This study
Δ*rsmA* Δ*rsmN* Δ*tseT_tsiT*	Deletion of *rsmA* (PA0905), *rsmN* (PA5183.1), *tseT* and *tsiT* (PA3907-08)	This study
Δ*rsmA* Δ*tle1_tli1ab*	Deletion of *rsmA* (PA0905), *tle1*, tli1a and tli1b (PA3290-92)	This study
Δ*rsmA* Δ*tle3_tli3*	Deletion of *rsmA* (PA0905), *tle3* and *tli3* (PA0259-60)	This study

Strain	**Features**	**Source**
Δ*rsmA* Δ*tle4_tli4*	Deletion of *rsmA* (PA0905), *tle4* and *tli4* (PA1509-10)	This study
Δ*rsmA* Δ*pldA_tli5a*	Deletion of *rsmA* (PA0905), *pldA* and *tli5a* (PA3487-88)	This study
Δ*rsmA* Δ*pldB_tli5b1-3*	Deletion of *rsmA* (PA0905), *pldB*, *tli5b1*, *tli5b2* and *tli5b3* (PA5086-89)	This study
Δ*rsmA* Δ*tseT_tsiT*	Deletion of *rsmA* (PA0905), *tseT* and *tsiT* (PA3907-08)	This study
Δ*rsmA* Δ*tseV_tsiV*	Deletion of *rsmA* (PA0905), *tseV* and *tsiV* (PA0821-22)	This study
Δ*rsmA* Δ*vgrG2b_vgrG2bi*	Deletion of *rsmA* (PA0905), *vgrG2b* and *vgrG2bi* (PA0261-62)	This study
Δ*rsmA* Δ*ampDh3_ampDh3i*	Deletion of *rsmA* (PA0905), *ampDh3* and *ampDh3i* (PA0807-08)	This study
Δ*rsmA* Δ*PA5264_PA5265*	Deletion of *rsmA* (PA0905), *PA5264* and *PA5265*	This study
Δ*rsmA* Δ*azu*	Deletion of *rsmA* (PA0905) and *azu* (PA4922)	This study
Δ*retS* Δ*tle1_tli1ab*	Deletion of *retS* (PA4856), *tle1*, *tli1a* and *tli1b* (PA3290-92)	This study
Δ*retS* Δ*pldA_tli5a*	Deletion of *retS* (PA4856), *pldA* and *tli5a* (PA3487-88)	This study
Δ*retS* Δ*pldB_tli5b1-3*	Deletion of *retS* (PA4856), *pldB*, *tli5b1*, *tli5b2* and *tli5b3* (PA5086-89)	This study
Δ*retS* Δ*tseT_tsiT*	Deletion of *retS* (PA4856), *tseT* and *tsiT* (PA3907-08)	This study
Δ*retS* Δ*ampDh3_ampDh3i*	Deletion of *retS* (PA4856), *ampDh3* and *ampDh3i* (PA0807-08)	This study
Δ*rsmA* Δ*PA2066_PA2067*	Deletion of *rsmA* (PA0905), *PA2066* and *PA2067*	Laboratory collection
Δ*rsmA* Δ*PA0256_PA0257*	Deletion of *rsmA* (PA0905), *PA0256* and *PA0257*	Laboratory collection
Δ*retS* Δ*pelA* Δ*pslBCD*	Deletion of *retS* (PA4856), *pelA* (PA3064) and *pslBCD* (PA2232-34)	This study
Δ*retS* Δ*pelA* Δ*pslBCD* Δ*tssB1*	Deletion of *retS* (PA4856), *pelA* (PA3064), *pslBCD* (PA2232-34) and *tssB1* (PA0083)	This study
Δ*retS* Δ*pelA* Δ*pslBCD* Δ*tse5_tsi5*	Deletion of *retS* (PA4856), *pelA* (PA3064), *pslBCD* (PA2232-34), *tse5* and *tsi5* (PA2683-84)	This study
Δ*rsmA* Δ*pelA* Δ*pslBCD*	Deletion of *rsmA* (PA0905), *pelA* (PA3064) and *pslBCD* (PA2232-34)	This study

Strain	Features	Source
Δ*rsmA* Δ*pelA* Δ*pslBCD* Δ*tssB1* Δ*tssB2* Δ*tssB3*	Deletion of *rsmA* (PA0905), *pelA* (PA3064), *pslBCD* (PA2232-34), *tssB1* (PA0083), *tssB2* (PA1657) and *tssB3* (PA2365)	This study
Δ*rsmA* Δ*pelA* Δ*pslBCD* Δ*tseT_tsiT*	Deletion of *rsmA* (PA0905), *pelA* (PA3064), *pslBCD* (PA2232-34), *tseT* and *tsiT* (PA3907-08)	This study
Δ*rsmA* Δ*pelA* Δ*pslBCD* Δ*pldB*_tli5b1-3	Deletion of *rsmA* (PA0905), *pelA* (PA3064), *pslBCD* (PA2232-34), *pldB*, *tli5b1*, *tli5b2* and *tli5b3* (PA5086-89)	This study
Δ*pilA*	Deletion of *pilA* (PA4525)	This study
Δ*fliC*	Deletion of *fliC* (PA1092)	This study
Δ*rsmA* Δ*pilA*	Deletion of *rsmA* (PA0905) and *pilA* (PA4525)	This study
Δ*rsmA* Δ*pilA* Δ*tssB1* Δ*tssB2* Δ*tssB3*	Deletion of *rsmA* (PA0905), *pilA* (PA4525), *tssB1* (PA0083), *tssB2* (PA1657) and *tssB3* (PA2365)	This study
Δ*rsmA* Δ*pilA* Δ*tse3_tsi3*	Deletion of *rsmA* (PA0905), *pilA* (PA4525), *tse3* and *tsi3* (PA3484-85)	This study
Δ*rsmA* Δ*pilA* Δ*tse5_tsi5*	Deletion of *rsmA* (PA0905), *pilA* (PA4525), *tse5* and *tsi5* (PA2683-84)	This study
Δ*rsmA* Δ*pilA* Δ*pldB*_tli5b1-3	Deletion of *rsmA* (PA0905), *pilA* (PA4525), *pldB*, tli5a, tli5b and tli5c (PA5086-89)	This study
Δ*rsmA* Δ*pilA* Δ*tseT_tsiT*	Deletion of *rsmA* (PA0905), *pilA* (PA4525), *tseT* and *tsiT* (PA3907-08)	This study
Δ*retS* Δ*pilA*	Deletion of *retS* (PA4856) and *pilA* (PA4525)	This study
E. coli DH5α	Strain used for cloning. F – endA1 glnV44 thi-. 1 recA1 relA1 gyrA96 deoR nupG purB20 ϕ80dlacZΔM15 Δ(lacZYA-argF)U169, hsdR17(rK - mK +), λ- .	Laboratory collection
E. coli C118lpir	train used for pKNG101 cloning and replication. Δ(ara-leu) araD ΔlacX74 galE galK-phoA20 thi-1 rpsE rpoB argE (ApR) recA1 Rfr λpir	(708)
E. coli 1047	Helper strain used for three-partner conjugation. (Km^R), oriColE1 RK2-Mob+ RK2- Tra+	(709)

Table 2.1: Bacterial strains used in this study. For simplicity, fluorescent tagged strain variant omitted.

Plasmid constructs	Features	Source
pCR-BluntII-TOPO	Blunt sub-cloning vector, Km^R	Invitrogen
pKNG101	Suicide vector, Sm^R	(710)

Plasmid constructs	**Features**	**Source**
pKNG101_*sadC*_ PAK_WT	Suicide vector to restore WT *sadC* (PA4332) from *P. aeruginosa* PAK, Sm^R	This study
pKNG101_Δ*sadC*_ PAK	Suicide vector to delete *sadC* (PA4332) from *P. aeruginosa* PAK, Sm^R	Laboratory collection
pKNG101_Δ*rsmN*	Suicide vector to delete *rsmN* (PA5183.1) from *P. aeruginosa*, Sm^R	This study
pKNG101_Δ*tssB1*	Suicide vector to delete *tssB1* (PA0083) from *P. aeruginosa*, Sm^R	Laboratory collection
pKNG101_Δ*tssB2*	Suicide vector to delete *tssB2* (PA1657) from *P. aeruginosa*, Sm^R	Laboratory collection
pKNG101_Δ*tssB3*	Suicide vector to delete *tssB3* (PA2365) from *P. aeruginosa*, Sm^R	Laboratory collection
pKNG101_Δ*tse1tsi1*	Suicide vector to delete *tse1* and *tsi1* (PA1844-45) from *P. aeruginosa*, Sm^R	Laboratory collection
pKNG101_Δ*tse2tsi2*	Suicide vector to delete *tse2* and *tsi2* (PA2702-03) from *P. aeruginosa*, Sm^R	Laboratory collection
pKNG101_Δ*tse3tsi3*	Suicide vector to delete *tse3* and *tsi3* (PA3484-85) from *P. aeruginosa*, Sm^R	Laboratory collection
pKNG101_Δ*tse4tsi4*	Suicide vector to delete *tse4* and *tsi4* (PA2774-75) from *P. aeruginosa*, Sm^R	Laboratory collection
pKNG101_Δ*tse5tsi5*	Suicide vector to delete *tse5* and *tsi5* (PA2683-84) from *P. aeruginosa*, Sm^R	This study
pKNG101_Δ*tse6tsi6*	Suicide vector to delete *tse6* and *tsi6* (PA0092-93) from *P. aeruginosa*, Sm^R	This study
pKNG101_Δ*tse7tsi7*	Suicide vector to delete *tse7* and *tsi7* (PA0099-0100) from *P. aeruginosa*, Sm^R	This study
pKNG101_Δ*tse8tsi8*	Suicide vector to delete *tse8* and *tsi8* (PA4163-64) from *P. aeruginosa*, Sm^R	This study
pKNG101_Δ*tle1tli1ab*	Suicide vector to delete *tle1*, *tli1a* and *tli1b* (PA3290-92) from *P. aeruginosa*, Sm^R	Laboratory collection
pKNG101_Δ*tle3tli3*	Suicide vector to delete *tle3* and *tli3* (PA0259-60) from *P. aeruginosa*, Sm^R	Laboratory collection
pKNG101_Δ*tle4tli4*	Suicide vector to delete *tle4* and *tli4* (PA1509-10) from *P. aeruginosa*, Sm^R	Laboratory collection
pKNG101_Δ*pldAtli5a*	Suicide vector to delete *pldA* and *tli5a* (PA3487-88) from *P. aeruginosa*, Sm^R	Laboratory collection
pKNG101_Δ*pldBtli5b1-3*	Suicide vector to delete *pldB*, *tli5b1*, *tli5b2* and *tli5B3* (PA5086-89) from *P. aeruginosa*, Sm^R	Laboratory collection
pKNG101_Δ*tseTtsiT*	Suicide vector to delete *tseT* and *tsiT* (PA3907-08) from *P. aeruginosa*, Sm^R	This study
pKNG101_Δ*tseVtsiV*	Suicide vector to delete *tseV* and *tsiV* (PA0821-22) from *P. aeruginosa*, Sm^R	This study

Plasmid constructs	**Features**	**Source**
pKNG101_Δ*vgrG2b*_ *vgrG2bi*	Suicide vector to delete *vgrG2b* and *vgrG2bi* (PA0261-62) from *P. aeruginosa*, Sm^R	Laboratory collection
pKNG101_Δ*ampDh3*_ *ampDh3i*	Suicide vector to delete *ampDh3* and *ampDh3i* (PA0807-08) from *P. aeruginosa*, Sm^R	This study
pKNG101_Δ*azu*	Suicide vector to delete *azu* (PA4922) from *P. aeruginosa*, Sm^R	This study
pKNG101_*tssB1* :mScarlet-I	Suicide vector to deliver *tssB1*-mScarlet-I fusion into *P. aeruginosa*, Sm^R	Laboratory collection
pKNG101_*tssB2* :sfGFP	Suicide vector to deliver *tssB2*-sfGFP fusion into *P. aeruginosa*, Sm^R	Laboratory collection
pKNG101_Δ*pilA*	Suicide vector to delete *pilA* (PA4525) from *P. aeruginosa*, Sm^R	This study
pKNG101_Δ*fliC*	Suicide vector to delete *fliC* (PA1092) from *P. aeruginosa*, Sm^R	This study
pKNG101_Δ*pppA*	Suicide vector to delete *pppA* (PA0075) from *P. aeruginosa*, Sm^R	Laboratory collection
pKNG101_Δ*pelA*	Suicide vector to delete *pelA* (PA3064) from *P. aeruginosa*, Sm^R	This study
pKNG101_Δ*pslBCD*	Suicide vector to delete *pslBCD* (PA2232-34) from *P. aeruginosa*, Sm^R	This study
pUCP22	Plasmid containing promoterless GFPmut3b, Gm^R	(711)
pUCP22_*tssA1*_ transcrip.	Plasmid containing GFPmut3b under *tssA1* transcirptional control, Gm^R	This study
pUCP22_*tssA1*_transl.	Plasmid containing GFPmut3b under *tssA1* translational control, Gm^R	This study
pUCP22_*tssA2*_ transcrip.	Plasmid containing GFPmut3b under *tssA2* transcirptional control, Gm^R	This study
pUCP22_*tssA2*_transl.	Plasmid containing GFPmut3b under *tssA2* translational control, Gm^R	This study
pUCP22_*tssB3*_ transcrip.	Plasmid containing GFPmut3b under *tssB3* transcirptional control, Gm^R	This study
pUCP22_*tssB3*_transl.	Plasmid containing GFPmut3b under *tssB3* translational control, Gm^R	This study
miniCTX-pX2-*mCherry*	mini-CTX suicide vector carrying mCherry under pX2 promoter (712), Tc^R	Knut Drescher Lab, Biozentrum University of Basel
miniCTX-pX2-*sfGFP*	mini-CTX suicide vector carrying sfGFPunder pX2 promoter, Tc^R	Knut Drescher Lab, Biozentrum University of Basel

Plasmid constructs	Features	Source
pCdrA-EGFP	C-di-GMP reporter of cdrA promoter in front of *egfp* in pPROBETT backbone, Tc^R	(713)
miniCTX-pARA	mini-CTX suicide vector with *araC* inducible promoter, empty vector Tc^R	Laboratory collection
miniCTX-pARA-PA2133	mini-CTX suicide vector with *araC* inducible promoter, carrying PA2133 Tc^R	Laboratory collection

Table 2.2: Plasmids used in this study.

Name	Sequence (5' - 3')	Description
Vector primers		
UpKn	CTCATCAGTGAAATCCAGGG	Primer flanking MCS of pKNG101
RpKn	CATATCACAACGTGCGTGGA	Primer flanking MCS of pKNG101
M13 Fw	TGTAAAACGACGGCCAGT	M13 forward sequencing primer
M13 Rw	CAGGAAACAGCTATGACC	M13 reverse sequencing primer
OAL1604	CGCGCGTAATACGACTCACT	Primer flanking MCS of mini-CTX plasmids
OAL1605	CCGTCCTTGCTGAATTAGCTT	Primer flanking MCS of mini-CTX plasmids
OAL5995	TGTTCTTTACGATGCCA	Primer flanking MCS of pUCP22 (to pair with M13Fw)
Construction of mutator plasmids and screening of gene deletions		
OAL3239	ATGATGGGCCCGCTCCAGGTTGAG CTGATTGAGGC	Constructing mutator for *rsmN* deletion P1 (*Sma*I)
OAL3240	CAACTCGTCGAAACCCATGTTCCG CGT	Constructing mutator for *rsmN* deletion P2
OAL3241	ATGGGTTTCGACGAGTTGAAGACG GCACCG	Constructing mutator for *rsmN* deletion P3
OAL3242	ATCATGGATCCTAATCGCGTTCGG CCTGCTG	Constructing mutator for *rsmN* deletion P1 (*Bam*HI)
OAL6642	GCTTGCCGAAGCTGATGTGT	Screening *rsmN* deletion
OAL6643	CTCGACGCTGGAGCAATGTT	Screening *rsmN* deletion
OAL2661	CGACCCCACCTTCCGTATCAAC	Screening *tssB1* deletion / fluorescent fusion
OAL2662	CGATGTAGCGGGAGTCCTCG	Screening *tssB1* deletion / fluorescent fusion
OAL1594	CAGGCGATGCGGGAAGTCGAAA	Screening *tssB2* deletion / fluorescent fusion
OAL1595	TCTGCCACTTGGCGAACTGC	Screening *tssB2* deletion / fluorescent fusion
OAL3149	GAAGGACTCCGACTCGATGAAC	Screening *tssB3* deletion
OAL3150	GACGTTCGACAGCTTCTCCA	Screening *tssB3* deletion

Name	**Sequence (5' - 3')**	**Description**
OAL1295	CACTTGGCGGTAAAGATCG	Screening *tse1tsi1* deletion
OAL1296	GATGGCCTGGATCACGTC	Screening *tse1tsi1* deletion
OAL1283	GCTGCTGCTCGGCCTGTTC	Screening *tse2tsi2* deletion
OAL1284	AGGCGCCTGAACTGTTCGT	Screening *tse2tsi2* deletion
OAL1345	CCATTACGCCGAACTCACC	Screening *tse3tsi3* deletion
OAL4465	CGGGGTGAAGGCGAGGAAGG	Screening *tse3tsi3* deletion
OAL4649	CCGACGCGGCGTAATAGG	Screening *tse4tsi4* deletion
OAL4650	CTGGATGCCCGGCCAGGC	Screening *tse4tsi4* deletion
OAL6254	ATTATAGTCGACCACGGGTCGCCT CGATCTTCACC	Constructing mutator for *tse5tsi5* deletion P1 (*Sal*I)
OAL6255	ATGAGCGGCGACGAGTGAGGCCGA CCC	Constructing mutator for *tse5tsi5* deletion P2
OAL6256	TCACTCGTCGCCGCTCATCTATCC ATCCTTCCTTG	Constructing mutator for *tse5tsi5* deletion P3
OAL6257	ATTATAGGGCCCGCAACGAGACGG TCAGGATCGGC	Constructing mutator for *tse5tsi5* deletion P4 (*Apa*I)
OAL6258	CAGCACGTCGGGGTGATC	Screening *tse5tsi5* deletion
OAL6259	ACGAGACGGTGCATGTGAAG	Screening *tse5tsi5* deletion
OAL6260	ATTATAGGATCCCAACAAGAGCAT CGGCCACGAC	Constructing mutator for *tse6tsi6* deletion P1 (*Bam*HI)
OAL6261	ATGGATGCGCTGCCCTGAGCGCAA CACC	Constructing mutator for *tse6tsi6* deletion P2
OAL6262	TCAGGGCAGCGCATCCATGCGTCG GTAC	Constructing mutator for *tse6tsi6* deletion P3
OAL6263	ATTATAGGGCCCCAGGAAAGCCTT GATTCGCGAGC	Constructing mutator for *tse6tsi6* deletion P4 (*Apa*I)
OAL3352	AGTTATACATCCACGCCGAGC	Screening *tse6tsi6* deletion
OAL3353	GAAAGGGGAGATGCGTGACA	Screening *tse6tsi6* deletion
OAL6264	ATTATAGGATCCCAACGGCTTCAT TCCCGGCG	Constructing mutator for *tse7tsi7* deletion P1 (*Bam*HI)
OAL6265	TGCTGGCCGTTGGCCATCAGGCAG CC	Constructing mutator for *tse7tsi7* deletion P2
OAL6266	ATGGCCAACGGCCAGCAATGGACG CG	Constructing mutator for *tse7tsi7* deletion P3
OAL6267	ATTATAGGGCCCGCCAAGGGCGGA CAGCAG	Constructing mutator for *tse7tsi7* deletion P4 (*Apa*I)
OAL3307	TGGAAGGCGAGCTGGGAC	Screening *tse7tsi7* deletion
OAL3308	TGCCAGGCGAGCAGCA	Screening *tse7tsi7* deletion
OAL6268	ATTATAGGATCCCGAGAGCAATCC GCGCAGC	Constructing mutator for *tse8tsi8* deletion P1 (*Bam*HI)
OAL6269	TCAGTCGCGCTCGATCATGCTGTC ACCGCC	Constructing mutator for *tse8tsi8* deletion P2

Name	**Sequence (5' - 3')**	**Description**
OAL6270	ATGATCGAGCGCGACTGAGCGCTTGCC	Constructing mutator for *tse8tsi8* deletion P3
OAL6271	ATTATAGGGCCCCGCATCGGCTACATGGTCCTG	Constructing mutator for *tse8tsi8* deletion P4 (*Apa*I)
OAL6272	CTGCACAGGTTGACGATGC	Screening *tse8tsi8* deletion
OAL6273	CGACAGCGAGTTCCACTACG	Screening *tse8tsi8* deletion
OAL4321	GCGCTGTTCAAATTGCTGGAG	Screening *tle1tli1ab* deletion
OAL4322	AGAACAGGCCAGGCATTCTAG	Screening *tle1tli1ab* deletion
OAL3293	CCGGGAAAGACGTTGAAGGA	Screening *tle3tli3* deletion
OAL3294	GTAGGTTCGGATGGCGGTAG	Screening *tle3tli3* deletion
OAL2586	GTTTTCAGCGACCCCTACCTC	Screening *tle4tli4* deletion
OAL2053	CCGCAGCAAACCCTCCAG	Screening *tle4tli4* deletion
OAL3231	CCGGGCAGAAGATGGTGATC	Screening *pldAtli5a* deletion
OAL3232	AGGACGATGCAATTGGTGGT	Screening *pldAtli5a* deletion
OAL3237	GAACTGGCCACCTTGCATTC	Screening *pldBtli5b1-3* deletion
OAL3238	GGGCGACGAGATCCATTTCA	Screening *pldBtli5b1-3* deletion
OAL6274	ATTATAGTCGACGCGCTGGAACAGGTCATGACC	Constructing mutator for *tseTtsiT* deletion P1 (*Sal*I)
OAL6275	TCAGCCGCGGCCGCTCATGCCGGTCTC	Constructing mutator for *tseTtsiT* deletion P2
OAL6276	ATGAGCGGCCGCGGCTGACGACGTACG	Constructing mutator for *tseTtsiT* deletion P3
OAL6277	ATTATAGGGCCCGGCCTGTAGGGCGAATAACCG	Constructing mutator for *tseTtsiT* deletion P4 (*Apa*I)
OAL6278	CATGGCCTCCTGGCTGTG	Screening *tseTtsiT* deletion
OAL6279	GCCGGGTGGCGATGAAG	Screening *tseTtsiT* deletion
OAL6548	ATTATAGGATCCCGAGTCTCGCACCGAGG	Constructing mutator for *tseVtsiV* deletion P1 (*Bam*HI)
OAL6549	ATGACCAAGCGCCTGTAGGGGCTTACG	Constructing mutator for *tseVtsiV* deletion P2
OAL6550	CTACAGGCGCTTGGTCATGTCGTAGCTGACC	Constructing mutator for *tseVtsiV* deletion P3
OAL6551	ATTATAACTAGTCCTTAACCGCAACAGCGTG	Constructing mutator for *tseVtsiV* deletion P4 (*Spe*I)
OAL6552	TCACCTTTGATAGCATCCTGGC	Screening *tseVtsiV* deletion
OAL6553	GTGACGCTGGGTAGTATCGG	Screening *tseVtsiV* deletion
OAL3320	TGAACTAGTGTAACGCTTGCGGATGATCTTG	Screening *vgrG2b vgrG2bi* deletion
OAL3321	CCCGACGACATTGATGGTGT	Screening *vgrG2b vgrG2bi* deletion
OAL6824	ATTATAGGATCCAGTAGCCGCTCTGTCGAGGGT	Constructing mutator for *ampDh3ampDh3i* deletion P1 (*Bam*HI)

Name	Sequence (5' - 3')	Description
OAL6825	TCAGCCATCGAGACCGCGATAGCT GTTGTAGTCGATGGTCAGCATGG	Constructing mutator for *ampDh3ampDh3i* deletion P2
OAL6826	GACTACAACAGCTATCGCGGTCTC GATGGCTGAGCATTG	Constructing mutator for *ampDh3ampDh3i* deletion P3
OAL6827	ATTATAACTAGTAACGCGGCGATC CTGATCGTC	Constructing mutator for *ampDh3ampDh3i* deletion P4 (*Spe*I)
OAL6671	CCGCTGGCACGACGCTAG	Screening *ampDh3 ampDh3i* deletion
OAL6672	ACCTGGCGATCGGCATCGT	Screening *ampDh3 ampDh3i* deletion
OAL6673	ATTATAACTAGTTGGCCTACAACA AGGACAACCAGG	Constructing mutator for PA5264 PA5265 deletion P1 (*Spe*I)
OAL6674	AGCGGATTCGAGCACTGATGCTGA GTTATTCCGC	Constructing mutator for PA5264 PA5265 deletion P2
OAL6675	TCAGTGCTCGAATCCGCTCATGCC TCGCTC	Constructing mutator for PA5264 PA5265 deletion P3
OAL6676	ATTATAGGATCCACATCGAGCACG ACCAGAAGATCC	Constructing mutator for PA5264 PA5265 deletion P4 (*Bam*HI)
OAL6677	TCATCGACCTGCCCGACC	Screening PA5264 PA5265 deletion
OAL6678	AAGACCCGCAGCGTCTTCA	Screening PA5264 PA5265 deletion
OAL6408	ATTATAATGCATCCTGGAACAACT GGCCGGC	Constructing mutator for *azu* deletion P1 (*Nsi*I)
OAL6409	ATGCTACGTCTGAAGTGATGCGCG AGCG	Constructing mutator for *azu* deletion P2
OAL6410	TCACTTCAGACGTAGCATGGAGCA GCCTC	Constructing mutator for *azu* deletion P3
OAL6411	ATTATAGGATCCCGATCTCGGCCT CCTGCAGG	Constructing mutator for *azu* deletion P4 (*Bam*HI)
OAL6412	AGCTGTATCCCTGCGAAGG	Screening *azu* deletion
OAL6413	GGCAAGGGCCAGAAGATCG	Screening *azu* deletion
OAL6941	ATTATAACTAGTCGGGAGCGCTAC AGTCGATGTG	Constructing mutator for restoring WT PAK *sadC* P1 (*Spe*I)
OAL6922	ATTATAGGATCCCCGGACGAACAC GGTGACGATC	Constructing mutator for restoring WT PAK *sadC* P4 (*Bam*HI)
OAL614	ATGGTCGGTACGGTTTTCAG	Screening *sadC* deletion / insertion
OAL615	CTCCACAGCAGCAGGTGCT	Screening *sadC* deletion / insertion
OAL6508	ATTATAGGATCCCGCATAGCACCC GGCAAG	Constructing mutator for *pilA* deletion P1 (*Bam*HI)
OAL6509	ATGAAAGCTGATAACTAAGGTGAT CGAAGGTG	Constructing mutator for *pilA* deletion P2
OAL6510	CTTAGTTATCAGCTTTCATGAATC TCTCCGT	Constructing mutator for *pilA* deletion P3
OAL6511	ATTATAGGTACCGTGTTGGCGGAC CAGCT	Constructing mutator for *pilA* deletion P4 (*Kpn*I)

Name	Sequence (5' - 3')	Description
OAL6512	GCCACAACCATCGCATCGG	Screening *pilA* deletion
OAL6513	CGACCAGAATCGCTTCGGTC	Screening *pilA* deletion
OAL6742	ATTATAATGCATCGTTCCAGGGAC TGGCTGGA	Constructing mutator for *fliC* deletion P1 (*Nsi*I)
OAL6743	TTAGCGCAGAAGGGCCATGGTGAT TTCCTCCAA	Constructing mutator for *fliC* deletion P2
OAL6744	ATGGCCCTTCTGCGCTAAGCCCGG GAAC	Constructing mutator for *fliC* deletion P3
OAL6745	ATATTAGGATCCAGGGCAAGCACC ATGCCAAGT	Constructing mutator for *fliC* deletion P4 (*Bam*HI)
OAL6746	TGGAGTACGGCGTGCTCG	Screening *fliC* deletion
OAL6747	CAGATCGGTGTAATCGGTCGAGC	Screening *fliC* deletion
OAL2645	AAGAGCCGGGTCGTGTCCGG	Screening *pppA* deletion
OAL2646	CGGGTCCTTGGCCAGCAACT	Screening *pppA* deletion
OAL6396	ATTATAATGCATCGCCAGGTCCGG CGCGTC	Constructing mutator for *pelA* deletion P1 (*Nsi*I)
OAL6397	ATGCGGTTCCAGGTGCGCGATGGC CAAC	Constructing mutator for *pelA* deletion P2
OAL6398	GCGCACCTGGAACCGCATGCCCAG CC	Constructing mutator for *pelA* deletion P3
OAL6399	ATTATAGGATCCGCGCGTGCGCCA AATG	Constructing mutator for *pelA* deletion P4 (*Bam*HI)
OAL6400	CCTGTTCGCCGCGCTC	Screening *pelA* deletion
OAL6401	CGCATGTTCTATTGGTCCACACC	Screening *pelA* deletion
OAL3197	GACTCCAAGGGGCCGGTGC	Constructing mutator for *pslBCD* deletion P1
OAL3198	TCAGCGATCGGCGTTCATCAGTAG ACT	Constructing mutator for *pslBCD* deletion P2
OAL3199	ATGAACGCCGATCGCTGAGGAGCG ACA	Constructing mutator for *pslBCD* deletion P3
OAL3200	AGGCGCTCGACCGCGGTGG	Constructing mutator for *pslBCD* deletion P4
OAL3196	GCGGCAATTGCCGGTGAACG	Screening *pslBCD* deletion
OAL3201	GCTCGGACAGGTCCTGCAGG	Screening *pslBCD* deletion
Construction of reporter plasmids		
OAL5919	TAATAAGGTACCGGTCAGCTGTCC CTGGTCCAGT	Constructing transcriptional / trasnational fusion for *tssA1* promoter (*Kpn*I)
OAL6365	ATTATAGGATCCGGCAGCCAGCAA AACGGGTAC	Constructing transcriptional fusion for *tssA1* promoter (*Bam*HI)

Name	Sequence (5' - 3')	Description
OAL5921	TAATAAGGTACCGCGCAGTAGTGT TCAGGCCAGT	Constructing transcriptional / trasnational fusion for *tssA2* promoter (*Kpn*I)
OAL6366	ATTATAGGATCCATGCGAGGAGAG CTTGCTCGAAT	Constructing transcriptional fusion for *tssA2* promoter (*Bam*HI)
OAL5923	TAATAAGGTACCCTCCATACCGCG AACTGCTGCC	Constructing transcriptional / trasnational fusion for *tssB3* promoter (*Kpn*I)
OAL6367	ATTATAGGATCCGTCCAGCTTGTG CTGCGTACTC	Constructing transcriptional fusion for *tssB3* promoter (*Bam*HI)
OAL6530	TTTACGCATGGCAGCCAGCAAAAC GG	Constructing translational fusion for *tssA1* promoter P2
OAL6531	CTGGCTGCCATGCGTAAAGGAGAA GAACTTTTCAC	Constructing translational fusion for *tssA1* promoter P3
OAL6532	GAGTCAGCTCAGCTAATAAGCTTA TTTGTAT	Constructing translational fusion for *tssA1* promoter P4
OAL6533	ATTATAGCATGCAATGCGAGGAGA GCTTGCTC	Constructing translational fusion for *tssA2* promoter (*Sph*I)
OAL6534	ATTATAGCATGCGGTCCAGCTTGT GCTGCG	Constructing translational fusion for *tssB3* promoter (*Sph*I)

Table 2.3: Primers used in this study. Enzymes indicated, where primers contain restriction digestion sites.

Bacteria were cultured in Lysogeny Broth (LB - Miller) (VWR), LB agar (1.2% w/v bacteriological agar) (VWR), or Tryptic Soy Broth (TSB) (Sigma). Unless specified otherwise, bacteria were grown at 37^{o}C. For long term storage strains were prepared with final concentration of 40% (v/v) glycerol and stored at -80^{o}C. Overnight cultures for use in experiments were inoculated directly from glycerol stocks. Where appropriate antibiotic supplement was added in the following concentrations - Streptomycin (2000μg/mL or 50μg/mL), Kanamycin (50μg/mL), Gentamicin (50μg/mL or 25μg/mL), Tetracycline (150μg/mL or 15μg/mL), for *E. coli* and *P. aeruginosa* correspondingly.

2.2 DNA manipulation

For purposes of use as template for construct cloning, *P. aeruginosa* PAO1 or PAK genomic DNA was used after isolation using PureLink Genomic DNA minikit (Invitrogen). Plasmids were purified using QIAprep spin miniprep kit (Qiagen). PCR and digestion products were purified using QIAquick PCR & Gel Cleanup kits (Qiagen). All of these used accordingly to manufacturers directions and purified DNA was eluted in autoclaved distilled dionised water. Nanodrop spectrophotometer was used to measure DNA concentrations.

Oligonucleotides used for gene cloning or screening purposes were purchased from Sigma. DNA fragments used for construction of mutators and expression reporter plasmids were cloned using KOD Hot Start DNA Polymerase (Novagen). Zero Blunt TOPO kit (Invitrogen) was used for ligation and further amplification of PCR products. Restriction enzymes - *Apa*I, *Bam*HI, *Blp*I, *Hind*III, *Kpn*I, *Nsi*I, *Sac*I, *Sal*I, *Spe*I, *Sph*I, *Xba*I by New England Biolabs (NEB) were used, with all reaction digestions performed according to manufacturers instructions. Constructs were ligated using T4 DNA ligase (NEB) according to manufacturers protocol. Sequences of plasmid constructs were verified using sequencing performed by GATC Biotech. Screening of mutant strains was performed via colony PCR using Taq polymerase. Gel electrophoresis for PCR samples were run on 1%(w/v) Trisacetate-EDTA (TAE) agarose gels, using SYBR Safe DNA Gel Stain for visualisation of DNA and NEB 1kb Plus DNA Ladder for size standards. DNA gels were imaged using the BioRad ChemiDoc XRS+.

2.3 Plasmid delivery

2.3.1 Transformation into competent cells

Plasmids were delivered to chemically competent *E. coli* via heat-shock transformation. To prepare competent cells for transformation, an *E. coli* overnight culture was sub-cultured into 50mL of LB with starting density of OD_{600} = 0.1 and grown at 37^{o}C until OD_{600} =0.6 to

OD_{600} =0.8 was reached. Cells are harvested via centrifugation (4000g, 4^{o}C, 10min). The pellet was resuspended in 25mL of ice-cold 50mM $CaCl_2$ + 15% (w/v) glycerol, incubated on ice for 30min and subsequently centrifuged (4000g, 4^{o}C, 10min). The pellet was resuspended in 2.5mL of ice-cold 50mM $CaCl_2$ + 15% (w/v) glycerol, aliquoted, snap frozen in liquid nitrogen and stored at -80^{o}C.

For heat-shock transformation, 50μL of competent cells are mixed with 10μL of plasmid ligation mix, Zero Blunt TOPO ligation mix or approx. 10ng of purified plasmid DNA. Competent cell and DNA mixtures were incubated on ice for 30min, heated at 42^{o}C for 2min (CC118λpir) or 45s (DH5α) and returned to ice for 1min. After heat shock bacteria are resuspended in 1mL of LB media and incubated with agitation at 37^{o}C for 1h. After recovery, *E. coli* cells were plated on LB agar supplemented with appropriate antibiotics and grown at 37^{o}C overnight.

2.3.2 Three partner conjugation

Plasmids were delivered into *P. aeruginosa* using three partner conjugation. Briefly, 20μL of overnight cultures of the *E. coli* donor (containing pKNG101 or miniCTX plasmids) and the helper strain 1047 (containing self-tansmissible pRK2013 (709)) were spotted on LB plate, dried and incubated at 37^{o}C for 2h. Aliquot of overnight culture of *P. aeruginosa* reciever strain was incubated at 43^{o}C for 2h. Subsequently, 40μL of reciever bacteria were spotted on the LB agar plate with donor-helper *E. coli* mix, after drying bacterial spots were incubated at 37^{o}C for 4h. After incubation, donor-helper-reciever mix was scraped up using a sterile 10μL inoculation loop, suspended in 1mL of TSB and incubated at 37^{o}C for 1h. Recovered bacteria mix was plated on Vogel-Bonner minimal (VBM) agar supplemented with antibiotics and grown at 37^{o}C until individual colonies appear (between 16h and 48h). Vogel-Bonner minimal medium [100 ml 10x stock: 200 mM magnesium sulfate heptahydrate, 2 g anhydrous citric acid, 10 g potassium phosphate dibasic and 3.5 g ammonium sodium phosphate dibasic tetrahydrate] was

pH adjusted to 7.0 and filter sterilised. To prepare VBM plates, concentrated VBM stock was added to 2% (w/v) bacteriological agar that was autoclaved prior to use.

2.3.3 Electroporation

Electroporation was used to deliver pUCP22 and CdrA reporter plasmids into *P. aeruginosa*. To prepare electrocompetent cells, 1.5mL aliquots of *P. aeruginosa* overnight cultures were pelleted (3min 8000rpm). Bacteria were washed twice in 300mM sucrose solution and subsequently resuspended in 1mL of 300mM sucrose. Purified plasmid and 400μL of electrocompetent cells were mixed and transferred to electroporation cuvette (BioRad Gene Pulser 0.2cm gap). After applying 2.5kV, 200Ω, 25μF pulse, 600μL of TSB was added and bacteria incubated at 37^{o}C for 1h. Recovered bacteria were plated on LB agar plates supplemented with an antibiotic.

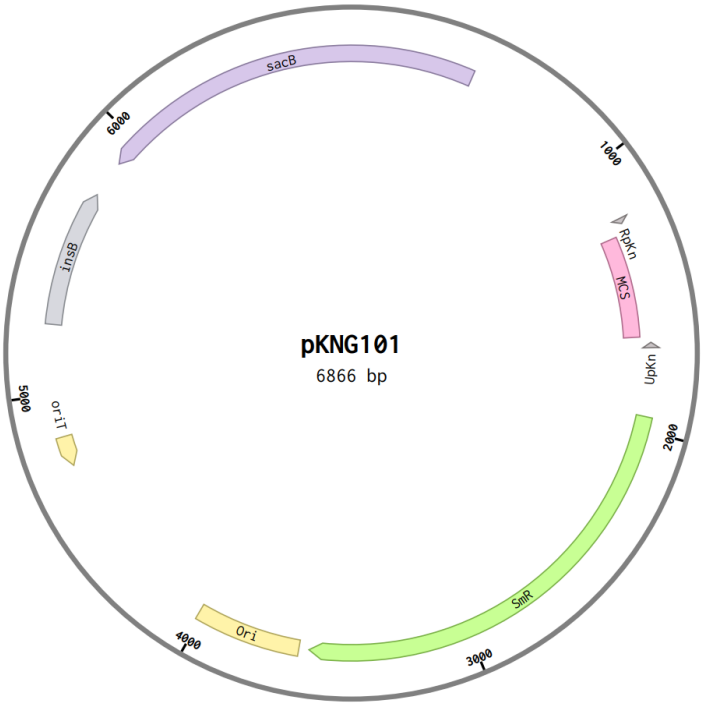

Figure 2.1: **Map of the pKNG101 plasmid.**
Plasmid features drawn to scale with locations of genes and features shown: Ori, origin of replication; oriT, origin of transfer; sacB, sucrose sensitivity inducing gene; SmR, streptomycin resistance gene; MCS, multi cloning site; UpKn / RpKn, primers for screening MCS inserts.

2.4 *P. aeruginosa* genomic manipulation

2.4.1 Gene deletions and fusions

Gene deletions and insertions of chimeric genes were performed though allelic exchange using a suicide vector pKNG101 (308) (Figure 2.1). Use of this plasmid allows to construct gene deletions or insert protein-fluorophore fusions in a specific site of interest and subsequently excise the vector resulting in seamless allele exchange (Figure 2.2). Vector integration into genome is guided by approximately 500bp upstream and 500bp downstream regions flanking sequence of interest. Deletions were constructed in frame leaving 9bp from the begging of the gene and 9bp from the end of the gene including the STOP codon, when deleting genes with overlapping open reading frames, exception was made to maintain full sequence of the overlapping gene. The constructs used for allelic exchange were assembled using splicing by overlap PCR.

pKNG101 encodes streptomycin resistance gene and *Bacillus subtilis* derived *sacB* gene that introduces sucrose sensitivity. Plasmid was delivered via three partner conjugation as described above and incorporation in genome was selected for by growth on streptomycin containing LB agar. Subsequently colonies are streaked on 20% (w/v) sucrose containing LB agar and grown at room temperature for 48 to 72h. This counter-selection process promotes excision of the vector, the resulting in strains that revert to the wild type genotype or contain only the alternative allele. Bacteria growing on sucrose containing media are replica-patched on LB and LB_{Sm2000} and screened via colony PCR to confirm the strain genotypes and ensure that new strain isolates are not streptomycin resistant.

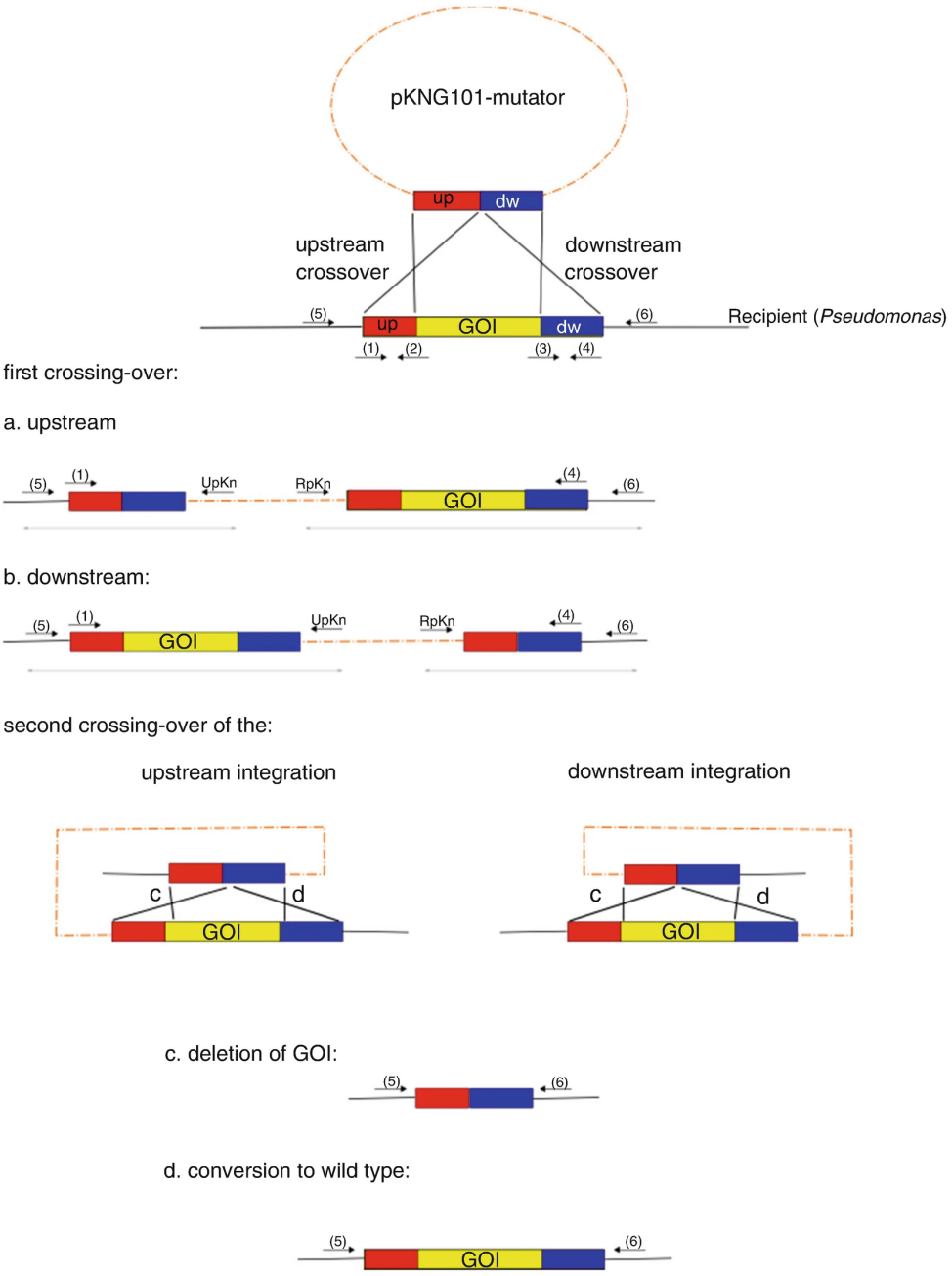

Figure 2.2: **Schematic of allelic exchange using pKNG101 plasmid.**
pKNG101 suicide vector carries an alternate deletion allele. Alternate allele constructed such that sequence of interest is flanked by 500bp upstream and downstream fragments that guide site specific integration. Primers used for construct assembly and screening labelled with numbers (1 to 4 for mutator construction, 5 and 6 for screening at the final modification stage). Vector primers designated as UpKn and RpKn. pKNG101 carrying deletion allele was delivered to *P. aeruginosa* through three partner conjugation. First crossover event was selected for through screening for antibiotic resistance and occurs upon plasmid integration into bacterial chromosome. Firs crossover even can can occur in upstream and downstream orientation. Following sucrose sensitivity mediate counter selection, second crossover event results in only one of the alleles remaining in the genome and only wild-type gene or gene deletion remains. This can be subsequently confirmed through a PCR screen. Adapted from (714), with a permission from Springer Nature.

2.4.2 Fluorescent tagging

Prior to use mixed macrocolony microscopy assay *P. aeruginosa* strains were tagged with fluorescent tags that are chromosomally integrated and constitutively expressed under pX2 promoter (712). This was done using miniCTX plasmids encoding sfGFP(pNUT1295) or mCherry (pNUT1108) (Figure 2.3) that were provided by Knut Drescher lab (Biozentrum Basel).

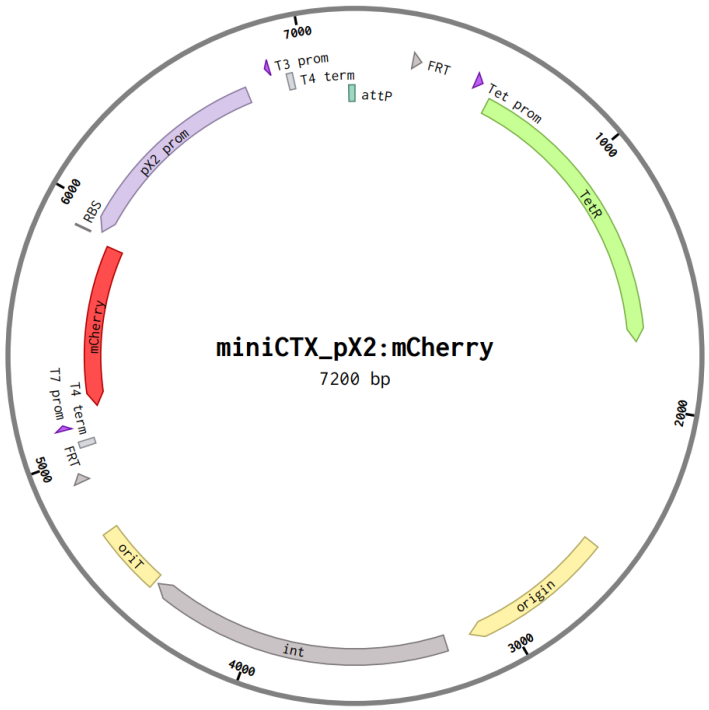

Figure 2.3: **Map of the miniCTX-pX2:mCherry plasmid.**
Plasmid features drawn to scale with locations of genes and features shown: Ori, origin of replication; oriT, origin of transfer; attP, fCTX attachment site; Int, fCTX integrase encoding gene; T3 prom / T7 prom, promoter sites; T4 term, T4 transcription terminator; FRT, Flp recombinase target site; TetR, Tetracycline resistance gene; Tet prom, tetracycline promoter; pX2 prom, promoter controlling fluorophore expression; RBS, Ribosome Binding Site; mCherry, gene encoding mCherry. sfGFP encoding miniCTX vector is equivalent with only difference being the fluorophore encoded.

2.4.3 Measuring gene expression using plasmid based reporters

Plasmid based transcriptional reporter fusions were used to asses gene expression levels. Promoter fragment region of +30bp to -500bp upstream of *tssA1*, *tssA2* and *tssB3* were amplified by PCR using *P. aeruginosa* PAO1 genomic DNA as template. Promoter fragments were placed into a pUCP22 plasmid (711) upstream of a gene encoding a stable green fluorescent protein

variant (GFPmut3b (715)) (Figure 2.4). Construct sequences were validated by sequencing and plasmids were delivered into *P. aeruginosa* by electroporation.

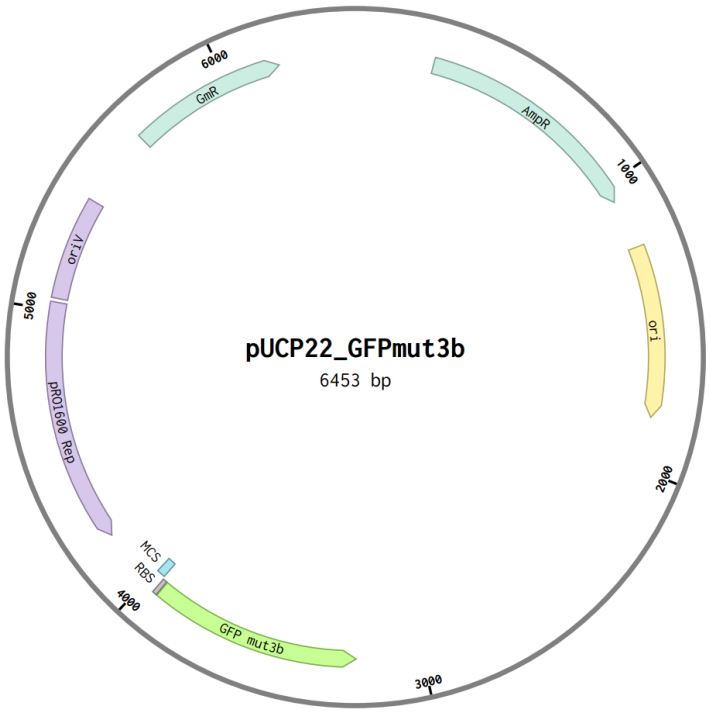

Figure 2.4: **Map of the pUCP22 plasmid.**
Plasmid features drawn to scale with locations of genes and features shown: Ori, origin of replication; pRO1600 Rep, *P. aeruginosa* pRO1600 plasmid replication protein; oriV, pRO1600 Rep dependent replication site; GmR, gentamicin resistance gene; AmpR, ampicillin resistance gene; RBS, ribosome binding site; MCS, multi cloning site; GFPmut3b, green fluorescent protein reporter.

Fluorescent reporter measurements were performed by growing *P. aeruginosa* strains statically in 48-well plates. *P. aeruginosa* overnight cultures were harvested by centrifugation (3min 8000rpm) and both supernatant and biofilm layer were discarded. Biofilm-free pellet was washed by re-suspending in PBS and subsequent centrifugation. After washing, pellet was resuspended in fresh PBS and bacterial concentration adjusted to $OD_{600} = 1.0$. 48-well plates containing 360μL of LB+ $Gent_{50}$ were inoculated with 40μL of bacterial culture. Promoter activity measurements were performed at 37^{o}C and 25^{o}C, without agitation. Measurements were performed using FLUOstar OMEGA plate reader, OD measurements were performed at 600nm, GFP measurements used 485nm excitation and 520nm emission filters.

2.5 CdrA reporter measurements

Relative c-di-GMP level measurements were performed using CdrA fluorescent reporter plasmid, where GFPmut3b is placed under promoter *cdrA* (713). Plasmids were delivered to bacterial strains using electroporation. Individual plasmid containing colonies were picked to start overnight cultures of bacteria to be used for assaying. Bacterial overnight cultures were harvested in 1.5mL microcentrifuge tube by centrifugation (3min 8000rpm). ECM layer accumulated on the top of the bacterial pellet was discarded with the supernatant. Minimal M63 media supplemented with casamino acids, glucose and L-arginine [2g/L $(NH_2)_2SO_4$, 13.6g/L KH_2PO_4, 0.5% (w/v) casamino acids, 0.5mg/L $FeSO_4$, 120mg/L $MgSO_4$, 0.2% (w/v) glucose,0.4% (w/v) L-arginine], components filer sterilised, where appropriate stored at 4^oC and media prepared in the day of use. Bacteria were washed by re-suspending in 1mL of M63 with L-arginine and subsequent centrifugation (3min 8000rpm). Clean cell pellets were resuspended in fresh M63 with L-arginine and bacterial concentration was adjusted to OD_{600} = 1.0. 96-well plates containing 180μL of M63 with L-arginine were inoculated with 20μL of bacterial culture. Bacteria were cultured at 37^oC for 24h. Measurements were performed using FLUOstar OMEGA plate reader, OD measurements were performed at 600nm, GFP measurements used 485nm excitation and 520nm emission filters.

2.6 Biofilm assay

Biofilm assays were performed in growing *P. aeruginosa* in 96-well plates in M63 media with supplemental L-arginine and stained using crystal violet solution (1% w/v). Bacteria from overnight cultures were aliquoted into 1.5mL microcentrifuge tubes, pelleted by centrifugation (3min 8000rpm). Biofilm-EPS layer accumulated on the top of the bacterial pellet was discarded with the supernatant. Bacteria are washed by resuspending in 1mL of PBS and subsequent centrifugation (3min 8000rpm). Clean cell pellets were resuspended in PBS and bacterial

concentration was adjusted to OD_{600} = 1.0. 96-well microtiter plate was filled with 190μL of M63 with L-arginine and each of the wells was inoculated with 10μL of bacteria. Plates were cultured statically at 37^{o}C for the time period specified in the corresponding figure description.

After incubation, the plate was inverted tipping out liquid culture and bacteria. The wells were washed with molecular biology grade water twice and left open over night to dry. Each well was filled with 200μL of 1% (w/v) crystal violet solution in water, placed on an orbital tilting table and left to stain at room temperature for 1h. After staining, the crystal violet solution was discarded and the plate washed in molecular biology grade water twice. Subsequently each well filled with 200μL of de-staining solution (20% acetic acid in molecular biology grade water). The plate was placed on an orbital tilting table and left to de-stain at room temperature for 15min. Absorbsance at 5955 nm was measured using a FLUOstar OMEGA plate reader.

2.7 Motility assays

2.7.1 Twitching assay

Twitching motility was assessed using a petri dish based assay. LB (Miller) solidified with 1% w/v agar was used as twitching assay media, prepared fresh on the day of assay set-up. Twitching plates were prepared by pouring 10mL of medium per standard perti dish. Once the agar was set, plates were dried under a flow hood for further 10 minutes. Using a pipette tip, individual bacterial colonies were picked from LB agar plates freshly cultured overnight. Twitching plates were inoculated by stabbing the pipette tip with bacteria through the agar to the bottom of the plate. After incubation at 37^{o}C for 24h agar was removed allowing for measurement of area of bacterial surface expansion. For purposes of imaging, twitching area was stained with 1% w/v crystal violet solution for 2-5min and gently rinsed using distilled water.

2.7.2 Swimming assay

Swimming motility was assessed using petri dish based assay. Swimming media consists of Tryptone (10g/L), NaCl (5g/L), and agar (3g/L). Media was prepared fresh on the day of the assay. Plates were prepared by pouring 25mL of media agar into standard petri dishes and dried under flow hood for 10min. Plates were inoculated by using a P10 pipette tip to inject 0.5μL of overnight culture under the surface of the agar. Plates were incubated 30^{o}C for 18h before measuring the swimming area.

2.7.3 Swarming assay

Swarming motility was assessed using petri dish based assay. Swarming was assayed on two distinct types of growth medium - defined media and nutrient rich media. Defined M8 medium with final concentration of - 6g/L $(NH_2)_2SO_4$, 3/L KH_2PO_4, 0.5g/L NaCl, 5g/L Agar, 11mM $MgSO_4$, 0.5% (w/v) casamino acids, 0.2% (w/v) glucose. Nutrient rich swarming media consists of LB with 0.5% (w/v) agar. Media was prepared on the day of use, standard plates with 25mL medium per plate prepared and dried under flow hood for approx. 15min. Plates were inoculated by spotting 5μL of overnight culture in the centre of a plate and incubated at 37^{o}C for 16h before swarming patterns imaged.

2.8 T6SS expression and activity assays

2.8.1 Protein sample preparation

For H1-T6SS component expression and secretion assays, overnight cultures were subcultured in 12mL of TSB with starting $OD_{600} = 0.1$ and grown at 37^{o}C for 5h. Cell lysate was prepared by harvesting culture volume equivalent to 1mL of $OD_{600} = 1.5$, pelleted by centrifugation (3min 8000rpm) and resuspended in 150μL of Laemmli buffer. Preparation of secretion samples was performed as in (536). Cell free supernatant was acquired by repeated centrifugation (20min,

4000g , 4^{o}C). Proteins from cell free supernatant were precipitated using 10% trichloracetic acid. Briefly, protein pellets were washed with 90% acetone, air dried and resuspended in Laemmli buffer. Both cell lysate and supernatant samples were boiled at 95^{o}C for 10min before loading onto SDS-PAGE gels for analysis via western blotting.

2.8.2 Western blotting

To asses protein presence and relative abundance in individual samples SDS-PAGE gels and subsequent western blotting were used. Samples were loaded on 12% acrylamide [0.375M Tris(pH 8.8), 0.1% SDS, 0.1% ammonium persulfate, 0.4% TMED] with a stacking gel of 5% acrylamide [0.265M Tris(pH6.8), 0.1% SDS, 0.1% ammonium persulfate, 0.1% TMED] and run in Tris-glycine-SDS buffer [0.3%(w/v) Tris, 1.44%(w/v) glycine, 0.01% SDS, pH 8.3] at 80V for 20min and at 130V until desired band separation achieved. As molecular weight standard Precision Plus Protein Kaleidoscope Prestrained Protein Standard (BioRad) was used.

For western blots, transfer to nitrocellulose membranes (Amersham Protran Western blotting membranes, pore size 0.2 µm) was performed at 24V, 0.18A for 45min using transfer buffer [10% Tris-glycine-SDS buffer, 20% ethanol]. Membrane blocking was performed at 4^{o}C overnight in blocking buffer [5% (w/v) milk powder in 1xTBST(50mM Tris, 150mM NaCl, pH 8.0, 0.1% Tween20)]. After blocking membrane was incubated with primary antibody (in corresponding blocking buffer) at room temperature for 1h. The membranes were washed in 1xTBST for 10min (3 times). Membranes were incubated with secondary antibodies (anti-mouse (for RpoB) or anti-rabbit(for Hcp1, Hcp2, Hcp3, TssB1, and TssB2)) for 1h at room temperature. After washing in 1xTBST for 10min (3 times), Novex ECL Chemiluminescent Substrate reagent mix (Millipore) was applied to membranes for approx. 1min and membranes were imaged using BioRad ChimiDoc Imaging System.

2.9 Competition assay

To numerically assess prey killing depending on individual T6SS toxins, *P. aeruginosa* - *P. aeruginosa* competition assays were performed. Prey strains were sensitised to individual T6SS toxins and carried a miniCTX fluorescent cassette that ensures tetracycline resistance. Strain backgrounds with active T6SS were used ($\Delta rsmA$ for H2-T6SS competition and $\Delta retS$ for H1-T6SS competition). As negative control attackers strains lacking a structural components from all 3 T6SSs were used ($\Delta rsmA\ \Delta tssB1\Delta tssB2\Delta tssB3$ for H2-T6SS competition and $\Delta retS$ $\Delta tssB1\Delta tssB2\Delta tssB3$ for H1-T6SS competition). Bacterial overnight cultures were harvested in 1.5mL eppendorfs by centrifugation (3min 8000rpm). Biofilm-EPS layer accumulated on the top of the bacterial pellet was discarded with the supernatant. Bacteria are washed by resuspending in 1mL of PBS and subsequent centrifugation (3min 8000rpm). Clean cell pellets were resuspended in PBS and bacterial concentration was adjusted to $OD_{600} = 3.0$. 100μL of prey and 100μL attacker bacteria were mixed, subsequently centrifuged (3min 8000rpm), 100μL of cell-free supernatant was removed and bacteria were resuspended in the remaining volume. 5μL of competition mix were spotted on LB 3% (w/v) agar, dried and grown for 24h (at 37^{o}C for H1-T6SS competition and at 25^{o}C for H2-T6SS competition). After growth competition spots were scraped up using a sterile 10μL loop, resuspended in 1mL of PBS and further dispersed by use of vortex shaker for 15 to 20min. For purposes of quantification, input mix and output bacterial mixes are serially diluted in PBS. Diluted prey:attacker mixes are spotted (20μL x3) on LB agar supplemented with 150ng/mL of tetracycline for prey selection. Input and output plates are grown at 37^{o}C overnight (or until individual countable colonies appear) and prey abundance in each of the competition mixes was quantified.

2.10 Microscopy

2.10.1 Whole colony microscopy

For purposes of whole colony imaging, bacteria are grown in 24-well tissue culture plates. Each of the wells was filled with 0.5mL of LB with 2% (w/v) bacteriological agar and are dried under a laminar flow hood for 2h. Bacteria overnight cultures were pelleted by centrifugation in 1.5mL microcentrifuge tubes (8000rpm 3min). After discarding both supernatant and ECM layer from the top of the pellet, bacteria were resuspended in PBS and centrifuged (8000rpm 3min). After washing bacteria, pellet was resuspended in PBS and cell density was adjusted to $OD_{600} = 1.0$. Prey and attacker bacteria were mixed at 1 to 1 ratio, subsequently diluted depending on the specific setup and 1μL of each mixed culture was spotted on agar in 24-well plate. After spots were dried, plate was sealed using parafilm and grown for 48h (at 37^{o}C for H1-T6SS and 25^{o}C for H2-T6SS experiments)

Macro-colony containing wells were imaged using an inverted widefield microscope Zeiss Axio Observer under LED illumination. Images were captured through the bottom of the plate and agar using a long working distance objectives (EC Plan-Neofluar 10x/0.30 Ph1 or 5x/0.16 Ph1EC Plan-Neofluar). (This yields images with a resolution where 1 pixel corresponds to approx. 1.3μm) All imaging was performed at the Facility for Imaging by Light Microscopy (FILM) at Imperial College London, UK.

2.10.2 Single cell microscopy

To prepare samples for microscopy at single cell resolution 1.5 mL of bacterial overnight were pelleted (3min 8000rpm). After discarding supernatant and biofilm fraction bacteria are washed by resuspended in PBS and subsequent centrifugation. Clean bacterial pellet was resuspended in PBS and bacterial concentration adjusted to $OD_{600} = 1.0$. Subsequently bacterial strains are mixed where appropriate and all samples are further diluted to total bacterial $OD_{600} = 0.05$

7μL of sample are spotted on LB agar and dried. LB agar with dried bacteria was inverted onto 35mm glass-bottom microscopy dishes (Mattek). Before imaging samples are incubated at 37^{o}C for 4h (unless otherwise specified). Images were acquired using Zeiss Axio Observer 7, with 100x oil immersion Plan-Apochromat objective. All imaging was performed at the Facility for Imaging by Light Microscopy (FILM) at Imperial College London, UK.

2.11 Data processing

Initial image processing including shading correction and tiling as well as histogram adjustment for purposes of generating display figures was done using ZEN lite (Zeiss). Single cell data analysis, mixed colony dimension measurements and further manual image analysis was performed using Fiji (ImageJ) (716). Analysis of spatial fluorescence signal distribution in mixed bacterial colonies, modelling result analysis and summery statistics and all experimental data plotting was by using Python3. When significance testing differences between 2 data sets, T test was used. When comparing multiple measurement groups, ANOVA was used for significance testing. Within the context of this thesis, technical replicates are regarded as measurements performed simultaneously using identical materials, for example, measurements of multiple wells within a single multiwell dish. While biological replicate refers to measurements performed independently from each other in timescale and in regards to consumable materials such as bacterial growth media.

2.11.1 Image analysis

Intermixing index was adapted from previous studies (717, 718). Briefly, intermixing index is defined as number of intersection events between the 2 populations in a circular section at a given distance from colony centre, correcting for circumference with a given radius. After image tile stitching performed using ZenBlue (Zeiss), colony central points were determined manually using Fiji (ImageJ) (716). Subsequently, histogram equalised images were used to calculate

relative signal intensity at a given radius from colony central point for each of the fluorescence channels, this was used to produce a barbarised matrix describing which of the strains is more abundant at a given location. (Relative signal intensity was normalised to colony central region.) This barbarised matrix was used to quantify number of intersection events between the 2 strains at a given distance from colony central point. Number of intersection events was normalised for circumference at a given radius to produce intermixing index. Elevation in intermixing index towards 1 indicates that both populations are equally abundant and distribution alternates, while trend towards 0 indicates that only one of the species is present or species are comparably more spatially segregated.

After performing histogram equalisation and manually determining the macrocolony central points, we determined the relative mean fluorescence signal intensity and its variation at different distances from the central point. To do this, we selected a set of pixels at a given distance from the central point and used these values to calculate the mean signal intensity and variance as a function of distance from the colony centre. We then compared the normalised fluorescent signal brightness corresponding to each species to determine the more abundant one. For spatially explicit relative prey abundance analysis, we performed this comparison for sets of pixels at different distances from the colony centre. To calculate the overall relative prey abundance, we performed the analysis for the entire outer colony region. We then used these values to test for statistical differences in relative prey abundance between T6SS+ and T6SS- parental strains using T test. Custom image analysis and statistical testing were performed using Python 3.

2.12 Modelling

Agent-based modelling framework - CellModeller by (682) was used with T6SS interactions implemented by (684). The associated articles contain full details in regard to equations dictating bacterial growth, specific equations governing biophysical interactions and details describing implementation of T6SS interactions, only select key details are highlighted below. The key

simulation parameters are listed in the Table 2.4.

Parameter	Value(s)	Source
Simulation initiation		
Inoculum radius*	110µm	
Inoculum density (OD)**	0.1, 8.0, 4.0, 2.0, 1.0, 0.5, 0.25, 0.125	
Attacker to prey ratio in inoculum	0.5, 0.45, 0.4, 0.35, 0.3, 0.25, 0.2, 0.15, 0.1, 0.05	
Biophysics		
Time step	0.025h	(682)
Cell growth drag	10	(682)
Max contacts	24	(682)
Number of sub-steps	8	(682)
Division orientation noise	0.10%	(682)
Cells parameters		
Cell radius	0.5µm	Estimated from single cell microscopy images
Target division length	3µm	Estimated from single cell microscopy images
Cell division noise	0.5	(683)
Maximum growth rate	1 h-1	(683)
T6SS parameters		
T6SS firing rate	1, 5, 25, 50, 100, 200	(684)
Toxin lethal dose	1, 5, 10, 20, 50	(684)
Toxin lysis delay (min)	3, 60, 120, >simulation time	(684)
Fraction of attacker population actively firing	1, 0.5, 0.25, 0.125, 0.0625	This study
Upfront T6SS cost	0	(576)
Cost per T6SS firing event	0.00001	(576)
Needle length	0.5µm	(576)
Minimum needle penetration	10nm	(684)

Table 2.4: **Simulation parameters.**
* 1µL spot drying on agar will result in inoculum area of 7.55 * 106 µm2 (Estimated from whole colony microscopy images)
** 2.04*105 colony forming units per 1µL of OD600=1.0 culture as per (719)

2.12.1 Cell growth and movement

Within the simulation framework, bacterial communities are represented as collections of rod-shaped cells, whose growth occurs via elongation until a set target size is reached and division via binary fission occurs producing 2 identical daughter cells. It is assumed that a constant source of nutrients is available, therefore bacterial growth is limited only by lack of physical space or via direct negative interactions. Bacteria simulated do not move actively, but cell arrangement changes due to bacteria pushing on each other during growth and as a result of random noise perturbations to ensure no overlap between cells.

2.12.2 T6SS interactions

T6SS firing is described as spatially explicit events. Each of the T6SS active cells are able to fire a set number of needles that are randomly distributed across the attacker cell. Number of firing events for each individual bacteria in each time-step are drawn from Poisson distribution where mean number of needles is parameterized accordingly to the specific setup. Each firing event carries an associated metabolic cost, specific maximum cell growth rate is reduced to "pay" set material penalty for each firing event. For purposes of simulations here, T6SS firing costs were set as negligibly low, as this has been shown to affect the specific optimum firing rate, but not the general "rules of engagement" and broader effect trends (684).

T6SS hit detection in detail described by (576), briefly, a test is performed to check weather a needle geometrically intersects any cell except for the one firing it. All T6SS hits within a simulation setup are assumed to deliver constant amount of identical toxin. Toxin mode of action is described by toxicity (Hits to kill), that determines the total dose of toxin reacquired to kill a sensitive cell and partial intoxication leads to proportional reduction in maximum prey growth rate. Another toxin characteristic is "lysis delay" that determines the time between cell death and the cell being removed from the simulation. As these setups allow for partial intoxication, gradual prey recovery is implemented, where prey cell's internal toxin pool undergoes exponential

decay over time.

2.12.3 Model setups and analysis

Initial simulation steps are set-up to reflect a scaled down inoculation of mixed bacterial colony experiments. A 1:1 mix of prey and attacker are randomly placed within a 110μm radius circular area at a density equivalent to OD_{600}=0.1. These simulations were restricted to 2D plane and run for a set number of time-steps (equivalent of 25h). Current models are parameterized with a set of parameters aimed at identifying overall beneficial interaction strategies, and inclusion of parameters characterising the exact interactions by *P. aeruginosa* will be added at a future date. The simulational run execution time of examples shown in results section ranges between 30min and 3h and is largely dependent on number of individual bacteria described and number of T6SS needles being fired.

Chapter 3

Role of c-di-GMP in regulation of *Pseudomonas aeruginosa* T6SS

3.1 Introduction

Pseudomonas aeruginosa adapts two distinct lifestyles - planktonic and biofilm, each characterised by a different gene expression profile (100). Transition between the two is modulated through the Gac-Rsm regulatory cascade and shift in c-di-GMP production (Figure 3.1). C-di-GMP is a commonly used second messenger central in determining whether bacteria adapt planktonic or biofilm-like behaviour, specifically regulating motility, production of extracellular matrix (ECM) components and expression of secretion system associated genes (102). Intracellular levels of c-di-GMP are controlled by diguanylate cyclases (DGCs) and phosphodiesterases (PDEs), that respectively produce or degrade this second messenger molecule. *P. aeruginosa* PAO1 genome encodes 40 such enzymes and many of these have been characterised to control different aspects of bacterial physiology (720), but the general association is that high level of c-di-GMP result in increased biofilm formation (Figure 3.1).

RetS is a sensory kinase whose gene is among the mutational hot-spots identified in genomes of *P. aeruginosa* clinical isolates (285, 54). Loss-of-function mutations in *retS* lead to a high

biofilm forming phenotype that is associated with increased c-di-GMP production, increased exopolysaccharide synthesis, and increased type VI secretion system (T6SS) activity, while both motility and type III secretion system (T3SS) activity are suppressed (167, 166, 172, 101). The direct regulatory impact of RetS is mediated through the Gac-Rsm regulatory cascade, which is reviewed in detail in the introduction section 1.2.3. Briefly, RsmA and RsmN are translational repressors that inhibit biofilm formation. The availability of RsmA/RsmN is modulated by sRNAs, the two main ones being RsmY and RsmZ, whose expression is under the

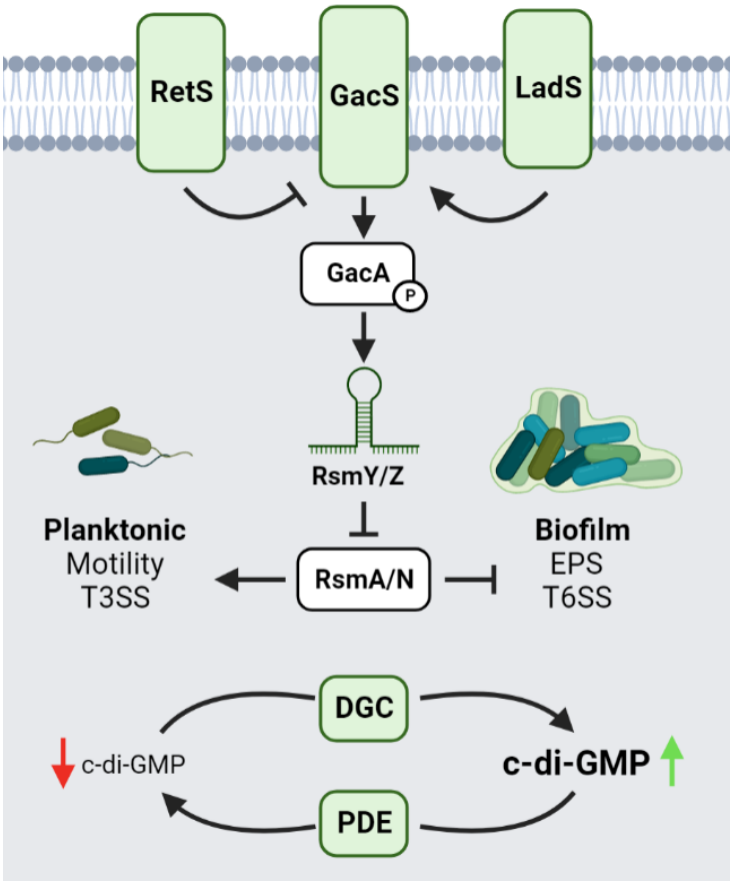

Figure 3.1: **Gac-Rsm cascade and c-di-GMP modulate *P. aeruginosa* planktonic-to-biofilm lifestyle switch.**
Schematic showing core components of Gac-Rsm pathway. RsmA and RsmN are orthologous translational repressors whose presence inhibits expression of biofilm associated genes features, such as extracellular matrix production or T6SS expression. The free RsmA/N pool is modulated by sRNAs RsmY and RsmZ. Expression of RsmY/Z is under control of GacS-GacA two component system. Sensory kinases RetS and LadS antagonistically act on GacS, indirectly influencing GacA phosphorilation state. Presence of LadS promotes biofilm formation, while active RetS represses biofilm formation. Amongst regulatory targets of the Gac-Rsm cascade are c-di-GMP metabolising DGC and PDE enzymes. Increase in c-di-GMP levels is generally associated with high biofilm producing phenotypes, while low intracellular c-di-GMP levels are associated with planktonic phenotype. Figure assembled using bioRender.

control of the GacS-GacA two-component system (123, 721). Upon ligand binding, active RetS interacts directly with GacS, this prevents GacS autophosphorylation and subsequent GacA phosphorylation (170, 169), and this is expected to result in high free RsmA/N abundance, and consequently, biofilm-associated genes are translationally repressed.

Loss of RetS results in high intracellular c-di-GMP levels and a subsequent hyperbiofilm-forming phenotype. This also correlates with an increase in the expression of T6SS, while the expression of T3SS is simultaneously down-regulated (101). T3SS is used for direct delivery of virulence factors to host cells and is a significant characteristic of *P. aeruginosa* acute infection (26). While increased T6SS activity is associated with chronic/ biofilm-like state. The Δ*retS*-dependent increase in c-di-GMP production is the result of the derepression of the gene encoding the DGC SadC, as removal of *sadC* reduces the intracellular levels of c-di-GMP and reverses the hyperbiofilm forming phenotype (110). In addition to this, increasing intracellular c-di-GMP levels through overproduction of diguanylate cyclases WspR and PA1120 also induces a similar change in the expression of T3SS/T6SS. While overexpression of PDE PA2133 reverts Δ*retS* strain towards a preferential T3SS expression (101).

Work by (101) describes how deletion of the gene encoding the sensory kinase RetS results in elevated c-di-GMP levels and subsequent phenotypic shift toward increased biofilm formation, and this work establishes the inverse control of the expression of T3SS and H1-T6SS. The direct impact of RetS-Gac-Rsm regulation on all three *P. aeruginosa* T6SSs is addressed in chapter 4 of this report. Here, we revisit the question of how changes in c-di-GMP level impact *P. aeruginosa* T6SS activity.

Aims of this chapter are:

- To validate previously characterised (101, 110) high biofilm phenotype introduced by deletion of *retS* and subsequent phenotypic reversal seen after removal of *sadC*.
- To test how changes in intracellular c-di-GMP levels impact expression and activity of all three *P. aeruginosa* T6SSs.

3.2 Results

3.2.1 Changes in relative c-di-GMP levels correlate with amounts of biofilm formed

Before assessing how changes in c-di-GMP level impact *P. aeruginosa* T6SS activity, we decided to validate phenotypes of the Δ*retS* and Δ*retS*Δ*sadC* strains in regard to biofilm formation and relative c-di-GMP production. We chose to use a fluorescent reporter based assay for assessment of relative intracellular c-di-GMP levels during cell growth. The *cdrA* reporter-carrying plasmid is based on fusion between the promoter region of *cdrA* with a *gfp* gene encoding green fluorescent protein and has been shown to reliably reflect intracellular c-di-GMP levels (713). The use of this reporter allowed us to validate that Δ*retS* strain displays substantial elevation in c-di-GMP levels compared to WT, while a subsequent deletion of *sadC* results in a stark drop in fluorescence levels that is indicative of a decrease in c-di-GMP levels below the detection limit of the assay (Figure 3.2 B). We simultaneously performed optical density measurements to assess strain growth dynamics, and these are indicative of Δ*retS* strain reaching much lower bacterial density within the culture (Figure 3.2 B). Although this observation could

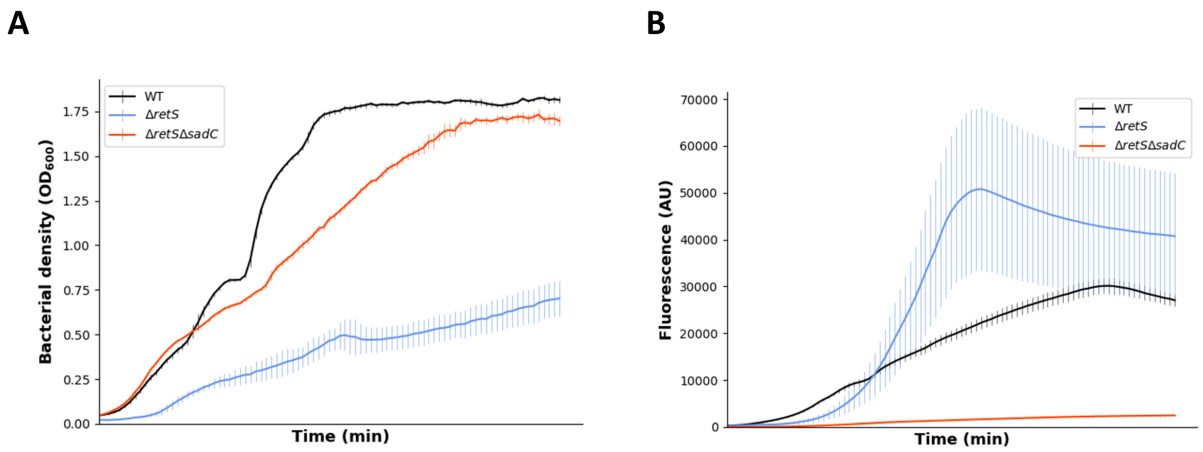

Figure 3.2: **Removal of SadC reverses high c-di-GMP phenotype of Δ*retS* mutant.** Comparative phenotype analysis of WT (PAK), Δ*retS*, and Δ*retS*Δ*sadC* strains. Relative c-di-GMP production level assessment as measured through use of a fluorescent CdrA reporter plasmid (A) and the corresponding strain growth dynamics (B). Showing mean (+SD) of 3 biological replicates.

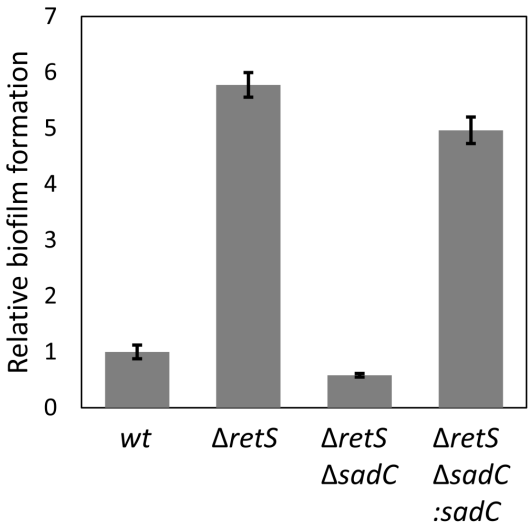

Figure 3.3: **Validation of biofilm phenotype resulting from *sadC* deletion.** Biofilm formation analysis compering WT (PAK), Δ*retS*, Δ*retS*Δ*sadC*, and Δ*retS*Δ*sadC::sadC* strains. Relative biofilm formation as measured through crystal violet staining after incubation at 37^{o}C for 6h. Showing mean (+SD) of 6 technical replicates.

suggest that the Δ*retS* strain has a substantial growth defect, this is not supported by existing literature and any further work conducted during this project; therefore, the low optical density observed here is likely to be a measurement artefact arising from a large fraction of the biomass accumulating on the walls of the microtiter dish in a form of biofilm.

As the Δ*retS* mutation is known to be hyperbiofilm forming, we chose to extend the strain phenotypic analysis by performing a biofilm assay. The high c-di-GMP mutant Δ*retS* produces nearly 6-fold more biofilm than WT, and this phenotype is reversed in the low c-di-GMP strain Δ*retS*Δ*sadC* (Figure 3.3). To validate the impact of *sadC* deletion, we next attempted to complement this phenotype. As heterologous expression of diguanylate cyclases is known to often result in highly aggregative phenotypes that are difficult to assay, we chose to restore WT *sadC* at the native locus. As expected, strain Δ*retS*Δ*sadC::sadC* forms biofilm at a level comparable to Δ*retS* mutant. After validating Δ*retS* and Δ*retS*Δ*sadC* mutants with respect to biofilm formation capabilities and relative intracellular c-di-GMP levels, we proceeded to use these strains to analyse how changes in c-di-GMP levels impact T6SS activity.

3.2.2 Loss of SadC results in decreased H1-T6SS activity while H2- and H3-T6SS expression is elevated

RetS is known to be involved in regulation of *P. aeruginosa* T6SSs and western blotting assaying of Hcp and TssB protein amounts in the cell, confirms that Δ*retS* strains display relative increase in T6SS protein expression as compared to WT (Figure 3.4). H1-T6SS and H2-T6SS activity can be assessed through use of secretion assay, where proteins present within the cell-free media fraction of a culture are precipitated and the amounts of secreted Hcp can be compared. Western blotting of the protein precipitate shows that both H1- and H2-T6SS activity is elevated upon loss of *retS*. Upon elevation in c-di-GMP resulting from *retS* deletion, H1-T6SS expression and activity is elevated compared to the WT, as seen by increase in TssB1 within the cell and Hcp1 both in the cell and supernatant (Figure 3.4 A). Subsequent decrease in c-di-GMP levels resulting from the removal of *sadC* does not result in a reduction in Hcp1 expression, but does lead to lower H1-T6SS activity, as suggested by the much decreased abundance of Hcp1 in the media fraction (Figure 3.4 A). A test western blot shows that reintroducing a WT *sadC* gene into Δ*retS*Δ*sadC* strain has no impact on Hcp1 expression, while H1-T6SS activity appears to

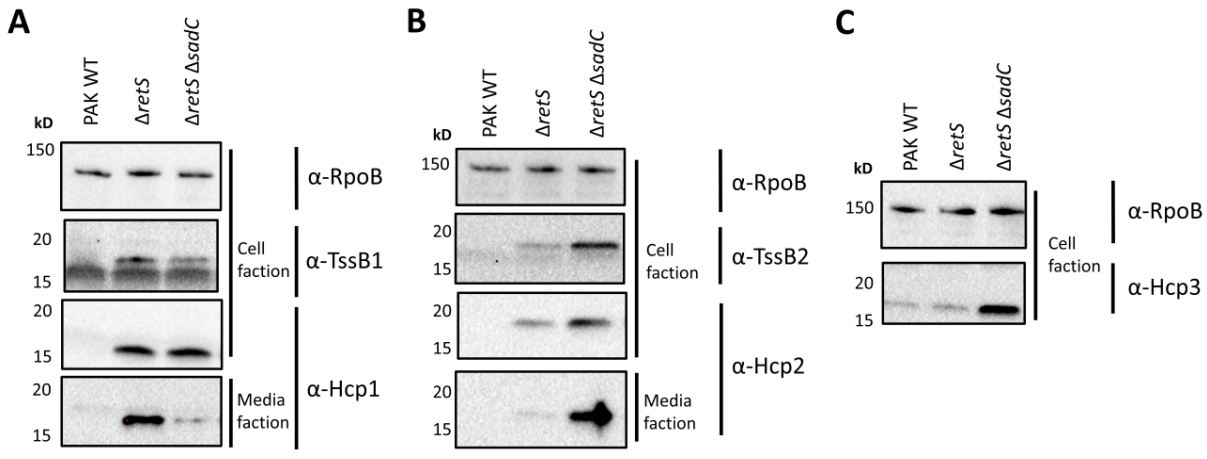

Figure 3.4: **SadC has inverse impact on H1-T6SS and H2-/H3-T6SS expression in *P. aeruginosa*.**
Comparative analysis of WT (PAK), Δ*retS*, and Δ*retS*Δ*sadC* strain T6SS expression and activity. Western blot analysis of T6SS expression and activity. For H1-T6SS (A) TssB1 and Hcp1 expression and Hcp1 secretion measured. For H2-T6SS (B) TssB2 and Hcp2 expression and Hcp2 secretion measured. For H2-T6SS (C) Hcp3 expression measured. Representative blots of 3 biological replicates. RNA polymerase (RpoB) used as a loading control.

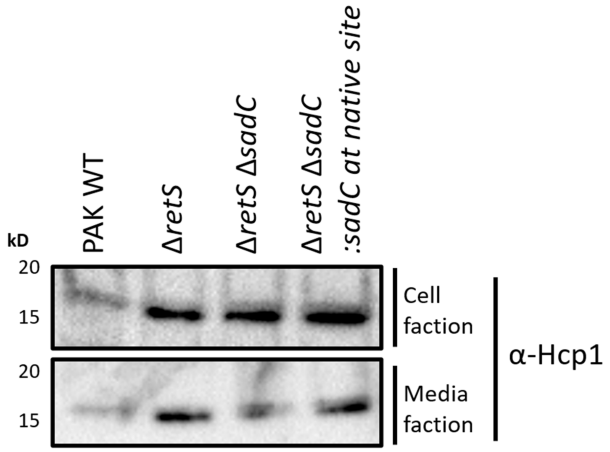

Figure 3.5: **Validation of phenotype resulting from *sadC* deletion.**
Western blot analysis of both Hcp1 expression and abundance in media compering WT (PAK), Δ*retS*, Δ*retS*Δ*sadC*, and Δ*retS*Δ*sadC::sadC* strains. 1 of 1 test blot shown.

be restored to the levels seen in Δ*retS* genetic context (Figure 3.5 A).

In the case of H2-T6SS, Δ*retS* strain displays both elevated system expression and activity, as reflected by increased TssB2 and Hcp2 abundance within the cells and corresponding elevation in Hcp2 abundance in media (Figure 3.4 D). Notably, the trend between H1-T6SS and H2-T6SS diverges in the case of Δ*retS*Δ*sadC*, as this strain displays an even further elevation in both H2-T6SS expression and activity as assessed through comparing relative levels of TssB2 and Hcp2 (Figure 3.2 D). When evaluating Hcp3 expression, a similar high expression trend is observed with the Δ*retS*Δ*sadC* mutant (Figure 3.4 E), assessment of secretion activity of the H3-T6SS was omitted as it is not reliably assayed under laboratory conditions used here.

3.2.3 *P. aeruginosa* T6SS activity is modulated by c-di-GMP levels

Next, we chose to assess whether the impact on H1- and H2-T6SS expression is specific and directly linked to SadC activity or a more general response to changes in c-di-GMP level. Therefore, we constructed a strain that allows to specifically lower c-di-GMP levels. To do this, we cloned the gene encoding a PDE, PA2133, under an arabinose inducible promoter and introduced this construct at the *attB* site on the chromosome of the Δ*retS* mutant strain. To confirm the functionality of the construct, we performed a biofilm assay and, as expected, the

expression of PA2133 results in a substantial decrease in both early and late biofilm formation far below what is observed in Δ*retS* strain carrying an empty vector control (Figure 3.6 B and D). Subsequently, we used this strain for assaying H1- and H2-T6SS expression and activity in a low c-di-GMP context.

Western blotting shows that similarly as in the case of Δ*retS*Δ*sadC*, the amount of Hcp1 within cells remains unchanged upon c-di-GMP level being lowered through PA2133 overexpression. Simultaneously, the Hcp1 abundance in media fraction is much lower, indicating that the activity of H1-T6SS is decreased (Figure 3.6 A). Next, we evaluated the low c-di-GMP

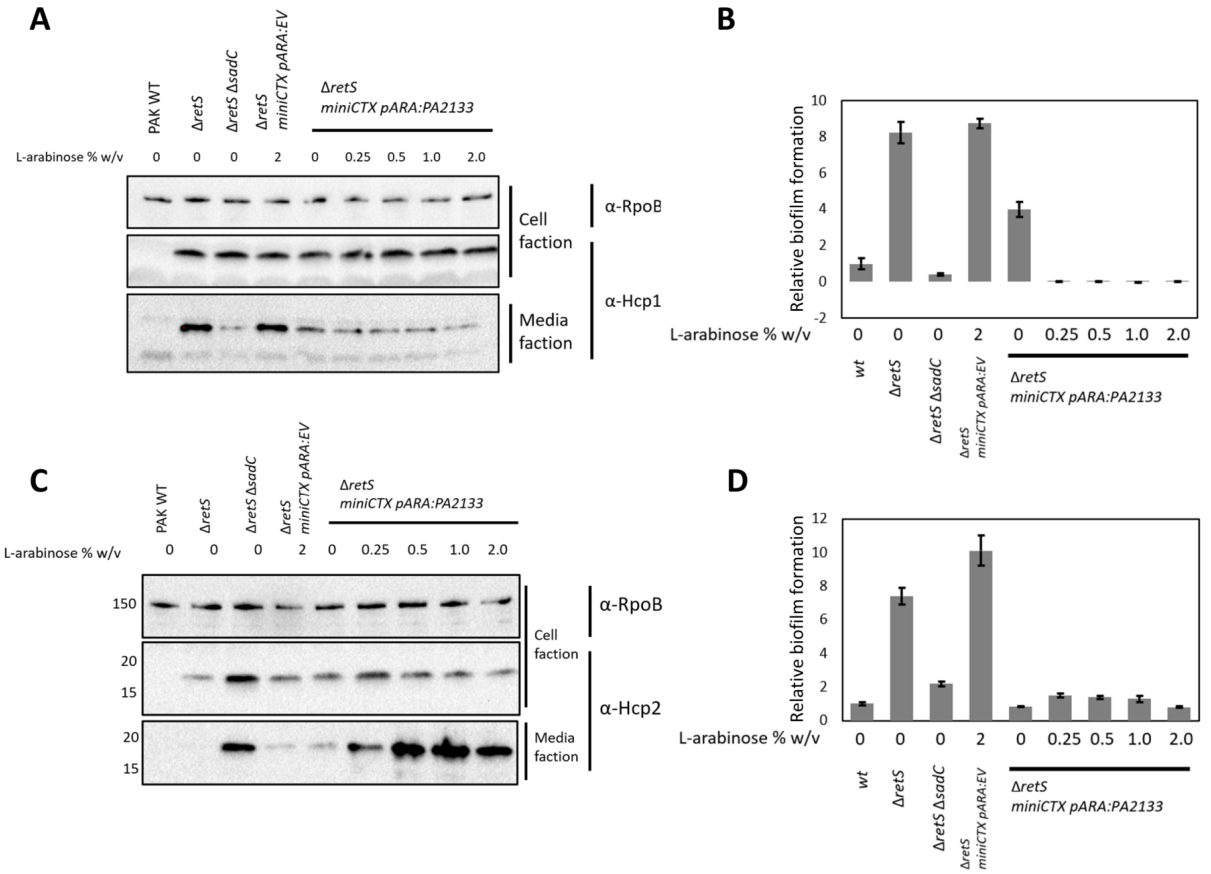

Figure 3.6: **The differential modulation of H1- and H2-T6SS activity is dependent on the global c-di-GMP levels.**
Western blot analysis of changes of both Hcp1 (A) and Hcp2 (B) expression and abundance in media as a result of decrease in PA2133 expression in response to induction of arabinose dependent promoter through gradual addition of L-arabinose at following concentrations : 0%; 0.25%; 0.25%; 0.5%; 1.0%; 2.0%. Showing a representative blot of 4 biological replicates. RNA polymerase (RpoB) used as control for equal sample loading.
Complementary analysis of strain early (6h) (**B**) and late (18h) (**D**) relative biofilm formation as measured through crystal violet staining. Showing mean (+SD) of 6 technical replicates.

impact on H2-T6SS, and western blotting showed a substantial increase in the amounts of Hcp2 found in the supernatant fraction (Figure 3.6 C). These results further support the observation that intracellular c-di-GMP levels have a differential impact on H1- and H2-T6SS expression and activity.

3.2.4 Mutation in *pppA* can "rescue" c-di-GMP mediated H1-T6SS firing impairment

The activity of H1-T6SS is under the control of the post-translational regulator PppA (569). Although the presence of PppA is not essential for the assembly and firing of H1-T6SS sheaths, it is essential for the repositioning of the H1-T6SS membrane and baseplate complexes within the cell, allowing bacteria to engage in retaliatory Tit-for-Tat firing (564, 531). The molecular details of signal sensing and Tit-for-Tat firing are described in further detail in introduction section 1.4.4. Loss of *pppA* has been shown to result in elevated Hcp1 secretion (569) and here we decided to test whether removal of PppA would rescue the low H1-T6SS secretion phenotype

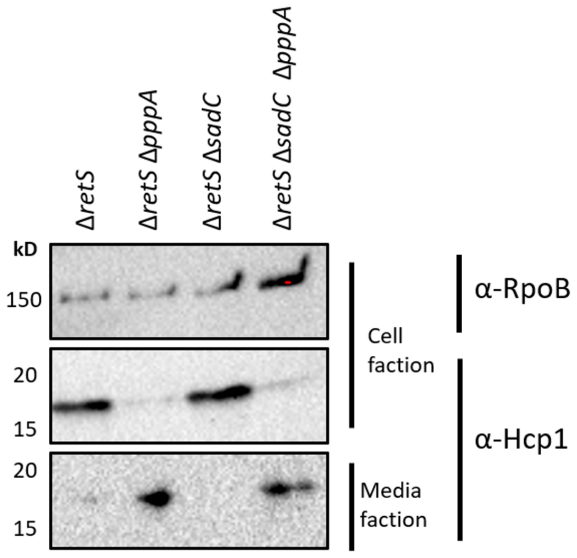

Figure 3.7: **Loss of PppA leads to constitutive H1-T6SS activation regardless of the intracellular c-di-GMP content.**
Western blot analysis of changes in Hcp1 abundance in cell and media fractions as a result of removal of post-translational regulator PppA. Showing a representative blot of 2 biological replicates.

observed in the Δ*retS*Δ*sadC* mutant strain. To do this, we used a Δ*retS*Δ*pppA* strain and subsequently introduced a *sadC* deletion. As expected, the loss of *pppA* results in an elevated activity of H1-T6SS to an extant where almost all Hcp1 produced in Δ*retS* strain is secreted in the supernatant (Figure 3.7). Notably, western blot analysis of the relative abundance of Hcp1 in whole cell lysate and supernatant fractions shows that deletion of *pppA* leads to an increase in H1-T6SS activity regardless of Δ*retS* or Δ*retS*Δ*sadC* regulatory context. These preliminary results show that the decrease in H1-T6SS activity resulting from low intracellular levels of c-di-GMP can be reversed by the introduction of an additional mutation in *pppA*.

3.3 Discussion

C-di-GMP is a widespread bacterial second messenger that mediates the transition between the planktonic and biofilm lifestyle. In *P. aeruginosa*, the biofilm lifestyle is associated with down-regulation of motility and virulence factors, while up-regulating extracellular matrix component production and T6SS activity (722, 1) (Figure 3.1). The Gac-Rsm cascade is central in *P. aeruginosa* transition towards biofilm-like gene expression pattern and is directly involved with the regulation of the expression of the three T6SS systems (723, 101). The Gac-Rsm system is under the control of the sensory kinase RetS, loss of RetS has been well characterised to result in increased intracellular c-di-GMP levels, promote biofilm formation and up-regulate T6SS expression (101, 167, 169). Here, the impact of intracellular c-di-GMP levels on T6SS activity is revisited.

RetS-dependent elevation in c-di-GMP levels has been linked to the activity of the diguanylate cyclase SadC (110). Here we were able to confirm that the relative elevation in intracellular c-di-GMP levels and biofilm formation observed in a Δ*retS* strain is reversed in the double mutant Δ*retS*Δ*sadC* (Figures 3.2B and 3.5C and D). Using these strains, we also make novel preliminary observations of the impact of the c-di-GMP level on the 3 *P. aeruginosa* T6SS systems. As expected, a Δ*retS* strain shows elevation in H1-T6SS expression and activity relative to WT, but western blotting indicates that subsequent deletion of *sadC* reduces Hcp1 secretion while expression remains unchanged (Figure 3.4 A). It is notable that although cellular Hcp1 levels are unaffected, western blotting indicates that H1-T6SS activity is much lower in the Δ*retS*Δ*sadC* than in a Δ*retS* background (Figure 3.4 A). Additionally, when intracellular c-di-GMP levels are reduced due to overexpression of PDE PA2133, a similar effect is observed (Figure 3.6 A) suggesting that global c-di-GMP may contribute to post-translational modulation of H1-T6SS activity.

P. aeruginosa H1-T6SS is under post-translational control of the PppA phosphatase (569, 531). PppA is not required for the assembly and firing of the H1-T6SS sheath to occur, but is

required for repositioning of the membrane complex and the ability of *P. aeruginosa* to engage in retaliatory Tit-for-Tat firing (564). We tested the impact of a Δ*pppA* mutation on H1-T6SS in both Δ*retS* and Δ*retS*Δ*sadC* strains (Figure 3.7) and preliminary western blotting results suggest the Δ*pppA* mutant strains will engage in constitutive H1-T6SS firing until most of the cellular Hcp1 pool is secreted into the media independently of the regulatory context and, notably, c-di-GMP levels. PppA has been shown to repress both the production of c-di-GMP and the T6SS protein expression in *Vibrio alginolyticus* (724), therefore validation of intracellular c-di-GMP levels in Δ*pppA* strains would be needed to further advance this study. Current results suggest that H1-T6SS firing is likely initiated independently of intracellular c-di-GMP levels and the lower H1-T6SS activity observed in Δ*retS*Δ*sadC* strains could be a result of subsequent interference with continued system re-assembly.

A general assumption derived from previous *P. aeruginosa* H1-T6SS studies is that increased c-di-GMP levels correlate with high T6SS activity and a decrease in c-di-GMP levels would result in lower expression of T6SS genes. Here we observe the opposite, although Δ*retS* strain displays higher expression and activity of H2-T6SS than WT, and system activity is even further elevated in low c-di-GMP strain Δ*retS*Δ*sadC* (Figure 3.4 B). With Hcp3 expression showing a similar trend of elevation in Δ*retS*Δ*sadC* context compared to Δ*retS* (Figure 3.2 E). The impact on H2-T6SS expression and activity is further corroborated as substantial elevation in the amounts of Hcp2 present in supernatant fraction is seen upon overexpression of c-di-GMP degrading PDE PA2133 (Figure 3.6). This observation of low levels of c-di-GMP that result in increased expression of T6SS in *P. aeruginosa* is quite novel, but it requires further experimental validation.

Currently, a few literature examples of T6SS activity inversely correlating with c-di-GMP levels exist. Heterologous over expression of *P. aeruginosa* DGCs SadC in *Agrobacterium tumefaciens* results in a substantial increase in the intracellular c-di-GMP levels and a corresponding decrease in T6SS expression (725). This work then further demonstrates that

high c-di-GMP levels suppress *A. tumefaciens* T6SS expression and ability to engage in effective inter-bacterial competition reliant on T6SS (725). In *Pseudomonas putida* two separate studies by (726) and (727) show that manipulation of c-di-GMP levels through DGC WspR or PDE BifA results in impact on K1-T6SS activity in a manner dependent on FleQ. FleQ is a c-di-GMP binding transcription factor that can act to both promote and repress expression of biofilm-associated genes in *P. aeruginosa* (119, 114, 116), additionally FleQ acts in conjunction with RpoN that has been shown to differentially regulate *P. aeruginosa* T6SSs (728). T6SS is also among the FleQ regulatory targets in *Pseudomonas fluorescens* suggesting an impact similar to the one observed in *P. putida* (729, 730, 731). Furthermore, a study by (732) observed that T6SS genes are among FleQ targets in *P. aeruginosa*. These observations suggest that a study of FleQ impact on H2- and H3-T6SS expression and activity in different regulatory context strains could be an investigative avenue to pursue when further addressing c-di-GMP level impact on *P. aeruginosa* T6SSs.

Chapter 4

The Gac-Rsm cascade modulates expression, activity and killing capacity of *Pseudomonas aeruginosa* T6SSs

4.1 Introduction

Pseudomonas aeruginosa is a bacterium capable of using a variety of diverse molecular tools to engage with its environment, host and other neighbouring organisms. Ability to take advantage of various niches requires bacteria to both sense their local environment and subsequently adjust the gene expression profile. Use of the type VI secretion system (T6SS) in *P. aeruginosa* is not constitutive and has been characterised to occur as part of a broader biofilm lifestyle jointly with increase in exopolysaccharide production, while simultaneously shifting away from producing acute virulence factors like the type III secretion system (T3SS) (100). The Gac-Rsm pathway is central in modulating this lifestyle transition, both acting directly and modulating the production of a secondary messenger c-di-GMP.

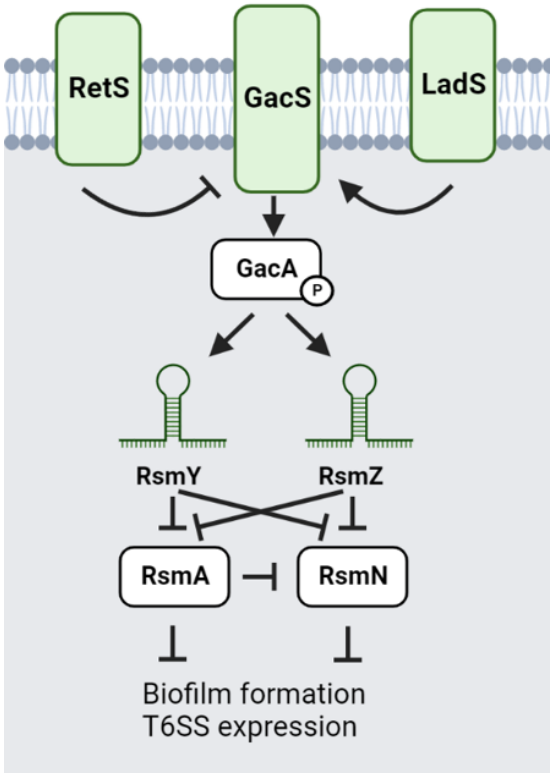

Figure 4.1: **Schematic of Gac-Rsm regulatory cascade core components.** Sensory kinase RetS represses action of GacS-GacA two component system, while sensory kinase LadS has an opposite effect. Upon phosphorylation of GacA, production of snRNAs RsmY and RsmZ is increased and translational repressors RsmA and RsmN are sequestered. In absence of RsmY and RsmZ, RsmA and RsmN translationally repress genes associated with T6SS and biofilm formation.

The chapter 6 looks at c-di-GMP level impact on T6SS expression and activity, while focus of this section is on the impact of Gac-Rsm cascade. Disruption of this pathway has been found to lead to a permanent shift towards biofilm-like phenotype and mutations involving this pathway are common in *P. aeruginosa* strains isolated from chronic lung infections (733, 59, 734).

The Gac-Rsm pathway plays a central role in *P. aeruginosa* T6SS regulation and is briefly described here (Figure 4.1). GacS-GacA two component system is present in genomes of a range of Gram-negative bacterial species and is commonly implicated in regulation of pathogenicity and virulence mechanisms (163). *P. aeruginosa* GacA response regulator induces the expression of sRNAs, RsmY and RsmZ (735, 149), which sequester two translational repressors, RsmA (123) and RsmN (131). To date, no ligands of the *P. aeruginosa* GacS sensor domain have been identified, but GacS acts to integrate signals from RetS and LadS sensory kinases (736, 163).

RetS is a histidine kinase and has been shown to affect the planktonic to biofilm switch primarily by acting through the Gac-Rsm cascade (167, 170). A known RetS ligand is mucin glycans and *P. aeruginosa* exposure to mucins results in decreased H1-T6SS expression and impaired competitive fitness (169). LadS responds to the presence of calcium ions and its impact on GacS is opposite to that of RetS, with loss of LadS resulting in increased virulence (126, 174, 737). Interactions between GacS, RetS, and LadS sensors determine the phosphorylation state of the GacA response regulator and the subsequent abundance of RsmY and RsmZ (163). The abundance of RsmY/Z within the cell is what determines amounts of free RsmA and RsmN available to act through binding to target mRNAs. RsmA and RsmN are translational regulators that belong to a broadly conserved CsrA regulator family (128). RsmA and RsmN have been shown to directly or indirectly impact expression of more than 500 genes this corresponding to nearly 10% of *P. aeruginosa* genome (123, 131, 122). Among the phenotypic features affected are production of extracellular matrix components, motility, virulence factors, and the T6SS.

The impact of RsmA has been broadly studied; it has been shown to directly repress synthesis of exopolysaccharides, secondary metabolites, and all three T6SSs (738, 723, 123). In addition, RsmA acts as a direct repressor of *rsmN* and *retS* genes that contribute feedback to the regulatory cascade (148). The phenotypic impact of RsmA can be observed in simple *rsmA* deletion strains, although both RsmA/N repressors share many regulatory targets, the *in vivo* role of the paralogue RsmN has been less well understood (122). Both RsmA/N share the same consensus sequence of AN**GGA**YG exposed as part of a stem-loop structure, but the affinity for individual mRNAs differs depending on the broader structural context (739). Genes encoding the T6SS component are distributed throughout the *P. aeruginosa* genome. The genes encoding structural T6SS components for each of the systems are grouped in a single cluster, while additional remote orphan clusters encode effector-immunity gene sets and additional copies of genes encoding T6SS spike components (Figure 1.20). Both RsmA and RsmN have been mapped to bind mRNAs corresponding to the 3 T6SS, in particular *tssA1*

and *fha1* for H1-T6SS, *tssA2* for H2-T6SS, and *tssB3* for H3-T6SS (723, 145, 122, 131, 135). Furthermore, control extends to T6SS orphan clusters that include *vgrG2a*, *vgrG2b*, *tse3* among others (145, 122). Altogether, RsmA and RsmN have both been shown to be involved in control of *P. aeruginosa* T6SS expression.

Here we aim to perform a comparative analysis of strains with mutations at different points within the Gac-Rsm cascade aiming to compile a set of strains with differentiated T6SS activity levels. This will then act as a basis for further investigation of impact of individual T6SS toxins and impact of graduated T6SS activity on competitive outcomes.

The objectives of the study are:

- To assess core T6SS promoter activity in *gac-rsm* mutant strains through the use of fluorescent reporters.
- To assess T6SS expression and activity of *gac-rsm* mutants through western blot analysis.
- To compare H1- and H2-T6SS mediated bacterial killing of different *gac-rsm* mutant strains.

4.2 The Gac-Rsm cascade modulates expression and activity of all 3 *P. aeruginosa* T6SSs

4.2.1 Gac-Rsm dependent changes in core T6SS promoter activity

We constructed a series of mutant strains that lack individual or combination of genes encoding proteins involved in the Gac-Rsm cascade. For this and following thesis sections work was performed using *P. aeruginosa* PAO1 (Lausanne) reference strain. The strain set constructed includes s with deletion of genes encoding the translational repressors RsmA and RsmN (both single and combined mutations), as well as strains lacking the gene encoding the histidine kinase RetS. With this mutant set we could assess whether differential impact might be observed when directly removing both repressors RsmA and RsmN or through upstream disruption of the cascade. We performed our analysis by assessing T6SS core promoter activity, using strains in which we introduced either transcriptional or translational fluorescent reporter plasmids. Reporter plasmids were constructed by cloning core T6SS promoters regions leading *tssA1*, *tssA2*, and *tssB3* upstream of GFPmut3b (272) (Figure 4.2).

Upon deletion of *rsmA* both transcriptional and translational reporter activity of all three

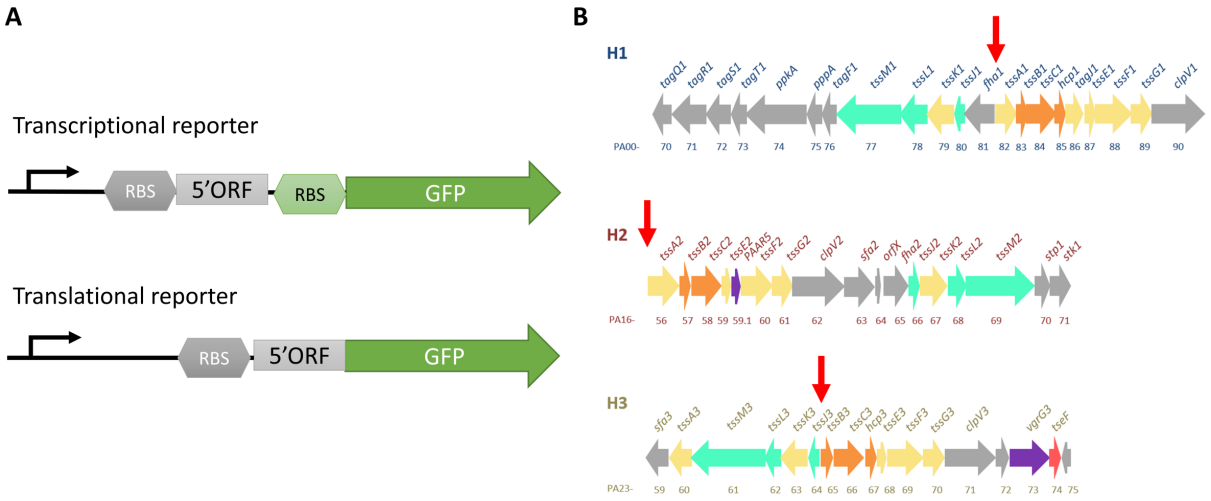

Figure 4.2: **Diagram of fluorescent T6SS promoter reporters.**
(**A**) Schematic of construction of transcriptional and translational promoter reporters. (**B**) Core gene clusters encoding structural components of H1-, H2-, and H3-T6SSs from *P. aeruginosa* PAO1 genome. Promoter regions used for reporter construction indicated with arrows in red.

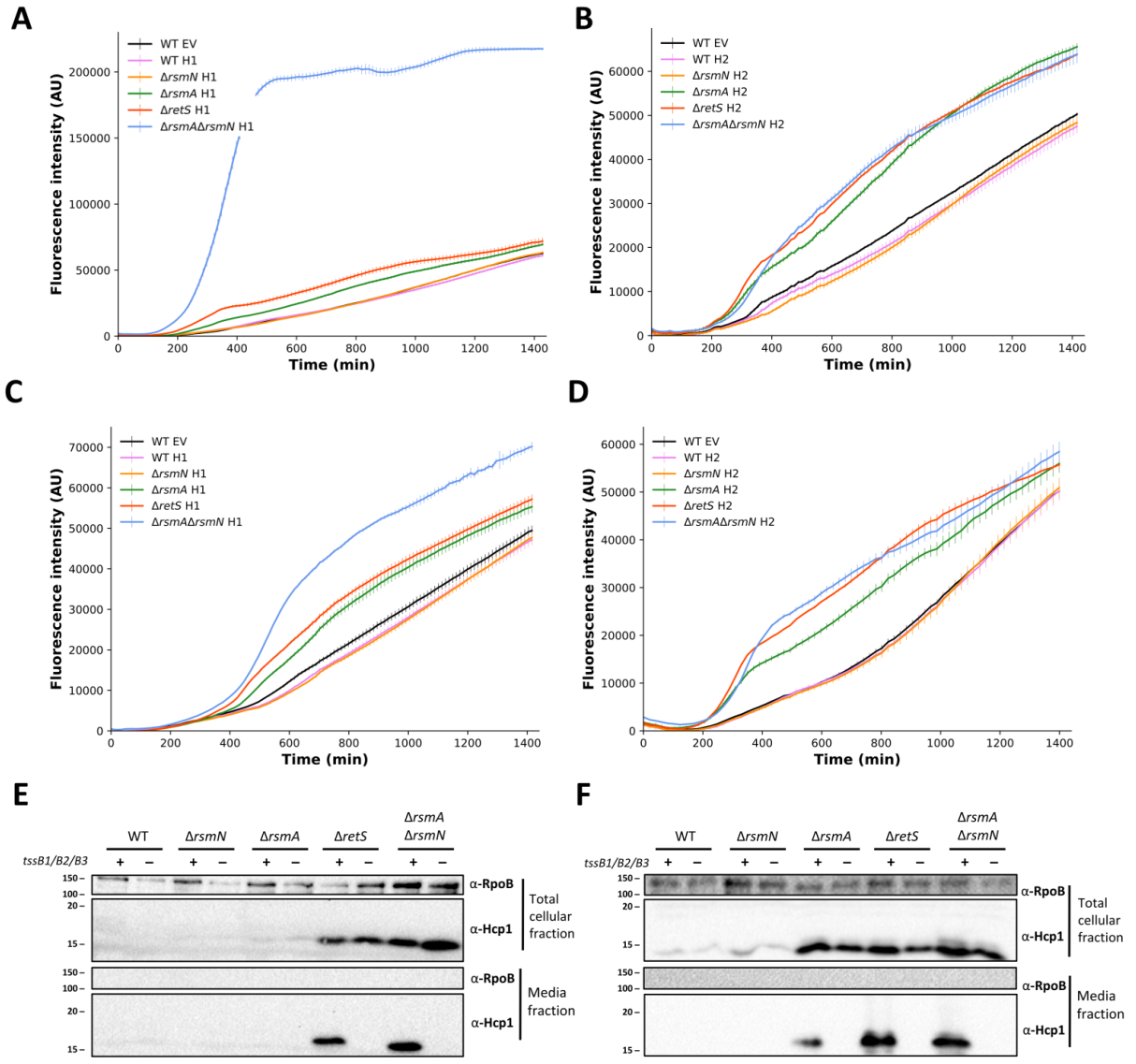

Figure 4.3: **Disruption of Gac-Rsm regulatory cascade results in graduated elevation in T6SS expression and activity.**
Analysis of T6SS promoter transcriptional (A and B) and translational (C and D) activity in WT, Δ*rsmN*, Δ*rsmA*, Δ*retS*, and Δ*rsmA*Δ*rsmN* strains. Left column shows H1-T6SS (*tssA1*) and right H2-T6SS (*tssA2*) promoter activity over growth time as measured by plasmid based GFPmut3b reporter fusions. All measurements performed at 37^{o}C, in static culture, each display item shows a mean +SD of 4 technical replicates that is representative of n = 3 biologically independent repeats.
Western blot analysis shown gradual elevation in of Hcp1 (E) and Hcp2 (F) levels in whole cell and supernatant fractions in WT, Δ*rsmN*, Δ*rsmA*, Δ*retS*, and Δ*rsmA*Δ*rsmN* strains. Presence or absence of *tssB1*, *tssB2*, and *tssB3* genes and correspondingly ability to assemble and fire T6SS sheaths is indicated by "+" or "–". A representative blot of 3 independent biological repeats shown here, for H1-T6SS activity assessment bacteria were cultured for 5h at 37^{o}C and for H2-T6SS for 18h at 25^{o}C. RNA polymerase (RpoB) used as lysis control.

systems is elevated (Figures 4.3 A, B, C, D and 4.4 A and B - green curve). Disrupting the Gac-Rsm cascade at an upstream position by removing the *retS* gene (RetS acts as a repressor)

results in further elevation in T6SS promoter activity (Figures 4.3, 4.4, and 4.5 red curve). Furthermore, the removal of the gene encoding RsmA ortholog RsmN does not appear to have a measurable impact on any of the promoter activity and the fluorescent signal intensity from Δ*rsmN* strains stays consistent with WT (Figures 4.3, 4.4, and 4.5 pink and orange curves). This indicates that unlike deletion of *rsmA*, removal of its ortholog *rsmN* has no measurable impact on T6SS promoter activity while RsmA is present.

Although T6SS promoter activity is high in a Δ*retS* context, it is notable that the strain with mutation in both *rsmA* and *rsmN* genes shows even further elevation in H1-T6SS promoter transcriptional and translational activity (Figures 4.3 and 4.5 blue curve). This indicating that RsmN does contribute to T6SS regulation in absence of RsmA. A particular feature of *P. aeruginosa* H2- and H3-T6SS expression reported previously by (723) is preferential expression at 25^{o}C rather than 37^{o}C (Figure 4.5). Therefore, we performed additional promoter activity measurements at 25^{o}C and this confirmed the prior observation as both *tssA2* and *tssB3* promoter reporters showed higher activity at 25^{o}C compared to 37^{o}C. It is also notable that independently of the growth conditions *gac-rsm* mutant strains display the same trend of differences in graduated promoter activity.

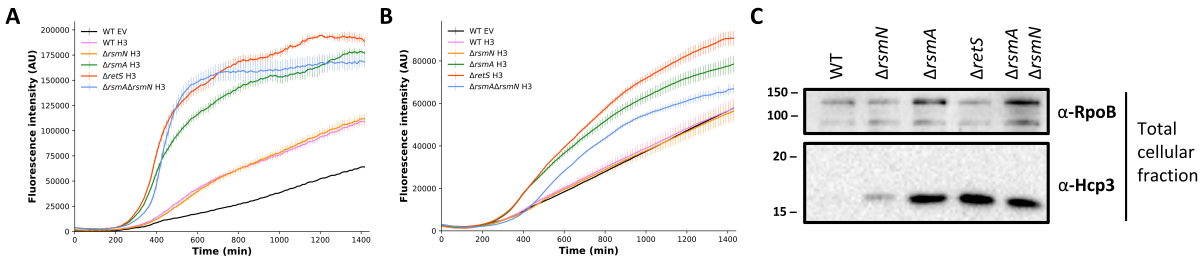

Figure 4.4: **Gac-Rsm mutant strains show graduated increase in H3-T6SS promoter activity and expression.**
Analysis of H3-T6SS (*tssB3*) promoter transcriptional (A) and translational (B) activity of WT, Δ*rsmN*, Δ*rsmA*, Δ*retS*, and Δ*rsmA*Δ*rsmN* strains. All measurements performed at 37^{o}C, in static culture, each display item shows a mean +SD of 4 technical replicates that is representative of n = 3 biologically independent repeats.
Complementary western blot analysis shows gradual elevation in of Hcp3 expression. A representative blot of 3 independent biological repeats shown here, for H3-T6SS activity assessment bacteria were cultured for 24h at 30^{o}C. RNA polymerase (RpoB) used as loading control.

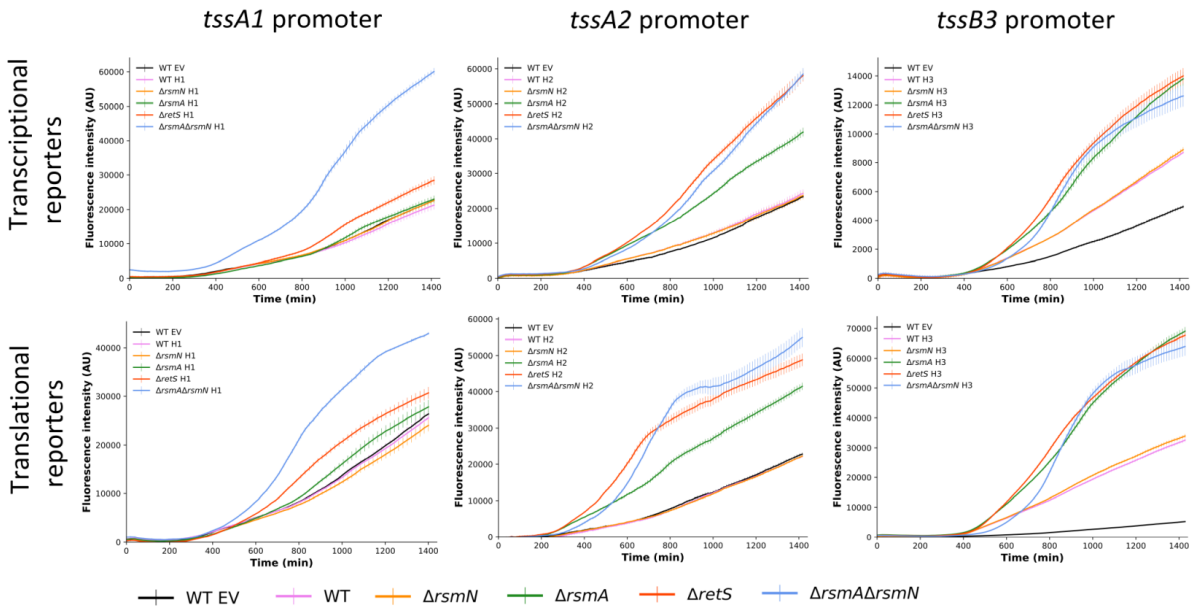

Figure 4.5: **Decrease in growth temperature results in elevated H2-T6SS and H3-T6SS promoter activity, while H1-T6SS promoter activity is decreased in Gac-Rsm regulatory cascade mutant strains.**
Analysis of T6SS promoter transcriptional (upper) and translational (lower) activity in WT, Δ*rsmN*, Δ*rsmA*, Δ*retS*, and Δ*rsmA*Δ*rsmN* strains. First column shows H1-T6SS (*tssA1*), middle H2-T6SS (*tssA2*), and last H3-T6SS (*tssB3*), promoter activity over growth time as measured by plasmid based GFPmut3b reporter fusions. All measurements performed at 25^{o}C, in static culture. Each display item shows a mean +SD of 4 technical replicates that is representative of n = 3 biologically independent repeats.

4.2.2 Gac-Rsm dependent elevation in Hcp abundance in cells and culture supernatant fraction

The measurements of promoter activity using fluorescent reporter fusions suggested that the level of T6SS expression could be progressively increased by interfering with the Gac-Rsm pathway. Here we assessed whether an increase in expression correlates with elevated activity, which means an increased level of T6SS-dependent secretion. An approach that allows for comparative assessment of T6SS activity is through quantifying the amounts of Hcp protein released into the culture supernatant through western blotting. The Hcp proteins are piled within the contractile sheath structure and are expelled from cells in large quantities once a firing event occurs. This analysis confirmed that similarly as in case of promoter activity, graduated elevation of both of Hcp1 and Hcp2 amounts from lowest to highest can be seen in

the cells of WT, Δ*rsmN*, Δ*rsmA*, Δ*retS*, and Δ*rsmA*Δ*rsmN* strains (Figure 4.3 E and F). To validate that release of Hcp in the medium is specific to system activity rather than a result of lysis, we included strains defective in T6SS activity due to deletion of genes encoding sheath proteins TssB1, TssB2, or TssB3. Removal of these genes ensures that the sheaths can no-longer be assembled, while the expression of the rest of the T6SS proteins likely remains unaffected. The analysis of Hcp1 and Hcp2 abundance in the media fraction shows that the increase in expression directly correlates with increased system activity. In regard to H1-T6SS, substantial amounts of Hcp1 are detected in the supernatant fraction of Δ*retS* strain culture with even further increase in case of Δ*rsmA*Δ*rsmN*, while T6SS activity in Δ*rsmA* strains is low by comparison (Figure 4.3 E). Hcp2 in the assaying conditions used here can be detected even in WT cell lysate, while Δ*rsmA*, Δ*retS*, and Δ*rsmA*Δ*rsmN* mutations are needed for consistent system activation, with graduation between the three mutants being less severe than seen in the case of H1-T6SS, but still displaying step-wise elevation in activity (Figure 4.3 F). Regarding H3-T6SS, Hcp3 expression in the cells is increased in a manner consistent with the promoter activity measurements (Figure 4.4 C), while analysis of Hcp3 presence in supernatant was omitted as it is not consistently detectable under current laboratory assay conditions. Overall, western blot analysis of Hcp protein amount in cell and medium fractions shows that graduated differences in promoter activation using our set of *gac-rsm* mutant strains directly correspond to increased protein production and T6SS activity as shown by western blotting.

4.2.3 *gac-rsm* mutants show increased TssBC sheath assembly dynamics

To further assess how regulatory cascade mutations influence T6SS activity at resolution of individual cells, dynamics of T6SS assembly and firing can be investigated using live cell imaging, where T6SS sheath proteins (TssB in case of this study) are fused with a fluorescent protein and this enables tracking of dynamics of individual sheath assembly (740, 547). We engineered and used *P. aeruginosa gac-rsm* mutant strains encoding *tssB1-mScarlet* fusion at the native locus to

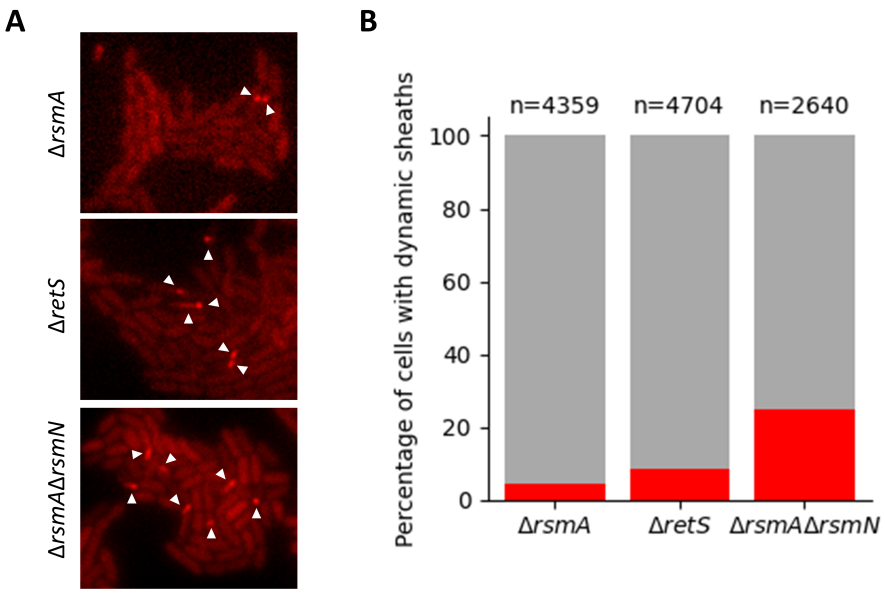

Figure 4.6: **Elevation in H1-T6SS expression and activity is reflected by increased dynamic sheath structure abundance.**
(A) Fluorescent images illustrating changes in H1-T6SS sheath abundance in Δ*rsmA*, Δ*retS*, and Δ*rsmA*Δ*rsmN* strains with chromosomal *tssB1::mScarlet-I* fusion at the native locus. (B) Quantification of percentage of the population with dynamic H1-T6SS sheath structures over 120s time-lapse. Image sets from 2 to 3 independent imaging session were analysed with total approx. 5000 to 6500 cells quantified for each strain shown. Bacterial culture of OD_{600}=0.05 was spotted LB agar and inverted onto cover glass, images taken after 3.5-4.5h incubation at 37^{o}C. An approx. 15.6 x 13 μm representative field of view shown.

assess differences in number of sheaths assembled (Figure 4.6). Time-lapse imaging of H1-T6SS sheath dynamics in Δ*rsmA* strains shows that approx. 4.2% of the population actively assemble sheaths and this number in doubled to 8.3% in Δ*retS* regulatory context (Figure 4.6 B). Even further elevation to 24.7% of the population engaging in active sheath assembly and firing can be seen in strain with mutations in both *rsmA* and *rsmN* genes (Figure 4.6 B). This elevation in dynamic sheath structure abundance directly correlates with increased Hcp1 abundance in secretome as assessed by western blotting (Figure 4.3 E). A notable feature of *P. aeruginosa* H1-T6SS sheath firing is the "Tit-for-Tat" or "duelling" behaviour first described by (564). As seen in Figure 4.6 A, many of the sheaths in neighbouring cells are assembled directly opposite of another sheath, at a site where previous injection just occurred. When quantifying the sheath abundance, it was notable that even in the case or Δ*rsmA*Δ*rsmN* mutant strain, that shows high level of Hcp1 secretion, only a fraction of the population is actively assembling and firing

H1-T6SS sheaths (Figure 4.6 B).

4.2.4 *gac-rsm* mutants show increased H1- and H2-T6SS-dependent competitiveness

Having established how mutations in genes encoding components of the Gac-Rsm cascade impact on T6SS *in vitro* activity, we proceeded to test whether this translates into graduated differences in strain competitive fitness. To assess T6SS-dependent killing, a surface-based competition assay can be used. This involves mixing an antibiotic resistance gene carrying T6SS sensitive prey bacterium with an attacker strain, that lacks the specific resistance gene. The bacterial mixture is placed on a medium-containing agar surface where both bacteria are co-cultured. Subsequently, bacteria are recovered and re-suspended in PBS, serially diluted and replica plated on antibiotic containing selective media that allows for specific recovery and quantification of prey abundance in different bacterial mixes. Strains lacking sheath proteins TssB1, TssB2, and TssB3 are used for negative control competition mixtures to ensure that changes in prey abundance observed are T6SS dependent. These assays are commonly performed with prey bacteria from different species, such as *E. coli* or *P. putida* (741). Here the aim is to compare *gac-rsm* mutant strains that different not only in the T6SS activity levels, but have also undergone a broader phenotypic shift. Within context of inter-species competition any non-T6SS-associated phenotypic changes are likely to act as a compounding factors and complicate interpretation of interspecies competition assay results. An alternative approach was taken here, where the various *gac-rsm* mutant strains are specifically sensitised to the attackers T6SS by deleting specific pairs of toxin-immunity genes. For assessment of H1-T6SS-dependent killing strains were sensitised to pore forming toxin Tse5, while nuclease TseT sensitive strains were used for assessment of H2-T6SS dependent killing. These toxins were chosen as comparative toxin potency assessment discussed in chapter 5 shows these to be the most effective for elimination of *P. aeruginosa* in an individual T6SS toxin-dependant manner. The T6SS toxin-sensitised

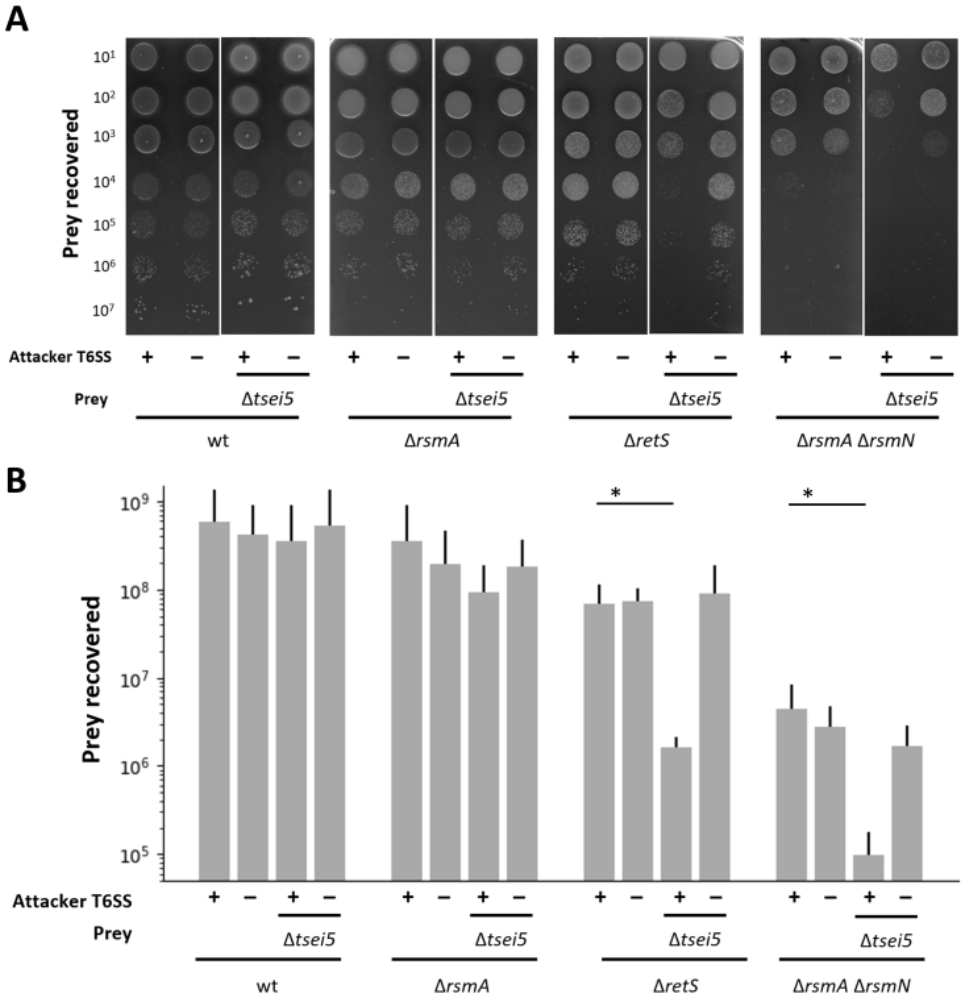

Figure 4.7: **Assessment of H1-T6SS toxin Tse5 mediated killing capacity of different Gac-Rsm mutants.**
Assessment of Tse5 mediated killing in different Gac-Rsm mutant strains. (**A**) Quantification of prey recovered on selective media. WT, Δ*rsmA*, Δ*retS*, and Δ*rsmA*Δ*rsmN* toxin sensitised strains with a parental strain of corresponding regulatory background. Using parental strains with active T6SS or mutation of Δ*tssB1*Δ*tssB2*Δ*tssB3* for T6SS- attacker strains as indicated. Showing images representative of three biological replicates.
(**B**) Corresponding numerical quantification of amount of prey recovered. Showing mean + SD of three biological replicates. Statistical testing performed using ANOVA and Tukey's tests, with $p<0.05$ indicated with a "*".

strains (Δ*tse5tsi5* or Δ*tseTtsiT*) were competed with the corresponding parental strains and the T6SS defective (Δ*tssB1*Δ*tssB2*Δ*tssB3*) counterparts. Use of this approach allowed to better compare differences in T6SS killing efficacy because of specific modulation in T6SS activity as competitors are otherwise isogenic.

The assessment of Hcp1 abundance in cells and media fraction through western blotting (Figure 4.3 E) indicates very low protein abundance in WT, Δ*rsmN*, and Δ*rsmA* strains. Here,

neither WT nor Δ*rsmA* strains sensitised to Tse5 action appear to be any less abundant than the control (Figure 4.7). Yet in Δ*retS* and Δ*rsmA*Δ*rsmN* mutant strains we previously observed much higher Hcp1 abundance in culture supernatant fractions (Figure 4.3 E) and accordingly a T6SS-dependent reduction in prey abundance within the competition mix is clearly detectable for both strains (Figure 4.7). It is notable that competition with Δ*retS* strains results in

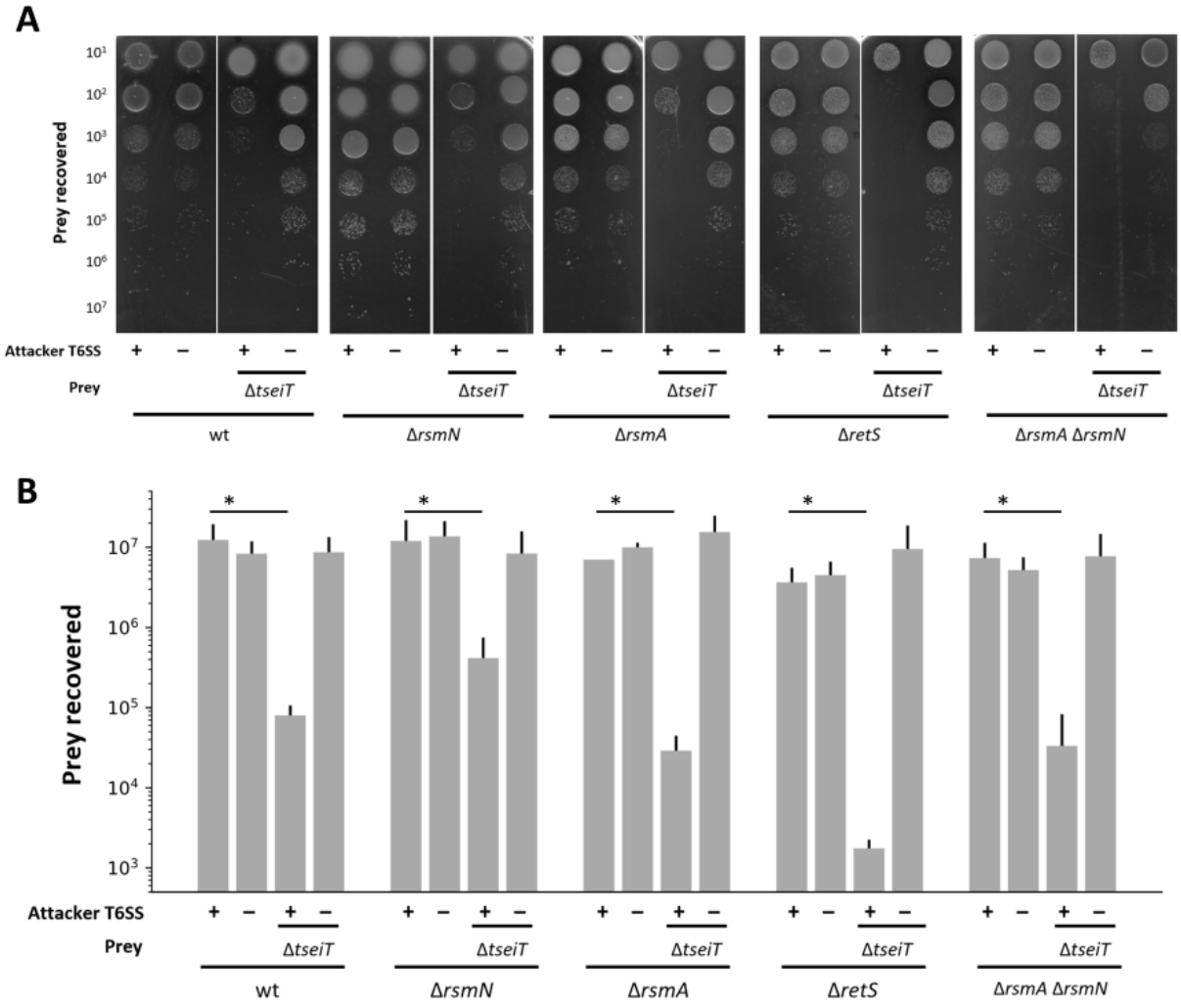

Figure 4.8: **Assessment of H2-T6SS toxin TseT mediated killing capacity of different Gac-Rsm mutants.**
Assessment of TseT mediated killing in different Gac-Rsm mutant strains. (**A**) Showing the amount of prey recovered on selective media. Competing WT, Δ*rsmN*, Δ*rsmA*, Δ*retS*, and Δ*rsmA*Δ*rsmN* toxin sensitised strains with a parental strain of corresponding regulatory background. Using parental strains with active T6SS or mutation of Δ*tssB1*Δ*tssB2*Δ*tssB3* for T6SS- attacker strains as indicated. Showing images representative of three biological replicates. (**B**) Corresponding numerical quantification of amount of prey recovered. Showing mean + SD of three biological replicates. Statistical testing performed using ANOVA and Tukey's tests, with $p<0.05$ indicated with a "*".

approximately 100-fold reduction in sensitive prey abundance, while only 10-fold reduction is consistently seen in Δ*rsmA*Δ*rsmN* context. When assessing H2-T6SS-dependent killing as mediated by nuclease TseT, stark differences in toxin sensitive bacteria abundance were detectable in all genetic contexts. Both WT and Δ*rsmN* strains show 10- to 100-fold reduction in toxin sensitive prey abundance, while in Δ*rsmA* context prey was nearly 150-fold less abundant in presence of a T6SS active (T6SS+) parental strain (Figure 4.8). This was broadly reflective of differences in Hcp2 levels detected in the supernatant using western blotting (Figure 4.3 F). An even further increase in H2-T6SS-dependent killing was seen in the Δ*retS* strain (Figure 4.8). This overall improvement in the ability to eliminate prey in a H2-T6SS-dependent manner compared to H1-T6SS does not necessarily reflect an improved killing, but may reflect the impact of the individual toxins used in the assay. Overall, competition assay relying on prey recovery broadly reflects the differences in T6SS activity of the *gac-rsm* mutant strains and further confirms that the disruption of the cascade at different points results in strains with different T6SS activity and thus ability to eliminate sensitive prey.

4.3 Discussion

The Gac-Rsm cascade is central in controlling transition towards increase in biofilm-associated gene expression, including control and increase in *P. aeruginosa* T6SS gene expression. This study evaluated the variation in T6SS expression and activity of strains with mutations at different positions within the Gac-Rsm pathway with the aim of compiling a set of strains with graduated T6SS activity that could be used for further studies of T6SS impact in competition. Loss of function mutations in both *rsmA* and *retS* genes have been shown to result in increased T6SS activity (172, 101, 723). RsmN has been shown to directly contribute to H1-T6SS translational activation (135, 149, 131, 145) and comparative analysis of Δ*retS* and Δ*rsmA*Δ*rsmN* *P. aeruginosa* PA14 strains through western blotting indicated higher activity levels in Δ*rsmA*Δ*rsmN* genetic context (598). In this study, we compared 4 strains with mutations affecting the Gas-Rsm regulatory cascade in regards to expression of all three *P. aeruginosa* T6SSs. These mutations are in the gene encoding the repressor RetS located at the top of the cascade, the downstream repressors RsmA and RsmN, and the combined Δ*rsmA*Δ*rsmN* mutant. This assessment provides a useful background to guide the choice of genetic context for future experimental design when performing *P. aeruginosa* T6SS studies investigating the impact of individual toxins (Chapter 5).

Here, we have combined promoter activity analysis with protein abundance assessment through western blotting and single-cell microscopy to investigate the impact of the Gac-Rsm cascade on *P. aeruginosa* T6SS. Both RsmA and RsmN have been shown to bind *P. aeruginosa* T6SS gene transcripts *in vitro* and *in vivo* (742, 739, 135). We have confirmed that, as expected from the existing literature, deletion of *rsmA* increases activity of all three T6SSs (723), while loss of *rsmN* alone does not have a notable impact on any of the T6SSs (Figures 4.3 and Figure 4.4). Comparative analysis of the impact of Δ*rsmA* and Δ*retS* on T6SS shows that the expression activity of each of the systems is further elevated if the Gac-Rsm cascade is disrupted at the sensory kinase level. More remarkably, even further H1-T6SS activation is

seen when comparing Δ*retS* and Δ*rsmA*Δ*rsmN* strains. With direct removal of both RsmA/N translational repressors, resulting in even further H1-T6SS activation than indirect de-repression through removal of RetS. Removal of RetS is likely to result in elevation of RsmY/Z production, but this does not guarantee that sRNAs will sequester all free RsmA and RsmN.

This study highlights the difference in T6SS activity between Δ*rsmA* and Δ*retS* strains, with Δ*retS* mutation resulting in consistently higher expression of the T6SS components and improved killing capacity of both H1- and H2-T6SS systems (Figures 4.7 and 4.8). This also points to the contribution of RsmN to the regulation of T6SS and that although Δ*rsmN* strains have been reported to display mild phenotypes (136, 135), the combination of Δ*rsmA*Δ*rsmN* mutations leads to a substantial phenotypic shift, with the impact on H1-T6SS being the most striking. The expression of *rsmN* is under regulatory control of RsmA (135, 743), and this provides a possible explanations of the somewhat mild Δ*rsmN* single deletion phenotypes, and this repressor could be more impactful and provide a compensatory mechanism upon loss of RsmA. Another factor contributing to the lesser *in vivo* impact of RsmN could be weaker target-binding and a requirement for dimer formation (122, 739). The results of a study that conducted transcriptome-wide mapping of RsmA/RsmN binding sites by (122) indicated that stabilisation through cross-linking was essential to detect RsmN binding sites, while RsmA binding was detectable without cross-linking; additionally, RsmA showed 5 times higher read enrichment for *tssA1* mRNA 5'UTR than RsmN. Both observations are indicative of RsmN forming weaker *in vivo* interactions with RNA targets. Yet, here we demonstrate that in the absence of RsmA, RsmN contributes to the repression of all three *P. aeruginosa* T6SSs. Additionally, further investigation avenue could focus on the phenotypic differences between Δ*retS* and Δ*rsmA*Δ*rsmN* strains. An avenue for this investigation would be to focus on impact of Rsm sRNAs. The two-component GacS-GacA system in *P. aeruginosa* is under direct control of RetS and appears to signal exclusively through RsmY and RsmZ (123), but the two sRNAs are not under exclusive control of GacA (152). Furthermore, additional sRNAs - RsmV and RsmW have been identified

and shown to interact with both RsmA and RsmN, but their regulatory contribution under physiological conditions remains unknown (157, 149).

Our data show that the level of T6SS activity can be upregulated in a kind of rheostat-like manner by manipulating distinct components of the Gac-Rsm network, and a progressive increase in the T6SS function is accompanied by a correlative increase in the level of secretion and impact on the survival of toxin sensitive prey bacteria. Overall the observations presented in this thesis chapter reinforce the idea that the Gac-Rsm cascade modulates the activity of T6SS and flag strains with gradually differentiated levels of T6SS activity that can be used as a tool for a further detailed study of how T6SS contributes to bacterial competition. In chapter 5 these strain set with graduated T6SS activity will be used to assess how differences in T6SS activity levels impact the whole community structure and to study the potency of T6SS toxins upon delivery at different doses.

Chapter 5

Individual *Pseudomonas aeruginosa* T6SS toxin mediated killing determines lineage distribution within communities

5.1 Introduction

Type VI secretion system (T6SS) is a molecular machine that is used to deliver effector proteins directly to adjacent cells. T6SS can be used to deliver effectors to host cells or nearby microbes, both bacteria and eukaryotes, such as fungi or amoebae (39, 514, 744). To mediate all of these interactions, the T6SS effectors display a high degree of functional versatility (354, 523). T6SS effectors are used to modify host cell behaviour, aiding with immune evasion and internalisation or to cause host cell death by other means (41, 611, 39). Alternatively, the system is used for direct competition with other microbes present within the niche killing or inhibiting growth of both bacterial or fungal cells (745). *Pseudomonas aeruginosa* T6SSs are notable for the high number of functionally diverse effectors that include anti-host and

antibacterial toxins as well as common good effectors that aid in metal ion uptake. Table 5.1 lists all effectors currently described in *P. aeruginosa* PAO1 and more are likely to be identified, as evidenced by the frequent addition of new entries to the list of toxins, with both systematic and unbiased identification approaches in use (555, 557). Most of the effectors identified to date are antibacterial toxins delivered by H1- and H2-T6SS. The functions of these toxins are biochemically diverse and target the integrity of the cell wall or membranes, as well as energy metabolism, protein production, or nucleic acids (584, 594, 40, 557, 559). A question that arises when looking at this effector diversity is how do these different toxins contribute to bacterial competition.

Studies evaluating the impact of individual T6SS toxins as delivered by producer bacteria are challenging in the context of bacteria such as *P. aeruginosa* that deliver a large and diverse set of T6SS effectors. In addition, studies of T6SS in *P. aeruginosa* generally rely on strains with regulatory mutations, often within the Gac-Rsm cascade, as T6SS expression is non-constituitive under laboratory conditions (Chapter 4). With these considerations, a study of individual effector impact within an interspecies context would prove not only exceedingly complex to perform from an engineering standpoint, but also provide challenges in interpretation due to the many compounding factors. Among these is the fact that the Gac-Rsm cascade not only affects T6SS activity but is central to regulating the transition from planktonic to biofilm lifestyle, involving hundreds of genes that include the production of extracellular matrix components and changes in bacterial motility (746, 122), factors known to influence the results of T6SS-dependent competition (650). It stands to reason that even in the context of competition between otherwise isogenic PAO1 WT and Gac-Rsm cascade mutant any competitive differences observed would be a result of not only increased T6SS activity, but a range of other compounding phenotypic differences. These considerations led us to an approach of studying impact of individual toxins in an isogenic context, where any changes in distribution of strains within bacterial communities are a result of actions of specific toxins as delivered by the attacker population.

	Effector	Cognate toxin immunity	Description	References
H1-T6SS	Tse1 (PA1844)	Tsi1 (PA1845)	Amidase that hydrolyses peptidoglycan crosslinks causing target cell lysis	(Hood *et al.*, 2010, Russell *et al.*, 2011)
	Tse2 (PA2702)	Tsi2 (PA2703)	NAD dependent ADP-ribosyltransferase that causes quiescence, toxic when expressed in eukaryotic cells	(Hood *et al.*, 2010, Li *et al.*, 2012, Robb *et al.*, 2016)
	Tse3 (PA3485)	Tsi3 (PA3485)	Muramidase that hydrolyses peptidoglycan backbone causing target cell lysis	(Hood *et al.*, 2010, Russell *et al.*, 2011)
	Tse4 (PA2774)	Tsi4 (PA2775)	Forms ion selective membrane pores that disrupt proton motive force	(Whitney *et al.*, 2014, LaCourse *et al.*, 2018)
	Tse5 /RhsP1 (PA2684)	Tsi5 /RhsP1i (PA2683.1)	Forms ion selective membrane pores resulting in loss of membrane potential, contains RHS and PAAR domains	(Hachani *et al.*, 2014, Whitney *et al.*, 2014, Gonzalez-Magana *et al.*, 2021)
	Tse6 (PA0093)	Tsi6 (PA0094)	NAD(P)+ glycohydrolase that depletes NAD(P)+ resulting in target bacteriostasis, contains PAAR domain	(Hachani *et al.*, 2014, Whitney *et al.*, 2014, Whitney *et al.*, 2015)
	Tse7 (PA0099)	Tsi7 (PA0100)	Tox-GHH2 nuclease, contains PAAR domain	(Hachani *et al.*, 2014, Pissaridou *et al.*, 2018)
	Tse8 (PA4163)	Tsi8 (PA4164)	Targets transamidosome complex disrupting protein synthesis	(Gonzalez-Magana *et al.*, 2020, Nolan *et al.*, 2021)
H2-T6SS	Tle1 (PA3290)	Tli1a (PA3291) Tli1b (PA3292)	Phospholipase A2 activity	(Russell *et al.*, 2013, Hu *et al.*, 2014, Flaugnatti *et al.*, 2016)
	Tle3 (PA0260)	Tli3 (PA0259)	Phospholipase	(Russell *et al.*, 2013, Berni *et al.*, 2019)
	Tle4 /TplE (PA1510)	Tli4 /TplEi (PA1509)	Phospholipase, contains PGAP1-like domain to aid internalisation into host cells and localisation at ER membrane inducing autophagy, both antibacterial and anti-host toxicity	(Russell *et al.*, 2013, Jiang *et al.*, 2014, Lu *et al.*, 2014)
	PldA /Tle5a (PA3487)	Tli5a (PA3488)	Phospholipase D with preference for PE (phosphatidylethanolamine) as substrate, activate PI3K/Akt pathway that promotes internalisation into host cells, both antibacterial and anti-host toxicity	(Wilderman *et al.*, 2001, Russell *et al.*, 2013, Jiang *et al.*, 2014, Spencer & Brown, 2015, Boulant *et al.*, 2018, Wettstadt *et al.*, 2019)
	PldB /Tle5b (PA5089)	$Tli5b_1$ (PA5088) $Tli5b_2$ (PA5087) $Tli5b_3$ (PA5086)	Phospholipase D, activates PI3K/Akt Pathway that promotes internalisation into host cells, both antibacterial and anti-host toxicity	(Russell *et al.*, 2013, Jiang *et al.*, 2014, Wettstadt *et al.*, 2019, Wen *et al.*, 2020)
	VgrG2b (PA0262)	VgrG2bi (PA0261)	Contains zinc- metallopeptidase domain, hydrolyses peptidoglycan in cell division plane causing target lysis. Interacts with α- and β-tubulins and γTuRC promoting internalisation into nonphagocytic cells, both antibacterial and anti-host toxicity	(Sana *et al.*, 2015, Berni *et al.*, 2019, Wood *et al.*, 2019)
	AmpDh3 (PA0807)	AmpDh3i (PA0808)	Cell wall remodelling amidase that contributes to β-lactam resistance, hydrolyses target cell peptidoglycan cross links	(Juan *et al.*, 2006, Zhang *et al.*, 2013, Wang *et al.*, 2020)
	TseT (PA3907)	TsiT (PA3908)	TOX-REase domain containing nuclease	(Burkinshaw *et al.*, 2018)
	TseV (PA0822)	TsiV (PA0821)	Putative VRR-NUC domain containing nuclease	(Wang *et al.*, 2021)
	PA5265	PA5264	Contains MIX (marker for type six effectors) motif	(Salomon *et al.*, 2014)
	PA2066	Unknown	Putative Hcp2 associated effector	(Howard *et al.*, 2021)
	Azu (PA4922)	-	Common good effector, copper binding and uptake	(Nar *et al.*, 1992, Han *et al.*, 2019)
	ModA (PA1863)	-	Common good effector, molybdite binding and uptake	(Self *et al.*, 2001, Wang *et al.*, 2021)
H3-T6SS	PA0256	Unknown	Putative Hcp3 associated effector	(Howard *et al.*, 2021)
	TseF (PA2374)	-	Common good effector, interacts with PQS and the siderophore receptor FptA aiding in iron uptake	(Lin *et al.*, 2017)

Table 5.1:
P. aeruginosa PAO1 T6SS effectors

The exact set of effectors differs between individual *P. aeruginosa* reference strains; here *P. aeruginosa* PAO1 was used to comprehensively engineer strains sensitised to each of the individual toxins listed in the Table 5.1 and this was done in a variety of regulatory backgrounds. To do so, we deleted specific cognate effector-immunity gene pairs in various regulatory backgrounds, enabling a comprehensive analysis of how delivery of individual toxins at different

doses results in increased competitive fitness.

The objectives of this chapter are:

- To develop an experimental setup that allows to assay how T6SS-dependent competition impacts lineage distribution in mixed communities.
- To assess individual T6SS toxin contribution to bacterial competition.
- To assess how graduated differences in T6SS firing behaviour translate into differences in bacterial competitiveness.
- To evaluate how changes in bacterial growth conditions impact T6SS-dependent competition outcome.
- To use theoretical modelling to evaluate the key parameters that determine the outcome of the T6SS-dependent competition.

5.2 Whole colony microscopy setup for imaging bacterial competition

To investigate how *P. aeruginosa* uses T6SS-toxins to shape the structure of whole communities, we took the approach of growing competing bacteria within mixed macrocolonies. This setup relies on placing a defined mix of fluorescently tagged bacteria on a media surface and once a macrocolony is established, spread and spatial distribution of sub-populations within the community can be visualised. This allows for assessment of not only the overall competition outcome by comparing the area occupied by the two competitors, but allows to look at the impact on lineage distribution within community. An experimental setup similar to the one employed here has been used in both bacterial and yeast systems to address questions on how the community structure is shaped by mechanistic interactions, positive interactions in form of cross-feeding or competition through both diffusible toxins and contact dependent inhibition (CDI) (416, 683, 747, 701, 700). Here, this setup has been adapted to assess how the use of individual T6SS toxins enables *P. aeruginosa* to restrict prey bacteria growth.

5.2.1 Bacterial distribution in mixed macrocolonies

To observe sub-population distribution within mixed macrocolony, bacterial strains are tagged with constructively expressed, chromosomally integrated fluorophores - here sfGFP or mCherry are used, then two isogenic PAO1 strains are mixed and grown on media agar until a macrocolony with 2 distinct regions is established. The central part of the colony corresponding to the placement of the inoculum droplet and bacteria in this area appear to be well mixed (Figure 5.1 A). It is also notable that after establishment sub-population distribution within the colony central region remains mostly unchanged during further growth (Figure 5.1 B). The outer colony region is made up of segments that are preferentially dominated by one of the strains within the mix. The number or segments in the outer colony region and the extent of

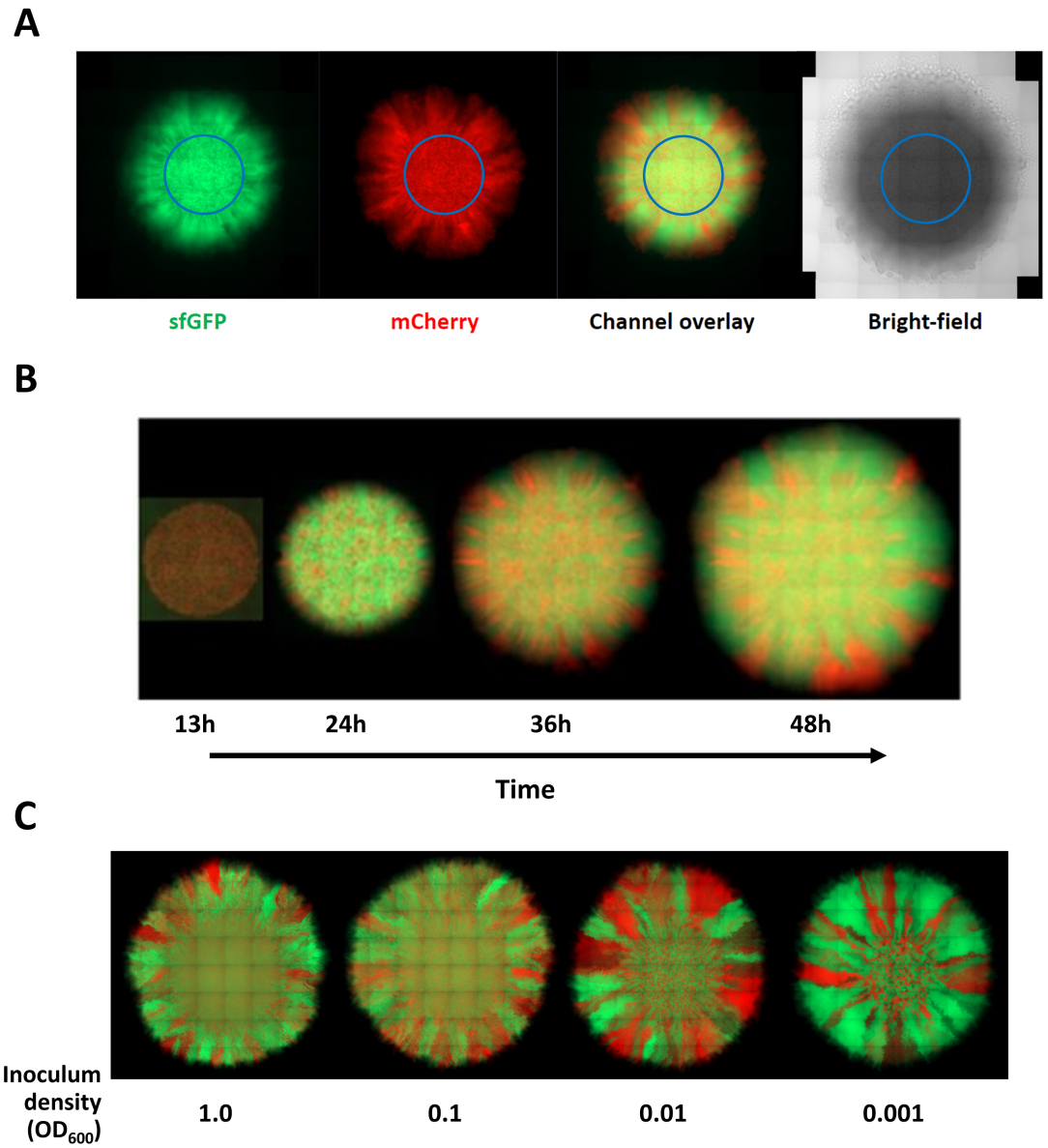

Figure 5.1: **Sub-population distribution within mixed macrocolony community.** Mixed lineage macrocolonies consist of two distinct regions, an intermixed central region corresponding to the inoculum placement and a segmented outer colony region. (**A**) Showing individual fluorescence channel images, corresponding overlay and bright-field images of a 24h old macrocolony of red (mCherry) and green (sfGFP) tagged Δ*rsmA* lineages. Location of inoculum spot indicated with a ring in blue. Inoculum density OD_{600}=0.01, strain ratio within mix of 1:1, bacteria cultured at 37^{o}C.
(**B**) Lineage range expansion within mixed bacterial colony. Fluorescent images of Δ*rsmA* lineage expansion within colony 13h, 24h, 36h, and 48h after inoculation. Inoculum density OD_{600}=0.01, strain ratio within mix of 1:1, bacteria cultured at 30^{o}C.
(**C**) Changes in sub-population spatial distribution depending on the bacterial density within inoculum. Showing fluorescent channel overlay images of 48h old mixed colonies consisting of Δ*rsmA* lineages. Inoculum density OD_{600} of 1.0, 0.1, 0.01, and 0.001, strain ratio within mix of 1:1, bacteria cultured at 37^{o}C for 48h.

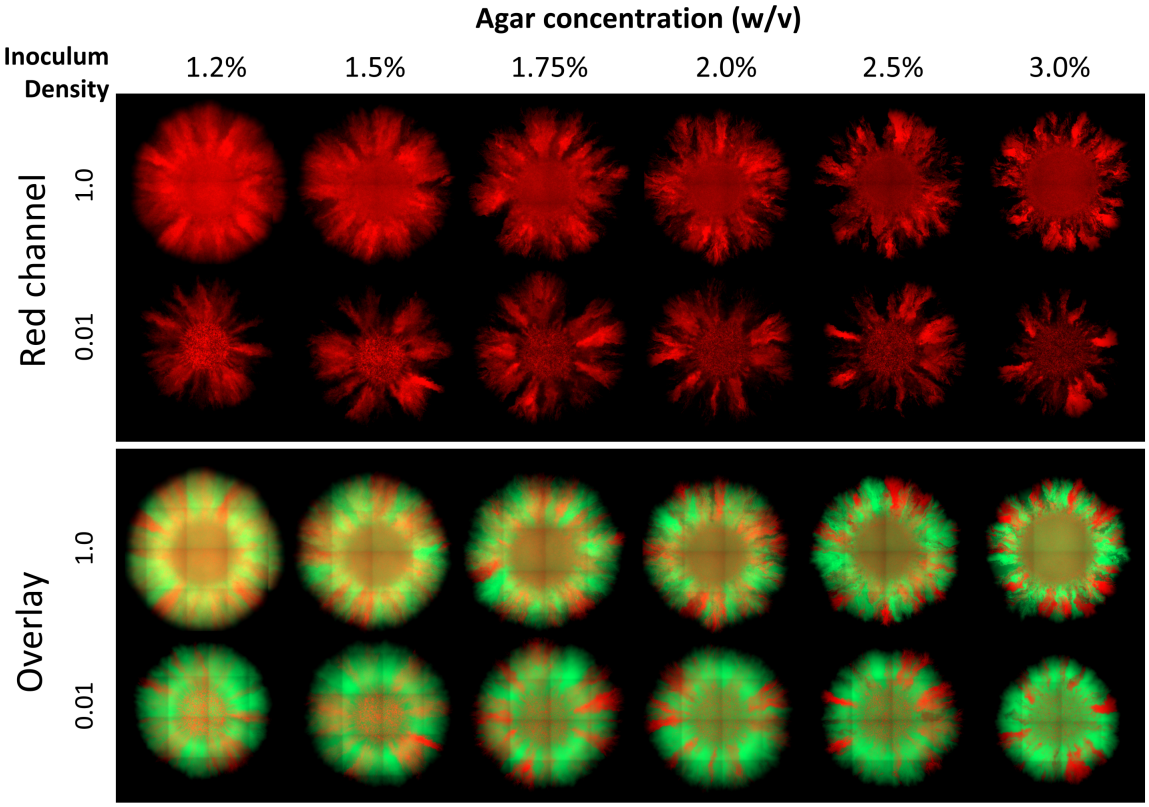

Figure 5.2: **Sub-population distribution within mixed macrocolonies is dependent on the media rigidity.**
Fluorescent images of lineage distribution within macrocolonies grown on LB with agar concentration (w/v) of 1.2%, 1.5%, 1.75%, 2.0%, 2.5%, 3.0%. Showing images of red fluorescent channel only and the corresponding overlay images. Communities established from inoculum with density of OD_{600}=1.0 or 0.01, grown at 37^{o}C for 48h. Showing 1 of 1 biological repeat set.

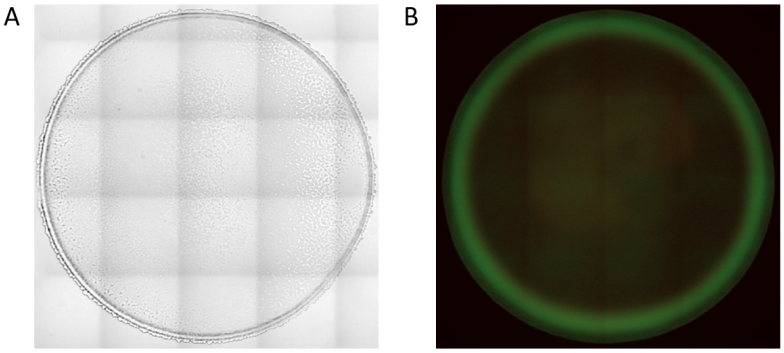

Figure 5.3: **Bacteria within a drying inoculum spot distribute accordingly to 'coffee stain' pattern.**
A ring indicative of higher bacterial density at the edge of inoculum spot can be seen both in bright-field (**A**) and fluorescent (**B**) images. Both images taken after 4h incubation at 37^{o}C, inoculum density OD_{600}=1.0 (**A**) and OD_{600}=3.0 (**B**).

strain intermixing in the outer colony region depends on the bacterial density in the inoculum (Figure 5.1 C). Growth conditions such as changes in temperature, ambient moisture and media

rigidity also notably affect sub-population distribution within macrocolonies (Figure 5.2). An increase in the concentration of media agar results in a corresponding elevation in substrate rigidity; bacterial colonies grown on increasingly more rigid media appear comparably smaller and less intermixed in the outer colony region. An additional feature observable in mixed macrocolony structures is an appearance of a ring at the location corresponding to the outer edge of the inoculum droplet (Figure 5.3). As a result of microfluidics effect termed "coffee stain" pattern, water from bacteria containing droplets evaporates in a manner that promotes bacterial aggregation at the edge of the drying droplet (748, 749). This increased bacterial density results in distinct population establishment conditions and differences in sub-population arrangement at this location can be observed in established communities.

5.2.2 Ability to actively fire T6SS is not sufficient to provide a competitive advantage.

First we chose to assess whether the ability to fire T6SS impacts the competitive fitness of the strain in an otherwise isogenic context. For this we used a strain with a triple deletion of *tssB1*, *tssB2*, and *tssB3* genes, that renders all T6SSs unable to fire, but does not interfere with

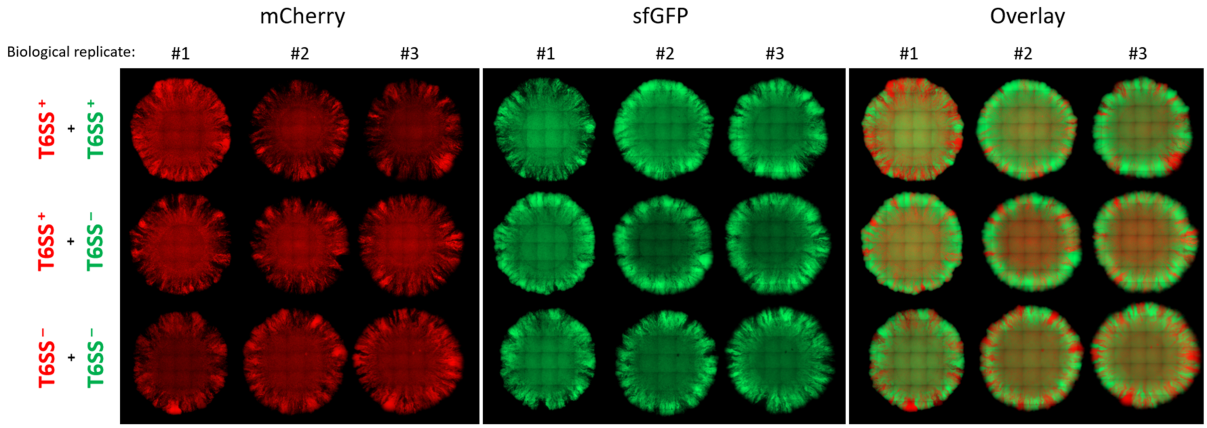

Figure 5.4: **Ability to actively fire T6SS does not provide a marked competitive advantage between otherwise isogenic *P. aeruginosa* strains.** Fluorescent images of whole bacterial colonies of bacteria mixes made up of T6SS+ (Δ*retS*) and T6SS– (Δ*retS*Δ*tssB1*Δ*tssB2*Δ*tssB3*) strains at 1:1 initial ratio and initial OD_{600}=1.0, showing individual channel and overlay images of 3 biological replicates of 48h old mixed macrocolonies incubated on LB with 2%(w/v) agar at 37^{o}C.

the production of T6SS components (Figure 4.3 E and F). Using a Δ*retS* mutant with high levels of T6SS activity, no competitive differences beyond expected inherent structural variation were seen when competing Δ*retS*Δ*tssB1*Δ*tssB2*Δ*tssB3* mutant with its parental Δ*retS* strain (Figure 5.4). This indicates that within the context of competition in macrocolony biofilm the metabolic costs resulting from the repeated assembly/disassembly process of T6SS are negligible. Additionally, these results emphasise the importance of the T6SS competition being dependent on successful toxin delivery rather than the effects of mechanical damage rendered through puncture by T6SS.

5.3 Delivery of individual T6SS toxins restricts prey expansion within macrocolonies.

The resistance to T6SS-mediated killing from sister cells results from the presence of a full set of effector immunity genes in both strains that make up the community. As simply firing T6SS does not provide an added competitive advantage, we decided to use this assay to study how competition mediated exclusively through individual T6SS effectors affects the bacterial distribution within the community. This can be done through systematically engineering strains sensitive to specific toxins by removing individual effector-immunity gene sets.

5.3.1 H1-T6SS toxin-mediated competition in different Gac-Rsm mutant strains

T6SS effector sets are highly variable not only between bacterial species, but also between commonly used reference strains. This study on the impact of individual T6SS effectors focusses on *P. aeruginosa* PAO1, with existing publications describing a total of 18 known effector-immunity gene pairs listed in Table 5.1. We systematically engineered strains sensitive to all 8 known H1-T6SS toxins, i.e. Tse1-Tse8 in a range of Gac-Rsm regulatory mutant strains. To

avoid self- and sister-cell intoxication, we removed both effector and cognate immunity genes (i.e. *tse1tsi1* - *tse8tsi8*). For purposes of assaying competition within mixed bacterial macrocolonies, strains sensitive to T6SS toxins were tagged with constitutively expressed mCherry (shown in red), while the parental strain with or without active T6SS was tagged with sfGFP (shown in green); this colour scheme remains consistent throughout the report (Figure 5.5).

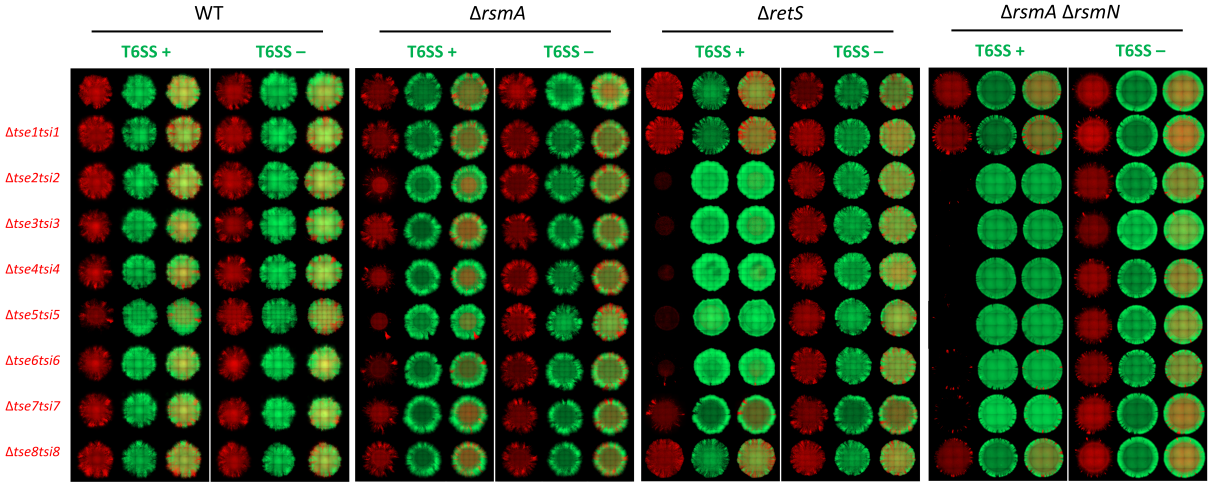

Figure 5.5: **Growth of H1-T6SS toxin sensitised strains is spatially restricted in a manner dependent on the specific toxin used and the level of H1-T6SS activity.** Representative image of 48h old mixed colonies of toxin sensitised bacteria in red in competition with T6SS+ or T6SS- ($\Delta tssB1\Delta tssB2\Delta tssB3$) strains of the same regulatory background in green. Upper lane contains a control mix of bacteria with full toxin-immunity gene sets, each of the following lanes contains strain sensitised to one of the H1-T6SS toxins from Tse1 to Tse8. Images sets (from left to right) of competitions of WT, $\Delta rsmA$, $\Delta retS$, and $\Delta rsmA\Delta rsmN$ regulatory background strains. For each of the experiment sets single fluorescence channel and overlay images showing distribution of sensitised prey in a mix with T6SS+ and subsequently T6SS- ($\Delta tssB1\Delta tssB2\Delta tssB3$) parental strain are shown. Strains contain constitutively expressed fluorescent proteins, toxin sensitised prey is labelled with mCherry (shown in red) and attacker with sfGFP (shown in green). All bacteria mixed at 1:1 ratio, inoculum OD_{600}=1.0, grown for 48h at 37°C on LB with 2% (w/v) agar.

WT *P. aeruginosa* PAO1 shows low levels of H1-T6SS activity (Figure 4.3E). In competition through prey recovery comparing the killing capacity of the Gac-Rsm mutant strains discussed previously, no measurable Tse5-dependent prey killing was seen when competing WT strains (Figure 4.7), but the scenario is somewhat different within the context of mixed macrocolony competition. When the WT strain sensitised to Tse5 is grown in the presence of T6SS+ WT attacker, the prey bacteria are restricted from expanding in the colony outer region (Figure 5.5). This growth defect is T6SS-dependent, as it does not occur when toxin-sensitive bacteria are

mixed with the parental strain T6SS Δ*tssB1*Δ*tssB2*Δ*tssB3*. Across multiple biological repeats, it can also be seen that sensitisation to Tse4 results in T6SS-dependent prey growth restriction, but to a lesser extent than Tse5. In the WT regulatory context, none of the other strains sensitised to individual toxins appear to be consistently growth restricted in a T6SS-dependent manner. However, it is notable that the delivery of a single pore-forming toxin Tse4 or Tse5 at doses as low as indicated by Gac/Rsm mutant H1-T6SS activity analysis provides a consistent competitive growth advantage.

The H1-T6SS activity is elevated within Δ*rsmA* genetic background (Figure 4.4E). In competition using toxin-sensitive Δ*rsmA* strains we see that use of five out of the eight H1-T6SS bacterial toxins results in prey growth restriction. Similarly as with WT strains, sensitivity to both of the pore-forming toxins, Tse4 and Tse5, results in prey growth being mostly limited to the colony central region. Furthermore, the delivery of NAD-dependent toxins Tse2 and Tse6, as well as nuclease Tse7, results in restriction of the prey bacteria to the central region of the colony. While use of peptidoglycan hydrolases Tse1 and Tse3, or Tse8, which impairs target protein synthesis by reducing the pool of available Asn-tRNA, does not result in a notable growth impairment of the sensitive Δ*rsmA* strains.

When assessing the contribution of individual H1-T6SS toxins in the context of Δ*retS* mutation, that was shown to result in further elevation of T6SS activity, even further growth restriction of toxin-sensitive bacteria becomes apparent. Regarding the toxins Tse2, Tse4, Tse5, and Tse6, all of which appeared to be sufficient to restrict prey bacteria growth to colony central region in Δ*rsmA* strains, within the context of Δ*retS* regulatory background result near complete prey elimination, with most replicates indicating that only trace amounts of toxin-sensitive bacteria remain in the colony central region. A notable difference between single H1-T6SS toxin-mediated competition in context of Δ*rsmA* and Δ*retS* strains is that sensitisation to peptidoglycan muramidase Tse3 leads to notable T6SS-dependent growth restriction in Δ*retS* context, while no impact is seen in Δ*rsmA* strain competition. Interestingly, in the case of

sensitisation to nuclease Tse7, in both Δ*rsmA* and Δ*retS* genetic context, toxin-sensitive strain growth is spatially restricted to the colony central region, but unlike in the case with the toxins mentioned above, the amounts of prey bacteria in the central region remain high, both in the presence of the T6SS+ and T6SS- parental strains.

Gac-Rsm mutant T6SS activity analysis revealed a that Δ*rsmA*Δ*rsmN* mutants show even further elevation of T6SS activity (Figure 4.4). Within the context of single toxin-mediated competition, all toxins providing a T6SS-dependent competitive advantage in Δ*retS* background strains appear to ensure nearly complete elimination of the sensitive bacteria, this being a further direct indication of the dose-dependent impact of H1-T6SS toxins mediated through elevation in T6SS activity. Notably, sensitisation to peptidoglycan hydrolase Tse1 or the transamidosome complex targeting Tse8, does not result in detectable growth disadvantage in any of the individual toxin-mediated competition assays performed. Both Tse1 and Tse8, have been demonstrated to be H1-T6SS-dependent antibacterial toxins (584, 557), but within the context of single toxin competition, remain ineffective in destroying prey, even when delivered in presumably high doses by Δ*rsmA*Δ*rsmN* strains, as indicated by the apparent dose response of the other toxins assessed. In case of single H1-T6SS toxin competition in Δ*rsmA*Δ*rsmN* strains, some other features in distribution of competitors emerge. In case of both Tse6 and Tse7 mediated competition, a clear T6SS-dependent growth restriction is observable when comparing prey abundance in presence of T6SS+ or T6SS- parental strains. What is notable is that unlike in any other regulatory context, where distribution of fluorescence signal indicates that any remaining prey bacteria is present in the colony central region, small amounts of surviving prey are present as segments in the outer colony regions, this effect being similar to one further addressed in the results section 6 looking at impact of type IV pili mediated impact on T6SS competition.

5.3.2 Analysis of changes in sensitive lineage spatial distribution upon T6SS attack

When conducting toxin-mediated T6SS competition within mixed macrocolonies, additional insights about competition within the context of growing communities can be observed. As the colonies grow by expanding laterally and established regions remain largely unchanged over time (Figure 5.1 B), analysis of spatial differences in the distribution of fluorescent signals within

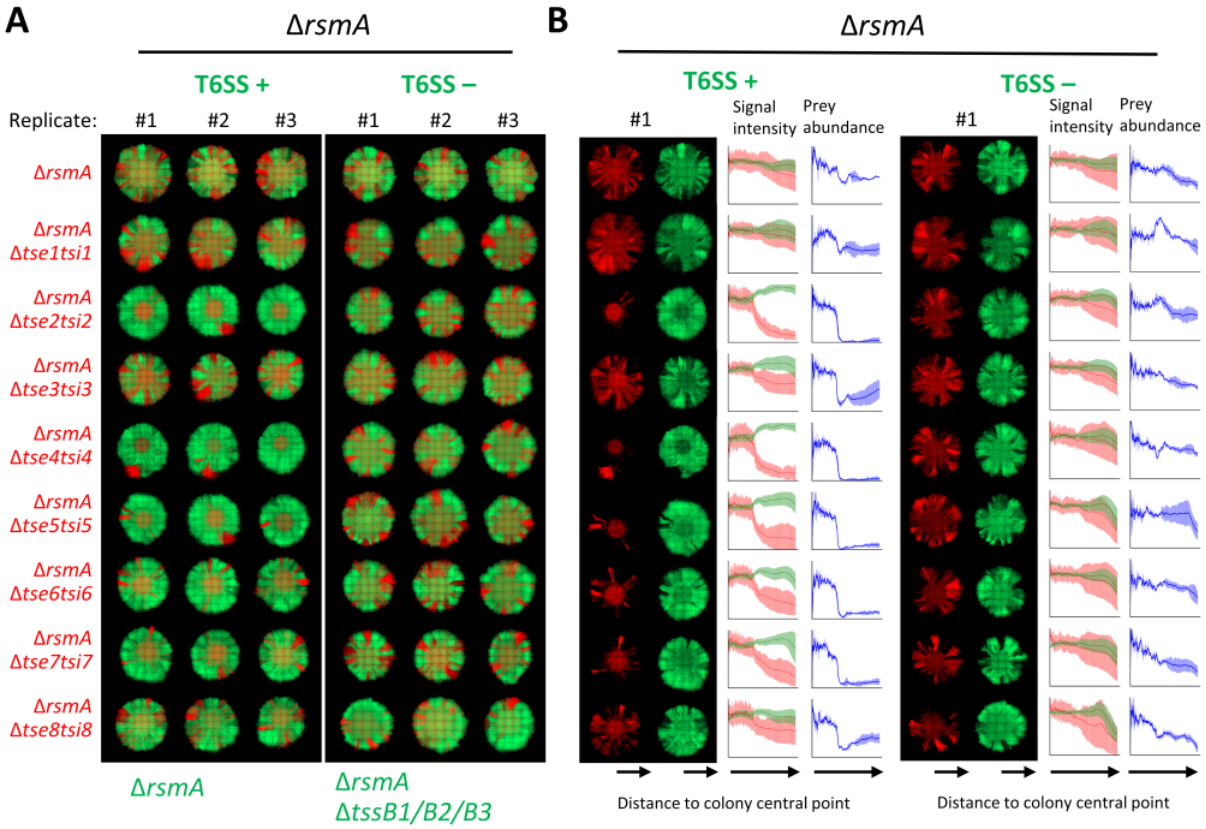

Figure 5.6: **T6SS toxin action impacts bacterial distribution within communities.** (**A**) Images of mixed bacterial macrocolonies consisting of H1-T6SS toxin sensitised bacteria (in red) in presence of T6SS+ (Δ) or T6SS- (Δ*rsmA* Δ*tssB1* Δ*tssB2* Δ*tssB3*) parental bacteria (in green). Upper lane contains a control mix of bacteria with full toxin-immunity gene sets, each of the following lanes contains strain sensitised to one of the H1-T6SS toxins from Tse1 to Tse8. Fluorescent channel overlay images show bacterial distribution within 3 replicate colonies. All bacteria mixed at 1 to 1 ratio with inoculum density of OD_{600}=0.01, grown for 48h at 37^{o}C on LB with 2% (w/v) agar. (**B**) Images showing distribution of individual strains corresponding to replicates #1 from panel (**A**) and the corresponding analysis of fluorescent signal distribution within the image. Columns 3 and 7 show the corresponding mean (+SD) relative fluorescence signal intensity for the each of the channels as function of distance from the colony central point (for image replicates #1). With columns 4 and 8 showing relative area occupied by prey as function of distance from the colony central point (mean of 3 replicate colonies +SD).

the final community can provide insight in how community develops over time. In cases where lineages in the outer colony region are well segregated, it is possible to measure the area of colony occupied by each of the strains within the mix. This more explicit analysis of spatial differences in the fluorescent signal was used to gain some further insight in H1-T6SS toxin-mediated killing within $\Delta rsmA$ regulatory context using a lower inoculum density setup that due to initial sub-population establishment promotes formation of more spatially segregated lineages.

When comparing the mean fluorescent signal brightness between the bacteria present or the area of colony occupied by each of the strains, it becomes apparent that sensitive prey is indeed not completely eliminated. Even in the example of Tse2-sensitised bacteria growth restriction shown in Figure 5.6B, some red fluorescent signal is present in the outer colony region although no large prey segments are apparent. In the cases of Tse5-, Tse6- or Tse7-mediated interactions, well segregated segments in the outer colony region are apparent, but rather than large increase in the relative area occupied, this is reflected in increased relative fluorescent signal variation. When comparing structures with small number of well-defined prey segments to the signal from Tse2 sensitive bacteria, mean relative fluorescence level differences in corresponding colony regions are small, but presence of segregated prey segments as compared to lack thereof is reflected by increase in relative fluorescence variation.

A notable feature of the competition within mixed macrocolonies is that the overall competitive outcome is primarily reflected in whether toxin-sensitive prey bacteria is able to expand beyond the inoculum area, rather than as a fraction of the total community area occupied, as this is likely to remain variable between communities (Figure 5.6A). Another point of note is that in this scenario of laterally expanding community, the number of prey segments formed or the size of remaining prey segments is not closely indicative of the relative toxin effectiveness and aspects of the overall prey population distribution. Individual segment width is likely more indicative of the fact that the particular fate of individual bacteria is subject

to local heterogeneity, but is not necessarily reflective of the overall competitive effectiveness (Figure 5.6A). It is also notable that although the low bacteria density setup used here allows for more detailed measurement of the lineage distribution, the competition outcomes are less robust overall, due to both inherently higher variation seen in communities established from sparse founder cell populations (700) and the impact of prior establishment on T6SS-mediated interactions addressed in more detail in the chapter 6.

5.3.3 T6SS toxins act synergistically

Two of the H1-T6SS toxins, Tse1 and Tse3, are peptidoglycan hydrolases, growth restrictive effect resulting from sensitisation to Tse3 is apparent in Δ*retS* and Δ*rsmA*Δ*rsmN* genetic context, while none of the Δ*tse1tsi1* strains tested appeared to be consistently growth restricted (Figure 5.5). Both of these toxins are amongst the most studied T6SS effectors, with Tse1 especially being known as one of the most potent toxins in some interspecies competition

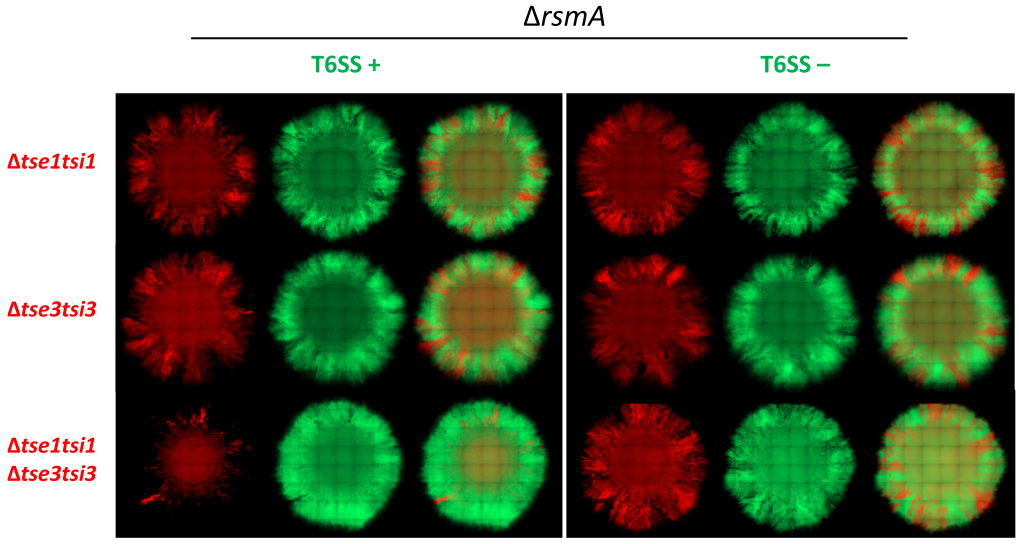

Figure 5.7: **T6SS toxins act synergistically to further restrict prey growth.** Representative fluorescent images of Δ*rsmA* strains sensitised to Tse1 or Tse3 individually (upper and middle rows correspondingly) and in combination (lower row). Both single fluorescence channel and overlay images showing distribution of sensitised prey in a mix with T6SS+ (Δ*rsmA*) on right and subsequently T6SS- (Δ*rsmA*Δ*tssB1*Δ*tssB2*Δ*tssB3*) parental strain on left. Strains contain constitutively expressed fluorescent proteins, prey labelled with mCherry (shown in red) and attacker with sfGFP (shown in green). All bacteria mixed at 1:1 ratio, inoculum OD_{600} = 1.0, grown for 48h at 37^{o}C on LB with 2% (w/v) agar, showing a representative image of a set of 3 replicates.

scenarios (582, 564, 584, 661). Nevertheless, in case of killing *P. aeruginosa*, analysis of different toxin-mediated competition suggests that toxins that alter the integrity of the peptidoglycan backbone (e.g. muramidase Tse3) may have a more severe impact on cell integrity than the ones targeting glycan crosslinks (e.g. amidase Tse1). Although neither Δ*rsmA*Δ*tse1tsi1* or Δ*rsmA*Δ*tse3tsi3* strains appear to be spatially restricted in the presence of the T6SS+ parental strain, simultaneous sensitisation to both Tse1 and Tse3 (Δ*rsmA*Δ*tse1tsi1* Δ*tse3tsi3*) leads to T6SS-dependent prey strain growth restriction (Figure 5.7). This is an excellent example of toxin synergy that emphasises the value of multiple toxin sets and additionally shows how effectors such as Tse1 that do not appear to be able to effectively kill *P. aeruginosa* even when delivered at high doses, could be a valuable part of the toxin set as a whole.

5.3.3.1 *P. aeruginosa* engages in effective H1-T6SS toxin-mediated competition under nutrient limitation

A significant broader question surrounding T6SS-mediated competition is the aspect of metabolic costs associated with the use of T6SS. T6SS is a molecular machine that fires proteins into target cells or surrounding media, and an assumption is that material costs associated with the use of T6SS are high due to the requirement of continuous synthesis of cargo proteins and energetic costs associated with the assembly and disassembly of the system. This type of expenditure is easily justified when competing for the occupancy of nutrient rich niches, but meta-genomics studies of marine bacteria have found that T6SSs are prevalent under nutrient poor niches (519), therefore a question of how nutrient limitation impacts T6SS-mediated killing is relevant. Additionally, we chose to test whether toxin-sensitive cells under nutrient-limiting conditions would be more vulnerable to killing by T6SS toxins targeting energy metabolism are more impactful under conditions where prey bacteria are under metabolic stress. Figure 5.8 shows a sub-set of H1-T6SS toxin sensitised Δ*retS* strains in a mix with both T6SS+ and T6SS- parental strain on M9 minimal media agar with glucose as a carbon source compared to the

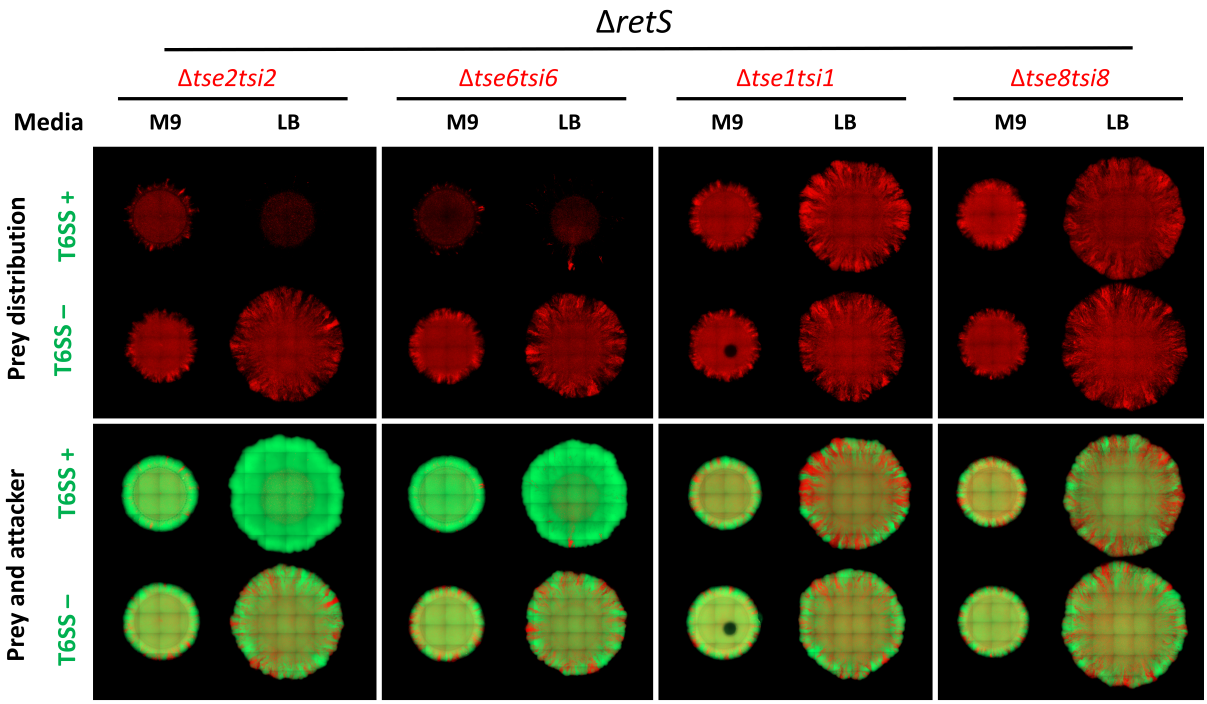

Figure 5.8: ***P. aeruginosa* is able to growth restrict H1-T6SS toxin-sensitive prey independently of nutrient limitation during competition.** Fluorescent images of mixed macrocolonies of Δ*retS* regulatory background toxin sensitised bacterial strains in competition with T6SS+ (Δ*retS*) and T6SS- (Δ*retS*Δ*tssB1*Δ*tssB2*Δ*tssB3*) parental strains. Showing mCherry tagged prey strain distribution (upper section in red) and fluorescent channel composite image with both prey and attacker (sfGFP shown in green) distribution in the lower set. Comparative competition sets with prey strains sensitised to Tse2, Tse6, Tse1, or Tse8, from left to right, with bacteria grown on defined minimal media (M9 with glucose as the sole carbon source) or rich media (LB agar). All bacteria mixed at 1:1 ratio, inoculum $OD_{600} = 1.0$, grown for 48h at 37^{o}C on M9 or LB with 2% (w/v) agar. Showing a representative image of a set of 3 replicates for bacterial colonies grown on LB agar and 1 of 1 test images for colonies grown on minimal media. Colony images shown to scale.

same competition mixes grown on nutrient rich LB agar. Strains sensitised to Tse2 and Tse6 were chosen as both of these toxins act by interfering with prey energy metabolism, and in both cases the prey strains appear to be spatially restricted independently of the growth medium. Furthermore, strains sensitive to Tse1 and Tse8 were chosen as sensitisation of either of the toxins did not show an effect in single toxin-mediated competition independently of H1-T6SS activity level (Figure 5.5). Tse8 impacts protein synthesis through targeting transamidosome complex (557), therefore we wanted to test whether this effector would be more impactful in media lacking amino acids. Neither sensitisation to Tse1 or Tse8 appeared to result in any prey growth restriction on defined media (Figure 5.8), with the main notable impact on

macrocolony experiments carried out in minimal media being the reduction in the size of the entire population, resulting from growth under conditions limited in nutrients. Although no additional compounding effects from growth in minimal media are observable, this confirms that *P. aeruginosa* is capable of using T6SS to eliminate sensitive prey even under nutrient restrictive conditions. Additionally, looking at the negative control competition mixes, it is observed that strains unable to actively fire T6SS (Δ*retS*Δ*tssB1*Δ*tssB2*Δ*tssB3*) do not appear to show a consistent increase in relative abundance under experimental conditions used here.

5.3.4 H1-T6SS toxin-mediated killing occurs independently of prey T6SS activity

P. aeruginosa H1-T6SS is used for response or Tit-for-tat firing (564). This describes a behaviour where a T6SS sheath is assembled in the location where an exogenous T6SS injection has just occurred. This response firing is described in further detail in the Introduction section 1.4.4. Bierefly, *P. aeruginosa* Tit-for-tat firing is mediated by the TagTSRQ-PppA-PpkA pathway (564, 579). Phosphatase PppA is H1-T6SS post-translational regulator and is essential for repositioning of the sheath assembly platform in response to the detection of a T6SS injection by TagTSRQ (569, 564, 573). This retaliatory firing means that upon provocation by external T6SS attack H1-T6SS firing rate increases and has been shown to lead to a more effective killing (576).

Taking this into account, we decided to test whether loss of T6SS activity in toxin-sensitive prey cells (Δ*rsmA* Δ*tsetsi* Δ*tssB1*Δ*tssB2*Δ*tssB3*) would result in any killing protection as a result of prey no longer "triggering/provoking" directed T6SS effector delivery. Looking at Tse2 or Tse5-mediated competition in the macrocolony competition assay assay, it appears that toxin-sensitive prey growth is equally spatially restricted independently of the prey T6SS activity under both conditions where competition is started by bacteria that are in close contact (inoculum OD_{600}=1.0) or bacteria are placed sparsely (inoculum OD_{600}=0.01) and able to establish before

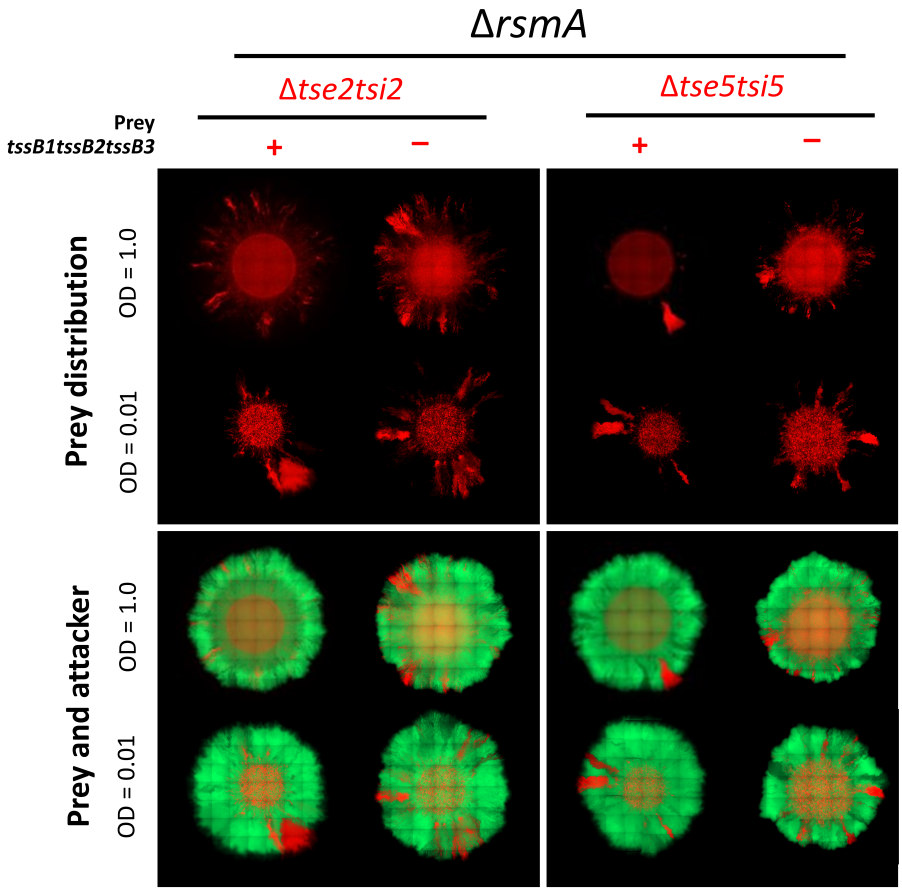

Figure 5.9: ***P. aeruginosa* used H1-T6SS to kill toxin-sensitive prey bacteria independently of active provocation by prey bacteria.** Fluorescent images of mixed macrocolonies of Δ*rsmA* regulatory background toxin sensitised bacterial strains in competition with T6SS+ (Δ*rsmA*) parental strain. Showing mCherry tagged prey strain distribution (upper section in red) and fluorescent channel composite image with both prey and attacker (sfGFP shown in green) distribution in the lower set. Comparative competition sets with prey strains sensitised to Tse2 on left or Tse5 on right. With first prey bacteria in the set being T6SS active (Δ*rsmA*) and the second being unable to actively fire any of the T6SSs (Δ*rsmA*Δ*tssB1*Δ*tssB2*Δ*tssB3*). Macrocolony competition set-up after inoculation from bacterial mixes of OD_{600} = 1.0 (upper) or OD_{600} = 0.01 (lower). All bacteria mixed at 1:1 ratio, grown for 48h at 37°C on LB with 2% (w/v) agar. Showing a representative image of a set of 3 replicates for bacterial colonies for prey bacteria with full set of *tssB* genes and 1 of 1 test images for colonies with (Δ*rsmA*Δ*tssB1*Δ*tssB2*Δ*tssB3*) prey.

directly competing (Figure 5.9). These experiments indicate that H1-T6SS, known as a primarily retaliatory T6SS system that specifically directs toxin injections, is able to effectively kill prey bacteria that do not directly provoke directed T6SS injections.

5.3.5 Loss of *pppA* results in elevated H1-T6SS firing, but does not change toxin-mediated competition outcome within a context of mixed bacterial macrocolonies

As the ability to specifically target T6SS attacks does not appear to be essential to effectively eliminate toxin-sensitive prey within the context of mixed macrocolonies, we decided to investigate how competition is affected by turning a retaliatory H1-T6SS into a constitutively firing Hcp pool limited system. Loss of PppA is known to increase H1-T6SS secretion activity (569) and result in bacteria that are no-longer able to participate in Tit-for-Tat firing (564), therefore we engineered Δ*pppA* mutations in Gac-Rsm mutant and toxin-sensitive strains. Gac-Rsm cascade modulates the expression of T6SS and the corresponding elevation in the activity of T6SS and associated ability to eliminate sensitive prey. Independently of the overall T6SS expression level, western blotting shows that matching pairs or T6SS+ and T6SS- (Δ*tssB1*) strains appear to maintain an equal Hcp1 pool within the cell (Figure 5.10 A). In strains lacking the post-translational regulator PppA, independently of the overall expression level of H1-T6SS, almost the entirity of Hcp1 pool is found in the media fraction (Figure 5.10 A). These results are consistent with the loss of PppA turning H1-T6SS in a constitutive firing system, where the overall levels of activity of the T6SS are limited by Hcp production.

The introduction of the Δ*pppA* mutation is known to increase the activity of the H1-T6SS system in the context of the secretion assay, but it remains somewhat unclear whether this translates into improved competitive fitness. To test how an increase in H1-T6SS activity resulting from *pppA* deletion affects bacterial killing, we constructed strains that are both sensitive to H1-T6SS toxins and lack *pppA*. Within mixed macrocolony competition, growth of Δ*retS* strains sensitised to Tse4 and Tse3 appear to be spatially restricted independently of the parental strain *pppA* presence. Similarly, no gain of ability to restrict prey growth through constitutive H1-T6SS firing was observed in case of Tse1 or Tse8 mediated competition (Figure 5.10). Taken together, these results indicate that an increase in T6SS activity as assessed

through a secretion assay is not always indicative of a corresponding improvement in killing.

At the same time, this does not provide sufficient evidence to conclude that the strains Δ*retS*

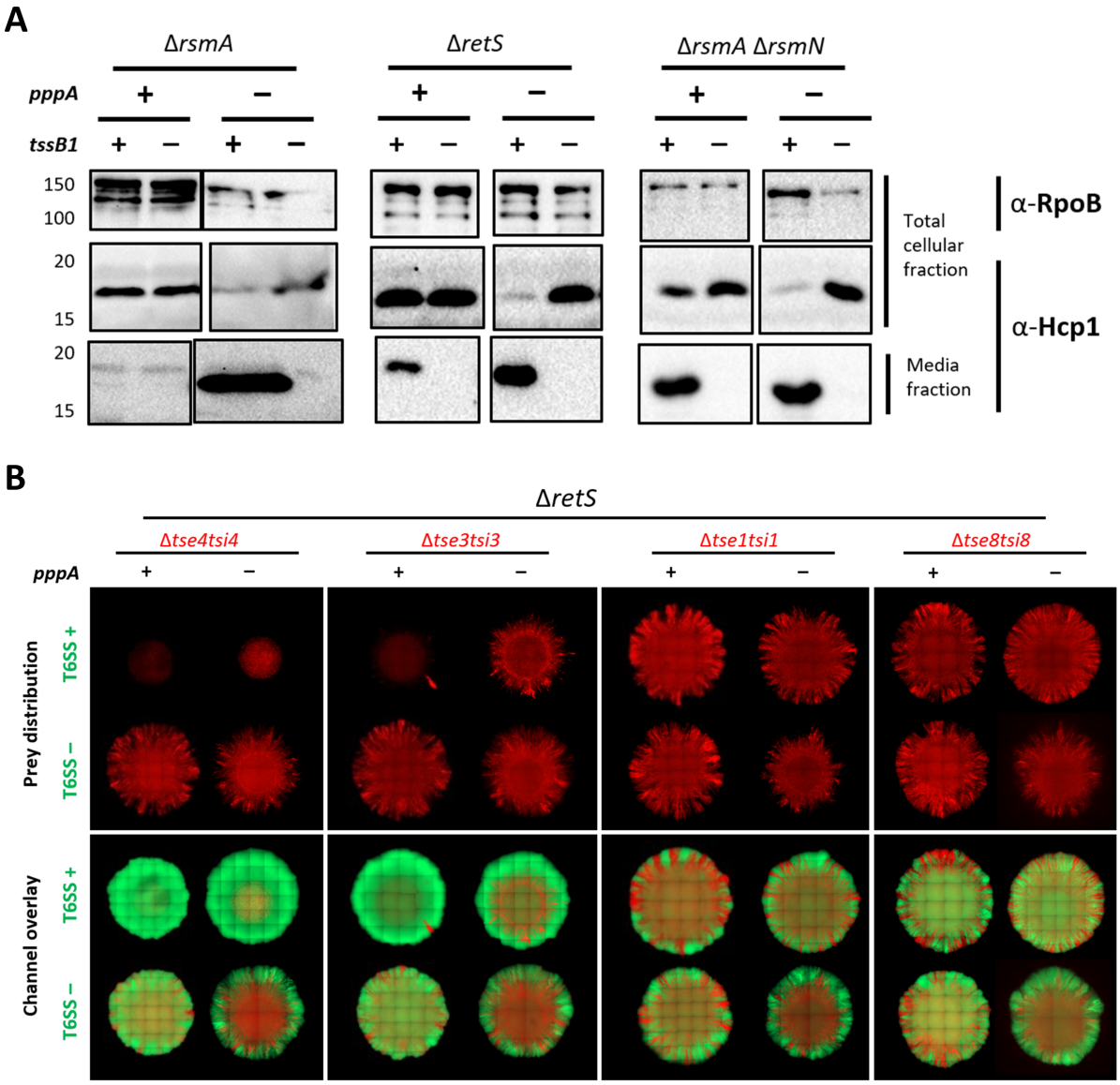

Figure 5.10: **Loss of post-translational regulator PppA results in increased H1-T6SS activity, but does not ensure improved competitive fitness.**
Western blot analysis showing how *pppA* deletion impacts relative Hcp1 abundance in cell and media fractions. Analysis of Δ*rsmA*, Δ*retS*, and Δ*rsmA*Δ*rsmN* strains with and without functional PppA or TssB1 indicated by "+" or "–". System component expression and activity assessed in bacteria cultured for 5h at 37^{o}C. Using RpoB as loading control.
Whole mixed colony competition assessing changes in toxin-sensitive prey lineage distribution depending on presence or absence of PppA. Prey strains sensitised to Tse4, Tse3, Tse1, and Tse8 in Δ*retS* genetic context (red). First colony in the set showing competition of PppA+ prey and attacker strains with second set of PppA- prey and attacker mix. Upper set of images shows prey distribution only with lower set containing fluorescent image composite showing both prey and attacker strain distribution. Upper lane in the set contains T6SS+ parental attacker strain (Δ*retS*), while lower set contains T6SS- attacker (Δ*retS*Δ*tssB1*). All bacteria mixed at 1:1 ratio, inoculum density of OD_{600}=1.0, grown for 48h at 37^{o}C on LB with 2% (w/v) agar.

and Δ*retS*Δ*pppA* are equally competitive. This is due to a number of assay limitations, such as potentially insufficient assay resolution. It is also possible that none of the toxins selected here were competition-limiting, hence any additional toxin dose delivered was unable to shift the balance of the broader competition dynamic. It is also possible that system activity in liquid culture is not reflective of H1-T6SS activity within surface growth based competition. Additionally, the ability to specifically target H1-T6SS injection may be a predeterminant of successful killing under other conditions, but in a community that is dense from establishment, this may be outweighed by a simple increase in activity.

5.4 Growth temperature dictates outcome of H2-T6SS-dependent competition

5.4.1 Low temperature promotes H2-T6SS sheath assembly

Analysis of T6SS promoter activity in Chapter 4 showed that decreasing the growth temperature from 37^{o}C to 25^{o}C results in H2- and H3-T6SS promoter activity increase. To complement the analysis of T6SS promoter activity, we investigated how changes in growth temperature impacts sheath assembly dynamics of H1- and H2-T6SS. For this, we engineered a Δ*retS* strain that encodes both *tssB1-mScarlet-I* and *tssB2-sfGFP* fusions at the native chromosome loci. This allows a simultaneous assessment of sheath assembly and firing events of both H1- and H2-T6SS (Figure 5.11). As previously described by (547) assembly and firing dynamics of these two systems are temporally distinct. H1-T6SS assembly and firing events take approximately 20s while a single round of H2-T6SS assembly-firing can extend to beyond 420s, with a notable fraction of H2-T6SS sheaths remaining present (547), but static during the whole duration of 7min imaging time-lapse. T6SS sheath dynamics observed under growth conditions in this study remain consistent with previously published, and this poses an experimental design challenge - due to fluorophore photo-bleaching and photo-toxicity, it becomes impractical to

perform imaging at a frequency required to capture the dynamics of H1-T6SS sheaths and to continue this for a sufficient period of time to observe the dynamics of H2-T6SS sheaths. Nevertheless, the differential temperature effect on the two T6SSs is best observed using a strain with double fluorescent tags, therefore we chose to employ imaging conditions optimised for capturing H1-T6SS dynamics aiming to asses the number of cells engaging in active H1-T6SS sheath assembly in a manner comparable with experiments in results section 4. Regarding the quantification of the H2-T6SS sheaths, we assessed the total number of H2-T6SS sheaths per 100 bacteria cells.

The abundance of the H1- and H2-T6SS sheaths changes depending on bacterial growth temperature, and similarly as observed with other methods, the effect is inverse. When grown at 37^{o}C, fewer than 1 TssB2-sfGFP structures was observed per 100 cells, while at 25^{o}C a stark increase with an average of 74 sheaths per 100 cells was seen, with many of cells containing multiple sheath structures (Figure 5.11 A and C). The temperature impact on H1-T6SS was considerably less severe, with approx. 14% of the bacteria actively assembling TssB1-mScarlet-I sheaths at 25^o C and this increased to approximately 24% at 37^{o}C (Figure 5.11 A and B).

5.4.2 Sensitivity to H2-T6SS toxins results in prey growth restriction at low temperatures

While H1-T6SS toxin-mediated competition in a mixed macrocolony context was assayed at 37^{o}C, for H2-T6SS we chose to carry out comparable experiments at both 25 and 37^{o}C to assess how the change in growth temperature impacts H2-T6SS toxin-mediated competition. For the study of H2-T6SS toxins, we constructed a set of 11 strains sensitised to every known toxin-immunity pair present in the PAO1 genome and as a control we added a prey strain lacking the H2-T6SS associated copper uptake protein Azu. When these toxin-sensitive strains were incubated with T6SS+ parental bacteria to monitor single toxin-mediated competition at 37^{o}C, none of the mixes resulted in consistent spatial restriction of the prey growth. When these

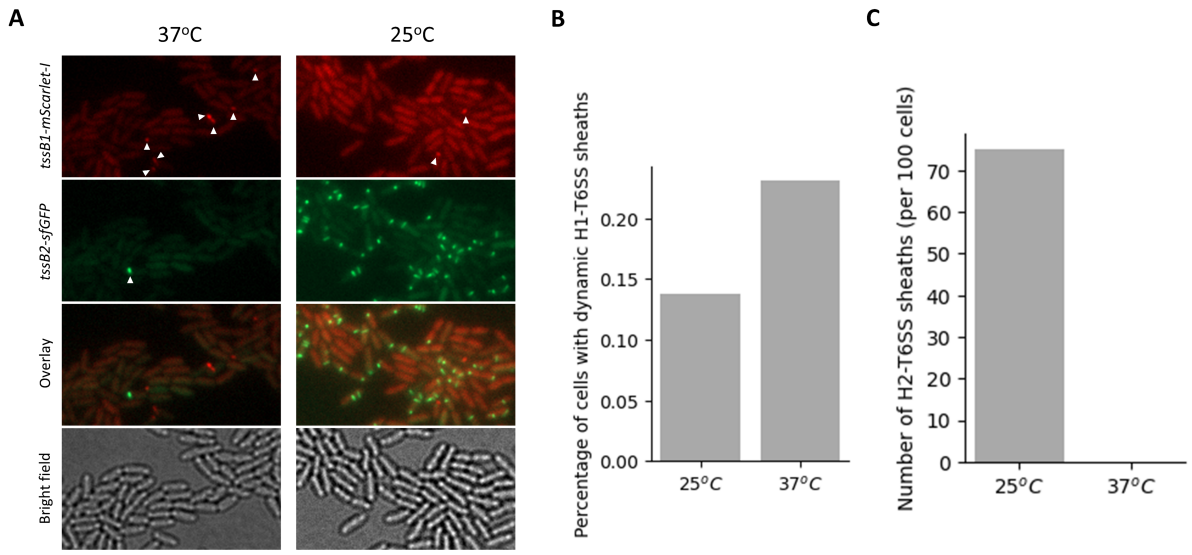

Figure 5.11: **Decrease in growth temperature promotes H2-T6SS sheath structure assembly.** H1-T6SS sheaths are preferentially assembled at 37^{o}C, while H2-T6SS activity increases if temperature is lowered to 25^{o}C. **A** Abundance of H1-T6SS (red) and H2-T6SS (green) sheath structures in Δ*retS* bacteria grown on LB agar at 37^{o}C and 25^{o}C. Corresponding quantification of bacteria with active H1-T6SS sheaths (**B**) and number of H2-T6SS sheaths per cell (**C**). A representative field of Δ*retS* regulatory mutant with *tssB1::mScarlet-I* and *tssB2::sfGFP* chromosomal fusions at native loci. Images from 2 independent imaging sessions analysed.

bacterial mixes were grown at 25^{o}C, a substantial impact of multiple of the toxins was seen, emphasising the importance of growth temperature impact on *P. aeruginosa* H2-T6SS activity (Figure 5.12).

As seen in Table 5.1, H2-T6SS delivers numerous functionally varied antibacterial toxins. The best represented functional class of antibacterial H2-T6SS effectors is phospholipases, with the PAO1 genome encoding - Tle1, Tle3, PldA (Tle5a) and PldB (Tle5b) (40). Within Δ*rsmA* genetic context individual use of three of these toxins appeared to provide a competitive advantage. Phospholipase Tle3 appears to be one of the most potent toxins associated with H2-T6SS and ensures almost complete prey elimination, while competition dependent on Tle4 or PldB results in sensitive strains being spatially restricted to the colony central region. No impact of Tle1 or PldA is seen within context Δ*rsmA* strain competition. Similarly as in the case with H1-T6SS, the H2-T6SS secretion activity is gradually elevated in Gac-Rsm cascade mutants, with both Δ*retS* and Δ*rsmA*Δ*rsmN* mutants displaying H2-T6SS activity higher than Δ*rsmA*

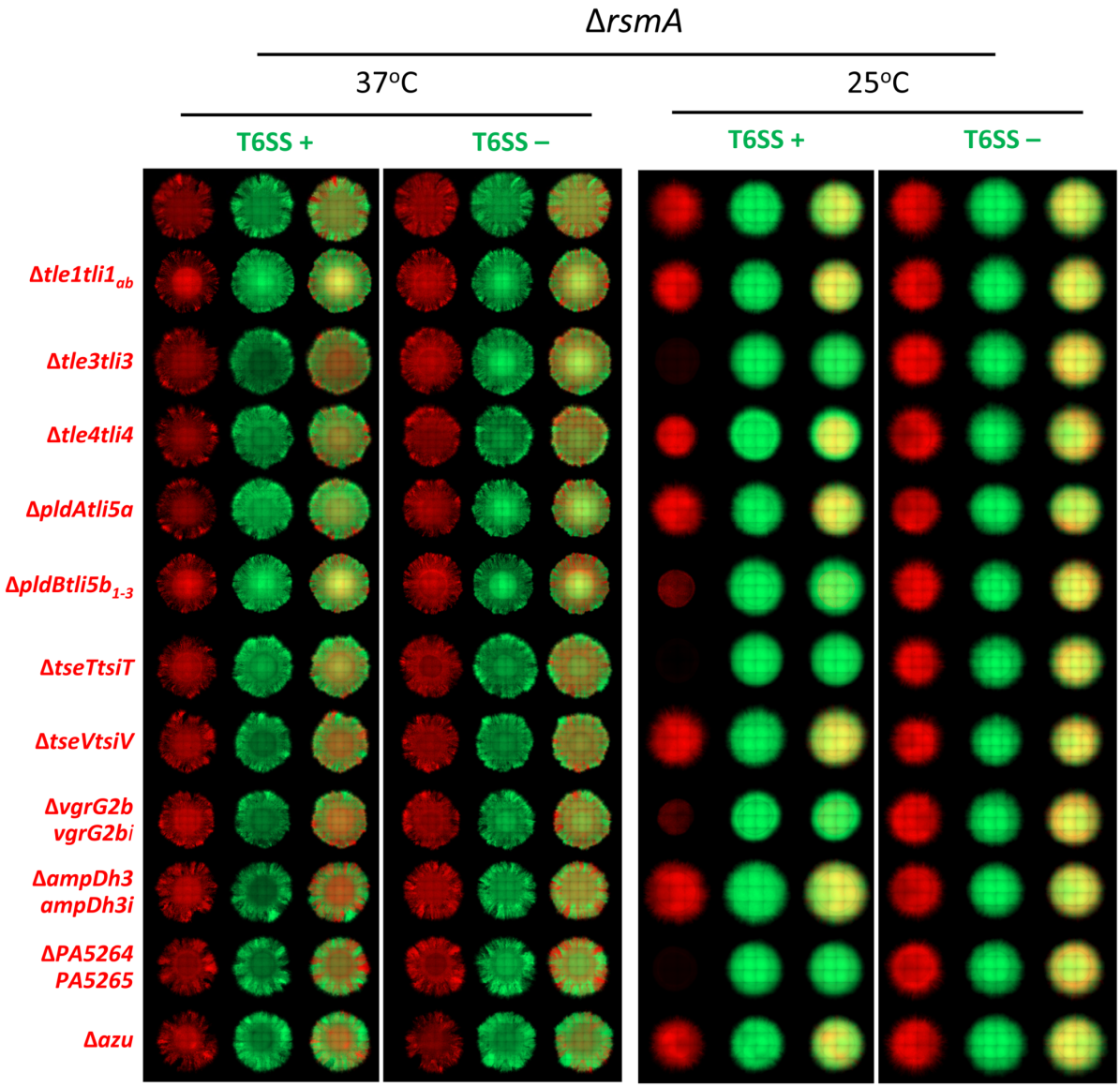

Figure 5.12: **Sensitivity to H2-T6SS toxins can be observed when growing colonies at 25^{o}C, but not 37^{o}C.** Representative images of 48h old mixed colonies of toxin sensitised Δ*rsmA* bacteria in red in competition with T6SS+ (Δ*rsmA*) or T6SS- (Δ*rsmA*Δ*tssB1*Δ*tssB2*Δ*tssB3*) parental strain in green. Upper lane contains a control mix of bacteria with full toxin-immunity gene sets, each of the following lanes contains strain sensitised to one of the H2-T6SS toxins in the following order: Tle1, Tle3, Tle4, PldA, PldB, TseT, TseV, VrgG2b, AmpDh3, PA5265, or common good effector Azu. Image sets of competitions show both single fluorescence channel and overlay images depicting distribution of sensitised prey in a mix with T6SS+ and subsequently T6SS- (Δ*tssB1*Δ*tssB2*Δ*tssB3*) parental strains at 2 different growth temperatures – 37^{o}C and 25^{o}C. Strains contain constitutively expressed fluorescent proteins, prey labelled with mCherry (shown in red) and attacker with sfGFP (shown in green). All bacteria mixed at 1:1 ratio, inoculum OD_{600}=1.0, grown for 48h, at 37^{o}C bacteria incubated on LB with 2% (w/v) agar, and at 25^{o}C bacteria incubated on LB with 1.2% (w/v) agar. Representative colony image of 3 biological replicates shown.

(Figure 4.3F). Therefore, we chose a subset of H2-T6SS effectors and engineered toxin-sensitive strains in Δ*retS* background to test whether elevated activity would translate into improved

ability to restrict prey growth. Bacterial competition in Δ*retS* regulatory context, shows that sensitisation to Tle1 or PldA leads to prey bacteria being restricted to the central region of the colony (Figure 5.13). The set of phospholipases show different levels of potency, some of the possible underlying reasons for this being linked to the specific type of catalytic activity (Table 5.1). Another likely factor is the differences in the expression levels of the individual effectors, as each of these toxins is encoded in a distinct orphan cluster (Figure 1.20).

Another common catalytic target of T6SS toxins is peptidoglycan; in addition to the

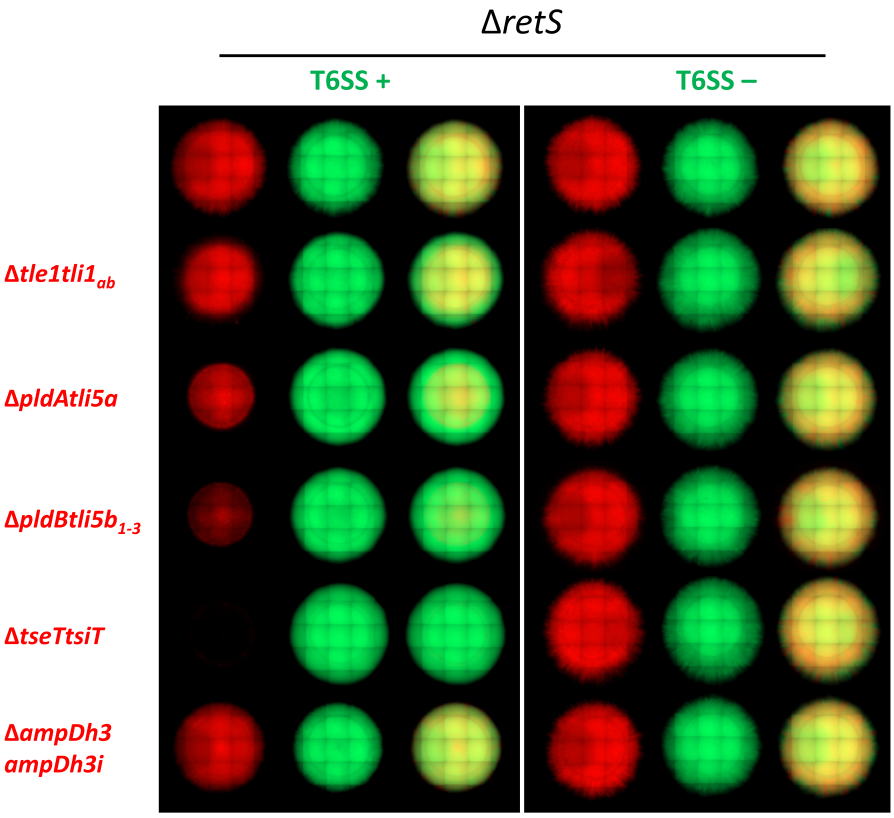

Figure 5.13: **Increased H2-T6SS toxin-mediated prey growth restriction can be observed in Δ*retS* strains.** Representative images of 48h old mixed colonies of toxin sensitised Δ*retS* bacteria in red in competition with T6SS+ (Δ*retS*) or T6SS- (Δ*retS*Δ*tssB1*Δ*tssB2*Δ*tssB3*) parental strain in green. Upper lane contains a control mix of bacteria with full toxin-immunity gene sets, each of the following lanes contains strain sensitised to one of the H2-T6SS toxins in the following order: Tle1, PldA, PldB, TseT, or AmpDh3. Image sets of competitions show both single fluorescence channel and overlay images depicting distribution of sensitised prey in a mix with T6SS+ and subsequently T6SS- (Δ*tssB1*Δ*tssB2*Δ*tssB3*) parental strains. Strains contain constitutively expressed fluorescent proteins, prey labelled with mCherry (shown in red) and attacker with sfGFP (shown in green). All bacteria mixed at 1:1 ratio, inoculum OD_{600}=1.0, grown for 48h at 25^{o}C on LB with 1.2% (w/v) agar. Showing a representative colony of 3 biological replicates shown.

two peptidoglycan hydrolases Tse1 and Tse3 delivered by H1-T6SS (584), another two toxins targeting peptidoglycan are associated with H2-T6SS. AmpDh3 is peptidoglycan hydrolase (587, 586) and sensitisation to this toxin does not appear to result in a measurable reduction in competitive fitness in the genetic context Δ*rsmA* or Δ*retS* (Figures 5.12 and 5.13). VgrG2b is a toxin that interferes with peptidoglycan biogenesis at the cell division plane (553) and delivery of this effector results in sensitive bacteria being restricted from spatially expanding within mixed community (Figure 5.12). Peptidoglycan hydrolases degrade the cell wall; therefore, toxins with this activity are expected to induce lysis and are typically expected to be highly potent and lytic toxins (582, 587, 358, 584). Yet, here these remain amongst some of the least effective toxins when it comes to elimination of *P. aeruginosa*, the mechanisms behind this remain an open question.

Our comparative analysis showed that the two most potent H2-T6SS toxins are the nuclease TseT and PA5265 (Figure 5.12). PA5265 is a toxin of unknown function that contains the MIX motif (645), likely to be indicative of interaction with VgrG. While bio-informatics analysis looking for additional conserved sequence or structure conserved motifs shows a presence of a trans-membrane domain resulting in predicted 750aa n-terminal non-cytoplasmic domain and 250aa c-terminal cytoplasmic domain, but no conserved features were found that would hint at the biochemical function of the effector through the alignment of the sequence or predicted structure (AlphaFold (750) predicted structure assessed through Dali (751) structure alignment). The link of PA5265 with H2-T6SS was established through genomic context (553), as the effector-immunity gene pair is encoded in a satellite cluster with *vgrG2b* and *hcpB* genes (Figure 1.20). With the antibacterial toxicity upon delivery by H2-T6SS specifically being first shown here, with the removal of the presumed effector immunity gene set PA5264-65 resulting in near complete T6SS-dependent elimination of prey.

The last T6SS effectors tested in this study are TseV, Azu, PA2066 and PA0256. Unlike in the case of nuclease TseT, the removal of the immunity gene associated with putative nuclease

TseV did not result in consistent spatial restriction of prey growth (Figure 5.12). Similarly, no T6SS-dependent growth restriction was observed in the case of removal of H2-T6SS associated PA2066 putative immunity PA2067 or H3-T6SS associated PA0256 putative immunity PA0257 (Figure 5.14). Both of these effectors have been linked to *P. aeruginosa* T6SSs through Hcp pull-down studies by (555), but the validation of antibacterial toxicity upon delivery by T6SS and identification of associated cognate immunities remains a question for future studies. Although the presence/absence of the common good effector Azu does not appear to have a measurable impact on the competitive outcome (Figure 5.12). For the purposes of testing here, Azu was chosen as a negative control, as, instead of antibacterial toxicity, this effector aids in copper uptake, and to further address the contribution of Azu to bacterial fitness, testing under copper

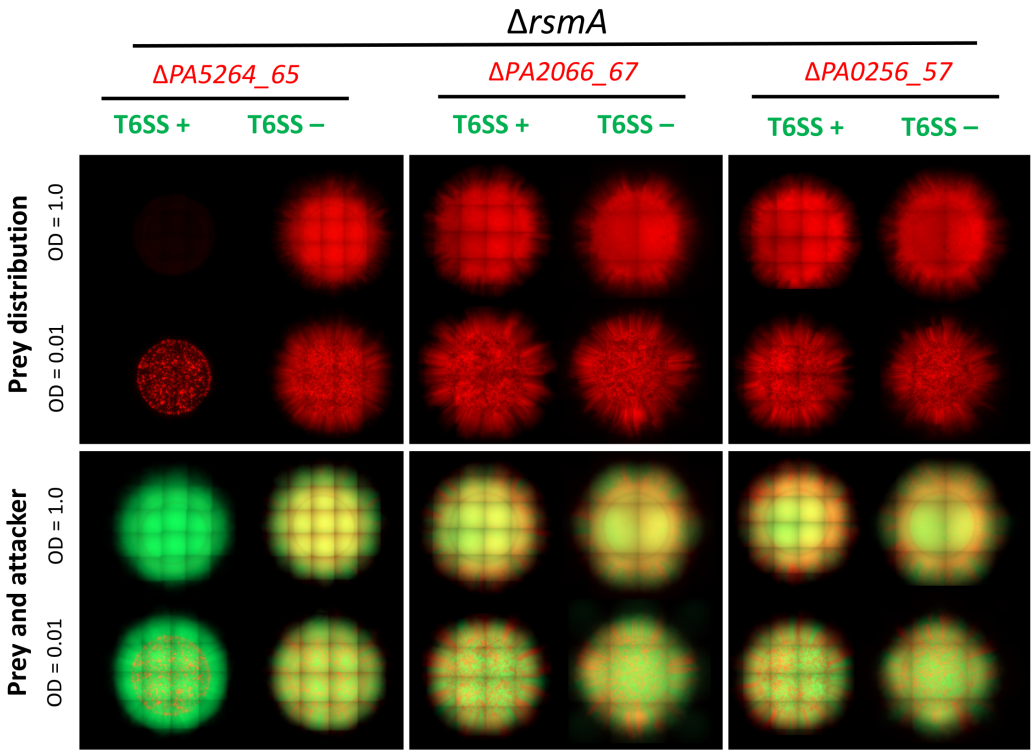

Figure 5.14: **Mixed macrocolony setup can be used to assess competitive impact of putative T6SS toxins.**
Mixed macrocolony images showing single channel and overlay fluorescent images of strains lacking a putative toxin-immunity gene pairs. In red (mCherry) are strain lacking *PA5264 PA5265*, *PA2066 PA2067*, and *PA0256 PA0257*, in presence of T6SS+ (Δ*rsmA*) or T6SS- (Δ*rsmA*Δ*tssB1*Δ*tssB2*Δ*tssB3*) parental strain in green (sfGFP). All bacteria mixed at 1:1 ratio, inoculum OD_{600}=1.0 or 0.01, grown for 48h at 25^{o}C on LB with 1.2% (w/v) agar. Showing a representative colony of 3 biological replicates for PA5264 mediated competition and 1 of 1 test images for PA2066 and PA0256 mediated competition.

limiting conditions should be performed.

5.4.3 Change in growth temperature has only minor impact on H1-T6SS toxin-mediated killing

As seen in the above sections, the H2-T6SS activity and ability to successfully eliminate prey is highly dependent on the growth temperature. Measurements of T6SS sheath assembly dynamics at both 25^{o}C and 37^{o}C, showed that the effect of temperature on the dynamics of the sheaths of H1 and H2-T6SS is inverse (Figure 5.11), therefore we extended our testing by assessing how shift in incubation temperature affects H1-T6SS toxin-mediated killing. For this experiment, the Tse2, Tse4, and Tse5 sensitised Δ*retS* strains were incubated with a T6SS+

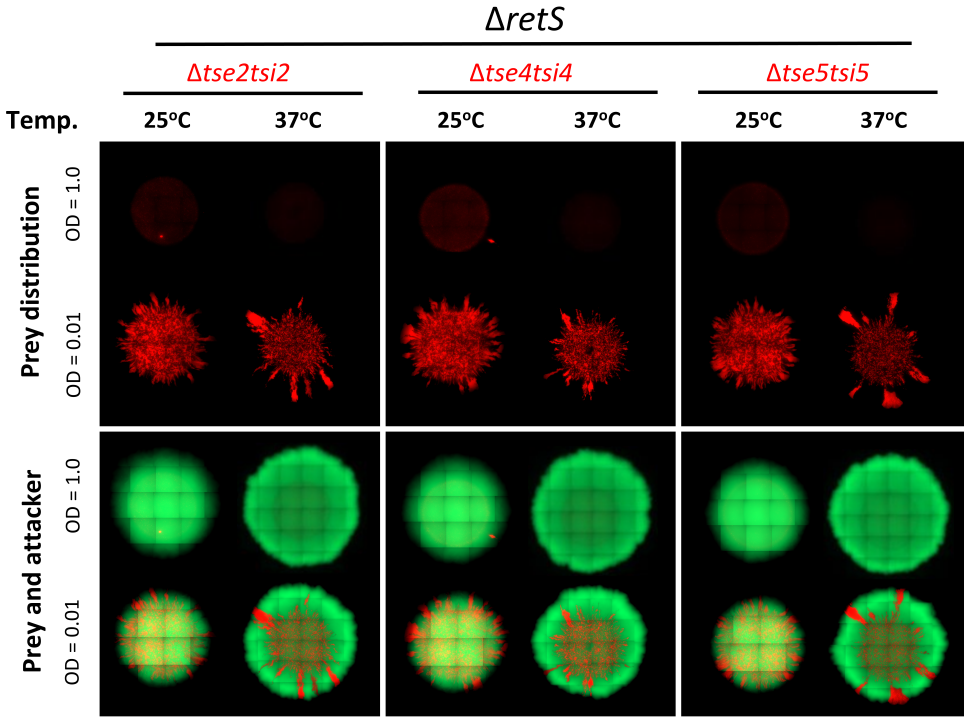

Figure 5.15: ***P. aeruginosa* is able to use H1-T6SS toxins to restrict sensitive prey growth at 25^{o}C.**
To assess growth temperature impact on H1-T6SS toxin-mediated killing toxin sensitised strains in red were mixed with parental T6SS+ attacker (green) and grown at both 25^{o}C and 37^{o}C. Mixed macrocolony images of Tse2 (Δ*retS*Δ*tse2tsi2*), Tse4 (Δ*retS*Δ*tse4tsi4*), and Tse5 (Δ*retS* Δ*tse5tsi5*) prey strain distribution in presence of Δ*retS* parental strain. Fluorescent channel overlay images showing both prey and attacker population distribution. Competition conducted in populations arising from both high (OD_{600} = 1.0 upper lane) and low (OD_{600} = 0.01 lower lane) density inoculum.

parental strains, setting up the competition at two distinct inoculum densities (Figure 5.15, negative control competition with T6SS- parental strain not shown). Independently of the toxin used, it appears that prey growth remains spatially restricted when high inoculum density competition mixes are incubated at 25^{o}C instead of 37^{o}C. Mixed colonies established at low inoculum densities do show that H1-T6SS toxin dependent competition provides limited benefit in this context, indicating that the lowered system activity after the temperature shift does translate into reduced competitiveness, but the temperature shift effect on H1-T6SS is much less severe than on H2-T6SS.

5.5 Theoretical model of T6SS interactions reveals how mode of toxin action is key determinant of competitive success

5.5.1 Toxin lysis rate and attacker firing dynamics determine competition outcome

After gaining an experimental understanding of key T6SS-dependent interactions parameters, such as different toxin potency or firing efficacy, we chose to use theoretical simulations to address how specific parameters contribute to the overall competition outcome. The use of theoretical simulations aids in interpretation of experimental data, by demonstrating how specific mechanistic interactions at a single-cell scale affect the whole populations. Additionally, this allows us to determine what are the key limiting factors in T6SS-mediated competition and under what factors such as increased T6SS firing rate increase competitiveness. An existing simulation platform CellModeller (682) has been previously used to investigate bacterial interactions in mixed colonies for both CDI (683) and T6SS (684). CellModeller is an agent-based modelling framework designed for studies of bacterial population development, in a manner that is comparable to population development within the context of flow-cell or surface growth (682). These studies mainly established the role of lytic toxins and the differential

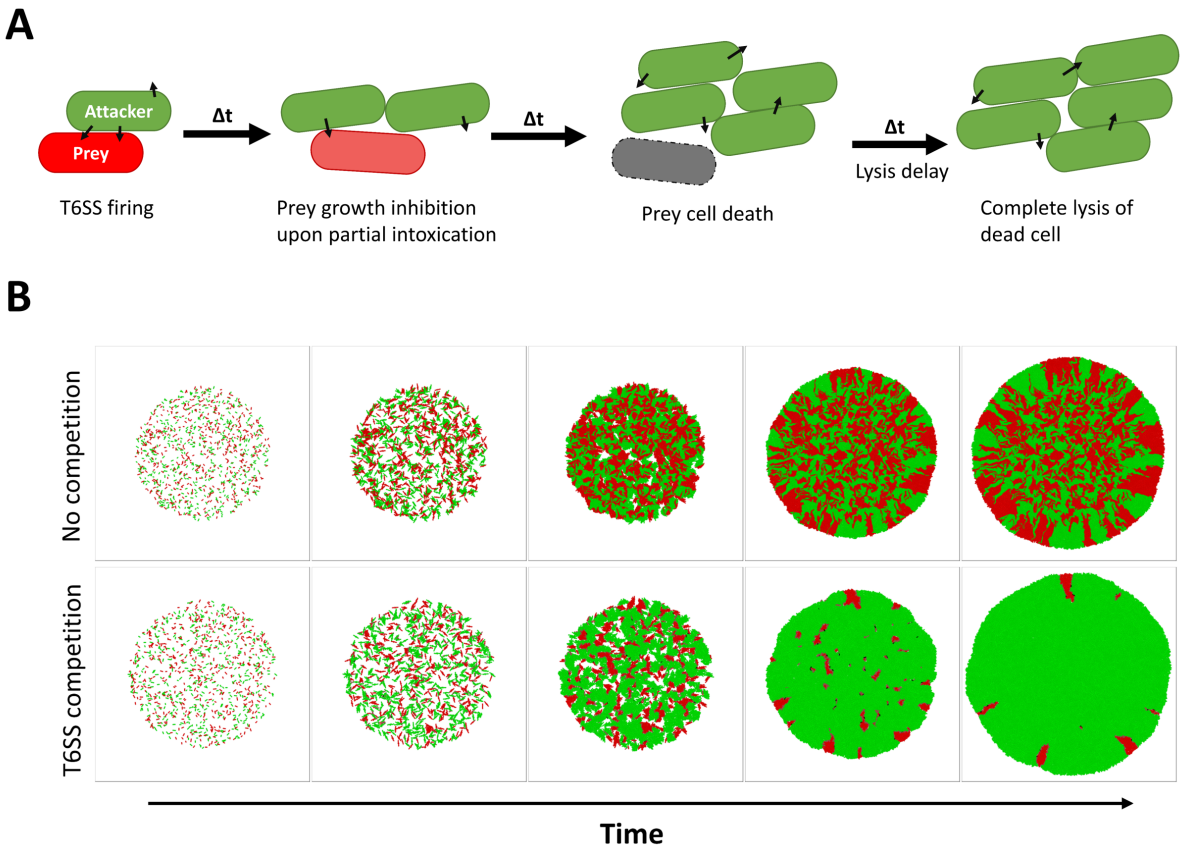

Figure 5.16: **Schematic of toxin-sensitive and attacker lineage fate in simulations.** (**A**) Schematic depicting types of bacteria represented within the model and their fate upon T6SS based interactions. T6SS+ attacker in green can fire a specified number of T6SSs in random directions and grows over time. Prey bacteria in red is susceptible to T6SS attacks, when prey is hit by T6SS its growth rate is reduced. Once certain threshold of T6SS attacks is reached prey cell dies (grey) and no further growth occurs. Dead prey cells remain in simulation until lysis defined by a certain delay is reached and are subsequently removed.
(**B**) Simulation of 2 mixed colony development over time with and without T6SS-mediated competition. Initially 1 to 1 mix of bacteria from both populations are randomly scattered on surface in circular inoculum zone. Bacterial growth occurs through elongation and division and in absence of active movement bacteria expand through rigid body interactions. At a whole colony scale, inoculum zone is filled by intermixed clonal clusters and further expansion is restricted by neighbouring cells exerting forces upon each other. Over simulation time-course radial expansion results in formation of distinct sectors in the region outside the inoculum area. In a mix with T6SS interactions, sensitive prey in red can be seen to initially establish in the colony centre, but over simulation time-course be gradually eliminated by T6SS+ attacker in green. Specific parameter space of simulations is shown in Table 2.4.

advantages of constitutive and retaliatory T6SS firing strategies. Our experimental data further suggest that the effectiveness of T6SS-based competition is determined by both the activity of T6SS and the type of toxins used.

We used CellModeller to build an agent-based model depicting bacterial growth and T6SS-

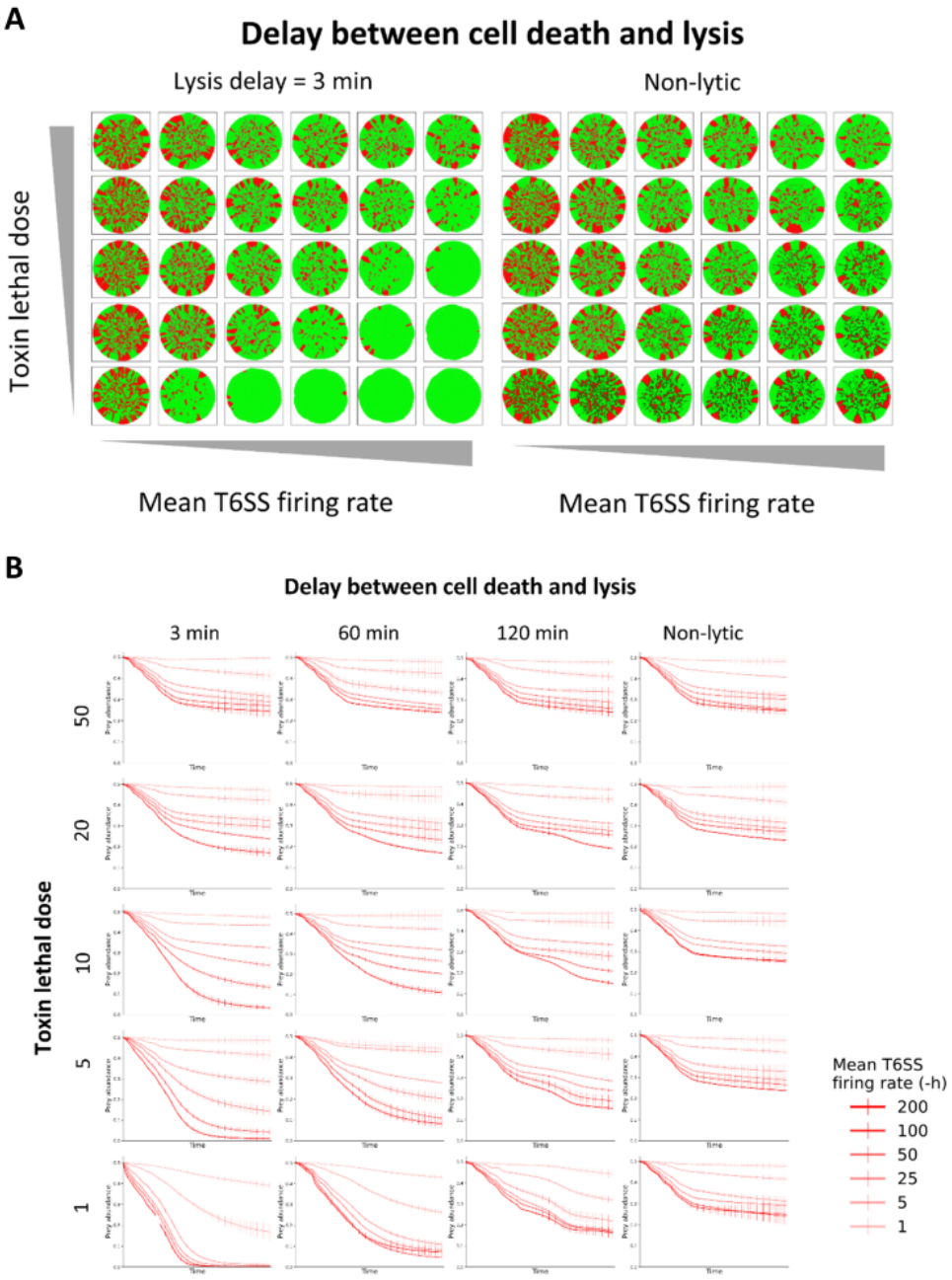

Figure 5.17: **Both toxin mode of action and T6SS firing rate determine population distribution within mixed bacterial communities.**
(**A**) Representative simulation outputs depicting interactions between 2 populations - sensitive prey in red and an attacker population in green. Showing interactions mediated trough lytic (3 min lysis delay) and non-lytic toxins, effects of toxin dose (number of T6SS hits) required to cause cell death with the lethal dose decreasing from the top row to the bottom row (50; 20; 10; 5; 1 T6SS hits), and effects of increase in mean T6SS firing rate by attacker population (1; 5; 25; 50; 100; 200 T6SS firing events per hour).
(**B**) Corresponding analysis of changes in relative prey abundance over simulation time-course depending on mean T6SS firing rate. Each of the columns contains simulation sets with increasing lysis delay from left to right. Each of the columns contains simulation set with differing toxin lethal dose, with highest at the top and lowest at the bottom.

based interactions. The key descriptors of the T6SS-mediated interactions are the frequency of attack and toxin mode of action (Figure 5.17). For purposes of biophysical simulations, T6SS toxins can be broadly characterised as lytic or non-lytic, here parameterised as having differing delay between cell death and removal from community. Additionally, different toxins are expected to have a different effective dose to inherent biochemical properties, and the number of individual toxin molecules delivered in a single firing event is likely to vary due to association with different T6SS components, as discussed in section 1.4.2. For simplicity, both of these effects are described by a single parameter – toxin lethal dose, which is the amount of toxin allowed to accumulate in any given prey cell before death occurs. All T6SS firing events that geometrically intersect a prey cell are assumed to deliver a fixed amount of given toxin; therefore, the lethal dose of toxin can be interpreted as the number of T6SS hits needed to kill an individual prey cell. The key characteristic of the attacker populations behaviour is described by changes in the mean T6SS firing rate, and it is assumed that the whole of the attacker population is participating in active competition. Variations in these parameters, such as having differing delay between cell death and lysis as well as differences in toxin lethal dose, demonstrates how the specific toxin mode of action impacts the competitive outcome at the whole population scale (Figure 5.16).

We used a systematic exploration of the parameter space describing the firing frequency of T6SS and the toxin mode of action to better understand the specific limiting factors determining the outcome of T6SS-mediated competition. For example, increased T6SS firing rate results in more effective prey killing, but the overall extent of prey elimination is determined by the effective dose of the toxin and the ability to lyse dead prey cells (Figure 5.17 A). Toxins that are effective at low doses (i.e. 1 or 5 T6SS hits) can enable effective prey elimination by attacker populations with a low T6SS firing rate (Figure 5.17 B lower rows) and additional increases in the amount of toxins delivered provide little to no additional competitive advantage. Highly lytic toxins enable near complete prey elimination if delivered at a sufficiently high rate, while a gradual increase in the delay between prey death event and lysis results in a protective effect (Figure

5.17 A and B). This matches observations described in previous work (684). If a high toxin load is reacquired for prey killing, the toxin lysis rate is no longer the key competition limiting factor (Figure 5.17B upper row). When a substantial amount of toxin needs to accumulate for prey elimination to occur, the specific mode of toxin action appears to be less important than delivering high amounts of the toxin. Similarly, when toxins are mainly non-lytic, decrease in the toxin effective dose has only a minor effect and the overall competition outcome is limited by the attacker firing rate (Figure 5.17B last column). An additional point of note is that doubling the T6SS firing rate does not result in doubled overall impact. As T6SS killing is highly localised, other factors such as the population geometry and, more specifically, ability to make direct contact with susceptible prey bacteria plays a significant role in determining the population level competitive outcome.

5.5.2 *P. aeruginosa* H1-T6SS-typical non-homogeneous firing behaviour is consistent with the ability to proficiently out-compete prey bacteria

To further corroborate our simulation results with mixed macrocolony experiments, a set of H1-T6SS toxin-mediated competition outcomes in different genetic backgrounds were selected. Figure 5.18 demonstrates a direct comparison of single-toxin-mediated competition in a set of strains with incrementally increasing T6SS activity levels - WT, Δ*rsmA*, Δ*retS*, and Δ*rsmA*Δ*rsmN*. A subset of toxins with different potency was selected from figure 5.5 - Tse1, Tse3, Tse2, and Tse5 - ranging in relative toxicity from the least to the most potent, respectively. The delivery of the pore-forming toxin Tse5 (597) results in restriction of prey expansion in the WT background and in strains with higher H1-T6SS activity such as Δ*retS* or Δ*rsmA*Δ*rsmN* prey almost entirely eliminated (Figure 5.18 A). Delivery of the ADP-ribostransferase toxin Tse2 (599) does not result in sensitive bacteria growth restriction in WT context, but an effect is notable in Δ*rsmA*, Δ*retS*, and Δ*rsmA*Δ*rsmN* strains. In case of peptidoglycan muramidase Tse3 (584) prey growth restriction appears to necessitate an even

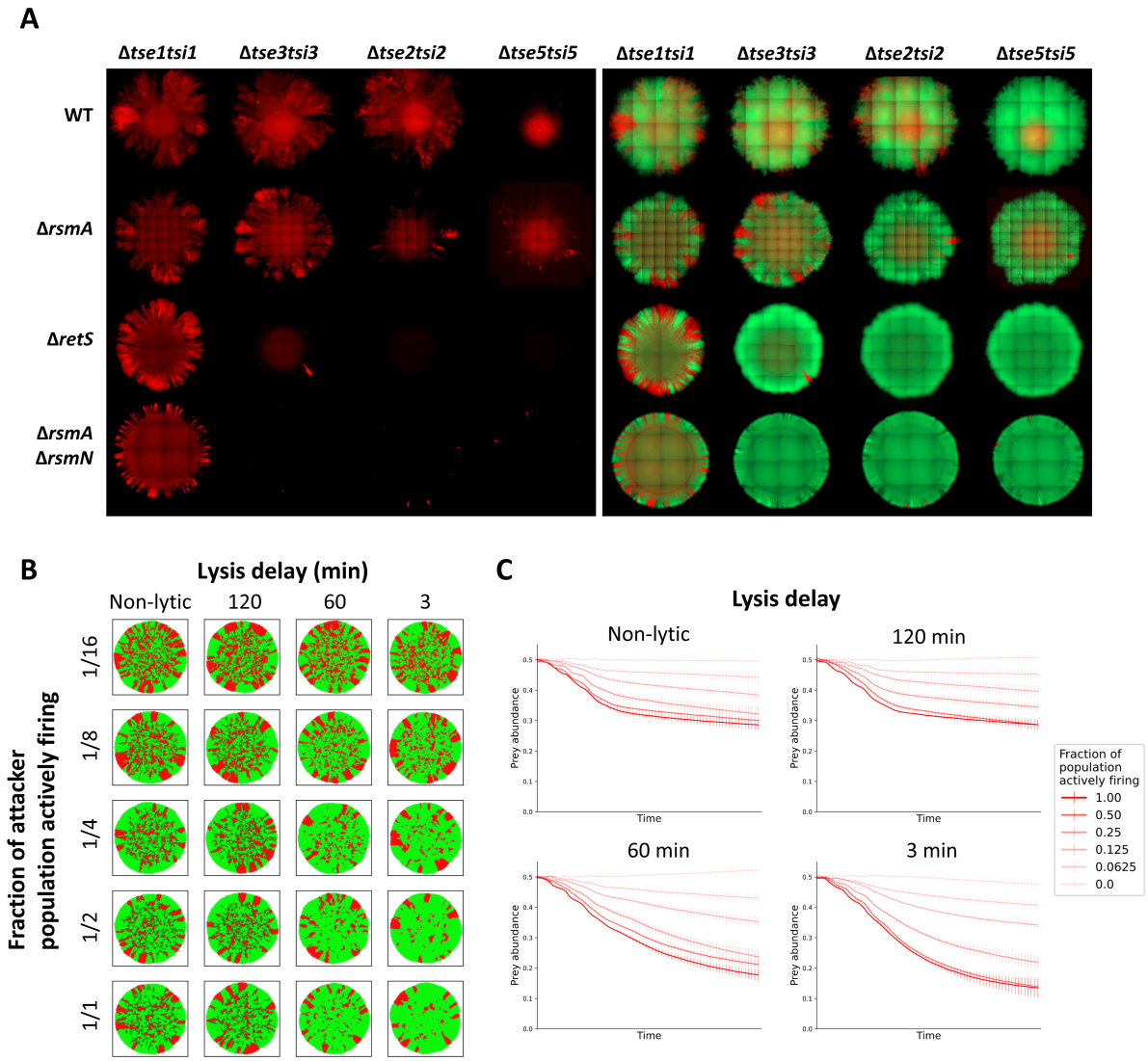

Figure 5.18: **T6SS toxin killing efficacy increases with elevation in T6SS activity.**
(**A**) Whole colony fluorescent microscopy image of T6SS sensitive strain distribution within colony a mix of T6SS+ parental strain. Corresponding fluorescent channel composite images showing toxin-sensitive bacteria in red and T6SS+ parental strain in green. Strains sensitised to individual H1-T6SS toxins in each of the columns in the following order: Tse1, Tse3, Tse2, and Tse5. Each row contains strains with different regulatory background in following order of ascending H1-T6SS activity: WT, Δ*rsmA*, Δ*retS*, and Δ*rsmA*Δ*rsmN*. Strains contain constitutively expressed fluorescent proteins, prey labelled with mCherry (red) and attacker with sfGFP (green). All bacteria mixed at 1:1 ratio, inoculum OD_{600} = 1.0, grown for 48h at 37°C on LB with 2% (w/v) agar.
(**B**) Representative simulation output of a mix of sensitive (red) and T6SS+ attacker (green) bacteria populations. Competition outcomes depending on different toxin lysis rate and changes of the fraction of the attacker population actively engaging in T6SS firing.
(**C**) Relative prey abundance over simulation time-course depending on differences in toxin lysis rate and fraction of attacker population engaging in T6SS firing, each of the plots corresponds to a column from panel **B**. (Toxin lethal dose = 5, initial seeding density = 1.0, mean +SD of n=10)

higher toxin dose, as competitive advantage can only be observed in Δ*retS* and Δ*rsmA*Δ*rsmN* strains. Simultaneously independently of the toxin dose delivered, in some cases, action of an individual effector will not result in a notable impact on prey expansion, as illustrated by peptidoglycan amidase Tse1 (584). This gradually differentiable change in competitive outcome can be directly compared with the theoretical model outcomes. Figure 5.18 shows how T6SS-dependent competition is affected by both attacker T6SS activity levels and toxin mode of action.

In our experiments assessing TssB1 sheath assembly dynamics (Figure 4.6), we noticed that even in the case of high secretion activity and killing proficiency at population scale, as in the case of Δ*rsmA*Δ*rsmN* strains, single cell analysis shows that only a quarter of the population actively participates active H1-T6SS firing (Figure 4.6 B). Therefore, we decided to simulate whether in cases where only fraction of the population actively participates in T6SS-mediated competition, a population-level competitive advantage is still observable. Comparing competition outcomes in mixtures where all or only 50% of the attacker population participate in the firing of T6SS showed that both can restrict prey growth to the same extent independently of toxin lysis ability (Figure 5.18 B and C). Reduction of the actively firing population to 25% will maintain approximately 80% of the maximum competitive advantage, while further decrease in the fraction of the population actively firing T6SS will result in gradual loss of the competitive advantage. We could thus conclude that non-homogenous T6SS firing by attacker population observed at single-cell level is consistent with the observations from whole mixed colony experiments, where these same strains proficiently kill sensitive prey bacteria.

5.6 Discussion

T6SS is a tool that can be utilised for inter-bacterial and bacteria-host interactions mediated through contact-dependent delivery of effector proteins. Analysis of currently available genome sequences show that genes encoding T6SSs are found in 20 to 30% of Gram-negatives (509, 510, 454). Additionally, it is not uncommon to find multiple distinct T6SSs encoded within the genome of a single species, with as many as 6 found in *Burkholderia sp.* (752). The complexity extends even further when it comes to effectors delivered by these systems. One of the best studied T6SS model systems is found in *V. cholera* and delivers 3 antibacterial toxins (580), while in other bacterial species such as *Serratia marcescens* it delivers at least 8 experimentally validated antibacterial and antifungal effectors (753, 514). Here, we have tackled the question of *P. aeruginosa* toxin multiplicity through a comprehensive and systematic analysis of the contribution of individual toxins to bacterial competition. We did this by comparing the impact of different toxic effectors and how competition efficacy is improved upon increase in the toxin load delivered. This was done using a mixed macrocolony assay that allows to assess how delivery of different toxins impacts sensitive lineage distribution within communities. By complementing mixed macrocolony experiments with theoretical simulations, we also addressed in what scenarios increase in T6SS toxin delivery rate provides an added competitive benefit.

5.6.1 Increase in T6SS firing results in improved killing

P. aeruginosa T6SS expression and activity is non-constitutive and each of the systems is activated only under specific conditions. A key regulator of T6SS expression and activity is the Gac-Rsm cascade, which, as part of modulating the transition to biofilm lifestyle, gradually increases the activity of the three T6SSs. Through the investigation of the impact of the Gac-Rsm cascade on H1-T6SS activity, it became apparent that even in cases of highly T6SS expressing and active $\Delta retS$ and $\Delta rsmA\Delta rsmN$ strains only a fraction of the population participates in active T6SS sheath assembly and firing (Figure 4.6). Nevertheless, both of these

strains are able to restrict toxin sensitive prey from expanding within populations. We further corroborated these observations using biophysical simulations that allowed us to confirm that attacker population where only a fraction of the population participates in T6SS-dependent attack is able to effectively eliminate toxin-sensitive prey (Figure 5.18). What is notable is that if only half of the population engages in active T6SS attack, prey growth is restricted to an extent comparable the case where the entire population is involved, and nearly 80% of the competitive advantage is attained by populations in which only 1 in 4 bacteria participate in active killing (Figure 5.18 C). A speculative explanation compatible with this observation is that this would be overall more cost effective. As some energetic investment is sufficient to provide most of the competitive benefit, there is no further evolutionary drive to further increase the T6SS attack rate. However, when comparing different strains of Gac-Rsm mutants, an increased T6SS activity does appear to result in a higher number of toxins being able to spatially restrict sensitive prey growth, as best illustrated by Figure 5.18A. Theoretical analysis of the factors determining T6SS-mediated competition outcome shows that although an increase in T6SS firing rate provides an additional competitive benefit, the main determinant of overall competition efficacy is the toxin mode of action (Figure 5.17 and (684)). Another point supporting the idea that increased T6SS firing does not necessarily translate into improved killing are the observations looking at $\Delta pppA$ strains. Loss of function *pppA* mutants display constitutive H1-T6SS firing, but do not appear to be measurably more effective when it comes to sensitive prey bacteria growth restriction within the context of whole mixed macrocolonies (Figure 5.10). Instead, the main determinant of the overall competitive outcome appears to be the toxin mode of action (Figure 5.17).

5.6.2 Differing toxin biochemical activity - importance of lytic toxins

Even though T6SS-associated toxins are highly varied in their specific biochemical function, they can be categorised into two broad classes by their impact on the target - lytic or

bacterostatic. Although this classification may be simplistic and most toxins exist on the spectrum between the two, this assumption allows us to make broad interpretations about general ecological rules on when it becomes advantageous to engage in direct bacterial competition. Lytic toxins, T6SS-dependent or delivered through other means, are able to cause disintegration of the target cell and this provides an opportunity to gain contact with a new susceptible prey cell (684). Toxins that disrupt the integrity of cell wall, through the degradation of peptidogycan or membrane as well as the formation of ion permeable pores are likely to result in rapid lysis of the target bacteria. Comparative analysis of H1-T6SS toxins showed that the two most potent toxins are pore forming Tse2 and Tse5, but surprisingly peptidoglycan hydrolases Tse1 and Tse3 are amongst some of the least potent toxins delivered by the system (Figure 5.5). Similarly, H2-T6SS-dependent peptidoglycan hydrolase AmpDh3 is one of the toxins that did not appear to provide competitive advantage under any of the conditions tested in this study (Figure 5.12 and 5.13). This is especially surprising as other comparative studies have positioned peptidoglycan hydrolases as a generally highly effective toxin class (754, 584, 358, 582). Tse1 has been identified as one of the most potent toxins in interspecies competition, being the specific effector that causes rounding of *V. cholera* cells (564) and is also notable for being able to degrade peptidoglycan of Gram-positive *B. subtilis* (661). This suggests that the insensitivity to Tse1 and Tse3 action could be specific to its target being *P. aeruginosa*. An existing example of evolved non-specific immunity against *P. aeruginosa* T6SS attack is *A. baumannii* use of the peptidoglycan editing enzyme RacK, that provides protection against T6SS attack (647).

Amongst the *P. aeruginosa* PAO1 H2-T6SS-associated toxins is a set of 5 phospholipases (40) with distinct specific catalytic targets and mechanisms of action (Table 5.1). In comparative toxin potency analysis, these phospholipases range from some of the least to the most effective effectors. Tle3 is amongst the most potent of H2-T6SS toxins, and both Tle4 and PldB also provide a measurable competitive advantage in $\Delta rsmA$ regulatory context (Figure 5.12), while to detect the impact of Tle1 and PldA use of $\Delta retS$ genetic context with higher system activity was

needed (Figure 5.13). Overall, phospholipase effectors are distributed over the entire comparative potency spectrum, this likely being a result of differences in the specific catalytic properties or enzymatic targets. Notably the most potent of the H2-T6SS toxins were effector of unknown function PA5264 and nuclease TseT (559) (Figure 5.12). Simultaneously H1-T6SS nuclease Tse7 (552) is one of the comparably less potent toxins (Figure 5.5). This comprehensive analysis reveals that broad sweeping predictions about toxin potency may be useful when identifying more general rules of engagement within competition, but may be less useful when making predictions surrounding effectiveness of individual toxins, as this is likely to be more dependent on specific context.

5.6.3 Toxin synergy

Both H1- and H2-T6SS are associated with delivery of numerous toxic effectors, but it is not entirely clear whether all of these effectors are delivered at once or whether killing at a highly local scale is the result of the action of an individual toxin. Previous studies looking at the expression of both core and orphan T6SS gene clusters appear to be co-regulated (723, 728) and therefore expressed under the same conditions. A factor that likely limits co-delivery is individual effector linkage with particular T6SS components. Cargo effectors can associate with Hcp and toxin-filled Hcp rings make up the internal barrel of the T6SS sheath structure (556, 555). Hcp is the most abundant of the T6SS proteins (755) and makes up the spear-like structure that exits a firing cell and enters neighbouring cells. It has also been shown that Hcp is transferred between cells in quantities sufficient to complement the absence of Hcp in the recipient cell (540). Therefore, it stands to reason that a potentially large number of Hcp-associated toxin molecules can be delivered to a target cell, and no limitation to the multiplicity of the Hcp-associated effectors being loaded within sheath at any one time is apparent. Alternatively, effectors can be associated with VgrG or PAAR proteins, both through direct binding or adaptor-mediated binding or as evolved domains that are a part of the effector (558, 559, 756). Each functional

T6SS spear will be topped with a VgrG trimer and a single PAAR protein (527, 538). Each of the 3 T6SSs in *P. aeruginosa* has a single and specific associated Hcp protein, which in the case of Hcp2 is encoded by 3 sequence conserved genes - *hcpA* (PA1512), *hcpB* (PA5267) and *hcpC* (PA0263) (Figure 1.20). Unlike with Hcp, both H1- and H2-T6SS have multiple associated PAAR and VgrG proteins (Figure 1.20). Individual effectors have been shown to associate with specific PAAR and VgrG proteins (553) and PAAR and VgrG protein combinations are not fully interchangeable (592, 553), so this places an overall theoretical limit on the possible co-delivered toxin combinations possible. What is notable from the comprehensive analysis of individual toxin efficacy here is that association with delivery by Hcp, VgrG or PAAR does not link with increased or decreased ability to eliminate sensitive prey growth. Hcp associated effectors have the highest theoretical potential to be delivered in large quantities, and while the Hcp1 associated effectors Tse2 and Tse4 are highly effective, Tse1 and Tse3 are some of the least potent H1-T6SS effectors. Furthermore, Hcp has been shown to provide protection against toxic effectors if the two are co-expressed, but presence of compatible Hcp clearly is not sufficient to provide protection against Tse2 or Tse4 impact in the absence of cognate immunity genes (Figure 5.5). Simultaneously, the most potent of the H1-T6SS effectors is pore forming Tse5, which contains a N-terminal PAAR domain (550, 551). This means that only a single effector molecule will be injected at any one time. Similarly, VgrG1a has been associated with delivery of both Tse6, a cytoplasmic acing NAD(P)+ degrading hydrolase (121) which is one of the relatively more effective H1-T6SS toxins. While VgrG1a associated Tse8 (557) is one of the toxins that failed to show any detectable killing independently of the doses delivered or competition growth conditions (Figures 5.5, 5.10 and 5.8). Regarding evolved T6SS effectors that contain both structural and effector domains, such as VgrG2b or PAAR containing Tse5 (550, 551), delivery of other effectors is likely to exclusively co-occur with these effectors. For example, VgrG2b contains a C-terminal toxin domain, but is also associated with delivery of lipase Tle3, peptidoglycan hydrolase AmpDh3 and common good effector Azu (358, 612, 625, 587). Therefore, when Tle3 or AmpDh3 are

injected into prey bacteria, these toxins will co-occur with VgrG2b, similarly loss of VgrG2b would interfere or entirely prevent delivery of these effectors.

A potential advantage of using a large set of toxins could be a more "energy efficient" mode of T6SS attack. If a single T6SS injection delivers a set of toxins with varied biochemical targets, then it stands to reason that the prey is less likely to have evolved immunity to every single one. Additionally, if the toxins delivered act synergistically it is possible that overall fewer firing events are required. In this study, we observed a striking example of toxin synergy, where the combined use of two peptidoglycan hydrolases enables effective prey growth restriction. When Δ*rsmA* bacteria were individually sensitised to Tse1 or Tse3 and mixed with T6SS+ parental strain, no consistent spatial restriction is observed. If a further step is taken to sensitise Δ*rsmA* to both Tse1 and Tse3 and the same experiment is performed, the growth of the toxin sensitive strain is restricted to only the central region of the colony (Figure 5.7). Tse1 is peptidoglycan amidase and its enzymatic target is peptidoglycan cross-links, while Tse3 is a muramidase that cleaves PG backbone. Although delivery of Tse3 does not appear to provide competitive advantage within context of WT or Δ*rsmA* strains, Δ*tse3tsi3* are growth restricted in Δ*retS* and Δ*rsmA*Δ*rsmN* context (Figure 5.5). The contribution of Tse1 becomes apparent only when combined with Tse3. This suggests that disruption of peptidoglycan backbone has a potentially more severe phenotype than cross-links.

5.6.4 Changes in growth conditions impact T6SS-mediated competition efficacy

Similarly as T6SS expression varies under different growth conditions, it stands to reason that competition outcomes are subject to the specific environmental conditions. Among the effectors delivered by T6SS are not only toxins, but also common good effectors that have the potential to help cope with nutritional limitations. These are proteins secreted by T6SS and aid in sequestering metal ions from the environment and three of these have been described

in *P. aeruginosa* to date - Azu, ModA and TseF (501, 625, 169). Furthermore, cells could be more or less vulnerable to action of specific toxin action depending on the specific growth conditions. Here we tested whether NAD(P)+ metabolism targeting Tse2 and Tse6 or protein synthesis disrupting Tse8 could be more impactful under nutrient limited conditions, but such effect was not detectable (Figure 5.8). But what this experiment allowed us to validate is that *P. aeruginosa* still produces and kills competitors using T6SS under nutrient limitation. This is an important aspect for T6SS-dependent interactions, as multiple literature examples linking T6SS-mediated killing as part of active predatory strategy have been shown (757). A notable feature of *P. aeruginosa* H2-T6SS is preferential expression when the growth temperature is lowered from 37^{o}C to 25^{o}C (723). This observation is further reinforced by experiments performed here where H2-T6SS toxin mediated killing was only observable at 25^{o}C (Figure 5.12).

5.6.5 Summary

P. aeruginosa T6SS delivers a cocktail of varied antibacterial toxins. One of the questions that emerges from this observation is why such multiplicity can be observed. Here, a systematic comparative toxin potency analysis was performed to assess the contribution of individual T6SS effectors in bacterial competition. We observed that the action of a single toxin can be sufficient to restrict spatial expansion of sensitive prey bacteria. Although low T6SS activity can be sufficient to prevent the expansion of prey beyond the inoculum area, a gradual increase in toxin dose delivered results in more toxins having a noticeable impact on prey growth and almost complete elimination of sensitive bacteria.

Chapter 6

Prey-attacker contact assortment determines T6SS mediated competition outcome

6.1 Introduction

Pseudomonas aeruginosa uses Type VI secretion system (T6SS) to deliver toxic effectors to adjacent microbes and compete for space within a biofilm niche. As we show in the chapter 5, the effectiveness of the T6SS attack depends on the delivery of toxic effectors. *P. aeruginosa* encodes more than 20 antibacterial toxins that vary between strains (Table 1.1). These toxins are varied in biochemistry and in cellular targets, in addition, a single injection of T6SS is likely to deliver a mixture of different ones. Although a prey bacteria may evolve defences against the action of few toxins, it appears somewhat unlikely that it would be possible to maintain specific defences against every single toxin within a large multiplicious set. Therefore, prey bacteria have evolved some more universal defence mechanisms that protect against T6SS attacks in general (650). T6SS defence mechanisms that are not dependent on specific immunity proteins include stress response-related damage repair (552, 356) and protection through spatial

separation (687, 695, 684).

T6SS-dependent competition relies on the bacteria from prey and attacker populations making direct cell-cell contact. This is due to the fact that most T6SS effectors lack intrinsic cell entry properties and therefore require direct delivery to the target cell (758, 351). Impact of cell-cell contact on T6SS and contact dependent inhibition (CDI) have been explored before and community architecture has been shown to impact the competitive outcomes (683, 684, 700). These studies have shown that one of the challenges for T6SS-mediated attacks is prior prey establishment (689, 687), where part of the existing resident population is able to shield others within the niche. This protection resulting from the accumulation of cell debris is termed the "corpse barrier" (684, 698). Here, we use a combination of biophysical simulations and the experimental setup established in the chapter 5 to address how the local population intermixing impacts competition at the whole community scale.

A distinct factor that impacts both the global community architecture and local cell-cell contacts is the amount of exopolysaccharides (EPS) present in biofilms. EPS production is known to have an impact on the structure of bacterial communities across a wide range of species. In the case of *E. coli* curli fibres and cellulose are responsible for the development of macroscopic wrinkly phenotypes (759), while *B. subtilis* colony wrinkling is a result of spatiotemporal differences in gene expression and matrix component production (760). The production of extracellular matrix by *B. subtilis* has been shown to provide protection from *Pseudomonas chlororaphis* T6SS attacks and promote co-existence while colonising plants (660). Rugose or wrinkled colony variants are also seen in *V. cholera* isolates and result from increased Vibrio **p**oly**s**accharide (VPS) production (761, 762). The presence of VPS and the biofilm matrix protein RbmA have been shown to protect from same-species and exogenous T6SS attacks (264, 763). *P. aeruginosa* clinical isolates also contain phenotypically distinct sub-populations termed rugose small-colony variants as a result of increased Pel and Psl production (61, 297, 328). This phenotype can be a result of a variety of pathoadaptive mutations, but is often seen to be the

result of increased c-di-GMP production and disruption of Gac-Rsm or associated regulatory cascades (764, 765, 766, 68). Persistence of *P. aeruginosa* lineages with these mutations is favoured, as the bacteria are better suited for survival in infection context, this including both host-pathogen and interactions with other organisms within the niche (67, 274). As we discussed in the chapters 3 and 4, *P. aeruginosa* T6SS expression and activity is modulated by both the Gac-Rsm cascade and c-di-GMP. Therefore, both EPS production and T6SS activity appear to be co-regulated in *P. aeruginosa*. A question of interest for this study are how changes in *P. aeruginosa* own EPS production impact the strain distribution in whole macrocolonies and what are the consequences for T6SS-mediated competition.

Another factor that impacts both the overall community architecture and local organisation is motility. Within the context of *P. aeruginosa* biofilms, type IV pili (T4P) have been shown to contribute to both adhesion and motility (30). T4P are proteins fibres extending from bacterial surface, that are used for both cell-cell adhesion and cell-surface adhesion (30, 205). Both of these functions are mediated trough the same mechanism – dynamic pili polymerisation and de-polymerisation that allows bacteria to exert force against the object that it adheres to (203, 206). When T4P adhere to substrate, this same mechanism is used to propel bacteria across the surface through a type of motility termed "twitching" (30). Both aggregation and active intermixing are factors that influence bacterial community organisation and therefore are likely to have implications on localised interactions. A recent study by (767) explores how T4P-mediated spatial segregation influences *Neisseria cinerea* T6SS-dependent competition. In case of *Neisseria* T4P appear to mediate specific adhesion dependent sorting, that results in non-piliated cell expulsion from the community (768, 769). Subsequently, this spatial segregation results in protection from T6SS-dependent killing (767). Here, we address how T4P impacts *P. aeruginosa* community organisation and see a distinct effect, where T4P is used primarily as a motility device. *P. aeruginosa* used T4P to actively intermix on both a local and global scale, and to expand across surfaces. Consequently we observe that loss of T4P leads to impairment

in *P. aeruginosa* T6SS toxin-dependent competition efficacy and observe how increased motility can aid with escape from contact-based killing.

The chapter 5 of this thesis focuses on how T6SS-dependent competition impacts sub-population distribution in mixed microbial communities. The focus is placed on impact of different T6SS toxins and how increase in T6SS activity results in gradual decrease in relative prey bacteria abundance. To modulate T6SS activity, we use strains with mutations within Gac-Rsm cascade, here we address how these mutations impact whole colony morphology. EPS and changes in motility influence community morphology and how this impacts T6SS mediated competition. Additionally we systematically assess how decrease in local contact intermixing resulting from loss of T4P interferes with T6SS mediated killing, as well as assesses how toxin sensitive prey can used T4P mediated surface motility to escape T6SS attack.

We aim to address the following questions:

- How disruption of Gac-Rsm regulatory cascade at different points impacts *P. aeruginosa* community organisation.
- How local contact assortment impacts T6SS-dependent competition outcomes.
- How loss of EPS impacts community organisation and T6SS-dependent competition outcomes.
- How loss of T4P impacts community organisation and T6SS-dependent competition outcomes.

6.2 Results

6.2.1 Inoculum composition determines the number of prey-attacker contacts within macrocolony and subsequent survival of T6SS sensitive prey

The most important prerequisite for T6SS-dependent killing is the formation of contact between bacteria from prey and attacking populations. Independently of how effective a toxin is at eliminating prey bacteria and independently on the T6SS firing frequency, these interactions are dependent on the T6SS wielding bacteria making contact with prey. If there is no contact between populations, no killing can occur, and conversely, the more contact between populations, the more effective killing can be expected to be. Here, a systematic approach using both biophysical simulations and a comparable experimental system is used to address how changes in local contact assortment influence T6SS-mediated competition.

Two straightforward approaches for manipulating inter-population contact assortment exist in the context of mixed macrocolony experiments. One is to manipulate the proportion of the competitors within the inoculum mix and the other is to adjust the starting population density. A study by (700) addresses how the competitive outcome in the context of mixed macrocolony is determined by the spatial configuration of individual bacterial cells at the point of population establishment. The main takeaways are that access to free space is a key factor determining whether a bacterial lineage is able to survive. Additionally, populations that arise from low density in founder cell inoculum are subject to more variation in the outcome of competition and spatial separation appears to be protective in active competition mediated both by diffusible and contact-based mechanisms (700, 683, 576, 416). Here these approaches are taken to more directly investigate how aspects such as spatial segregation prior establishment influence the overall competitive outcome. And to establish how aspects such as increased local intermixing influence T6SS competition specifically and how these observations could be generalised to all contact-based bacterial competition systems. Additionally, this systematic investigation of

changes in competition effectiveness changes resulting from manipulation of inoculum density provides a valuable reference point that can later be used to comparatively investigate how other factors such as changes in motility influence competition outcome.

6.2.1.1 Inoculum density and strain ratio determines local contact assortment

To explore how the inter-population contact assortment is affected by density and strain ratio in the starting population a set of theoretical simulations without T6SS interactions was used (Figure 6.2). In the context of these biophysical simulations set up here, the movement of bacteria is the result of neighbouring bacteria physically pushing adjacent cells and this movement being opposed by viscous drag (770). Both changes in inoculum density and initial strain mixing ratio are factors that affect whether individual bacteria are preferentially surrounded by one of the species in the mix or whether sub-populations are highly locally intermixed.

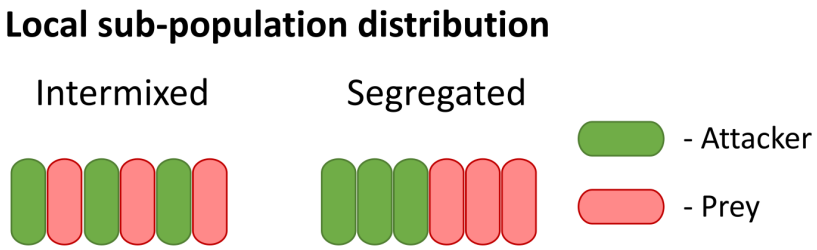

Figure 6.1: **A schematic showing locally intermixed and spatially segregated communities.**
Depiction of locally intermixed bacterial populations on the left and spatially segregated populations on the right.

Upon the establishment of a dense community departure from a 1 to 1 mixing ratio and decrease in inoculum density, both result in a gradual decrease in local contact assortment (6.2 A and B), but the two approaches have distinct effects on population time resolved dynamics. A decrease in the initial bacterial density will result in a smaller overall population at a given time point and a delay before the establishment of a dense community (Figure 6.2 C and D) while changes in initial mixing ratio will not affect the overall growth dynamics in the absence

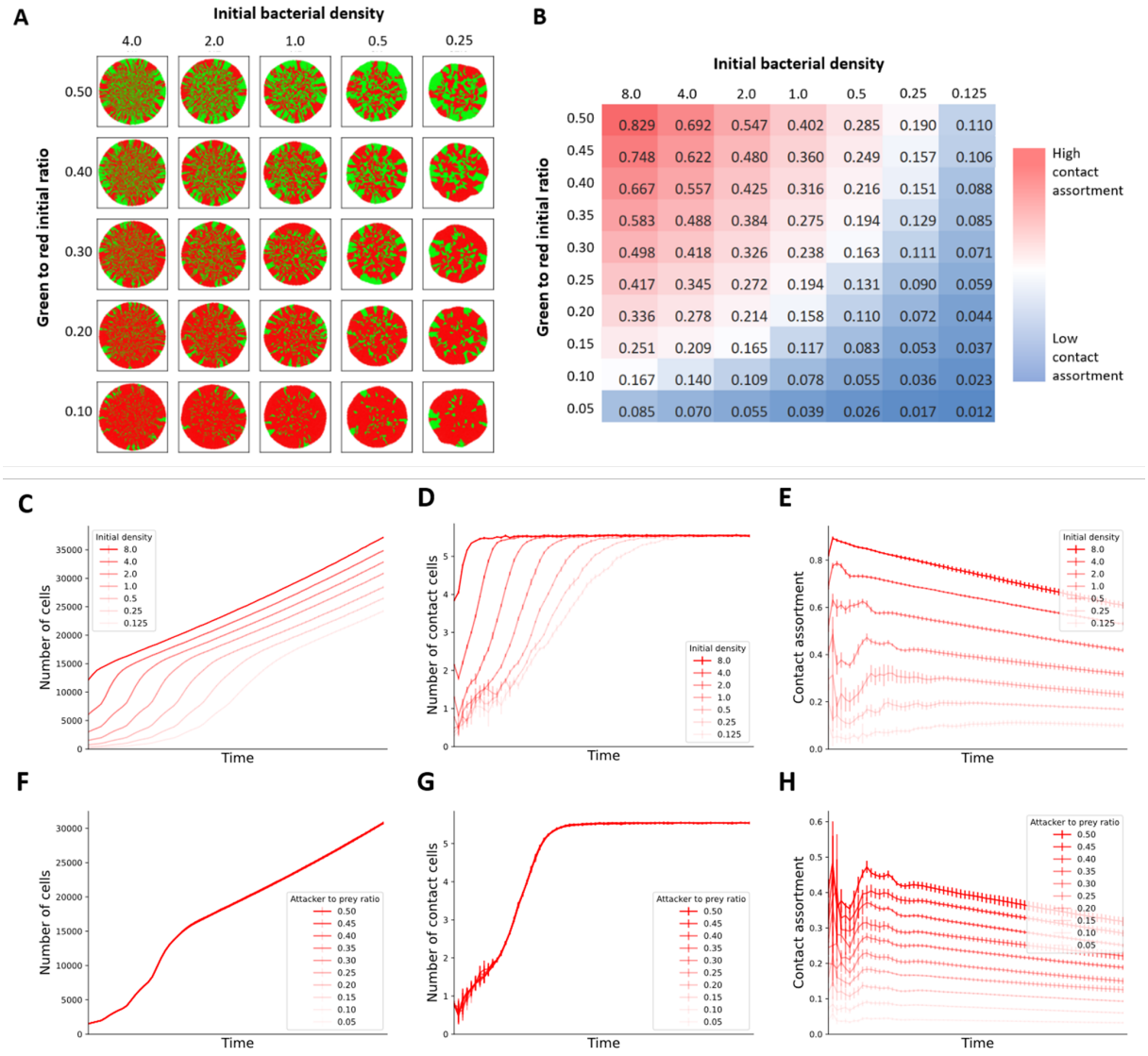

Figure 6.2: **Inoculum composition determines prey/attacker population contact assortment within macrocolony.**
(**A**) Representative simulation outputs showing changes in species distribution resulting from variation in initial density and mixing ratio of cells from two populations.
(**B**) Changes in localised agent intermixing as interspecies contact assortment resulting from variation in initial density and mixing ratio of cells in simulation setup.
Time resolved changes in interspecies contact assortment are determined by both inoculum density and initial ratio of strains in the mix. (**C**) and (**F**) Total number of cells over simulation time-course. (**D**) and (**G**) Total number of contact cells within 2D plane over simulation time-course. (**E**) and (**H**) Interspecies contact assortment over simulation time-course (**C**), (**D**), and (**E**) Effect of variation in initial density. (**F**), (**G**), and (**H**) Effect of variation in species mixing ratio. (No T6SS interactions, mean +SD of n=5)

of competition (Figure 6.2 F and G). Once dense community is established, an individual cell forms an average of 5.53 contacts in 2D plane. The contact assortment index indicates the level of local intermixing of sub-populations (Figure 6.1); upon an increase in the initial bacterial

density, the contact assortment index tends towards 1, indicating a high number of interspecies contacts, while the decrease in seeding density allows for initial sub-population establishment results segregation with fewer interspecies contacts (Figure 6.2 A, B, and E). The number of interspecies contacts formed is also influenced by the proportion of prey to attacker in the inoculum mix, with the 1 to 1 mixing ratio resulting in the highest contact assortment and with gradual decrease in contact assortment as species mixing ratio in initial population departs from 1 to 1. Independently of inoculum composition, the contact assortment will gradually decrease during later population expansion where most of the growth occurs through further clonal expansion at the outer edge of a colony (Figure 6.2 E and H).

In conclusion, changes in the bacterial density within the establishment population impact not only species contact assortment, but also the overall population establishment dynamics. Using this approach, impacts of prior population establishment and attacker population's ability to clear and actively invade pre-established prey can be investigated. Although maintaining 1 to 1 strain ratio enables easier measurement of changes in competitive outcome assessed experimentally, changing this mixing ratio allows to more directly pinpoint impact of changes in contact assortment (Figure 6.2 F, G, and H). As the competitor mixing ratio departs from 1 to 1 (or 50%) a directly proportional drop in the contact assortment is seen (Figure 6.2 B and H). Next, we used both experimental and theoretical competition, to see how changes in prey-attacker contact assortment impact T6SS-mediated competition.

6.2.1.2 Effectiveness of T6SS killing is determined by the initial bacterial seeding density

The prior establishment or creation of spatial separation is one of the immunity-independent mechanisms that bacteria employ to protect from T6SS (687, 695). To address how prior establishment mediated spatial population segregation impacts *P. aeruginosa* T6SS-dependent competition, we combined biophysical models with experimental data of toxin Tse5-mediated

competition using a set of Gac-Rsm mutant strains with gradually modulated T6SS activity levels (Figure 5.18). Theoretical modelling here is an extension of the work described in the chapter 5.5 of this thesis. The simulations describe interactions between two bacterial populations that grow on a surface in two dimensions. One of the populations is sensitive to killing by T6SS, while the other is parameterised to fire T6SS in random directions at a previously specified frequency. After T6SS firing occurs, all of the T6SS "needles" intersecting prey bacteria are accounted for, if a prey bacteria has received more T6SS "hits" than it can tolerate then prey death occurs. The number of T6SS hits (or the toxin dose) required to kill a prey bacteria and the time delay between prey death and complete lysis are parameterised to describe both highly lytic and non-lytic toxins, as well as highly potent and less potent toxins. The impact of different toxin mode of action and T6SS firing behaviours is addressed in more detail in chapter 5.5 of the thesis.

We used theoretical simulations to assess how changes in inoculum density impact competition mediated through both highly lytic or non-lytic toxins (Figure 6.3). Theoretical modelling shows that decrease in initial cell density results in gradual increase in prey survival (Figure 6.3 A and B). The degree of restriction in prey growth is directly proportional to the attacker population's T6SS firing rate. The ability to entirely eliminate the prey population rather than just spatially restrict prey population is determined by the type of toxin used, lytic toxins enable the removal of any pre-established prey cells, as the susceptible population is eliminated even in cases of low initial density, i.e. $OD_{600equivalent}$=0.25 (Figure 6.3 A). The scenario differs if competition is mediated through entirely non-lytic toxins (Figure 6.3 B), if sufficiently high amounts of a toxin are delivered, clear prey killing can be seen, but no clearance of the dead bacteria occurs. In a scenario with the highest inoculum density, i.e. $OD_{600equivalent}$=4.0, dead prey cells are seen in the initial placement area, while if the inoculum density is halved, prey population segments are allowed to expand in the outer regions of the colony, as bacteria in the centre of the segment are protected by a barrier of dead kin, this

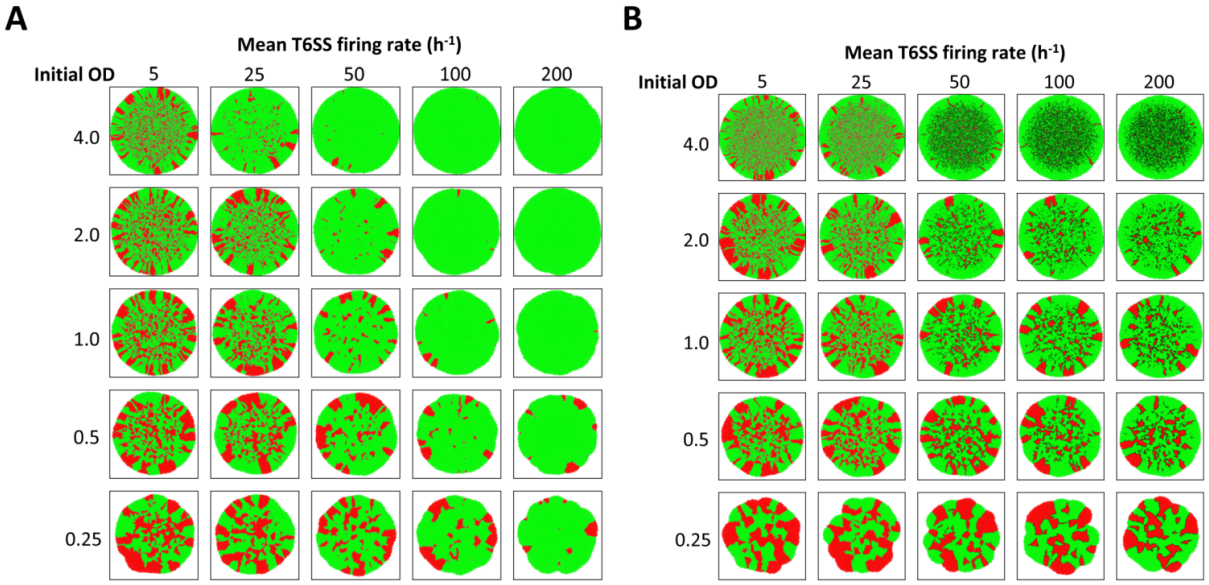

Figure 6.3: **Theoretical modelling shows that decrease in founding population density allows for toxin sensitive bacteria survival.**
Representative simulation outputs showing how decrease in initial bacterial density promotes prey (red) survival within a mixed population. Competition outcomes depending on attacker populations (green) mean T6SS firing rate within context of highly lytic toxins (**A** where toxin lethal dose = 5, lysis delay = 3 min) or non-lytic toxins (**B** where toxin lethal dose = 5). Changes in prey (red) and attacker (green) population distribution at the simulation endpoint shown subject to variations in initial population density ($OD_{600_{equivalent}}$ = 4.0; 2.0; 1.0; 0.5; 0.25) and mean attacker firing rate (5; 25; 50; 100; 200 firing events per hour). Decrease in initial bacterial density promotes prey survival independently of the type of toxin employed, with increase in T6SS attack rate directly correlating with decreased abundance of prey bacteria. The spatial distribution of remaining prey in cases of effective competition being determined by the type of toxin used.

protective effect has previously been termed a "corpse barrier" (684) (Figure 6.4).

To confirm the protective effects of prior prey establishment experimentally, we setup a mixed macrocolony experiments using the H1-T6SS toxin Tse5. We chose this toxin as comparative analysis in the chapter 5 established that it is the most potent of H1-T6SS associated antibacterial effectors. The bacterial density within the inoculum was varied between OD_{600} 0.001 to 1 (Figure 6.5 A and B). We also used strains with mutations in the Gac-Rsm cascade for competition setup with differentiated T6SS firing rates. In chapters 4 and 5, we established that WT, Δ*rsmA*, Δ*retS*, and Δ*rsmA*Δ*rsmN* mutant strains show gradually elevated T6SS activity, and this allows us to match the firing T6SS firing rate in simulation parameter space.

We observed that at the highest initial density, i.e. OD_{600}=1, the prey does not expand

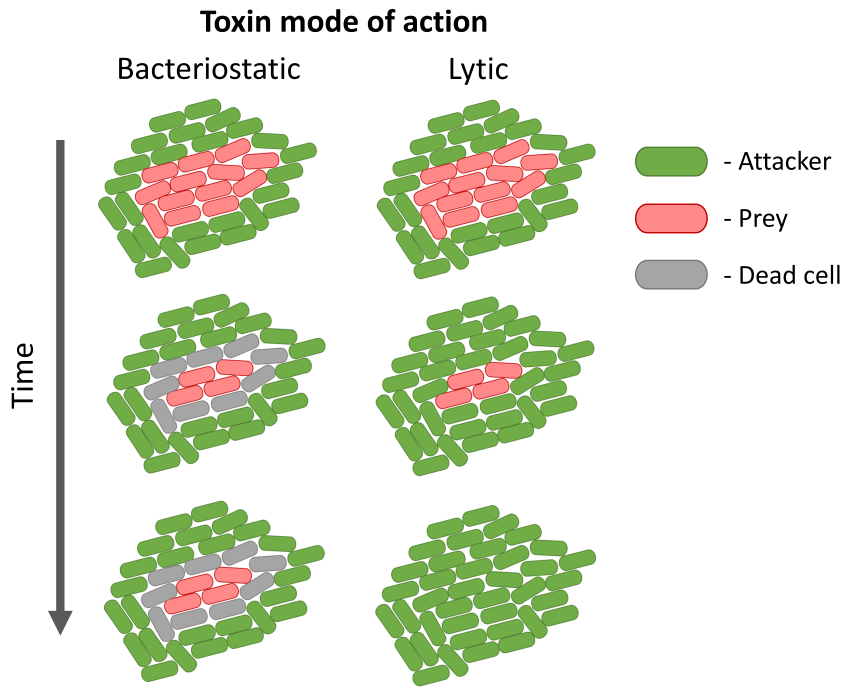

Figure 6.4: **Schematic showing protective effect provided through "corpse barrier".** Diagram showing competition population development over time. Bacteria in green are in a contact-dependent manner killing bacteria in red. On the right, competition occurs trough use of a lytic toxin, that enables immediate removal of dead prey bacteria allowing access to further prey population and resulting in gradual complete elimination of red population. On the left, competition occurs through non-lytic toxins. Although attacking population is able to kill most of the prey bacteria, dead bacteria are not removed and form a protective barrier. This "corpse barrier" shield remaining prey bacteria from killing and enables persistence.

if the colony is made up of strains with the highest H1-T6SS firing activity ($\Delta retS$ and $\Delta rsmA\Delta rsmN$), while a small amount of bacteria grew in the outer colony regions when attacker populations T6SS activity was relatively low (WT and $\Delta rsmA$ strains). In bacterial colonies established from sparsely distributed bacteria, i.e. $OD_{600} = 0.001$, sensitive bacteria appear to be present at comparable frequencies independently of the attacker's T6SS activity status, even in the context of the high H1-T6SS activity of $\Delta retS$ and $\Delta rsmA\Delta rsmN$ mixes, prey bacteria are highly abundant (Figure 6.5 A and B, lower lines). This is a scenario comparable to simulation outcomes evaluating impact of non-lytic toxins on established populations, where prior establishment plays a more notable role in determining the extent of prey survival rather than further increasing the frequency of T6SS attack, where doubling the toxin injection rate is of little added benefit (Figures 6.3 and 6.5). It is also notable that surviving prey bacteria will

be preferentially found in the colony central region, emphasising that true complete clearance of existing sensitive bacteria is more challenging than hindrance of further expansion.

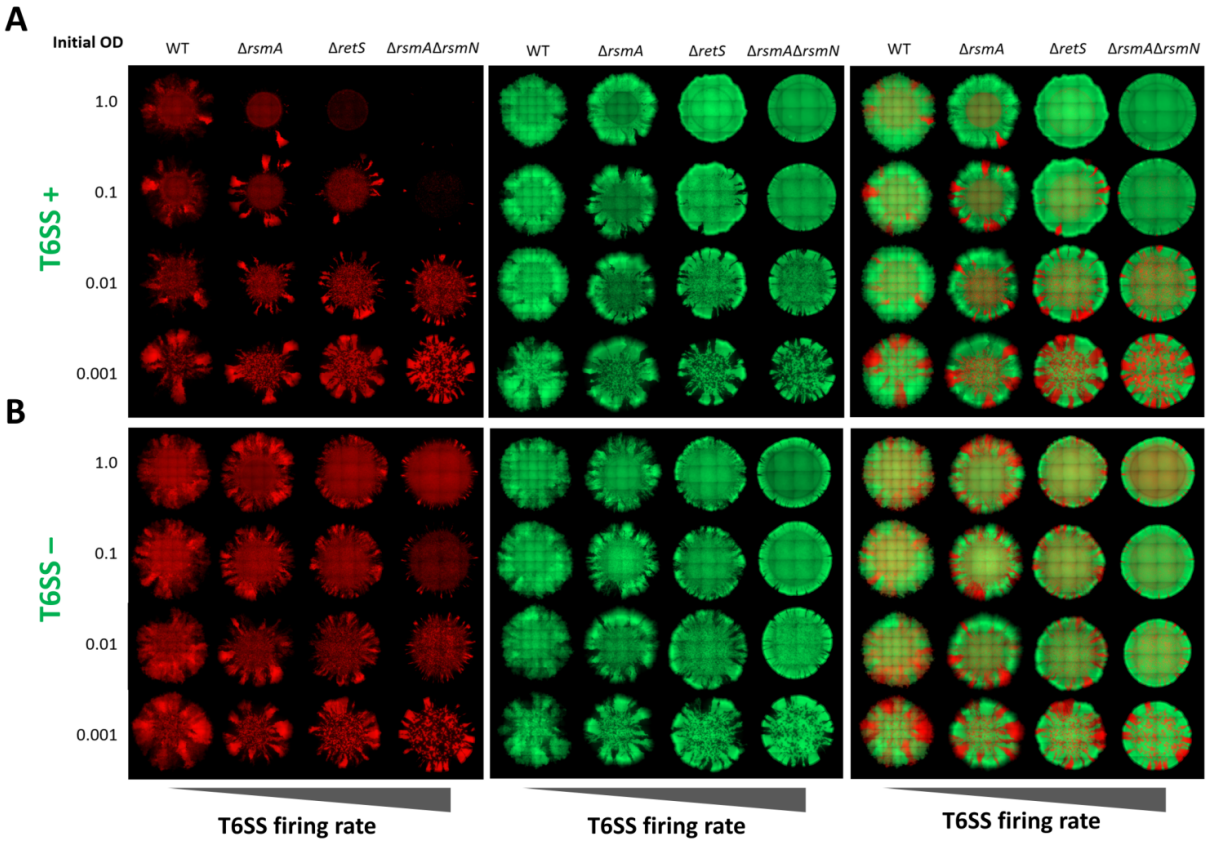

Figure 6.5: **Low inoculum density allows for establishment and survival of toxin sensitive prey.** Tse5 mediated competition outcomes in context of strains with differing T6SS activity levels of populations inoculated from different initial density. Representative images of 48h old mixed colonies of Tse5 sensitised bacteria (red) in competition with T6SS+ (**A**) or T6SS- parental strain (**B**) of the same regulatory background (green). Mixed bacterial colonies of WT, Δ*rsmA*, Δ*retS*, and Δ*rsmA*Δ*rsmN* strains in different columns and altered inoculum densities in different rows. First set of images shows prey distribution only and second set shows corresponding fluorescent channel overlay of both prey and attacker populations. Stains lacking *tssB1*, *tssB2*, and *tssB3* genes used for negative control mixed colony setup (**B**). Strains contain constitutively expressed fluorescent proteins, prey labelled with mCherry (shown in red) and attacker with sfGFP (shown in green). Isogenic bacterial strains tagged with mCherry (red) and sfGFP (green) fluorophores were mixed at 1 to 1 ratio and after adjusting inoculum density (OD_{600} = 1.0; 0.1; 0.01; 0.001) spotted on LB agar, images of whole macrocolonies acquired after 48h incubation at 37^{o}C on LB with 2% (w/v) agar.

6.2.1.3 Effectiveness of T6SS killing is determined by the initial prey-attacker cells ratio

Manipulation of relative strain abundance during the experiment set-up allows to directly change the extent of local inter- vs intra-population contact formation without affecting the overall population growth dynamics (Figure 6.2). Manipulation of the ratio of prey to attacker is also a commonly used methodological optimisation approach when conducting competition assays to investigate T6SS, CDI, or other contact-based and contact-independent bacterial interactions (683, 684, 416). Here, the direct impact of increased prey-attacker contacts formation on the outcomes of T6SS-dependent killing is addressed in a manner similar to the above investigation on the protective role provided by prior prey establishment.

Theoretical simulations were once again used to specifically address the extent of protection

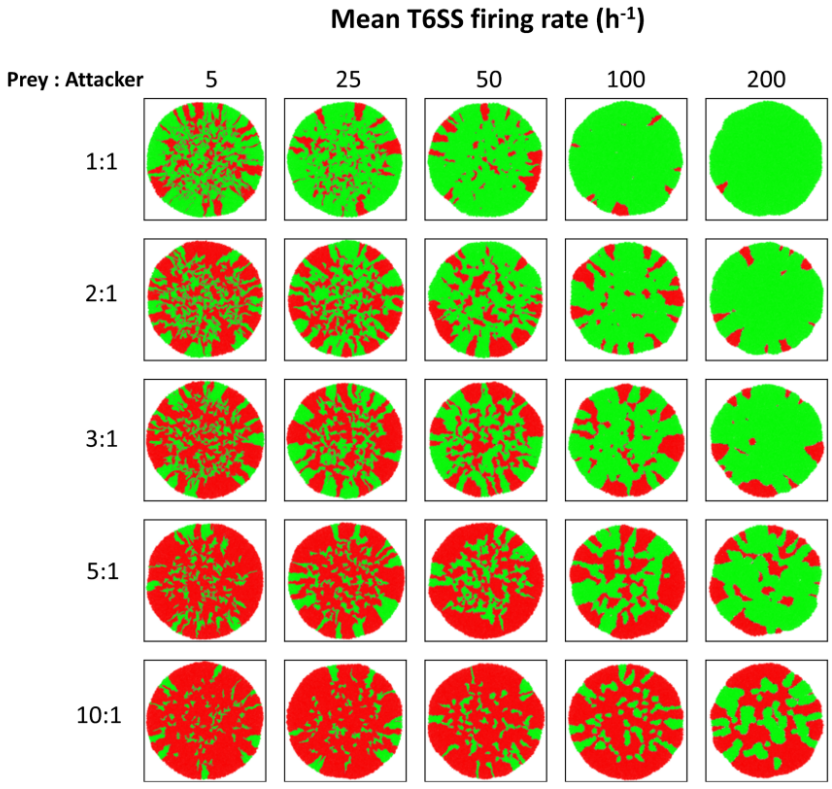

Figure 6.6: **Decrease in inter-population contacts protects T6SS sensitive prey.** A set of representative simulation outputs showing how changes in competition lineage ratio within initial population affect prey (red) survival. Impact of competition mediated through fast lysing toxins (lethal dose = 5, lysis delay = 3 min) delivered at different rates (5; 25; 50; 100; 200 firing events per hour).

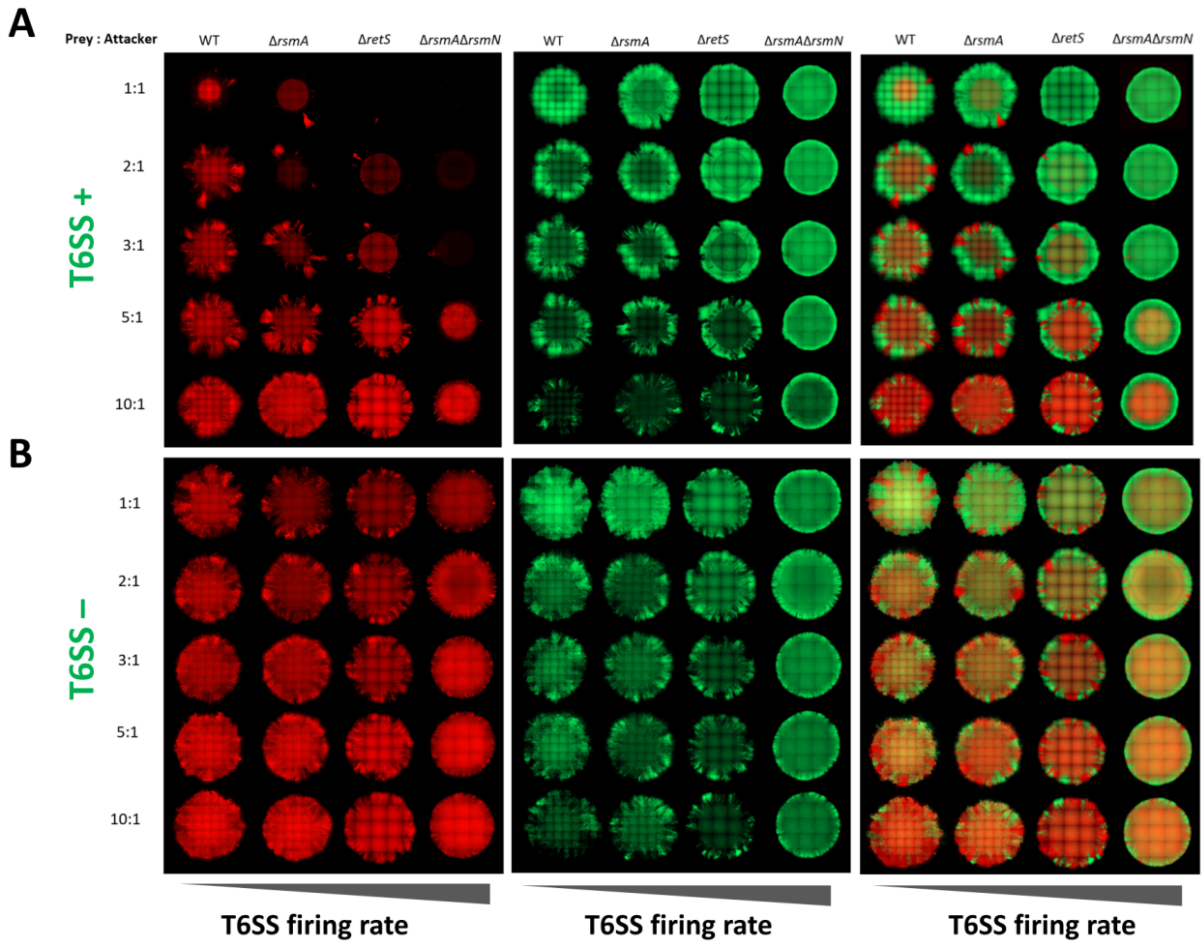

Figure 6.7: **Decrease in inter-population contacts protects T6SS sensitive prey.** Tse5 mediated competition outcomes in context of strains with differing T6SS activity levels. Each of the columns correspond to WT, Δ*rsmA*, Δ*retS*, and Δ*rsmA*Δ*rsmN* regulatory background strains in the given order. Sowing a set of individual fluorescent channel images of prey distribution only (in red) and fluorescent channel overlay images of both prey in a mix with T6SS+ (**B**) and T6SS- (**D**) parental strains. Each of the rows contains a set of representative images of colonies set up with a different prey to attacker ratio in the inoculum. Isogenic regulatory background prey to attacker strains mixed at the following ratios from the top row: 1:1, 2:1, 3:1, 5:1, 10:1. Showing 1 representative colony of a set of 3 biological repeats.
Strains tagged with constitutively expressed fluorescent proteins, prey labelled with mCherry (red) and attacker with sfGFP (green). Inoculum density OD_{600} = 1.0, with prey to attacker mixing ratio as specified, spotted on LB agar, images of whole macrocolonies taken after 48h incubation at 37°C on LB with 2% (w/v) agar.

provided by the reduction in local contact assortment (Figure 6.6). As the prey-to-attacker proportion in inoculum departs from 1 to 1 towards 10 to 1, a gradual increase in prey survival can be observed, with effect remaining proportional to attacker T6SS firing proficiency (Figure 6.6). This is also supported experimentally using Tse5-dependent competition and Gac-Rsm mutant strains with incrementally differing H1-T6SS activity levels (Figure 6.7). When the

species ratio is 1:1, prey bacteria are readily growth-restricted in all genetic backgrounds. However, the attacker advantage is progressively lost as the relative prey abundance in inoculum increases, with only the highest T6SS activity strains ($\Delta rsmA\Delta rsmN$) strains being able to spatially restrict sensitive prey expansion in a scenario where inoculum contains 10 toxin sensitive bacteria for every cell in the attacker population. Furthermore, while $\Delta rsmA\Delta rsmN$ strain competition results in near total prey elimination if bacteria are mixed at 1:1 ratio, large amounts of sensitive bacteria are present at the inoculum region when mixed at 5:1 or 10:1 ratio (Figure 6.7 B). To test whether this same approach would enable detection of single toxin-mediated killing by toxins that appeared otherwise ineffective at prey growth restriction we set up an experiment where Tse1 sensitive bacteria ($\Delta retS\ \Delta tse1tsi1$) are mixed with increasing amounts of toxin

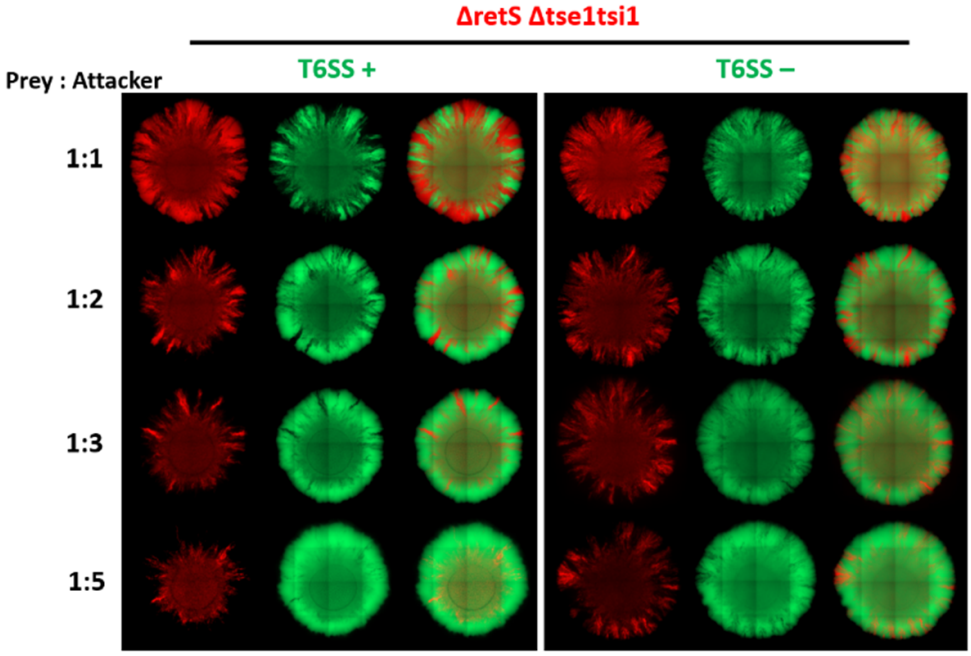

Figure 6.8: **Increased opportunity for toxin injection does not ensure improved killing.** A set of mixed macrocolonies of Tse1 sensitive prey ($\Delta retS\ \Delta tse1tsi1$) in presence of T6SS+ ($\Delta retS$) or T6SS- parental strain ($\Delta retS\ \Delta tssB1\ \Delta tssB2\ \Delta tssB3$). Showing both individual fluorescence channel images of toxin sensitive prey (red), attacker population (green) distribution, and the corresponding fluorescent channel overlay images. Assessing how increasing relative amount of attacker bacteria within the mix impacts Tse1 sensitive prey strain spatial distribution. From upper row prey to attacker population ratio in the inoculum mix is as follows - 1:1; 1:2; 1:3; 1:5. Showing 1 of 1 test competition outcome.
Strains tagged with constitutively expressed fluorescent proteins, prey labelled with mCherry (red) and attacker with sfGFP (green). Inoculum density OD_{600} = 1.0, with prey to attacker mixing ratio as specified, spotted on LB agar, images of whole macrocolonies taken after 48h incubation at 37^{o}C on LB with 2% (w/v) agar.

carrying parental strain ($\Delta retS$). We chose Tse1-dependent competition, as this peptidoglycan hydrolase appeared to be unable to restrict the growth of prey bacteria in any of the assays conducted in Chapter 5. As seen in Figure 5.18, isogenic Tse1 mediated T6SS competition in mixed colonies of 1 to 1 prey to attacker mix did not result in consistent prey growth spatial restriction independently of the strain regulatory context. Skewing the competition in a manner where any sensitive bacteria is exposed to a higher number of cells capable of delivering T6SS injection carrying Tse1 by adjusting prey-attacker ratio to 1 to 5, only slight increases in T6SS-dependent spatial restriction can be seen in the outer colony region, while the abundance of prey bacteria in the central colony region is unaffected (Figure 6.8). This further emphasises that adequate prey-attacker mixing is essential for success of contact-based competition, the overall limiting factor remains bacterial ability to deliver a potent toxin.

In summary, as T6SS-mediated competition is entirely dependent on prey and attacker populations making close contact, bacterial distribution at the local scale will have a notable impact on the overall competitive outcome. T6SS killing will be most effective when populations are highly intermixed, while spatial segregation through prior establishment provides universal protection against contact-dependent killing. Additionally, if a prey bacteria is exposed to a higher number of T6SS wielding attackers, this provides additional opportunities for toxin injection to occur, but it appears that the specific toxins employed remain the competition limiting factor.

6.2.2 Lineages in mixed macrocolonies formed by *gac-rsm* mutants show different levels of intermixing

The Gac-Rsm regulatory cascade modulates *P. aeruginosa* T6SS activity as part of a broader planktonic to biofilm lifestyle switch involving changes in expression of hundreds of genes. Among direct and indirect regulatory targets are genes related to motility, adhesion, polysaccharide production (122, 123, 131). Alteration in the expression of biofilm formation

associated genes is known to impact the overall architecture of bacterial communities (328). Therefore, we decided to assess how disruption of Gac-Rsm regulatory cascade impacts sub-population organisation within mixed macrocolonies. Subsequently, this study will be expanded to assess how specific phenotypic features under control of Gac-Rsm cascade, specifically Type IV pili-dependent motility and EPS production, impact community organisation and T6SS-dependent competition.

The bacterial lineage distribution within mixed macrocolonies is subject to both inoculum composition and specific growth conditions, as discussed in chapter 5. The above simulation set in Figure 6.2 shows how decrease in inoculum population density reduces sub-population intermixing. Here, we tested how lineage distribution within mixed communities consisting of isogenic strains changes subject to variation in initial population density (Figure 6.9). For this we used a *P. aeruginosa* strain set with mutation at different points in the Gac-Rsm cascade - WT, Δ*rsmA*, Δ*retS*, and Δ*rsmA*Δ*rsmN*. The extent of lineage intermixing in the central region of the colony decreases as the overall bacterial density in inoculum is lowered from OD_{600}=1.0 to 0.001 (Figure 6.9 B). In colonies established from low density inoculum, i.e. OD_{600}=0.001, distinct monoclonal patches can be seen in the colony central region (Figure 6.9 A, C, and D, last columns). This lineage spatial segregation is reflected by increased relative fluorescent signal variation (Figure 6.9 E, last column) and corresponding decrease in population intermixing measured in the central colony region (Figure 6.9 B). This spatial segregation in colonies established from sparse initial populations is a result of individual bacteria being able to form monoclonal micro-colonies before encountering adjacent populations and shows that once establishment has occurred, adjacent lineages will not fully intermix. Communities that are initially dense, i.e. inoculum OD_{600}=1.0, appear to be consistently more intermixed once established (Figure 6.9 B and F), this observation directly matching with simulation outcomes (Figure 6.2).

Within the context of surface-based macrocolony growth setup, once a community is

established in the inoculum zone most of the further growth proceeds through lateral expansion.

Only bacteria at the very edge of the community are able to expand into adjacent empty space,

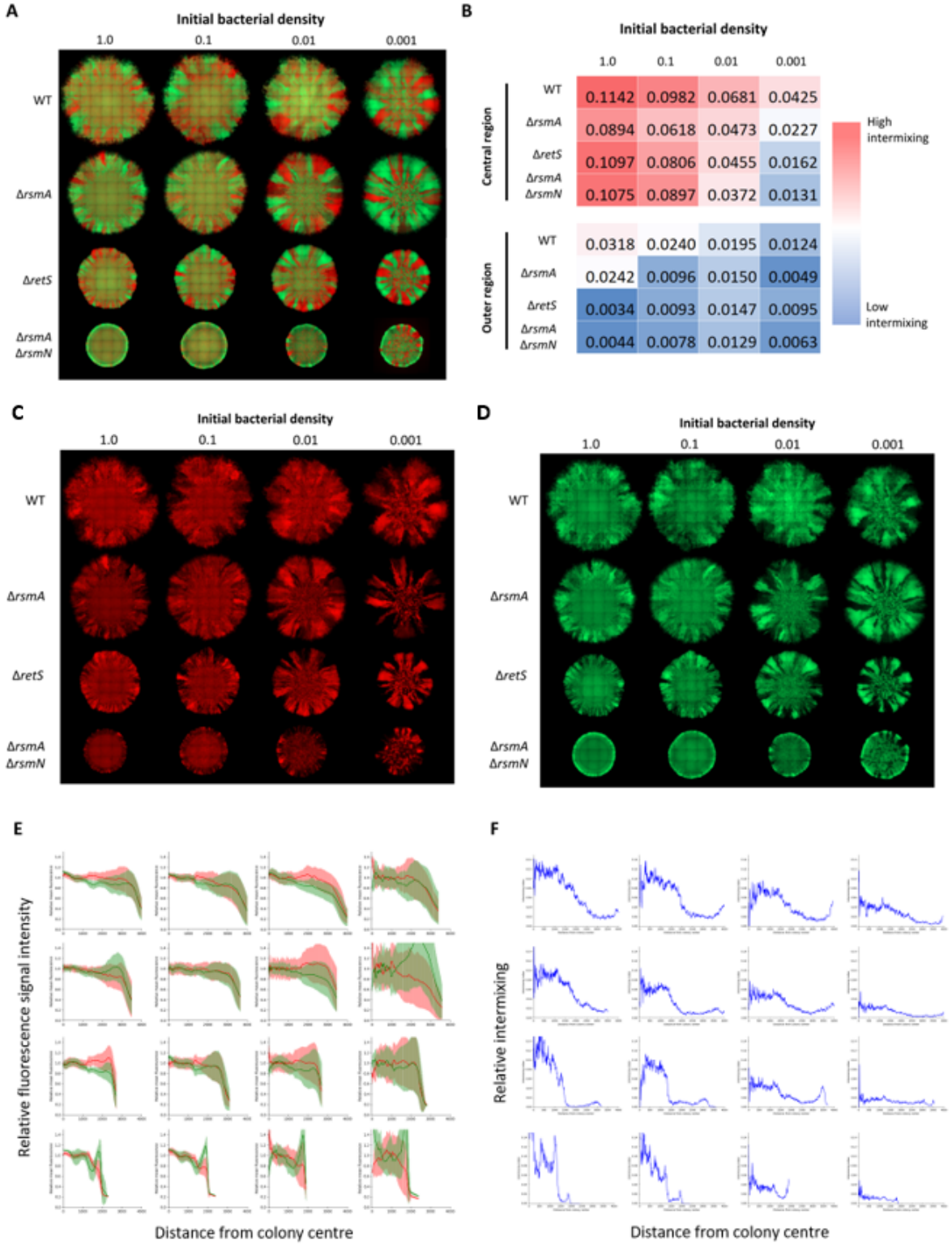

Figure 6.9: **Colony morphology is determined by strain regulatory background and bacterial density in inoculum.**

Figure 6.9 *(previous page)*: **Colony morphology is determined by strain regulatory background and bacterial density in inoculum.** (**A**) Set of representative fluorescence composite images of mixed bacterial colonies of WT, Δ*rsmA*, Δ*retS*, and Δ*rsmA*Δ*rsmN* strains with altered inoculum densities. Isogenic bacterial strains tagged with mCherry (red) and sfGFP (green) fluorophores were mixed at 1 to 1 ratio and after adjusting inoculum density (OD_{600} = 1.0; 0.1; 0.01; 0.001) spotted on LB agar. Images of whole macrocolonies taken after 48h incubation at 37^{o}C show 2 morphologically distinct regions - highly mixed inner region corresponding to inoculum zone and an outer region where spatial segregation of the sub-populations is apparent. Representative images of 3 biological replicates shown, with the corresponding individual fluorescence channel images in panels (**C**) and (**D**). (**B**) Mean relative sub-population intermixing measurements of the colony central and outer regions for the corresponding images. Increase in fluorescence signal variance and decreased intermixing are indicative of sub-population segregation in outer colony regions. Spatially resolved relative mean signal intensity + SD of individual fluorescence channels (**E**) and relative intermixing (**F**) are calculated for circular sections taken at increasing distance from colony central point.

and this leads to formation of segmented outer colony edge. Sub-population segregation and corresponding decrease in bacterial intermixing in outer colony regions is a subject both to changes in inoculum density and strain genetic context, with Δ*retS* and Δ*rsmA*Δ*rsmN* mutant strains forming communities that are less locally intermixed. In addition to this, morphology of whole colonies is subject to disruption in Gac-Rsm regulatory cascade, with both Δ*retS* and Δ*rsmA*Δ*rsmN* strains producing smaller more aggregative colonies (Figure 6.9). The likely reasons for this phenotypic shift towards aggregation being Gac-Rsm mutation mediated changes in biofilm formation.

6.2.3 *P. aeruginosa* EPS impact on strain distribution in macrocolonies

6.2.3.1 Loss of EPS has minor impact on mixed macrocolony structure.

To study how loss of EPS impacts *P. aeruginosa* community organisation in mixed macrocolonies, we constructed a set of strains that are unable to produce Pel or Psl, by removing both *pelA* and *pslBCD* genes (61, 771). As *P. aeruginosa* PAO1 is a low alginate producing strain (273), loss of Pel and Psl effectively renders these strains as EPS free mutants. Then to observe how this affects the distribution of bacterial lineages within the community, we tagged both EPS+ (Δ*retS*) and EPS- (Δ*retS*Δ*pelA*Δ*pslBCD*) strains with constructively expressed

mCherry (in red) or sfGFP (in green) fluorophores and subsequently used these strains to set up mixed macrocolony experiments (Figure 6.10). Similarly as above, mixed macrocolonies were inoculated from bacterial mixes ranging in density from OD_{600} = 1.0 to 0.001. In the cases of both EPS+ with EPS+ (Figure 6.10 A first set) and EPS- with EPS- (Figure 6.10 A fourth set), both red and green tagged lineages are equally intermixed, with further sub-population segregation occurring as inoculum density is gradually decreased. The equal distribution of lineages within these communities is expected, as both of the strains within the set are entirely isogenic, aside form the fluorescent tag. Unexpectedly, the mixed macrocolonies containing both EPS+ and EPS- strains show only minor impact on the lineage distribution within community, with the EPS- strains appearing to take up slightly increased area of the colony (Figure 6.10 second and third columns). Altrough, further assessment would be needed to pinpoint mechanistic reason behind the changes in population distribution, likely explanations are changes in the cell-cell adhesion resulting from the loss of EPS or an indirect impact stemming from changes in motility. Although only minor impact of loss of EPS on the sub-population distribution was seen, we proceeded to test how this would impact T6SS-mediated competition.

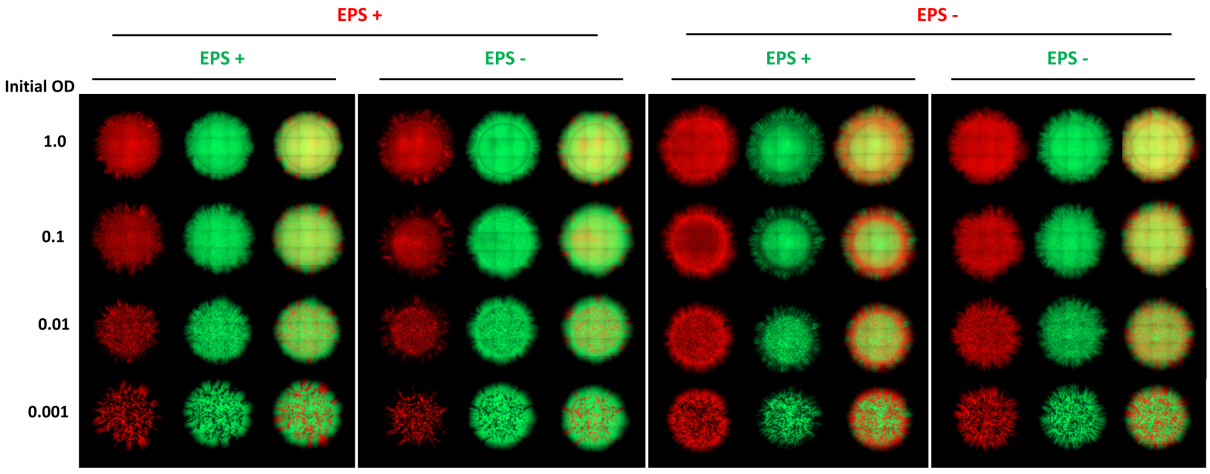

Figure 6.10: **Loss of EPS has minor impact on sub-population distribution within bacterial macrocolonies.** Mixed macrocolony communities made up of off EPS+ ($\Delta retS$) and EPS- ($\Delta retS$ $\Delta pelA$ $\Delta pslBCD$) bacterial strains tagged with mCherry (red) and sfGFP (green) fluorophores. Showing both individual fluorescent channel and overlay images for mixes of EPS+ and EPS+ strains in the first column, deferentially tagged EPS+ and EPS- mixes in the middle 2 image sets, and EPS- and EPS- strains in the forth column.

Changes in EPS production have been shown to impact T6SS mediated competition in *V. cholerae*, *E. coli*, *Klebsiella* and other bacterial species (264, 560, 650). Although the exact mechanistic details behind EPS dependent protection from T6SS attacks are yet to be fully elucidated, the simplest proposed mechanisms could be changes in cell-cell adhesion or presence of EPS resulting in increased distance between cells, preventing T6SS injection. To test how loss of EPS would impact *P. aeruginosa* T6SS-mediated competition within mixed macrocolony context, we constructed mutants sensitised to the H1-T6SS toxin Tse5, in both EPS+ (Δ*retS*Δ*tse5tsi5*::mCherry) and EPS- (Δ*retS*Δ*pelA*Δ*pslBCD*Δ*tse5tsi5*::mCherry) genetic context. These strains were labelled with constitutively expressed mCherry (shown in red) and competed these with both EPS+ (Δ*retS*::sfGFP) and EPS- (Δ*retS*Δ*pelA*Δ*pslBCD*::sfGFP) parental strains. These competitions were carried out within populations with initial bacterial densities ranging from OD_{600} = 1.0 to 0.001, in order to better capture minor changes in relative competitive fitness (Figure 6.11).

As seen in the section 5, strains sensitised to Tse5 are restricted from growth when in a mix with T6SS+ parental strain. Here we observe that this prey growth restriction occurs

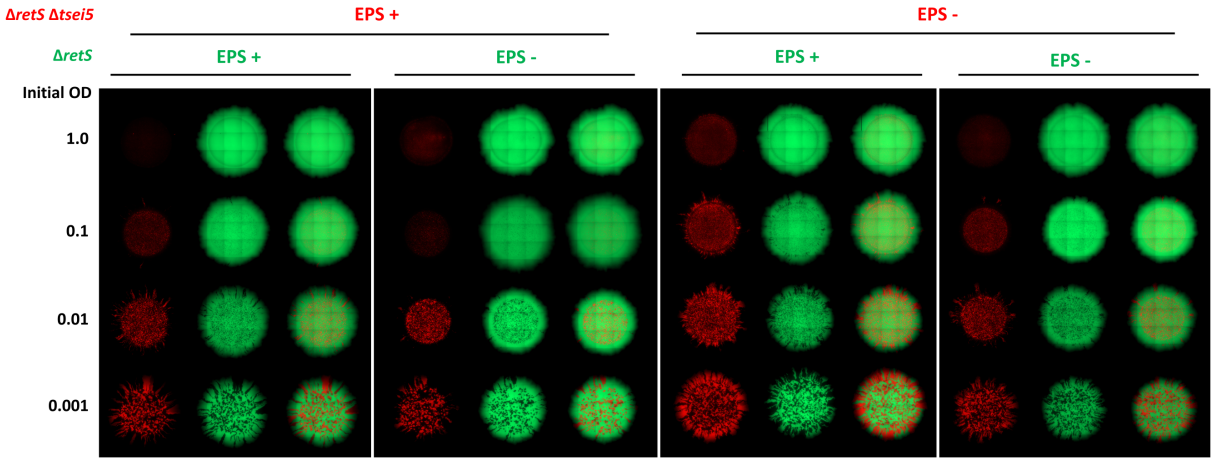

Figure 6.11: **Loss of EPS has minor impact on Tse5-dependent competition.** Assessing impact of prey and attacker population EPS status impact on the H1-T6SS toxin Tse5 mediated competition outcome. Mixed bacterial macrocolonies of Tse5 sensitised prey bacteria (Δ*retS* Δ*tse5tsi5*) in red (mCherry) in presence of T6SS+ attacker population. For both (**A**) and (**B**) bacteria were mixed at 1 to 1 ratio and after adjusting inoculum density (OD_{600} = 1.0; 0.1; 0.01; 0.001) spotted on LB with 2% (w/v) agar, images of whole macrocolonies taken after 48h incubation at 37^{o}C.

independently of the EPS status of the attacker population. The prey bacteria being mainly detectable within the colony central region and prey abundance increase when competition occurs in initially sparse community (Figure 6.11 B, OD_{600}=0.01 or 0.001). Within the context of EPS- prey and EPS+ attacker mix, a slight increase in abundance of toxin sensitive bacteria is seen, suggesting a potential impairment in the delivery of T6SS by the EPS+ attacker (Figure 6.11 third image set). Comparing this to the mixed colonies where populations are not engaged in active T6SS competition, a similar increase in abundance of EPS- lineages in presence of EPS+ strains can be seen (Figure 6.10 second and third image set). This suggests, that although a slight competitive advantage between the two strains can be seen, these results do not show clear EPS-mediated protection during T6SS competition. This is further emphasised when

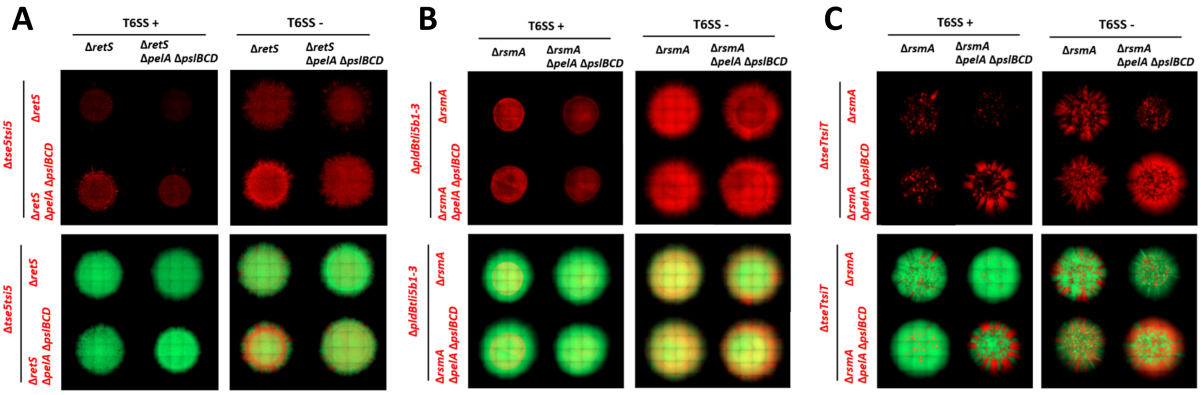

Figure 6.12: **Loss of EPS has minor impact on *P. aeruginosa* T6SS-dependent competition.** Images of mixed macrocolonies of strains sensitised to Tse5 ($\Delta retS\ \Delta tse5tsi5$) (**A**), PldB ($\Delta rsmA\ \Delta pldBtli5b_{1-3}$) (**B**), or TseT $\Delta rsmA\ \Delta tseTtsiT$ (**C**) toxins in red (mCherry). In competition with the corresponding T6SS+ and T6SS- parental strains. To asses impact of EPS in otherwise isogenic T6SS toxin mediated competition, each of the panels contains individual red channel images showing toxin sensitive prey distribution in presence of T6SS+ (left) or T6SS- (right) attacker strain in the upper two rows. Corresponding overlay images showing distribution of both toxin sensitive prey (in red) and T6SS attacker population in green (sfGFP) shown in the lower two rows. Attacker populations with active T6SS used in competition shown on the left and T6SS- ($\Delta tssB1\ \Delta tssB2\ \Delta tssB3$) on the right. Each of the four image panels contains mixes of EPS+ and EPS- ($\Delta pelA\ \Delta pslBCD$) strains, with EPS+ prey in the upper lane and EPS- upper in the lower lane, while mixes in the first column contain EPS+ attacker strains and mixes in the second column contain matching EPS- strains. Bacterial inoculum mixes of OD_{600}=1.0 (**B**), 0.1 (**A**), or 0.001 (**C**) used in competition set-up. H1-T6SS toxin (Tse5) mediated competition conducted on LB with 2.0% (w/v) agar at 37^{o}C for 48h, while H2-T6SS toxin (PldB and TseT) mediated competition conducted on LB with 1.2% (w/v) agar at 25^{o}C for 48h. 1 of 1 colony test images shown for the mixed colonies containing EPS- strains, consistent relative fluorescent channel brightness within image sets, while colonies shown are not to scale.

Tse5 sensitive strain (Δ*retS* Δ*pelA* Δ*pslBCD* Δ*tse5tsi5*) cultured in presence of T6SS- parental strains with and without EPS (Figure 6.12 A), where a similar trend in prey abundance is seen.

As H1- and H2-T6SSs are active under different growth conditions, have distinct dynamics and toxin repertoire, we next chose to test impact of removal of EPS on H2-T6SS toxin mediated competition. For this we chose phospholipse effector PldB and seemingly the most effective of the the H2-T6SS toxins - nuclease TseT. We conducted both of these competition using Δ*rsmA* regulatory background strains, as both of these toxins can be used to effectively restrict sensitive prey growth in this regulatory context (Chapter 5). In case of PldB-mediated competition, both EPS+ and EPS- prey strains appear to be slightly less abundant in presence of T6SS+ EPS- attacker strain (Δ*rsmA* Δ*pelA* Δ*pslBCD*) (Figure 6.12 B). While in case of TseT-mediated competition (Figure 6.12 C), survival of EPS- prey population seems to be favoured independently of attacker populations T6SS activity status. Taken altogether, these results suggest that although loss of Pel and Psl does impact sub-population distribution within context of mixed macrocolonies, this does not translate into clear impact on *P. aeruginosa* T6SS-mediated competition.

6.2.4 Type IV pili impact on bacterial intermixing

6.2.4.1 Gac-Rsm cascade mutants display decreased motility

Details surrounding regulation by Gac-Rsm cascade are described in chapter 1.2.3. Among the regulatory targets of RsmA/RsmN are motility genes encoding both flagella and type 4 pili (T4P) (122). Comparative analysis of Gac-Rsm mutant strains show graduated impairment in twitching and swimming motility (Described in more detail in chapter 1.2.4) as well as distinct swarming phenotypes (Figure 6.13). Regarding T4P-mediated surface twitching motility (Figure 6.13 A), Δ*rsmA*, Δ*retS* and Δ*rsmA*Δ*rsmN* mutants all showed a significant impairment in surface colonisation (Figure 6.13A). Especially notable is Δ*rsmA*Δ*rsmN* mutant strain that shows about 90% reduction in relative attachment area, with phenotypic impairment to this

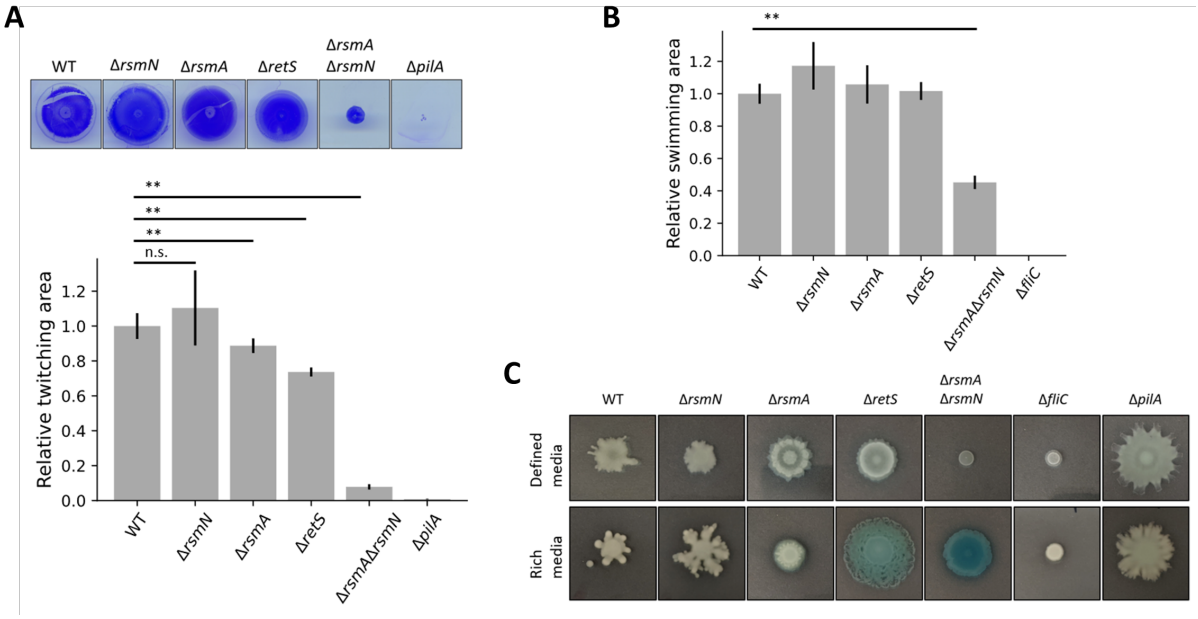

Figure 6.13: **Disruption of Gac-Rsm cascade results in impairment in both T4P and flagella dependent motility.**
Comparative analysis in the relative twitching (**A**), swimming (**B**) and swarming motility of Gac-Rsm mutants compared to WT. (**A**) Showing images comparing strain twitching zones as seen by crystal violet staining and corresponding quantification of the relative twitching zone area, using T4P- mutant (Δ*pilA*) as negative control. (Mean + SD of n=5 biological repeats)
(**B**) Relative changes in swimming area as measured through agar based swimming assay. Using flagella-less (Δ*fliC*) mutant as negative control. (Mean + SD of n=3 biological repeats) ANOVA in combination with Tukey's test used for statistical testing in panels (A) and (B), with "**" designating $p<0.05$.
(**C**) Changes in agar surface swarming assay pattern subject to mutations in Gac-Rsm cascade and loss of T4P or flagella as assessed on minimal (M8 with glucose as carbon source) or nutrient rich media (LB agar) surface.

extent being somewhat visually apparent. Regarding flagella-mediated swimming motility (Figure 6.13 B), only *rsmArsmN* strain shows a significant reduction in relative swimming area to approx 45% of WT. Dependent both on flagella and T4P swarming is a coordinated group movement on viscous surfaces (180, 772, 181). Assessment of different swarming phenotypes is somewhat more complex, due to high phenotypic sensitivity to the exact growth conditions. Here comparative swarming screen on both minimal and nutrient rich media surfaces was performed (Figure 6.13 C). *P. aeruginosa* PAO1 WT is known to form some branching dendrite structures (773) and same is observed here, while loss of flagella (Δ*fliC*) results in bacteria being unable to expand on surface. Mutations in Gac-Rsm pathway have an impact on the swarming phenotype, but interpretation of this is not straightforward. Δ*rsmA*, Δ*retS* and Δ*rsmA*Δ*rsmN* mutant

strains appear to have lost characteristic dendrite structures, but this does not necessarily result in a smaller area being occupied, as in the case of Δ*retS*. It is also notable that Δ*rsmA*Δ*rsmN* mutant strain entirely fails to expand when grown on minimal media suggesting that deletion of both *rsmA* and *rsmN* results in growth defect, while under nutrient rich conditions same strain is able to expand to a comparably larger area than WT or Δ*rsmA* strains (Figure 6.13 C). Taken together, this confirms that the disruption of the Gac-Rsm cascade has an impact on *P. aeruginosa* motility and this is likely to be one of the factors contributing to the changes in the mixed macrocolony morphology observed in Figure 6.9.

6.2.4.2 Loss of T4P results in decreased strain intermixing at both single-cell and whole-colony scale

T4P are adherent protein fibres protruding from the bacterial cell surface, these pili are dynamically assembled and disassembled and this allows bacteria to exert force against the object it adheres to. The use of this single mechanism allows T4P to mediate both aggregation, in cases where pili mediate cell-cell interactions, and surface motility, in case of pili-surface adhesion. Both bacterial aggregation and active surface motility are factors that impact the mixing of bacterial populations at a local and a whole population scale in distinct ways. To assess how loss of T4P impacts *P. aeruginosa* lineage spatial organisation we engineered T4P defective strains by deleting *pilA* - a gene encoding the mayor T4P pilin, rendering these bacteria non-motile (Figure 6.13A). *P. aeruginosa* loss of T4P (Δ*pilA*) results in reduced strain intermixing at single-cell scale (Figure 6.14). In the population made up of differentially fluorescently labelled T4P mutants, single lineage clusters are observable within colony central region and clear clonal expansion lineages can be seen at the population expansion front. Under the same conditions T4P+ cells appear more intermixed, as individual bacteria from one strain are mostly surrounded by members of the other population.

The loss of T4P also impacts the structure of the population as a whole. As seen at single

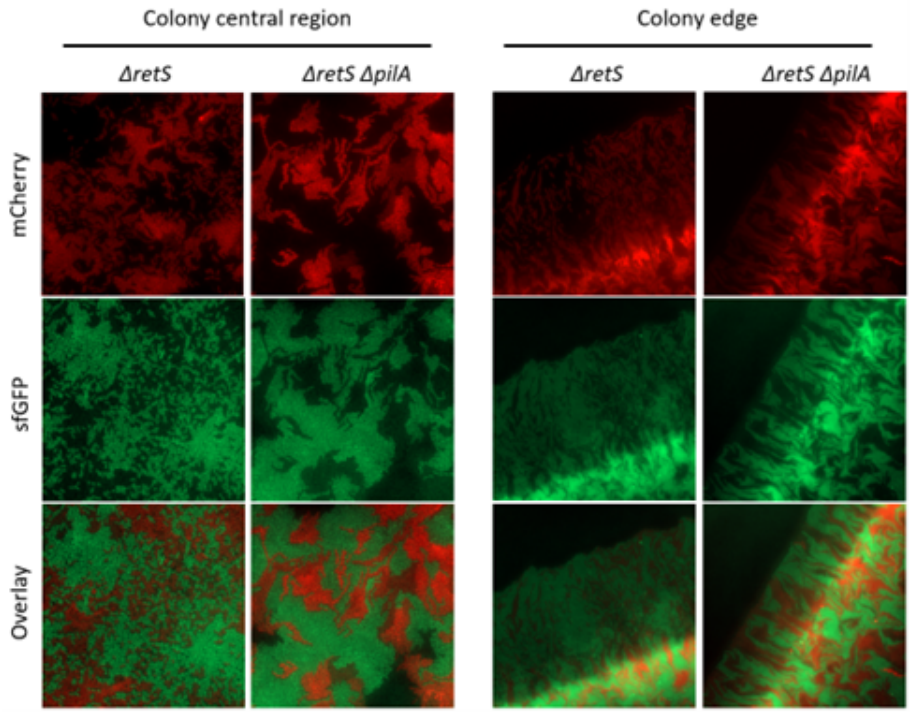

Figure 6.14: **Loss of T4P results in reduced local intermixing at single-cell scale.** T4P+ (Δ*retS*) and T4P- (Δ*retS* Δ*pilA*) bacteria distribution while grown in the interface between LB agar and cover glass. Mixes of isogenic strains with distinct mCherry and sfGFP tags show that loss of T4P results in bacteria localising in monoclonal clusters, while T4P+ strains appear comparably intermixed in both colony central region and at the laterally expanding growth front. Both single fluorescent channel and corresponding image overlays shown.

cell scale *P. aeruginosa* growth on surface is not entirely dependent on expansion through physical interactions but also involves active intermixing using T4P (Figure 6.14). At a scale of whole bacterial communities T4P- strains form smaller colonies (Figure 6.15). Similarly, to Δ*rsmA*Δ*rsmN* mutants (Figure 6.9), outer laterally expanding macrocolony regions of Δ*pilA* mixed colonies are reduced in size and sub-populations appear to form defined segments even in colonies established from high density inoculum (Figure 6.15). This reduction in bacterial ability to expand on rigid agar surfaces or to intermix when grown in interface between media agar and cover glass suggest that *P. aeruginosa* uses T4P to both actively intermix locally and to expand the population overall.

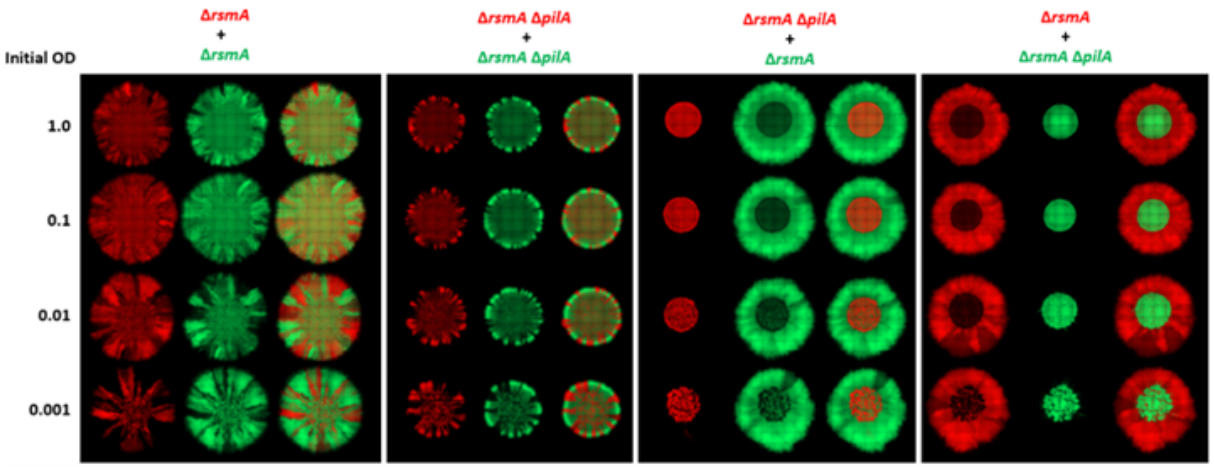

Figure 6.15: **T4P mediate *P. aeruginosa* lineage lateral expansion on surfaces.** Mixed bacterial macrocolonies of T4P+ ($\Delta rsmA$) and T4P- ($\Delta rsmA$ $\Delta pilA$) mutant strains tagged with constitutive mCherry (red) and sfGFP (green) tags. Showing single fluorescence channel and overlay images of T4P+ and T4P+, T4P- and T4P-, T4P- and T4P+ mixed colonies, displayed to scale. Strains mixed at 1 to 1 ratio and after adjusting inoculum density (OD = 1.0; 0.1; 0.01; 0.001) spotted on LB with 2% (w/v) agar and incubated at 37^{o}C for 48h before imaging.

6.2.4.3 Surface growth and active intermixing promotes H1-T6SS sheath assembly and firing

P. aeruginosa H1-T6SS is a retaliatory/ response firing system, meaning that sheath structures are often assembled in response to a prior injection. *P. aeruginosa* uses TagPQRS-PpkA-PppA pathway (further described in Chapter 1.4.4) to sense exogenous T6SS injections and subsequently positions membrane and baseplate complex such that further T6SS assembly/firing events are directed towards the site of injection. Such retaliatory firing events can also be triggered by T6SS injections from kin cells and are termed "duelling" (564).

As H1-T6SS activity is promoted by kin cell T6SS injection, we reasoned that the firing activity of the system would likely be increased when bacteria are grown on a surface where they are in contact with each other rather than in liquid media. To test this, we used a strain with fluorescent tagged sheath proteins (*tssB1:mScarlet-I*), that allows for assessment of T6SS dynamics at single cell resolution. To examine the sheath dynamics of *P. aeruginosa* growing on the surface at single cell resolution a set-up was used where bacteria are spotted on LB agar

pad, once the inoculum is dried, the agar pad is inverted onto a microscopy dish with cover-glass bottom. By further culturing this bacteria T6SS sheath dynamics of bacteria grown on surface can be assessed.

Figure 6.16 compares both H1- and H2-T6SS sheath abundance in liquid culture and bacteria grown on agar surface and an inverse effect is observable. A comparably much higher number of cells with TssB1-sfGFP sheath structures are seen when bacteria are grown on the surface. In case of TssB2-sfGFP sheaths, the opposite is the case, as reported by (547) bacteria sampled from liquid culture will often contain multiple H2-T6SS sheaths forming "zebra" like pattern. When the same bacterial strain was assessed in this study when bacteria was grown on agar surface as described above, only few of the bacteria assembled sheath structures. These observations confirm that increased cell-cell contact likely contributes to T6SS activity in case of retaliatory systems, as seen with H1-T6SS. The reasons behind relatively lower H2-T6SS activity are less obvious, but a possible explanation could be differences in the overall physiology and growth dynamics of bacteria on surface and liquid culture.

An additional factor to be considered for bacteria that grow on a surface is the extent of active intermixing that occurs and how this impacts firing dynamics of retaliatory T6SSs. Figure 6.16 illustrates a scenario, where H1-T6SS sheath firing is increasingly propagated if bacteria are motile and actively intermix with kin cells. Time series in Figure 6.16 captures a cluster of bacteria where initially no active H1-T6SS sheath assembly is observable, but some the cells appear to be actively moving on growth surface. At 79s mark a fluorescent foci can be observed indicating start of a T6SS sheath assembly within the cell highlighted in white. The sheath is fully assembled and a firing event towards cell in yellow has occurred at 85s mark, subsequently a "response" sheath assembly occurs in the cell in yellow and another T6SS sheath is reassembled in the initial "trigger" cell, while simultaneously both of these bacteria move relative to each other. At time point 125s bacteria in yellow can be seen to have "triggered" a response sheath assembly event in bacteria in blue, while at time point 159s cell in white appears to have triggered

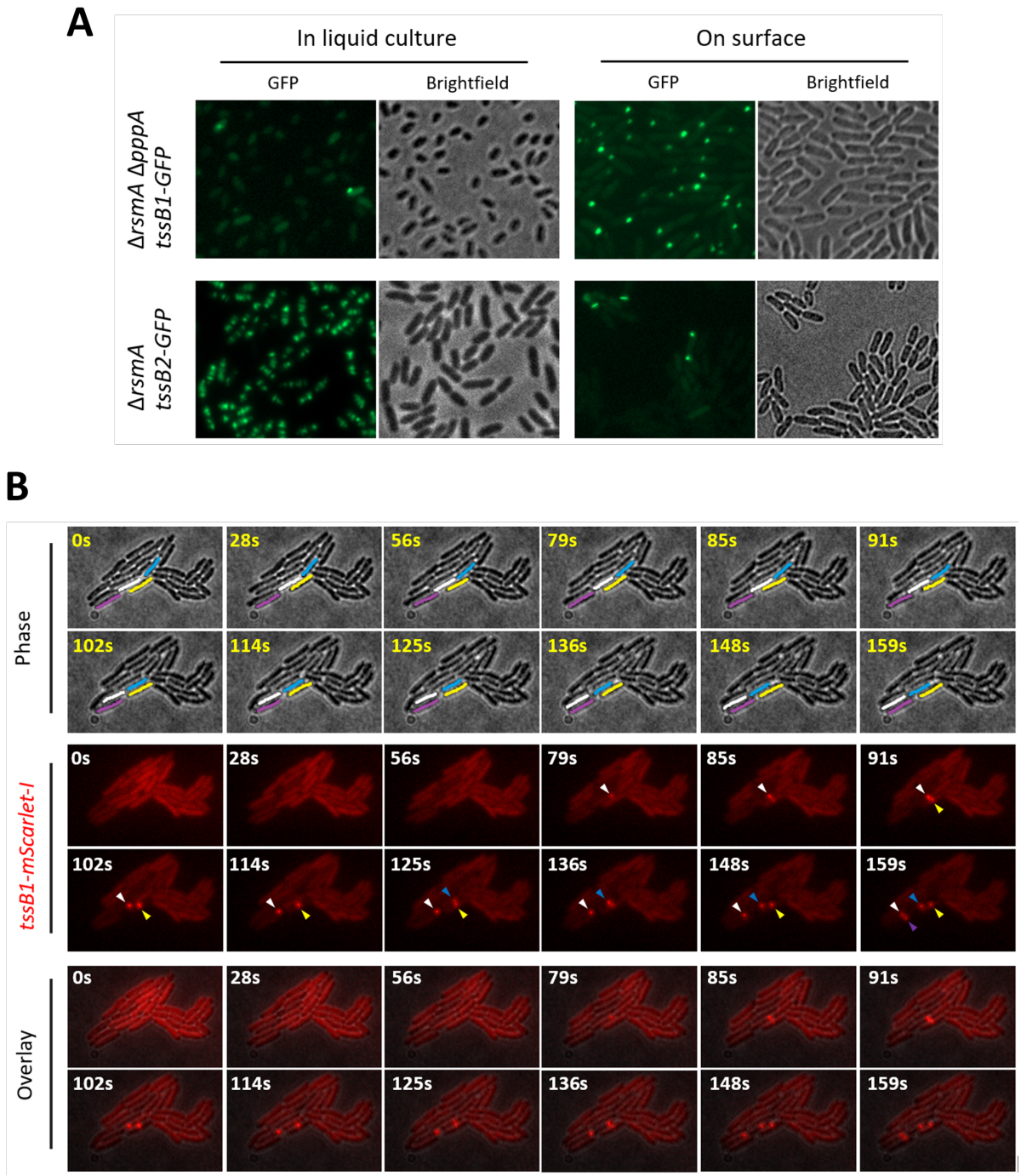

Figure 6.16: **Contact with kin cells and active intermixing promotes assembly and firing of H1-T6SS sheaths.** (**A**) H1-T6SS and H2-T6SS sheath abundance in compared between growth in liquid culture and on agar surface. H1-T6SS sheath abundance measured in Δ*rsmA*Δ*pppAtssB1:sfGFP* strain, grown on agar surface at 37^{o}C for 4h or in liquid culture until mid-exponential phase. H2-T6SS sheath abundance measured in Δ*rsmAtssB2:sfGFP* growing at 25^{o}C on surface for 4h or in liquid culture at 25^{o}C for 18h. (**B**) H1-T6SS sheath "duelling" dynamics over time in actively mixing bacterial cluster. Dynamics of sheath assembly in PAK Δ*retStssB1:mScarlet-I* strain grown for 3.5h at 37^{o}C on LB agar surface.

a response firing event from bacteria in purple. These time-lapse snapshots illustrate how in a scenario where bacteria are actively moving H1-T6SS sheath firing is propagated through the same mechanism that would lead to kin cell "duelling" in a static bacteria population. Overall this indicates that active bacterial intermixing contributes to propagation of active H1-T6SS firing within clonal populations of sister-cells.

6.2.4.4 Loss of T4P interferes with *P. aeruginosa* T6SS-dependent competition

As T6SS competition relies on an attacker being able to establish contact with toxin-sensitive prey bacteria, we decided to test how loss of ability to actively intermix and expand on surfaces impacts T6SS-mediated killing in a whole colony context. To do this, we chose to test the impact of the loss pili on both H1-T6SS-mediated and H2-T6SS-mediated competition using the most potent toxin from each of the systems, Tse5 and TseT. This competition was conducted using Δ*rsmA* strains as both Tse5 and TseT show a consistent ability to spatially restrict prey growth, while unlike Δ*retS* or Δ*rsmA*Δ*rsmN*, Δ*rsmA* colonies are not obviously aggregative and show only minor twitching impairments, thus providing an opportunity for the best differential between T4P+ and T4P- competition. In case of T4P+ strains, growth of TseT-sensitive bacteria was entirely restricted in colonies with high density inoculum, i.e. OD_{600}= 1.0 or 0.1, while at lower densities small amounts of prey were present in the colony central region (Figure 6.17 A). In contrast, in competition between two T4P- prey and attacker strains, TseT-sensitised bacteria were detectable in colonies with higher inoculum density. In cases of competition at low inoculum densities, i.e. OD_{600}= 0.001 or 0.01, where prey bacteria have an opportunity to establish before encountering population delivering TseT, competition using T4P- strains shows little to no spatial restriction, while within T4P+ strain context prey growth is readily restricted. In context of Tse5-mediated competition similar observations can be made, at comparable inoculum densities colonies consisting of T4P+ strains appear to be more conducive to T6SS-dependent sensitive prey growth restriction than comparable T4P- communities (Figure 6.17 B). Clear Tse5-

mediated killing is observable at all inoculum densities in T4P+ colonies, while Tse5 delivery appears to have only minor effect in T4P- context. This indicates that ability to actively intermix using T4P is contributing to *P. aeruginosa* contact mediated killing proficiency and is used to at least in part overcome the defence provided by spatial segregation resulting from prior establishment.

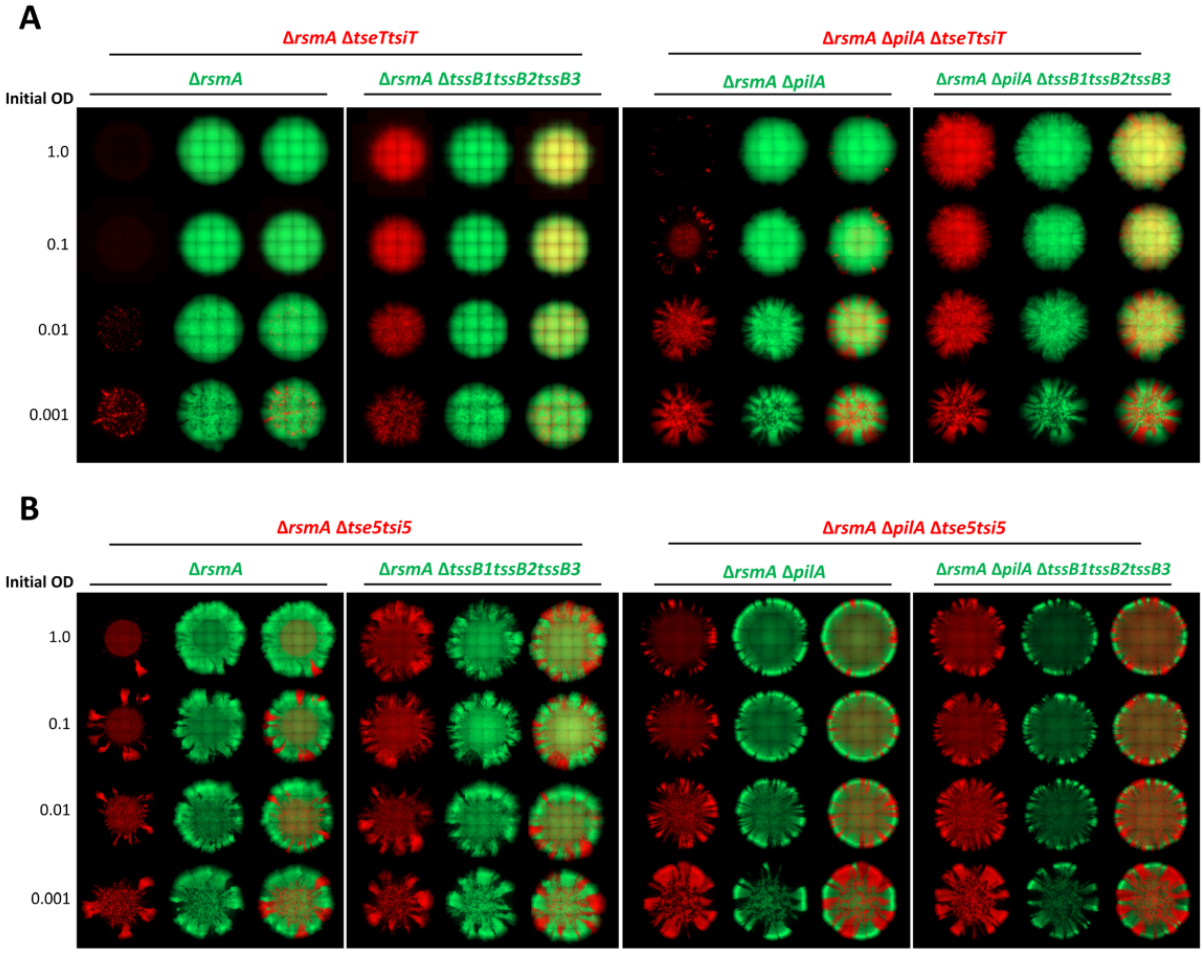

Figure 6.17: **Loss of T4P negatively impacts *P. aeruginosa* T6SS-mediated killing.** Assessing effectiveness of H1-T6SS (**A**) and H2-T6SS (**B**) toxin mediated killing in mixed macrocolony communities made up of off T4P+ ($\Delta rsmA$) and T4P- ($\Delta rsmA$ $\Delta pilA$). Prey bacteria sensitised to TseT ($\Delta rsmA \Delta tseTtsiT$) (**A**) or Tse5 ($\Delta rsmA \Delta tse5tsi5$) (**B**) in tagged with mCherry (red) and attacker population with sfGFP (green) fluorophores. Both single fluorescent channel and corresponding composite images. For both (**A**) and (**B**) bacteria were mixed at 1 to 1 ratio and after adjusting inoculum density (OD_{600} = 1.0; 0.1; 0.01; 0.001) spotted on LB agar, images of whole macrocolonies taken after 48h incubation at 25^{o}C for TseT competition and 37^{o}C for Tse5 competition. Showing 1 of 1 test images for panel **A** and panel **B** pili mutant strain competition. Showing representative images of 3 biological replicates for the $\Delta rsmA \Delta tse5tsi5$ prey competition.

6.2.4.5 Toxin sensitive prey strains use T4P to escape immobile attacker population

The loss of T4P is detrimental to the *P. aeruginosa* ability to eliminate T6SS sensitive prey in an otherwise isogenic context (Figure 6.17). Strains lacking *pilA* form smaller colonies, indicating that the impairment in surface motility interferes with the expansion of the population on the rigid surface of agar specifically (Figure 6.15), as this strain remains able to expand proficiently on surfaces under swarming conditions (Figure 6.13 C). In mixed colonies containing both T4P+ and T4P- strains, bacteria lacking T4P are present in the inoculum region and the laterally expanding colony edge is exclusively occupied by T4P+ strains and the overall size of the colony is comparable to T4P+ colonies (Figure 6.15). This sub-population distribution is consistent with the observation that T4P are likely the primary *P. aeruginosa* mode of active expansion within the context of macrocolony assay as only the motile (T4P+) populations are able to expand in the outer colony regions.

Within a mixed community containing both T4P+ and T4P- strains these sub-populations appear to spatially segregate (Figure 6.15), therefore we tested how this reduction in sub-population intermixing impacts *P. aeruginosa* T6SS-mediated killing. For this we chose two H1-T6SS toxins, Tse3 and Tse5, as well as two H2-T6SS toxins, PldB and TseT, using this approach we were able to test the impact of toxins of different potency, as delivered by two different systems in competition that occurs in distinct growth conditions. A similar scenario emerges independently of the toxin used or the T6SS system delivering it, when the mixed colony is made up of pili defective prey and attacker strains, prey growth appears to be less restricted than in cases of T4P+ competitors (Figure 6.18). If T4P- toxin sensitive bacteria are grown in presence of T4P+ attacker population, T6SS-dependent growth restriction is observable. In both PldB and TseT mediated competition, T4P- prey grown in presence of T4P+ attacker is almost entirely eliminated, with the exception being that the prey bacteria appear to survive at the very edge of the inoculum spot (Figure 6.18 C and D). It is known that as a result of the

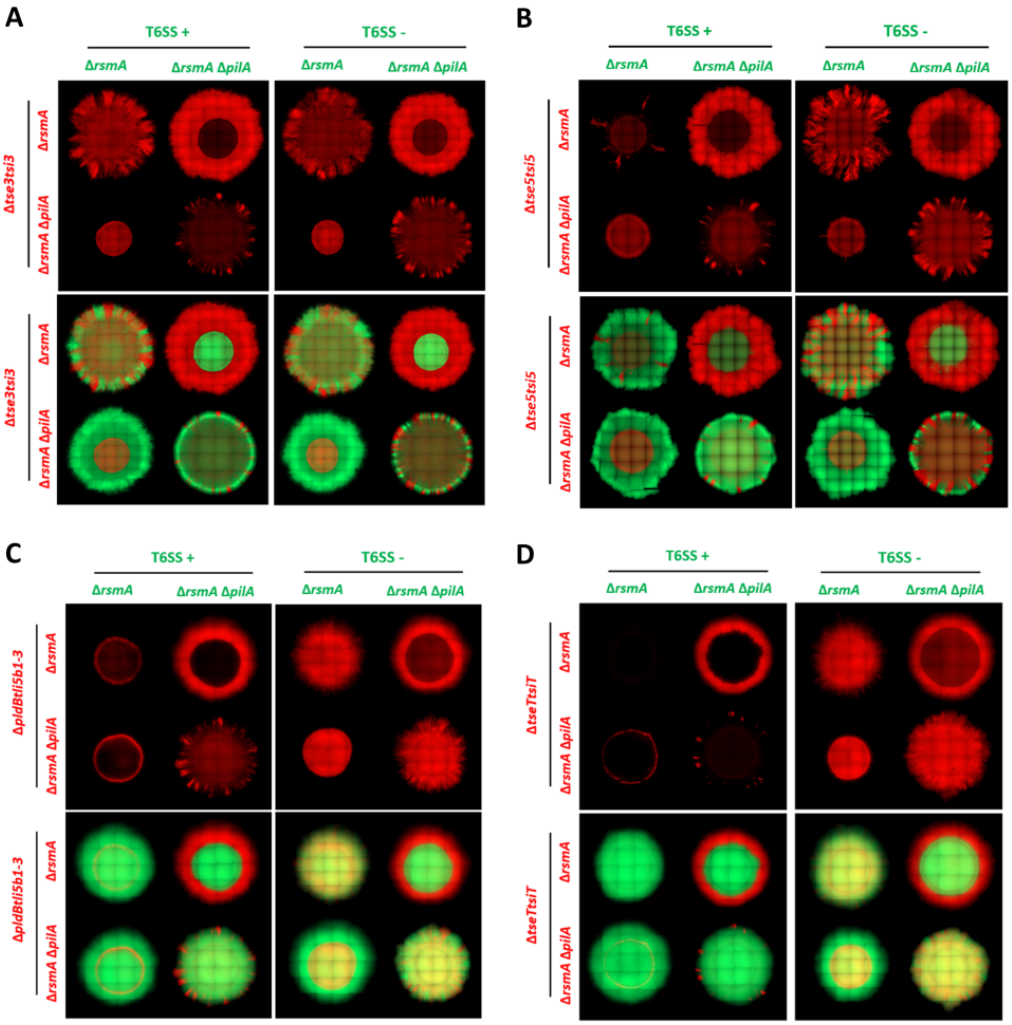

Figure 6.18: **Toxin sensitive prey bacteria can escape H1- and H2-T6SS attack using type IV pili.**
Images of mixed macrocolonies of strains sensitised to Tse3 (Δ*rsmA* Δ*tse3tsi3*) (**A**), Tse5 (Δ*rsmA* Δ*tse5tsi5*) (**B**), PldB (Δ*rsmA* Δ*pldBtli5b*$_{1-3}$) (**C**), or TseT Δ*rsmA* Δ*tseTtsiT* (**D**) toxins in red (mCherry). In competition with T6SS+ (Δ*rsmA*) and T6SS- (Δ*rsmA* Δ*tssB1* Δ*tssB2* Δ*tssB3*) parental strains with and without functional T4P aiming to asses impact of T4P in otherwise isogenic individual T6SS toxin mediated competition. Each of the panels contains individual red channel images showing toxin sensitive prey distribution in presence of T6SS+ (left) or T6SS- (right) attacker strain in the upper two rows. Corresponding overlay images showing distribution of both toxin sensitive prey (red) and T6SS attacker population in green (sfGFP) shown in the lower two rows. Attacker populations with active T6SS (Δ*rsmA*) used in competition shown on the left and T6SS- (Δ*rsmA* Δ*tssB1* Δ*tssB2* Δ*tssB3*) on the right. Each of the four image panels contains mixes of T4P+ and T4P- (Δ*pilA*) strains, with T4P+ prey in the upper lane and T4P- upper in the lower lane, while mixes in the first column contain T4P+ attacker strains and mixes in the second column contain T4P- strains. Bacterial inoculum mixes of OD_{600}=1.0 used in competition set-up. H1-T6SS toxin (Tse3 and Tse5) mediated competition conducted on LB with 2.0% (w/v) agar at 37^{o}C for 48h, while H2-T6SS toxin (PldB and TseT) mediated competition conducted on LB with 1.2% (w/v) agar at 25^{o}C for 48h. 1 of 1 colony test images shown for the mixed colonies containing T4P- strains, consistent relative fluorescent channel brightness within image sets, while colonies shown are not to scale.

microfluidics phenomenon termed “coffee ring effect” bacteria aggregate at the edge of a fluid droplet (749, 702), therefore a possible explanation for prey survival at the edge of inoculum spot seen here is that the T4P+ cells remain unable to intermix with a dense non-motile T4P- population and this results in subsequent failure to eliminate sensitive bacteria.

When evaluating the contribution of T4P within mixed macrocolonies of bacteria interacting through T6SS, the most striking outcome can be observed when T4P+ toxin sensitive prey strain is mixed with T4P- attacker population (Figure 6.18). T4P-defective attacker populations ($\Delta rsmA$ $\Delta pilA$) remain capable of eliminating prey in the colony central region to the same or potentially slightly higher extent than their T4P+ counterparts (Figure 6.18), but toxin sensitive prey is able to escape and grow in the colony outer edge to the same extent as in absence of T6SS-mediated attack. The T4P-mediated escape from prey occurs even in the case of highly effective toxins, such as illustrated by $\Delta rsmA\Delta tseTtsiT$ prey growth in presence of $\Delta rsmA\Delta pilA$ attacker population. These experimental observations position T4P as a complementary tool in *P. aeruginosa* contact-based competition, where the ability to actively intermix and form contacts between prey-attacker populations aids attacking bacteria, while prey bacteria population benefits from ability to "run away" from an attacker that is slower to expand.

6.3 Discussion

6.3.1 Gac-Rsm cascade modulates gradual changes in whole community structure

T6SS is only one of many tools that *P. aeruginosa* uses to compete for existence within a niche. The use of T6SS for host interactions, bacterial competition, or nutrient acquisition is part of a far broader lifestyle shift. *P. aeruginosa* possesses 3 T6SS systems and, rather than constitutively expressed and assembled, each of these systems is activated under specific conditions. As explored in chapters 3 and 4, all three T6SSs are under the control of the Gac-Rsm regulatory cascade, and disruption of network functionality results in a graduated increase in T6SS activation. In chapter 5 we show how this translates into what could be considered a dose-response in increased competitive fitness (Figure 5.18). Although *P. aeruginosa* T6SS is under the control of the Gac-Rsm cascade, this cascade is in no way specific for regulation of T6SS alone. Gac-Rsm cascade together with c-di-GMP-mediated regulation introduces what has been characterised as planktonic/biofilm lifestyle switch involving changes in the expression of virulence factors, motility devices, LPS, and extracellular matrix substances (100, 1). Similarly, as disruption in Gac-Rsm cascade results in gradual elevation in T6SS expression and activity, here we see that these same strains appear to display incremented phenotypic variation in motility and aggregation (Figure 6.13) leading to communities made up of these strains differing in lineage organisation within communities and overall aggregation (Figure 6.9). When evaluating the impact of T6SS-mediated interactions in *P. aeruginosa* it becomes increasingly important to consider what compounding effects influence the competition for space. The previous sections have addressed the specifics of modulation of T6SS firing and the contribution of various toxins; here, broader T6SS-nonspecific competition aspects are considered.

We consider how changes in the composition of the founding community affect T6SS-

mediated competition. We comprehensively assess how prior establishment provides protection to toxin-sensitive prey populations and to what extent this can be overcome by active intermixing. Additionally, this study is the first demonstration of how T4P-mediated motility aids in contact-based prey killing and how the use of twitching motility allows for sensitive prey escape even in cases of highly efficient killing.

6.3.2 Local contact assortment is a key determinant of population level competitive success

T6SS-mediated bacterial competition is contact-dependent, as bacterial killing relies on toxic effectors being injected directly into adjacently located competitors. The ability to deliver presumably ready-to-function protein effectors directly to the site of action positions T6SS as a highly efficient weapon. At the same time, this aspect of the system functionality makes T6SS-mediated competition vulnerable to simple and ubiquitous defence - protection through spatial separation (650). Not only competition through use of T6SS, but all highly local interactions are dependent on the lineage distribution within communities and sub-population prior establishment.

Here, through the use of both theoretical simulation and experimental mixed macrocolony assay, we have demonstrated how aspects such as increased local contact assortment are a key contributor in T6SS-mediated killing. As seen both by increasing inoculum density and modulating the competitor ratio within the mix, the most effective T6SS toxin-mediated prey growth restriction is observable when the maximum number of sensitive cells are directly exposed to the attacker population (Figure 6.5 and 6.7). Although perhaps it is unsurprising to observe that the success of highly local competition is reliant on establishing inter-population contacts, it does emphasise that bacterial competitive success within complex communities is likely dependent not only on use of efficacious direct competition tools, but also on many compounding factors. One of the biggest challenges for T6SS-dependent niche takeover is overcoming prior

establishment, as T6SS proficient bacterial species has to make direct contact with resident flora for killing to occur. If sensitive prey bacteria is present in sufficient amounts, the fraction of population directly exposed to attack may act as a shield preventing the killing of others. Protection from T6SS through spatial separation has also been previously observed in both cases of T6SS (687, 695) and CDI mediated competition (774, 683). This emphasises the importance of using highly lytic toxins that enable effective removal of dead competitor cells accumulated (684). A mechanism known to contribute to protection through spatial separation is production of EPS. The presence of EPS has long been known to protect bacteria within biofilm community from external biotic and abiotic stresses (259, 1), but is also emerging as a non-immunity protective tool against T6SS attacks (650).

6.3.3 EPS impact on *P. aeruginosa* community structure and T6SS-mediated interactions

A defining feature of biofilm communities is the presence of extracellular matrix (ECM) that contains not only EPS, but also eDNA and extracellular proteins. ECM provides an overall structural support allowing for development of microbial communities and encases the bacteria found in the community providing protection from the environment. This also results in increased biomass and bulk within the extracellular space, and as direct cell-cell contact is disrupted, this has the potential to interfere with T6SS needle injections. As EPS is a major component of ECM, impact of this on T6SS-mediated inter-bacterial competition has been addressed in multiple prior studies. The protective role of EPS in the case of T6SS-mediated attacks was first studied in *Vibrio cholerae* where Vibrio PolySaccharide (VPS) provides protection from exogenous and near-isogenous T6SS attackers, without interfering with the VPS producers ability to compete using T6SS (264). It was proposed that the protection is a result of the surrounding capsule-like barrier formed by the VPS (775, 776). A more recent study has also identified the ECM protein RmbA as having a similar protective function within

V. cholerae biofilms (763). Another case of immunity-independent T6SS protection is seen in *E. coli*, where *V. cholerae* T6SS toxin injection induced expression of both osmotic-response genes and promoted synthesis of colanic acid capsule (650). If the protection provided by EPS is simply the result of spatial separation, bacterial genera known for the production of protective EPS capsules such as *Klebsiella* (777), are of interest. Unlike most EPS seen in *Pseudomonas* or *Vibrio* species, *Klebsiella* capsule consists of dense, surface attached polysaccharide layer that provides spatial separation and therefore poses a somewhat obvious problem for contact-based interactions. *Klebsiella* capsule it is known to interfere with immune complement binding and prevent *Klebsiella pneumoniae* infection clearance (778). The presence of capsule polysacharides has recently been shown to protect gut commensal *Klebsiella* species from exogenous T6SS attacks (560). Unlike in the case where self-produced EPS interferes with *Campylobacter jejuni* T6SS injection into red blood cells (657), *Klebsiella sp.* and, same as other capsular polysaccharide producing bacteria such as *Acinetobacter sp.* or *Burkholderia sp.*, remain amongst T6SS proficient bacteria (779, 780, 781, 782, 27, 783). This shows that formation of EPS barrier surrounding a cell, even what appears to be a formidable one as in case of *Klebsiella* capsule, does not exclude bacteria from participation in contact-mediated interactions with its surroundings, and therefore mechanism behind EPS interference with T6SS is likely somewhat more complex.

In case of *P. aeruginosa*, where EPS and T6SS production is co-regulated, increased presence of EPS seems to in no way interfere with contact-mediated competition, instead these strains are increasingly proficient T6SS killers. In *P. aeruginosa* PAO1, the two dominant exopolysaccharides are Pel and Psl, whose expression is under direct control of Gac-Rsm cascade. In the chapter 5 we showed how mutations in Gac-Rsm cascade result in graduated modulation in T6SS activity and killing effectiveness, here we show how these same regulatory mutations lead to graduated changes in community organisation even in absence of T6SS competition (Figure 6.9). We observed an impact on community organisation, within the mixed macrocolony competition setup where strains lacking EPS were able to occupy a comparatively larger area. Notably,

this loss of EPS failed to translate in any consistent and meaningful impact on T6SS-mediated competition (Figures 6.11 and 6.12). As the interplay between T6SS-mediated interactions and presence of EPS appears to be widespread in other species, this was likely a result of the nature of these exoploysaccharides. Therefore, the question comes down to how exactly EPS affects the local bacterial community structure. Rather than simply resulting in bulk within the extracellular space, *P. aeruginosa* Pel and Psl aid in cell-cell cohesion, that is likely to result in closer packing at local scale and aggregation at whole colony level. At a level of individual bacteria EPS aid in cell-cell adhesion, while at a level of whole bacterial communities, acting together with eDNA and extracellular proteins, EPS provides mechanical support enabling formation of complex mature biofilm structures (784, 246, 259, 328). Therefore, as much as loss of EPS could reduce the amount of physical barriers that have a potential to interfere with T6SS needles in the inter-cellular space, EPS- bacteria will not be necessarily packed closer as a result of decrease in the specific cell-cell adhesion, and this may have additional implications on bacterial motility (211).

6.3.4 T4P in *P. aeruginosa* communities - attachment, intermixing and escape

As discussed in more detail in section 1.3.3, specific cell-cell adhesion is a requisite component for killing using contact-dependent killing (CDI) (785). But it stands to reason that both specific and more general adhesion would impact any bacterial interactions reliant on close contact, this includes T6SS. *Myxococcus xanthus* possesses T6SS-associated antennae-like structures that have been proposed to function in specific target binding through a mechanism resembling phage binding specific receptor proteins (786). A study that engineered T6SS to effectively kill in liquid culture took an approach of adding surface nanobodies that allowed T6SS+ bacteria to adhere to specific target cells in a manner resembling CDI (787). An example of naturally occurring specific attachment aiding in T6SS-mediated killing has been identified in *Vibrio fischeri*, where

a T6SS-associated lipoprotein TasL promotes cell-cell attachment (788). Increased adhesion is likely to result in higher number of close and prolonged contacts between adjacent bacteria, and its somewhat apparent how this would aid in contact-dependent competition. No specific adhesion mechanisms have been associated with *P. aeruginosa* T6SSs, but the contributions of generic cell-cell adhesion and aggregation mechanisms is of interest in this study.

Cell-cell adhesion within the context of *P. aeruginosa* biofilms is mediated through multiple mechanisms, including EPS components, extracellular matrix proteins, such as CdrA that links Psl strands, or T4P-mediated direct cell-cell attachment (211, 789, 326). The role of EPS is addressed above, while of specific interest here is T4P, a tool that bacteria use both for cell-cell adhesion and surface-based motility, as both directly impact community structure at local and global scale. T4P have been shown to be responsible for directed *P. aeruginosa* surface motility towards and intermixing with *Staphylococcus aureus* (218). Here we observed that loss of T4P resulted in bacteria growing in monoclonal clusters at single cell scale, while increase in local mixing was observable in a bacterial lawn formed by T4P+ lineages (Figure 6.14). Motility within community leads to lineage intermixing and this results with more individual bacteria transiently exposed to interspecies contacts, providing more potential opportunities to deliver a toxins through T6SS injection. A key characteristic of H1-T6SS is repeated retaliatory firing and often rapid and repeated T6SS sheath reassembly (564). This has been shown to be a favourable competitive strategy (576) and a consequence of inter-population contacts being transient limits opportunities for repeated T6SS injection. Our near isogenic mixed colony experimental setup is well suited to address how specific mechanistic changes impact the overall competitive outcomes. When comparing T6SS toxin-mediated killing in mixed macrocolonies, loss of T4P results in improved prey population survival (Figure 6.17). This leads to a conclusion that in the case of *P. aeruginosa*, ability to actively intermix and establish contacts with prey population is a key component of T6SS-dependent competitive success.

Here we observed *pilA* mutants at both single cell and whole colony scale, concluding that

T4P aid in strain intermixing in isogenic context (Figure 6.14 and 6.15). Furthermore when T4P+ and T4P- strains are co-cultured spatial segregation of the two bacterial populations occurs, with only T4P+ population being able to successfully expand on growth surface. This is somewhat unusual as a similar study assessing impact of T4P on sub-population distribution in whole mixed colonies focusing on another bacterial species *Neisseria gonorrhoeae* shows the opposite effect. In a mix of T4P+ and T4P- strains, *N. gonorrhoeae* lacking pili are found in the colony outer region (768). This has been attributed to a somewhat ubiquitous adhesion-based sorting mechanism resulting in phase separation (769). In the case of *N. gonorrhoeae* loss of pili results in reduced adhesion and T4P- sub-population is expelled to the outer colony edge (768). A previous study looking at T4P contribution to *P. aeruginosa* swarming has also noted that in a mix of T4P+ and T4P- bacteria, the strains lacking pili are preferentially found at the leading edge of a swarming population (180). Altogether it appears that both presence of T4P and specific growth conditions play a role in determining sub-population distribution within a bacterial community and within mixed macrocolonies T4P are a motility device used for lateral expansion.

Within mixed community containing both T4P+ and T4P- strains sub-populations appear to spatially segregate, therefore we tested how this reduction in sub-population intermixing impacts T6SS-mediated killing in case of *P. aeruginosa* mixed colony setup. A previous study assessing T4P impact on *Neisseria cinerea* T6SS-mediated killing within whole colony context observed that in cells that lose T4P, this sub-population escaped otherwise proficient T6SS killing through adhesion-mediated sorting (767). In this study the opposite is observed (Figure 6.18), in a mix where T4P- prey sensitive to a T6SS effector is in presence of T6SS+ attacker, sensitive bacteria are almost entirely eliminated. The exception is that some of the prey bacteria appears to survive at the very edge of the inoculum spot, where bacteria aggregate at the edge of a fluid droplet due to a microfluidics phenomenon termed “coffee ring effect” (702), a possible explanation for prey survival here being the T4P+ cell inability to intermix with a dense T4P-

population and subsequently failing to eliminate the sensitive bacteria. In a mix where T4P+ toxins sensitive prey bacteria are in presence of T6SS+ attacker lacking T4P, the prey bacteria are eliminated from the colony central region, but able to expand and grow in the colony outer edge to the same extent as in absence of T6SS-mediated attack. This T4P-mediated impact on T6SS-dependent killing in *P. aeruginosa* also extends to H1-T6SS and this supports the idea that the effect observed here is likely mechanistic and universal rather than specific to the strain or even the type of contact based killing system used. The pili impact on *P. aeruginosa* T6SS-mediated interactions is consistent with T4P being used as a surface motility device. T4P are a complementary tool that an attacking population can use to actively intermix, this leading to a quantifiable improvement in T6SS killing. This study adds to the evidence of T4P being an important determinant of contact-mediated competition success, with preferential adhesion towards prey cells or surface being the factors determining population organisation within the community, with preferential aggregation or active expansion being the two fates for T4P+ bacteria populations. This choice between aggregation or motility also determines bacterial fate under contact-based attack, while motile prey bacteria appear to minimise interspecies contacts and escape T6SS attacks through segregation, with two underlying mechanisms being - prey "running" from a non-motile attacker or prey escaping through loss of T4P as the attacker cells are no longer able to "hold onto" susceptible prey.

6.3.5 Summary

Establishment of contact between prey and attacker population is a key component for effective T6SS-mediated competition success. Clearance of even highly vulnerable prey populations is challenging if enough of prey bacteria are already present. Alternatively, sensitive bacteria can survive when escaping through active motility. This also highlights that simple increase in T6SS attack frequency or use of set of diverse and potent toxins can in some scenarios be of little added benefit and use of complementary tools such as T4P to actively

intermix within communities is of importance. Naturally occurring microbial communities are highly complex and consist of tens or hundreds of species. Due to the high complexity of the these systems, the specific interactions occurring within these communities are often difficult to detangle. Systematic studies like this one offer an opportunity to focus on how specific aspects such as changes in local contact assortment or surface motility contribute to the overall community organisation and what are the consequences on direct bacterial competition. Work like this can be subsequently used to aid in interpretation of more complex interactions occurring in polymicrobial context.

Chapter 7

Discussion

There is a wide range of various ecological niches, and each is occupied by organisms adapted for existence within the particular conditions (352, 790). These ecological niches are rarely exclusively occupied by a single species, instead most microbes exist as a part of complex interacting polymicrobial communities (229, 791). *Pseudomonas aeruginosa* is a highly adaptive opportunistic pathogen able to shift its gene expression profile to adapt to a range of environmental conditions and actively compete for space and resources. This includes proficiency as a pathogen that is capable of causing both acute and chronic infections, while also not being constrained by exclusive existence in a narrow niche (1). *P. aeruginosa* possesses a range of complex molecular tools that enable this bacterium to take advantage of opportunities such as invading immunocompromised host niches and subsequently escaping clearance (26, 792). These tools include a range of virulence factors, protein secretion systems, motility devices, and many other mechanisms, such as iron acquisition via siderophores or molecules promoting biofilm formation (26). Ability to use specific tools when needed requires sensor and regulator networks, that enables bacteria to gather information about its environment and subsequently integrate this information to coordinate an appropriate response trough changing gene expression profile (100, 1). One of these tools in the Type VI secretion system (T6SS) that can be used for interactions with host, surrounding bacteria or to simply export proteins into extracellular

milieu. In this thesis we address how the activity of *P. aeruginosa* T6SS is modulated, and how this translates into different competitive outcomes. We conducted a comprehensive study of impact of individual T6SS effectors within context of competition in mixed macrocolonies and showed how the ability to intermix is a key predeterminant for T6SS-dependent competition outcomes.

7.1 Impact of regulatory network on T6SS expression and activity

The expression of *P. aeruginosa* T6SS has been associated with existence in biofilms. *P. aeruginosa* biofilm formation is subject of a range of regulators, two key ones being Gac-Rsm regulatory cascade and modulation of gene expression through c-di-GMP. c-di-GMP regulation is widespread across many bacterial genera and is commonly found to modulate a range of biological processes (102), in *P. aeruginosa* up-regulation of c-di-GMP production marks transition towards biofilm formation (746, 103). A study by (101) connected high intracellular c-di-GMP levels with down-regulation in virulence mediated through Type III secretion system (T3SS) and simultaneous up-regulation in expression of H1-T6SS. This and a subsequent study by (110) establishes the link between biofilms and high H1-T6SS expression. Here we expand on this by performing a preliminary analysis of c-di-GMP impact on both H1- and H2-T6SS activity and observe an inverse impact (Chapter 3). As expected, high c-di-GMP mutant strains show high H1-T6SS expression and activity, but subsequent drop in c-di-GMP levels appears to impact only the activity of the system while expression remains intact (Figure 3.4). Simultaneously, H2-T6SS expression and activity appears to be elevated in a low c-di-GMP regulatory context. This second observation was unexpected, as increased H2-T6SS expression was observed in strains that exhibited a low biofilm formation phenotype (Figure 3.6). In *P. aeruginosa* T6SS has been seen to be elevated under biofilm conditions (568, 101), but low c-di-GMP levels have been

shown to promote T6SS activity in other bacterial species such as *Agrobacterium tumefaciens*, *Pseudomonas putida* and *Pseudomonas fluorescens* (725, 727, 730).

These observations of c-di-GMP impact were made in strains that lack the sensory kinase RetS. RetS modulates the action of the Gac-Rsm regulatory pathway that is responsible for the transition between planktonic and biofilm-like gene expression profiles (166, 125). The regulatory impact of the Gac-Rsm cascade is exerted through the translational repressors RsmA and RsmN (123). RsmA/RsmN both directly and indirectly impact expression of genes encoding components for each of the three T6SSs (124, 122). Both RsmA and RetS have been previously shown to modulate T6SS expression and activity (723, 101), and unlike in the case of differential impact by c-di-GMP, expression of all three systems appear to be repressed by Gac-Rsm cascade. Here we assessed a set of strains with mutations in genes encoding Gac-Rsm pathway components and this enabled us to compile a strain set with gradually modulated T6SS activity levels. RsmA has been characterised as controlling the expression of all three T6SS clusters (723), while *in vivo* function of paralogue RsmN has been less well characterised. Here we were able to use promoter activity measurements to validate that in absence of RsmA, RsmN does repress all three of the T6SSs (Figures 4.3 and 4.4). We then further saw that graduated differences in promoter activity translate into graduated differences in protein expression and T6SS activity. We also note, that although strain with mutation in the gene encoding sensory kinase RetS show high T6SS activity, even further activity and corresponding improvement in the ability to kill sensitive bacteria is seen if both RsmA and RsmN are removed (Figures 4.6 and 5.18). Subsequently, this set of strains with modulated T6SS activity was used in a systematic evaluation of differential impact of toxins with entirely distinct biochemical activities.

7.2 T6SS toxins are the key determinants of the overall competitive success

The T6SS effectors dictate the impact of this molecular tool. Unlike many other simpler protein export systems that secrete cargo intro extracellular milieu, T6SS can be used to deliver effectors directly into adjacent cells (793). And the molecular makeup of the system enables for effector delivery to be indiscriminate, unlike in the case of systems such as CDI (794), no requirement for recognition of specific binding features on target cell surface exists, instead T6SS spear is topped by a spike that allows for puncture of target cell membrane and effector translocation. But unlike in the cases of tailocin impact (436), adjacent cell puncture by T6SS is not sufficient to deal damage 5.4. Instead, T6SS impact is entirely dependent on the type of effectors delivered. The effector proteins can have different impacts and encompass antibacterial, anti-eukaryotic or common good molecules (Figure 5.5). Additionally, T6SS modular makeup allows for an individual bacteria to encode and deliver a variety of effectors, with *P. aeruginosa* T6SSs delivering more than 20 effectors (Table 1.1).

Prior studies have focused on characterisation of individual T6SS effector biochemical activity or mode of delivery (Table 1.1), while studies such as the one conducted by (594) look at toxin differential impact depending on the growth conditions and changes in factors such as pH or osmolarity. Here we conducted a comprehensive investigation of how action of individual toxins shapes bacterial community structure. To assess a community-wide impact of T6SS toxins, we adapted a macrocolony imaging approach where two bacterial populations are mixed and competition of sub-populations can be evaluated (Figure 5.1). We observe that potency of T6SS effectors is highly variable, but in cases of pore forming toxins, such as Tse5, even delivery in low doses seen in *P. aeruginosa* PAO1 WT enables attacking population to restrict prey spatial expansion (Figure 5.5). In strains with higher T6SS activity, we see that most of the characterised T6SS effectors are able restrict prey bacteria expansion ($\Delta rsmA$), while a

near complete elimination of sensitive bacteria can only be achieved when the attacker's T6SS firing frequency is further elevated ($\Delta retS$ or $\Delta rsmA\Delta rsmN$). This is an important observation, as we show that an increase in the dose of toxin delivered directly translates into improved killing (Figures 5.18). It is also notable that some of the effectors, specifically peptidoglycan amidase Tse1 and tarnsamidosome targeting Tse8, acting individually do not appear to be effective against sensitised *P. aeruginosa* prey (Figure 5.5). But in case of Tse1 we note that this effector still contributes to the effector set as a whole, as combined use of Tse1 and Tse3 is more effective for sensitive bacteria growth restriction than individual toxins (Figure 5.7). Through the combined use of biophysical simulations and mixed macrocolony experiments, we also demonstrate that although an increase in the firing rate of T6SS contributes to improved competitiveness, the specific mode of action of the toxin is the main limiting factor in contact-based competition (Figures 5.17). This being in a general agreement with previous studies that emphasise importance of lytic toxins in competition reliant on cell-cell contact (684).

7.3 Active intermixing aids with effective T6SS killing

T6SS-dependent bacterial competition is reliant on the formation of direct contact between competing bacteria. Spatial separation of competitors due to prior establishment or emerging during competition has been demonstrated to aid in prey survival when exposed to an otherwise effective T6SS attack (701, 416, 683, 700). Through the use of biophysical simulations and experiments, we demonstrate that increased contact assortment promotes prey elimination (Figures 6.2, 6.5, and 6.7). Conversely, prior establishment reduces interspecies contact surface and allows for prey populations to persist even when exposed to attack by highly effective toxins (Figures 6.3 and 6.5). These observations emphasise the impact of specific community architecture on direct competition.

Since contact is an essential component of T6SS-dependent competition, factors that promote contact events may have a drastic impact on the competition outcome. We show that type IV

pili (T4P) that are known to contribute to both adhesion and surface motility (30), promote intermixing on both a single cell scale and at a whole population level (Figures 6.14 and 6.15). Notably, we see that loss of the ability to intermix using T4P is detrimental to the ability to kill using T6SS toxins (Figure 6.17). We extend this even further by assessing how T6SS-dependent killing in a mix of motile and non-motile bacteria and show that motile *P. aeruginosa* populations can escape T6SS attack by moving away from the attacking population (Figure 6.18). Although, T4P-dependent adhesion-mediated sorting has been demonstrated to interfere with T6SS-dependent competition in *Neisseria sp.* (767), in *P. aeruginosa* T4P impact appears to be a result of surface motility, rather than adhesion. Altogether it thus appears that presence/absence of T4P, specific growth conditions and T6SS-dependent effective competition play a role in determining sub-population distribution within a bacterial community and this may drastically vary from one bacterial species to another. This opens up questions for further investigation of how factors such as motility and adhesion impact not only community organisation but also T6SS-dependent competition outcomes in a polymicrobial context.

7.4 Conclusion

Every study model, both experimental and theoretical, is limited by the fact that only specific environmental conditions and a limited number of parameters can be considered. As such, making predictions on the outcome of a competition happening within complex host niches remains challenging. The best known *P. aeruginosa* infection scenario is within the context of cystic fibrosis lung, where it is a part of a polymicrobial community (795, 86). A notable aspect of *P. aeruginosa* pathogenesis is that once this bacterium invades the community, it is able persist for years and its presence appears to largely define how the community behaves overall (796, 1). The full complexity of natural communities is unlikely to be entirely recapitulated in minimal ecological systems used experimentally. However, experimental systems are well suited for evaluation of how mechanistic factors and individual molecular tolls influence

bacterial competition dynamics. Here, we took an approach of engineering a system that enables manipulation of T6SS activity to investigate how specific toxic effectors impact can change the overall community organisation and how complementary tools such as T4P impact competition outcome. We believe that recording the contribution of individual elements, and that is one major advance provided by studies as the one we conducted here, is essential for construction of large and comprehensive datasets. These can be used in conjunction with theoretical tools to gain further understanding of what rules govern the outcome of competition in polymicrobial context within natural niches. If the T6SS is a key machine in the resolution of microbial competition, genomic approaches showed that despite a broad distribution across phyla and species, there is no rule on who does or does not pose a T6SS (522). Trying to figure out the benefit for bacteria of having or not a T6SS would only make sense if we understand which toxins are delivered by these systems, and what are their impact on preys. Further studies should also assess the distribution of cell lineages within the three dimensions of a biofilm (763) which will further complexify the heterogeneity of the environment and how cells respond and adapt within the different layers of a biofilm. And expand by performing competition that includes other organisms that *P. aeruginosa* encounters within infection niche.

Bibliography

[1] M. F. Moradali, S. Ghods, and B. H. Rehm. Pseudomonas aeruginosa lifestyle: A paradigm for adaptation, survival, and persistence. *Front Cell Infect Microbiol*, 7:39, 2017. doi: 10.3389/fcimb.2017.00039.

[2] S. Crone, M. Vives-Florez, L. Kvich, A. M. Saunders, M. Malone, M. H. Nicolaisen, E. Martinez-Garcia, C. Rojas-Acosta, M. Catalina Gomez-Puerto, H. Calum, M. Whiteley, R. Kolter, and T. Bjarnsholt. The environmental occurrence of pseudomonas aeruginosa. *APMIS*, 128(3):220–231, 2020. doi: 10.1111/apm.13010.

[3] J. Klockgether, N. Cramer, L. Wiehlmann, C. F. Davenport, and B. Tummler. Pseudomonas aeruginosa genomic structure and diversity. *Front Microbiol*, 2:150, 2011. doi: 10.3389/fmicb.2011.00150.

[4] C. K. Stover, X. Q. Pham, A. L. Erwin, S. D. Mizoguchi, P. Warrener, M. J. Hickey, F. S. Brinkman, W. O. Hufnagle, D. J. Kowalik, M. Lagrou, R. L. Garber, L. Goltry, E. Tolentino, S. Westbrock-Wadman, Y. Yuan, L. L. Brody, S. N. Coulter, K. R. Folger, A. Kas, K. Larbig, R. Lim, K. Smith, D. Spencer, G. K. Wong, Z. Wu, I. T. Paulsen, J. Reizer, M. H. Saier, R. E. Hancock, S. Lory, and M. V. Olson. Complete genome sequence of pseudomonas aeruginosa pao1, an opportunistic pathogen. *Nature*, 406(6799): 959–64, 2000. doi: 10.1038/35023079.

[5] J. Labaer, Q. Qiu, A. Anumanthan, W. Mar, D. Zuo, T. V. Murthy, H. Taycher, A. Halleck, E. Hainsworth, S. Lory, and L. Brizuela. The pseudomonas aeruginosa pa01 gene collection. *Genome Res*, 14(10B):2190–200, 2004. doi: 10.1101/gr.2482804.

[6] A. Vasquez-Rifo, I. Veksler-Lublinsky, Z. Cheng, F. M. Ausubel, and V. Ambros. The pseudomonas aeruginosa accessory genome elements influence virulence towards caenorhabditis elegans. *Genome Biol*, 20(1):270, 2019. doi: 10.1186/s13059-019-1890-1.

[7] B. Valot, C. Guyeux, J. Y. Rolland, K. Mazouzi, X. Bertrand, and D. Hocquet. What it takes to be a pseudomonas aeruginosa? the core genome of the opportunistic pathogen updated. *PLoS One*, 10(5):e0126468, 2015. doi: 10.1371/journal.pone.0126468.

[8] E. Alm, K. Huang, and A. Arkin. The evolution of two-component systems in bacteria reveals different strategies for niche adaptation. *PLoS Comput Biol*, 2(11):e143, 2006. doi: 10.1371/journal.pcbi.0020143.

[9] Agnes Rodrigue, Yves Quentin, Andree Lazdunski, Vincent Mejean, and Maryline Foglino. Two-component systems in pseudomonas aeruginosa: why so many? *RENDS IN MICROBIOLOGY*, 8(11):498–504, 2000.

[10] J. Trouillon, L. Imbert, A. M. Villard, T. Vernet, I. Attree, and S. Elsen. Determination of the two-component systems regulatory network reveals core and accessory regulations across pseudomonas aeruginosa lineages. *Nucleic Acids Res*, 49(20):11476–11490, 2021. doi: 10.1093/nar/gkab928.

[11] E. Potvin, F. Sanschagrin, and R. C. Levesque. Sigma factors in pseudomonas aeruginosa. *FEMS Microbiol Rev*, 32(1):38–55, 2008. doi: 10.1111/j.1574-6976.2007.00092.x.

[12] S. Schulz, D. Eckweiler, A. Bielecka, T. Nicolai, R. Franke, A. Dotsch, K. Hornischer, S. Bruchmann, J. Duvel, and S. Haussler. Elucidation of sigma factor-associated networks in pseudomonas aeruginosa reveals a modular architecture with limited and function-specific crosstalk. *PLoS Pathog*, 11(3):e1004744, 2015. doi: 10.1371/journal.ppat.1004744.

[13] T. Wang, W. Sun, L. Fan, C. Hua, N. Wu, S. Fan, J. Zhang, X. Deng, and J. Yan. An atlas of the binding specificities of transcription factors in pseudomonas aeruginosa directs prediction of novel regulators in virulence. *Elife*, 10, 2021. doi: 10.7554/eLife.61885.

[14] M. Gomez-Lozano, R. L. Marvig, C. Molina-Santiago, P. M. Tribelli, J. L. Ramos, and S. Molin. Diversity of small rnas expressed in pseudomonas species. *Environ Microbiol Rep*, 7(2):227–36, 2015. doi: 10.1111/1758-2229.12233.

[15] D. M. P. De Oliveira, B. M. Forde, T. J. Kidd, P. N. A. Harris, M. A. Schembri, S. A. Beatson, D. L. Paterson, and M. J. Walker. Antimicrobial resistance in eskape pathogens. *Clin Microbiol Rev*, 33(3), 2020. doi: 10.1128/CMR.00181-19.

[16] S. S. Magill, J. R. Edwards, W. Bamberg, Z. G. Beldavs, G. Dumyati, M. A. Kainer, R. Lynfield, M. Maloney, L. McAllister-Hollod, J. Nadle, S. M. Ray, D. L. Thompson, L. E. Wilson, S. K. Fridkin, Infections Emerging Infections Program Healthcare-Associated, and Team Antimicrobial Use Prevalence Survey. Multistate point-prevalence survey of health care-associated infections. *N Engl J Med*, 370(13):1198–208, 2014. doi: 10.1056/NEJMoa1306801.

[17] D. Reynolds and M. Kollef. The epidemiology and pathogenesis and treatment of pseudomonas aeruginosa infections: An update. *Drugs*, 81(18):2117–2131, 2021. doi: 10.1007/s40265-021-01635-6.

[18] L. Cuthbertson, A. W. Walker, A. E. Oliver, G. B. Rogers, D. W. Rivett, T. H. Hampton, A. Ashare, J. S. Elborn, A. De Soyza, M. P. Carroll, L. R. Hoffman, C. Lanyon, S. M. Moskowitz, G. A. O'Toole, J. Parkhill, P. J. Planet, C. C. Teneback, M. M. Tunney, J. B. Zuckerman, K. D. Bruce, and C. J. van der Gast. Lung function and microbiota diversity in cystic fibrosis. *Microbiome*, 8(1):45, 2020. doi: 10.1186/s40168-020-00810-3.

[19] S. Fischer, J. Klockgether, M. Gonzalez Sorribes, M. Dorda, L. Wiehlmann, and B. Tummler. Sequence diversity of the pseudomonas aeruginosa population in loci that

undergo microevolution in cystic fibrosis airways. *Access Microbiol*, 3(12):000286, 2021. doi: 10.1099/acmi.0.000286.

[20] J. E. Pittman, E. H. Calloway, M. Kiser, J. Yeatts, S. D. Davis, M. L. Drumm, M. S. Schechter, M. W. Leigh, M. Emond, A. Van Rie, and M. R. Knowles. Age of pseudomonas aeruginosa acquisition and subsequent severity of cystic fibrosis lung disease. *Pediatr Pulmonol*, 46(5):497–504, 2011. doi: 10.1002/ppul.21397.

[21] M. I. Metzger, S. Y. Graeber, M. Stahl, O. Sommerburg, M. A. Mall, A. H. Dalpke, and S. Boutin. A volatile and dynamic longitudinal microbiome is associated with less reduction in lung function in adolescents with cystic fibrosis. *Front Cell Infect Microbiol*, 11:763121, 2021. doi: 10.3389/fcimb.2021.763121.

[22] N. Acosta, B. Waddell, A. Heirali, R. Somayaji, M. G. Surette, M. L. Workentine, H. R. Rabin, and M. D. Parkins. Cystic fibrosis patients infected with epidemic pseudomonas aeruginosa strains have unique microbial communities. *Front Cell Infect Microbiol*, 10: 173, 2020. doi: 10.3389/fcimb.2020.00173.

[23] P. Karami, P. Mohajeri, R. Yousefi Mashouf, M. Karami, M. H. Yaghoobi, D. Dastan, and M. Y. Alikhani. Molecular characterization of clinical and environmental pseudomonas aeruginosa isolated in a burn center. *Saudi J Biol Sci*, 26(7):1731–1736, 2019. doi: 10.1016/j.sjbs.2018.07.009.

[24] M. Garcia-Clemente, D. de la Rosa, L. Maiz, R. Giron, M. Blanco, C. Olveira, R. Canton, and M. A. Martinez-Garcia. Impact of pseudomonas aeruginosa infection on patients with chronic inflammatory airway diseases. *J Clin Med*, 9(12), 2020. doi: 10.3390/jcm9123800.

[25] S. Reig, A. Le Gouellec, and S. Bleves. What is new in the anti-pseudomonas aeruginosa clinical development pipeline since the 2017 who alert? *Front Cell Infect Microbiol*, 12: 909731, 2022. doi: 10.3389/fcimb.2022.909731.

[26] I. Jurado-Martin, M. Sainz-Mejias, and S. McClean. Pseudomonas aeruginosa: An audacious pathogen with an adaptable arsenal of virulence factors. *Int J Mol Sci*, 22 (6), 2021. doi: 10.3390/ijms22063128.

[27] C. Liao, X. Huang, Q. Wang, D. Yao, and W. Lu. Virulence factors of pseudomonas aeruginosa and antivirulence strategies to combat its drug resistance. *Front Cell Infect Microbiol*, 12:926758, 2022. doi: 10.3389/fcimb.2022.926758.

[28] S. M. Huszczynski, J. S. Lam, and C. M. Khursigara. The role of pseudomonas aeruginosa lipopolysaccharide in bacterial pathogenesis and physiology. *Pathogens*, 9(1), 2019. doi: 10.3390/pathogens9010006.

[29] J. Haiko and B. Westerlund-Wikstrom. The role of the bacterial flagellum in adhesion and virulence. *Biology (Basel)*, 2(4):1242–67, 2013. doi: 10.3390/biology2041242.

[30] L. L. Burrows. Pseudomonas aeruginosa twitching motility: type iv pili in action. *Annu Rev Microbiol*, 66:493–520, 2012. doi: 10.1146/annurev-micro-092611-150055.

[31] Q. Duan, M. Zhou, L. Zhu, and G. Zhu. Flagella and bacterial pathogenicity. *J Basic Microbiol*, 53(1):1–8, 2013. doi: 10.1002/jobm.201100335.

[32] M. Garcia, E. Morello, J. Garnier, C. Barrault, M. Garnier, C. Burucoa, J. C. Lecron, M. Si-Tahar, F. X. Bernard, and C. Bodet. Pseudomonas aeruginosa flagellum is critical for invasion, cutaneous persistence and induction of inflammatory response of skin epidermis. *Virulence*, 9(1):1163–1175, 2018. doi: 10.1080/21505594.2018.1480830.

[33] A. R. Hauser. The type iii secretion system of pseudomonas aeruginosa: infection by injection. *Nat Rev Microbiol*, 7(9):654–65, 2009. doi: 10.1038/nrmicro2199.

[34] H. Selim, T. E. E. Radwan, and A. M. Reyad. Regulation of t3ss synthesis, assembly and secretion in pseudomonas aeruginosa. *Arch Microbiol*, 204(8):468, 2022. doi: 10.1007/s00203-022-03068-5.

[35] S. M. Rangel, L. K. Logan, and A. R. Hauser. The adp-ribosyltransferase domain of the effector protein exos inhibits phagocytosis of pseudomonas aeruginosa during pneumonia. *mBio*, 5(3):e01080–14, 2014. doi: 10.1128/mBio.01080-14.

[36] D. M. Foulkes, K. McLean, A. S. Haneef, D. G. Fernig, C. Winstanley, N. Berry, and S. B. Kaye. Pseudomonas aeruginosa toxin exou as a therapeutic target in the treatment of bacterial infections. *Microorganisms*, 7(12), 2019. doi: 10.3390/microorganisms7120707.

[37] M. Jain, D. Ramirez, R. Seshadri, J. F. Cullina, C. A. Powers, G. S. Schulert, M. Bar-Meir, C. L. Sullivan, S. A. McColley, and A. R. Hauser. Type iii secretion phenotypes of pseudomonas aeruginosa strains change during infection of individuals with cystic fibrosis. *J Clin Microbiol*, 42(11):5229–37, 2004. doi: 10.1128/JCM.42.11.5229-5237.2004.

[38] Edsnf Sarges, Y. C. Rodrigues, I. P. Furlaneto, M. V. H. de Melo, Gldc Brabo, K. C. M. Lopes, Ajpg Quaresma, Lngc Lima, and K. V. B. Lima. Pseudomonas aeruginosa type iii secretion system virulotypes and their association with clinical features of cystic fibrosis patients. *Infect Drug Resist*, 13:3771–3781, 2020. doi: 10.2147/IDR.S273759.

[39] J. Monjaras Feria and M. A. Valvano. An overview of anti-eukaryotic t6ss effectors. *Front Cell Infect Microbiol*, 10:584751, 2020. doi: 10.3389/fcimb.2020.584751.

[40] A. B. Russell, M. LeRoux, K. Hathazi, D. M. Agnello, T. Ishikawa, P. A. Wiggins, S. N. Wai, and J. D. Mougous. Diverse type vi secretion phospholipases are functionally plastic antibacterial effectors. *Nature*, 496(7446):508–12, 2013. doi: 10.1038/nature12074.

[41] F. Jiang, N. R. Waterfield, J. Yang, G. Yang, and Q. Jin. A pseudomonas aeruginosa type vi secretion phospholipase d effector targets both prokaryotic and eukaryotic cells. *Cell Host Microbe*, 15(5):600–10, 2014. doi: 10.1016/j.chom.2014.04.010.

[42] F. Jiang, X. Wang, B. Wang, L. Chen, Z. Zhao, N. R. Waterfield, G. Yang, and Q. Jin. The pseudomonas aeruginosa type vi secretion pgap1-like effector induces host autophagy by activating endoplasmic reticulum stress. *Cell Rep*, 16(6):1502–1509, 2016. doi: 10.1016/j.celrep.2016.07.012.

[43] L. S. Terada, K. A. Johansen, S. Nowbar, A. I. Vasil, and M. L. Vasil. Pseudomonas aeruginosa hemolytic phospholipase c suppresses neutrophil respiratory burst activity. *Infect Immun*, 67(5):2371–6, 1999. doi: 10.1128/IAI.67.5.2371-2376.1999.

[44] S. Hall, C. McDermott, S. Anoopkumar-Dukie, A. J. McFarland, A. Forbes, A. V. Perkins, A. K. Davey, R. Chess-Williams, M. J. Kiefel, D. Arora, and G. D. Grant. Cellular effects of pyocyanin, a secreted virulence factor of pseudomonas aeruginosa. *Toxins (Basel)*, 8 (8), 2016. doi: 10.3390/toxins8080236.

[45] B. Ryall, J. C. Davies, R. Wilson, A. Shoemark, and H. D. Williams. Pseudomonas aeruginosa, cyanide accumulation and lung function in cf and non-cf bronchiectasis patients. *Eur Respir J*, 32(3):740–7, 2008. doi: 10.1183/09031936.00159607.

[46] P. Cornelis and J. Dingemans. Pseudomonas aeruginosa adapts its iron uptake strategies in function of the type of infections. *Front Cell Infect Microbiol*, 3:75, 2013. doi: 10.3389/fcimb.2013.00075.

[47] M. E. Davey, N. C. Caiazza, and G. A. O'Toole. Rhamnolipid surfactant production affects biofilm architecture in pseudomonas aeruginosa pao1. *J Bacteriol*, 185(3):1027–36, 2003. doi: 10.1128/JB.185.3.1027-1036.2003.

[48] L. Chrzanowski, L. Lawniczak, and K. Czaczyk. Why do microorganisms produce rhamnolipids? *World J Microbiol Biotechnol*, 28(2):401–19, 2012. doi: 10.1007/s11274-011-0854-8.

[49] J. Lee and L. Zhang. The hierarchy quorum sensing network in pseudomonas aeruginosa. *Protein Cell*, 6(1):26–41, 2015. doi: 10.1007/s13238-014-0100-x.

[50] J. Chadha, K. Harjai, and S. Chhibber. Revisiting the virulence hallmarks of pseudomonas aeruginosa: a chronicle through the perspective of quorum sensing. *Environ Microbiol*, 24 (6):2630–2656, 2022. doi: 10.1111/1462-2920.15784.

[51] H. Venter, R. Mowla, T. Ohene-Agyei, and S. Ma. Rnd-type drug e ffl ux pumps from gram-negative bacteria: molecular mechanism and inhibition. *Front Microbiol*, 6:377, 2015. doi: 10.3389/fmicb.2015.00377.

[52] O. Ciofu and T. Tolker-Nielsen. Tolerance and resistance of pseudomonas aeruginosa biofilms to antimicrobial agents-how p. aeruginosa can escape antibiotics. *Front Microbiol*, 10:913, 2019. doi: 10.3389/fmicb.2019.00913.

[53] J. Lopez, P. M. Ly, and M. F. Feldman. The tip of the vgrg spike is essential to functional type vi secretion system assembly in acinetobacter baumannii. *mBio*, 11(1), 2020. doi: 10.1128/mBio.02761-19.

[54] R. L. Marvig, L. M. Sommer, S. Molin, and H. K. Johansen. Convergent evolution and adaptation of pseudomonas aeruginosa within patients with cystic fibrosis. *Nat Genet*, 47 (1):57–64, 2015. doi: 10.1038/ng.3148.

[55] C. Lopez-Causape, L. M. Sommer, G. Cabot, R. Rubio, A. A. Ocampo-Sosa, H. K. Johansen, J. Figuerola, R. Canton, T. J. Kidd, S. Molin, and A. Oliver. Evolution of the pseudomonas aeruginosa mutational resistome in an international cystic fibrosis clone. *Sci Rep*, 7(1):5555, 2017. doi: 10.1038/s41598-017-05621-5.

[56] A. San Millan. Evolution of plasmid-mediated antibiotic resistance in the clinical context. *Trends Microbiol*, 26(12):978–985, 2018. doi: 10.1016/j.tim.2018.06.007.

[57] J. P. Horcajada, M. Montero, A. Oliver, L. Sorli, S. Luque, S. Gomez-Zorrilla, N. Benito, and S. Grau. Epidemiology and treatment of multidrug-resistant and extensively drug-resistant pseudomonas aeruginosa infections. *Clin Microbiol Rev*, 32(4), 2019. doi: 10.1128/CMR.00031-19.

[58] D. Subedi, A. K. Vijay, G. S. Kohli, S. A. Rice, and M. Willcox. Comparative genomics of clinical strains of pseudomonas aeruginosa strains isolated from different geographic sites. *Sci Rep*, 8(1):15668, 2018. doi: 10.1038/s41598-018-34020-7.

[59] K. M. Hall, Z. F. Pursell, and L. A. Morici. The role of the pseudomonas aeruginosa hypermutator phenotype on the shift from acute to chronic virulence during respiratory infection. *Front Cell Infect Microbiol*, 12:943346, 2022. doi: 10.3389/fcimb.2022.943346.

[60] B. Pritt, L. O'Brien, and W. Winn. Mucoid pseudomonas in cystic fibrosis. *Am J Clin Pathol*, 128(1):32–4, 2007. doi: 10.1309/KJRPC7DD5TR9NTDM.

[61] M. Starkey, J. H. Hickman, L. Ma, N. Zhang, S. De Long, A. Hinz, S. Palacios, C. Manoil, M. J. Kirisits, T. D. Starner, D. J. Wozniak, C. S. Harwood, and M. R. Parsek. Pseudomonas aeruginosa rugose small-colony variants have adaptations that likely promote persistence in the cystic fibrosis lung. *J Bacteriol*, 191(11):3492–503, 2009. doi: 10.1128/JB.00119-09.

[62] C. J. Jones and D. J. Wozniak. Psl produced by mucoid pseudomonas aeruginosa contributes to the establishment of biofilms and immune evasion. *mBio*, 8(3), 2017. doi: 10.1128/mBio.00864-17.

[63] S. Malhotra, D. H. Limoli, A. E. English, M. R. Parsek, and D. J. Wozniak. Mixed communities of mucoid and nonmucoid pseudomonas aeruginosa exhibit enhanced resistance to host antimicrobials. *mBio*, 9(2), 2018. doi: 10.1128/mBio.00275-18.

[64] D. W. Martin, M. J. Schurr, M. H. Mudd, J. R. Govan, B. W. Holloway, and V. Deretic. <mechanism of conversion to mucoidy in pseudomonas aeruginosa infecting cystic fibrosis patients.pdf>. *Proc Natl Acad Sci U S A*, 90(18):8377–81, 1993. doi: 10.1073/pnas.90.18.8377.

[65] B. Ryall, M. Carrara, J. E. Zlosnik, V. Behrends, X. Lee, Z. Wong, K. E. Lougheed, and H. D. Williams. The mucoid switch in pseudomonas aeruginosa represses quorum sensing systems and leads to complex changes to stationary phase virulence factor regulation. *PLoS One*, 9(5):e96166, 2014. doi: 10.1371/journal.pone.0096166.

[66] L. Camus, F. Vandenesch, and K. Moreau. From genotype to phenotype: adaptations of pseudomonas aeruginosa to the cystic fibrosis environment. *Microb Genom*, 7(3), 2021. doi: 10.1099/mgen.0.000513.

[67] M. J. Pestrak, S. B. Chaney, H. C. Eggleston, S. Dellos-Nolan, S. Dixit, S. S. Mathew-Steiner, S. Roy, M. R. Parsek, C. K. Sen, and D. J. Wozniak. Pseudomonas aeruginosa rugose small-colony variants evade host clearance, are hyper-inflammatory, and persist in multiple host environments. *PLoS Pathog*, 14(2):e1006842, 2018. doi: 10.1371/journal.ppat.1006842.

[68] A. Xu, X. Zhang, T. Wang, F. Xin, L. Z. Ma, J. Zhou, W. Dong, and M. Jiang. Rugose small colony variant and its hyper-biofilm in pseudomonas aeruginosa: Adaption, evolution, and biotechnological potential. *Biotechnol Adv*, 53:107862, 2021. doi: 10.1016/j.biotechadv.2021.107862.

[69] J. R. Aeschlimann. The role of multidrug efflux pumps in the antibiotic resistance of pseudomonas aeruginosa and other gram-negative bacteria. insights from the society of infectious diseases pharmacists. *Pharmacotherapy*, 23(7):916–24, 2003. doi: 10.1592/phco.23.7.916.32722.

[70] Z. Ma, C. Xu, X. Zhang, D. Wang, X. Pan, H. Liu, G. Zhu, F. Bai, Z. Cheng, W. Wu, and Y. Jin. A mexr mutation which confers aztreonam resistance to pseudomonas aeruginosa. *Front Microbiol*, 12:659808, 2021. doi: 10.3389/fmicb.2021.659808.

[71] S. Chevalier, E. Bouffartigues, J. Bodilis, O. Maillot, O. Lesouhaitier, M. G. J. Feuilloley, N. Orange, A. Dufour, and P. Cornelis. Structure, function and regulation of pseudomonas aeruginosa porins. *FEMS Microbiol Rev*, 41(5):698–722, 2017. doi: 10.1093/femsre/fux020.

[72] Christopher JL Murray, Kevin Shunji Ikuta, Fablina Sharara, Lucien Swetschinski, Gisela Robles Aguilar, Authia Gray, Chieh Han, Catherine Bisignano, Puja Rao, Eve Wool, Sarah C Johnson, Annie J Browne, Michael Give Chipeta, Frederick Fell, Sean Hackett, Georgina Haines-Woodhouse, Bahar H Kashef Hamadani, Emmanuelle A P Kumaran, Barney McManigal, Ramesh Agarwal, Samuel Akech, Samuel Albertson, John Amuasi, Jason Andrews, Aleskandr Aravkin, Elizabeth Ashley, Freddie Bailey, Stephen Baker, Buddha Basnyat, Adrie Bekker, Rose Bender, Adhisivam Bethou, Julia Bielicki, Suppawat Boonkasidecha, James Bukosia, Cristina Carvalheiro, Carlos Castaneda-Orjuela, Vilada Chansamouth, Suman Chaurasia, Sara Chiurchiu, Fazle Chowdhury, Aislinn J Cook, Ben Cooper, Tim R Cressey, Elia Criollo-Mora, Matthew Cunningham, Saffiatou Darboe, Nicholas P J Day, Maia De Luca, Klara Dokova, Angela Dramowski, Susanna J Dunachie, Tim Eckmanns, Daniel Eibach, Amir Emami, Nicholas Feasey, Natasha Fisher-Pearson, Karen Forrest, Denise Garrett, Petra Gastmeier, Ababi Zergaw Giref, Rachel Claire Greer, Vikas Gupta, Sebastian Haller, Andrea Haselbeck, Simon I Hay, Marianne Holm, Susan Hopkins, Kenneth C Iregbu, Jan Jacobs, Daniel Jarovsky, Fatemeh Javanmardi, Meera Khorana, Niranjan Kissoon, Elsa Kobeissi, Tomislav Kostyanev, Fiorella Krapp, Ralf Krumkamp, Ajay Kumar, Hmwe Hmwe Kyu, Cherry Lim, Direk Limmathurotsakul, Michael James Loftus, Miles Lunn, Jianing Ma, Neema Mturi, Tatiana

Munera-Huertas, Patrick Musicha, Marisa Marcia Mussi-Pinhata, Tomoka Nakamura, Ruchi Nanavati, Sushma Nangia, Paul Newton, Chanpheaktra Ngoun, Amanda Novotney, Davis Nwakanma, Christina W Obiero, Antonio Olivas-Martinez, Piero Olliaro, Ednah Ooko, et al. Global burden of bacterial antimicrobial resistance in 2019: a systematic analysis. *Lancet*, 399(10325):629–655, 2022. doi: 10.1016/s0140-6736(21)02724-0.

[73] C. L. Tooke, P. Hinchliffe, E. C. Bragginton, C. K. Colenso, V. H. A. Hirvonen, Y. Takebayashi, and J. Spencer. beta-lactamases and beta-lactamase inhibitors in the 21st century. *J Mol Biol*, 431(18):3472–3500, 2019. doi: 10.1016/j.jmb.2019.04.002.

[74] F. Liu, J. Mao, W. Kong, Q. Hua, Y. Feng, R. Bashir, and T. Lu. Interaction variability shapes succession of synthetic microbial ecosystems. *Nat Commun*, 11(1):309, 2020. doi: 10.1038/s41467-019-13986-6.

[75] P. S. Saudagar, S. A. Survase, and R. S. Singhal. Clavulanic acid: a review. *Biotechnol Adv*, 26(4):335–51, 2008. doi: 10.1016/j.biotechadv.2008.03.002.

[76] L. Poirel, A. Jayol, and P. Nordmann. Polymyxins: Antibacterial activity, susceptibility testing, and resistance mechanisms encoded by plasmids or chromosomes. *Clin Microbiol Rev*, 30(2):557–596, 2017. doi: 10.1128/CMR.00064-16.

[77] M. A. Farha and E. D. Brown. Drug repurposing for antimicrobial discovery. *Nat Microbiol*, 4(4):565–577, 2019. doi: 10.1038/s41564-019-0357-1.

[78] D. Leitsch. A review on metronidazole: an old warhorse in antimicrobial chemotherapy. *Parasitology*, 146(9):1167–1178, 2019. doi: 10.1017/S0031182017002025.

[79] V. Loustaud-Ratti, M. Debette-Gratien, J. Jacques, S. Alain, P. Marquet, D. Sautereau, A. Rousseau, and P. Carrier. Ribavirin: Past, present and future. *World J Hepatol*, 8(2): 123–30, 2016. doi: 10.4254/wjh.v8.i2.123.

[80] Y. Yuan, X. Yang, Q. Zeng, H. Li, R. Fu, L. Du, W. Liu, Y. Zhang, X. Zhou, Y. Chu, X. Zhang, and K. Zhao. Repurposing dimetridazole and ribavirin to disarm pseudomonas aeruginosa virulence by targeting the quorum sensing system. *Front Microbiol*, 13:978502, 2022. doi: 10.3389/fmicb.2022.978502.

[81] S. Naseer, E. A. Weinstein, D. B. Rubin, K. Suvarna, X. Wei, K. Higgins, A. Goodwin, S. H. Jang, D. Iarikov, J. Farley, and S. Nambiar. Us food and drug administration (fda): Benefit-risk considerations for cefiderocol (fetroja(r)). *Clin Infect Dis*, 72(12):e1103–e1111, 2021. doi: 10.1093/cid/ciaa1799.

[82] FDA. Fetroja (cefiderocol) for injection, for intravenous use initial u.s. approval: 2019, 2019.

[83] T. J. O'Brien, W. Figueroa, and M. Welch. Decreased efficacy of antimicrobial agents in a polymicrobial environment. *ISME J*, 16(7):1694–1704, 2022. doi: 10.1038/s41396-022-01218-7.

[84] M. J. Bottery, J. L. Matthews, A. J. Wood, H. K. Johansen, J. W. Pitchford, and V. P. Friman. Inter-species interactions alter antibiotic efficacy in bacterial communities. *ISME J*, 16(3):812–821, 2022. doi: 10.1038/s41396-021-01130-6.

[85] M. D. Macia, E. Rojo-Molinero, and A. Oliver. Antimicrobial susceptibility testing in biofilm-growing bacteria. *Clin Microbiol Infect*, 20(10):981–90, 2014. doi: 10.1111/1469-0691.12651.

[86] E. Reece, P. H. A. Bettio, and J. Renwick. Polymicrobial interactions in the cystic fibrosis airway microbiome impact the antimicrobial susceptibility of pseudomonas aeruginosa. *Antibiotics (Basel)*, 10(7), 2021. doi: 10.3390/antibiotics10070827.

[87] J. Tasse, D. Croisier, S. Badel-Berchoux, P. Chavanet, T. Bernardi, C. Provot, and F. Laurent. Preliminary results of a new antibiotic susceptibility test against biofilm installation in device-associated infections: the antibiofilmogram(r). *Pathog Dis*, 74(6), 2016. doi: 10.1093/femspd/ftw057.

[88] D. L. Wannigama, C. Hurst, P. Hongsing, L. Pearson, T. Saethang, N. Chantaravisoot, U. Singkham-In, S. Luk-In, R. J. Storer, and T. Chatsuwan. A rapid and simple method for routine determination of antibiotic sensitivity to biofilm populations of pseudomonas aeruginosa. *Ann Clin Microbiol Antimicrob*, 19(1):8, 2020. doi: 10.1186/s12941-020-00350-6.

[89] L. Thieme, A. Hartung, K. Tramm, M. Klinger-Strobel, K. D. Jandt, O. Makarewicz, and M. W. Pletz. Mbec versus mbic: the lack of differentiation between biofilm reducing and inhibitory effects as a current problem in biofilm methodology. *Biol Proced Online*, 21:18, 2019. doi: 10.1186/s12575-019-0106-0.

[90] R. M. Pinto, F. A. Soares, S. Reis, C. Nunes, and P. Van Dijck. Innovative strategies toward the disassembly of the eps matrix in bacterial biofilms. *Front Microbiol*, 11:952, 2020. doi: 10.3389/fmicb.2020.00952.

[91] N. Blanco-Cabra, B. Paetzold, T. Ferrar, R. Mazzolini, E. Torrents, L. Serrano, and L. Luch-Senar M. Characterization of different alginate lyases for dissolving pseudomonas aeruginosa biofilms. *Sci Rep*, 10(1):9390, 2020. doi: 10.1038/s41598-020-66293-2.

[92] E. D. Avila-Calderon, M. D. S. Ruiz-Palma, M. G. Aguilera-Arreola, N. Velazquez-Guadarrama, E. A. Ruiz, Z. Gomez-Lunar, S. Witonsky, and A. Contreras-Rodriguez. Outer membrane vesicles of gram-negative bacteria: An outlook on biogenesis. *Front Microbiol*, 12:557902, 2021. doi: 10.3389/fmicb.2021.557902.

[93] X. Liu, J. Xiao, S. Wang, J. Zhou, J. Qin, Z. Jia, Y. Wang, Z. Wang, Y. Zhang, and H. Hao. Research progress on bacterial membrane vesicles and antibiotic resistance. *Int J Mol Sci*, 23(19), 2022. doi: 10.3390/ijms231911553.

[94] A. Patil, R. Banerji, P. Kanojiya, S. Koratkar, and S. Saroj. Bacteriophages for eskape: role in pathogenicity and measures of control. *Expert Rev Anti Infect Ther*, 19(7):845–865, 2021. doi: 10.1080/14787210.2021.1858800.

[95] Z. Chegini, A. Khoshbayan, M. Taati Moghadam, I. Farahani, P. Jazireian, and A. Shariati. Bacteriophage therapy against pseudomonas aeruginosa biofilms: a review. *Ann Clin Microbiol Antimicrob*, 19(1):45, 2020. doi: 10.1186/s12941-020-00389-5.

[96] F. Micoli, F. Bagnoli, R. Rappuoli, and D. Serruto. The role of vaccines in combatting antimicrobial resistance. *Nat Rev Microbiol*, 19(5):287–302, 2021. doi: 10.1038/s41579-020-00506-3.

[97] M. Killough, A. M. Rodgers, and R. J. Ingram. Pseudomonas aeruginosa: Recent advances in vaccine development. *Vaccines (Basel)*, 10(7), 2022. doi: 10.3390/vaccines10071100.

[98] C. Adlbrecht, R. Wurm, P. Depuydt, H. Spapen, J. A. Lorente, T. Staudinger, J. Creteur, C. Zauner, A. Meier-Hellmann, P. Eller, M. V. Laenen, Z. Molnar, I. Varkonyi, B. Schaaf, M. Hejja, V. Sramek, H. Schneider, N. Kanesa-Thasan, S. Eder-Lingelbach, A. Klingler, K. Dubischar, N. Wressnigg, and J. Rello. Efficacy, immunogenicity, and safety of ic43 recombinant pseudomonas aeruginosa vaccine in mechanically ventilated intensive care patients-a randomized clinical trial. *Crit Care*, 24(1):74, 2020. doi: 10.1186/s13054-020-2792-z.

[99] M. P. Moore, I. L. Lamont, D. Williams, S. Paterson, I. Kukavica-Ibrulj, N. P. Tucker, D. T. D. Kenna, J. F. Turton, J. Jeukens, L. Freschi, B. A. Wee, N. J. Loman, S. Holden, S. Manzoor, P. Hawkey, K. W. Southern, M. J. Walshaw, R. C. Levesque, J. L. Fothergill, and C. Winstanley. Transmission, adaptation and geographical spread of the pseudomonas aeruginosa liverpool epidemic strain. *Microb Genom*, 7(3), 2021. doi: 10.1099/mgen.0.000511.

[100] M. Valentini, D. Gonzalez, D. A. Mavridou, and A. Filloux. Lifestyle transitions and adaptive pathogenesis of pseudomonas aeruginosa. *Curr Opin Microbiol*, 41:15–20, 2018. doi: 10.1016/j.mib.2017.11.006.

[101] J. A. Moscoso, H. Mikkelsen, S. Heeb, P. Williams, and A. Filloux. The pseudomonas aeruginosa sensor rets switches type iii and type vi secretion via c-di-gmp signalling. *Environ Microbiol*, 13(12):3128–38, 2011. doi: 10.1111/j.1462-2920.2011.02595.x.

[102] U. Jenal, A. Reinders, and C. Lori. Cyclic di-gmp: second messenger extraordinaire. *Nat Rev Microbiol*, 15(5):271–284, 2017. doi: 10.1038/nrmicro.2016.190.

[103] D. G. Ha and G. A. O'Toole. c-di-gmp and its effects on biofilm formation and dispersion: a pseudomonas aeruginosa review. *Microbiol Spectr*, 3(2):MB–0003–2014, 2015. doi: 10.1128/microbiolspec.MB-0003-2014.

[104] R. Hengge. Principles of c-di-gmp signalling in bacteria. *Nat Rev Microbiol*, 7(4):263–73, 2009. doi: 10.1038/nrmicro2109.

[105] U. Romling, M. Y. Galperin, and M. Gomelsky. Cyclic di-gmp: the first 25 years of a universal bacterial second messenger. *Microbiol Mol Biol Rev*, 77(1):1–52, 2013. doi: 10.1128/MMBR.00043-12.

[106] H. Kulasakara, V. Lee, A. Brencic, N. Liberati, J. Urbach, S. Miyata, D. G. Lee, A. N. Neely, M. Hyodo, Y. Hayakawa, F. M. Ausubel, and S. Lory. Analysis of pseudomonas aeruginosa diguanylate cyclases and phosphodiesterases reveals a role for bis-(3'-5')-cyclic-gmp in virulence. *Proc Natl Acad Sci U S A*, 103(8):2839–44, 2006. doi: 10.1073/pnas.0511090103.

[107] L. O'Neal, C. Baraquet, Z. Suo, J. E. Dreifus, Y. Peng, T. L. Raivio, D. J. Wozniak, C. S. Harwood, and M. R. Parsek. The wsp system of pseudomonas aeruginosa links surface sensing and cell envelope stress. *Proc Natl Acad Sci U S A*, 119(18):e2117633119, 2022. doi: 10.1073/pnas.2117633119.

[108] Z. T. Guvener and C. S. Harwood. Subcellular location characteristics of the pseudomonas aeruginosa ggdef protein, wspr, indicate that it produces cyclic-di-gmp in response to growth on surfaces. *Mol Microbiol*, 66(6):1459–73, 2007. doi: 10.1111/j.1365-2958.2007.06008.x.

[109] J. H. Merritt, K. M. Brothers, S. L. Kuchma, and G. A. O'Toole. Sadc reciprocally influences biofilm formation and swarming motility via modulation of exopolysaccharide production and flagellar function. *J Bacteriol*, 189(22):8154–64, 2007. doi: 10.1128/JB.00585-07.

[110] J. A. Moscoso, T. Jaeger, M. Valentini, K. Hui, U. Jenal, and A. Filloux. The diguanylate cyclase sadc is a central player in gac/rsm-mediated biofilm formation in pseudomonas aeruginosa. *J Bacteriol*, 196(23):4081–8, 2014. doi: 10.1128/JB.01850-14.

[111] R. R. McCarthy, M. J. Mazon-Moya, J. A. Moscoso, Y. Hao, J. S. Lam, C. Bordi, S. Mostowy, and A. Filloux. Cyclic-di-gmp regulates lipopolysaccharide modification and contributes to pseudomonas aeruginosa immune evasion. *Nat Microbiol*, 2:17027, 2017. doi: 10.1038/nmicrobiol.2017.27.

[112] S. L. Kuchma, K. M. Brothers, J. H. Merritt, N. T. Liberati, F. M. Ausubel, and G. A. O'Toole. Bifa, a cyclic-di-gmp phosphodiesterase, inversely regulates biofilm formation and swarming motility by pseudomonas aeruginosa pa14. *J Bacteriol*, 189(22):8165–78, 2007. doi: 10.1128/JB.00586-07.

[113] J. B. Andersen, K. N. Kragh, L. D. Hultqvist, M. Rybtke, M. Nilsson, T. H. Jakobsen, M. Givskov, and T. Tolker-Nielsen. Induction of native c-di-gmp phosphodiesterases leads to dispersal of pseudomonas aeruginosa biofilms. *Antimicrob Agents Chemother*, 65(4), 2021. doi: 10.1128/AAC.02431-20.

[114] J. W. Hickman and C. S. Harwood. Identification of fleq from pseudomonas aeruginosa as a c-di-gmp-responsive transcription factor. *Mol Microbiol*, 69(2):376–89, 2008. doi: 10.1111/j.1365-2958.2008.06281.x.

[115] S. H. Chou and M. Y. Galperin. Diversity of cyclic di-gmp-binding proteins and mechanisms. *J Bacteriol*, 198(1):32–46, 2016. doi: 10.1128/JB.00333-15.

[116] B. Y. Matsuyama, P. V. Krasteva, C. Baraquet, C. S. Harwood, H. Sondermann, and M. V. Navarro. Mechanistic insights into c-di-gmp-dependent control of the biofilm regulator fleq from pseudomonas aeruginosa. *Proc Natl Acad Sci U S A*, 113(2):E209–18, 2016. doi: 10.1073/pnas.1523148113.

[117] C. Baraquet and C. S. Harwood. Cyclic diguanosine monophosphate represses bacterial flagella synthesis by interacting with the walker a motif of the enhancer-binding protein fleq. *Proc Natl Acad Sci U S A*, 110(46):18478–83, 2013. doi: 10.1073/pnas.1318972110.

[118] C. Baraquet and C. S. Harwood. Fleq dna binding consensus sequence revealed by studies of fleq-dependent regulation of biofilm gene expression in pseudomonas aeruginosa. *J Bacteriol*, 198(1):178–86, 2016. doi: 10.1128/JB.00539-15.

[119] C. Baraquet, K. Murakami, M. R. Parsek, and C. S. Harwood. The fleq protein from pseudomonas aeruginosa functions as both a repressor and an activator to control gene expression from the pel operon promoter in response to c-di-gmp. *Nucleic Acids Res*, 40 (15):7207–18, 2012. doi: 10.1093/nar/gks384.

[120] R. Jain, O. Sliusarenko, and B. I. Kazmierczak. Interaction of the cyclic-di-gmp binding protein fimx and the type 4 pilus assembly atpase promotes pilus assembly. *PLoS Pathog*, 13(8):e1006594, 2017. doi: 10.1371/journal.ppat.1006594.

[121] J. C. Whitney, D. Quentin, S. Sawai, M. LeRoux, B. N. Harding, H. E. Ledvina, B. Q. Tran, H. Robinson, Y. A. Goo, D. R. Goodlett, S. Raunser, and J. D. Mougous. An interbacterial nad(p)(+) glycohydrolase toxin requires elongation factor tu for delivery to target cells. *Cell*, 163(3):607–19, 2015. doi: 10.1016/j.cell.2015.09.027.

[122] K. Chihara, L. Barquist, K. Takasugi, N. Noda, and S. Tsuneda. Global identification of rsma/n binding sites in pseudomonas aeruginosa by in vivo uv clip-seq. *RNA Biol*, 18(12): 2401–2416, 2021. doi: 10.1080/15476286.2021.1917184.

[123] A. Brencic and S. Lory. Determination of the regulon and identification of novel mrna targets of pseudomonas aeruginosa rsma. *Mol Microbiol*, 72(3):612–32, 2009. doi: 10.1111/j.1365-2958.2009.06670.x.

[124] A. Brencic, K. A. McFarland, H. R. McManus, S. Castang, I. Mogno, S. L. Dove, and S. Lory. The gacs/gaca signal transduction system of pseudomonas aeruginosa acts exclusively through its control over the transcription of the rsmy and rsmz regulatory small rnas. *Mol Microbiol*, 73(3):434–45, 2009. doi: 10.1111/j.1365-2958.2009.06782.x.

[125] F. Fadel, V. Bassim, V. I. Francis, S. L. Porter, T. Botzanowski, P. Legrand, M. M. Perez, Y. Bourne, S. Cianferani, and F. Vincent. Insights into the atypical autokinase activity of the pseudomonas aeruginosa gacs histidine kinase and its interaction with rets. *Structure*, 30(9):1285–1297 e5, 2022. doi: 10.1016/j.str.2022.06.002.

[126] G. Chambonnier, L. Roux, D. Redelberger, F. Fadel, A. Filloux, M. Sivaneson, S. de Bentzmann, and C. Bordi. The hybrid histidine kinase lads forms a multicomponent

signal transduction system with the gacs/gaca two-component system in pseudomonas aeruginosa. *PLoS Genet*, 12(5):e1006032, 2016. doi: 10.1371/journal.pgen.1006032.

[127] C. Pourciau, Y. J. Lai, M. Gorelik, P. Babitzke, and T. Romeo. Diverse mechanisms and circuitry for global regulation by the rna-binding protein csra. *Front Microbiol*, 11:601352, 2020. doi: 10.3389/fmicb.2020.601352.

[128] P. M. Sobrero and C. Valverde. Comparative genomics and evolutionary analysis of rna-binding proteins of the csra family in the genus pseudomonas. *Front Mol Biosci*, 7:127, 2020. doi: 10.3389/fmolb.2020.00127.

[129] P. Gutierrez, Y. Li, M. J. Osborne, E. Pomerantseva, Q. Liu, and K. Gehring. Solution structure of the carbon storage regulator protein csra from escherichia coli. *J Bacteriol*, 187(10):3496–501, 2005. doi: 10.1128/JB.187.10.3496-3501.2005.

[130] T. Romeo, M. Gong, M. Y. Liu, and A. M. Brun-Zinkernagel. <jbacter00057-0178.pdf>. *J Bacteriol*, 175(15):4744–55, 1993. doi: 10.1128/jb.175.15.4744-4755.1993.

[131] M. Romero, H. Silistre, L. Lovelock, V. J. Wright, K. G. Chan, K. W. Hong, P. Williams, M. Camara, and S. Heeb. Genome-wide mapping of the rna targets of the pseudomonas aeruginosa riboregulatory protein rsmn. *Nucleic Acids Res*, 46(13):6823–6840, 2018. doi: 10.1093/nar/gky324.

[132] A. K. Dubey, C. S. Baker, T. Romeo, and P. Babitzke. Rna sequence and secondary structure participate in high-affinity csra-rna interaction. *RNA*, 11(10):1579–87, 2005. doi: 10.1261/rna.2990205.

[133] K. Lapouge, M. Schubert, F. H. Allain, and D. Haas. Gac/rsm signal transduction pathway of gamma-proteobacteria: from rna recognition to regulation of social behaviour. *Mol Microbiol*, 67(2):241–53, 2008. doi: 10.1111/j.1365-2958.2007.06042.x.

[134] O. Duss, E. Michel, N. Diarra dit Konte, M. Schubert, and F. H. Allain. Molecular basis for the wide range of affinity found in csr/rsm protein-rna recognition. *Nucleic Acids Res*, 42(8):5332–46, 2014. doi: 10.1093/nar/gku141.

[135] J. N. Marden, M. R. Diaz, W. G. Walton, C. J. Gode, L. Betts, M. L. Urbanowski, M. R. Redinbo, T. L. Yahr, and M. C. Wolfgang. An unusual csra family member operates in series with rsma to amplify posttranscriptional responses in pseudomonas aeruginosa. *Proc Natl Acad Sci U S A*, 110(37):15055–60, 2013. doi: 10.1073/pnas.1307217110.

[136] E. R. Morris, G. Hall, C. Li, S. Heeb, R. V. Kulkarni, L. Lovelock, H. Silistre, M. Messina, M. Camara, J. Emsley, P. Williams, and M. S. Searle. Structural rearrangement in an rsma/csra ortholog of pseudomonas aeruginosa creates a dimeric rna-binding protein, rsmn. *Structure*, 21(9):1659–71, 2013. doi: 10.1016/j.str.2013.07.007.

[137] M. Schubert, K. Lapouge, O. Duss, F. C. Oberstrass, I. Jelesarov, D. Haas, and F. H. Allain. Molecular basis of messenger rna recognition by the specific bacterial repressing clamp rsma/csra. *Nat Struct Mol Biol*, 14(9):807–13, 2007. doi: 10.1038/nsmb1285.

[138] N. Figueroa-Bossi, A. Schwartz, B. Guillemardet, F. D'Heygere, L. Bossi, and M. Boudvillain. Rna remodeling by bacterial global regulator csra promotes rho-dependent transcription termination. *Genes Dev*, 28(11):1239–51, 2014. doi: 10.1101/gad.240192.114.

[139] K. Suzuki, P. Babitzke, S. R. Kushner, and T. Romeo. Identification of a novel regulatory protein (csrd) that targets the global regulatory rnas csrb and csrc for degradation by rnase e. *Genes Dev*, 20(18):2605–17, 2006. doi: 10.1101/gad.1461606.

[140] A. V. Yakhnin, C. S. Baker, C. A. Vakulskas, H. Yakhnin, I. Berezin, T. Romeo, and P. Babitzke. Csra activates flhdc expression by protecting flhdc mrna from rnase e-mediated cleavage. *Mol Microbiol*, 87(4):851–66, 2013. doi: 10.1111/mmi.12136.

[141] A. Renda, S. Poly, Y. J. Lai, A. Pannuri, H. Yakhnin, A. H. Potts, P. C. Bevilacqua, T. Romeo, and P. Babitzke. Csra-mediated translational activation of ymda expression in escherichia coli. *mBio*, 11(5), 2020. doi: 10.1128/mBio.00849-20.

[142] C. Blumer, S. Heeb, G. Pessi, and D. Haas. Global gaca-steered control of cyanide and exoprotease production in pseudomonas fluorescens involves specific ribosome binding sites. *Proc Natl Acad Sci U S A*, 96(24):14073–8, 1999. doi: 10.1073/pnas.96.24.14073.

[143] G. Pessi, F. Williams, Z. Hindle, K. Heurlier, M. T. Holden, M. Camara, D. Haas, and P. Williams. The global posttranscriptional regulator rsma modulates production of virulence determinants and n-acylhomoserine lactones in pseudomonas aeruginosa. *J Bacteriol*, 183(22):6676–83, 2001. doi: 10.1128/JB.183.22.6676-6683.2001.

[144] E. Burrowes, C. Baysse, C. Adams, and F. O'Gara. Influence of the regulatory protein rsma on cellular functions in pseudomonas aeruginosa pao1, as revealed by transcriptome analysis. *Microbiology (Reading)*, 152(Pt 2):405–418, 2006. doi: 10.1099/mic.0.28324-0.

[145] M. J. Gebhardt, T. K. Kambara, K. M. Ramsey, and S. L. Dove. Widespread targeting of nascent transcripts by rsma in pseudomonas aeruginosa. *Proc Natl Acad Sci U S A*, 117 (19):10520–10529, 2020. doi: 10.1073/pnas.1917587117.

[146] C. J. Jones, D. Newsom, B. Kelly, Y. Irie, L. K. Jennings, B. Xu, D. H. Limoli, J. J. Harrison, M. R. Parsek, P. White, and D. J. Wozniak. Chip-seq and rna-seq reveal an amrz-mediated mechanism for cyclic di-gmp synthesis and biofilm development by pseudomonas aeruginosa. *PLoS Pathog*, 10(3):e1003984, 2014. doi: 10.1371/journal.ppat.1003984.

[147] H. Huang, X. Shao, Y. Xie, T. Wang, Y. Zhang, X. Wang, and X. Deng. An integrated genomic regulatory network of virulence-related transcriptional factors in pseudomonas aeruginosa. *Nat Commun*, 10(1):2931, 2019. doi: 10.1038/s41467-019-10778-w.

[148] J. M. Corley, P. Intile, and T. L. Yahr. Direct inhibition of rets synthesis by rsma contributes to homeostasis of the pseudomonas aeruginosa gac/rsm signaling system. *J Bacteriol*, 204(3):e0058021, 2022. doi: 10.1128/jb.00580-21.

[149] K. H. Janssen, M. R. Diaz, C. J. Gode, M. C. Wolfgang, and T. L. Yahr. Rsmv, a small noncoding regulatory rna in pseudomonas aeruginosa that sequesters rsma and rsmf from target mrnas. *J Bacteriol*, 200(16), 2018. doi: 10.1128/JB.00277-18.

[150] J. O'Callaghan, F. J. Reen, C. Adams, and F. O'Gara. Low oxygen induces the type iii secretion system in pseudomonas aeruginosa via modulation of the small rnas rsmz and rsmy. *Microbiology (Reading)*, 157(Pt 12):3417–3428, 2011. doi: 10.1099/mic.0.052050-0.

[151] S. Chakravarty, C. N. Melton, A. Bailin, T. L. Yahr, and G. G. Anderson. Pseudomonas aeruginosa magnesium transporter mgte inhibits type iii secretion system gene expression by stimulating rsmyz transcription. *J Bacteriol*, 199(23), 2017. doi: 10.1128/JB.00268-17.

[152] P. Pusic, E. Sonnleitner, and U. Blasi. Specific and global rna regulators in pseudomonas aeruginosa. *Int J Mol Sci*, 22(16), 2021. doi: 10.3390/ijms22168632.

[153] K. H. Janssen, J. M. Corley, L. Djapgne, J. T. Cribbs, D. Voelker, Z. Slusher, R. Nordell, E. E. Regulski, B. I. Kazmierczak, E. W. McMackin, and T. L. Yahr. Hfq and srna 179 inhibit expression of the pseudomonas aeruginosa camp-vfr and type iii secretion regulons. *mBio*, 11(3), 2020. doi: 10.1128/mBio.00363-20.

[154] W. Liu, M. Li, L. Jiao, P. Wang, and Y. Yan. Pmra/pmrb two-component system regulation of lipa expression in pseudomonas aeruginosa pao1. *Front Microbiol*, 8:2690, 2017. doi: 10.3389/fmicb.2017.02690.

[155] S. Castang, H. R. McManus, K. H. Turner, and S. L. Dove. H-ns family members function coordinately in an opportunistic pathogen. *Proc Natl Acad Sci U S A*, 105(48):18947–52, 2008. doi: 10.1073/pnas.0808215105.

[156] O. E. Petrova and K. Sauer. A novel signaling network essential for regulating pseudomonas aeruginosa biofilm development. *PLoS Pathog*, 5(11):e1000668, 2009. doi: 10.1371/journal.ppat.1000668.

[157] C. L. Miller, M. Romero, S. L. Karna, T. Chen, S. Heeb, and K. P. Leung. Rsmw, pseudomonas aeruginosa small non-coding rsma-binding rna upregulated in biofilm versus planktonic growth conditions. *BMC Microbiol*, 16(1):155, 2016. doi: 10.1186/s12866-016-0771-y.

[158] M. Gomez-Lozano, R. L. Marvig, S. Molin, and K. S. Long. Genome-wide identification of novel small rnas in pseudomonas aeruginosa. *Environ Microbiol*, 14(8):2006–16, 2012. doi: 10.1111/j.1462-2920.2012.02759.x.

[159] U. A. Ochsner, P. J. Wilderman, A. I. Vasil, and M. L. Vasil. <molecular microbiology - 2002 - ochsner - genechip expression analysis of the iron starvation response in pseudomonas.pdf>. *Mol Microbiol*, 45(5):1277–87, 2002. doi: 10.1046/j.1365-2958.2002.03084.x.

[160] G. M. Patriquin, E. Banin, C. Gilmour, R. Tuchman, E. P. Greenberg, and K. Poole. Influence of quorum sensing and iron on twitching motility and biofilm formation in pseudomonas aeruginosa. *J Bacteriol*, 190(2):662–71, 2008. doi: 10.1128/JB.01473-07.

[161] O. Wurtzel, D. R. Yoder-Himes, K. Han, A. A. Dandekar, S. Edelheit, E. P. Greenberg, R. Sorek, and S. Lory. The single-nucleotide resolution transcriptome of pseudomonas

aeruginosa grown in body temperature. *PLoS Pathog*, 8(9):e1002945, 2012. doi: 10.1371/journal.ppat.1002945.

[162] V. I. Francis, E. M. Waters, S. E. Finton-James, A. Gori, A. Kadioglu, A. R. Brown, and S. L. Porter. Multiple communication mechanisms between sensor kinases are crucial for virulence in pseudomonas aeruginosa. *Nat Commun*, 9(1):2219, 2018. doi: 10.1038/s41467-018-04640-8.

[163] Huihui Song, Yuying Li, and Yan Wang. Two-component system gacs/gaca, a global response regulator of bacterial physiological behaviors. *Engineering Microbiology*, 3(1), 2023. doi: 10.1016/j.engmic.2022.100051.

[164] A. Ali-Ahmad, O. Bornet, F. Fadel, Y. Bourne, F. Vincent, C. Bordi, F. Guerlesquin, and C. Sebban-Kreuzer. Nmr assignments of the gacs histidine-kinase periplasmic detection domain from pseudomonas aeruginosa pao1. *Biomol NMR Assign*, 11(1):25–28, 2017. doi: 10.1007/s12104-016-9714-7.

[165] A. Ali-Ahmad, F. Fadel, C. Sebban-Kreuzer, M. Ba, G. D. Pelissier, O. Bornet, F. Guerlesquin, Y. Bourne, C. Bordi, and F. Vincent. Structural and functional insights into the periplasmic detector domain of the gacs histidine kinase controlling biofilm formation in pseudomonas aeruginosa. *Sci Rep*, 7(1):11262, 2017. doi: 10.1038/s41598-017-11361-3.

[166] I. Ventre, A. L. Goodman, I. Vallet-Gely, P. Vasseur, C. Soscia, S. Molin, S. Bleves, A. Lazdunski, S. Lory, and A. Filloux. Multiple sensors control reciprocal expression of pseudomonas aeruginosa regulatory rna and virulence genes. *Proc Natl Acad Sci U S A*, 103(1):171–6, 2006. doi: 10.1073/pnas.0507407103.

[167] A. L. Goodman, B. Kulasekara, A. Rietsch, D. Boyd, R. S. Smith, and S. Lory. A signaling network reciprocally regulates genes associated with acute infection and chronic persistence in pseudomonas aeruginosa. *Dev Cell*, 7(5):745–54, 2004. doi: 10.1016/j.devcel.2004.08.020.

[168] W. Kong, L. Chen, J. Zhao, T. Shen, M. G. Surette, L. Shen, and K. Duan. Hybrid sensor kinase pa1611 in pseudomonas aeruginosa regulates transitions between acute and chronic infection through direct interaction with rets. *Mol Microbiol*, 88(4):784–97, 2013. doi: 10.1111/mmi.12223.

[169] B. X. Wang, K. M. Wheeler, K. C. Cady, S. Lehoux, R. D. Cummings, M. T. Laub, and K. Ribbeck. Mucin glycans signal through the sensor kinase rets to inhibit virulence-associated traits in pseudomonas aeruginosa. *Curr Biol*, 31(1):90–102 e7, 2021. doi: 10.1016/j.cub.2020.09.088.

[170] K. M. Ryan Kaler, J. C. Nix, and F. D. Schubot. Rets inhibits pseudomonas aeruginosa biofilm formation by disrupting the canonical histidine kinase dimerization interface of gacs. *J Biol Chem*, 297(4):101193, 2021. doi: 10.1016/j.jbc.2021.101193.

[171] N. Cramer, J. Klockgether, K. Wrasman, M. Schmidt, C. F. Davenport, and B. Tummler. Microevolution of the major common pseudomonas aeruginosa clones c and pa14 in cystic fibrosis lungs. *Environ Microbiol*, 13(7):1690–704, 2011. doi: 10.1111/j.1462-2920.2011.02483.x.

[172] J. D. Mougous, M. E. Cuff, S. Raunser, A. Shen, M. Zhou, C. A. Gifford, A. L. Goodman, G. Joachimiak, C. L. Ordonez, S. Lory, T. Walz, A. Joachimiak, and J. J. Mekalanos. A virulence locus of pseudomonas aeruginosa encodes a protein secretion apparatus. *Science*, 312(5779):1526–30, 2006. doi: 10.1126/science.1128393.

[173] O. Francetic. Tagging the type vi secretion system. *Nat Microbiol*, 3(11):1190–1191, 2018. doi: 10.1038/s41564-018-0277-5.

[174] U. N. Broder, T. Jaeger, and U. Jenal. Lads is a calcium-responsive kinase that induces acute-to-chronic virulence switch in pseudomonas aeruginosa. *Nat Microbiol*, 2:16184, 2016. doi: 10.1038/nmicrobiol.2016.184.

[175] H. Mikkelsen, R. McMullan, and A. Filloux. The pseudomonas aeruginosa reference strain pa14 displays increased virulence due to a mutation in lads. *PLoS One*, 6(12):e29113, 2011. doi: 10.1371/journal.pone.0029113.

[176] A. Y. Bhagirath, S. P. Pydi, Y. Li, C. Lin, W. Kong, P. Chelikani, and K. Duan. Characterization of the direct interaction between hybrid sensor kinases pa1611 and rets that controls biofilm formation and the type iii secretion system in pseudomonas aeruginosa. *ACS Infect Dis*, 3(2):162–175, 2017. doi: 10.1021/acsinfecdis.6b00153.

[177] V. I. Francis, E. C. Stevenson, and S. L. Porter. Two-component systems required for virulence in pseudomonas aeruginosa. *FEMS Microbiol Lett*, 364(11), 2017. doi: 10.1093/femsle/fnx104.

[178] M. Bouteiller, C. Dupont, Y. Bourigault, X. Latour, C. Barbey, Y. Konto-Ghiorghi, and A. Merieau. Pseudomonas flagella: Generalities and specificities. *Int J Mol Sci*, 22(7), 2021. doi: 10.3390/ijms22073337.

[179] A. Be'er and G. Ariel. A statistical physics view of swarming bacteria. *Mov Ecol*, 7:9, 2019. doi: 10.1186/s40462-019-0153-9.

[180] M. E. Anyan, A. Amiri, C. W. Harvey, G. Tierra, N. Morales-Soto, C. M. Driscoll, M. S. Alber, and J. D. Shrout. Type iv pili interactions promote intercellular association and moderate swarming of pseudomonas aeruginosa. *Proc Natl Acad Sci U S A*, 111(50): 18013–8, 2014. doi: 10.1073/pnas.1414661111.

[181] T. Kohler, L. K. Curty, F. Barja, C. van Delden, and J. C. Pechere. Swarming of pseudomonas aeruginosa is dependent on cell-to-cell signaling and requires flagella and pili. *J Bacteriol*, 182(21):5990–6, 2000. doi: 10.1128/JB.182.21.5990-5996.2000.

[182] L. Xin, Y. Zeng, S. Sheng, R. A. Chea, Q. Liu, H. Y. Li, L. Yang, L. Xu, K. H. Chiam, and Z. X. Liang. Regulation of flagellar motor switching by c-di-gmp

phosphodiesterases in pseudomonas aeruginosa. *J Biol Chem*, 294(37):13789–13799, 2019. doi: 10.1074/jbc.RA119.009009.

[183] B. J. Laventie, M. Sangermani, F. Estermann, P. Manfredi, R. Planes, I. Hug, T. Jaeger, E. Meunier, P. Broz, and U. Jenal. A surface-induced asymmetric program promotes tissue colonization by pseudomonas aeruginosa. *Cell Host Microbe*, 25(1):140–152 e6, 2019. doi: 10.1016/j.chom.2018.11.008.

[184] M. Klausen, A. Heydorn, P. Ragas, L. Lambertsen, A. Aaes-Jorgensen, S. Molin, and T. Tolker-Nielsen. Biofilm formation by pseudomonas aeruginosa wild type, flagella and type iv pili mutants. *Mol Microbiol*, 48(6):1511–24, 2003. doi: 10.1046/j.1365-2958.2003.03525.x.

[185] J. Overhage, M. Bains, M. D. Brazas, and R. E. Hancock. Swarming of pseudomonas aeruginosa is a complex adaptation leading to increased production of virulence factors and antibiotic resistance. *J Bacteriol*, 190(8):2671–9, 2008. doi: 10.1128/JB.01659-07.

[186] S. R. Coleman, D. Pletzer, and R. E. W. Hancock. Contribution of swarming motility to dissemination in a pseudomonas aeruginosa murine skin abscess infection model. *J Infect Dis*, 224(4):726–733, 2021. doi: 10.1093/infdis/jiaa778.

[187] M. Grognot and K. M. Taute. More than propellers: how flagella shape bacterial motility behaviors. *Curr Opin Microbiol*, 61:73–81, 2021. doi: 10.1016/j.mib.2021.02.005.

[188] M. Tian, Z. Wu, R. Zhang, and J. Yuan. A new mode of swimming in singly flagellated pseudomonas aeruginosa. *Proc Natl Acad Sci U S A*, 119(14):e2120508119, 2022. doi: 10.1073/pnas.2120508119.

[189] S. Nakamura and T. Minamino. Flagella-driven motility of bacteria. *Biomolecules*, 9(7), 2019. doi: 10.3390/biom9070279.

[190] J. S. Schuhmacher, K. M. Thormann, and G. Bange. How bacteria maintain location and number of flagella? *FEMS Microbiol Rev*, 39(6):812–22, 2015. doi: 10.1093/femsre/fuv034.

[191] Q. Cai, Z. Li, Q. Ouyang, C. Luo, and V. D. Gordon. Singly flagellated pseudomonas aeruginosa chemotaxes efficiently by unbiased motor regulation. *mBio*, 7(2):e00013, 2016. doi: 10.1128/mBio.00013-16.

[192] I. Sampedro, R. E. Parales, T. Krell, and J. E. Hill. Pseudomonas chemotaxis. *FEMS Microbiol Rev*, 39(1):17–46, 2015. doi: 10.1111/1574-6976.12081.

[193] A. Ortega, I. B. Zhulin, and T. Krell. Sensory repertoire of bacterial chemoreceptors. *Microbiol Mol Biol Rev*, 81(4), 2017. doi: 10.1128/MMBR.00033-17.

[194] J. Lacal, C. Garcia-Fontana, F. Munoz-Martinez, J. L. Ramos, and T. Krell. Sensing of environmental signals: classification of chemoreceptors according to the size of their ligand binding regions. *Environ Microbiol*, 12(11):2873–84, 2010. doi: 10.1111/j.1462-2920.2010.02325.x.

[195] M. A. Matilla, D. Martin-Mora, J. A. Gavira, and T. Krell. Pseudomonas aeruginosa as a model to study chemosensory pathway signaling. *Microbiol Mol Biol Rev*, 85(1), 2021. doi: 10.1128/MMBR.00151-20.

[196] H. Wu, J. Kato, A. Kuroda, T. Ikeda, N. Takiguchi, and H. Ohtake. Identification and characterization of two chemotactic transducers for inorganic phosphate in pseudomonas aeruginosa. *J Bacteriol*, 182(12):3400–4, 2000. doi: 10.1128/JB.182.12.3400-3404.2000.

[197] K. Taguchi, H. Fukutomi, A. Kuroda, J. Kato, and H. Ohtake. Genetic identification of chemotactic transducers for amino acids in pseudomonas aeruginosa. *Microbiology (Reading)*, 143 (Pt 10):3223–3229, 1997. doi: 10.1099/00221287-143-10-3223.

[198] J. A. Reyes-Darias, Y. Yang, V. Sourjik, and T. Krell. Correlation between signal input and output in pcta and pctb amino acid chemoreceptor of pseudomonas aeruginosa. *Mol Microbiol*, 96(3):513–25, 2015. doi: 10.1111/mmi.12953.

[199] M. A. Matilla, F. Velando, A. Tajuelo, D. Martin-Mora, W. Xu, V. Sourjik, J. A. Gavira, and T. Krell. Chemotaxis of the human pathogen pseudomonas aeruginosa to the neurotransmitter acetylcholine. *mBio*, 13(2):e0345821, 2022. doi: 10.1128/mbio.03458-21.

[200] R. R. Lovewell, S. M. Hayes, G. A. O'Toole, and B. Berwin. Pseudomonas aeruginosa flagellar motility activates the phagocyte pi3k/akt pathway to induce phagocytic engulfment. *Am J Physiol Lung Cell Mol Physiol*, 306(7):L698–707, 2014. doi: 10.1152/ajplung.00319.2013.

[201] M. Schniederberend, J. F. Williams, E. Shine, C. Shen, R. Jain, T. Emonet, and B. I. Kazmierczak. Modulation of flagellar rotation in surface-attached bacteria: A pathway for rapid surface-sensing after flagellar attachment. *PLoS Pathog*, 15(11):e1008149, 2019. doi: 10.1371/journal.ppat.1008149.

[202] J. L. Berry and V. Pelicic. Exceptionally widespread nanomachines composed of type iv pilins: the prokaryotic swiss army knives. *FEMS Microbiol Rev*, 39(1):134–54, 2015. doi: 10.1093/femsre/fuu001.

[203] B. Maier and G. C. L. Wong. How bacteria use type iv pili machinery on surfaces. *Trends Microbiol*, 23(12):775–788, 2015. doi: 10.1016/j.tim.2015.09.002.

[204] Y. Nguyen, S. Sugiman-Marangos, H. Harvey, S. D. Bell, C. L. Charlton, M. S. Junop, and L. L. Burrows. Pseudomonas aeruginosa minor pilins prime type iva pilus assembly and promote surface display of the pily1 adhesin. *J Biol Chem*, 290(1):601–11, 2015. doi: 10.1074/jbc.M114.616904.

[205] L. Craig, K. T. Forest, and B. Maier. Type iv pili: dynamics, biophysics and functional consequences. *Nat Rev Microbiol*, 17(7):429–440, 2019. doi: 10.1038/s41579-019-0195-4.

[206] A. Beaussart, A. E. Baker, S. L. Kuchma, S. El-Kirat-Chatel, G. A. O'Toole, and Y. F. Dufrene. Nanoscale adhesion forces of pseudomonas aeruginosa type iv pili. *ACS Nano*, 8 (10):10723–33, 2014. doi: 10.1021/nn5044383.

[207] C. Holz, D. Opitz, L. Greune, R. Kurre, M. Koomey, M. A. Schmidt, and B. Maier. Multiple pilus motors cooperate for persistent bacterial movement in two dimensions. *Phys Rev Lett*, 104(17):178104, 2010. doi: 10.1103/PhysRevLett.104.178104.

[208] B. Maier, L. Potter, M. So, C. D. Long, H. S. Seifert, and M. P. Sheetz. <pnas.242523299.pdf>. *Proc Natl Acad Sci U S A*, 99(25):16012–7, 2002. doi: 10.1073/pnas.242523299.

[209] M. D. Johnson, C. K. Garrett, J. E. Bond, K. A. Coggan, M. C. Wolfgang, and M. R. Redinbo. Pseudomonas aeruginosa pily1 binds integrin in an rgd- and calcium-dependent manner. *PLoS One*, 6(12):e29629, 2011. doi: 10.1371/journal.pone.0029629.

[210] K. H. Piepenbrink. Dna uptake by type iv filaments. *Front Mol Biosci*, 6:1, 2019. doi: 10.3389/fmolb.2019.00001.

[211] H. Patel and D. Gajjar. Cell adhesion and twitching motility influence strong biofilm formation in pseudomonas aeruginosa. *Biofouling*, 38(3):235–249, 2022. doi: 10.1080/08927014.2022.2054703.

[212] S. Burdman, O. Bahar, J. K. Parker, and L. De La Fuente. Involvement of type iv pili in pathogenicity of plant pathogenic bacteria. *Genes (Basel)*, 2(4):706–35, 2011. doi: 10.3390/genes2040706.

[213] K. N. Cowles and Z. Gitai. Surface association and the mreb cytoskeleton regulate pilus production, localization and function in pseudomonas aeruginosa. *Mol Microbiol*, 76(6): 1411–26, 2010. doi: 10.1111/j.1365-2958.2010.07132.x.

[214] A. J. Merz, M. So, and M. P. Sheetz. Pilus retraction powers bacterial twitching motility. *Nature*, 407(6800):98–102, 2000. doi: 10.1038/35024105.

[215] M. L. Gibiansky, J. C. Conrad, F. Jin, V. D. Gordon, D. A. Motto, M. A. Mathewson, W. G. Stopka, D. C. Zelasko, J. D. Shrout, and G. C. Wong. Bacteria use type iv pili to walk upright and detach from surfaces. *Science*, 330(6001):197, 2010. doi: 10.1126/science.1194238.

[216] J. C. Conrad, M. L. Gibiansky, F. Jin, V. D. Gordon, D. A. Motto, M. A. Mathewson, W. G. Stopka, D. C. Zelasko, J. D. Shrout, and G. C. Wong. Flagella and pili-mediated near-surface single-cell motility mechanisms in p. aeruginosa. *Biophys J*, 100(7):1608–16, 2011. doi: 10.1016/j.bpj.2011.02.020.

[217] M. J. Kuhn, L. Tala, Y. F. Inclan, R. Patino, X. Pierrat, I. Vos, Z. Al-Mayyah, H. Macmillan, Jr. Negrete, J., J. N. Engel, and A. Persat. Mechanotaxis directs pseudomonas aeruginosa twitching motility. *Proc Natl Acad Sci U S A*, 118(30), 2021. doi: 10.1073/pnas.2101759118.

[218] D. H. Limoli, E. A. Warren, K. D. Yarrington, N. P. Donegan, A. L. Cheung, and G. A. O'Toole. Interspecies interactions induce exploratory motility in pseudomonas aeruginosa. *Elife*, 8, 2019. doi: 10.7554/eLife.47365.

[219] L. M. Nolan, L. C. McCaughey, J. Merjane, L. Turnbull, and C. B. Whitchurch. Chpc controls twitching motility-mediated expansion of pseudomonas aeruginosa biofilms in response to serum albumin, mucin and oligopeptides. *Microbiology (Reading)*, 166(7): 669–678, 2020. doi: 10.1099/mic.0.000911.

[220] H. C. Flemming and S. Wuertz. Bacteria and archaea on earth and their abundance in biofilms. *Nat Rev Microbiol*, 17(4):247–260, 2019. doi: 10.1038/s41579-019-0158-9.

[221] H. C. Flemming, P. Baveye, T. R. Neu, P. Stoodley, U. Szewzyk, J. Wingender, and S. Wuertz. Who put the film in biofilm? the migration of a term from wastewater engineering to medicine and beyond. *NPJ Biofilms Microbiomes*, 7(1):10, 2021. doi: 10.1038/s41522-020-00183-3.

[222] L. Procopio. The role of biofilms in the corrosion of steel in marine environments. *World J Microbiol Biotechnol*, 35(5):73, 2019. doi: 10.1007/s11274-019-2647-4.

[223] C. M. Narayanan and Vikas Narayan. Biological wastewater treatment and bioreactor design: a review. *Sustainable Environment Research*, 29(1), 2019. doi: 10.1186/s42834-019-0036-1.

[224] Z. Wang, Y. Shen, and M. Haapasalo. Dynamics of dissolution, killing, and inhibition of dental plaque biofilm. *Front Microbiol*, 11:964, 2020. doi: 10.3389/fmicb.2020.00964.

[225] M. Alhede, K. N. Kragh, K. Qvortrup, M. Allesen-Holm, M. van Gennip, L. D. Christensen, P. O. Jensen, A. K. Nielsen, M. Parsek, D. Wozniak, S. Molin, T. Tolker-Nielsen, N. Hoiby, M. Givskov, and T. Bjarnsholt. Phenotypes of non-attached pseudomonas aeruginosa aggregates resemble surface attached biofilm. *PLoS One*, 6(11): e27943, 2011. doi: 10.1371/journal.pone.0027943.

[226] X. Raynaud and N. Nunan. Spatial ecology of bacteria at the microscale in soil. *PLoS One*, 9(1):e87217, 2014. doi: 10.1371/journal.pone.0087217.

[227] K. Sauer, P. Stoodley, D. M. Goeres, L. Hall-Stoodley, M. Burmolle, P. S. Stewart, and T. Bjarnsholt. The biofilm life cycle: expanding the conceptual model of biofilm formation. *Nat Rev Microbiol*, 20(10):608–620, 2022. doi: 10.1038/s41579-022-00767-0.

[228] J. Jo, A. Price-Whelan, and L. E. P. Dietrich. Gradients and consequences of heterogeneity in biofilms. *Nat Rev Microbiol*, 2022. doi: 10.1038/s41579-022-00692-2.

[229] S. Elias and E. Banin. Multi-species biofilms: living with friendly neighbors. *FEMS Microbiol Rev*, 36(5):990–1004, 2012. doi: 10.1111/j.1574-6976.2012.00325.x.

[230] H. L. Roder, J. Herschend, J. Russel, M. F. Andersen, J. S. Madsen, S. J. Sorensen, and M. Burmolle. Enhanced bacterial mutualism through an evolved biofilm phenotype. *ISME J*, 12(11):2608–2618, 2018. doi: 10.1038/s41396-018-0165-2.

[231] M. Li, I. Le Trong, M. A. Carl, E. T. Larson, S. Chou, J. A. De Leon, S. L. Dove, R. E. Stenkamp, and J. D. Mougous. Structural basis for type vi secretion effector

recognition by a cognate immunity protein. *PLoS Pathog*, 8(4):e1002613, 2012. doi: 10.1371/journal.ppat.1002613.

[232] P. Williams and M. Camara. Quorum sensing and environmental adaptation in pseudomonas aeruginosa: a tale of regulatory networks and multifunctional signal molecules. *Curr Opin Microbiol*, 12(2):182–91, 2009. doi: 10.1016/j.mib.2009.01.005.

[233] K. Craig, B. R. Johnson, and A. Grunden. Leveraging pseudomonas stress response mechanisms for industrial applications. *Front Microbiol*, 12:660134, 2021. doi: 10.3389/fmicb.2021.660134.

[234] L. C. Simoes, I. B. Gomes, H. Sousa, A. Borges, and M. Simoes. Biofilm formation under high shear stress increases resilience to chemical and mechanical challenges. *Biofouling*, 38(1):1–12, 2022. doi: 10.1080/08927014.2021.2006189.

[235] Lakshmi Machineni. Effects of biotic and abiotic factors on biofilm growth dynamics and their heterogeneous response to antibiotic challenge. *Journal of Biosciences*, 45(1), 2020. doi: 10.1007/s12038-020-9990-3.

[236] Y. Cheng, J. K. H. Yam, Z. Cai, Y. Ding, L. H. Zhang, Y. Deng, and L. Yang. Population dynamics and transcriptomic responses of pseudomonas aeruginosa in a complex laboratory microbial community. *NPJ Biofilms Microbiomes*, 5(1):1, 2019. doi: 10.1038/s41522-018-0076-z.

[237] H. M. Kurkjian, M. J. Akbari, and B. Momeni. The impact of interactions on invasion and colonization resistance in microbial communities. *PLoS Comput Biol*, 17(1):e1008643, 2021. doi: 10.1371/journal.pcbi.1008643.

[238] C. Moser, P. O. Jensen, K. Thomsen, M. Kolpen, M. Rybtke, A. S. Lauland, H. Trostrup, and T. Tolker-Nielsen. Immune responses to pseudomonas aeruginosa biofilm infections. *Front Immunol*, 12:625597, 2021. doi: 10.3389/fimmu.2021.625597.

[239] W. Yin, Y. Wang, L. Liu, and J. He. Biofilms: The microbial "protective clothing" in extreme environments. *Int J Mol Sci*, 20(14), 2019. doi: 10.3390/ijms20143423.

[240] K. Sauer. The genomics and proteomics of biofilm formation. *Genome Biol*, 4(6):219, 2003. doi: 10.1186/gb-2003-4-6-219.

[241] P. Stoodley, K. Sauer, D. G. Davies, and J. W. Costerton. Biofilms as complex differentiated communities. *Annu Rev Microbiol*, 56:187–209, 2002. doi: 10.1146/annurev.micro.56.012302.160705.

[242] G. A. O'Toole and R. Kolter. Flagellar and twitching motility are necessary for pseudomonas aeruginosa biofilm development. *Mol Microbiol*, 30(2):295–304, 1998. doi: 10.1046/j.1365-2958.1998.01062.x.

[243] A. Boehm, M. Kaiser, H. Li, C. Spangler, C. A. Kasper, M. Ackermann, V. Kaever, V. Sourjik, V. Roth, and U. Jenal. Second messenger-mediated adjustment of bacterial swimming velocity. *Cell*, 141(1):107–16, 2010. doi: 10.1016/j.cell.2010.01.018.

[244] I. Hug, S. Deshpande, K. S. Sprecher, T. Pfohl, and U. Jenal. Second messenger-mediated tactile response by a bacterial rotary motor. *Science*, 358(6362):531–534, 2017. doi: 10.1126/science.aan5353.

[245] K. Gupta, C. N. Marques, O. E. Petrova, and K. Sauer. Antimicrobial tolerance of pseudomonas aeruginosa biofilms is activated during an early developmental stage and requires the two-component hybrid sags. *J Bacteriol*, 195(21):4975–87, 2013. doi: 10.1128/JB.00732-13.

[246] K. M. Colvin, Y. Irie, C. S. Tart, R. Urbano, J. C. Whitney, C. Ryder, P. L. Howell, D. J. Wozniak, and M. R. Parsek. The pel and psl polysaccharides provide pseudomonas aeruginosa structural redundancy within the biofilm matrix. *Environ Microbiol*, 14(8): 1913–28, 2012. doi: 10.1111/j.1462-2920.2011.02657.x.

[247] Aishwarya Vetrivel, Monica Ramasamy, Preethi Vetrivel, Santhi Natchimuthu, Shobana Arunachalam, Gon-Sup Kim, and Rajeswari Murugesan. Pseudomonas aeruginosa biofilm formation and its control. *Biologics*, 1(3):312–336, 2021. doi: 10.3390/biologics1030019.

[248] A. Penesyan, I. T. Paulsen, S. Kjelleberg, and M. R. Gillings. Three faces of biofilms: a microbial lifestyle, a nascent multicellular organism, and an incubator for diversity. *NPJ Biofilms Microbiomes*, 7(1):80, 2021. doi: 10.1038/s41522-021-00251-2.

[249] L. K. Jennings, J. E. Dreifus, C. Reichhardt, K. M. Storek, P. R. Secor, D. J. Wozniak, K. B. Hisert, and M. R. Parsek. Pseudomonas aeruginosa aggregates in cystic fibrosis sputum produce exopolysaccharides that likely impede current therapies. *Cell Rep*, 34(8): 108782, 2021. doi: 10.1016/j.celrep.2021.108782.

[250] Anna Christine Trego, Simon Mills, and Gavin Collins. Granular biofilms: Function, application, and new trends as model microbial communities. *Critical Reviews in Environmental Science and Technology*, 51(15):1702–1725, 2020. doi: 10.1080/10643389.2020.1769433.

[251] D. Lebeaux, A. Chauhan, O. Rendueles, and C. Beloin. From in vitro to in vivo models of bacterial biofilm-related infections. *Pathogens*, 2(2):288–356, 2013. doi: 10.3390/pathogens2020288.

[252] D. Schleheck, N. Barraud, J. Klebensberger, J. S. Webb, D. McDougald, S. A. Rice, and S. Kjelleberg. Pseudomonas aeruginosa pao1 preferentially grows as aggregates in liquid batch cultures and disperses upon starvation. *PLoS One*, 4(5):e5513, 2009. doi: 10.1371/journal.pone.0005513.

[253] L. Hall-Stoodley, J. W. Costerton, and P. Stoodley. Bacterial biofilms: from the natural environment to infectious diseases. *Nat Rev Microbiol*, 2(2):95–108, 2004. doi: 10.1038/nrmicro821.

[254] P. R. Secor, L. A. Michaels, A. Ratjen, L. K. Jennings, and P. K. Singh. Entropically driven aggregation of bacteria by host polymers promotes antibiotic tolerance in

pseudomonas aeruginosa. *Proc Natl Acad Sci U S A*, 115(42):10780–10785, 2018. doi: 10.1073/pnas.1806005115.

[255] K. N. Kragh, J. B. Hutchison, G. Melaugh, C. Rodesney, A. E. Roberts, Y. Irie, P. O. Jensen, S. P. Diggle, R. J. Allen, V. Gordon, and T. Bjarnsholt. Role of multicellular aggregates in biofilm formation. *mBio*, 7(2):e00237, 2016. doi: 10.1128/mBio.00237-16.

[256] A. Bidossi, M. Bottagisio, P. Savadori, and E. De Vecchi. Identification and characterization of planktonic biofilm-like aggregates in infected synovial fluids from joint infections. *Front Microbiol*, 11:1368, 2020. doi: 10.3389/fmicb.2020.01368.

[257] S. Dastgheyb, J. Parvizi, I. M. Shapiro, N. J. Hickok, and M. Otto. Effect of biofilms on recalcitrance of staphylococcal joint infection to antibiotic treatment. *J Infect Dis*, 211 (4):641–50, 2015. doi: 10.1093/infdis/jiu514.

[258] H. C. Flemming and J. Wingender. The biofilm matrix. *Nat Rev Microbiol*, 8(9):623–33, 2010. doi: 10.1038/nrmicro2415.

[259] L. Karygianni, Z. Ren, H. Koo, and T. Thurnheer. Biofilm matrixome: Extracellular components in structured microbial communities. *Trends Microbiol*, 28(8):668–681, 2020. doi: 10.1016/j.tim.2020.03.016.

[260] E. E. Mann and D. J. Wozniak. Pseudomonas biofilm matrix composition and niche biology. *FEMS Microbiol Rev*, 36(4):893–916, 2012. doi: 10.1111/j.1574-6976.2011.00322.x.

[261] L. Hobley, C. Harkins, C. E. MacPhee, and N. R. Stanley-Wall. Giving structure to the biofilm matrix: an overview of individual strategies and emerging common themes. *FEMS Microbiol Rev*, 39(5):649–69, 2015. doi: 10.1093/femsre/fuv015.

[262] R. Singh, S. Sahore, P. Kaur, A. Rani, and P. Ray. Penetration barrier contributes to bacterial biofilm-associated resistance against only select antibiotics, and exhibits genus-, strain- and antibiotic-specific differences. *Pathog Dis*, 74(6), 2016. doi: 10.1093/femspd/ftw056.

[263] N. Billings, M. Millan, M. Caldara, R. Rusconi, Y. Tarasova, R. Stocker, and K. Ribbeck. The extracellular matrix component psl provides fast-acting antibiotic defense in pseudomonas aeruginosa biofilms. *PLoS Pathog*, 9(8):e1003526, 2013. doi: 10.1371/journal.ppat.1003526.

[264] J. Toska, B. T. Ho, and J. J. Mekalanos. Exopolysaccharide protects vibrio cholerae from exogenous attacks by the type 6 secretion system. *Proc Natl Acad Sci U S A*, 115(31): 7997–8002, 2018. doi: 10.1073/pnas.1808469115.

[265] B. W. Peterson, Y. He, Y. Ren, A. Zerdoum, M. R. Libera, P. K. Sharma, A. J. van Winkelhoff, D. Neut, P. Stoodley, H. C. van der Mei, and H. J. Busscher. Viscoelasticity of biofilms and their recalcitrance to mechanical and chemical challenges. *FEMS Microbiol Rev*, 39(2):234–45, 2015. doi: 10.1093/femsre/fuu008.

[266] E. S. Gloag, S. Fabbri, D. J. Wozniak, and P. Stoodley. Biofilm mechanics: Implications in infection and survival. *Biofilm*, 2:100017, 2020. doi: 10.1016/j.bioflm.2019.100017.

[267] Z. Qin, L. Yang, D. Qu, S. Molin, and T. Tolker-Nielsen. Pseudomonas aeruginosa extracellular products inhibit staphylococcal growth, and disrupt established biofilms produced by staphylococcus epidermidis. *Microbiology (Reading)*, 155(Pt 7):2148–2156, 2009. doi: 10.1099/mic.0.028001-0.

[268] A. Ghafoor, I. D. Hay, and B. H. Rehm. Role of exopolysaccharides in pseudomonas aeruginosa biofilm formation and architecture. *Appl Environ Microbiol*, 77(15):5238–46, 2011. doi: 10.1128/AEM.00637-11.

[269] Iain D. Hay, Zahid Ur Rehman, Aamir Ghafoor, and Bernd H. A. Rehm. Bacterial biosynthesis of alginates. *Journal of Chemical Technology and Biotechnology*, 85(6):752–759, 2010. doi: 10.1002/jctb.2372.

[270] W. S. Chang, M. van de Mortel, L. Nielsen, G. Nino de Guzman, X. Li, and L. J. Halverson. Alginate production by pseudomonas putida creates a hydrated microenvironment and contributes to biofilm architecture and stress tolerance under water-limiting conditions. *J Bacteriol*, 189(22):8290–9, 2007. doi: 10.1128/JB.00727-07.

[271] R. G. Doggett. Incidence of mucoid pseudomonas aeruginosa from clinical sources. *Appl Microbiol*, 18(5):936–7, 1969. doi: 10.1128/am.18.5.936-937.1969.

[272] M. Hentzer, G. M. Teitzel, G. J. Balzer, A. Heydorn, S. Molin, M. Givskov, and M. R. Parsek. Alginate overproduction affects pseudomonas aeruginosa biofilm structure and function. *J Bacteriol*, 183(18):5395–401, 2001. doi: 10.1128/JB.183.18.5395-5401.2001.

[273] D. J. Wozniak, T. J. Wyckoff, M. Starkey, R. Keyser, P. Azadi, G. A. O'Toole, and M. R. Parsek. <pnas.1231792100.pdf>. *Proc Natl Acad Sci U S A*, 100(13):7907–12, 2003. doi: 10.1073/pnas.1231792100.

[274] S. Periasamy, H. A. Nair, K. W. Lee, J. Ong, J. Q. Goh, S. Kjelleberg, and S. A. Rice. Pseudomonas aeruginosa pao1 exopolysaccharides are important for mixed species biofilm community development and stress tolerance. *Front Microbiol*, 6:851, 2015. doi: 10.3389/fmicb.2015.00851.

[275] S. L. Heltshe, U. Khan, V. Beckett, A. Baines, J. Emerson, D. B. Sanders, R. L. Gibson, W. Morgan, and M. Rosenfeld. Longitudinal development of initial, chronic and mucoid pseudomonas aeruginosa infection in young children with cystic fibrosis. *J Cyst Fibros*, 17 (3):341–347, 2018. doi: 10.1016/j.jcf.2017.10.008.

[276] J. A. Simpson, S. E. Smith, and R. T. Dean. <mic-134-1-29.pdf>. *J Gen Microbiol*, 134 (1):29–36, 1988. doi: 10.1099/00221287-134-1-29.

[277] J. G. Leid, C. J. Willson, M. E. Shirtliff, D. J. Hassett, M. R. Parsek, and A. K. Jeffers. The exopolysaccharide alginate protects pseudomonas aeruginosa biofilm bacteria from ifn-gamma-mediated macrophage killing. *J Immunol*, 175(11):7512–8, 2005. doi: 10.4049/jimmunol.175.11.7512.

[278] C. A. McCaslin, D. N. Petrusca, C. Poirier, K. A. Serban, G. G. Anderson, and I. Petrache. Impact of alginate-producing pseudomonas aeruginosa on alveolar macrophage apoptotic cell clearance. *J Cyst Fibros*, 14(1):70–77, 2015. doi: 10.1016/j.jcf.2014.06.009.

[279] Z. Pang, R. Raudonis, B. R. Glick, T. J. Lin, and Z. Cheng. Antibiotic resistance in pseudomonas aeruginosa: mechanisms and alternative therapeutic strategies. *Biotechnol Adv*, 37(1):177–192, 2019. doi: 10.1016/j.biotechadv.2018.11.013.

[280] B. Cao, L. Christophersen, K. Thomsen, M. Sonderholm, T. Bjarnsholt, P. O. Jensen, N. Hoiby, and C. Moser. Antibiotic penetration and bacterial killing in a pseudomonas aeruginosa biofilm model. *J Antimicrob Chemother*, 70(7):2057–63, 2015. doi: 10.1093/jac/dkv058.

[281] Giovanna Pulcrano, Dora Vita Iula, Valeria Raia, Fabio Rossano, and Maria Rosaria Catania. Different mutations in muca gene of pseudomonas aeruginosa mucoid strains in cystic fibrosis patients and their effect on algu gene expression. *NEW MICROBIOLOGICA*, (35):295–305, 2012.

[282] A. D. Valderrey, M. J. Pozuelo, P. A. Jimenez, M. D. Macia, A. Oliver, and R. Rotger. Chronic colonization by pseudomonas aeruginosa of patients with obstructive lung diseases: cystic fibrosis, bronchiectasis, and chronic obstructive pulmonary disease. *Diagn Microbiol Infect Dis*, 68(1):20–7, 2010. doi: 10.1016/j.diagmicrobio.2010.04.008.

[283] I. Y. Jung, S. J. Jeong, K. M. Lee, J. Y. Ahn, N. S. Ku, S. H. Han, J. Y. Choi, D. Yong, S. S. Yoon, Y. G. Song, S. H. Jeong, J. M. Kim, and K. Lee. Risk factors for mortality in patients with pseudomonas aeruginosa pneumonia: Clinical impact of muca gene mutation. *Respir Med*, 140:27–31, 2018. doi: 10.1016/j.rmed.2018.05.017.

[284] N. Candido Cacador, C. Paulino da Costa Capizzani, L. A. Gomes Monteiro Marin Torres, R. Galetti, O. Ciofu, A. L. da Costa Darini, and N. Hoiby. Adaptation of pseudomonas aeruginosa to the chronic phenotype by mutations in the algtmucabd operon in isolates from brazilian cystic fibrosis patients. *PLoS One*, 13(11):e0208013, 2018. doi: 10.1371/journal.pone.0208013.

[285] R. La Rosa, E. Rossi, A. M. Feist, H. K. Johansen, and S. Molin. Compensatory evolution of pseudomonas aeruginosa's slow growth phenotype suggests mechanisms of adaptation in cystic fibrosis. *Nat Commun*, 12(1):3186, 2021. doi: 10.1038/s41467-021-23451-y.

[286] W. Wu, H. Badrane, S. Arora, H. V. Baker, and S. Jin. Muca-mediated coordination of type iii secretion and alginate synthesis in pseudomonas aeruginosa. *J Bacteriol*, 186(22): 7575–85, 2004. doi: 10.1128/JB.186.22.7575-7585.2004.

[287] V. Decoin, M. Gallique, C. Barbey, F. Le Mauff, C. D. Poc, M. G. Feuilloley, N. Orange, and A. Merieau. A pseudomonas fluorescens type 6 secretion system is related to mucoidy, motility and bacterial competition. *BMC Microbiol*, 15:72, 2015. doi: 10.1186/s12866-015-0405-9.

[288] W. Panmanee, S. Su, M. J. Schurr, G. W. Lau, X. Zhu, Z. Ren, C. T. McDaniel, L. J. Lu, D. E. Ohman, D. A. Muruve, R. J. Panos, H. D. Yu, T. B. Thompson, B. S. Tseng, and D. J. Hassett. The anti-sigma factor muca of pseudomonas aeruginosa: Dramatic differences of a muca22 vs. a deltamuca mutant in anaerobic acidified nitrite sensitivity of planktonic and biofilm bacteria in vitro and during chronic murine lung infection. *PLoS One*, 14(6):e0216401, 2019. doi: 10.1371/journal.pone.0216401.

[289] M. S. Byrd, I. Sadovskaya, E. Vinogradov, H. Lu, A. B. Sprinkle, S. H. Richardson, L. Ma, B. Ralston, M. R. Parsek, E. M. Anderson, J. S. Lam, and D. J. Wozniak. Genetic and biochemical analyses of the pseudomonas aeruginosa psl exopolysaccharide reveal overlapping roles for polysaccharide synthesis enzymes in psl and lps production. *Mol Microbiol*, 73(4):622–38, 2009. doi: 10.1111/j.1365-2958.2009.06795.x.

[290] L. Friedman and R. Kolter. Two genetic loci produce distinct carbohydrate-rich structural components of the pseudomonas aeruginosa biofilm matrix. *J Bacteriol*, 186(14):4457–65, 2004. doi: 10.1128/JB.186.14.4457-4465.2004.

[291] K. D. Jackson, M. Starkey, S. Kremer, M. R. Parsek, and D. J. Wozniak. Identification of psl, a locus encoding a potential exopolysaccharide that is essential for pseudomonas aeruginosa pao1 biofilm formation. *J Bacteriol*, 186(14):4466–75, 2004. doi: 10.1128/JB.186.14.4466-4475.2004.

[292] L. Ma, M. Conover, H. Lu, M. R. Parsek, K. Bayles, and D. J. Wozniak. Assembly and development of the pseudomonas aeruginosa biofilm matrix. *PLoS Pathog*, 5(3):e1000354, 2009. doi: 10.1371/journal.ppat.1000354.

[293] S. C. Chew, B. Kundukad, T. Seviour, J. R. van der Maarel, L. Yang, S. A. Rice, P. Doyle, and S. Kjelleberg. Dynamic remodeling of microbial biofilms by functionally distinct exopolysaccharides. *mBio*, 5(4):e01536–14, 2014. doi: 10.1128/mBio.01536-14.

[294] L. Ma, K. D. Jackson, R. M. Landry, M. R. Parsek, and D. J. Wozniak. Analysis of pseudomonas aeruginosa conditional psl variants reveals roles for the psl polysaccharide in adhesion and maintaining biofilm structure postattachment. *J Bacteriol*, 188(23):8213–21, 2006. doi: 10.1128/JB.01202-06.

[295] J. Overhage, M. Schemionek, J. S. Webb, and B. H. Rehm. Expression of the psl operon in pseudomonas aeruginosa pao1 biofilms: Psla performs an essential function in biofilm formation. *Appl Environ Microbiol*, 71(8):4407–13, 2005. doi: 10.1128/AEM.71.8.4407-4413.2005.

[296] Y. Irie, B. R. Borlee, J. R. O'Connor, P. J. Hill, C. S. Harwood, D. J. Wozniak, and M. R. Parsek. Self-produced exopolysaccharide is a signal that stimulates biofilm formation in pseudomonas aeruginosa. *Proc Natl Acad Sci U S A*, 109(50):20632–6, 2012. doi: 10.1073/pnas.1217993109.

[297] K. M. Colvin, V. D. Gordon, K. Murakami, B. R. Borlee, D. J. Wozniak, G. C. Wong, and M. R. Parsek. The pel polysaccharide can serve a structural and protective role in

the biofilm matrix of pseudomonas aeruginosa. *PLoS Pathog*, 7(1):e1001264, 2011. doi: 10.1371/journal.ppat.1001264.

[298] M. S. Byrd, B. Pang, M. Mishra, W. E. Swords, and D. J. Wozniak. The pseudomonas aeruginosa exopolysaccharide psl facilitates surface adherence and nf-kappab activation in a549 cells. *mBio*, 1(3), 2010. doi: 10.1128/mBio.00140-10.

[299] Y. Irie, A. E. L. Roberts, K. N. Kragh, V. D. Gordon, J. Hutchison, R. J. Allen, G. Melaugh, T. Bjarnsholt, S. A. West, and S. P. Diggle. The pseudomonas aeruginosa psl polysaccharide is a social but noncheatable trait in biofilms. *mBio*, 8(3), 2017. doi: 10.1128/mBio.00374-17.

[300] U. Singkham-In, P. Phuengmaung, J. Makjaroen, W. Saisorn, T. Bhunyakarnjanarat, T. Chatsuwan, C. Chirathaworn, W. Chancharoenthana, and A. Leelahavanichkul. Chlorhexidine promotes psl expression in pseudomonas aeruginosa that enhances cell aggregation with preserved pathogenicity demonstrates an adaptation against antiseptic. *Int J Mol Sci*, 23(15), 2022. doi: 10.3390/ijms23158308.

[301] S. N. Stoner, J. J. Baty, and J. A. Scoffield. Pseudomonas aeruginosa polysaccharide psl supports airway microbial community development. *ISME J*, 16(7):1730–1739, 2022. doi: 10.1038/s41396-022-01221-y.

[302] J. Wang, X. Liu, K. Yu, M. Liu, J. Qu, Y. Liu, Z. Cai, K. Wang, C. Zhuo, L. Yang, and Y. Zhang. Psl-dependent cooperation contributes to drug resistance of pseudomonas aeruginosa in dual-species biofilms with acinetobacter baumannii. *ACS Infect Dis*, 8(1): 129–136, 2022. doi: 10.1021/acsinfecdis.1c00416.

[303] M. Mishra, M. S. Byrd, S. Sergeant, A. K. Azad, M. R. Parsek, L. McPhail, L. S. Schlesinger, and D. J. Wozniak. Pseudomonas aeruginosa psl polysaccharide reduces neutrophil phagocytosis and the oxidative response by limiting complement-mediated opsonization. *Cell Microbiol*, 14(1):95–106, 2012. doi: 10.1111/j.1462-5822.2011.01704.x.

[304] A. J. Morris, L. Jackson, Y. Cw Yau, C. Reichhardt, T. Beaudoin, S. Uwumarenogie, K. M. Guttman, P. Lynne Howell, M. R. Parsek, L. R. Hoffman, D. Nguyen, A. DiGiandomenico, D. S. Guttman, D. J. Wozniak, and V. J. Waters. The role of psl in the failure to eradicate pseudomonas aeruginosa biofilms in children with cystic fibrosis. *NPJ Biofilms Microbiomes*, 7(1):63, 2021. doi: 10.1038/s41522-021-00234-3.

[305] V. A. Ray, P. J. Hill, C. K. Stover, S. Roy, C. K. Sen, L. Yu, D. J. Wozniak, and A. DiGiandomenico. Anti-psl targeting of pseudomonas aeruginosa biofilms for neutrophil-mediated disruption. *Sci Rep*, 7(1):16065, 2017. doi: 10.1038/s41598-017-16215-6.

[306] L. K. Jennings, K. M. Storek, H. E. Ledvina, C. Coulon, L. S. Marmont, I. Sadovskaya, P. R. Secor, B. S. Tseng, M. Scian, A. Filloux, D. J. Wozniak, P. L. Howell, and M. R. Parsek. Pel is a cationic exopolysaccharide that cross-links extracellular dna in the pseudomonas aeruginosa biofilm matrix. *Proc Natl Acad Sci U S A*, 112(36):11353–8, 2015. doi: 10.1073/pnas.1503058112.

[307] L. Friedman and R. Kolter. Genes involved in matrix formation in pseudomonas aeruginosa pa14 biofilms. *Mol Microbiol*, 51(3):675–90, 2004. doi: 10.1046/j.1365-2958.2003.03877.x.

[308] P. Vasseur, I. Vallet-Gely, C. Soscia, S. Genin, and A. Filloux. The pel genes of the pseudomonas aeruginosa pak strain are involved at early and late stages of biofilm formation. *Microbiology (Reading)*, 151(Pt 3):985–997, 2005. doi: 10.1099/mic.0.27410-0.

[309] E. S. Gloag, G. K. German, P. Stoodley, and D. J. Wozniak. Viscoelastic properties of pseudomonas aeruginosa variant biofilms. *Sci Rep*, 8(1):9691, 2018. doi: 10.1038/s41598-018-28009-5.

[310] B. Yang, Y. Jiang, Y. Jin, F. Bai, Z. Cheng, and W. Wu. Pseudomonas aeruginosa oligoribonuclease controls tolerance to polymyxin b by regulating pel exopolysaccharide production. *Antimicrob Agents Chemother*, 66(3):e0207221, 2022. doi: 10.1128/AAC.02072-21.

[311] C. B. Whitchurch, T. Tolker-Nielsen, P. C. Ragas, and J. S. Mattick. Extracellular dna required for bacterial biofilm formation. *Science*, 295(5559):1487, 2002. doi: 10.1126/science.295.5559.1487.

[312] E. Secchi, G. Savorana, A. Vitale, L. Eberl, R. Stocker, and R. Rusconi. The structural role of bacterial edna in the formation of biofilm streamers. *Proc Natl Acad Sci U S A*, 119(12):e2113723119, 2022. doi: 10.1073/pnas.2113723119.

[313] D. M. Dominiak, J. L. Nielsen, and P. H. Nielsen. Extracellular dna is abundant and important for microcolony strength in mixed microbial biofilms. *Environ Microbiol*, 13(3): 710–21, 2011. doi: 10.1111/j.1462-2920.2010.02375.x.

[314] S. Wang, X. Liu, H. Liu, L. Zhang, Y. Guo, S. Yu, D. J. Wozniak, and L. Z. Ma. The exopolysaccharide psl-edna interaction enables the formation of a biofilm skeleton in pseudomonas aeruginosa. *Environ Microbiol Rep*, 7(2):330–40, 2015. doi: 10.1111/1758-2229.12252.

[315] E. S. Gloag, L. Turnbull, A. Huang, P. Vallotton, H. Wang, L. M. Nolan, L. Mililli, C. Hunt, J. Lu, S. R. Osvath, L. G. Monahan, R. Cavaliere, I. G. Charles, M. P. Wand, M. L. Gee, R. Prabhakar, and C. B. Whitchurch. Self-organization of bacterial biofilms is facilitated by extracellular dna. *Proc Natl Acad Sci U S A*, 110(28):11541–6, 2013. doi: 10.1073/pnas.1218898110.

[316] Søren Molin and Tim Tolker-Nielsen. Gene transfer occurs with enhanced efficiency in biofilms and induces enhanced stabilisation of the biofilm structure. *Current Opinion in Biotechnology*, 14(3):255–261, 2003. doi: 10.1016/s0958-1669(03)00036-3.

[317] J. M. Ghigo. Natural conjugative plasmids induce bacterial biofilm development. *Nature*, 412(6845):442–5, 2001. doi: 10.1038/35086581.

[318] LM Nolan, L Turnbull, M Katrib, SR Osvath, D Losa, JJ Lazenby, and CB Whitchurch. Pseudomonas aeruginosa is capable of natural transformation in

biofilms. *Microbiology*, 10:995–1003, 2020. doi: 10.1099/mic.0.000956. URL http://dx.doi.org/10.1099/mic.0.000956.

[319] T. Das, S. Sehar, L. Koop, Y. K. Wong, S. Ahmed, K. S. Siddiqui, and M. Manefield. Influence of calcium in extracellular dna mediated bacterial aggregation and biofilm formation. *PLoS One*, 9(3):e91935, 2014. doi: 10.1371/journal.pone.0091935.

[320] M. Wilton, L. Charron-Mazenod, R. Moore, and S. Lewenza. Extracellular dna acidifies biofilms and induces aminoglycoside resistance in pseudomonas aeruginosa. *Antimicrob Agents Chemother*, 60(1):544–53, 2016. doi: 10.1128/AAC.01650-15.

[321] W. C. Chiang, M. Nilsson, P. O. Jensen, N. Hoiby, T. E. Nielsen, M. Givskov, and T. Tolker-Nielsen. Extracellular dna shields against aminoglycosides in pseudomonas aeruginosa biofilms. *Antimicrob Agents Chemother*, 57(5):2352–61, 2013. doi: 10.1128/AAC.00001-13.

[322] L. Turnbull, M. Toyofuku, A. L. Hynen, M. Kurosawa, G. Pessi, N. K. Petty, S. R. Osvath, G. Carcamo-Oyarce, E. S. Gloag, R. Shimoni, U. Omasits, S. Ito, X. Yap, L. G. Monahan, R. Cavaliere, C. H. Ahrens, I. G. Charles, N. Nomura, L. Eberl, and C. B. Whitchurch. Explosive cell lysis as a mechanism for the biogenesis of bacterial membrane vesicles and biofilms. *Nat Commun*, 7:11220, 2016. doi: 10.1038/ncomms11220.

[323] S. Sarkar. Release mechanisms and molecular interactions of pseudomonas aeruginosa extracellular dna. *Appl Microbiol Biotechnol*, 104(15):6549–6564, 2020. doi: 10.1007/s00253-020-10687-9.

[324] A. L. Ibanez de Aldecoa, O. Zafra, and J. E. Gonzalez-Pastor. Mechanisms and regulation of extracellular dna release and its biological roles in microbial communities. *Front Microbiol*, 8:1390, 2017. doi: 10.3389/fmicb.2017.01390.

[325] B. R. Borlee, A. D. Goldman, K. Murakami, R. Samudrala, D. J. Wozniak, and M. R. Parsek. Pseudomonas aeruginosa uses a cyclic-di-gmp-regulated adhesin to reinforce the biofilm extracellular matrix. *Mol Microbiol*, 75(4):827–42, 2010. doi: 10.1111/j.1365-2958.2009.06991.x.

[326] C. Reichhardt, H. M. Jacobs, M. Matwichuk, C. Wong, D. J. Wozniak, and M. R. Parsek. The versatile pseudomonas aeruginosa biofilm matrix protein cdra promotes aggregation through different extracellular exopolysaccharide interactions. *J Bacteriol*, 202(19), 2020. doi: 10.1128/JB.00216-20.

[327] C. Reichhardt, C. Wong, D. Passos da Silva, D. J. Wozniak, and M. R. Parsek. Cdra interactions within the pseudomonas aeruginosa biofilm matrix safeguard it from proteolysis and promote cellular packing. *mBio*, 9(5), 2018. doi: 10.1128/mBio.01376-18.

[328] J. J. Harrison, H. Almblad, Y. Irie, D. J. Wolter, H. C. Eggleston, T. E. Randall, J. O. Kitzman, B. Stackhouse, J. C. Emerson, S. McNamara, T. J. Larsen, J. Shendure, L. R. Hoffman, D. J. Wozniak, and M. R. Parsek. Elevated exopolysaccharide levels in

pseudomonas aeruginosa flagellar mutants have implications for biofilm growth and chronic infections. *PLoS Genet*, 16(6):e1008848, 2020. doi: 10.1371/journal.pgen.1008848.

[329] M. Kilian, I. L. Chapple, M. Hannig, P. D. Marsh, V. Meuric, A. M. Pedersen, M. S. Tonetti, W. G. Wade, and E. Zaura. The oral microbiome - an update for oral healthcare professionals. *Br Dent J*, 221(10):657–666, 2016. doi: 10.1038/sj.bdj.2016.865.

[330] D. N. Frank and N. R. Pace. Gastrointestinal microbiology enters the metagenomics era. *Curr Opin Gastroenterol*, 24(1):4–10, 2008. doi: 10.1097/MOG.0b013e3282f2b0e8.

[331] K. Bisht, J. Baishya, and C. A. Wakeman. Pseudomonas aeruginosa polymicrobial interactions during lung infection. *Curr Opin Microbiol*, 53:1–8, 2020. doi: 10.1016/j.mib.2020.01.014.

[332] F. J. Whelan, B. Waddell, S. A. Syed, S. Shekarriz, H. R. Rabin, M. D. Parkins, and M. G. Surette. Culture-enriched metagenomic sequencing enables in-depth profiling of the cystic fibrosis lung microbiota. *Nat Microbiol*, 5(2):379–390, 2020. doi: 10.1038/s41564-019-0643-y.

[333] R. A. Khanolkar, S. T. Clark, P. W. Wang, D. M. Hwang, Y. C. W. Yau, V. J. Waters, and D. S. Guttman. Ecological succession of polymicrobial communities in the cystic fibrosis airways. *mSystems*, 5(6), 2020. doi: 10.1128/mSystems.00809-20.

[334] D. Rodriguez Amor and M. Dal Bello. Bottom-up approaches to synthetic cooperation in microbial communities. *Life (Basel)*, 9(1), 2019. doi: 10.3390/life9010022.

[335] A. M. Sousa, I. Machado, A. Nicolau, and M. O. Pereira. Improvements on colony morphology identification towards bacterial profiling. *J Microbiol Methods*, 95(3):327–35, 2013. doi: 10.1016/j.mimet.2013.09.020.

[336] A. M. Sousa, M. O. Pereira, and A. Lourenco. Morphocol: An ontology-based knowledgebase for the characterisation of clinically significant bacterial colony morphologies. *J Biomed Inform*, 55:55–63, 2015. doi: 10.1016/j.jbi.2015.03.007.

[337] G. Carvalho, D. Balestrino, C. Forestier, and J. D. Mathias. How do environment-dependent switching rates between susceptible and persister cells affect the dynamics of biofilms faced with antibiotics? *NPJ Biofilms Microbiomes*, 4:6, 2018. doi: 10.1038/s41522-018-0049-2.

[338] L. Kern, S. K. Abdeen, A. A. Kolodziejczyk, and E. Elinav. Commensal inter-bacterial interactions shaping the microbiota. *Curr Opin Microbiol*, 63:158–171, 2021. doi: 10.1016/j.mib.2021.07.011.

[339] W. Harcombe. Novel cooperation experimentally evolved between species. *Evolution*, 64 (7):2166–72, 2010. doi: 10.1111/j.1558-5646.2010.00959.x.

[340] S. Rakoff-Nahoum, K. R. Foster, and L. E. Comstock. The evolution of cooperation within the gut microbiota. *Nature*, 533(7602):255–9, 2016. doi: 10.1038/nature17626.

[341] H. Bachmann, F. J. Bruggeman, D. Molenaar, F. Branco Dos Santos, and B. Teusink. Public goods and metabolic strategies. *Curr Opin Microbiol*, 31:109–115, 2016. doi: 10.1016/j.mib.2016.03.007.

[342] O. X. Cordero, L. A. Ventouras, E. F. DeLong, and M. F. Polz. Public good dynamics drive evolution of iron acquisition strategies in natural bacterioplankton populations. *Proc Natl Acad Sci U S A*, 109(49):20059–64, 2012. doi: 10.1073/pnas.1213344109.

[343] J. D. Palmer and K. R. Foster. <science.abn5093.pdf>. *Science*, 376(6593):581–582, 2022. doi: 10.1126/science.abn5093.

[344] K. Z. Coyte, J. Schluter, and K. R. Foster. The ecology of the microbiome: Networks, competition, and stability. *Science*, 350(6261):663–6, 2015. doi: 10.1126/science.aad2602.

[345] H. J. Wu and E. Wu. The role of gut microbiota in immune homeostasis and autoimmunity. *Gut Microbes*, 3(1):4–14, 2012. doi: 10.4161/gmic.19320.

[346] F. Malard, J. Dore, B. Gaugler, and M. Mohty. Introduction to host microbiome symbiosis in health and disease. *Mucosal Immunol*, 14(3):547–554, 2021. doi: 10.1038/s41385-020-00365-4.

[347] A. I. Celis and D. A. Relman. Competitors versus collaborators: Micronutrient processing by pathogenic and commensal human-associated gut bacteria. *Mol Cell*, 78(4):570–576, 2020. doi: 10.1016/j.molcel.2020.03.032.

[348] E. H. Crost, L. E. Tailford, G. Le Gall, M. Fons, B. Henrissat, and N. Juge. Utilisation of mucin glycans by the human gut symbiont ruminococcus gnavus is strain-dependent. *PLoS One*, 8(10):e76341, 2013. doi: 10.1371/journal.pone.0076341.

[349] A. F. Rosenthal, J. S. Griffin, M. Wagner, A. I. Packman, O. Balogun, and G. F. Wells. Morphological analysis of pore size and connectivity in a thick mixed-culture biofilm. *Biotechnol Bioeng*, 115(9):2268–2279, 2018. doi: 10.1002/bit.26729.

[350] C. Lambert, K. A. Morehouse, C. Y. Chang, and R. E. Sockett. Bdellovibrio: growth and development during the predatory cycle. *Curr Opin Microbiol*, 9(6):639–44, 2006. doi: 10.1016/j.mib.2006.10.002.

[351] S. B. Peterson, S. K. Bertolli, and J. D. Mougous. The central role of interbacterial antagonism in bacterial life. *Curr Biol*, 30(19):R1203–R1214, 2020. doi: 10.1016/j.cub.2020.06.103.

[352] E. T. Granato, T. A. Meiller-Legrand, and K. R. Foster. The evolution and ecology of bacterial warfare. *Curr Biol*, 29(11):R521–R537, 2019. doi: 10.1016/j.cub.2019.04.024.

[353] D. Gonzalez and D. A. I. Mavridou. Making the best of aggression: The many dimensions of bacterial toxin regulation. *Trends Microbiol*, 27(11):897–905, 2019. doi: 10.1016/j.tim.2019.05.009.

[354] L. P. Allsopp, P. Bernal, L. M. Nolan, and A. Filloux. Causalities of war: The connection between type vi secretion system and microbiota. *Cell Microbiol*, 22(3):e13153, 2020. doi: 10.1111/cmi.13153.

[355] S. Heilbronner, B. Krismer, H. Brotz-Oesterhelt, and A. Peschel. The microbiome-shaping roles of bacteriocins. *Nat Rev Microbiol*, 19(11):726–739, 2021. doi: 10.1038/s41579-021-00569-w.

[356] S. J. Hersch, K. Manera, and T. G. Dong. Defending against the type six secretion system: beyond immunity genes. *Cell Rep*, 33(2):108259, 2020. doi: 10.1016/j.celrep.2020.108259.

[357] A. T. Nguyen, J. W. Jones, M. Camara, P. Williams, M. A. Kane, and A. G. Oglesby-Sherrouse. Cystic fibrosis isolates of pseudomonas aeruginosa retain iron-regulated antimicrobial activity against staphylococcus aureus through the action of multiple alkylquinolones. *Front Microbiol*, 7:1171, 2016. doi: 10.3389/fmicb.2016.01171.

[358] T. E. Wood, S. A. Howard, A. Forster, L. M. Nolan, E. Manoli, N. P. Bullen, H. C. L. Yau, A. Hachani, R. D. Hayward, J. C. Whitney, W. Vollmer, P. S. Freemont, and A. Filloux. The pseudomonas aeruginosa t6ss delivers a periplasmic toxin that disrupts bacterial cell morphology. *Cell Rep*, 29(1):187–201 e7, 2019. doi: 10.1016/j.celrep.2019.08.094.

[359] S. S. Abby, J. Cury, J. Guglielmini, B. Neron, M. Touchon, and E. P. Rocha. Identification of protein secretion systems in bacterial genomes. *Sci Rep*, 6:23080, 2016. doi: 10.1038/srep23080.

[360] J. Grijpstra, J. Arenas, L. Rutten, and J. Tommassen. Autotransporter secretion: varying on a theme. *Res Microbiol*, 164(6):562–82, 2013. doi: 10.1016/j.resmic.2013.03.010.

[361] I. Meuskens, A. Saragliadis, J. C. Leo, and D. Linke. Type v secretion systems: An overview of passenger domain functions. *Front Microbiol*, 10:1163, 2019. doi: 10.3389/fmicb.2019.01163.

[362] J. P. Allen and A. R. Hauser. Diversity of contact-dependent growth inhibition systems of pseudomonas aeruginosa. *J Bacteriol*, 201(14), 2019. doi: 10.1128/JB.00776-18.

[363] S. K. Aoki, R. Pamma, A. D. Hernday, J. E. Bickham, B. A. Braaten, and D. A. Low. Contact-dependent inhibition of growth in escherichia coli. *Science*, 309(5738):1245–8, 2005. doi: 10.1126/science.1115109.

[364] S. K. Aoki, E. J. Diner, C. T. de Roodenbeke, B. R. Burgess, S. J. Poole, B. A. Braaten, A. M. Jones, J. S. Webb, C. S. Hayes, P. A. Cotter, and D. A. Low. A widespread family of polymorphic contact-dependent toxin delivery systems in bacteria. *Nature*, 468(7322): 439–42, 2010. doi: 10.1038/nature09490.

[365] B. J. Cuthbert, C. S. Hayes, and C. W. Goulding. Functional and structural diversity of bacterial contact-dependent growth inhibition effectors. *Front Mol Biosci*, 9:866854, 2022. doi: 10.3389/fmolb.2022.866854.

[366] P. S. Choi and H. D. Bernstein. Sequential translocation of an escherchia coli two-partner secretion pathway exoprotein across the inner and outer membranes. *Mol Microbiol*, 75 (2):440–51, 2010. doi: 10.1111/j.1365-2958.2009.06993.x.

[367] J. Mazar and P. A. Cotter. New insight into the molecular mechanisms of two-partner secretion. *Trends Microbiol*, 15(11):508–15, 2007. doi: 10.1016/j.tim.2007.10.005.

[368] S. J. Poole, E. J. Diner, S. K. Aoki, B. A. Braaten, C. t'Kint de Roodenbeke, D. A. Low, and C. S. Hayes. Identification of functional toxin/immunity genes linked to contact-dependent growth inhibition (cdi) and rearrangement hotspot (rhs) systems. *PLoS Genet*, 7(8):e1002217, 2011. doi: 10.1371/journal.pgen.1002217.

[369] Z. C. Ruhe, J. Y. Nguyen, J. Xiong, S. Koskiniemi, C. M. Beck, B. R. Perkins, D. A. Low, and C. S. Hayes. Cdia effectors use modular receptor-binding domains to recognize target bacteria. *mBio*, 8(2), 2017. doi: 10.1128/mBio.00290-17.

[370] Z. C. Ruhe, P. Subramanian, K. Song, J. Y. Nguyen, T. A. Stevens, D. A. Low, G. J. Jensen, and C. S. Hayes. Programmed secretion arrest and receptor-triggered toxin export during antibacterial contact-dependent growth inhibition. *Cell*, 175(4):921–933 e14, 2018. doi: 10.1016/j.cell.2018.10.033.

[371] J. L. Willett, G. C. Gucinski, J. P. Fatherree, D. A. Low, and C. S. Hayes. Contact-dependent growth inhibition toxins exploit multiple independent cell-entry pathways. *Proc Natl Acad Sci U S A*, 112(36):11341–6, 2015. doi: 10.1073/pnas.1512124112.

[372] H. H. Lin, A. Filloux, and E. M. Lai. Role of recipient susceptibility factors during contact-dependent interbacterial competition. *Front Microbiol*, 11:603652, 2020. doi: 10.3389/fmicb.2020.603652.

[373] R. J. Allen and B. Waclaw. Bacterial growth: a statistical physicist's guide. *Rep Prog Phys*, 82(1):016601, 2019. doi: 10.1088/1361-6633/aae546.

[374] R. P. Morse, K. C. Nikolakakis, J. L. Willett, E. Gerrick, D. A. Low, C. S. Hayes, and C. W. Goulding. Structural basis of toxicity and immunity in contact-dependent growth inhibition (cdi) systems. *Proc Natl Acad Sci U S A*, 109(52):21480–5, 2012. doi: 10.1073/pnas.1216238110.

[375] E. C. Garcia, M. S. Anderson, J. A. Hagar, and P. A. Cotter. Burkholderia bcpa mediates biofilm formation independently of interbacterial contact-dependent growth inhibition. *Mol Microbiol*, 89(6):1213–25, 2013. doi: 10.1111/mmi.12339.

[376] K. Nikolakakis, S. Amber, J. S. Wilbur, E. J. Diner, S. K. Aoki, S. J. Poole, A. Tuanyok, P. S. Keim, S. Peacock, C. S. Hayes, and D. A. Low. The toxin/immunity network of burkholderia pseudomallei contact-dependent growth inhibition (cdi) systems. *Mol Microbiol*, 84(3):516–29, 2012. doi: 10.1111/j.1365-2958.2012.08039.x.

[377] M. S. Anderson, E. C. Garcia, and P. A. Cotter. The burkholderia bcpaiob genes define unique classes of two-partner secretion and contact dependent growth inhibition systems. *PLoS Genet*, 8(8):e1002877, 2012. doi: 10.1371/journal.pgen.1002877.

[378] C. Mercy, B. Ize, S. P. Salcedo, S. de Bentzmann, and S. Bigot. Functional characterization of pseudomonas contact dependent growth inhibition (cdi) systems. *PLoS One*, 11(1): e0147435, 2016. doi: 10.1371/journal.pone.0147435.

[379] J. A. Melvin, J. R. Gaston, S. N. Phillips, M. J. Springer, C. W. Marshall, R. M. Q. Shanks, and J. M. Bomberger. Pseudomonas aeruginosa contact-dependent growth inhibition plays dual role in host-pathogen interactions. *mSphere*, 2(6), 2017. doi: 10.1128/mSphere.00336-17.

[380] J. P. Allen, E. A. Ozer, G. Minasov, L. Shuvalova, O. Kiryukhina, K. J. F. Satchell, and A. R. Hauser. A comparative genomics approach identifies contact-dependent growth inhibition as a virulence determinant. *Proc Natl Acad Sci U S A*, 117(12):6811–6821, 2020. doi: 10.1073/pnas.1919198117.

[381] T. R. D. Costa, L. Harb, P. Khara, L. Zeng, B. Hu, and P. J. Christie. Type iv secretion systems: Advances in structure, function, and activation. *Mol Microbiol*, 115(3):436–452, 2021. doi: 10.1111/mmi.14670.

[382] Z. Ding, K. Atmakuri, and P. J. Christie. The outs and ins of bacterial type iv secretion substrates. *Trends Microbiol*, 11(11):527–35, 2003. doi: 10.1016/j.tim.2003.09.004.

[383] C. Gonzalez-Rivera, M. Bhatty, and P. J. Christie. Mechanism and function of type iv secretion during infection of the human host. *Microbiol Spectr*, 4(3), 2016. doi: 10.1128/microbiolspec.VMBF-0024-2015.

[384] D. P. Souza, G. U. Oka, C. E. Alvarez-Martinez, A. W. Bisson-Filho, G. Dunger, L. Hobeika, N. S. Cavalcante, M. C. Alegria, L. R. Barbosa, R. K. Salinas, C. R. Guzzo, and C. S. Farah. Bacterial killing via a type iv secretion system. *Nat Commun*, 6:6453, 2015. doi: 10.1038/ncomms7453.

[385] G. G. Sgro, G. U. Oka, D. P. Souza, W. Cenens, E. Bayer-Santos, B. Y. Matsuyama, N. F. Bueno, T. R. Dos Santos, C. E. Alvarez-Martinez, R. K. Salinas, and C. S. Farah. Bacteria-killing type iv secretion systems. *Front Microbiol*, 10:1078, 2019. doi: 10.3389/fmicb.2019.01078.

[386] M. J. Sheedlo, M. D. Ohi, D. B. Lacy, and T. L. Cover. Molecular architecture of bacterial type iv secretion systems. *PLoS Pathog*, 18(8):e1010720, 2022. doi: 10.1371/journal.ppat.1010720.

[387] E. Grohmann, P. J. Christie, G. Waksman, and S. Backert. Type iv secretion in gram-negative and gram-positive bacteria. *Mol Microbiol*, 107(4):455–471, 2018. doi: 10.1111/mmi.13896.

[388] K. Mace, A. K. Vadakkepat, A. Redzej, N. Lukoyanova, C. Oomen, N. Braun, M. Ukleja, F. Lu, T. R. D. Costa, E. V. Orlova, D. Baker, Q. Cong, and G. Waksman. Cryo-em structure of a type iv secretion system. *Nature*, 607(7917):191–196, 2022. doi: 10.1038/s41586-022-04859-y.

[389] G. Koraimann. Spread and persistence of virulence and antibiotic resistance genes: A ride on the f plasmid conjugation module. *EcoSal Plus*, 8(1), 2018. doi: 10.1128/ecosalplus.ESP-0003-2018.

[390] Y. G. Li and P. J. Christie. The agrobacterium virb/vird4 t4ss: Mechanism and architecture defined through in vivo mutagenesis and chimeric systems. *Curr Top Microbiol Immunol*, 418:233–260, 2018. doi: 10.1007/82$_2$018$_9$4.

[391] K. Stingl, S. Muller, G. Scheidgen-Kleyboldt, M. Clausen, and B. Maier. Composite system mediates two-step dna uptake into helicobacter pylori. *Proc Natl Acad Sci U S A*, 107(3): 1184–9, 2010. doi: 10.1073/pnas.0909955107.

[392] A. A. Rambow-Larsen and A. A. Weiss. Temporal expression of pertussis toxin and ptl secretion proteins by bordetella pertussis. *J Bacteriol*, 186(1):43–50, 2004. doi: 10.1128/JB.186.1.43-50.2004.

[393] M. Naumann, O. Sokolova, N. Tegtmeyer, and S. Backert. Helicobacter pylori: A paradigm pathogen for subverting host cell signal transmission. *Trends Microbiol*, 25(4):316–328, 2017. doi: 10.1016/j.tim.2016.12.004.

[394] E. Bayer-Santos, W. Cenens, B. Y. Matsuyama, G. U. Oka, G. Di Sessa, I. D. V. Mininel, T. L. Alves, and C. S. Farah. The opportunistic pathogen stenotrophomonas maltophilia utilizes a type iv secretion system for interbacterial killing. *PLoS Pathog*, 15(9):e1007651, 2019. doi: 10.1371/journal.ppat.1007651.

[395] M. Daffe and H. Marrakchi. Unraveling the structure of the mycobacterial envelope. *Microbiol Spectr*, 7(4), 2019. doi: 10.1128/microbiolspec.GPP3-0027-2018.

[396] M. Rohde. The gram-positive bacterial cell wall. *Microbiol Spectr*, 7(3), 2019. doi: 10.1128/microbiolspec.GPP3-0044-2018.

[397] E. N. Houben, K. V. Korotkov, and W. Bitter. Take five - type vii secretion systems of mycobacteria. *Biochim Biophys Acta*, 1843(8):1707–16, 2014. doi: 10.1016/j.bbamcr.2013.11.003.

[398] A. M. Abdallah, N. C. Gey van Pittius, P. A. Champion, J. Cox, J. Luirink, C. M. Vandenbroucke-Grauls, B. J. Appelmelk, and W. Bitter. Type vii secretion–mycobacteria show the way. *Nat Rev Microbiol*, 5(11):883–91, 2007. doi: 10.1038/nrmicro1773.

[399] M. Unnikrishnan, C. Constantinidou, T. Palmer, and M. J. Pallen. The enigmatic esx proteins: Looking beyond mycobacteria. *Trends Microbiol*, 25(3):192–204, 2017. doi: 10.1016/j.tim.2016.11.004.

[400] K. S. H. Beckham, C. Ritter, G. Chojnowski, D. S. Ziemianowicz, E. Mullapudi, M. Rettel, M. M. Savitski, S. A. Mortensen, J. Kosinski, and M. Wilmanns. Structure of the mycobacterial esx-5 type vii secretion system pore complex. *Sci Adv*, 7(26), 2021. doi: 10.1126/sciadv.abg9923.

[401] C. M. Bunduc, D. Fahrenkamp, J. Wald, R. Ummels, W. Bitter, E. N. G. Houben, and T. C. Marlovits. Structure and dynamics of a mycobacterial type vii secretion system. *Nature*, 593 (7859):445–448, 2021. doi: 10.1038/s41586-021-03517-z.

[402] A. Rivera-Calzada, N. Famelis, O. Llorca, and S. Geibel. Type vii secretion systems: structure, functions and transport models. *Nat Rev Microbiol*, 19(9):567–584, 2021. doi: 10.1038/s41579-021-00560-5.

[403] N. Famelis, A. Rivera-Calzada, G. Degliesposti, M. Wingender, N. Mietrach, J. M. Skehel, R. Fernandez-Leiro, B. Bottcher, A. Schlosser, O. Llorca, and S. Geibel. Architecture of the mycobacterial type vii secretion system. *Nature*, 576(7786):321–325, 2019. doi: 10.1038/s41586-019-1633-1.

[404] H. R. Tran, D. W. Grebenc, T. A. Klein, and J. C. Whitney. Bacterial type vii secretion: An important player in host-microbe and microbe-microbe interactions. *Mol Microbiol*, 115(3): 478–489, 2021. doi: 10.1111/mmi.14680.

[405] J. Sun, A. Siroy, R. K. Lokareddy, A. Speer, K. S. Doornbos, G. Cingolani, and M. Niederweis. The tuberculosis necrotizing toxin kills macrophages by hydrolyzing nad. *Nat Struct Mol Biol*, 22(9):672–8, 2015. doi: 10.1038/nsmb.3064.

[406] Z. Cao, M. G. Casabona, H. Kneuper, J. D. Chalmers, and T. Palmer. The type vii secretion system of staphylococcus aureus secretes a nuclease toxin that targets competitor bacteria. *Nat Microbiol*, 2:16183, 2016. doi: 10.1038/nmicrobiol.2016.183.

[407] C. G. Korea, G. Balsamo, A. Pezzicoli, C. Merakou, S. Tavarini, F. Bagnoli, D. Serruto, and M. Unnikrishnan. Staphylococcal esx proteins modulate apoptosis and release of intracellular staphylococcus aureus during infection in epithelial cells. *Infect Immun*, 82(10):4144–53, 2014. doi: 10.1128/IAI.01576-14.

[408] M. Tassinari, T. Doan, M. Bellinzoni, M. Chabalier, M. Ben-Assaya, M. Martinez, Q. Gaday, P. M. Alzari, E. Cascales, R. Fronzes, and F. Gubellini. The antibacterial type vii secretion system of bacillus subtilis: Structure and interactions of the pseudokinase yukc/essb. *mBio*, 13 (5):e0013422, 2022. doi: 10.1128/mbio.00134-22.

[409] K. Gerdes, P. B. Rasmussen, and S. Molin. Unique type of plasmid maintenance function: postsegregational killing of plasmid-free cells. *Proc Natl Acad Sci U S A*, 83(10):3116–20, 1986. doi: 10.1073/pnas.83.10.3116.

[410] T. Ogura and S. Hiraga. Mini-f plasmid genes that couple host cell division to plasmid proliferation. *Proc Natl Acad Sci U S A*, 80(15):4784–8, 1983. doi: 10.1073/pnas.80.15.4784.

[411] S. J. Unterholzner, B. Poppenberger, and W. Rozhon. Toxin-antitoxin systems: Biology, identification, and application. *Mob Genet Elements*, 3(5):e26219, 2013. doi: 10.4161/mge.26219.

[412] D. Jurenas, N. Fraikin, F. Goormaghtigh, and L. Van Melderen. Biology and evolution of bacterial toxin-antitoxin systems. *Nat Rev Microbiol*, 20(6):335–350, 2022. doi: 10.1038/s41579-021-00661-1.

[413] G. Singh, M. Yadav, C. Ghosh, and J. S. Rathore. Bacterial toxin-antitoxin modules: classification, functions, and association with persistence. *Curr Res Microb Sci*, 2:100047, 2021. doi: 10.1016/j.crmicr.2021.100047.

[414] Z. C. Ruhe, D. A. Low, and C. S. Hayes. Polymorphic toxins and their immunity proteins: Diversity, evolution, and mechanisms of delivery. *Annu Rev Microbiol*, 74:497–520, 2020. doi: 10.1146/annurev-micro-020518-115638.

[415] P. Bernard and M. Couturier. Cell killing by the f plasmid ccdb protein involves poisoning of dna-topoisomerase ii complexes. *J Mol Biol*, 226(3):735–45, 1992. doi: 10.1016/0022-2836(92)90629-x.

[416] V. Celik Ozgen, W. Kong, A. E. Blanchard, F. Liu, and T. Lu. Spatial interference scale as a determinant of microbial range expansion. *Sci Adv*, 4(11):eaau0695, 2018. doi: 10.1126/sciadv.aau0695.

[417] R. Leplae, D. Geeraerts, R. Hallez, J. Guglielmini, P. Dreze, and L. Van Melderen. Diversity of bacterial type ii toxin-antitoxin systems: a comprehensive search and functional analysis of novel families. *Nucleic Acids Res*, 39(13):5513–25, 2011. doi: 10.1093/nar/gkr131.

[418] Si-Ping Zhang, Qian Wang, Shuo-Wei Quan, Xiao-Quan Yu, Yong Wang, Ding-Ding Guo, Liang Peng, Hu-Yuan Feng, and Yong-Xing He. Type ii toxin–antitoxin system in bacteria: activation, function, and mode of action. *Biophysics Reports*, 6(2-3):68–79, 2020. doi: 10.1007/s41048-020-00109-8.

[419] A. Simons, K. Alhanout, and R. E. Duval. Bacteriocins, antimicrobial peptides from bacterial origin: Overview of their biology and their impact against multidrug-resistant bacteria. *Microorganisms*, 8(5), 2020. doi: 10.3390/microorganisms8050639.

[420] Andre Gratia and Pierre Fredericq. Diversite des souches antibiotiques de b. coli et etendue variable de leur champ d'action. *Comptes Rendus des Séances de la Societe de Biologie et de ses Filiales*, 140, 1946.

[421] E. Cascales, S. K. Buchanan, D. Duche, C. Kleanthous, R. Lloubes, K. Postle, M. Riley, S. Slatin, and D. Cavard. Colicin biology. *Microbiol Mol Biol Rev*, 71(1):158–229, 2007. doi: 10.1128/MMBR.00036-06.

[422] M. Zimina, O. Babich, A. Prosekov, S. Sukhikh, S. Ivanova, M. Shevchenko, and S. Noskova. Overview of global trends in classification, methods of preparation and application of bacteriocins. *Antibiotics (Basel)*, 9(9), 2020. doi: 10.3390/antibiotics9090553.

[423] D. F. Benitez-Chao, A. Leon-Buitimea, J. A. Lerma-Escalera, and J. R. Morones-Ramirez. Bacteriocins: An overview of antimicrobial, toxicity, and biosafety assessment by in vivo models. *Front Microbiol*, 12:630695, 2021. doi: 10.3389/fmicb.2021.630695.

[424] F. Jacob. Induced biosynthesis and mode of action of a pyocine, antibiotic produced by pseudomonas aeruginosa. *Ann Inst Pasteur (Paris)*, 86(2):149–60, 1954.

[425] Y. Michel-Briand and C. Baysse. The pyocins of pseudomonas aeruginosa. *Biochimie*, 84(5-6): 499–510, 2002. doi: 10.1016/s0300-9084(02)01422-0.

[426] D. Scholl. Phage tail-like bacteriocins. *Annu Rev Virol*, 4(1):453–467, 2017. doi: 10.1146/annurev-virology-101416-041632.

[427] N. M. I. Taylor, M. J. van Raaij, and P. G. Leiman. Contractile injection systems of bacteriophages and related systems. *Mol Microbiol*, 108(1):6–15, 2018. doi: 10.1111/mmi.13921.

[428] M. G. Ghequire and R. De Mot. Ribosomally encoded antibacterial proteins and peptides from pseudomonas. *FEMS Microbiol Rev*, 38(4):523–68, 2014. doi: 10.1111/1574-6976.12079.

[429] H. Matsui, Y. Sano, H. Ishihara, and T. Shinomiya. Regulation of pyocin genes in pseudomonas aeruginosa by positive (prtn) and negative (prtr) regulatory genes. *J Bacteriol*, 175(5):1257–63, 1993. doi: 10.1128/jb.175.5.1257-1263.1993.

[430] J. Penterman, P. K. Singh, and G. C. Walker. Biological cost of pyocin production during the sos response in pseudomonas aeruginosa. *J Bacteriol*, 196(18):3351–9, 2014. doi: 10.1128/JB.01889-14.

[431] A. L. Hynen, J. J. Lazenby, G. M. Savva, L. C. McCaughey, L. Turnbull, L. M. Nolan, and C. B. Whitchurch. Multiple holins contribute to extracellular dna release in pseudomonas aeruginosa biofilms. *Microbiology (Reading)*, 167(2), 2021. doi: 10.1099/mic.0.000990.

[432] T. Kohler, V. Donner, and C. van Delden. Lipopolysaccharide as shield and receptor for r-pyocin-mediated killing in pseudomonas aeruginosa. *J Bacteriol*, 192(7):1921–8, 2010. doi: 10.1128/JB.01459-09.

[433] Senjuti Saha, Chidozie D. Ojobor, Erik Mackinnon, Olesia I. North, Joseph Bondy-Denomy, Joseph S. Lam, Alexander W. Ensminger, Karen L. Maxwell, and Alan R. Davidson. F-type pyocins are diverse non-contractile phage tail-like weapons for killing pseudomonas aeruginosa. *bioRxiv*, 2021. doi: 10.1101/2021.02.16.431561.

[434] A. J. Salazar, M. Sherekar, J. Tsai, and J. C. Sacchettini. R pyocin tail fiber structure reveals a receptor-binding domain with a lectin fold. *PLoS One*, 14(2):e0211432, 2019. doi: 10.1371/journal.pone.0211432.

[435] K. Ikeda, M. Kageyama, and F. Egami. Studies of a pyocin. ii. mode of production of the pyocin. *J Biochem*, 55:54–8, 1964. doi: 10.1093/oxfordjournals.jbchem.a127840.

[436] A. Fraser, N. S. Prokhorov, F. Jiao, B. M. Pettitt, S. Scheuring, and P. G. Leiman. Quantitative description of a contractile macromolecular machine. *Sci Adv*, 7(24), 2021. doi: 10.1126/sciadv.abf9601.

[437] Y. J. Heo, I. Y. Chung, K. B. Choi, and Y. H. Cho. R-type pyocin is required for competitive growth advantage between pseudomonas aeruginosa strains. *J Microbiol Biotechnol*, 17(1):180–5, 2007.

[438] S. Carim, A. L. Azadeh, A. E. Kazakov, M. N. Price, P. J. Walian, L. M. Lui, T. N. Nielsen, R. Chakraborty, A. M. Deutschbauer, V. K. Mutalik, and A. P. Arkin. Systematic discovery of pseudomonad genetic factors involved in sensitivity to tailocins. *ISME J*, 15(8):2289–2305, 2021. doi: 10.1038/s41396-021-00921-1.

[439] S. A. Morse, B. V. Jones, and P. G. Lysko. Pyocin inhibition of neisseria gonorrhoeae: mechanism of action. *Antimicrob Agents Chemother*, 18(3):416–23, 1980. doi: 10.1128/AAC.18.3.416.

[440] R. D. Waite and M. A. Curtis. Pseudomonas aeruginosa pao1 pyocin production affects population dynamics within mixed-culture biofilms. *J Bacteriol*, 191(4):1349–54, 2009. doi: 10.1128/JB.01458-08.

[441] M. Kageyama and F. Egami. On the purification and some properties of a pyocin, a bacteriocin produced by pseudomonas aeruginosa. *Life Sci (1962)*, 1:471–6, 1962. doi: 10.1016/0024-3205(62)90055-3.

[442] A. Jayawardene and H. Farkas-Himsley. Particulate nature of vibriocin: a bacteriocin from vibrio comma. *Nature*, 219(5149):79–80, 1968. doi: 10.1038/219079a0.

[443] E. Strauch, H. Kaspar, C. Schaudinn, P. Dersch, K. Madela, C. Gewinner, S. Hertwig, J. Wecke, and B. Appel. Characterization of enterocoliticin, a phage tail-like bacteriocin, and its effect on pathogenic yersinia enterocolitica strains. *Appl Environ Microbiol*, 67(12):5634–42, 2001. doi: 10.1128/AEM.67.12.5634-5642.2001.

[444] D. Gebhart, S. R. Williams, K. A. Bishop-Lilly, G. R. Govoni, K. M. Willner, A. Butani, S. Sozhamannan, D. Martin, L. C. Fortier, and D. Scholl. Novel high-molecular-weight, r-type bacteriocins of clostridium difficile. *J Bacteriol*, 194(22):6240–7, 2012. doi: 10.1128/JB.01272-12.

[445] R. Zink, M. J. Loessner, and S. Scherer. Characterization of cryptic prophages (monocins) in listeria and sequence analysis of a holin/endolysin gene. *Microbiology (Reading)*, 141 (Pt 10): 2577–84, 1995. doi: 10.1099/13500872-141-10-2577.

[446] Seiga Ito, Makoto Kageyama, and Fujio Egami. Isolation and characterization of pyocins from several strains of pseudomonas aeruginosa. *The Journal of General and Applied Microbiology*, 16(3):205–214, 1970. doi: $10.2323/\text{jgam.16.3}_2\text{05}$.

[447] Connor Sharp, James Bray, Nicholas G. Housden, Martin C. J. Maiden2, and Colin Kleanthous. Diversity and distribution of nuclease bacteriocins in bacterial genomes revealed using hidden markov models. *PLoS Comput Biol*, 13(7):e1005652, 2017.

[448] M. G. Ghequire, A. Garcia-Pino, E. K. Lebbe, S. Spaepen, R. Loris, and R. De Mot. Structural determinants for activity and specificity of the bacterial toxin llpa. *PLoS Pathog*, 9(2):e1003199, 2013. doi: 10.1371/journal.ppat.1003199.

[449] H. Barreteau, A. Bouhss, M. Fourgeaud, J. L. Mainardi, T. Touze, F. Gerard, D. Blanot, M. Arthur, and D. Mengin-Lecreulx. Human- and plant-pathogenic pseudomonas species produce bacteriocins exhibiting colicin m-like hydrolase activity towards peptidoglycan precursors. *J Bacteriol*, 191(11):3657–64, 2009. doi: 10.1128/JB.01824-08.

[450] A. H. Parret and R. De Mot. Bacteria killing their own kind: novel bacteriocins of pseudomonas and other gamma-proteobacteria. *Trends Microbiol*, 10(3):107–12, 2002. doi: 10.1016/s0966-842x(02)02307-7.

[451] B. H. Rasouliha, H. Ling, C. L. Ho, and M. W. Chang. A predicted immunity protein confers resistance to pyocin s5 in a sensitive strain of pseudomonas aeruginosa. *Chembiochem*, 14(18): 2444–6, 2013. doi: 10.1002/cbic.201300410.

[452] M. I. Rojas, G. S. Cavalcanti, K. McNair, S. Benler, A. T. Alker, A. G. Cobian-Guemes, M. Giluso, K. Levi, F. Rohwer, B. A. Bailey, S. Beyhan, R. A. Edwards, and N. J. Shikuma. A distinct contractile injection system gene cluster found in a majority of healthy adult human microbiomes. *mSystems*, 5(4), 2020. doi: 10.1128/mSystems.00648-20.

[453] R. Bhattacharjee, A. Nandi, A. Sinha, H. Kumar, D. Mitra, A. Mojumdar, P. Patel, E. Jha, S. Mishra, P. K. Rout, P. K. Panda, M. Suar, and S. K. Verma. Phage-tail-like bacteriocins as a biomedical platform to counter anti-microbial resistant pathogens. *Biomed Pharmacother*, 155: 113720, 2022. doi: 10.1016/j.biopha.2022.113720.

[454] A. M. Geller, I. Pollin, D. Zlotkin, A. Danov, N. Nachmias, W. B. Andreopoulos, K. Shemesh, and A. Levy. The extracellular contractile injection system is enriched in environmental microbes and associates with numerous toxins. *Nat Commun*, 12(1):3743, 2021. doi: 10.1038/s41467-021-23777-7.

[455] C. Chen, X. Yang, and X. Shen. Confirmed and potential roles of bacterial t6sss in the intestinal ecosystem. *Front Microbiol*, 10:1484, 2019. doi: 10.3389/fmicb.2019.01484.

[456] G. Yang, A. J. Dowling, U. Gerike, R. H. ffrench Constant, and N. R. Waterfield. Photorhabdus virulence cassettes confer injectable insecticidal activity against the wax moth. *J Bacteriol*, 188 (6):2254–61, 2006. doi: 10.1128/JB.188.6.2254-2261.2006.

[457] F. Jiang, J. Shen, J. Cheng, X. Wang, J. Yang, N. Li, N. Gao, and Q. Jin. N-terminal signal peptides facilitate the engineering of pvc complex as a potent protein delivery system. *Sci Adv*, 8(17):eabm2343, 2022. doi: 10.1126/sciadv.abm2343.

[458] I. Vlisidou, A. Hapeshi, J. R. Healey, K. Smart, G. Yang, and N. R. Waterfield. The photorhabdus asymbiotica virulence cassettes deliver protein effectors directly into target eukaryotic cells. *Elife*, 8, 2019. doi: 10.7554/eLife.46259.

[459] M. R. Hurst, S. S. Beard, T. A. Jackson, and S. M. Jones. Isolation and characterization of the serratia entomophila antifeeding prophage. *FEMS Microbiol Lett*, 270(1):42–8, 2007. doi: 10.1111/j.1574-6968.2007.00645.x.

[460] M. R. H. Hurst, A. Beattie, S. A. Jones, A. Laugraud, C. van Koten, and L. Harper. Serratia proteamaculans strain agr96x encodes an antifeeding prophage (tailocin) with activity against grass grub (costelytra giveni) and manuka beetle (pyronota species) larvae. *Appl Environ Microbiol*, 84(10), 2018. doi: 10.1128/AEM.02739-17.

[461] N. J. Shikuma, M. Pilhofer, G. L. Weiss, M. G. Hadfield, G. J. Jensen, and D. K. Newman. Marine tubeworm metamorphosis induced by arrays of bacterial phage tail-like structures. *Science*, 343(6170):529–33, 2014. doi: 10.1126/science.1246794.

[462] C. F. Ericson, F. Eisenstein, J. M. Medeiros, K. E. Malter, G. S. Cavalcanti, R. W. Zeller, D. K. Newman, M. Pilhofer, and N. J. Shikuma. A contractile injection system stimulates tubeworm metamorphosis by translocating a proteinaceous effector. *Elife*, 8, 2019. doi: 10.7554/eLife.46845.

[463] E. V. Prazdnova, A. V. Gorovtsov, N. G. Vasilchenko, M. P. Kulikov, V. N. Statsenko, A. A. Bogdanova, A. G. Refeld, Y. A. Brislavskiy, V. A. Chistyakov, and M. L. Chikindas. Quorum-sensing inhibition by gram-positive bacteria. *Microorganisms*, 10(2), 2022. doi: 10.3390/microorganisms10020350.

[464] F. Hemmati, R. Salehi, R. Ghotaslou, H. Samadi Kafil, A. Hasani, P. Gholizadeh, R. Nouri, and M. Ahangarzadeh Rezaee. Quorum quenching: A potential target for antipseudomonal therapy. *Infect Drug Resist*, 13:2989–3005, 2020. doi: 10.2147/IDR.S263196.

[465] B. Remy, S. Mion, L. Plener, M. Elias, E. Chabriere, and D. Daude. Interference in bacterial quorum sensing: A biopharmaceutical perspective. *Front Pharmacol*, 9:203, 2018. doi: 10.3389/fphar.2018.00203.

[466] S. Kimura, K. Tateda, Y. Ishii, M. Horikawa, S. Miyairi, N. Gotoh, M. Ishiguro, and K. Yamaguchi. Pseudomonas aeruginosa las quorum sensing autoinducer suppresses growth and biofilm production in legionella species. *Microbiology (Reading)*, 155(Pt 6):1934–1939, 2009. doi: 10.1099/mic.0.026641-0.

[467] N. Hosono Honda, S. Kimura, K. Tateda, M. Horikawa, C. Ueda, Y. Ishii, M. Ishiguro, S. Miyairi, and K. Yamaguchi. Roles of pseudomonas aeruginosa autoinducers and their degradation products, tetramic acids, in bacterial survival and behavior in ecological niches. *Microbes Environ*, 26(2):160–4, 2011. doi: 10.1264/jsme2.me10198.

[468] C. A. Lowery, J. Park, C. Gloeckner, M. M. Meijler, R. S. Mueller, H. I. Boshoff, R. L. Ulrich, 3rd Barry, C. E., D. H. Bartlett, V. V. Kravchenko, G. F. Kaufmann, and K. D. Janda. Defining the mode of action of tetramic acid antibacterials derived from pseudomonas aeruginosa quorum sensing signals. *J Am Chem Soc*, 131(40):14473–9, 2009. doi: 10.1021/ja9056079.

[469] L. Biswas and F. Gotz. Molecular mechanisms of staphylococcus and pseudomonas interactions in cystic fibrosis. *Front Cell Infect Microbiol*, 11:824042, 2021. doi: 10.3389/fcimb.2021.824042.

[470] M. Toyofuku, T. Nakajima-Kambe, H. Uchiyama, and N. Nomura. The effect of a cell-to-cell communication molecule, pseudomonas quinolone signal (pqs), produced by p. aeruginosa on other bacterial species. *Microbes Environ*, 25(1):1–7, 2010. doi: 10.1264/jsme2.me09156.

[471] J. D. Desai and I. M. Banat. Microbial production of surfactants and their commercial potential. *Microbiol Mol Biol Rev*, 61(1):47–64, 1997. doi: 10.1128/mmbr.61.1.47-64.1997.

[472] A. V. Sotirova, D. I. Spasova, D. N. Galabova, E. Karpenko, and A. Shulga. Rhamnolipid-biosurfactant permeabilizing effects on gram-positive and gram-negative bacterial strains. *Curr Microbiol*, 56(6):639–44, 2008. doi: 10.1007/s00284-008-9139-3.

[473] T. L. Wood, T. Gong, L. Zhu, J. Miller, D. S. Miller, B. Yin, and T. K. Wood. Rhamnolipids from pseudomonas aeruginosa disperse the biofilms of sulfate-reducing bacteria. *NPJ Biofilms Microbiomes*, 4:22, 2018. doi: 10.1038/s41522-018-0066-1.

[474] A. Bhattacharjee, T. D. Nusca, and A. I. Hochbaum. Rhamnolipids mediate an interspecies biofilm dispersal signaling pathway. *ACS Chem Biol*, 11(11):3068–3076, 2016. doi: 10.1021/acschembio.6b00750.

[475] H. Chong and Q. Li. Microbial production of rhamnolipids: opportunities, challenges and strategies. *Microb Cell Fact*, 16(1):137, 2017. doi: 10.1186/s12934-017-0753-2.

[476] K. K. Sekhon Randhawa and P. K. Rahman. Rhamnolipid biosurfactants-past, present, and future scenario of global market. *Front Microbiol*, 5:454, 2014. doi: 10.3389/fmicb.2014.00454.

[477] B. G. Gdaniec, F. Bonini, F. Prodon, T. Braschler, T. Kohler, and C. van Delden. Pseudomonas aeruginosa rhamnolipid micelles deliver toxic metabolites and antibiotics into staphylococcus aureus. *iScience*, 25(1):103669, 2022. doi: 10.1016/j.isci.2021.103669.

[478] C. Blumer and D. Haas. Mechanism, regulation, and ecological role of bacterial cyanide biosynthesis. *Arch Microbiol*, 173(3):170–7, 2000. doi: 10.1007/s002039900127.

[479] G. Pessi and D. Haas. Transcriptional control of the hydrogen cyanide biosynthetic genes hcnabc by the anaerobic regulator anr and the quorum-sensing regulators lasr and rhlr in pseudomonas aeruginosa. *J Bacteriol*, 182(24):6940–9, 2000. doi: 10.1128/JB.182.24.6940-6949.2000.

[480] H. Yan, K. L. Asfahl, N. Li, F. Sun, J. Xiao, D. Shen, A. A. Dandekar, and M. Wang. Conditional quorum-sensing induction of a cyanide-insensitive terminal oxidase stabilizes cooperating populations of pseudomonas aeruginosa. *Nat Commun*, 10(1):4999, 2019. doi: 10.1038/s41467-019-13013-8.

[481] O. Ozkaya, R. Balbontin, I. Gordo, and K. B. Xavier. Cheating on cheaters stabilizes cooperation in pseudomonas aeruginosa. *Curr Biol*, 28(13):2070–2080 e6, 2018. doi: 10.1016/j.cub.2018.04.093.

[482] J. Yan, W. Liu, J. Cai, Y. Wang, D. Li, H. Hua, and H. Cao. Advances in phenazines over the past decade: Review of their pharmacological activities, mechanisms of action, biosynthetic pathways and synthetic strategies. *Mar Drugs*, 19(11), 2021. doi: 10.3390/md19110610.

[483] L. Zhang, X. Tian, S. Kuang, G. Liu, C. Zhang, and C. Sun. Antagonistic activity and mode of action of phenazine-1-carboxylic acid, produced by marine bacterium pseudomonas aeruginosa pa31x, against vibrio anguillarum in vitro and in a zebrafish in vivo model. *Front Microbiol*, 8: 289, 2017. doi: 10.3389/fmicb.2017.00289.

[484] S. G. Tupe, R. R. Kulkarni, F. Shirazi, D. G. Sant, S. P. Joshi, and M. V. Deshpande. Possible mechanism of antifungal phenazine-1-carboxamide from pseudomonas sp. against dimorphic fungi benjaminiella poitrasii and human pathogen candida albicans. *J Appl Microbiol*, 118(1): 39–48, 2015. doi: 10.1111/jam.12675.

[485] Mohamed N. F. Hamad, Diaa A. Marrez, and Sherien M. R. El-Sherbieny. Toxicity evaluation and antimicrobial activity of purified pyocyanin from pseudomonas aeruginosa. *Biointerface Research in Applied Chemistry*, 10(6):6974–6990, 2020. doi: 10.33263/briac106.69746990.

[486] Patrick Abou Raji El Feghali and Tarek Nawas. Pyocyanin: A powerful inhibitor of bacterial growth and biofilm formation. *Madridge Journal of Case Reports and Studies*, 3(1):101–107, 2018. doi: 10.18689/mjcrs-1000125.

[487] T. Sudhakar and S. Karpagam. Antifungal efficacy of pyocyanin produced from bioindicators of nosocomial hazards. *International Conference on Green technology and environmental Conservation (GTEC-2011)*, pages 224–229, 2011. doi: 10.1109/GTEC.2011.6167673.

[488] T. Das and M. Manefield. Pyocyanin promotes extracellular dna release in pseudomonas aeruginosa. *PLoS One*, 7(10):e46718, 2012. doi: 10.1371/journal.pone.0046718.

[489] L. A. Meirelles and D. K. Newman. Both toxic and beneficial effects of pyocyanin contribute to the lifecycle of pseudomonas aeruginosa. *Mol Microbiol*, 110(6):995–1010, 2018. doi: 10.1111/mmi.14132.

[490] D. K. Morales, N. J. Jacobs, S. Rajamani, M. Krishnamurthy, J. R. Cubillos-Ruiz, and D. A. Hogan. Antifungal mechanisms by which a novel pseudomonas aeruginosa phenazine toxin kills candida albicans in biofilms. *Mol Microbiol*, 78(6):1379–92, 2010. doi: 10.1111/j.1365-2958.2010.07414.x.

[491] S. Dharni, Sanchita, A. Samad, A. Sharma, and D. D. Patra. The interaction pattern between a homology model of 40s ribosomal s9 protein of rhizoctonia solani and 1-hydroxyphenaize by docking study. *Biomed Res Int*, 2014:682946, 2014. doi: 10.1155/2014/682946.

[492] S. Higgins, S. Heeb, G. Rampioni, M. P. Fletcher, P. Williams, and M. Camara. Differential regulation of the phenazine biosynthetic operons by quorum sensing in pseudomonas aeruginosa pao1-n. *Front Cell Infect Microbiol*, 8:252, 2018. doi: 10.3389/fcimb.2018.00252.

[493] O. Cunrath, G. Graulier, A. Carballido-Lopez, J. Perard, A. Forster, V. A. Geoffroy, P. Saint Auguste, D. Bumann, G. L. A. Mislin, I. Michaud-Soret, I. J. Schalk, and P. Fechter. The pathogen pseudomonas aeruginosa optimizes the production of the siderophore pyochelin upon environmental challenges. *Metallomics*, 12(12):2108–2120, 2020. doi: 10.1039/d0mt00029a.

[494] D. J. Sexton and M. Schuster. Nutrient limitation determines the fitness of cheaters in bacterial siderophore cooperation. *Nat Commun*, 8(1):230, 2017. doi: 10.1038/s41467-017-00222-2.

[495] C. Adler, N. S. Corbalan, M. R. Seyedsayamdost, M. F. Pomares, R. E. de Cristobal, J. Clardy, R. Kolter, and P. A. Vincent. Catecholate siderophores protect bacteria from pyochelin toxicity. *PLoS One*, 7(10):e46754, 2012. doi: 10.1371/journal.pone.0046754.

[496] M. G. Sartorio, E. J. Pardue, M. F. Feldman, and M. F. Haurat. Bacterial outer membrane vesicles: From discovery to applications. *Annu Rev Microbiol*, 75:609–630, 2021. doi: 10.1146/annurev-micro-052821-031444.

[497] S. Combo, S. Mendes, K. M. Nielsen, G. J. da Silva, and S. Domingues. The discovery of the role of outer membrane vesicles against bacteria. *Biomedicines*, 10(10), 2022. doi: 10.3390/biomedicines10102399.

[498] C. Schwechheimer and M. J. Kuehn. Outer-membrane vesicles from gram-negative bacteria: biogenesis and functions. *Nat Rev Microbiol*, 13(10):605–19, 2015. doi: 10.1038/nrmicro3525.

[499] A. G. L. Evans, H. M. Davey, A. Cookson, H. Currinn, G. Cooke-Fox, P. J. Stanczyk, and D. E. Whitworth. Predatory activity of myxococcus xanthus outer-membrane vesicles and

properties of their hydrolase cargo. *Microbiology (Reading)*, 158(Pt 11):2742–2752, 2012. doi: 10.1099/mic.0.060343-0.

[500] J. L. Kadurugamuwa and T. J. Beveridge. Bacteriolytic effect of membrane vesicles from pseudomonas aeruginosa on other bacteria including pathogens: conceptually new antibiotics. *J Bacteriol*, 178(10):2767–74, 1996. doi: 10.1128/jb.178.10.2767-2774.1996.

[501] J. Lin, W. Zhang, J. Cheng, X. Yang, K. Zhu, Y. Wang, G. Wei, P. Y. Qian, Z. Q. Luo, and X. Shen. A pseudomonas t6ss effector recruits pqs-containing outer membrane vesicles for iron acquisition. *Nat Commun*, 8:14888, 2017. doi: 10.1038/ncomms14888.

[502] T. Wang, X. Du, L. Ji, Y. Han, J. Dang, J. Wen, Y. Wang, Q. Pu, M. Wu, and H. Liang. Pseudomonas aeruginosa t6ss-mediated molybdate transport contributes to bacterial competition during anaerobiosis. *Cell Rep*, 35(2):108957, 2021. doi: 10.1016/j.celrep.2021.108957.

[503] L. M. Mashburn and M. Whiteley. Membrane vesicles traffic signals and facilitate group activities in a prokaryote. *Nature*, 437(7057):422–5, 2005. doi: 10.1038/nature03925.

[504] J. M. Bomberger, D. P. Maceachran, B. A. Coutermarsh, S. Ye, G. A. O'Toole, and B. A. Stanton. Long-distance delivery of bacterial virulence factors by pseudomonas aeruginosa outer membrane vesicles. *PLoS Pathog*, 5(4):e1000382, 2009. doi: 10.1371/journal.ppat.1000382.

[505] J. D. Cecil, N. Sirisaengtaksin, N. M. O'Brien-Simpson, and A. M. Krachler. Outer membrane vesicle-host cell interactions. *Microbiol Spectr*, 7(1), 2019. doi: 10.1128/microbiolspec.PSIB-0001-2018.

[506] K. Koeppen, T. H. Hampton, M. Jarek, M. Scharfe, S. A. Gerber, D. W. Mielcarz, E. G. Demers, E. L. Dolben, J. H. Hammond, D. A. Hogan, and B. A. Stanton. A novel mechanism of host-pathogen interaction through srna in bacterial outer membrane vesicles. *PLoS Pathog*, 12(6): e1005672, 2016. doi: 10.1371/journal.ppat.1005672.

[507] A. T. Jan. Outer membrane vesicles (omvs) of gram-negative bacteria: A perspective update. *Front Microbiol*, 8:1053, 2017. doi: 10.3389/fmicb.2017.01053.

[508] S. Pukatzki, A. T. Ma, D. Sturtevant, B. Krastins, D. Sarracino, W. C. Nelson, J. F. Heidelberg, and J. J. Mekalanos. <identification of a conserved bacterial protein secretion system in vibrio cholerae using the dictyostelium hos.pdf>. *Proc Natl Acad Sci U S A*, 103(5):1528–33, 2006. doi: 10.1073/pnas.0510322103.

[509] L. E. Bingle, C. M. Bailey, and M. J. Pallen. Type vi secretion: a beginner's guide. *Curr Opin Microbiol*, 11(1):3–8, 2008. doi: 10.1016/j.mib.2008.01.006.

[510] F. Boyer, G. Fichant, J. Berthod, Y. Vandenbrouck, and I. Attree. Dissecting the bacterial type vi secretion system by a genome wide in silico analysis: what can be learned from available microbial genomic resources? *BMC Genomics*, 10:104, 2009. doi: 10.1186/1471-2164-10-104.

[511] S. Morgado and A. C. Vicente. Diversity and distribution of type vi secretion system gene clusters in bacterial plasmids. *Sci Rep*, 12(1):8249, 2022. doi: 10.1038/s41598-022-12382-3.

[512] B. Jana, K. Keppel, and D. Salomon. Engineering a customizable antibacterial t6ss-based platform in vibrio natriegens. *EMBO Rep*, 22(11):e53681, 2021. doi: 10.15252/embr.202153681.

[513] Tong-Tong Pei, Yumin Kan, Zeng Hang Wang, Ming Xuan Tang, Hao Li, Shuangquan Yan, Yang Cui, Hao Yu Zheng, Han Luo, Xiaoye Liang, and Tao Dong. Delivery of an rhs family nuclease effector reveals direct penetration of the gram positive cell envelope by a type vi secretion system in acidovorax citrulli. *mLife*, 1(1):66–78, 2022. doi: 10.1002/mlf2.12007.

[514] K. Trunk, J. Peltier, Y. C. Liu, B. D. Dill, L. Walker, N. A. R. Gow, M. J. R. Stark, J. Quinn, H. Strahl, M. Trost, and S. J. Coulthurst. The type vi secretion system deploys antifungal effectors against microbial competitors. *Nat Microbiol*, 3(8):920–931, 2018. doi: 10.1038/s41564-018-0191-x.

[515] A. Hachani, T. E. Wood, and A. Filloux. Type vi secretion and anti-host effectors. *Curr Opin Microbiol*, 29:81–93, 2016. doi: 10.1016/j.mib.2015.11.006.

[516] M. I. Steele and N. A. Moran. Evolution of interbacterial antagonism in bee gut microbiota reflects host and symbiont diversification. *mSystems*, 6(3), 2021. doi: 10.1128/mSystems.00063-21.

[517] A. M. Suria, S. Smith, L. Speare, Y. Chen, I. Chien, E. G. Clark, M. Krueger, A. M. Warwick, H. Wilkins, and A. N. Septer. Prevalence and diversity of type vi secretion systems in a model beneficial symbiosis. *Front Microbiol*, 13:988044, 2022. doi: 10.3389/fmicb.2022.988044.

[518] Jinshui Lin, Lei Xu, Jianshe Yang, Zhuo Wang, and Xihui Shen. Beyond dueling: roles of the type vi secretion system in microbiome modulation, pathogenesis and stress resistance. *Stress Biology*, 1(1), 2021. doi: 10.1007/s44154-021-00008-z.

[519] M. W. Kempnich and M. P. Sison-Mangus. Presence and abundance of bacteria with the type vi secretion system in a coastal environment and in the global oceans. *PLoS One*, 15(12):e0244217, 2020. doi: 10.1371/journal.pone.0244217.

[520] R. Gallegos-Monterrosa and S. J. Coulthurst. The ecological impact of a bacterial weapon: microbial interactions and the type vi secretion system. *FEMS Microbiol Rev*, 45(6), 2021. doi: 10.1093/femsre/fuab033.

[521] L. Lin, P. D. Ringel, A. Vettiger, L. Durr, and M. Basler. Dna uptake upon t6ss-dependent prey cell lysis induces sos response and reduces fitness of acinetobacter baylyi. *Cell Rep*, 29(6): 1633–1644 e4, 2019. doi: 10.1016/j.celrep.2019.09.083.

[522] R. Unni, K. L. Pintor, A. Diepold, and D. Unterweger. Presence and absence of type vi secretion systems in bacteria. *Microbiology (Reading)*, 168(4), 2022. doi: 10.1099/mic.0.001151.

[523] S. Coulthurst. The type vi secretion system: a versatile bacterial weapon. *Microbiology (Reading)*, 165(5):503–515, 2019. doi: 10.1099/mic.0.000789.

[524] L. Speare, A. G. Cecere, K. R. Guckes, S. Smith, M. S. Wollenberg, M. J. Mandel, T. Miyashiro, and A. N. Septer. Bacterial symbionts use a type vi secretion system to eliminate

competitors in their natural host. *Proc Natl Acad Sci U S A*, 115(36):E8528–E8537, 2018. doi: 10.1073/pnas.1808302115.

[525] G. Caballero-Flores, J. M. Pickard, and G. Nunez. Microbiota-mediated colonization resistance: mechanisms and regulation. *Nat Rev Microbiol*, 2022. doi: 10.1038/s41579-022-00833-7.

[526] V. S. Nguyen, B. Douzi, E. Durand, A. Roussel, E. Cascales, and C. Cambillau. Towards a complete structural deciphering of type vi secretion system. *Curr Opin Struct Biol*, 49:77–84, 2018. doi: 10.1016/j.sbi.2018.01.007.

[527] A. Zoued, Y. R. Brunet, E. Durand, M. S. Aschtgen, L. Logger, B. Douzi, L. Journet, C. Cambillau, and E. Cascales. Architecture and assembly of the type vi secretion system. *Biochim Biophys Acta*, 1843(8):1664–73, 2014. doi: 10.1016/j.bbamcr.2014.03.018.

[528] E. Durand, V. S. Nguyen, A. Zoued, L. Logger, G. Pehau-Arnaudet, M. S. Aschtgen, S. Spinelli, A. Desmyter, B. Bardiaux, A. Dujeancourt, A. Roussel, C. Cambillau, E. Cascales, and R. Fronzes. Biogenesis and structure of a type vi secretion membrane core complex. *Nature*, 523(7562):555–60, 2015. doi: 10.1038/nature14667.

[529] C. Felisberto-Rodrigues, E. Durand, M. S. Aschtgen, S. Blangy, M. Ortiz-Lombardia, B. Douzi, C. Cambillau, and E. Cascales. Towards a structural comprehension of bacterial type vi secretion systems: characterization of the tssj-tssm complex of an escherichia coli pathovar. *PLoS Pathog*, 7(11):e1002386, 2011. doi: 10.1371/journal.ppat.1002386.

[530] Y. Cherrak, C. Rapisarda, R. Pellarin, G. Bouvier, B. Bardiaux, F. Allain, C. Malosse, M. Rey, J. Chamot-Rooke, E. Cascales, R. Fronzes, and E. Durand. Biogenesis and structure of a type vi secretion baseplate. *Nat Microbiol*, 3(12):1404–1416, 2018. doi: 10.1038/s41564-018-0260-1.

[531] D. Liebl, M. Robert-Genthon, V. Job, V. Cogoni, and I. Attree. Baseplate component tssk and spatio-temporal assembly of t6ss in pseudomonas aeruginosa. *Front Microbiol*, 10:1615, 2019. doi: 10.3389/fmicb.2019.01615.

[532] Y. R. Brunet, A. Zoued, F. Boyer, B. Douzi, and E. Cascales. The type vi secretion tssefgk-vgrg phage-like baseplate is recruited to the tssjlm membrane complex via multiple contacts and serves as assembly platform for tail tube/sheath polymerization. *PLoS Genet*, 11(10):e1005545, 2015. doi: 10.1371/journal.pgen.1005545.

[533] Y. J. Park, K. D. Lacourse, C. Cambillau, F. DiMaio, J. D. Mougous, and D. Veesler. Structure of the type vi secretion system tssk-tssf-tssg baseplate subcomplex revealed by cryo-electron microscopy. *Nat Commun*, 9(1):5385, 2018. doi: 10.1038/s41467-018-07796-5.

[534] E. R. Ballister, A. H. Lai, R. N. Zuckermann, Y. Cheng, and J. D. Mougous. In vitro self-assembly of tailorable nanotubes from a simple protein building block. *Proc Natl Acad Sci U S A*, 105(10):3733–8, 2008. doi: 10.1073/pnas.0712247105.

[535] N. S. Lossi, E. Manoli, A. Forster, R. Dajani, T. Pape, P. Freemont, and A. Filloux. The hsib1c1 (tssb-tssc) complex of the pseudomonas aeruginosa type vi secretion system forms a bacteriophage tail sheathlike structure. *J Biol Chem*, 288(11):7536–7548, 2013. doi: 10.1074/jbc.M112.439273.

[536] A. Hachani, N. S. Lossi, A. Hamilton, C. Jones, S. Bleves, D. Albesa-Jove, and A. Filloux. Type vi secretion system in pseudomonas aeruginosa: secretion and multimerization of vgrg proteins. *J Biol Chem*, 286(14):12317–27, 2011. doi: 10.1074/jbc.M110.193045.

[537] M. M. Shneider, S. A. Buth, B. T. Ho, M. Basler, J. J. Mekalanos, and P. G. Leiman. Paar-repeat proteins sharpen and diversify the type vi secretion system spike. *Nature*, 500(7462): 350–353, 2013. doi: 10.1038/nature12453.

[538] N. Flaugnatti, C. Rapisarda, M. Rey, S. G. Beauvois, V. A. Nguyen, S. Canaan, E. Durand, J. Chamot-Rooke, E. Cascales, R. Fronzes, and L. Journet. Structural basis for loading and inhibition of a bacterial t6ss phospholipase effector by the vgrg spike. *EMBO J*, 39(11):e104129, 2020. doi: 10.15252/embj.2019104129.

[539] D. Jurenas and L. Journet. Activity, delivery, and diversity of type vi secretion effectors. *Mol Microbiol*, 115(3):383–394, 2021. doi: 10.1111/mmi.14648.

[540] A. Vettiger and M. Basler. Type vi secretion system substrates are transferred and reused among sister cells. *Cell*, 167(1):99–110 e12, 2016. doi: 10.1016/j.cell.2016.08.023.

[541] A. Vettiger, J. Winter, L. Lin, and M. Basler. The type vi secretion system sheath assembles at the end distal from the membrane anchor. *Nat Commun*, 8:16088, 2017. doi: 10.1038/ncomms16088.

[542] M. Brackmann, J. Wang, and M. Basler. Type vi secretion system sheath inter-subunit interactions modulate its contraction. *EMBO Rep*, 19(2):225–233, 2018. doi: 10.15252/embr.201744416.

[543] G. Bonemann, A. Pietrosiuk, A. Diemand, H. Zentgraf, and A. Mogk. Remodelling of vipa/vipb tubules by clpv-mediated threading is crucial for type vi protein secretion. *EMBO J*, 28(4): 315–25, 2009. doi: 10.1038/emboj.2008.269.

[544] S. Nazarov, J. P. Schneider, M. Brackmann, K. N. Goldie, H. Stahlberg, and M. Basler. Cryo-em reconstruction of type vi secretion system baseplate and sheath distal end. *EMBO J*, 37(4), 2018. doi: 10.15252/embj.201797103.

[545] A. Zoued, C. J. Cassaro, E. Durand, B. Douzi, A. P. Espana, C. Cambillau, L. Journet, and E. Cascales. Structure-function analysis of the tssl cytoplasmic domain reveals a new interaction between the type vi secretion baseplate and membrane complexes. *J Mol Biol*, 428(22):4413–4423, 2016. doi: 10.1016/j.jmb.2016.08.030.

[546] J. P. Schneider, S. Nazarov, R. Adaixo, M. Liuzzo, P. D. Ringel, H. Stahlberg, and M. Basler. Diverse roles of tssa-like proteins in the assembly of bacterial type vi secretion systems. *EMBO J*, 38(18):e100825, 2019. doi: 10.15252/embj.2018100825.

[547] P. Bernal, R. C. D. Furniss, S. Fecht, R. C. Y. Leung, L. Spiga, D. A. I. Mavridou, and A. Filloux. A novel stabilization mechanism for the type vi secretion system sheath. *Proc Natl Acad Sci U S A*, 118(7), 2021. doi: 10.1073/pnas.2008500118.

[548] S. R. Dix, H. J. Owen, R. Sun, A. Ahmad, S. Shastri, H. L. Spiewak, D. J. Mosby, M. J. Harris, S. L. Batters, T. A. Brooker, S. B. Tzokov, S. E. Sedelnikova, P. J. Baker, P. A. Bullough, D. W. Rice, and M. S. Thomas. Structural insights into the function of type vi secretion system tssa subunits. *Nat Commun*, 9(1):4765, 2018. doi: 10.1038/s41467-018-07247-1.

[549] Y. G. Santin, T. Doan, R. Lebrun, L. Espinosa, L. Journet, and E. Cascales. In vivo tssa proximity labelling during type vi secretion biogenesis reveals taga as a protein that stops and holds the sheath. *Nat Microbiol*, 3(11):1304–1313, 2018. doi: 10.1038/s41564-018-0234-3.

[550] A. Hachani, L. P. Allsopp, Y. Oduko, and A. Filloux. The vgrg proteins are "a la carte" delivery systems for bacterial type vi effectors. *J Biol Chem*, 289(25):17872–84, 2014. doi: 10.1074/jbc.M114.563429.

[551] John C. Whitney, Christina M. Beck, Young Ah Goo, Alistair B. Russell, Brittany N. Harding, Justin A. De Leon, David A. Cunningham, Bao Q. Tran, David A. Low, David R. Goodlett, Christopher S. Hayes, and Joseph D. Mougous. Genetically distinct pathways guide effector export through the type vi secretion system. *Molecular Microbiology*, 92(3):529–542, 2014. doi: 10.1111/mmi.12571.

[552] P. Pissaridou, L. P. Allsopp, S. Wettstadt, S. A. Howard, D. A. I. Mavridou, and A. Filloux. The pseudomonas aeruginosa t6ss-vgrg1b spike is topped by a paar protein eliciting dna damage to bacterial competitors. *Proc Natl Acad Sci U S A*, 115(49):12519–12524, 2018. doi: 10.1073/pnas.1814181115.

[553] T. E. Wood, S. A. Howard, S. Wettstadt, and A. Filloux. Paar proteins act as the 'sorting hat' of the type vi secretion system. *Microbiology (Reading)*, 165(11):1203–1218, 2019. doi: 10.1099/mic.0.000842.

[554] J. Ma, Z. Pan, J. Huang, M. Sun, C. Lu, and H. Yao. The hcp proteins fused with diverse extended-toxin domains represent a novel pattern of antibacterial effectors in type vi secretion systems. *Virulence*, 8(7):1189–1202, 2017. doi: 10.1080/21505594.2017.1279374.

[555] S. A. Howard, R. C. D. Furniss, D. Bonini, H. Amin, P. Paracuellos, D. Zlotkin, T. R. D. Costa, A. Levy, D. A. I. Mavridou, and A. Filloux. The breadth and molecular basis of hcp-driven type vi secretion system effector delivery. *mBio*, 12(3):e0026221, 2021. doi: 10.1128/mBio.00262-21.

[556] J. M. Silverman, D. M. Agnello, H. Zheng, B. T. Andrews, M. Li, C. E. Catalano, T. Gonen, and J. D. Mougous. Haemolysin coregulated protein is an exported receptor and chaperone of type vi secretion substrates. *Mol Cell*, 51(5):584–93, 2013. doi: 10.1016/j.molcel.2013.07.025.

[557] L. M. Nolan, A. K. Cain, T. Clamens, R. C. D. Furniss, E. Manoli, M. A. Sainz-Polo, G. Dougan, D. Albesa-Jove, J. Parkhill, D. A. I. Mavridou, and A. Filloux. Identification of tse8 as a type vi secretion system toxin from pseudomonas aeruginosa that targets the bacterial transamidosome to inhibit protein synthesis in prey cells. *Nat Microbiol*, 6(9):1199–1210, 2021. doi: 10.1038/s41564-021-00950-8.

[558] D. Quentin, S. Ahmad, P. Shanthamoorthy, J. D. Mougous, J. C. Whitney, and S. Raunser. Mechanism of loading and translocation of type vi secretion system effector tse6. *Nat Microbiol*, 3(10):1142–1152, 2018. doi: 10.1038/s41564-018-0238-z.

[559] B. J. Burkinshaw, X. Liang, M. Wong, A. N. H. Le, L. Lam, and T. G. Dong. A type vi secretion system effector delivery mechanism dependent on paar and a chaperone-co-chaperone complex. *Nat Microbiol*, 3(5):632–640, 2018. doi: 10.1038/s41564-018-0144-4.

[560] N. Flaugnatti, S. Isaac, L. F. Lemos Rocha, S. Stutzmann, O. Rendueles, C. Stoudmann, N. Vesel, M. Garcia-Garcera, A. Buffet, T. G. Sana, E. P. C. Rocha, and M. Blokesch. Human commensal gut proteobacteria withstand type vi secretion attacks through immunity protein-independent mechanisms. *Nat Commun*, 12(1):5751, 2021. doi: 10.1038/s41467-021-26041-0.

[561] X. Liang, T. T. Pei, H. Li, H. Y. Zheng, H. Luo, Y. Cui, M. X. Tang, Y. J. Zhao, P. Xu, and T. Dong. Vgrg-dependent effectors and chaperones modulate the assembly of the type vi secretion system. *PLoS Pathog*, 17(12):e1010116, 2021. doi: 10.1371/journal.ppat.1010116.

[562] H. H. Lin, M. Yu, M. K. Sriramoju, S. D. Hsu, C. T. Liu, and E. M. Lai. A high-throughput interbacterial competition screen identifies clpap in enhancing recipient susceptibility to type vi secretion system-mediated attack by agrobacterium tumefaciens. *Front Microbiol*, 10:3077, 2019. doi: 10.3389/fmicb.2019.03077.

[563] C. Jones, A. Hachani, E. Manoli, and A. Filloux. An rhs gene linked to the second type vi secretion cluster is a feature of the pseudomonas aeruginosa strain pa14. *J Bacteriol*, 196(4): 800–10, 2014. doi: 10.1128/JB.00863-13.

[564] M. Basler, B. T. Ho, and J. J. Mekalanos. Tit-for-tat: type vi secretion system counterattack during bacterial cell-cell interactions. *Cell*, 152(4):884–94, 2013. doi: 10.1016/j.cell.2013.01.042.

[565] T. Boulant, Y. M. Boudehen, A. Filloux, P. Plesiat, T. Naas, and L. Dortet. Higher prevalence of plda, a pseudomonas aeruginosa trans-kingdom h2-type vi secretion system effector, in clinical isolates responsible for acute infections and in multidrug resistant strains. *Front Microbiol*, 9: 2578, 2018. doi: 10.3389/fmicb.2018.02578.

[566] B. Lesic, M. Starkey, J. He, R. Hazan, and L. G. Rahme. Quorum sensing differentially regulates pseudomonas aeruginosa type vi secretion locus i and homologous loci ii and iii, which are required for pathogenesis. *Microbiology (Reading)*, 155(Pt 9):2845–2855, 2009. doi: 10.1099/mic.0.029082-0.

[567] H. Li, X. Zhou, Y. Huang, B. Liao, L. Cheng, and B. Ren. Reactive oxygen species in pathogen clearance: The killing mechanisms, the adaption response, and the side effects. *Front Microbiol*, 11:622534, 2020. doi: 10.3389/fmicb.2020.622534.

[568] L. Chen, Y. Zou, A. A. Kronfl, and Y. Wu. Type vi secretion system of pseudomonas aeruginosa is associated with biofilm formation but not environmental adaptation. *Microbiologyopen*, 9(3): e991, 2020. doi: 10.1002/mbo3.991.

[569] J. D. Mougous, C. A. Gifford, T. L. Ramsdell, and J. J. Mekalanos. Threonine phosphorylation post-translationally regulates protein secretion in pseudomonas aeruginosa. *Nat Cell Biol*, 9(7): 797–803, 2007. doi: 10.1038/ncb1605.

[570] J. S. Lin, P. Pissaridou, H. H. Wu, M. D. Tsai, A. Filloux, and E. M. Lai. Tagf-mediated repression of bacterial type vi secretion systems involves a direct interaction with the cytoplasmic protein fha. *J Biol Chem*, 293(23):8829–8842, 2018. doi: 10.1074/jbc.RA117.001618.

[571] A. Ostrowski, F. R. Cianfanelli, M. Porter, G. Mariano, J. Peltier, J. J. Wong, J. R. Swedlow, M. Trost, and S. J. Coulthurst. Killing with proficiency: Integrated post-translational regulation of an offensive type vi secretion system. *PLoS Pathog*, 14(7):e1007230, 2018. doi: 10.1371/journal.ppat.1007230.

[572] F. Hsu, S. Schwarz, and J. D. Mougous. Tagr promotes ppka-catalysed type vi secretion activation in pseudomonas aeruginosa. *Mol Microbiol*, 72(5):1111–25, 2009. doi: 10.1111/j.1365-2958.2009.06701.x.

[573] J. S. Lin, H. H. Wu, P. H. Hsu, L. S. Ma, Y. Y. Pang, M. D. Tsai, and E. M. Lai. Fha interaction with phosphothreonine of tssl activates type vi secretion in agrobacterium tumefaciens. *PLoS Pathog*, 10(3):e1003991, 2014. doi: 10.1371/journal.ppat.1003991.

[574] M. G. Casabona, J. M. Silverman, K. M. Sall, F. Boyer, Y. Coute, J. Poirel, D. Grunwald, J. D. Mougous, S. Elsen, and I. Attree. An abc transporter and an outer membrane lipoprotein participate in posttranslational activation of type vi secretion in pseudomonas aeruginosa. *Environ Microbiol*, 15(2):471–86, 2013. doi: 10.1111/j.1462-2920.2012.02816.x.

[575] Y. C. Lin, M. D. Sekedat, W. C. Cornell, G. M. Silva, C. Okegbe, A. Price-Whelan, C. Vogel, and L. E. P. Dietrich. Phenazines regulate nap-dependent denitrification in pseudomonas aeruginosa biofilms. *J Bacteriol*, 200(9), 2018. doi: 10.1128/JB.00031-18.

[576] W. P. J. Smith, M. Brodmann, D. Unterweger, Y. Davit, L. E. Comstock, M. Basler, and K. R. Foster. The evolution of tit-for-tat in bacteria via the type vi secretion system. *Nat Commun*, 11(1):5395, 2020. doi: 10.1038/s41467-020-19017-z.

[577] F. Kamal, X. Liang, K. Manera, T. T. Pei, H. Kim, L. G. Lam, A. Pun, S. J. Hersch, and T. G. Dong. Differential cellular response to translocated toxic effectors and physical penetration by the type vi secretion system. *Cell Rep*, 31(11):107766, 2020. doi: 10.1016/j.celrep.2020.107766.

[578] B. T. Ho, T. G. Dong, and J. J. Mekalanos. A view to a kill: the bacterial type vi secretion system. *Cell Host Microbe*, 15(1):9–21, 2014. doi: 10.1016/j.chom.2013.11.008.

[579] A. S. Stolle, B. T. Meader, J. Toska, and J. J. Mekalanos. Endogenous membrane stress induces t6ss activity in pseudomonas aeruginosa. *Proc Natl Acad Sci U S A*, 118(1), 2021. doi: 10.1073/pnas.2018365118.

[580] T. G. Dong, B. T. Ho, D. R. Yoder-Himes, and J. J. Mekalanos. Identification of t6ss-dependent effector and immunity proteins by tn-seq in vibrio cholerae. *Proc Natl Acad Sci U S A*, 110(7): 2623–8, 2013. doi: 10.1073/pnas.1222783110.

[581] A. B. Russell, S. B. Peterson, and J. D. Mougous. Type vi secretion system effectors: poisons with a purpose. *Nat Rev Microbiol*, 12(2):137–48, 2014. doi: 10.1038/nrmicro3185.

[582] A. Radkov, A. L. Sapiro, S. Flores, C. Henderson, H. Saunders, R. Kim, S. Massa, S. Thompson, C. Mateusiak, J. Biboy, Z. Zhao, L. M. Starita, W. L. Hatleberg, W. Vollmer, A. B. Russell, J. P. Simorre, S. Anthony-Cahill, P. Brzovic, B. Hayes, and S. Chou. Antibacterial potency of type vi amidase effector toxins is dependent on substrate topology and cellular context. *Elife*, 11, 2022. doi: 10.7554/eLife.79796.

[583] R. D. Hood, P. Singh, F. Hsu, T. Guvener, M. A. Carl, R. R. Trinidad, J. M. Silverman, B. B. Ohlson, K. G. Hicks, R. L. Plemel, M. Li, S. Schwarz, W. Y. Wang, A. J. Merz, D. R. Goodlett, and J. D. Mougous. A type vi secretion system of pseudomonas aeruginosa targets a toxin to bacteria. *Cell Host Microbe*, 7(1):25–37, 2010. doi: 10.1016/j.chom.2009.12.007.

[584] A. B. Russell, R. D. Hood, N. K. Bui, M. LeRoux, W. Vollmer, and J. D. Mougous. Type vi secretion delivers bacteriolytic effectors to target cells. *Nature*, 475(7356):343–7, 2011. doi: 10.1038/nature10244.

[585] C. Juan, B. Moya, J. L. Perez, and A. Oliver. Stepwise upregulation of the pseudomonas aeruginosa chromosomal cephalosporinase conferring high-level beta-lactam resistance involves three ampd homologues. *Antimicrob Agents Chemother*, 50(5):1780–7, 2006. doi: 10.1128/AAC.50.5.1780-1787.2006.

[586] W. Zhang, M. Lee, D. Hesek, E. Lastochkin, B. Boggess, and S. Mobashery. Reactions of the three ampd enzymes of pseudomonas aeruginosa. *J Am Chem Soc*, 135(13):4950–3, 2013. doi: 10.1021/ja400970n.

[587] T. Wang, Z. Hu, X. Du, Y. Shi, J. Dang, M. Lee, D. Hesek, S. Mobashery, M. Wu, and H. Liang. A type vi secretion system delivers a cell wall amidase to target bacterial competitors. *Mol Microbiol*, 114(2):308–321, 2020. doi: 10.1111/mmi.14513.

[588] H. Hu, H. Zhang, Z. Gao, D. Wang, G. Liu, J. Xu, K. Lan, and Y. Dong. Structure of the type vi secretion phospholipase effector tle1 provides insight into its hydrolysis and membrane targeting. *Acta Crystallogr D Biol Crystallogr*, 70(Pt 8):2175–85, 2014. doi: 10.1107/S1399004714012899.

[589] N. Flaugnatti, T. T. Le, S. Canaan, M. S. Aschtgen, V. S. Nguyen, S. Blangy, C. Kellenberger, A. Roussel, C. Cambillau, E. Cascales, and L. Journet. A phospholipase a1 antibacterial type vi secretion effector interacts directly with the c-terminal domain of the vgrg spike protein for delivery. *Mol Microbiol*, 99(6):1099–118, 2016. doi: 10.1111/mmi.13292.

[590] P. J. Wilderman, A. I. Vasil, Z. Johnson, and M. L. Vasil. Genetic and biochemical analyses of a eukaryotic-like phospholipase d of pseudomonas aeruginosa suggest horizontal acquisition and a role for persistence in a chronic pulmonary infection model. *Mol Microbiol*, 39(2):291–303, 2001. doi: 10.1046/j.1365-2958.2001.02282.x.

[591] C. Spencer and H. A. Brown. Biochemical characterization of a pseudomonas aeruginosa phospholipase d. *Biochemistry*, 54(5):1208–18, 2015. doi: 10.1021/bi501291t.

[592] S. Wettstadt, T. E. Wood, S. Fecht, and A. Filloux. Delivery of the pseudomonas aeruginosa phospholipase effectors plda and pldb in a vgrg- and h2-t6ss-dependent manner. *Front Microbiol*, 10:1718, 2019. doi: 10.3389/fmicb.2019.01718.

[593] D. Lu, Y. Zheng, N. Liao, L. Wei, B. Xu, X. Liu, and J. Liu. The structural basis of the tle4-tli4 complex reveals the self-protection mechanism of h2-t6ss in pseudomonas aeruginosa. *Acta Crystallogr D Biol Crystallogr*, 70(Pt 12):3233–43, 2014. doi: 10.1107/S1399004714023967.

[594] K. D. LaCourse, S. B. Peterson, H. D. Kulasekara, M. C. Radey, J. Kim, and J. D. Mougous. Conditional toxicity and synergy drive diversity among antibacterial effectors. *Nat Microbiol*, 3 (4):440–446, 2018. doi: 10.1038/s41564-018-0113-y.

[595] A. Gonzalez-Magana, M. A. Sainz-Polo, G. Pretre, R. Capuni, M. Lucas, J. Altuna, I. Montanchez, P. Fucini, and D. Albesa-Jove. Structural insights into pseudomonas aeruginosatype six secretion system exported effector 8. *J Struct Biol*, 212(3):107651, 2020. doi: 10.1016/j.jsb.2020.107651.

[596] S. Kim, T. J. Jeon, A. Oberai, D. Yang, J. J. Schmidt, and J. U. Bowie. Transmembrane glycine zippers: physiological and pathological roles in membrane proteins. *Proc Natl Acad Sci U S A*, 102(40):14278–83, 2005. doi: 10.1073/pnas.0501234102.

[597] A. Gonzalez-Magana, J. Altuna, M. Queralt-Martin, E. Largo, C. Velazquez, I. Montanchez, P. Bernal, A. Alcaraz, and D. Albesa-Jove. The p. aeruginosa effector tse5 forms membrane pores disrupting the membrane potential of intoxicated bacteria. *Commun Biol*, 5(1):1189, 2022. doi: 10.1038/s42003-022-04140-y.

[598] S. Ahmad, B. Wang, M. D. Walker, H. R. Tran, P. J. Stogios, A. Savchenko, R. A. Grant, A. G. McArthur, M. T. Laub, and J. C. Whitney. An interbacterial toxin inhibits target cell growth by synthesizing (p)ppapp. *Nature*, 575(7784):674–678, 2019. doi: 10.1038/s41586-019-1735-9.

[599] C. S. Robb, M. Robb, F. E. Nano, and A. B. Boraston. The structure of the toxin and type six secretion system substrate tse2 in complex with its immunity protein. *Structure*, 24(2):277–84, 2016. doi: 10.1016/j.str.2015.11.012.

[600] A. Goni-Moreno, J. Kim, and V. de Lorenzo. Cellshape: A user-friendly image analysis tool for quantitative visualization of bacterial cell factories inside. *Biotechnol J*, 12(2), 2017. doi: 10.1002/biot.201600323.

[601] N. P. Bullen, D. Sychantha, S. S. Thang, P. H. Culviner, M. Rudzite, S. Ahmad, V. S. Shah, A. Filloux, G. Prehna, and J. C. Whitney. An adp-ribosyltransferase toxin kills bacterial cells by modifying structured non-coding rnas. *Mol Cell*, 82(18):3484–3498 e11, 2022. doi: 10.1016/j.molcel.2022.08.015.

[602] X. Yang, M. Long, and X. Shen. Effector(-)immunity pairs provide the t6ss nanomachine its offensive and defensive capabilities. *Molecules*, 23(5), 2018. doi: 10.3390/molecules23051009.

[603] P. C. Kirchberger, D. Unterweger, D. Provenzano, S. Pukatzki, and Y. Boucher. Sequential displacement of type vi secretion system effector genes leads to evolution of diverse immunity gene arrays in vibrio cholerae. *Sci Rep*, 7:45133, 2017. doi: 10.1038/srep45133.

[604] A. G. Wexler, Y. Bao, J. C. Whitney, L. M. Bobay, J. B. Xavier, W. B. Schofield, N. A. Barry, A. B. Russell, B. Q. Tran, Y. A. Goo, D. R. Goodlett, H. Ochman, J. D. Mougous, and A. L.

Goodman. Human symbionts inject and neutralize antibacterial toxins to persist in the gut. *Proc Natl Acad Sci U S A*, 113(13):3639–44, 2016. doi: 10.1073/pnas.1525637113.

[605] B. D. Ross, A. J. Verster, M. C. Radey, D. T. Schmidtke, C. E. Pope, L. R. Hoffman, A. M. Hajjar, S. B. Peterson, E. Borenstein, and J. D. Mougous. Human gut bacteria contain acquired interbacterial defence systems. *Nature*, 575(7781):224–228, 2019. doi: 10.1038/s41586-019-1708-z.

[606] S. Y. Ting, D. E. Bosch, S. M. Mangiameli, M. C. Radey, S. Huang, Y. J. Park, K. A. Kelly, S. K. Filip, Y. A. Goo, J. K. Eng, M. Allaire, D. Veesler, P. A. Wiggins, S. B. Peterson, and J. D. Mougous. Bifunctional immunity proteins protect bacteria against ftsz-targeting adp-ribosylating toxins. *Cell*, 175(5):1380–1392 e14, 2018. doi: 10.1016/j.cell.2018.09.037.

[607] H. Wen, G. Liu, Z. Geng, H. Zhang, Y. Li, Z. She, and Y. Dong. Structure and saxs studies unveiled a novel inhibition mechanism of the pseudomonas aeruginosa t6ss tset-tsit complex. *Int J Biol Macromol*, 188:450–459, 2021. doi: 10.1016/j.ijbiomac.2021.08.029.

[608] H. Wen, Z. Geng, Z. Gao, Z. She, and Y. Dong. Characterization of the pseudomonas aeruginosa t6ss pldb immunity proteins pa5086, pa5087 and pa5088 explains a novel stockpiling mechanism. *Acta Crystallogr F Struct Biol Commun*, 76(Pt 5):222–227, 2020. doi: 10.1107/S2053230X2000566X.

[609] X. Y. Yang, Z. Q. Li, Z. She, Z. Geng, J. H. Xu, Z. Q. Gao, and Y. H. Dong. Structural analysis of pseudomonas aeruginosa h3-t6ss immunity proteins. *FEBS Lett*, 590(16):2787–96, 2016. doi: 10.1002/1873-3468.12291.

[610] A. B. Russell, P. Singh, M. Brittnacher, N. K. Bui, R. D. Hood, M. A. Carl, D. M. Agnello, S. Schwarz, D. R. Goodlett, W. Vollmer, and J. D. Mougous. A widespread bacterial type vi secretion effector superfamily identified using a heuristic approach. *Cell Host Microbe*, 11(5): 538–49, 2012. doi: 10.1016/j.chom.2012.04.007.

[611] T. G. Sana, C. Baumann, A. Merdes, C. Soscia, T. Rattei, A. Hachani, C. Jones, K. L. Bennett, A. Filloux, G. Superti-Furga, R. Voulhoux, and S. Bleves. Internalization of pseudomonas aeruginosa strain pao1 into epithelial cells is promoted by interaction of a t6ss effector with the microtubule network. *mBio*, 6(3):e00712, 2015. doi: 10.1128/mBio.00712-15.

[612] B. Berni, C. Soscia, S. Djermoun, B. Ize, and S. Bleves. A type vi secretion system trans-kingdom effector is required for the delivery of a novel antibacterial toxin in pseudomonas aeruginosa. *Front Microbiol*, 10:1218, 2019. doi: 10.3389/fmicb.2019.01218.

[613] G. Suarez, J. C. Sierra, T. E. Erova, J. Sha, A. J. Horneman, and A. K. Chopra. A type vi secretion system effector protein, vgrg1, from aeromonas hydrophila that induces host cell toxicity by adp ribosylation of actin. *J Bacteriol*, 192(1):155–68, 2010. doi: 10.1128/JB.01260-09.

[614] A. T. Ma and J. J. Mekalanos. In vivo actin cross-linking induced by vibrio cholerae type vi secretion system is associated with intestinal inflammation. *Proc Natl Acad Sci U S A*, 107(9): 4365–70, 2010. doi: 10.1073/pnas.0915156107.

[615] D. F. Aubert, H. Xu, J. Yang, X. Shi, W. Gao, L. Li, F. Bisaro, S. Chen, M. A. Valvano, and F. Shao. A burkholderia type vi effector deamidates rho gtpases to activate the pyrin inflammasome and trigger inflammation. *Cell Host Microbe*, 19(5):664–74, 2016. doi: 10.1016/j.chom.2016.04.004.

[616] B. Wan, Q. Zhang, J. Ni, S. Li, D. Wen, J. Li, H. Xiao, P. He, H. Y. Ou, J. Tao, Q. Teng, J. Lu, W. Wu, and Y. F. Yao. Type vi secretion system contributes to enterohemorrhagic escherichia coli virulence by secreting catalase against host reactive oxygen species (ros). *PLoS Pathog*, 13 (3):e1006246, 2017. doi: 10.1371/journal.ppat.1006246.

[617] T. Wang, M. Si, Y. Song, W. Zhu, F. Gao, Y. Wang, L. Zhang, W. Zhang, G. Wei, Z. Q. Luo, and X. Shen. Type vi secretion system transports zn2+ to combat multiple stresses and host immunity. *PLoS Pathog*, 11(7):e1005020, 2015. doi: 10.1371/journal.ppat.1005020.

[618] D. L. Clemens, B. Y. Lee, and M. A. Horwitz. The francisella type vi secretion system. *Front Cell Infect Microbiol*, 8:121, 2018. doi: 10.3389/fcimb.2018.00121.

[619] M. Brodmann, R. F. Dreier, P. Broz, and M. Basler. Francisella requires dynamic type vi secretion system and clpb to deliver effectors for phagosomal escape. *Nat Commun*, 8:15853, 2017. doi: 10.1038/ncomms15853.

[620] Huili Li, Boguang Sun, Xianhui Ning, Shuai Jiang, and Li Sun. A comparative analysis of edwardsiella tarda-induced transcriptome profiles in raw264.7 cells reveals new insights into the strategy of bacterial immune evasion. *International Journal of Molecular Sciences*, 20(22), 2019. doi: 10.3390/ijms20225724.

[621] H. Chen, D. Yang, F. Han, J. Tan, L. Zhang, J. Xiao, Y. Zhang, and Q. Liu. The bacterial t6ss effector evpp prevents nlrp3 inflammasome activation by inhibiting the ca(2+)-dependent mapk-jnk pathway. *Cell Host Microbe*, 21(1):47–58, 2017. doi: 10.1016/j.chom.2016.12.004.

[622] P. Bernal, L. P. Allsopp, A. Filloux, and M. A. Llamas. The pseudomonas putida t6ss is a plant warden against phytopathogens. *ISME J*, 11(4):972–987, 2017. doi: 10.1038/ismej.2016.169.

[623] L. Zhang, J. Xu, J. Xu, H. Zhang, L. He, and J. Feng. Tssb is essential for virulence and required for type vi secretion system in ralstonia solanacearum. *Microb Pathog*, 74:1–7, 2014. doi: 10.1016/j.micpath.2014.06.006.

[624] D. Y. Shyntum, J. Theron, S. N. Venter, L. N. Moleleki, I. K. Toth, and T. A. Coutinho. Pantoea ananatis utilizes a type vi secretion system for pathogenesis and bacterial competition. *Mol Plant Microbe Interact*, 28(4):420–31, 2015. doi: 10.1094/MPMI-07-14-0219-R.

[625] Y. Han, T. Wang, G. Chen, Q. Pu, Q. Liu, Y. Zhang, L. Xu, M. Wu, and H. Liang. A pseudomonas aeruginosa type vi secretion system regulated by cuer facilitates copper acquisition. *PLoS Pathog*, 15(12):e1008198, 2019. doi: 10.1371/journal.ppat.1008198.

[626] L. Fito-Boncompte, A. Chapalain, E. Bouffartigues, H. Chaker, O. Lesouhaitier, G. Gicquel, A. Bazire, A. Madi, N. Connil, W. Veron, L. Taupin, B. Toussaint, P. Cornelis, Q. Wei, K. Shioya, E. Deziel, M. G. Feuilloley, N. Orange, A. Dufour, and S. Chevalier. Full

virulence of pseudomonas aeruginosa requires oprf. *Infect Immun*, 79(3):1176–86, 2011. doi: 10.1128/IAI.00850-10.

[627] J. M. Meyer. Exogenous siderophore-mediated iron uptake in pseudomonas aeruginosa: possible involvement of porin oprf in iron translocation. *J Gen Microbiol*, 138(5):951–8, 1992. doi: 10.1099/00221287-138-5-951.

[628] R. G. Ankenbauer and H. N. Quan. Fpta, the fe(iii)-pyochelin receptor of pseudomonas aeruginosa: a phenolate siderophore receptor homologous to hydroxamate siderophore receptors. *J Bacteriol*, 176(2):307–19, 1994. doi: 10.1128/jb.176.2.307-319.1994.

[629] A. Kulp and M. J. Kuehn. Biological functions and biogenesis of secreted bacterial outer membrane vesicles. *Annu Rev Microbiol*, 64:163–84, 2010. doi: 10.1146/annurev.micro.091208.073413.

[630] S. Perinet, J. Jeukens, I. Kukavica-Ibrulj, M. M. Ouellet, S. J. Charette, and R. C. Levesque. Molybdate transporter modabc is important for pseudomonas aeruginosa chronic lung infection. *BMC Res Notes*, 9:23, 2016. doi: 10.1186/s13104-016-1840-x.

[631] William T. Self, Amy M. Grunden, Adnan Hasona, and Keelnatham T. Shanmugam. <1-s2.0-s0923250801012025-main.pdf>. *Research in Microbiology*, 152(3-4):311–321, 2001. doi: 10.1016/s0923-2508(01)01202-5.

[632] H. Nar, A. Messerschmidt, R. Huber, M. Vandekamp, and G. W. Canters. Crystal-structure of pseudomonas-aeruginosa apo-azurin at 1.85 angstrom resolution. *Febs Letters*, 306(2-3):119–124, 1992. doi: Doi 10.1016/0014-5793(92)80981-L.

[633] X. Yang, H. Liu, Y. Zhang, and X. Shen. Roles of type vi secretion system in transport of metal ions. *Front Microbiol*, 12:756136, 2021. doi: 10.3389/fmicb.2021.756136.

[634] M. Si, C. Zhao, B. Burkinshaw, B. Zhang, D. Wei, Y. Wang, T. G. Dong, and X. Shen. Manganese scavenging and oxidative stress response mediated by type vi secretion system in burkholderia thailandensis. *Proc Natl Acad Sci U S A*, 114(11):E2233–E2242, 2017. doi: 10.1073/pnas.1614902114.

[635] M. Si, Y. Wang, B. Zhang, C. Zhao, Y. Kang, H. Bai, D. Wei, L. Zhu, L. Zhang, T. G. Dong, and X. Shen. The type vi secretion system engages a redox-regulated dual-functional heme transporter for zinc acquisition. *Cell Rep*, 20(4):949–959, 2017. doi: 10.1016/j.celrep.2017.06.081.

[636] D. DeShazer. A novel contact-independent t6ss that maintains redox homeostasis via zn(2+) and mn(2+) acquisition is conserved in the burkholderia pseudomallei complex. *Microbiol Res*, 226:48–54, 2019. doi: 10.1016/j.micres.2019.05.007.

[637] X. Zhu, C. Feng, L. Zhou, Z. Li, Y. Zhang, and J. Pan. Impacts of ser/thr protein kinase stk1 on the proteome, twitching motility, and competitive advantage in pseudomonas aeruginosa. *Front Microbiol*, 12:738690, 2021. doi: 10.3389/fmicb.2021.738690.

[638] R. J. Lin, M. Capage, and C. W. Hill. A repetitive dna sequence, rhs, responsible for duplications within the escherichia coli k-12 chromosome. *J Mol Biol*, 177(1):1–18, 1984. doi: 10.1016/0022-2836(84)90054-8.

[639] S. Koskiniemi, J. G. Lamoureux, K. C. Nikolakakis, C. t'Kint de Roodenbeke, M. D. Kaplan, D. A. Low, and C. S. Hayes. Rhs proteins from diverse bacteria mediate intercellular competition. *Proc Natl Acad Sci U S A*, 110(17):7032–7, 2013. doi: 10.1073/pnas.1300627110.

[640] J. Alcoforado Diniz, Y. C. Liu, and S. J. Coulthurst. Molecular weaponry: diverse effectors delivered by the type vi secretion system. *Cell Microbiol*, 17(12):1742–51, 2015. doi: 10.1111/cmi.12532.

[641] M. Starsta, D. L. Hammarlof, M. Waneskog, S. Schlegel, F. Xu, A. Heden Gynna, M. Borg, S. Herschend, and S. Koskiniemi. Rhs-elements function as type ii toxin-antitoxin modules that regulate intra-macrophage replication of salmonella typhimurium. *PLoS Genet*, 16(2):e1008607, 2020. doi: 10.1371/journal.pgen.1008607.

[642] O. Stempler, A. K. Baidya, S. Bhattacharya, G. B. Malli Mohan, E. Tzipilevich, L. Sinai, G. Mamou, and S. Ben-Yehuda. Interspecies nutrient extraction and toxin delivery between bacteria. *Nat Commun*, 8(1):315, 2017. doi: 10.1038/s41467-017-00344-7.

[643] A. Jamet and X. Nassif. New players in the toxin field: polymorphic toxin systems in bacteria. *mBio*, 6(3):e00285–15, 2015. doi: 10.1128/mBio.00285-15.

[644] D. Zhang, R. F. de Souza, V. Anantharaman, L. M. Iyer, and L. Aravind. <1745-6150-7-18.pdf>. *Biol Direct*, 7:18, 2012. doi: 10.1186/1745-6150-7-18.

[645] D. Salomon, L. N. Kinch, D. C. Trudgian, X. Guo, J. A. Klimko, N. V. Grishin, H. Mirzaei, and K. Orth. Marker for type vi secretion system effectors. *Proc Natl Acad Sci U S A*, 111(25): 9271–6, 2014. doi: 10.1073/pnas.1406110111.

[646] B. Jana, C. M. Fridman, E. Bosis, and D. Salomon. A modular effector with a dnase domain and a marker for t6ss substrates. *Nat Commun*, 10(1):3595, 2019. doi: 10.1038/s41467-019-11546-6.

[647] N. H. Le, K. Peters, A. Espaillat, J. R. Sheldon, J. Gray, G. Di Venanzio, J. Lopez, B. Djahanschiri, E. A. Mueller, S. W. Hennon, P. A. Levin, I. Ebersberger, E. P. Skaar, F. Cava, W. Vollmer, and M. F. Feldman. <sciadv.abb5614.pdf>. *Sci Adv*, 6(30):eabb5614, 2020. doi: 10.1126/sciadv.abb5614.

[648] B. Lories, S. Roberfroid, L. Dieltjens, D. De Coster, K. R. Foster, and H. P. Steenackers. Biofilm bacteria use stress responses to detect and respond to competitors. *Curr Biol*, 30(7):1231–1244 e4, 2020. doi: 10.1016/j.cub.2020.01.065.

[649] T. Dorr, L. Alvarez, F. Delgado, B. M. Davis, F. Cava, and M. K. Waldor. A cell wall damage response mediated by a sensor kinase/response regulator pair enables beta-lactam tolerance. *Proc Natl Acad Sci U S A*, 113(2):404–9, 2016. doi: 10.1073/pnas.1520333113.

[650] S. J. Hersch, N. Watanabe, M. S. Stietz, K. Manera, F. Kamal, B. Burkinshaw, L. Lam, A. Pun, M. Li, A. Savchenko, and T. G. Dong. Envelope stress responses defend against type six secretion

system attacks independently of immunity proteins. *Nat Microbiol*, 5(5):706–714, 2020. doi: 10.1038/s41564-020-0672-6.

[651] Z. Podlesek and D. Zgur Bertok. The dna damage inducible sos response is a key player in the generation of bacterial persister cells and population wide tolerance. *Front Microbiol*, 11:1785, 2020. doi: 10.3389/fmicb.2020.01785.

[652] J. T. Hespanhol, D. E. Sanchez-Limache, G. G. Nicastro, L. Mead, E. E. Llontop, G. Chagas-Santos, C. S. Farah, R. F. de Souza, R. D. S. Galhardo, A. Lovering, and E. Bayer-Santos. <elife-82437-v1.pdf>. *Elife*, 11, 2022. doi: 10.7554/eLife.82437.

[653] A. Vaishampayan and E. Grohmann. Antimicrobials functioning through ros-mediated mechanisms: Current insights. *Microorganisms*, 10(1), 2021. doi: 10.3390/microorganisms10010061.

[654] T. G. Dong, S. Dong, C. Catalano, R. Moore, X. Liang, and J. J. Mekalanos. Generation of reactive oxygen species by lethal attacks from competing microbes. *Proc Natl Acad Sci U S A*, 112(7):2181–6, 2015. doi: 10.1073/pnas.1425007112.

[655] D. Storey, A. McNally, M. Astrand, J. Sa-Pessoa Graca Santos, I. Rodriguez-Escudero, B. Elmore, L. Palacios, H. Marshall, L. Hobley, M. Molina, V. J. Cid, T. A. Salminen, and J. A. Bengoechea. Klebsiella pneumoniae type vi secretion system-mediated microbial competition is phopq controlled and reactive oxygen species dependent. *PLoS Pathog*, 16(3):e1007969, 2020. doi: 10.1371/journal.ppat.1007969.

[656] S. W. Seo, D. Kim, R. Szubin, and B. O. Palsson. Genome-wide reconstruction of oxyr and soxrs transcriptional regulatory networks under oxidative stress in escherichia coli k-12 mg1655. *Cell Rep*, 12(8):1289–99, 2015. doi: 10.1016/j.celrep.2015.07.043.

[657] N. M. Bleumink-Pluym, L. B. van Alphen, L. I. Bouwman, M. M. Wosten, and J. P. van Putten. Identification of a functional type vi secretion system in campylobacter jejuni conferring capsule polysaccharide sensitive cytotoxicity. *PLoS Pathog*, 9(5):e1003393, 2013. doi: 10.1371/journal.ppat.1003393.

[658] O. Rendueles, L. Travier, P. Latour-Lambert, T. Fontaine, J. Magnus, E. Denamur, and J. M. Ghigo. Screening of escherichia coli species biodiversity reveals new biofilm-associated antiadhesion polysaccharides. *mBio*, 2(3):e00043–11, 2011. doi: 10.1128/mBio.00043-11.

[659] M. J. Powers, E. Sanabria-Valentin, A. A. Bowers, and E. A. Shank. Inhibition of cell differentiation in bacillus subtilis by pseudomonas protegens. *J Bacteriol*, 197(13):2129–2138, 2015. doi: 10.1128/JB.02535-14.

[660] C. Molina-Santiago, J. R. Pearson, Y. Navarro, M. V. Berlanga-Clavero, A. M. Caraballo-Rodriguez, D. Petras, M. L. Garcia-Martin, G. Lamon, B. Haberstein, F. M. Cazorla, A. de Vicente, A. Loquet, P. C. Dorrestein, and D. Romero. The extracellular matrix protects bacillus subtilis colonies from pseudomonas invasion and modulates plant co-colonization. *Nat Commun*, 10(1):1919, 2019. doi: 10.1038/s41467-019-09944-x.

[661] Alicia I. Perez-Lorente, Carlos Molina-Santiago, Antonio de Vicente, and Diego Romero. Sporulation activated via sigma w protects bacillus from a tse1 peptidoglycan hydrolase t6ss effector. 2022. doi: 10.1101/2022.02.23.481616.

[662] N. H. Le, V. Pinedo, J. Lopez, F. Cava, and M. F. Feldman. Killing of gram-negative and gram-positive bacteria by a bifunctional cell wall-targeting t6ss effector. *Proc Natl Acad Sci U S A*, 118(40), 2021. doi: 10.1073/pnas.2106555118.

[663] C. D. Nadell, K. Drescher, and K. R. Foster. Spatial structure, cooperation and competition in biofilms. *Nat Rev Microbiol*, 14(9):589–600, 2016. doi: 10.1038/nrmicro.2016.84.

[664] D. K. H. Rode, P. K. Singh, and K. Drescher. Multicellular and unicellular responses of microbial biofilms to stress. *Biol Chem*, 401(12):1365–1374, 2020. doi: 10.1515/hsz-2020-0213.

[665] H. C. Flemming, J. Wingender, U. Szewzyk, P. Steinberg, S. A. Rice, and S. Kjelleberg. Biofilms: an emergent form of bacterial life. *Nat Rev Microbiol*, 14(9):563–75, 2016. doi: 10.1038/nrmicro.2016.94.

[666] N. I. van den Berg, D. Machado, S. Santos, I. Rocha, J. Chacon, W. Harcombe, S. Mitri, and K. R. Patil. Ecological modelling approaches for predicting emergent properties in microbial communities. *Nat Ecol Evol*, 6(7):855–865, 2022. doi: 10.1038/s41559-022-01746-7.

[667] K. Nagarajan, C. Ni, and T. Lu. Agent-based modeling of microbial communities. *ACS Synth Biol*, 11(11):3564–3574, 2022. doi: 10.1021/acssynbio.2c00411.

[668] S. Koshy-Chenthittayil, L. Archambault, D. Senthilkumar, R. Laubenbacher, P. Mendes, and A. Dongari-Bagtzoglou. Agent based models of polymicrobial biofilms and the microbiome-a review. *Microorganisms*, 9(2), 2021. doi: 10.3390/microorganisms9020417.

[669] R. Hartmann, P. K. Singh, P. Pearce, R. Mok, B. Song, F. Diaz-Pascual, J. Dunkel, and K. Drescher. Emergence of three-dimensional order and structure in growing biofilms. *Nat Phys*, 15(3):251–256, 2019. doi: 10.1038/s41567-018-0356-9.

[670] A. Persat, C. D. Nadell, M. K. Kim, F. Ingremeau, A. Siryaporn, K. Drescher, N. S. Wingreen, B. L. Bassler, Z. Gitai, and H. A. Stone. The mechanical world of bacteria. *Cell*, 161(5):988–997, 2015. doi: 10.1016/j.cell.2015.05.005.

[671] F. L. Hellweger, R. J. Clegg, J. R. Clark, C. M. Plugge, and J. U. Kreft. Advancing microbial sciences by individual-based modelling. *Nat Rev Microbiol*, 14(7):461–71, 2016. doi: 10.1038/nrmicro.2016.62.

[672] L. Pacciani-Mori, A. Giometto, S. Suweis, and A. Maritan. Dynamic metabolic adaptation can promote species coexistence in competitive microbial communities. *PLoS Comput Biol*, 16(5): e1007896, 2020. doi: 10.1371/journal.pcbi.1007896.

[673] S. Estrela, A. Sanchez-Gorostiaga, J. C. Vila, and A. Sanchez. Nutrient dominance governs the assembly of microbial communities in mixed nutrient environments. *Elife*, 10, 2021. doi: 10.7554/eLife.65948.

[674] 3rd Marsland, R., W. Cui, and P. Mehta. A minimal model for microbial biodiversity can reproduce experimentally observed ecological patterns. *Sci Rep*, 10(1):3308, 2020. doi: 10.1038/s41598-020-60130-2.

[675] J. J. Winkle, O. A. Igoshin, M. R. Bennett, K. Josic, and W. Ott. Modeling mechanical interactions in growing populations of rod-shaped bacteria. *Phys Biol*, 14(5):055001, 2017. doi: 10.1088/1478-3975/aa7bae.

[676] J. Naylor, H. Fellermann, Y. Ding, W. K. Mohammed, N. S. Jakubovics, J. Mukherjee, C. A. Biggs, P. C. Wright, and N. Krasnogor. Simbiotics: A multiscale integrative platform for 3d modeling of bacterial populations. *ACS Synth Biol*, 6(7):1194–1210, 2017. doi: 10.1021/acssynbio.6b00315.

[677] J. Purswani, R. C. Romero-Zaliz, A. M. Martin-Platero, I. M. Guisado, J. Gonzalez-Lopez, and C. Pozo. Bsocial: Deciphering social behaviors within mixed microbial populations. *Front Microbiol*, 8:919, 2017. doi: 10.3389/fmicb.2017.00919.

[678] S. S. Jang, K. T. Oishi, R. G. Egbert, and E. Klavins. Specification and simulation of synthetic multicelled behaviors. *ACS Synth Biol*, 1(8):365–74, 2012. doi: 10.1021/sb300034m.

[679] M. Gutierrez, P. Gregorio-Godoy, G. Perez Del Pulgar, L. E. Munoz, S. Saez, and A. Rodriguez-Paton. A new improved and extended version of the multicell bacterial simulator gro. *ACS Synth Biol*, 6(8):1496–1508, 2017. doi: 10.1021/acssynbio.7b00003.

[680] Aidan P. Thompson, H. Metin Aktulga, Richard Berger, Dan S. Bolintineanu, W. Michael Brown, Paul S. Crozier, Pieter J. in 't Veld, Axel Kohlmeyer, Stan G. Moore, Trung Dac Nguyen, Ray Shan, Mark J. Stevens, Julien Tranchida, Christian Trott, and Steven J. Plimpton. Lammps - a flexible simulation tool for particle-based materials modeling at the atomic, meso, and continuum scales. *Computer Physics Communications*, 271, 2022. doi: 10.1016/j.cpc.2021.108171.

[681] A. Bogdanowski, T. Banitz, L. K. Muhsal, C. Kost, and K. Frank. Mccomedy: A user-friendly tool for next-generation individual-based modeling of microbial consumer-resource systems. *PLoS Comput Biol*, 18(1):e1009777, 2022. doi: 10.1371/journal.pcbi.1009777.

[682] T. J. Rudge, P. J. Steiner, A. Phillips, and J. Haseloff. Computational modeling of synthetic microbial biofilms. *ACS Synth Biol*, 1(8):345–52, 2012. doi: 10.1021/sb300031n.

[683] M. J. Bottery, I. Passaris, C. Dytham, A. J. Wood, and M. W. van der Woude. Spatial organization of expanding bacterial colonies is affected by contact-dependent growth inhibition. *Curr Biol*, 29(21):3622–3634 e5, 2019. doi: 10.1016/j.cub.2019.08.074.

[684] W. P. J. Smith, A. Vettiger, J. Winter, T. Ryser, L. E. Comstock, M. Basler, and K. R. Foster. The evolution of the type vi secretion system as a disintegration weapon. *PLoS Biol*, 18(5): e3000720, 2020. doi: 10.1371/journal.pbio.3000720.

[685] T. G. Sana, B. Berni, and S. Bleves. The t6sss of pseudomonas aeruginosa strain pao1 and their effectors: Beyond bacterial-cell targeting. *Front Cell Infect Microbiol*, 6:61, 2016. doi: 10.3389/fcimb.2016.00061.

[686] M. C. Anderson, P. Vonaesch, A. Saffarian, B. S. Marteyn, and P. J. Sansonetti. Shigella sonnei encodes a functional t6ss used for interbacterial competition and niche occupancy. *Cell Host Microbe*, 21(6):769–776 e3, 2017. doi: 10.1016/j.chom.2017.05.004.

[687] D. B. Borenstein, P. Ringel, M. Basler, and N. S. Wingreen. Established microbial colonies can survive type vi secretion assault. *PLoS Comput Biol*, 11(10):e1004520, 2015. doi: 10.1371/journal.pcbi.1004520.

[688] L. Xiong, R. Cooper, and L. S. Tsimring. Coexistence and pattern formation in bacterial mixtures with contact-dependent killing. *Biophys J*, 114(7):1741–1750, 2018. doi: 10.1016/j.bpj.2018.02.012.

[689] L. McNally, E. Bernardy, J. Thomas, A. Kalziqi, J. Pentz, S. P. Brown, B. K. Hammer, P. J. Yunker, and W. C. Ratcliff. Killing by type vi secretion drives genetic phase separation and correlates with increased cooperation. *Nat Commun*, 8:14371, 2017. doi: 10.1038/ncomms14371.

[690] J. L. Wilmoth, P. W. Doak, A. Timm, M. Halsted, J. D. Anderson, M. Ginovart, C. Prats, X. Portell, S. T. Retterer, and M. Fuentes-Cabrera. A microfluidics and agent-based modeling framework for investigating spatial organization in bacterial colonies: The case of pseudomonas aeruginosa and h1-type vi secretion interactions. *Front Microbiol*, 9:33, 2018. doi: 10.3389/fmicb.2018.00033.

[691] A. E. Blanchard and T. Lu. Bacterial social interactions drive the emergence of differential spatial colony structures. *BMC Syst Biol*, 9:59, 2015. doi: 10.1186/s12918-015-0188-5.

[692] T. G. Sana, N. Flaugnatti, K. A. Lugo, L. H. Lam, A. Jacobson, V. Baylot, E. Durand, L. Journet, E. Cascales, and D. M. Monack. Salmonella typhimurium utilizes a t6ss-mediated antibacterial weapon to establish in the host gut. *Proc Natl Acad Sci U S A*, 113(34):E5044–51, 2016. doi: 10.1073/pnas.1608858113.

[693] W. Zhao, F. Caro, W. Robins, and J. J. Mekalanos. Antagonism toward the intestinal microbiota and its effect on vibrio cholerae virulence. *Science*, 359(6372):210–213, 2018. doi: 10.1126/science.aap8775.

[694] C. Bongrand, E. J. Koch, S. Moriano-Gutierrez, O. X. Cordero, M. McFall-Ngai, M. F. Polz, and E. G. Ruby. A genomic comparison of 13 symbiotic vibrio fischeri isolates from the perspective of their host source and colonization behavior. *ISME J*, 10(12):2907–2917, 2016. doi: 10.1038/ismej.2016.69.

[695] M. Wong, X. Liang, M. Smart, L. Tang, R. Moore, B. Ingalls, and T. G. Dong. Microbial herd protection mediated by antagonistic interaction in polymicrobial communities. *Appl Environ Microbiol*, 82(23):6881–6888, 2016. doi: 10.1128/AEM.02210-16.

[696] B. Momeni, K. A. Brileya, M. W. Fields, and W. Shou. Strong inter-population cooperation leads to partner intermixing in microbial communities. *Elife*, 2:e00230, 2013. doi: 10.7554/eLife.00230.

[697] S. C. Booth and S. A. Rice. Influence of interspecies interactions on the spatial organization of dual species bacterial communities. *Biofilm*, 2:100035, 2020. doi: 10.1016/j.bioflm.2020.100035.

[698] G. Steinbach, C. Crisan, S. L. Ng, B. K. Hammer, and P. J. Yunker. Accumulation of dead cells from contact killing facilitates coexistence in bacterial biofilms. *J R Soc Interface*, 17(173): 20200486, 2020. doi: 10.1098/rsif.2020.0486.

[699] T. G. Sana, K. A. Lugo, and D. M. Monack. T6ss: The bacterial "fight club" in the host gut. *PLoS Pathog*, 13(6):e1006325, 2017. doi: 10.1371/journal.ppat.1006325.

[700] L. Eigentler, M. Kalamara, G. Ball, C. E. MacPhee, N. R. Stanley-Wall, and F. A. Davidson. Founder cell configuration drives competitive outcome within colony biofilms. *ISME J*, 16(6): 1512–1522, 2022. doi: 10.1038/s41396-022-01198-8.

[701] J. van Gestel, F. J. Weissing, O. P. Kuipers, and A. T. Kovacs. Density of founder cells affects spatial pattern formation and cooperation in bacillus subtilis biofilms. *ISME J*, 8(10):2069–79, 2014. doi: 10.1038/ismej.2014.52.

[702] David Yanni, Arben Kalziqi, Jacob Thomas, Siu Lung Ng, Skanda Vivek, William C. Ratcliff, Brian K. Hammer, and Peter J. Yunker. Life in the coffee-ring how evaporation-driven density gradients dictate the outcome of inter-bacterial competition. *arXiv*, 1707.03472, 2017. doi: 10.48550/arXiv.1707.03472.

[703] Sean C. Booth, William P. J. Smith, and Kevin R. Foster. Bows and swords: why bacteria carry short and long-range weapons. *bioRxiv*, 2022. doi: 10.1101/2022.10.13.512033.

[704] K. Nakayama, K. Takashima, H. Ishihara, T. Shinomiya, M. Kageyama, S. Kanaya, M. Ohnishi, T. Murata, H. Mori, and T. Hayashi. The r-type pyocin of pseudomonas aeruginosa is related to p2 phage, and the f-type is related to lambda phage. *Mol Microbiol*, 38(2):213–31, 2000. doi: 10.1046/j.1365-2958.2000.02135.x.

[705] M. Lazzaro, M. F. Feldman, and E. Garcia Vescovi. A transcriptional regulatory mechanism finely tunes the firing of type vi secretion system in response to bacterial enemies. *mBio*, 8(4), 2017. doi: 10.1128/mBio.00559-17.

[706] R. Guillemette, B. Ushijima, M. Jalan, C. C. Hase, and F. Azam. Insight into the resilience and susceptibility of marine bacteria to t6ss attack by vibrio cholerae and vibrio coralliilyticus. *PLoS One*, 15(1):e0227864, 2020. doi: 10.1371/journal.pone.0227864.

[707] Yuexia Luna Lin, Stephanie N. Smith, Eva Kanso, Alecia N. Septer, and Chris H. Rycroft. A subcellular biochemical model for t6ss dynamics reveals winning competitive strategies. *bioRxiv*, 2021. doi: 10.1101/2021.07.17.452664.

[708] M. Herrero, V. de Lorenzo, and K. N. Timmis. Transposon vectors containing non-antibiotic resistance selection markers for cloning and stable chromosomal insertion of foreign genes in gram-negative bacteria. *J Bacteriol*, 172(11):6557–67, 1990. doi: 10.1128/jb.172.11.6557-6567.1990.

[709] D. H. Figurski and D. R. Helinski. Replication of an origin-containing derivative of plasmid rk2 dependent on a plasmid function provided in trans. *Proc Natl Acad Sci U S A*, 76(4):1648–52, 1979. doi: 10.1073/pnas.76.4.1648.

[710] K. Kaniga, I. Delor, and G. R. Cornelis. A wide-host-range suicide vector for improving reverse genetics in gram-negative bacteria: inactivation of the blaa gene of yersinia enterocolitica. *Gene*, 109(1):137–41, 1991. doi: 10.1016/0378-1119(91)90599-7.

[711] M. Hentzer, K. Riedel, T. B. Rasmussen, A. Heydorn, J. B. Andersen, M. R. Parsek, S. A. Rice, L. Eberl, S. Molin, N. Hoiby, S. Kjelleberg, and M. Givskov. Inhibition of quorum sensing in pseudomonas aeruginosa biofilm bacteria by a halogenated furanone compound. *Microbiology (Reading)*, 148(Pt 1):87–102, 2002. doi: 10.1099/00221287-148-1-87.

[712] J. Thibault, E. Faudry, C. Ebel, I. Attree, and S. Elsen. Anti-activator exsd forms a 1 to 1 complex with exsa to inhibit transcription of type iii secretion operons. *J Biol Chem*, 284(23): 15762–70, 2009. doi: 10.1074/jbc.M109.003533.

[713] M. T. Rybtke, B. R. Borlee, K. Murakami, Y. Irie, M. Hentzer, T. E. Nielsen, M. Givskov, M. R. Parsek, and T. Tolker-Nielsen. Fluorescence-based reporter for gauging cyclic di-gmp levels in pseudomonas aeruginosa. *Appl Environ Microbiol*, 78(15):5060–9, 2012. doi: 10.1128/AEM.00414-12.

[714] D. Muhl and A. Filloux. Site-directed mutagenesis and gene deletion using reverse genetics. *Methods Mol Biol.*, 521-39(1149), 2014. doi: 10.1007/978-1-4939-0473-$0_4$0.

[715] Brendan P. Cormack, Raphael H. Valdivia, and Stanley Falkow. Facs-optimized mutants of the green fluorescent protein (gfp). *Gene*, 173(1):33–38, 1996. ISSN 0378-1119. Flourescent Proteins and Applications.

[716] J. Schindelin, I. Arganda-Carreras, E. Frise, V. Kaynig, M. Longair, T. Pietzsch, S. Preibisch, C. Rueden, S. Saalfeld, B. Schmid, J. Y. Tinevez, D. J. White, V. Hartenstein, K. Eliceiri, P. Tomancak, and A. Cardona. Fiji: an open-source platform for biological-image analysis. *Nat Methods*, 9(7):676–82, 2012. doi: 10.1038/nmeth.2019.

[717] F. Goldschmidt, R. R. Regoes, and D. R. Johnson. Successive range expansion promotes diversity and accelerates evolution in spatially structured microbial populations. *ISME J*, 11(9):2112–2123, 2017. doi: 10.1038/ismej.2017.76.

[718] M. Wang, X. Chen, Y. Ma, Y. Q. Tang, D. R. Johnson, Y. Nie, and X. L. Wu. Type iv pilus shapes a 'bubble-burst' pattern opposing spatial intermixing of two interacting bacterial populations. *Microbiol Spectr*, 10(1):e0194421, 2022. doi: 10.1128/spectrum.01944-21.

[719] Dong-ju Kim,. Relation of microbial biomass to counting units for Pseudomonas aeruginosa. *African Journal of Microbiology Research*, 6(21):4620–4622, jun 2012. ISSN 1996-0808. doi: 10.5897/ajmr10.902.

[720] K. Eilers, J. Kuok Hoong Yam, R. Morton, A. Mei Hui Yong, J. Brizuela, C. Hadjicharalambous, X. Liu, M. Givskov, S. A. Rice, and A. Filloux. Phenotypic and integrated analysis of a comprehensive pseudomonas aeruginosa pao1 library of mutants lacking cyclic-di-gmp-related genes. *Front Microbiol*, 13:949597, 2022. doi: 10.3389/fmicb.2022.949597.

[721] C. Valverde, S. Heeb, C. Keel, and D. Haas. Rsmy, a small regulatory rna, is required in concert with rsmz for gaca-dependent expression of biocontrol traits in pseudomonas fluorescens cha0. *Mol Microbiol*, 50(4):1361–79, 2003. doi: 10.1046/j.1365-2958.2003.03774.x.

[722] M. Whiteley, M. G. Bangera, R. E. Bumgarner, M. R. Parsek, G. M. Teitzel, S. Lory, and E. P. Greenberg. Gene expression in pseudomonas aeruginosa biofilms. *Nature*, 413(6858):860–4, 2001. doi: 10.1038/35101627.

[723] L. P. Allsopp, T. E. Wood, S. A. Howard, F. Maggiorelli, L. M. Nolan, S. Wettstadt, and A. Filloux. Rsma and amrz orchestrate the assembly of all three type vi secretion systems in pseudomonas aeruginosa. *Proc Natl Acad Sci U S A*, 114(29):7707–7712, 2017. doi: 10.1073/pnas.1700286114.

[724] L. Sheng, Y. Lv, Q. Liu, Q. Wang, and Y. Zhang. Connecting type vi secretion, quorum sensing, and c-di-gmp production in fish pathogen vibrio alginolyticus through phosphatase pppa. *Vet Microbiol*, 162(2-4):652–662, 2013. doi: 10.1016/j.vetmic.2012.09.009.

[725] R. R. McCarthy, M. Yu, K. Eilers, Y. C. Wang, E. M. Lai, and A. Filloux. Cyclic di-gmp inactivates t6ss and t4ss activity in agrobacterium tumefaciens. *Mol Microbiol*, 112(2):632–648, 2019. doi: 10.1111/mmi.14279.

[726] Z. Wang, X. Huang, Y. Liu, G. Yang, Y. Liu, and X. Zhang. Gacs/gaca activates pyoluteorin biosynthesis through gac/rsm-rsme cascade and rsma/rsme-driven feedback loop in pseudomonas protegens h78. *Mol Microbiol*, 105(6):968–985, 2017. doi: 10.1111/mmi.13749.

[727] H. Nie, Y. Xiao, M. Song, N. Wu, Q. Peng, W. Duan, W. Chen, and Q. Huang. Wsp system oppositely modulates antibacterial activity and biofilm formation via fleq-flen complex in pseudomonas putida. *Environ Microbiol*, 24(3):1543–1559, 2022. doi: 10.1111/1462-2920.15905.

[728] L. P. Allsopp, A. C. Z. Collins, E. Hawkins, T. E. Wood, and A. Filloux. Rpon/sfa2-dependent activation of the pseudomonas aeruginosa h2-t6ss and its cognate arsenal of antibacterial toxins. *Nucleic Acids Res*, 50(1):227–243, 2022. doi: 10.1093/nar/gkab1254.

[729] E. Blanco-Romero, M. Redondo-Nieto, F. Martinez-Granero, D. Garrido-Sanz, M. I. Ramos-Gonzalez, M. Martin, and R. Rivilla. Genome-wide analysis of the fleq direct regulon in pseudomonas fluorescens f113 and pseudomonas putida kt2440. *Sci Rep*, 8(1):13145, 2018. doi: 10.1038/s41598-018-31371-z.

[730] E. Blanco-Romero, D. Duran, D. Garrido-Sanz, R. Rivilla, M. Martin, and M. Redondo-Nieto. Transcriptomic analysis of pseudomonas ogarae f113 reveals the antagonistic roles of amrz and fleq during rhizosphere adaption. *Microb Genom*, 8(1), 2022. doi: 10.1099/mgen.0.000750.

[731] D. Duran, P. Bernal, D. Vazquez-Arias, E. Blanco-Romero, D. Garrido-Sanz, M. Redondo-Nieto, R. Rivilla, and M. Martin. Pseudomonas fluorescens f113 type vi secretion systems mediate bacterial killing and adaption to the rhizosphere microbiome. *Sci Rep*, 11(1):5772, 2021. doi: 10.1038/s41598-021-85218-1.

[732] T. Zhou, J. Huang, Z. Liu, Q. Lin, Z. Xu, and L. H. Zhang. The two-component system fles/fler represses h1-t6ss via cyclic di-gmp signaling in pseudomonas aeruginosa. *Appl Environ Microbiol*, 88(2):e0165521, 2022. doi: 10.1128/AEM.01655-21.

[733] K. M. Sall, M. G. Casabona, C. Bordi, P. Huber, S. de Bentzmann, I. Attree, and S. Elsen. A gacs deletion in pseudomonas aeruginosa cystic fibrosis isolate cha shapes its virulence. *PLoS One*, 9(4):e95936, 2014. doi: 10.1371/journal.pone.0095936.

[734] S. Feliziani, R. L. Marvig, A. M. Lujan, A. J. Moyano, J. A. Di Rienzo, H. Krogh Johansen, S. Molin, and A. M. Smania. Coexistence and within-host evolution of diversified lineages of hypermutable pseudomonas aeruginosa in long-term cystic fibrosis infections. *PLoS Genet*, 10 (10):e1004651, 2014. doi: 10.1371/journal.pgen.1004651.

[735] C. Bordi, M. C. Lamy, I. Ventre, E. Termine, A. Hachani, S. Fillet, B. Roche, S. Bleves, V. Mejean, A. Lazdunski, and A. Filloux. Regulatory rnas and the hptb/rets signalling pathways fine-tune pseudomonas aeruginosa pathogenesis. *Mol Microbiol*, 76(6):1427–43, 2010. doi: 10.1111/j.1365-2958.2010.07146.x.

[736] X. Latour. The evanescent gacs signal. *Microorganisms*, 8(11), 2020. doi: 10.3390/microorganisms8111746.

[737] H. Mikkelsen, M. Sivaneson, and A. Filloux. Key two-component regulatory systems that control biofilm formation in pseudomonas aeruginosa. *Environ Microbiol*, 13(7):1666–81, 2011. doi: 10.1111/j.1462-2920.2011.02495.x.

[738] Y. Irie, A. La Mensa, V. Murina, V. Hauryliuk, T. Tenson, and V. Shingler. Hfq-assisted rsma regulation is central to pseudomonas aeruginosa biofilm polysaccharide pel expression. *Front Microbiol*, 11:482585, 2020. doi: 10.3389/fmicb.2020.482585.

[739] K. H. Schulmeyer, M. R. Diaz, T. B. Bair, W. Sanders, C. J. Gode, A. Laederach, M. C. Wolfgang, and T. L. Yahr. Primary and secondary sequence structure requirements for recognition and discrimination of target rnas by pseudomonas aeruginosa rsma and rsmf. *J Bacteriol*, 198(18):2458–69, 2016. doi: 10.1128/JB.00343-16.

[740] M. Basler and J. J. Mekalanos. Type 6 secretion dynamics within and between bacterial cells. *Science*, 337(6096):815, 2012. doi: 10.1126/science.1222901.

[741] A. Hachani, N. S. Lossi, and A. Filloux. A visual assay to monitor t6ss-mediated bacterial competition. *J Vis Exp*, (73):e50103, 2013. doi: 10.3791/50103.

[742] T. Romeo and P. Babitzke. Global regulation by csra and its rna antagonists. *Microbiol Spectr*, 6(2), 2018. doi: 10.1128/microbiolspec.RWR-0009-2017.

[743] F. Jean-Pierre, J. Tremblay, and E. Deziel. Broth versus surface-grown cells: Differential regulation of rsmy/z small rnas in pseudomonas aeruginosa by the gac/hptb system. *Front Microbiol*, 7:2168, 2016. doi: 10.3389/fmicb.2016.02168.

[744] J. Zheng, B. Ho, and J. J. Mekalanos. Genetic analysis of anti-amoebae and anti-bacterial activities of the type vi secretion system in vibrio cholerae. *PLoS One*, 6(8):e23876, 2011. doi: 10.1371/journal.pone.0023876.

[745] R. E. Hernandez, R. Gallegos-Monterrosa, and S. J. Coulthurst. Type vi secretion system effector proteins: Effective weapons for bacterial competitiveness. *Cell Microbiol*, 22(9):e13241, 2020. doi: 10.1111/cmi.13241.

[746] M. Valentini, B. J. Laventie, J. Moscoso, U. Jenal, and A. Filloux. The diguanylate cyclase hsbd intersects with the hptb regulatory cascade to control pseudomonas aeruginosa biofilm and motility. *PLoS Genet*, 12(10):e1006354, 2016. doi: 10.1371/journal.pgen.1006354.

[747] O. Hallatschek, P. Hersen, S. Ramanathan, and D. R. Nelson. Genetic drift at expanding frontiers promotes gene segregation. *Proc Natl Acad Sci U S A*, 104(50):19926–30, 2007. doi: 10.1073/pnas.0710150104.

[748] T. Xu, M. L. Lam, and T. H. Chen. Discrete element model for suppression of coffee-ring effect. *Sci Rep*, 7:42817, 2017. doi: 10.1038/srep42817.

[749] T. Andac, P. Weigmann, S. K. P. Velu, E. Pince, G. Volpe, G. Volpe, and A. Callegari. Active matter alters the growth dynamics of coffee rings. *Soft Matter*, 15(7):1488–1496, 2019. doi: 10.1039/c8sm01350k.

[750] J. Jumper, R. Evans, A. Pritzel, T. Green, M. Figurnov, O. Ronneberger, K. Tunyasuvunakool, R. Bates, A. Zidek, A. Potapenko, A. Bridgland, C. Meyer, S. A. A. Kohl, A. J. Ballard, A. Cowie, B. Romera-Paredes, S. Nikolov, R. Jain, J. Adler, T. Back, S. Petersen, D. Reiman, E. Clancy, M. Zielinski, M. Steinegger, M. Pacholska, T. Berghammer, S. Bodenstein, D. Silver, O. Vinyals, A. W. Senior, K. Kavukcuoglu, P. Kohli, and D. Hassabis. Highly accurate protein structure prediction with alphafold. *Nature*, 596(7873):583–589, 2021. doi: 10.1038/s41586-021-03819-2.

[751] L. Holm. Dali and the persistence of protein shape. *Protein Sci*, 29(1):128–140, 2020. doi: 10.1002/pro.3749.

[752] A. A. Angus, C. M. Agapakis, S. Fong, S. Yerrapragada, P. Estrada-de los Santos, P. Yang, N. Song, S. Kano, J. Caballero-Mellado, S. M. de Faria, F. D. Dakora, G. Weinstock, and A. M. Hirsch. Plant-associated symbiotic burkholderia species lack hallmark strategies required in mammalian pathogenesis. *PLoS One*, 9(1):e83779, 2014. doi: 10.1371/journal.pone.0083779.

[753] S. L. Murdoch, K. Trunk, G. English, M. J. Fritsch, E. Pourkarimi, and S. J. Coulthurst. The opportunistic pathogen serratia marcescens utilizes type vi secretion to target bacterial competitors. *J Bacteriol*, 193(21):6057–69, 2011. doi: 10.1128/JB.05671-11.

[754] A. Vermassen, S. Leroy, R. Talon, C. Provot, M. Popowska, and M. Desvaux. Cell wall hydrolases in bacteria: Insight on the diversity of cell wall amidases, glycosidases and peptidases toward peptidoglycan. *Front Microbiol*, 10:331, 2019. doi: 10.3389/fmicb.2019.00331.

[755] L. Lin, E. Lezan, A. Schmidt, and M. Basler. Abundance of bacterial type vi secretion system components measured by targeted proteomics. *Nat Commun*, 10(1):2584, 2019. doi: 10.1038/s41467-019-10466-9.

[756] E. Durand, C. Cambillau, E. Cascales, and L. Journet. Vgrg, tae, tle, and beyond: the versatile arsenal of type vi secretion effectors. *Trends Microbiol*, 22(9):498–507, 2014. doi: 10.1016/j.tim.2014.06.004.

[757] S. Gupta, S. Ray, A. Khan, A. China, D. Das, and A. I. Mallick. The cost of bacterial predation via type vi secretion system leads to predator extinction under environmental stress. *iScience*, 24(12):103507, 2021. doi: 10.1016/j.isci.2021.103507.

[758] B. Chassaing and E. Cascales. Antibacterial weapons: Targeted destruction in the microbiota. *Trends Microbiol*, 26(4):329–338, 2018. doi: 10.1016/j.tim.2018.01.006.

[759] D. O. Serra, A. M. Richter, and R. Hengge. Cellulose as an architectural element in spatially structured escherichia coli biofilms. *J Bacteriol*, 195(24):5540–54, 2013. doi: 10.1128/JB.00946-13.

[760] S. Srinivasan, I. D. Vladescu, S. A. Koehler, X. Wang, M. Mani, and S. M. Rubinstein. Matrix production and sporulation in bacillus subtilis biofilms localize to propagating wave fronts. *Biophys J*, 114(6):1490–1498, 2018. doi: 10.1016/j.bpj.2018.02.002.

[761] S. Beyhan and F. H. Yildiz. Smooth to rugose phase variation in vibrio cholerae can be mediated by a single nucleotide change that targets c-di-gmp signalling pathway. *Mol Microbiol*, 63(4): 995–1007, 2007. doi: 10.1111/j.1365-2958.2006.05568.x.

[762] J. C. Fong and F. H. Yildiz. The rbmbcdef gene cluster modulates development of rugose colony morphology and biofilm formation in vibrio cholerae. *J Bacteriol*, 189(6):2319–30, 2007. doi: 10.1128/JB.01569-06.

[763] J. K. Teschler, E. Jimenez-Siebert, H. Jeckel, P. K. Singh, J. H. Park, S. Pukatzki, C. D. Nadell, K. Drescher, and F. H. Yildiz. Vxrb influences antagonism within biofilms by controlling competition through extracellular matrix production and type 6 secretion. *mBio*, 13(4):e0188522, 2022. doi: 10.1128/mbio.01885-22.

[764] J. G. Malone. Role of small colony variants in persistence of pseudomonas aeruginosa infections in cystic fibrosis lungs. *Infect Drug Resist*, 8:237–47, 2015. doi: 10.2147/IDR.S68214.

[765] Y. Irie, M. Starkey, A. N. Edwards, D. J. Wozniak, T. Romeo, and M. R. Parsek. Pseudomonas aeruginosa biofilm matrix polysaccharide psl is regulated transcriptionally by rpos and post-transcriptionally by rsma. *Mol Microbiol*, 78(1):158–72, 2010. doi: 10.1111/j.1365-2958.2010.07320.x.

[766] E. S. Gloag, C. W. Marshall, D. Snyder, G. R. Lewin, J. S. Harris, A. Santos-Lopez, S. B. Chaney, M. Whiteley, V. S. Cooper, and D. J. Wozniak. Pseudomonas aeruginosa interstrain dynamics and selection of hyperbiofilm mutants during a chronic infection. *mBio*, 10(4), 2019. doi: 10.1128/mBio.01698-19.

[767] R. Custodio, R. M. Ford, C. J. Ellison, G. Liu, G. Mickute, C. M. Tang, and R. M. Exley. Type vi secretion system killing by commensal neisseria is influenced by expression of type four pili. *Elife*, 10, 2021. doi: 10.7554/eLife.63755.

[768] R. Zollner, E. R. Oldewurtel, N. Kouzel, and B. Maier. Phase and antigenic variation govern competition dynamics through positioning in bacterial colonies. *Sci Rep*, 7(1):12151, 2017. doi: 10.1038/s41598-017-12472-7.

[769] E. R. Oldewurtel, N. Kouzel, L. Dewenter, K. Henseler, and B. Maier. Differential interaction forces govern bacterial sorting in early biofilms. *Elife*, 4, 2015. doi: 10.7554/eLife.10811.

[770] T. J. Rudge, F. Federici, P. J. Steiner, A. Kan, and J. Haseloff. Cell polarity-driven instability generates self-organized, fractal patterning of cell layers. *ACS Synth Biol*, 2(12):705–14, 2013. doi: 10.1021/sb400030p.

[771] S. L. Chua, K. Sivakumar, M. Rybtke, M. Yuan, J. B. Andersen, T. E. Nielsen, M. Givskov, T. Tolker-Nielsen, B. Cao, S. Kjelleberg, and L. Yang. C-di-gmp regulates pseudomonas aeruginosa stress response to tellurite during both planktonic and biofilm modes of growth. *Sci Rep*, 5:10052, 2015. doi: 10.1038/srep10052.

[772] N. C. Darnton, L. Turner, S. Rojevsky, and H. C. Berg. Dynamics of bacterial swarming. *Biophys J*, 98(10):2082–90, 2010. doi: 10.1016/j.bpj.2010.01.053.

[773] J. Tremblay and E. Deziel. Improving the reproducibility of pseudomonas aeruginosa swarming motility assays. *J Basic Microbiol*, 48(6):509–15, 2008. doi: 10.1002/jobm.200800030.

[774] M. S. Anderson, E. C. Garcia, and P. A. Cotter. Kind discrimination and competitive exclusion mediated by contact-dependent growth inhibition systems shape biofilm community structure. *PLoS Pathog*, 10(4):e1004076, 2014. doi: 10.1371/journal.ppat.1004076.

[775] J. C. Fong, A. Rogers, A. K. Michael, N. C. Parsley, W. C. Cornell, Y. C. Lin, P. K. Singh, R. Hartmann, K. Drescher, E. Vinogradov, L. E. Dietrich, C. L. Partch, and F. H. Yildiz. Structural dynamics of rbma governs plasticity of vibrio cholerae biofilms. *Elife*, 6, 2017. doi: 10.7554/eLife.26163.

[776] S. N. Wai, Y. Mizunoe, A. Takade, S. I. Kawabata, and S. I. Yoshida. Vibrio cholerae o1 strain tsi-4 produces the exopolysaccharide materials that determine colony morphology, stress resistance, and biofilm formation. *Appl Environ Microbiol*, 64(10):3648–55, 1998. doi: 10.1128/AEM.64.10.3648-3655.1998.

[777] Olaya Rendueles. Deciphering the role of the capsule ofklebsiella pneumoniaeduring pathogenesis: A cautionary tale. *Molecular Microbiology*, 113(5):883–888, 2020. doi: 10.1111/mmi.14474.

[778] D. J. Doorduijn, S. H. Rooijakkers, W. van Schaik, and B. W. Bardoel. Complement resistance mechanisms of klebsiella pneumoniae. *Immunobiology*, 221(10):1102–9, 2016. doi: 10.1016/j.imbio.2016.06.014.

[779] J. Lennings, T. E. West, and S. Schwarz. The burkholderia type vi secretion system 5: Composition, regulation and role in virulence. *Front Microbiol*, 9:3339, 2018. doi: 10.3389/fmicb.2018.03339.

[780] S. L. Reckseidler-Zenteno, D. F. Viteri, R. Moore, E. Wong, A. Tuanyok, and D. E. Woods. Characterization of the type iii capsular polysaccharide produced by burkholderia pseudomallei. *J Med Microbiol*, 59(Pt 12):1403–1414, 2010. doi: 10.1099/jmm.0.022202-0.

[781] H. L. Spiewak, S. Shastri, L. Zhang, S. Schwager, L. Eberl, A. C. Vergunst, and M. S. Thomas. Burkholderia cenocepacia utilizes a type vi secretion system for bacterial competition. *Microbiologyopen*, page e774, 2019. doi: 10.1002/mbo3.774.

[782] J. Tickner, S. Hawas, M. Totsika, and J. J. Kenyon. The wzi outer membrane protein mediates assembly of a tight capsular polysaccharide layer on the acinetobacter baumannii cell surface. *Sci Rep*, 11(1):21741, 2021. doi: 10.1038/s41598-021-01206-5.

[783] T. Merciecca, S. Bornes, L. Nakusi, S. Theil, O. Rendueles, C. Forestier, and S. Miquel. Role of klebsiella pneumoniae type vi secretion system (t6ss) in long-term gastrointestinal colonization. *Sci Rep*, 12(1):16968, 2022. doi: 10.1038/s41598-022-21396-w.

[784] B. Deng, S. Ghatak, S. Sarkar, K. Singh, P. Das Ghatak, S. S. Mathew-Steiner, S. Roy, S. Khanna, D. J. Wozniak, D. W. McComb, and C. K. Sen. Novel bacterial diversity and fragmented edna identified in hyperbiofilm-forming pseudomonas aeruginosa rugose small colony variant. *iScience*, 23(2):100827, 2020. doi: 10.1016/j.isci.2020.100827.

[785] Z. C. Ruhe, L. Townsley, A. B. Wallace, A. King, M. W. Van der Woude, D. A. Low, F. H. Yildiz, and C. S. Hayes. Cdia promotes receptor-independent intercellular adhesion. *Mol Microbiol*, 98 (1):175–92, 2015. doi: 10.1111/mmi.13114.

[786] Y. W. Chang, L. A. Rettberg, D. R. Ortega, and G. J. Jensen. In vivo structures of an intact type vi secretion system revealed by electron cryotomography. *EMBO Rep*, 18(7):1090–1099, 2017. doi: 10.15252/embr.201744072.

[787] S. Y. Ting, E. Martinez-Garcia, S. Huang, S. K. Bertolli, K. A. Kelly, K. J. Cutler, E. D. Su, H. Zhi, Q. Tang, M. C. Radey, M. Raffatellu, S. B. Peterson, V. de Lorenzo, and J. D. Mougous. Targeted depletion of bacteria from mixed populations by programmable adhesion with antagonistic competitor cells. *Cell Host Microbe*, 28(2):313–321 e6, 2020. doi: 10.1016/j.chom.2020.05.006.

[788] L. Speare, M. Woo, A. K. Dunn, and A. N. Septer. A putative lipoprotein mediates cell-cell contact for type vi secretion system-dependent killing of specific competitors. *mBio*, 13(2): e0308521, 2022. doi: 10.1128/mbio.03085-21.

[789] Gavin Melaugh, Vincent Martinez, Perrin Baker, Preston Hill, P. Lynne Howell, Daniel J. Wozniak, and Rosalind J. Allen. Distinct types of multicellular aggregates in pseudomonas aeruginosa liquid cultures. 2022. doi: 10.1101/2022.05.18.492589.

[790] F. Baquero, T. M. Coque, J. C. Galan, and J. L. Martinez. The origin of niches and species in the bacterial world. *Front Microbiol*, 12:657986, 2021. doi: 10.3389/fmicb.2021.657986.

[791] M. G. J. de Vos, M. Zagorski, A. McNally, and T. Bollenbach. Interaction networks, ecological stability, and collective antibiotic tolerance in polymicrobial infections. *Proc Natl Acad Sci U S A*, 114(40):10666–10671, 2017. doi: 10.1073/pnas.1713372114.

[792] S. Qin, W. Xiao, C. Zhou, Q. Pu, X. Deng, L. Lan, H. Liang, X. Song, and M. Wu. Pseudomonas aeruginosa: pathogenesis, virulence factors, antibiotic resistance, interaction with host, technology advances and emerging therapeutics. *Signal Transduct Target Ther*, 7(1):199, 2022. doi: 10.1038/s41392-022-01056-1.

[793] T. R. Costa, C. Felisberto-Rodrigues, A. Meir, M. S. Prevost, A. Redzej, M. Trokter, and G. Waksman. Secretion systems in gram-negative bacteria: structural and mechanistic insights. *Nat Rev Microbiol*, 13(6):343–59, 2015. doi: 10.1038/nrmicro3456.

[794] C. S. Hayes, S. Koskiniemi, Z. C. Ruhe, S. J. Poole, and D. A. Low. Mechanisms and biological roles of contact-dependent growth inhibition systems. *Cold Spring Harb Perspect Med*, 4(2), 2014. doi: 10.1101/cshperspect.a010025.

[795] F. Jean-Pierre, A. Vyas, T. H. Hampton, M. A. Henson, and G. A. O'Toole. One versus many: Polymicrobial communities and the cystic fibrosis airway. *mBio*, 12(2), 2021. doi: 10.1128/mBio.00006-21.

[796] S. Malhotra, Jr. Hayes, D., and D. J. Wozniak. Cystic fibrosis and pseudomonas aeruginosa: the host-microbe interface. *Clin Microbiol Rev*, 32(3), 2019. doi: 10.1128/CMR.00138-18.

Appendix - Image permissions

CCC Marketplace

Order Number: 1327913
Order Date: 25 Feb 2023

Payment Information

Marta Rudzite
marta.rudzite18@imperial.ac.uk
Payment method: Invoice

Billing Address:
Marta Rudzite
Imperial College London
South Kensington Campus, Flowers Buildin
London, Select... SW7 2AZ
United Kingdom

+44 7541011945
marta.rudzite18@imperial.ac.uk

Customer Location:
Marta Rudzite
Imperial College London
South Kensington Campus, Flowers Buildin
London, Select... SW7 2AZ
United Kingdom

Order Details

1. Journal of bacteriology : JB

Billing Status: Open

Article: Diversity of Contact-Dependent Growth Inhibition Systems of Pseudomonas aeruginosa

Order License ID	1327913-1	**Type of use**	Republish in a thesis/dissertation
Order detail status	Completed		
ISSN	1098-5530	**Publisher**	AMERICAN SOCIETY FOR MICROBIOLOGY
		Portion	Image/photo/illustration

0.00 USD
Republication Permission

LICENSED CONTENT

Publication Title	Journal of bacteriology : JB	**Rightsholder**	American Society for Microbiology - Journals
Article Title	Diversity of Contact-Dependent Growth Inhibition Systems of Pseudomonas aeruginosa	**Publication Type**	e-Journal
		Issue	14
		Volume	201
		URL	https://journals.asm.org/journal/jb
Author/Editor	American Society for Microbiology.		
Date	01/01/1916		
Language	English		
Country	United States of America		

REQUEST DETAILS

Portion Type	Image/photo/illustration

Number of Images / Photos / Illustrations	1	**Distribution**	U.K. and Commonwealth (excluding Canada)
Format (select all that apply)	Print, Electronic	**Translation**	Original language of publication
Who Will Republish the Content?	Academic institution	**Copies for the Disabled?**	No
Duration of Use	Life of current edition	**Minor Editing Privileges?**	Yes
Lifetime Unit Quantity	Up to 499	**Incidental Promotional Use?**	No
Rights Requested	Main product	**Currency**	USD

NEW WORK DETAILS

Title	Type VI secretion system mediated competition in Pseudomonas aeruginosa: modulation of system activity, contribution of individual toxins and bacterial intermixing.	**Institution Name**	Imperial College London
		Expected Presentation Date	2023-02-28
Instructor Name	Alain Filloux		

ADDITIONAL DETAILS

The Requesting Person/Organization to Appear on the License	Marta Rudzitw

REQUESTED CONTENT DETAILS

Title, Description or Numeric Reference of the Portion(s)	Figure 1	**Title of the Article/Chapter the Portion Is From**	Diversity of Contact-Dependent Growth Inhibition Systems of Pseudomonas aeruginosa
Editor of Portion(s)	Allen, Jonathan P.; Hauser, Alan R.	**Author of Portion(s)**	Allen, Jonathan P.; Hauser, Alan R.
Volume of Serial or Monograph	201		
Page or Page Range of Portion	1	**Issue, if Republishing an Article From a Serial**	14
		Publication Date of Portion	2019-07-15

SPRINGER NATURE LICENSE
TERMS AND CONDITIONS

Feb 23, 2023

This Agreement between Imperial College London -- Marta Rudzite ("You") and Springer Nature ("Springer Nature") consists of your license details and the terms and conditions provided by Springer Nature and Copyright Clearance Center.

License Number	5494851180294
License date	Feb 23, 2023
Licensed Content Publisher	Springer Nature
Licensed Content Publication	Nature Reviews Microbiology
Licensed Content Title	The biofilm life cycle: expanding the conceptual model of biofilm formation
Licensed Content Author	Karin Sauer et al
Licensed Content Date	Aug 3, 2022
Type of Use	Thesis/Dissertation
Requestor type	academic/university or research institute
Format	print and electronic
Portion	figures/tables/illustrations
Number of figures/tables/illustrations	2
High-res required	no
Will you be translating?	no

Circulation/distribution	1 - 29
Author of this Springer Nature content	no
Title	Type VI secretion system mediated competition in Pseudomonas aeruginosa: modulation of system activity, contribution of individual toxins and bacterial intermixing.
Institution name	Imperial College London
Expected presentation date	Feb 2023
Portions	Figures 1 and 5
Requestor Location	Imperial College London South Kensington Campus, Flowers Buildin London, Select... SW7 2AZ United Kingdom Attn: Imperial College London
Total	0.00 USD

Terms and Conditions

Springer Nature Customer Service Centre GmbH Terms and Conditions

The following terms and conditions ("Terms and Conditions") together with the terms specified in your [RightsLink] constitute the License ("License") between you as Licensee and Springer Nature Customer Service Centre GmbH as Licensor. By clicking 'accept' and completing the transaction for your use of the material ("Licensed Material"), you confirm your acceptance of and obligation to be bound by these Terms and Conditions.

1. Grant and Scope of License

1. 1. The Licensor grants you a personal, non-exclusive, non-transferable, non-sublicensable, revocable, world-wide License to reproduce, distribute, communicate to the public, make available, broadcast, electronically transmit or create derivative works using the Licensed Material for the purpose(s) specified in your RightsLink Licence Details only. Licenses are granted for the specific use requested in the order and for no other use, subject to these Terms and Conditions. You acknowledge and agree that the rights granted to you under this License do not include the right to modify, edit, translate, include in collective works, or create derivative works of the

SPRINGER NATURE LICENSE
TERMS AND CONDITIONS

Dec 27, 2022

This Agreement between Imperial College London -- Marta Rudzite ("You") and Springer Nature ("Springer Nature") consists of your license details and the terms and conditions provided by Springer Nature and Copyright Clearance Center.

License Number	5457191385234
License date	Dec 27, 2022
Licensed Content Publisher	Springer Nature
Licensed Content Publication	Nature Reviews Microbiology
Licensed Content Title	Principles of c-di-GMP signalling in bacteria
Licensed Content Author	Regine Hengge
Licensed Content Date	Dec 31, 1969
Type of Use	Thesis/Dissertation
Requestor type	academic/university or research institute
Format	print and electronic
Portion	figures/tables/illustrations
Number of figures/tables/illustrations	1
Will you be translating?	no
Circulation/distribution	1 - 29

Author of this Springer Nature content	no
Title	Type VI secretion system mediated competition in Pseudomonas aeruginosa: modulation of system activity, contribution of individual toxins and bacterial intermixing.
Institution name	Imperial College London
Expected presentation date	Feb 2023
Portions	figure 1
Requestor Location	Imperial College London South Kensington Campus, Flowers Buildin London, Select... SW7 2AZ United Kingdom Attn: Imperial College London
Total	0.00 USD

Terms and Conditions

Springer Nature Customer Service Centre GmbH Terms and Conditions

The following terms and conditions ("Terms and Conditions") together with the terms specified in your [RightsLink] constitute the License ("License") between you as Licensee and Springer Nature Customer Service Centre GmbH as Licensor. By clicking 'accept' and completing the transaction for your use of the material ("Licensed Material"), you confirm your acceptance of and obligation to be bound by these Terms and Conditions.

1. Grant and Scope of License

1. 1. The Licensor grants you a personal, non-exclusive, non-transferable, non-sublicensable, revocable, world-wide License to reproduce, distribute, communicate to the public, make available, broadcast, electronically transmit or create derivative works using the Licensed Material for the purpose(s) specified in your RightsLink Licence Details only. Licenses are granted for the specific use requested in the order and for no other use, subject to these Terms and Conditions. You acknowledge and agree that the rights granted to you under this License do not include the right to modify, edit, translate, include in collective works, or create derivative works of the Licensed Material in whole or in part unless expressly stated in your RightsLink Licence Details. You may use the Licensed Material only as permitted under this Agreement and will not reproduce, distribute, display, perform, or otherwise use or exploit any Licensed Material in any way, in whole or in part, except as expressly

ELSEVIER LICENSE
TERMS AND CONDITIONS

Feb 23, 2023

This Agreement between Imperial College London -- Marta Rudzite ("You") and Elsevier ("Elsevier") consists of your license details and the terms and conditions provided by Elsevier and Copyright Clearance Center.

License Number	5494851420460
License date	Feb 23, 2023
Licensed Content Publisher	Elsevier
Licensed Content Publication	Current Opinion in Microbiology
Licensed Content Title	Commensal inter-bacterial interactions shaping the microbiota
Licensed Content Author	Lara Kern,Suhaib K Abdeen,Aleksandra A Kolodziejczyk,Eran Elinav
Licensed Content Date	Oct 1, 2021
Licensed Content Volume	63
Licensed Content Issue	n/a
Licensed Content Pages	14
Start Page	158
End Page	171
Type of Use	reuse in a thesis/dissertation
Portion	figures/tables/illustrations

Number of figures/tables/illustrations	1
Format	both print and electronic
Are you the author of this Elsevier article?	No
Will you be translating?	No
Title	Type VI secretion system mediated competition in Pseudomonas aeruginosa: modulation of system activity, contribution of individual toxins and bacterial intermixing.
Institution name	Imperial College London
Expected presentation date	Feb 2023
Portions	Figure 1
Requestor Location	Imperial College London South Kensington Campus, Flowers Buildin London, Select... SW7 2AZ United Kingdom Attn: Imperial College London
Publisher Tax ID	GB 494 6272 12
Total	0.00 USD
Terms and Conditions	

INTRODUCTION

1. The publisher for this copyrighted material is Elsevier. By clicking "accept" in connection with completing this licensing transaction, you agree that the following terms and conditions apply to this transaction (along with the Billing and Payment terms and conditions established by Copyright Clearance Center, Inc. ("CCC"), at the time that you opened your Rightslink account and that are available at any time at http://myaccount.copyright.com).

GENERAL TERMS

SPRINGER NATURE LICENSE
TERMS AND CONDITIONS

Feb 23, 2023

This Agreement between Imperial College London -- Marta Rudzite ("You") and Springer Nature ("Springer Nature") consists of your license details and the terms and conditions provided by Springer Nature and Copyright Clearance Center.

License Number	5494850642959
License date	Feb 23, 2023
Licensed Content Publisher	Springer Nature
Licensed Content Publication	Nature Reviews Microbiology
Licensed Content Title	Type IV pili: dynamics, biophysics and functional consequences
Licensed Content Author	Lisa Craig et al
Licensed Content Date	Apr 15, 2019
Type of Use	Thesis/Dissertation
Requestor type	academic/university or research institute
Format	electronic
Portion	figures/tables/illustrations
Number of figures/tables/illustrations	1
High-res required	no
Will you be translating?	no

Circulation/distribution	1 - 29
Author of this Springer Nature content	no
Title	Type VI secretion system mediated competition in Pseudomonas aeruginosa: modulation of system activity, contribution of individual toxins and bacterial intermixing.
Institution name	Imperial College London
Expected presentation date	Feb 2023
Portions	Figure 5
Requestor Location	Imperial College London South Kensington Campus, Flowers Buildin London, Select... SW7 2AZ United Kingdom Attn: Imperial College London
Total	0.00 USD

Terms and Conditions

Springer Nature Customer Service Centre GmbH Terms and Conditions

The following terms and conditions ("Terms and Conditions") together with the terms specified in your [RightsLink] constitute the License ("License") between you as Licensee and Springer Nature Customer Service Centre GmbH as Licensor. By clicking 'accept' and completing the transaction for your use of the material ("Licensed Material"), you confirm your acceptance of and obligation to be bound by these Terms and Conditions.

1. Grant and Scope of License

1. 1. The Licensor grants you a personal, non-exclusive, non-transferable, non-sublicensable, revocable, world-wide License to reproduce, distribute, communicate to the public, make available, broadcast, electronically transmit or create derivative works using the Licensed Material for the purpose(s) specified in your RightsLink Licence Details only. Licenses are granted for the specific use requested in the order and for no other use, subject to these Terms and Conditions. You acknowledge and agree that the rights granted to you under this License do not include the right to modify, edit, translate, include in collective works, or create derivative works of the

JOHN WILEY AND SONS LICENSE
TERMS AND CONDITIONS

Feb 23, 2023

This Agreement between Imperial College London -- Marta Rudzite ("You") and John Wiley and Sons ("John Wiley and Sons") consists of your license details and the terms and conditions provided by John Wiley and Sons and Copyright Clearance Center.

License Number	5494861117937
License date	Feb 23, 2023
Licensed Content Publisher	John Wiley and Sons
Licensed Content Publication	Molecular Microbiology
Licensed Content Title	Type IV secretion in Gram-negative and Gram-positive bacteria
Licensed Content Author	Steffen Backert, Gabriel Waksman, Peter J. Christie, et al
Licensed Content Date	Jan 18, 2018
Licensed Content Volume	107
Licensed Content Issue	4
Licensed Content Pages	17
Type of use	Dissertation/Thesis
Requestor type	University/Academic

Format	Print and electronic
Portion	Figure/table
Number of figures/tables	1
Will you be translating?	No
Title	Type VI secretion system mediated competition in Pseudomonas aeruginosa: modulation of system activity, contribution of individual toxins and bacterial intermixing.
Institution name	Imperial College London
Expected presentation date	Feb 2023
Portions	Summary figure
Requestor Location	Imperial College London South Kensington Campus, Flowers Buildin London, Select... SW7 2AZ United Kingdom Attn: Imperial College London
Publisher Tax ID	EU826007151
Total	0.00 USD

Terms and Conditions

TERMS AND CONDITIONS

This copyrighted material is owned by or exclusively licensed to John Wiley & Sons, Inc. or one of its group companies (each a"Wiley Company") or handled on behalf of a society with which a Wiley Company has exclusive publishing rights in relation to a particular work (collectively "WILEY"). By clicking "accept" in connection with completing this licensing transaction, you agree that the following terms and conditions apply to this transaction (along with the billing and payment terms and conditions established by the Copyright Clearance Center Inc., ("CCC's Billing and Payment terms and conditions"), at the time that

ELSEVIER LICENSE
TERMS AND CONDITIONS

Feb 23, 2023

This Agreement between Imperial College London -- Marta Rudzite ("You") and Elsevier ("Elsevier") consists of your license details and the terms and conditions provided by Elsevier and Copyright Clearance Center.

License Number	5494870484911
License date	Feb 23, 2023
Licensed Content Publisher	Elsevier
Licensed Content Publication	Current Opinion in Structural Biology
Licensed Content Title	Towards a complete structural deciphering of Type VI secretion system
Licensed Content Author	Van Son Nguyen,Badreddine Douzi,Eric Durand,Alain Roussel,Eric Cascales,Christian Cambillau
Licensed Content Date	Apr 1, 2018
Licensed Content Volume	49
Licensed Content Issue	n/a
Licensed Content Pages	8
Start Page	77
End Page	84
Type of Use	reuse in a thesis/dissertation
Portion	figures/tables/illustrations

Number of figures/tables/illustrations	1
Format	both print and electronic
Are you the author of this Elsevier article?	No
Will you be translating?	No
Title	Type VI secretion system mediated competition in Pseudomonas aeruginosa: modulation of system activity, contribution of individual toxins and bacterial intermixing.
Institution name	Imperial College London
Expected presentation date	Feb 2023
Portions	FIgure 4
Requestor Location	Imperial College London South Kensington Campus, Flowers Buildin London, Select... SW7 2AZ United Kingdom Attn: Imperial College London
Publisher Tax ID	GB 494 6272 12
Total	0.00 USD
Terms and Conditions	

INTRODUCTION

1. The publisher for this copyrighted material is Elsevier. By clicking "accept" in connection with completing this licensing transaction, you agree that the following terms and conditions apply to this transaction (along with the Billing and Payment terms and conditions established by Copyright Clearance Center, Inc. ("CCC"), at the time that you opened your Rightslink account and that are available at any time at http://myaccount.copyright.com).

GENERAL TERMS

Marketplace

Order Confirmation

Thank you, your order has been placed. An email confirmation has been sent to you. Your order license details and printable licenses will be available within 24 hours. Please access Manage Account for final order details.

This is not an invoice. Please go to manage account to access your order history and invoices.

CUSTOMER INFORMATION

Payment by invoice: You can cancel your order until the invoice is generated by contacting customer service.

Billing Address

Marta Rudzite
Imperial College London
South Kensington Campus, Flowers Buildin
London, Select... SW7 2AZ
United Kingdom

+44 7541011945
marta.rudzite18@imperial.ac.uk

Customer Location

Marta Rudzite
Imperial College London
South Kensington Campus, Flowers Buildin
London, Select... SW7 2AZ
United Kingdom

PO Number (optional)

N/A

Payment options

Invoice

PENDING ORDER CONFIRMATION

Confirmation Number: Pending

Order Date: 27-Feb-2023

1. Annual review of virology

0.00 USD

Order License ID	Pending	**Publisher**	Annual Reviews
ISSN	2327-0578	**Portion**	Chart/graph/table/figure
Type of Use	Republish in a thesis/dissertation		

LICENSED CONTENT

Publication Title	Annual review of virology	**Rightsholder**	Annual Reviews, Inc.
Date	01/01/2014	**Publication Type**	e-Journal
Language	English	**URL**	http://www.annualreviews.org/journal/virology
Country	United States of America		

REQUEST DETAILS

Portion Type	Chart/graph/table/figure	**Distribution**	U.K. and Commonwealth (excluding Canada)
Number of Charts / Graphs / Tables / Figures Requested	1	**Translation**	Original language of publication
Format (select all that apply)	Electronic	**Copies for the Disabled?**	No
Who Will Republish the Content?	Academic institution	**Minor Editing Privileges?**	Yes
Duration of Use	Life of current edition	**Incidental Promotional Use?**	No
Lifetime Unit Quantity	Up to 499	**Currency**	USD
Rights Requested	Main product		

NEW WORK DETAILS

Title	Type VI secretion system mediated competition in Pseudomonas aeruginosa: modulation of system activity, contribution of individual toxins and bacterial intermixing	**Institution Name**	Imperial College London
		Expected Presentation Date	2023-02-28
Instructor Name	Alain FIlloux		

ADDITIONAL DETAILS

Order Reference Number	N/A	**The Requesting Person/Organization to Appear on the License**	Marta Rudzite

REQUESTED CONTENT DETAILS

Title, Description or Numeric Reference of the Portion(s)	Figure 3	**Title of the Article/Chapter the Portion Is From**	N/A
Editor of Portion(s)	N/A	**Author of Portion(s)**	N/A
Volume of Serial or Monograph	N/A	**Issue, if Republishing an Article From a Serial**	N/A
Page or Page Range of Portion	1	**Publication Date of Portion**	2014-01-01

Total Items: 1

Total Due: 0.00 USD

Accepted: Marketplace Permissions General Terms and Conditions and any applicable Publisher Terms and Conditions

SPRINGER NATURE LICENSE
TERMS AND CONDITIONS

Feb 23, 2023

This Agreement between Imperial College London -- Marta Rudzite ("You") and Springer Nature ("Springer Nature") consists of your license details and the terms and conditions provided by Springer Nature and Copyright Clearance Center.

License Number	5494871024222
License date	Feb 23, 2023
Licensed Content Publisher	Springer Nature
Licensed Content Publication	Nature Reviews Microbiology
Licensed Content Title	Type VI secretion system effectors: poisons with a purpose
Licensed Content Author	Alistair B. Russell et al
Licensed Content Date	Jan 2, 2014
Type of Use	Thesis/Dissertation
Requestor type	academic/university or research institute
Format	print and electronic
Portion	figures/tables/illustrations
Number of figures/tables/illustrations	1
High-res required	no
Will you be translating?	no

Circulation/distribution	1 - 29
Author of this Springer Nature content	no
Title	Type VI secretion system mediated competition in Pseudomonas aeruginosa: modulation of system activity, contribution of individual toxins and bacterial intermixing.
Institution name	Imperial College London
Expected presentation date	Feb 2023
Portions	Figure 1
Requestor Location	Imperial College London South Kensington Campus, Flowers Buildin London, Select... SW7 2AZ United Kingdom Attn: Imperial College London
Total	0.00 USD

Terms and Conditions

Springer Nature Customer Service Centre GmbH Terms and Conditions

The following terms and conditions ("Terms and Conditions") together with the terms specified in your [RightsLink] constitute the License ("License") between you as Licensee and Springer Nature Customer Service Centre GmbH as Licensor. By clicking 'accept' and completing the transaction for your use of the material ("Licensed Material"), you confirm your acceptance of and obligation to be bound by these Terms and Conditions.

1. Grant and Scope of License

1. 1. The Licensor grants you a personal, non-exclusive, non-transferable, non-sublicensable, revocable, world-wide License to reproduce, distribute, communicate to the public, make available, broadcast, electronically transmit or create derivative works using the Licensed Material for the purpose(s) specified in your RightsLink Licence Details only. Licenses are granted for the specific use requested in the order and for no other use, subject to these Terms and Conditions. You acknowledge and agree that the rights granted to you under this License do not include the right to modify, edit, translate, include in collective works, or create derivative works of the

SPRINGER NATURE LICENSE
TERMS AND CONDITIONS

Feb 23, 2023

This Agreement between Imperial College London -- Marta Rudzite ("You") and Springer Nature ("Springer Nature") consists of your license details and the terms and conditions provided by Springer Nature and Copyright Clearance Center.

License Number	5494870663850
License date	Feb 23, 2023
Licensed Content Publisher	Springer Nature
Licensed Content Publication	Nature Microbiology
Licensed Content Title	Mechanism of loading and translocation of type VI secretion system effector Tse6
Licensed Content Author	Dennis Quentin et al
Licensed Content Date	Sep 3, 2018
Type of Use	Thesis/Dissertation
Requestor type	academic/university or research institute
Format	print and electronic
Portion	figures/tables/illustrations
Number of figures/tables/illustrations	2
High-res required	no
Will you be translating?	no

Circulation/distribution	1 - 29
Author of this Springer Nature content	no
Title	Type VI secretion system mediated competition in Pseudomonas aeruginosa: modulation of system activity, contribution of individual toxins and bacterial intermixing.
Institution name	Imperial College London
Expected presentation date	Feb 2023
Portions	Figures 1 and 2
Requestor Location	Imperial College London South Kensington Campus, Flowers Buildin London, Select... SW7 2AZ United Kingdom Attn: Imperial College London
Total	0.00 USD

Terms and Conditions

Springer Nature Customer Service Centre GmbH Terms and Conditions

The following terms and conditions ("Terms and Conditions") together with the terms specified in your [RightsLink] constitute the License ("License") between you as Licensee and Springer Nature Customer Service Centre GmbH as Licensor. By clicking 'accept' and completing the transaction for your use of the material ("Licensed Material"), you confirm your acceptance of and obligation to be bound by these Terms and Conditions.

1. Grant and Scope of License

1. 1. The Licensor grants you a personal, non-exclusive, non-transferable, non-sublicensable, revocable, world-wide License to reproduce, distribute, communicate to the public, make available, broadcast, electronically transmit or create derivative works using the Licensed Material for the purpose(s) specified in your RightsLink Licence Details only. Licenses are granted for the specific use requested in the order and for no other use, subject to these Terms and Conditions. You acknowledge and agree that the rights granted to you under this License do not include the right to modify, edit, translate, include in collective works, or create derivative works of the

SPRINGER NATURE LICENSE
TERMS AND CONDITIONS

Feb 23, 2023

This Agreement between Imperial College London -- Marta Rudzite ("You") and Springer Nature ("Springer Nature") consists of your license details and the terms and conditions provided by Springer Nature and Copyright Clearance Center.

License Number	5494880038375
License date	Feb 23, 2023
Licensed Content Publisher	Springer Nature
Licensed Content Publication	Nature
Licensed Content Title	An interbacterial toxin inhibits target cell growth by synthesizing (p)ppApp
Licensed Content Author	Shehryar Ahmad et al
Licensed Content Date	Nov 6, 2019
Type of Use	Thesis/Dissertation
Requestor type	academic/university or research institute
Format	print and electronic
Portion	figures/tables/illustrations
Number of figures/tables/illustrations	1
High-res required	no
Will you be translating?	no

Circulation/distribution	1 - 29
Author of this Springer Nature content	no
Title	Type VI secretion system mediated competition in Pseudomonas aeruginosa: modulation of system activity, contribution of individual toxins and bacterial intermixing.
Institution name	Imperial College London
Expected presentation date	Feb 2023
Portions	Figure 1
Requestor Location	Imperial College London South Kensington Campus, Flowers Buildin London, Select... SW7 2AZ United Kingdom Attn: Imperial College London
Total	0.00 USD

Terms and Conditions

Springer Nature Customer Service Centre GmbH Terms and Conditions

The following terms and conditions ("Terms and Conditions") together with the terms specified in your [RightsLink] constitute the License ("License") between you as Licensee and Springer Nature Customer Service Centre GmbH as Licensor. By clicking 'accept' and completing the transaction for your use of the material ("Licensed Material"), you confirm your acceptance of and obligation to be bound by these Terms and Conditions.

1. Grant and Scope of License

1. 1. The Licensor grants you a personal, non-exclusive, non-transferable, non-sublicensable, revocable, world-wide License to reproduce, distribute, communicate to the public, make available, broadcast, electronically transmit or create derivative works using the Licensed Material for the purpose(s) specified in your RightsLink Licence Details only. Licenses are granted for the specific use requested in the order and for no other use, subject to these Terms and Conditions. You acknowledge and agree that the rights granted to you under this License do not include the right to modify, edit, translate, include in collective works, or create derivative works of the

ELSEVIER LICENSE
TERMS AND CONDITIONS

Dec 27, 2022

This Agreement between Imperial College London -- Marta Rudzite ("You") and Elsevier ("Elsevier") consists of your license details and the terms and conditions provided by Elsevier and Copyright Clearance Center.

License Number	5457180523376
License date	Dec 27, 2022
Licensed Content Publisher	Elsevier
Licensed Content Publication	Current Opinion in Microbiology
Licensed Content Title	Lifestyle transitions and adaptive pathogenesis of Pseudomonas aeruginosa
Licensed Content Author	Martina Valentini,Diego Gonzalez,Despoina AI Mavridou,Alain Filloux
Licensed Content Date	Feb 1, 2018
Licensed Content Volume	41
Licensed Content Issue	n/a
Licensed Content Pages	6
Start Page	15
End Page	20
Type of Use	reuse in a thesis/dissertation
Portion	figures/tables/illustrations

Number of figures/tables/illustrations	2
Format	both print and electronic
Are you the author of this Elsevier article?	No
Will you be translating?	No
Title	Type VI secretion system mediated competition in Pseudomonas aeruginosa: modulation of system activity, contribution of individual toxins and bacterial intermixing.
Institution name	Imperial College London
Expected presentation date	Feb 2023
Portions	Figures 1 and 2
Requestor Location	Imperial College London South Kensington Campus, Flowers Buildin London, Select... SW7 2AZ United Kingdom Attn: Imperial College London
Publisher Tax ID	GB 494 6272 12
Total	0.00 USD
Terms and Conditions	

INTRODUCTION

1. The publisher for this copyrighted material is Elsevier. By clicking "accept" in connection with completing this licensing transaction, you agree that the following terms and conditions apply to this transaction (along with the Billing and Payment terms and conditions established by Copyright Clearance Center, Inc. ("CCC"), at the time that you opened your Rightslink account and that are available at any time at http://myaccount.copyright.com).

GENERAL TERMS

SPRINGER NATURE LICENSE
TERMS AND CONDITIONS

May 02, 2023

This Agreement between Imperial College London -- Marta Rudzite ("You") and Springer Nature ("Springer Nature") consists of your license details and the terms and conditions provided by Springer Nature and Copyright Clearance Center.

License Number	5535491052361
License date	Apr 24, 2023
Licensed Content Publisher	Springer Nature
Licensed Content Publication	Springer eBook
Licensed Content Title	Site-Directed Mutagenesis and Gene Deletion Using Reverse Genetics
Licensed Content Author	Daniela Muhl, Alain Filloux
Licensed Content Date	Jan 1, 2014
Type of Use	Thesis/Dissertation
Requestor type	academic/university or research institute
Format	electronic
Portion	figures/tables/illustrations
Number of figures/tables/illustrations	1
Will you be translating?	no
Circulation/distribution	1 - 29

Author of this Springer Nature content	no
Title	Type VI secretion system mediated competition in Pseudomonas aeruginosa: modulation of system activity, contribution of individual toxins and bacterial intermixing.
Institution name	Imperial College London
Expected presentation date	May 2023
Portions	Figure 6
Requestor Location	Imperial College London South Kensington Campus, Flowers Buildin London, Select... SW7 2AZ United Kingdom Attn: Imperial College London
Total	0.00 USD

Terms and Conditions

Springer Nature Customer Service Centre GmbH Terms and Conditions

The following terms and conditions ("Terms and Conditions") together with the terms specified in your [RightsLink] constitute the License ("License") between you as Licensee and Springer Nature Customer Service Centre GmbH as Licensor. By clicking 'accept' and completing the transaction for your use of the material ("Licensed Material"), you confirm your acceptance of and obligation to be bound by these Terms and Conditions.

1. Grant and Scope of License

1. 1. The Licensor grants you a personal, non-exclusive, non-transferable, non-sublicensable, revocable, world-wide License to reproduce, distribute, communicate to the public, make available, broadcast, electronically transmit or create derivative works using the Licensed Material for the purpose(s) specified in your RightsLink Licence Details only. Licenses are granted for the specific use requested in the order and for no other use, subject to these Terms and Conditions. You acknowledge and agree that the rights granted to you under this License do not include the right to modify, edit, translate, include in collective works, or create derivative works of the Licensed Material in whole or in part unless expressly stated in your RightsLink Licence Details. You may use the Licensed Material only as permitted under this Agreement and will not reproduce, distribute, display, perform, or otherwise use or

exploit any Licensed Material in any way, in whole or in part, except as expressly permitted by this License.

1. 2. You may only use the Licensed Content in the manner and to the extent permitted by these Terms and Conditions, by your RightsLink Licence Details and by any applicable laws.

1. 3. A separate license may be required for any additional use of the Licensed Material, e.g. where a license has been purchased for print use only, separate permission must be obtained for electronic re-use. Similarly, a License is only valid in the language selected and does not apply for editions in other languages unless additional translation rights have been granted separately in the License.

1. 4. Any content within the Licensed Material that is owned by third parties is expressly excluded from the License.

1. 5. Rights for additional reuses such as custom editions, computer/mobile applications, film or TV reuses and/or any other derivative rights requests require additional permission and may be subject to an additional fee. Please apply to journalpermissions@springernature.com or bookpermissions@springernature.com for these rights.

2. Reservation of Rights

Licensor reserves all rights not expressly granted to you under this License. You acknowledge and agree that nothing in this License limits or restricts Licensor's rights in or use of the Licensed Material in any way. Neither this License, nor any act, omission, or statement by Licensor or you, conveys any ownership right to you in any Licensed Material, or to any element or portion thereof. As between Licensor and you, Licensor owns and retains all right, title, and interest in and to the Licensed Material subject to the license granted in Section 1.1. Your permission to use the Licensed Material is expressly conditioned on you not impairing Licensor's or the applicable copyright owner's rights in the Licensed Material in any way.

3. Restrictions on use

3. 1. Minor editing privileges are allowed for adaptations for stylistic purposes or formatting purposes provided such alterations do not alter the original meaning or intention of the Licensed Material and the new figure(s) are still accurate and representative of the Licensed Material. Any other changes including but not limited to, cropping, adapting, and/or omitting material that affect the meaning, intention or moral rights of the author(s) are strictly prohibited.

3. 2. You must not use any Licensed Material as part of any design or trademark.

3. 3. Licensed Material may be used in Open Access Publications (OAP), but any such reuse must include a clear acknowledgment of this permission visible at the same time as the figures/tables/illustration or abstract and which must indicate that the Licensed Material is not part of the governing OA license but has been reproduced with permission. This may be indicated according to any standard referencing system but must include at a minimum 'Book/Journal title, Author, Journal Name (if applicable), Volume (if applicable), Publisher, Year, reproduced with permission from SNCSC'.

4. STM Permission Guidelines

4. 1. An alternative scope of license may apply to signatories of the STM Permissions Guidelines ("STM PG") as amended from time to time and made available at

https://www.stm-assoc.org/intellectual-property/permissions/permissions-guidelines/.

4. 2. For content reuse requests that qualify for permission under the STM PG, and which may be updated from time to time, the STM PG supersede the terms and conditions contained in this License.

4. 3. If a License has been granted under the STM PG, but the STM PG no longer apply at the time of publication, further permission must be sought from the Rightsholder. Contact journalpermissions@springernature.com or bookpermissions@springernature.com for these rights.

5. Duration of License

5. 1. Unless otherwise indicated on your License, a License is valid from the date of purchase ("License Date") until the end of the relevant period in the below table:

Reuse in a medical communications project	Reuse up to distribution or time period indicated in License
Reuse in a dissertation/thesis	Lifetime of thesis
Reuse in a journal/magazine	Lifetime of journal/magazine
Reuse in a book/textbook	Lifetime of edition
Reuse on a website	1 year unless otherwise specified in the License
Reuse in a presentation/slide kit/poster	Lifetime of presentation/slide kit/poster. Note: publication whether electronic or in print of presentation/slide kit/poster may require further permission.
Reuse in conference proceedings	Lifetime of conference proceedings
Reuse in an annual report	Lifetime of annual report
Reuse in training/CME materials	Reuse up to distribution or time period indicated in License
Reuse in newsmedia	Lifetime of newsmedia
Reuse in coursepack/classroom materials	Reuse up to distribution and/or time period indicated in license

6. Acknowledgement

6. 1. The Licensor's permission must be acknowledged next to the Licensed Material in print. In electronic form, this acknowledgement must be visible at the same time as the figures/tables/illustrations or abstract and must be hyperlinked to the journal/book's homepage.

6. 2. Acknowledgement may be provided according to any standard referencing system and at a minimum should include "Author, Article/Book Title, Journal name/Book imprint, volume, page number, year, Springer Nature".

7. Reuse in a dissertation or thesis

7. 1. Where 'reuse in a dissertation/thesis' has been selected, the following terms apply: Print rights of the Version of Record are provided for; electronic rights for use only on institutional repository as defined by the Sherpa guideline (www.sherpa.ac.uk/romeo/) and only up to what is required by the awarding institution.

7. 2. For theses published under an ISBN or ISSN, separate permission is required. Please contact journalpermissions@springernature.com or bookpermissions@springernature.com for these rights.

7. 3. Authors must properly cite the published manuscript in their thesis according to current citation standards and include the following acknowledgement: '*Reproduced with permission from Springer Nature*'.

8. License Fee

You must pay the fee set forth in the License Agreement (the "License Fees"). All amounts payable by you under this License are exclusive of any sales, use, withholding, value added or similar taxes, government fees or levies or other assessments. Collection and/or remittance of such taxes to the relevant tax authority shall be the responsibility of the party who has the legal obligation to do so.

9. Warranty

9. 1. The Licensor warrants that it has, to the best of its knowledge, the rights to license reuse of the Licensed Material. **You are solely responsible for ensuring that the material you wish to license is original to the Licensor and does not carry the copyright of another entity or third party (as credited in the published version).** If the credit line on any part of the Licensed Material indicates that it was reprinted or adapted with permission from another source, then you should seek additional permission from that source to reuse the material.

9. 2. EXCEPT FOR THE EXPRESS WARRANTY STATED HEREIN AND TO THE EXTENT PERMITTED BY APPLICABLE LAW, LICENSOR PROVIDES THE LICENSED MATERIAL "AS IS" AND MAKES NO OTHER REPRESENTATION OR WARRANTY. LICENSOR EXPRESSLY DISCLAIMS ANY LIABILITY FOR ANY CLAIM ARISING FROM OR OUT OF THE CONTENT, INCLUDING BUT NOT LIMITED TO ANY ERRORS, INACCURACIES, OMISSIONS, OR DEFECTS CONTAINED THEREIN, AND ANY IMPLIED OR EXPRESS WARRANTY AS TO MERCHANTABILITY OR FITNESS FOR A PARTICULAR PURPOSE. IN NO EVENT SHALL LICENSOR BE LIABLE TO YOU OR ANY OTHER PARTY OR ANY OTHER PERSON OR FOR ANY SPECIAL, CONSEQUENTIAL, INCIDENTAL, INDIRECT, PUNITIVE, OR EXEMPLARY DAMAGES, HOWEVER CAUSED, ARISING OUT OF OR IN CONNECTION WITH THE DOWNLOADING, VIEWING OR USE OF THE LICENSED MATERIAL REGARDLESS OF THE FORM OF ACTION, WHETHER FOR BREACH OF CONTRACT, BREACH OF WARRANTY, TORT, NEGLIGENCE, INFRINGEMENT OR OTHERWISE (INCLUDING, WITHOUT LIMITATION, DAMAGES BASED ON LOSS OF PROFITS, DATA, FILES, USE, BUSINESS OPPORTUNITY OR CLAIMS OF THIRD PARTIES), AND WHETHER OR NOT THE PARTY HAS BEEN ADVISED OF THE POSSIBILITY OF SUCH DAMAGES. THIS LIMITATION APPLIES NOTWITHSTANDING ANY FAILURE OF ESSENTIAL PURPOSE OF ANY LIMITED REMEDY PROVIDED HEREIN.

10. Termination and Cancellation

10. 1. The License and all rights granted hereunder will continue until the end of the applicable period shown in Clause 5.1 above. Thereafter, this license will be terminated and all rights granted hereunder will cease.

10. 2. Licensor reserves the right to terminate the License in the event that payment is not received in full or if you breach the terms of this License.

11. General

11. 1. The License and the rights and obligations of the parties hereto shall be construed, interpreted and determined in accordance with the laws of the Federal Republic of Germany without reference to the stipulations of the CISG (United Nations Convention on Contracts for the International Sale of Goods) or to Germany´s choice-of-law principle.

11. 2. The parties acknowledge and agree that any controversies and disputes arising out of this License shall be decided exclusively by the courts of or having jurisdiction for Heidelberg, Germany, as far as legally permissible.

11. 3. This License is solely for Licensor's and Licensee's benefit. It is not for the benefit of any other person or entity.

Questions? For questions on Copyright Clearance Center accounts or website issues please contact springernaturesupport@copyright.com or +1-855-239-3415 (toll free in the US) or +1-978-646-2777. For questions on Springer Nature licensing please visit https://www.springernature.com/gp/partners/rights-permissions-third-party-distribution

Other Conditions:

Version 1.4 - Dec 2022

Questions? customercare@copyright.com.